



**Using GEMMs to investigate
novel therapeutic strategies for colorectal cancer**

Meera Raja

Cardiff University

Ph. D

2009-2013



Declarations

This work has not been submitted in substance for any other degree or award at this or any other university or place of learning, nor is being submitted concurrently in candidature for any degree or other award.

This thesis is being submitted in partial fulfilment of the requirements for the degree of PhD.

This thesis is the result of my own independent work/investigation, except where otherwise stated. Other sources are acknowledged by explicit references. The views expressed are my own.

I hereby give consent for my thesis, if accepted, to be available for photocopying and for inter-library loan, and for the title and summary to be made available to outside organisations.

I hereby give consent for my thesis, if accepted, to be available for photocopying and for inter-library loans after expiry of a bar on access previously approved by the Academic Standards & Quality Committee.

Signed.....(Candidate)

Date.....

Acknowledgements

First and foremost, I must thank my supervisors- Professor Alan Clarke for his scientific wisdom, advice and guidance during this time and Dr Paul Shaw for his support, constant enthusiasm and optimism. I would like to thank both for providing an interesting project and a stimulating start to my scientific career. I would also like to thank Tenovus, in particular the Jane Hodge foundation for kindly funding my studentship.

For their assistance with reagents and data analysis, I would like to thank Professor Chris McGuigan, Dr Stephanie Rats and Dr Sahar Kandhil from the Welsh school of pharmacy who synthesised and provided ProTide agents, and to Professor Jan Balzarini (Rega Institute) for kindly providing MCF7 and MCF7TDX cell lines. I would like to thank former PhD students in the Clarkson lab, Alison Wakefield and Syn Kok for assistance with tissue culture experiments, and I would also like to thank Dr Geraint Williams (School of Medicine, Cardiff University) for providing expertise with histopathology and for the many patient hours spent at the microscope.

Much of the research presented in this thesis would not have been possible without the technical assistance of a number of individuals. In particular, Derek Scarborough and Mark Isaac for their excellent histology services and without whom I would have endured many laborious hours of tissue slicing. I would like to thank the PCR dream team: Mark Bishop and Lucie Stocking, and more recently, Matt Zverev and Elaine Taylor for their assistance with genotyping and ear clipping. I must also thank Matt in particular, for taking over the many hours of gavaging during my final year to allow me to finish data analysis and start the write-up. I would also like to thank Emma Davies, Lili Ordonez and Trevor Hay who spent many hours in the basement, kindly gavaging for me during my holidays and to Valerie Meniel for her selfless assistance both in the lab and the basement.

I would also like to thank Dr Trevor Hay, for his input and assistance in collecting data presented in chapter 7, who has been a pleasure to work with. To Tanya Davies, a final year undergraduate student who conducted some of the scoring and IHCs presented in chapter 3. I would also like to thank Lucie, Emma and Val for their kind friendship, support and advice within the lab but also from various corners of the country! Finally I would like to thank all the members of the ARC group and everyone on the 4th and 5th floor of BIOSI3 who were not mentioned in person, but made my experience an enjoyable one, filled with lots of wine, cake and popcorn!

On a personal note, I am indebted to my family, in particular my parents, brother and sister-in law for their unconditional support and encouragement to fulfil my academic goals, in particular my father who I wish was here today. I would like to thank my long suffering partner Chris for his love and endless support, providing a mostly stress-free and happy home, but mainly for putting up with me through the last 4 years. Finally, I would also like to thank Chris's parents Tim and Ruth for their support, in particular for funding a very enjoyable 'writing holiday' which helped me beat the thesis blues.

Table of contents

Declarations	ii
Acknowledgements	iii
List of figures	xi
List of Tables	xvii
Abbreviations and Definitions	xix
Abstract	1
1 General Introduction	3
1.1 Colorectal cancer	3
1.1.1 Colorectal cancer statistics and causes.....	3
1.1.2 TNM classification of colorectal cancer.....	4
1.1.3 Current therapeutic strategies for patients with CRC.....	5
1.2 Intestinal biology and maintenance of homeostasis	6
1.2.1 Basic anatomy and function of the intestines.....	6
1.2.2 Small intestine and large intestine histology.....	9
1.2.3 The intestinal stem cell.....	10
1.3 The stem cell niche and maintenance of homeostasis	13
1.3.1 The Canonical Wnt signalling pathway.....	13
1.3.2 The Hedgehog signalling pathway.....	14
1.3.3 The TFG β /BMP signalling pathway.....	15
1.3.4 The Notch signalling pathway.....	17
1.3.5 Colorectal Cancer stem cells.....	20
1.4 The genetic model of colorectal cancer progression	22
1.5 Novel targeted therapeutic strategies in pre-clinical and clinical development for CRC	26
1.5.1 Targeting developmental pathways and cancer stem cells: Wnt, Notch and Hedgehog pathways.....	26
1.5.2 Mitogen-Activated Protein Kinase Pathway (MAPK/ERK) pathway.....	29
1.5.3 Phosphoinositide-3-kinase (PI3K) pathway.....	32
1.5.4 Anti-cancer prodrugs.....	37
1.6 Preclinical mouse models of colorectal cancer and their value to study translational research	38
1.6.1 Genetically engineered mouse models as useful tools for translational research.....	38
1.6.2 Overview of conditional transgenesis techniques.....	41
1.6.3 Modelling colorectal cancer in the mouse.....	43

1.7	Aims and Objectives	44
2	Materials and Methods	46
2.1	Experimental Animals	46
2.1.1	Animal Husbandry	46
2.1.2	Colony Maintenance	46
2.1.3	Breeding	46
2.1.4	Genetic Mouse Models	46
2.2	Experimental Procedures	49
2.2.1	Ear Biopsies	49
2.2.2	Administration of Tamoxifen	49
2.2.3	Administration of beta-Naphthoflavone and Tamoxifen	49
2.2.4	Treatment strategy for NVP-BEZ235 and MEK162	49
2.2.5	Treatment strategy for BVDU ProTide compounds	52
2.2.6	Administration of BrdU	53
2.3	Polymerase Chain Reaction (PCR) genotyping	53
2.3.1	DNA extraction from ear biopsies	53
2.3.2	Generic PCR genotyping protocol	53
2.3.3	Visualisation of PCR products	54
2.4	Tissue sample preparation	56
2.4.1	Dissection of Organs	56
2.4.2	Dissection of intestines	56
2.5	Fixation of tissues	56
2.5.1	Formalin fixation	56
2.5.2	Methacarn fixation of intestines	57
2.5.3	Processing of fixed tissue	57
2.5.4	Sectioning of fixed tissue	57
2.6	Histological Analysis	57
2.6.1	Preparation of sections for staining or IHC	57
2.6.2	Immunohistochemistry	58
2.6.3	Generic IHC protocol	58
2.6.4	Haematoxylin and Eosin (H&E) stain	62
2.7	Scoring	62
2.7.1	Apoptosis and mitosis scoring	62
2.7.2	BrdU Scoring	62
2.7.3	Cleaved caspase 3 scoring	62
2.7.4	Tumour severity grading	62
2.8	Protein Extraction and Western Blot Analysis	65
2.8.1	Protein extraction	65

2.8.2	Determination of protein concentration	65
2.8.3	Preparation of protein samples for western blot analysis.....	66
2.8.4	Casting of polyacrylamide gels.....	66
2.8.5	SDS-PAGE	67
2.8.6	Protein transfer to nitrocellulose membrane	68
2.8.7	Primary and Secondary antibody probing on nitrocellulose membrane.....	68
2.8.8	Signal detection.....	68
2.8.9	Confirmation of equal loading	69
2.8.10	Densitometry Analysis.....	69
2.9	<i>Maintenance and culture of cells</i>	71
2.9.1	Experimental cell lines	71
2.9.2	Maintenance of cell lines	71
2.9.3	Long term cell storage.....	71
2.9.4	Collection of cells for RNA extraction	72
2.9.5	Cell Titer Blue cell viability assay.....	72
2.9.6	Colony forming assay	73
2.10	<i>RNA extraction and Gene expression analysis</i>	73
2.10.1	RNA isolation and quantification	73
2.10.2	Homogenisation of cells.....	73
2.10.3	RNA extraction and purification.....	74
2.10.4	DNase treatment.....	74
2.10.5	cDNA synthesis.....	74
2.10.6	Design of quantitative real-time (qRT) PCR primers	75
2.10.7	Syber green gene expression analysis.....	76
2.10.8	Analysis of qRT-PCR data.....	76
2.11	<i>Data Analysis and Statistical analysis</i>	77
2.11.1	Mann Whitney U test	77
2.11.2	Kaplan Meier survival analysis	77
3	<i>Evaluating MEK and PI3K/mTOR inhibition in the Wnt activated, Apc^{f/+} tumour model</i> 77	
3.1	<i>Introduction</i>	77
3.2	<i>Results</i>	78
3.2.1	Mek inhibitor MEK162 elicits no anti-tumour effect on Apc ^{f/+} colon polyps however, in small intestinal tumours increases proliferation and apoptosis.....	78
3.2.2	MEK162 reduces MAPK signalling through pERK and also reduces PI3K signalling 82	
3.2.3	Continuous MEK162 treatment increases longevity of Apc ^{f/+} mice	85
3.2.4	The acute effects of NVP-BEZ235 in Apc ^{f/+} colon polyps and SITs	87
3.2.5	NVP-BEZ235 preferentially reduces signalling downstream mTOR and not PI3K	88

3.2.6	NVP-BEZ235 significantly increases survival of $Apc^{f/+}$ mice	93
3.2.7	Analysis of tumour burden in $Apc^{f/+}$ mice on various treatments.....	95
3.2.8	Comparison of MAPK and PI3K activation in colonic and small intestinal tumours in alternative models of intestinal cancer.....	99
3.3	Discussion	102
3.3.1	MEK inhibition by MEK162 increases survival of $Apc^{f/+}$ mice and results in tumour growth stasis	102
3.3.2	NVP-BEZ235 treatment in $Apc^{f/+}$ mice also increases longevity of mice and prevents tumour progression	104
3.4	Summary	106
3.5	Further work	106
3.5.1	Further investigation of anti-tumour effects of MEK162 and NVP-BEZ235 in $Apc^{f/+}$ mice	106
3.5.2	Acute and chronic combination therapy in $Apc^{f/+}$ mice	106
4	Investigating PI3K/mTOR inhibition and MEK inhibition in the $Apc^{f/+}$ $Pten^{f/f}$ colorectal cancer mouse model	108
4.1	Introduction	108
4.2	Results	109
4.2.1	NVP-BEZ235 reduces proliferation, induces apoptosis and leads to inhibition of the PI3K and mTOR signalling cascade in $Apc^{f/+}$ $Pten^{f/f}$ tumours	109
4.2.2	Long term PI3K/mTOR inhibition through NVP-BEZ235 leads to a significant increase in survival of $Apc^{f/+}$ $Pten^{f/f}$ mice.....	117
4.2.3	Acute MEK inhibition through MEK162 reduces MAPK signaling and cellular proliferation in $Apc^{f/+}$ $Pten^{f/f}$ tumours, but reduces apoptosis and increases PI3K signalling	119
4.2.4	Chronic MEK162 treatment has no effect on longevity of $Apc^{f/+}$ $Pten^{f/f}$ mice .	126
4.2.5	The sequence of NVP-BEZ235 and MEK162 administration is crucial for combined inhibition of PI3K and MAPK signalling in $Apc^{f/+}$ $Pten^{f/f}$ mice	127
4.2.6	Combination strategy 2 results in prolonged inhibition of the PI3K/mTOR and MAPK signalling cascades.....	135
4.2.7	Combined PI3K/mTOR and MEK inhibition increases longevity of $Apc^{f/+}$ $Pten^{f/f}$ mice.....	139
4.2.8	Tumour burden analysis of $Apc^{f/+}$ $Pten^{f/f}$ mice on long term treatments	143
4.3	Discussion	148
4.3.1	NVP-BEZ235 leads to inhibition of PI3K and mTOR signalling whilst imposing anti-proliferative and pro-apoptotic effects in $Pten$ deficient small intestinal tumours and long term, substantially increasing longevity of mice.....	148
4.3.2	MEK inhibition through MEK162 reduces MAPK signalling in $Pten$ deficient tumours, however does not increase survival of mice potentially through increased PI3K signalling	150
4.3.3	Sequencing of PI3K/mTOR and MEK inhibitors is crucial for concomitant inhibition of signalling cascades.....	151

4.3.4	Summary	154
4.4	Further work	154
4.4.1	Mechanisms of resistance to chronic single agent NVP-BEZ235	154
4.4.2	Further evaluation of the differential sensitivities to acute combination treatment	154
5	Investigating MEK inhibition and PI3K/mTOR inhibition in the $Apc^{f/+}$ $Kras^{LSL/+}$ colorectal cancer mouse model	156
5.1	Introduction	156
5.2	Results	158
5.2.1	MEK162 results in a pro-apoptotic effect in $Apc^{f/+}$ $Kras^{LSL/+}$ tumours and reduces MAPK signalling through reduced phosphorylated ERK	158
5.2.2	MEK162 increases survival of $Apc^{f/+}$ $Kras^{LSL/+}$ mice	169
5.2.3	NVP-BEZ235 increases apoptosis in Kras mutant tumours and reduces signalling downstream PI3K and mTOR	170
5.2.4	NVP-BEZ235 significantly increases longevity of $Apc^{f/+}$ $Kras^{LSL/+}$ mice	181
5.2.5	Investigating the varied combination strategies in Kras mutant colon polyps and small intestinal tumours	183
5.2.6	Long term combination results in an additive increase in survival in $Apc^{f/+}$ $Kras^{LSL/+}$ mice	192
5.2.7	Analysis of tumour burden following treatment in $Apc^{f/+}$ $Kras^{LSL/+}$ mice	197
5.3	Discussion	205
5.3.1	MEK inhibition lead to increased PI3K signalling in Kras mutant tumours, however still increases survival of $Apc^{f/+}$ $Kras^{LSL/+}$ mice	205
5.3.2	PI3K/mTOR inhibition through NVP-BEZ235 significantly increased survival of $Apc^{f/+}$ $Kras^{LSL/+}$ mice however, leads to increased tumour burden	208
5.3.3	Combination treatment leads to an additive increase in longevity for $Apc^{f/+}$ $Kras^{LSL/+}$ mice	211
5.4	Summary	213
5.5	Further work	214
5.5.1	Further investigation of mechanisms underlying the immediate response of Kras mutant tumours to combination therapy	214
5.5.2	Further investigation to toxic effects of combination in $Apc^{f/+}$ $Kras^{LSL/+}$ mice and not $Apc^{f/+}$ $Pten^{f/f}$ mice	214
5.5.3	Mechanisms of resistance to combination strategy	215
6	Investigating PI3K/mTOR inhibition and MEK inhibition in the $Apc^{f/+}$ $Pten^{f/f}$ $Kras^{LSL/+}$ colorectal cancer mouse model	216
6.1	Introduction	216
6.2	Results	217
6.2.1	NVP-BEZ235 increases apoptosis in $Apc^{f/+}$ $Pten^{f/f}$ $Kras^{LSL/+}$ tumours, inhibits PI3K and mTOR signalling, however also reduces MAPK signalling	217
6.2.2	Chronic NVP-BEZ235 significantly increases longevity of $Apc^{f/+}$ $Pten^{f/f}$ $Kras^{LSL/+}$ mice	224

6.2.3	MEK162 increases cleaved caspase 3 in Apc ^{f/+} Pten ^{f/f} Kras ^{LSL/+} tumours and prolonged inhibition of MAPK signalling, however also leads to modulation of PI3K/mTOR signalling	226
6.2.4	Chronic MEK162 has no beneficial effect on survival of Apc ^{f/+} Pten ^{f/f} Kras ^{LSL/+} mice.....	231
6.2.5	Investigation of short term combination treatment in Apc ^{f/+} Pten ^{f/f} Kras ^{LSL/+} tumours.....	233
6.2.6	Further analysis of combination strategy 2 in Apc ^{f/+} Pten ^{f/f} Kras ^{LSL/+} tumours..	240
6.2.7	Chronic treatment of combined NVP-BEZ235 and MEK162 results in a synergistic survival benefit in Apc ^{f/+} Pten ^{f/f} Kras ^{LSL/+} mice	244
6.2.8	Tumour burden analysis of Apc ^{f/+} Pten ^{f/f} Kras ^{LSL/+} mice on various treatments	249
6.3	Discussion	255
6.3.1	The effects of acute and chronic NVP-BEZ235 in Apc ^{f/+} Pten ^{f/f} Kras ^{LSL/+} mice ...	255
6.3.2	MEK inhibition induces favourable anti-tumour and pharmacodynamic effects however does not increase survival of Apc ^{f/+} Pten ^{f/f} Kras ^{LSL/+} mice.....	257
6.3.3	Combination therapy synergistically increases survival of Apc ^{f/+} Pten ^{f/f} Kras ^{LSL/+} mice.....	259
6.4	Summary.....	261
6.5	Further work	262
6.5.1	Further investigation of feedback mechanisms in Apc ^{f/+} Pten ^{f/f} Kras ^{LSL/+} tumours	262
6.5.2	Further evaluation of synergy between NVP-BEZ235 and MEK162 in Apc ^{f/+} Pten ^{f/f} Kras ^{LSL/+} mice	262
6.5.3	Mechanisms of resistance to chronic PI3K and combination therapy.....	262
7	Characterisation and delivery of anti-cancer 'ProTide' agents into a mouse model of colorectal cancer.....	264
7.1	Introduction	264
7.2	Results.....	268
7.2.1	Cell viability assay of thymectacin phosphoramidates in MCF7 and MCF7TDX cell lines.....	268
7.2.2	Colony forming assay of selected thymectacin ProTides in MCF7 and MCF7TDX cell lines.....	272
7.2.3	In vivo anti-tumour effects of thymectacin and selected ProTide agents	274
7.2.4	Long term treatment of lead ProTide agents in the Apc ^{f/+} Pten ^{f/f} tumour model	279
7.2.5	Investigation of chronic 5-FU treatment.....	281
7.3	Discussion	287
7.3.1	In vitro and in vivo characterisation of ProTide compounds	287
7.3.2	Alternative mechanisms of resistance to 5-FU	289
7.4	Summary.....	291
7.5	Further work	292

7.5.1	Further in vivo investigations of ProTides agents	292
7.5.2	Modulation of 5-FU in the Apc ^{f/+} Pten ^{f/f} tumour model.....	292
8	<i>General Discussion</i>	294
8.1	<i>The use of genetically engineered mouse models for pre-clinical studies</i>	294
8.1.1	PI3K/mTOR inhibitor treatment in increasing lifespan of GEMMs	295
8.1.2	Pten deletion as a marker of non-response to MEK inhibitor treatment.....	297
8.1.3	Combinatorial therapy in Kras mutant and Pten deficient tumour settings	298
8.1.4	The MRC FOCUS 4 trial	300
8.1.5	The drug discovery and development process applied to 5-FU.....	302
	<i>Bibliography</i>	304

List of figures

Figure 1.1 Structure of the small and large intestine	8
Figure 1.2 Schematic diagram of the small intestine.....	12
Figure 1.3 Schematic representations of four main signalling pathways which regulate small intestinal homeostasis	19
Figure 1.4 Schematic outlining Fearon and Vogelstein model of colorectal cancer progression	25
Figure 1.5 Schematic representation of the MAPK and PI3K signalling cascades	36
Figure 2.1 Schematic representation of transgenic mouse techniques used in this thesis	48
Figure 2.2 Schematic description of treatment regimes used in this thesis.....	50
Figure 2.3 Stages of colon tumour progression.....	63
Figure 2.4 Stages of intestinal tumour progression.....	64
Figure 3.1 The anti-tumour effects of MEK162, characterised by scoring of histological mitosis and apoptosis in $Apc^{f/+}$ colon polyps and small intestine tumours.....	80
Figure 3.2 MEK162 has no effect on BrdU positive cells in $Apc^{f/+}$ colon polyps or small intestine tumours (SITs) but increased cleaved caspase 3 in SITs only	81
Figure 3.3 IHC reveals MEK162 reduces MAPK and PI3K signalling in colon polyps 4 hours post exposure.....	83
Figure 3.4 IHC for pERK, pAKT473 and pS6RP in small intestinal tumours 4 hrs following a single dose of MEK162	84
Figure 3.5 Kaplan Meier survival analysis of $Apc^{f/+}$ mice on twice daily 30mg/kg MEK162 and vehicle controls from 220 days post induction.....	86
Figure 3.6 The anti-tumour effects of NVP-BEZ235, determined by scoring of histological mitosis and apoptosis in $Apc^{f/+}$ colon polyps and small intestine tumours	89
Figure 3.7 BrdU scoring revealed no significant alterations following NVP-BEZ235 treatment, cleaved caspase 3 scoring showed no significant differences in colon polyps but a significant reduction in small intestine tumours.....	90
Figure 3.8 Immunostaining for PI3K pathway effectors reveals a reduction in levels of pS6RP only and no effect on MAPK signalling in colon polyps, in response to NVP-BEZ235	91
Figure 3.9 IHC for PI3K pathway and MAPK pathway effectors in small intestine tumours 4 hours post exposure to NVP-BEZ235	92
Figure 3.10 Kaplan Meier survival analysis of $Apc^{f/+}$ mice on twice daily 35mg/kg NVP-BEZ235 and vehicle controls from 220 days post induction.....	94
Figure 3.11 Analysis of colon tumour burden in $Apc^{f/+}$ mice on various treatments.	97

Figure 3.12 Analysis of small intestinal tumour (SIT) burden in $Apc^{f/+}$ mice on various treatments.	98
Figure 3.13 Western blot analysis indicating activation of PI3K and MAPK signalling in additional models of intestinal cancer.....	101
Figure 4.1 NVP-BEZ235 does not alter levels of mitosis and apoptosis in $Apc^{f/+}$ $Pten^{f/f}$ small intestine tumours.....	112
Figure 4.2 NVP-BEZ235 reduces the number of cycling cells and induces apoptosis through cleaved caspase 3 in $Apc^{f/+}$ $Pten^{f/f}$ small intestine tumours.....	113
Figure 4.3 NVP-BEZ235 reduces PI3K and mTOR signalling in $Apc^{f/+}$ $Pten^{f/f}$ small intestine tumours 4 hours post exposure	114
Figure 4.4 Schematic showing the effects of NVP-BEZ235 on PI3K/mTOR and MAPK pathway components as detected through western blot analysis.....	116
Figure 4.5 Kaplan-Meier survival analysis of $Apc^{f/+}$ $Pten^{f/f}$ mice on NVP-BEZ235 compared to vehicle controls.....	118
Figure 4.6 MEK162 resulted in a reduction of apoptotic bodies in $Apc^{f/+}$ $Pten^{f/f}$ small intestine tumours.....	120
Figure 4.7 MEK162 lead to a reduction in the number of BrdU positive cells however, no alterations in cleaved caspase 3 were detected in $Apc^{f/+}$ $Pten^{f/f}$ small intestine tumours.....	121
Figure 4.8 MEK162 leads to inhibition of MAPK signalling through pERK in $Apc^{f/+}$ $Pten^{f/f}$ small intestine tumours, however leads to differential modulation of PI3K and mTOR signalling ...	124
Figure 4.9 MEK162 leads to a significant increase in p110 α 24 hours post exposure in $Apc^{f/+}$ $Pten^{f/f}$ small intestine tumours	125
Figure 4.10 Schematic showing the effects of MEK162 on PI3K/mTOR and MAPK pathway components as detected by western blot analysis	126
Figure 4.11 Kaplan-Meier survival analysis of $Apc^{f/+}$ $Pten^{f/f}$ mice on MEK162 compared to vehicle controls.....	127
Figure 4.12 Sequencing of combination is important for anti-tumour effects in $Apc^{f/+}$ $Pten^{f/f}$ small intestine tumours	132
Figure 4.13 Sequencing of combination is important for anti-tumour effects in $Apc^{f/+}$ $Pten^{f/f}$ small intestine tumours	133
Figure 4.14 Sequencing of combination is crucial for combined inhibition of PI3K/mTOR and MAPK signalling in $Apc^{f/+}$ $Pten^{f/f}$ small intestine tumours.....	134
Figure 4.15 Biological effects of combo 2, 24 hours following NVP-BEZ235 exposure in $Apc^{f/+}$ $Pten^{f/f}$ small intestine tumours..	136

Figure 4.16 Sequencing of combination is crucial for prolonged inhibition of PI3K/mTOR and MAPK signalling in Apc ^{f/+} Pten ^{f/f} small intestine tumours.....	138
Figure 4.17 Twice-daily combo 2 administration resulted in significant weight loss in wild type mice.....	141
Figure 4.18 Kaplan-Meier survival analysis of Apc ^{f/+} Pten ^{f/f} mice on combination therapy compared to vehicle and single agent controls	142
Figure 4.19 Analysis of tumour burden in Apc ^{f/+} Pten ^{f/f} mice	146
Figure 4.20 Incidence of liver tumours in Apc ^{f/+} Pten ^{f/f} mice on long term treatment	147
Figure 5.1 MEK162 had no effect on mitosis but increased apoptosis in Apc ^{f/+} Kras ^{LSL/+} colon polyps and small intestinal tumours	161
Figure 5.2 MEK162 also increased BrdU positive cells in small intestinal tumours (SITs) and cleaved caspase 3 staining in colon polyps	162
Figure 5.3 MEK162 reduces MAPK signalling in Apc ^{f/+} Kras ^{LSL/+} colon polyps , however leads to modulation of PI3K and mTOR signalling.	164
Figure 5.4 reduces MAPK signalling in Apc ^{f/+} Kras ^{LSL/+} small intestine tumours (SITs) and partial inhibition of PI3K and mTOR signalling.	165
Figure 5.5 Schematic showing the effects of MEK162 on MAPK and PI3K/mTOR pathway components in Apc ^{f/+} Kras ^{LSL/+} colon polyps detected through western blot analysis	168
Figure 5.6 Schematic showing the effects of MEK162 on MAPK and PI3K/mTOR pathway components in Apc ^{f/+} Kras ^{LSL/+} SITs detected through western blotting.	168
Figure 5.7 Kaplan-Meier survival analysis of Apc ^{f/+} Kras ^{LSL/+} mice receiving MEK162 compared to vehicle controls.....	170
Figure 5.8 NVP-BE2235 significantly increases apoptosis in Apc ^{f/+} Kras ^{LSL/+} colon polyps and small intestine tumours, but elicits no significant anti-proliferative effects.	173
Figure 5.9 Further anti-tumour evaluation of NVP-BE2235 revealed an increased pro-apoptotic effect in Apc ^{f/+} Kras ^{LSL/+} colon polyps and small intestine tumours	174
Figure 5.10 NVP-BE2235 significantly reduces signalling downstream PI3K and mTOR in Apc ^{f/+} Kras ^{LSL/+} colon polyps.....	178
Figure 5.11 Figure 5.9 NVP-BE2235 significantly reduces signalling downstream PI3K and mTOR in Apc ^{f/+} Kras ^{LSL/+} small intestine tumours	179
Figure 5.12 Schematic showing the effects of NVP-BE2235 on PI3K/mTOR and MAPK pathway components in Apc ^{f/+} Kras ^{LSL/+} colon polyps and SITs detected through western blotting.....	180
Figure 5.13 Kaplan-Meier survival analysis of Apc ^{f/+} Kras ^{LSL/+} mice receiving chronic NVP-BE2235 treatment compared to vehicle controls.....	182

Figure 5.14 Anti-tumour effects of different combination strategies in $Apc^{f/+}$ $Kras^{LSL/+}$ colon polyps and small intestinal tumours	185
Figure 5.15 BrdU and cleaved caspase 3 scoring of three combination strategies in $Apc^{f/+}$ $Kras^{LSL/+}$ colon polyps and small intestinal tumours	186
Figure 5.16 sequencing of combination has no differential effect on signalling in $Apc^{f/+}$ $Kras^{LSL/+}$ colon polyps..	190
Figure 5.17 sequencing of combination has no differential effect on signalling in $Apc^{f/+}$ $Kras^{LSL/+}$ small intestinal tumours..	191
Figure 5.18 Combination treatment was found to induce toxicity in $Apc^{f/+}$ $Kras^{LSL/+}$ mice.....	194
Figure 5.19 Kaplan-Meier survival analysis of $Apc^{f/+}$ $Kras^{LSL/+}$ mice receiving long term combination treatment (Combo R1) compared to single agent NVP-BEZ235, MEK162 and vehicle controls	195
Figure 5.20 Kaplan-Meier survival analysis of $Apc^{f/+}$ $Kras^{LSL/+}$ mice receiving reduced combination treatment (Combo R2) long term compared to reduced single agent NVP-BEZ235 and MEK162, and vehicle controls.....	196
Figure 5.21 Colon tumour burden analysis of $Apc^{f/+}$ $Kras^{LSL/+}$ mice on all long term treatments.	203
Figure 5.22 Small intestinal tumour burden analysis of $Apc^{f/+}$ $Kras^{LSL/+}$ mice on all long term treatments	204
Figure 6.1 NVP-BEZ235 results in a pro-apoptotic effect in $Apc^{f/+}$ $Pten^{f/f}$ $Kras^{LSL/+}$ small intestinal tumours 4 hours following exposure, but no effect on mitosis.....	219
Figure 6.2 NVP-BEZ235 increases the number of cycling cells, but also increases apoptosis through cleaved caspase 3 in $Apc^{f/+}$ $Pten^{f/f}$ $Kras^{LSL/+}$ lesions	220
Figure 6.3 NVP-BEZ235 reduces PI3K and mTOR signalling in $Apc^{f/+}$ $Pten^{f/f}$ $Kras^{LSL/+}$ tumours 4 hours after exposure, however increases signalling at a 24 hour time point.....	222
Figure 6.4 Schematic showing the effects of NVP-BEZ235 on PI3K/mTOR and MAPK pathway components as detected by western blot analysis.....	223
Figure 6.5 Kaplan-Meier survival analysis of $Apc^{f/+}$ $Pten^{f/f}$ $Kras^{LSL/+}$ mice on NVP-BEZ235 compared to vehicle controls	225
Figure 6.6 MEK162 has no effect on levels of mitosis or apoptosis in $Apc^{f/+}$ $Pten^{f/f}$ $Kras^{LSL/+}$ small intestine tumours.....	227
Figure 6.7 MEK162 significantly increases the number of BrdU positive cells and cleaved caspase 3 staining in $Apc^{f/+}$ $Pten^{f/f}$ $Kras^{LSL/+}$ small intestine tumours.....	228

Figure 6.8 MEK162 induced prolonged inhibition of MAPK signalling in $Apc^{f/+}$ $Pten^{f/f}$ $Kras^{LSL/+}$ tumours and reduced PI3K signalling 4 hours after exposure, but increased levels of PI3K/mTOR signalling at the 24 hour time point	230
Figure 6.9 Schematic showing the effects of MEK162 on MAPK and PI3K/mTOR pathway components as detected by western blot analysis.....	231
Figure 6.10 Kaplan-Meier survival analysis of $Apc^{f/+}$ $Pten^{f/f}$ $Kras^{LSL/+}$ mice on MEK162 compared to vehicle controls.....	232
Figure 6.11 All three combination strategies resulted in a pro-apoptotic effect in $Apc^{f/+}$ $Pten^{f/f}$ $Kras^{LSL/+}$ but no effect on proliferation	235
Figure 6.12 All combination strategies increased BrdU positive cells and cleaved caspase 3 staining in $Apc^{f/+}$ $Pten^{f/f}$ $Kras^{LSL/+}$ tumours.....	236
Figure 6.13 sequencing of combination results in differential inhibition of signalling downstream PI3K/mTOR and MEK in $Apc^{f/+}$ $Pten^{f/f}$ $Kras^{LSL/+}$ tumours	239
Figure 6.14 Biological effects of combo 2 24 hours post exposure in $Apc^{f/+}$ $Pten^{f/f}$ $Kras^{LSL/+}$ small intestinal tumours.....	241
Figure 6.15 Combo 2 led to inhibition of MAPK signalling but increased PI3K signalling 24 hours following exposure.....	243
Figure 6.16 Toxicity of combination treatment in $Apc^{f/+}$ $Pten^{f/f}$ $Kras^{LSL/+}$ mice.....	246
Figure 6.17 Kaplan-Meier survival analysis of $Apc^{f/+}$ $Pten^{f/f}$ $Kras^{LSL/+}$ mice on combination treatment (combo R1) compared to single agent treatment and vehicle controls.....	247
Figure 6.18 Kaplan-Meier survival analysis of $Apc^{f/+}$ $Pten^{f/f}$ $Kras^{LSL/+}$ mice on further reduced combo 2 (Combo R2) dose compared to vehicle, MEK162 T-D and NVP-BE235 O-D controls	248
Figure 6.19 Tumour burden analysis of $Apc^{f/+}$ $Pten^{f/f}$ $Kras^{LSL/+}$ mice on all long term treatments	253
Figure 6.20 Ulceration of tumours in $Apc^{f/+}$ $Pten^{f/f}$ $Kras^{LSL/+}$ mice on long term treatments	254
Figure 7.1 Schematic summarising metabolism of 5-FU	266
Figure 7.2 Schematic summarising the concept of using ProTide BVDU to target upregulated TS in 5-FU resistant cells.	267
Figure 7.3 Increased expression of TS in MCF7TDX cancer cells	270
Figure 7.4 Colony forming assay comparing cell growth in MCF7 and MCF7TDX cells	273
Figure 7.5 Assessment of anti-proliferative and pro-apoptotic effects in $Apc^{f/+}$ $Pten^{f/f}$ tumours following short term treatment of selected ProTides and thymectacin.	276

Figure 7.6 BrdU and cleaved caspase 3 scoring in $Apc^{f/+}$ $Pten^{f/f}$ tumours following short term treatment of selected ProTides and thymectacin.	277
Figure 7.7 Kaplan Meier survival analysis of $Apc^{f/+}$ $Pten^{f/f}$ mice on long term CPF472, CPF3172 or thymectacin treatment.....	280
Figure 7.8 Increased expression of TS in $Apc^{f/+}$ $Pten^{f/f}$ small intestinal tumours in comparison with normal small intestinal tissue.	283
Figure 7.9 Kaplan Meier survival analysis of $Apc^{f/+}$ $Pten^{f/f}$ mice on long term 5-FU treatment.	284
Figure 7.10 quantitative-RTPCR analysis of individual untreated $Apc^{f/+}$ $Pten^{f/f}$ tumours in comparison with those exposed to 50mg/kg 5-FU treatment from day 60 post induction for varied periods of time.....	285
Figure 7.11 quantitative-RTPCR analysis of individual untreated $Apc^{f/+}$ $Pten^{f/f}$ tumours in comparison with those exposed to 50mg/kg 5-FU treatment from day 50 post induction for varied periods of time	286
Figure 8.1 Outline of the MRC-FOCUS 4 phase II clinical trial	301

List of Tables

Table 1.1 Outline of TNM system used to stage colorectal cancers.....	4
Table 2.1 Outline of transgenic mice used in this thesis	47
Table 2.2 Outline of chronic treatment start points for each mouse model used in this study	51
Table 2.3 Primer sequences used for gene specific PCRs.....	54
Table 2.4 Outline of PCR reaction mixtures, cycling conditions	55
Table 2.5 Outline of PCR product sizes	55
Table 2.6 Outline of antibodies and conditions for immunohistochemistry (IHC).....	61
Table 2.7 Scoring system used for grade severity of lesions	63
Table 2.8 Recipes for resolving and stacking gels.....	67
Table 2.9 Recipes for buffers used during SDS-PAGE	67
Table 2.10 Outline of antibodies and conditions for protein analysis.....	70
Table 2.11 Outline of primer sequences used for qRT-PCR analysis	75
Table 4.1 Raw densitometry values from western blot analysis of pooled Apc ^{f/+} Pten ^{f/f} SITs 4 hours post exposure to NVP-BEZ235	115
Table 4.2 Raw densitometry values from western blot analysis of pooled Apc ^{f/+} Pten ^{f/f} SITs 8 and 24 hours post exposure to NVP-BEZ235	115
Table 4.3 Outline of raw densitometry values from western blot analysis of pooled Apcf/+ Ptenf/f SITs 4 hours post exposure to MEK162	122
Table 4.4 Outline of raw densitometry values from western blot analysis of pooled Apcf/+ Ptenf/f SITs 24 hours post exposure to MEK162	122
Table 4.5 Outline of combination dosing strategies utilised for short term pharmacodynamic and anti-tumour evaluations	128
Table 4.6 Outline of raw densitometry values from western blot analysis of pooled Apc ^{f/+} Pten ^{f/f} SITs 4 hours post exposure to combo 1	130
Table 4.7 Outline of raw densitometry values from western blot analysis of pooled Apc ^{f/+} Pten ^{f/f} SITs 4 hours post exposure to combo 2 and combo 3	130
Table 4.8 Outline of raw densitometry values from western blot analysis of pooled Apc ^{f/+} Pten ^{f/f} SITs 24 hours post exposure to combo 2	137
Table 5.1 Outline of raw densitometry values from western blot analysis of Apc ^{f/+} Kras ^{LSL/+} colon polys 4 hours post exposure to MEK162.....	166
Table 5.2 Outline of raw densitometry values from western blot analysis of Apc ^{f/+} Kras ^{LSL/+} colon polyps 24 hours post exposure to MEK162.....	166

Table 5.3 Outline of raw densitometry values from western blot analysis of Apc ^{f/+} Kras ^{LSL/+} SITs 4 hours post exposure to MEK162	167
Table 5.4 Outline of raw densitometry values from western blot analysis of Apc ^{f/+} Kras ^{LSL/+} colon polyps 24 hours post exposure to MEK162.....	167
Table 5.5 Outline of raw densitometry values from western blot analysis of Apc ^{f/+} Kras ^{LSL/+} colon polyps 4 hours post exposure to NVP-BEZ235	175
Table 5.6 Outline of raw densitometry values from western blot analysis of Apc ^{f/+} Kras ^{LSL/+} colon polyps 24 hours post exposure to NVP-BEZ235	175
Table 5.7 Outline of raw densitometry values from western blot analysis of Apc ^{f/+} Kras ^{LSL/+} SITs 4 hours post exposure to NVP-BEZ235	176
Table 5.8 Outline of raw densitometry values from western blot analysis of Apc ^{f/+} Kras ^{LSL/+} SITs 24 hours post exposure to NVP-BEZ235	176
Table 5.9 Outline of raw densitometry values from western blot analysis of Apc ^{f/+} Kras ^{LSL/+} colon polyps 4 hours post exposure to combo 1 and combo 2	187
Table 5.10 Outline of raw densitometry values from western blot analysis of Apc ^{f/+} Kras ^{LSL/+} colon polyps 4 hours post exposure to combo 3	188
Table 5.11 Raw densitometry values from western blot analysis of Apc ^{f/+} Kras ^{LSL/+} SITs 4 hours post exposure to combo 1 and combo 2	189
Table 5.12 Raw densitometry values from western blot analysis of Apc ^{f/+} Kras ^{LSL/+} SITs 4 hours post exposure to combo 3	189
Table 6.1 Outline of raw densitometry values from western blot analysis of pooled Apc ^{f/+} Pten ^{f/f} Kras ^{LSL/+} SITs 4 and 24 hours post exposure to NVP-BEZ235	221
Table 6.2 Outline of raw densitometry values from western blot analysis of pooled Apc ^{f/+} Pten ^{f/f} Kras ^{LSL/+} SITs 4 and 24 hours post exposure to MEK162.....	229
Table 6.3 Outline of raw densitometry values from western blot analysis of pooled Apc ^{f/+} Pten ^{f/f} Kras ^{LSL/+} SITs 4 hours post exposure to combo 1 and combo 2.....	237
Table 6.4 Outline of raw densitometry values from western blot analysis of pooled Apc ^{f/+} Pten ^{f/f} Kras ^{LSL/+} SITs 4 hours post exposure to combo 3.....	238
Table 6.5 Outline of raw densitometry values from western blot analysis of pooled Apc ^{f/+} Pten ^{f/f} Kras ^{LSL/+} SITs 24 hours post exposure to combo 2	242
Table 7.1 IC50 values (µM) of ProTide compounds assessed by cell viability assay	271
Table 7.2 Summary of short term in vitro and in vivo anti-tumour effects of selected ProTides and thymectacin.....	278

Abbreviations and Definitions

Symbols		D	
°C	Degrees Celsius	DAB	3,3'-diaminobenzidine
µg	Micrograms	dATP	Deoxyadenosine Triphosphate
µl	Microlitres	DCAMKL-1	Doublecortin and Calcium/Calmodulin-dependent Protein Kinase-Like-1
µm	Micrometre	DCC	Deleted in Colorectal Cancer
µM	Micromolar	dCTP	Deoxycytidine Triphosphate
<hr/>		ddH₂O	double distilled water
A		dGTP	Deoxyguanosine Triphosphate
ABC	Avidin Biotin Complex	Dhh	Desert Hedgehog
Ah	Aryl Hydrocarbon	dH₂O	deionised water
AKT	Thymoma viral oncogene Homolog 1	Disp	Dispatched
ALDH1	Aldehyde dehydrogenase 1	DLL	Delta-like
APC	Adenomatous Polyposis Coli	DNA	Deoxyribonucleic Acid
AXIN	Axis Inhibitor	DNase	Deoxyribonuclease
<hr/>		dNTP	Deoxynucleotide Triphosphate
B		DPD	Dihydropyrimidine dehydrogenase
BCA	Bicinchoninic Acid	DSH	Dishevelled
Bmi1	polycomb ring finger oncogene	DTT	Dithiothreitol
BMP	Bone Morphogenic Protein	dTTP	Deoxythymidine Triphosphate
BMPRI/II	Bone Morphogenic Receptor type 1/II	dTMP	deoxythymidine monophosphate
bp	Base Pair	dUMP	deoxyuridine monophosphate
BrdU	5-Bromo-2-deoxyuridine	<hr/>	
BSA	Bovine Serum Albumin	E	
BVDU	Brivudin	ECL	Electrochemiluminescence
BVdUMP	BVDU monophosphate	EDTA	Ethylenediamine Tetra-acetic acid
<hr/>		EGFR	Epidermal growth factor receptor
C		elf4E	Eukaryotic translation initiation factor 4E
CBP	CREB-binding protein	EpCAM	Epithelial Cell Adhesion Molecule
cDNA	complementary deoxyribonucleic acid	EphB	Ephrin type B receptor
C-myc	cellular myelocytomatosis oncogene	ER	Estrogen Receptor
Cre	Causes recombination	ERK	Extracellular regulated MAP kinase
CRC	Colorectal Cancer		
CBC cells	Crypt-Base-Columnar cells		
COX	Cyclogenase		
CSL	CBF1/RBP-Jk/Suppressor of Hairless/LAG-1		
CreER	Cre recombinase-Estrogen receptor fusion transgene		
Cr	Cycle Time		
<hr/>			

ES cells	Embryonic Stem cells	JPS	Juvenile Polyposis Syndrome
<hr/>		<hr/>	
F		K	
FAK	Focal Adhesion Kinase	KDa	Kilodaltons
FAP	Familial Adenomatous Polyposis	KRAS	Kirsten RAS
FdUMP	fluorodeoxyuridine monophosphate	Kv	Kilovolts
<hr/>		<hr/>	
FdUTP	fluorodeoxyuridine triphosphate	L	
FLP	flippase	L	Litre
FOXO	Forkhead box proteins	LOH	loss of heterozygosity
FRT	FLP Recognition Target	loxP	Locus of crossover of Bacteriophage P1
FTI	Farnesyltransferase inhibitors	Lgr5	Leucine-rich repeat-containing G protein coupled receptor 5
FUTP	fluorouridine triphosphate	<hr/>	
<hr/>		<hr/>	
G		M	
gDNA	genomic DNA	mAb	Monoclonal antibody
GDP	Guanosine Diphosphate	MAPK	Mitogen Activated Protein Kinase
Gli	Glioma-associated oncogene homolog	MEK	Mitogen Activated Erk Kinase
GSI	Gamma-secretase inhibitor	mg	Milligrams
GSK-3	Glycogen Synthase Kinase-3	MIN	Multiple Intestinal Neoplasia
GTP	Guanosine Triphosphate	mins	minutes
	GTPase Guanosine Triphosphatase	MLH1	MutL homolog 1
<hr/>		mm	Millimetre
H		MMR	Mismatch Repair
H&E	Haematoxylin and Eosin	MRC	Medical Research Council
HNPCC	Hereditary Nonpolyposis Colorectal Cancer	MSH2	MutS E.Coli homolog of 2
Hopx	Homeodomain-only protein	MSI	Microsatellite instability
Hr	Hour		mTERT mouse telomerase reverse transcriptase
HRAS	Harvey RAS	mTOR	mammalian target of rapamycin
HRP	Horse Radish Peroxidase	<hr/>	
HSV	Herpes Simplex Virus	<hr/>	
<hr/>		<hr/>	
I		N	
IGF-1	Insulin-Like Growth Factor-1	NCID	Notch Receptor Intracellular Domain
IHC	Immunohistochemistry	NGS	Normal Goat Serum
Ihh	Indian Hedgehog	NOD/SCID	Non-obese diabetic/severe Combined immunodeficient
i.p.	Intraperitoneal		
IRS	Insulin receptor substrate	NO-ASA	Nitric oxide donating aspirin
<hr/>		NRAS	Neuroblastoma RAS
J		NRS	Normal Rabbit Serum
Jag	Jagged	NSAID	Non-steroidal anti-inflammatory drugs
JNK	c-Jun N-terminal Kinase		
<hr/>		<hr/>	

O		TA	Transit-Amplifying
Olfm4	Olfactomedin 4	Taq	DNA polymerase from <i>Thermus aquaticus</i>
<hr/>		TBE	Tris Borate EDTA
P		Tcf/Lef	T-cell factor and Lymphoid enhancer factor
PCR	Polymerase Chain Reaction	TDX	Tomudex
PDK	Phosphoinositide-dependent Protein Kinase 1	Tert	Telomerase reverse transcriptase
PKA	Protein Kinase A	TEMED	N,N,N',N'-teramethylethylenediamine
PLL	Poly-L-Lysine	tetO	Tet Operon
PI3K	Phosphatidylinositol-3-Kinase	tetR	tetracycline repressor protein
PIP₂	phosphatidylinositol (4,5)-bisphosphate	TGFR	Transforming Growth Factor Receptor
PIP₃	phosphatidylinositol (3,4,5)- Trisphosphate	TK	Thymidine Kinase
Ptch	Patched	TNM	Tumour-Node-Metastasis
PTEN	Phosphatase and tensin homolog deleted on chromosome ten	TP	Thymidylate Phosphorylase
<hr/>		TS	Thymidylate synthase
Q		tTA	Tetracycline-controlled Transactivator
qRT	Quantitative Real-Time	<hr/>	
R		U	
RAS	Rat sarcoma viral oncogene homolog	UICC	Union for International Cancer Control
RNA	Ribonucleic Acid	UV	Ultra Violet
RNase	Ribonuclease	<hr/>	
RPM	Revolutions Per Minute	V	Volts
rtTA	reverse Tetracycline-controlled Transactivator	V	Volts
RTK	Receptor Tyrosine Kinase	v/v	volume per volume
<hr/>		VEGF	Vascular endothelial growth Factor
S		VZV	Varicella Zoster Virus
S6K	Ribosomal protein S6	<hr/>	
SD	Standard deviation	W	
SDS	Sodium Dodecyl Sulphate	w/v	weight per volume
SDS-PAGE	SDS- Polyacrylamide Gel Electrophoresis	WT	Wild Type
secs	Seconds	Wnt	Wingless-type murine mammary tumour virus Integration site family
Smad	Mothers against decapentapleigic homolog	<hr/>	
Smo	Smoothened	X	
SOS	Sevenless homolog	x g	times gravity
Shh	Sonic Hedgehog	<hr/>	
<hr/>		123	
T		3HTdR	Tritiated Thymidine
		5-FU	5-fluorouracil
		4E-BP1	4E-binding protein 1

Abstract

Despite recent advances in the clinic to integrate novel targeted therapeutic agents into standard therapy, colorectal cancer (CRC) remains a significant cause of mortality. The high attrition rate of novel compounds at phase III clinical trials for CRC, has been attributed to limited information from pre-clinical strategies, in particular, the use of inadequate xenograft models. In response, this thesis aimed to utilise robust and relevant genetically engineered mouse models of CRC to evaluate a number of novel therapeutic strategies.

Whilst mutations in the tumour suppressor APC are crucial for initiation of CRC, mutations which lead to activation of the PI3K and MAPK signalling pathways, such as through loss of the tumour suppressor protein PTEN and activation of oncogenic KRAS, have been implicated in promoting progression of CRC. As such, combinations of these genetic alterations within the murine intestine, using the Cre-LoxP system, lead to differing mouse models of invasive intestinal adenocarcinoma. This thesis reports therapeutic targeting of the PI3K and MAPK signalling pathways using the dual PI3K and mTOR inhibitor NVP-BEZ235, and the MEK inhibitor MEK162, respectively. For this, compounds were initially evaluated for pharmacodynamic and anti-tumour effects through short term exposure experiments. These analyses yielded a range of effects, some of which appeared predictive of long term efficacy, others which were contradictory and some which revealed novel feedback mechanisms. Furthermore, these agents were assessed in a long term therapeutic setting to evaluate the effect of continuous treatment on longevity and tumour burden of tumour models. Here, whilst dual PI3K/mTOR inhibition significantly increased longevity of all mouse models, MEK inhibition was only effective in the Apc and Apc Kras mutant settings, identifying Pten loss as a marker of non-response to MEK inhibition, independently and also in the Kras mutant setting. Furthermore, analysis of the combination therapy in short term settings identified scheduling of these agents to be key to achieve concomitant pathway inhibition, particularly in the Apc Pten deficient tumour setting. Ultimately, when evaluated in a long term setting, although the combination therapy displayed no further benefit in the Pten deficient setting, this had additive benefits in the Kras mutant setting and synergistic benefits in the Pten Kras mutant setting.

Nevertheless despite the promise of targeted therapy, standard chemotherapeutic agents such as 5-fluorouracil (5-FU) remain the backbone of therapy for CRC, regardless of only moderate benefits of 10-15% in advanced tumour settings. Furthermore, resistance to 5-FU predominantly through upregulation of the enzyme thymidylate synthase (TS) frequently

occurs in human tumours. Investigations reported here aimed to target tumours with upregulated TS using novel analogues of the anti-viral agent Brivudin (BVDU), metabolites of which are converted to anti-cancer metabolites by TS.

Initially, *In vitro* characterisation of a small library of compounds reported here identified a number of potent compounds. Following further *in vitro* characterisation and short term evaluation in the Apc Pten tumour model of invasive adenocarcinoma, two lead compounds: CPF472 and CPF3172 were taken forward for long term experiments. Subsequently, this study evaluated and identified compounds which showed increased efficacy in the TS upregulated setting.

Taken together, the investigations presented in this thesis highlight the utility of appropriate mouse models in evaluating novel therapeutic strategies and generating clinically relevant hypotheses.

1 General Introduction

1.1 Colorectal cancer

1.1.1 Colorectal cancer statistics and causes

Although significant advances have recently been made to improve outcomes of patients with early and advanced colorectal cancer (CRC), it remains the third most common cancer worldwide after breast and lung cancer (Cancer Research UK, 2013). With more than 16,000 deaths annually in the UK, CRC accounts for approximately 10% of female and 11% of male cancer deaths. Bowel cancer mortality rates are strongly related to age with 80% of all deaths occurring in people aged 65 and over. This relationship is largely a consequence of mild early symptoms (for example bloating and diarrhoea) of the disease and hence late detection i.e. often when the disease has metastasised (Cancer Research UK, 2013).

CRC is traditionally split into hereditary and sporadic. Hereditary conditions contribute between 20-25% of bowel cancers namely through Familial Adenomatous Polyposis (FAP) and Hereditary non-polyposis colorectal cancer (HNPCC or Lynch Syndrome)(de la Chapelle, 2004). FAP results in hundreds to thousands of adenomas throughout the bowel and if left untreated this will lead to near 100% penetrance of CRC. HNPCC is associated with germ line mutations of mismatch repair genes with a penetrance of 80% for colorectal cancer (de la Chapelle, 2004, Fearnhead et al., 2002).

The high incidence of sporadic bowel cancer is largely attributed to environmental factors including poor diet, obesity, increased alcohol consumption and smoking (Cancer research UK, 2013). High intake of red meat and processed meat has been consistently linked to increased risk of bowel cancer with a recent study estimating that 18% of all cases in 2010 were linked to high consumption of red meat and processed meat (Parkin, 2011). Epidemiology data has also suggested that obesity remains an increasing risk factor for developing CRC in the western world (Moghaddam et al., 2007). Importantly, many studies have shown an inverse correlation linking colorectal cancer risk with intake of vegetables, physical exercise as well as non-steroidal anti-inflammatory drugs and hormone replacement therapy (Watson and Collins, 2011).

1.1.2 TNM classification of colorectal cancer

The gold standard for CRC prognostication remains pathological staging through the Tumour-Node-Metastasis (TNM) system, modified from the Duke's system initially proposed by Cuthbert Dukes in 1932 (Walther et al., 2009). This system assesses the size and invasion of the primary tumour (T), pathological review of tumour cells in surrounding lymph nodes (N) and local or distant spread of tumour i.e. metastasis (M) (Wolpin and Mayer, 2008) (summarised in table 1.1). Additional clinical and pathological features are often used to further assess prognosis and risk of recurrence including poorly differentiated histology, lymphovascular invasion and high pre-operative carcinoembryonic antigen levels (Steinberg et al., 1986, Wanebo et al., 1978).

UICC/TNM		Duke's
Stage 0	Carcinoma in situ	A
Stage I	No nodal involvement, no distant metastasis	
	Tumour invades submucosa (T1, N0, M0)	
	Tumour invades muscularis propria (T2, N0, M0)	
Stage II	No nodal involvement, no distant metastasis	B
	Tumour invades subserosa (T3, N0, M0)	
	Tumour invades into other organs (T4, N0, M0)	
Stage III	No nodal involvement, no distant metastasis	C
	1-3 regional lymph nodes involved (any T, N1, M0)	
	4 or more regional lymph nodes involved (any T1, N2, M0)	
Stage IV	Distant metastasis (any T or N, M1)	D

Table 1-1 Outline of system used to stage colorectal cancers, adapted from Cancer Research UK, Stats 2013

1.1.3 *Current therapeutic strategies for patients with CRC*

Clinical options for CRC patients primarily involve tumour and metastasis resection in conjunction with radiotherapy or chemotherapy. These are either used in the neoadjuvant setting to shrink the tumour prior to surgery or alternatively, in the adjuvant setting (after surgery) to prevent recurrence.

In terms of chemotherapy, 5-fluorouracil (5-FU) remains the cornerstone of systemic treatment for CRC patients. Developed by Charles Heidelberger in 1957, 5-FU is a fluorinated pyrimidine that functions by inhibiting Thymidylate synthase (TS), the rate-limiting enzyme in pyrimidine nucleotide synthesis (Sobrero et al., 2000). Despite 5-FU being the most widely used anti-cancer therapy to treat the disease, its' efficacy as a monotherapy remains modest, with 10-15% response rates and an overall median survival of around 8 months (Johnston and Kaye, 2001). 5-FU is now most commonly administered with leucovorin, a reduced folate, thought to stabilize interactions between 5-FU and TS (Zhang et al., 1992). A meta-analysis of 19 randomized trials found that 20% of metastatic CRC patients receiving 5-FU with leucovorin, had a 50% reduction in tumour size and median survival had increased from 6 to 12 months (Thirion et al., 2004) compared to 5-FU alone.

Over the past 15 years, significant advances have been made in the treatment of metastatic colorectal cancer, with the approval of 3 new cytotoxic agents. This includes the topoisomerase I inhibitor irinotecan (Pfizer), the platinum compound oxaliplatin (Sanofi-Aventis) and the oral prodrug of fluorouracil capecitabine (Roche). Randomized clinical trials have shown improvements in progression-free and overall survival when irinotecan was added to 5-FU and leucovorin (Douillard and Group, 2000). Similarly, the addition of oxaliplatin to 5-FU and leucovorin increased tumour response rates and disease-free survival rates (Giacchetti et al., 2000). Importantly, patients receiving all three cytotoxics-fluorouracil, irinotecan and oxaliplatin had an increased median survival of approximately 20 months (Grothey and Goldberg, 2004).

Despite the improvements described above, anti-cancer therapy is largely limited by the damage it inflicts on normal tissues. Therefore, the search for agents which specifically target tumour cells whilst sparing normal cells is often described as one of the 'holy grails' of cancer research (Keefe and Bateman, 2012). In light of this, the addition of targeted agents for the treatment of metastatic CRC has been implemented to further improve clinical outcomes. Bevacizumab (Genentech), a human monoclonal antibody against the vascular endothelial

growth factor (VEGF), is currently being evaluated in addition with standard chemotherapeutic schedules, to target the key signalling pathway which mediates angiogenesis, an essential process in tumour development. Initial studies have shown the addition of bevacizumab to fluoruracil and leucovorin prolonged median overall survival after failure of an irinotecan containing regime. Despite this, toxicity issues similar to those observed with chemotherapy alone, remain with bevacizumab treatment. (Kabbinar et al., 2005, Glusker et al., 2006, Guijarro-Muñoz et al., 2013). Additionally to targeting VEGF, antibodies against the Epidermal growth factor receptor (EGFR) have been integrated into current therapeutic strategies for CRC, given that EGFR is overexpressed in 70% of CRCs (Resnick et al., 2004). Cetuximab (ImClone) and panitumumab (Amgen) are monoclonal antibodies against EGFR, a transmembrane glycoprotein involved in stimulating cellular growth, proliferation and inhibiting programmed cell death (Scaltriti and Baselga, 2006). Both molecules bind to the extracellular domain of EGFR whereby leading to inhibition of downstream signalling. Promisingly, cetuximab has shown efficacy in patients with irinotecan-refractory metastatic CRC as well as improvements in progression-free survival and overall survival as a weekly treatment for patients that progressed on 5-FU, irinotecan and oxaliplatin (Jonker et al., 2007). Despite this, extensive retrospective analysis of clinical trials has identified that mutations downstream EGFR signalling mediate non-response to cetuximab and panitumumab (further discussed in section 1.5.2 and 1.5.3), limiting the population of patients which benefit from this treatment.

Therefore, whilst substantial advances have been made over the last decade to integrate targeted biological agents into the treatment of CRC, they have had little impact on the crucial 5-year survival rates (Jonker et al., 2007). Hence, efforts are continuing to develop a variety of agents targeting processes involved in colorectal tumour development, in the hope to vastly improve patient outcomes.

1.2 *Intestinal biology and maintenance of homeostasis*

1.2.1 *Basic anatomy and function of the intestines*

The intestines are part of the digestive system where they play a key role in the digestion and absorption of nutrients, water and form a part of the body's defence to ingested pathogens. The intestinal structure consists of a tube extending from the stomach to the anus. The small intestine has three segments, the duodenum (receives chyme-partly digested material, from

the stomach and digestive secretions from the pancreas and liver), the jejunum (responsible for the chemical digestion and nutrient absorption) and the ileum (controls flow of material to the large intestine via the caecum). The surface of the small intestine is covered in a single layer of epithelial cells that form invaginations called crypts of Lieberkühn (commonly called crypts) deep in the lamina propria. From these, finger-like projections called villi are formed and these function to increase the surface area for nutrient absorption (Figure 1.1). The lamina propria forms a support of mesenchymal (stromal) fibroblasts around the crypts and also extends up to the top of the villus. This contains an extensive network of capillaries which carry absorbed nutrients and a lacteal which transports material too large to be absorbed, including lipids packaged as lipoproteins. The small intestine wall is made up of a layer of smooth muscle which is responsible for peristalsis, an important muscle movement which increases absorption of nutrients and movement of material through the intestine (Figure 1.1) (L et al., 1989, H, 2006, Williams et al., 1989, Martini, 2006).

The large intestine is made up of the caecum, colon, rectum and the anal canal. The caecum collects and stores material from the ileum and is also the region of the large intestine where the appendix is located. The reabsorption of water is the main function of the colon and it is also where faecal material is stored prior to ejection from the body through the rectum and the anal canal. The large intestine is made up of a single layer of columnar epithelial cells like the small intestine, however unlike the small intestine, the cells form a flat surface of epithelium and don't have raised villi (Figure 1.1) (Williams et al. 1989, Martini 2006).

Small intestine structure



Large intestine structure



Figure 1.1 Structure of the small and large intestine

The small intestine is a single epithelial layer made up finger-like projections called villi and invaginations called crypts, supported by stromal fibroblasts and surrounded by a layer of smooth muscle. The large intestine is also a single epithelial layer but is only made up of crypts which consist of enteroendocrine and goblet cells.

1.2.2 *Small intestine and large intestine histology*

The epithelial layer of the small intestine undergoes rapid renewal every 5-6 days in humans and every 2-3 days in the mouse, a process which is driven by the proliferative compartment found in crypts (Creamer, 1967, Wright and Alison, 1984). The intestinal stem cells are located at the bottom of the crypt and give rise to their progeny, transit-amplifying cells. These cells divide 4-5 times before terminally differentiating as they migrate up the villus where they are subsequently shed into the lumen (Hall et al., 1994, Grossmann et al., 2002), with the exception of paneth cells which migrate downwards and occupy the base of the crypt (Figure 1.2). The main differentiated cell types found in the small intestine include absorptive enterocytes, secretory goblet, enteroendocrine cells and Paneth cells, and to a lesser extent, M cells (membranous or microfold cells), cup cells and tuft cells. Enterocytes are the most abundant cell type in the small and large intestine. They are tightly packed specialised cells which function to maintain cell polarity and to provide a barrier to microbes. Also, their apical surfaces are covered in microvilli to maximise surface area for absorption of nutrients. Goblet cells are secretory cells located near the crypt-villus junction and all along the villus. They primarily function to lubricate and protect the epithelium from the mechanical stress of material movement by secreting mucin but also by secreting trefoil proteins to aid repair of damaged tissue. Enteroendocrine cells are also secretory cells found along the villus and secrete hormones to maintain vital gut function. Paneth cells are long-lived secretory cells which escape migration and reside at the bottom of the crypt intercalated between the crypt base columnar cells. Here, they are responsible for innate immunity and function by secreting defensins and anti-microbials such as lysozyme (Williams et al. 1989, Martini 2006).

The often over-looked M cells, cup cells and tuft cells are also found in the intestinal epithelium. M cells are microbial trafficking cells, primarily found overlying Peyer's patches. These cells possess an unusual membrane structure which allows presentation of microbes to the underlying lymphocytes, macrophages and dendritic cells, and therefore provide a layer of interphase between immune cells and the luminal content (Owen and Jones, 1974). Also found in the intestine are elusive wine glass-shaped cup cells. These have a shorter brush border than other columnar cells and express Vimentin, much like M cells (filament protein which is a mesenchymal cell marker) however, their function remains largely unidentified (Ramirez and Gebert, 2003). Finally, tuft cells (also known as brush cells) are on rare occasions found in both crypts and villi of the small intestinal epithelium. The role of these cells was largely unknown until recent studies by Gerbe et al revealed them to be of a secretory lineage,

a source of prostanoids, prostaglandins, the largest source of opioids and β -endorphins in the intestine. It is hypothesised that tuft cells contribute to essential maintenance of homeostasis in the intestine as well as vasoconstriction, peristalsis and pain detection (Gerbe et al., 2009, Gerbe et al., 2011).

The colonic mucosa also consists of a single epithelial layer which consists of differentiated absorptive cells termed colonocytes, enteroendocrine cells and goblet cells which are the most abundant cell type comprising up to 50% of the large intestine epithelium (Figure 1.1). Similarly to the small intestine, stem cells are found at the base of the crypt, however unlike the small intestine, the large intestine is completely devoid of paneth cells (Williams et al., 1989).

1.2.3 The intestinal stem cell

In the adult, stem cells are defined as pluripotent cells that maintain their own capacity for long-term self-renewal (Siminovitch and Axelrad, 1963). In all organs, stem cells are vital for tissue maintenance and homeostasis and it is hypothesised that the accumulation of mutations in these cells may result in the tumour-initiating cells that give rise to cancers. However, intestinal stem cells are thought to possess a number of protective mechanisms in order to prevent neoplastic growth. These include their propensity to be slow-cycling (quiescent) (Orford and Scadden, 2008), their ability to selectively sort damaged DNA to pass onto daughter cells which differentiate and migrate up the villus, and lastly their ability to readily undergo programmed cell death (apoptosis) after genetic insult (Potten et al., 1978).

The location of the intestinal stem cell has been a widely debated issue in the field. The classical model put forward by Potten and colleagues described the location of the stem cells in the +4 cell region, relative to the base of the crypt. This was evidenced by a number of DNA labelling (using tritiated thymidine- $^3\text{HTdR}$ which incorporates into DNA during S phase) and irradiation experiments (to cause genetic insult) which showed the $^3\text{HTdR}$ was incorporated into the DNA of stem cells that underwent regeneration, and could be visualised a number of weeks later (Potten 1974). This led to the identification of potential stem cell markers that were predominantly expressed in the +4 region including, *mushashi-1* (Potten et al., 2003), *Bmi1* (the polycomb ring finger oncogene) (Sangiorgi and Capecchi, 2008), *doublecortin* and *calcium/calmodulin-dependent protein kinase-like-1* (*DCAMKL-1*) (May et al., 2008) and *CD133* (*Prominin-1*) (Zhu et al., 2009) to study stem cell functionality. Functional lineage tracing experiments using conditional transgenic techniques in the mouse revealed that *Bmi1* positive

cells can generate all intestinal cell types and a single Bmi1 positive cell can generate organoid structures when cultured *in vitro* (Sangiorgi and Capecchi, 2008). Since then, a number of other markers for the quiescent +4 cell have been identified including, the homeobox protein Hopx (Takeda et al., 2011), telomerase reverse transcriptase Tert (Montgomery et al., 2011) and the pan-ErbB inhibitor Lrig1 (Powell et al., 2012). More recently however, a plethora of new evidence demonstrated that the previously identified crypt based columnar cells (CBC cells) (Cheng and Leblond, 1974) can function as intestinal stem cells. Lineage tracing experiments identified the Wnt target gene leucine-rich repeat containing G-protein coupled receptor 5 (Lgr5) expressing CBC cells were actively cycling, and capable of generating all epithelial lineages over a 2 month period (Barker et al., 2007). Furthermore, when isolated and cultured *in vitro*, Lgr5 positive cells were able to generate organoid structures (Sato et al., 2009).

Together, the two areas of evidence led to the hypothesis of two pools of small intestinal stem cells, one quiescent pool in Bmi1 expressing cells at the +4 position and a second, in actively cycling Lgr5 expressing CBC cells. This model proposes the two populations have separate but cooperative functional roles as reciprocal back-up systems to provide a high rate of self-renewal and flexible damage repair for the small intestine (Li and Clevers, 2010). Despite the validity of highly complex lineage tracing and *in vitro* culture experiments which gave rise to this hypothesis, a number of studies failed to corroborate the previous findings of specific markers of the quiescent '+4' stem cell mentioned above, in particular, a study which failed to recapitulate the phenotype reported from Bmi1 driven lineage tracing experiments (Muñoz et al., 2012). This study conducted a transcriptome and proteomic analysis of Lgr5 positive CBC cells and found high levels of Bmi1, Hopx, Tert and Lrig1 in the Lgr5 positive cells and no specific enrichment of these markers in the Lgr5 negative stem cell zone. Whilst the authors argue that the presence and function of a quiescent stem cell pool cannot be excluded, they implying these markers solely cannot be used to identify the cells accurately. Instead, the authors allude to a concept first postulated by Cheng and Leblond and Potten and colleagues. This concept hypothesised that the transit amplifying cells above the stem cell zone may display plasticity when damaged and may be able to revert to stem cells to aid the regeneration process.

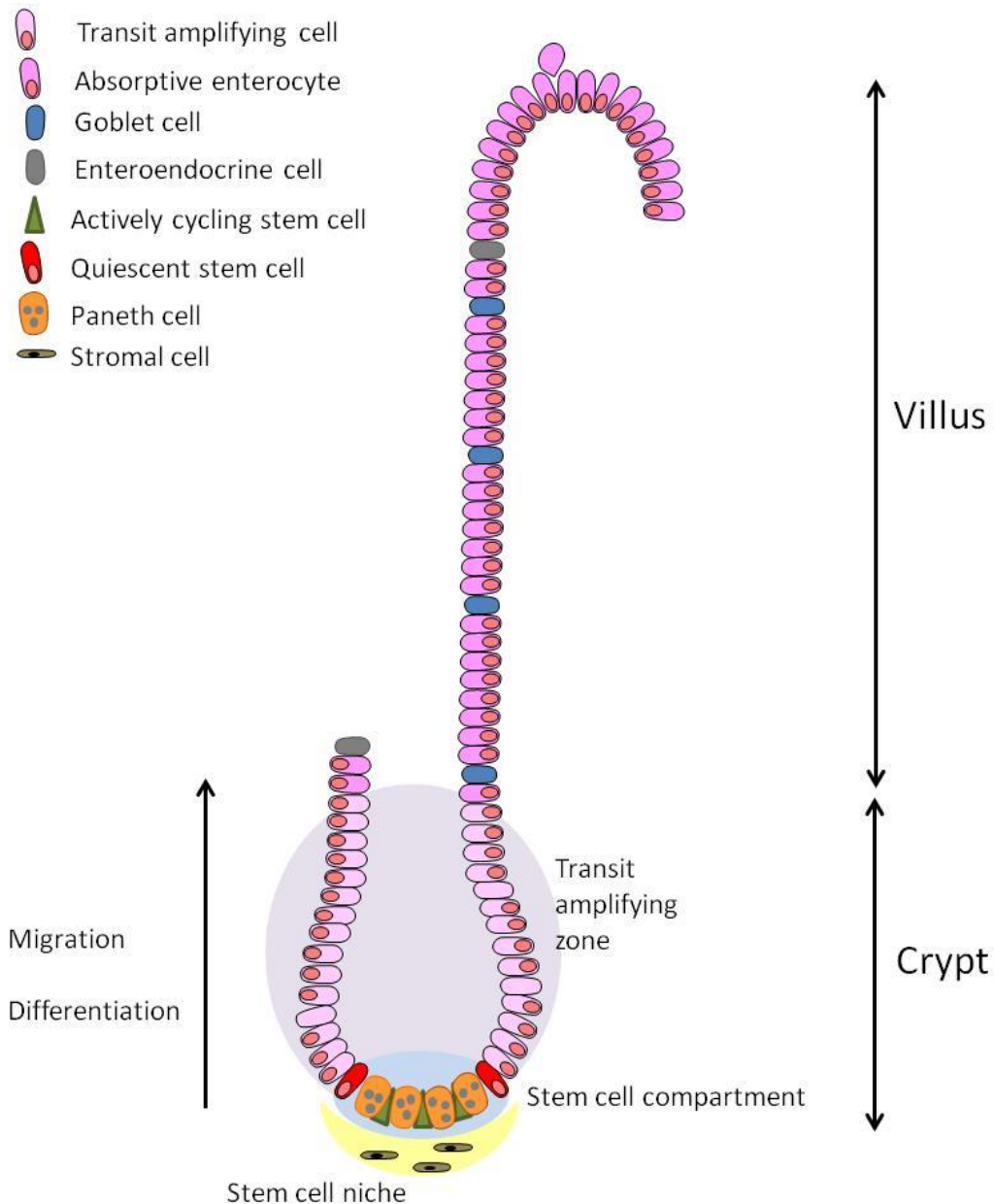


Figure 1.2 Schematic diagram of the small intestine

The small intestinal epithelium is made up of two compartments, the crypt and transit amplifying zone where stem cells and their progeny reside, and the villus, which constitutes differentiated cell types. Stem cells located at the bottom of the crypt give rise to immature progenitor cells which terminally differentiate as they migrate up the villus, before being shed into the lumen, with the exception of Paneth cells which migrate downwards and occupy the base of the crypt. The stem cell compartment found at the base of the crypt consists of paneth cells and stromal fibroblasts to create the stem cell niche.

1.3 The stem cell niche and maintenance of homeostasis

The stem cell niche can be defined as a local tissue microenvironment that hosts and influences the behaviour and characteristics of stem cells in order to maintain the balance between self-renewal and differentiation in the intestine, and therefore maintain homeostasis (Fuchs et al., 2004). This includes interactions between stromal fibroblasts found in the lamina propria through short-range signalling as well as interactions with the basement membrane and neighbouring epithelial cells. A number of signalling pathways have been implicated in maintenance of intestinal homeostasis and are discussed in detail below.

1.3.1 The Canonical Wnt signalling pathway

The Wnt signalling pathway plays an important role in regulation of cell proliferation and differentiation in a number of tissues including the skin, blood, brain and intestine. The canonical Wnt pathway, which regulates the ability of the β -catenin driven activation of target genes is better characterized and is strongly associated with initiation of colorectal cancer. The pathway is controlled at the cell membrane by Wnt ligands which bind to frizzled receptors (7 pass transmembrane proteins). In the absence of cognate ligand, the protein dishevelled (Dsh) is recruited to the receptor preventing it inhibiting degradation of the transcriptional activator β -catenin in the cytoplasm by a destruction complex. This complex consists of Axis inhibitor (Axin) and adenomatous polyposis coli (Apc) proteins which form a scaffold and allow phosphorylation of β -catenin by glycogen synthase kinase 3 β (Gsk3 β). Phosphorylation marks the β -catenin protein for ubiquitination and subsequent proteosomal degradation. Binding of Wnt ligands to the receptor releases the Dsh protein from the receptor which is then able to bind to the destruction complex and prevent phosphorylation of β -catenin (summarised in Figure 1.3). This allows β -catenin to accumulate and enter the nucleus where it interacts with members of the T-cell factor and Lymphoid enhancer factor (Tcf/Lef) family to activate transcription of various Wnt target genes (reviewed in (Clevers, 2006).

A number of elegant studies using mouse models have demonstrated the importance of precise Wnt signalling, for regulation of cell proliferation and maintenance of intestinal homeostasis. Initially, the role of Wnt signalling in the intestinal epithelium was determined by genetic alterations in Apc and β -catenin. This was shown to result in nuclear accumulation of β -catenin, constitutive activation of target genes associated with proliferation and subsequent formation of intestinal adenomas (Harada et al., 1999, Andreu et al., 2005). Similarly, homozygous loss of Apc in the intestine also resulted in rapid activation of the Wnt pathway

(Sansom et al., 2004). Accumulation of nuclear β -catenin here conferred a 'crypt progenitor' phenotype which led to mislocalisation of paneth cells, and increased proliferation and migration. Not surprisingly, inhibition of Wnt signalling has been shown to result in arrested epithelial cell proliferation, through ectopic expression of the secreted Wnt inhibitor Dickkopf1 (Dkk1) (Pinto et al., 2003) and can also lead to loss of the whole proliferative compartment as evidenced by deletion of the transcription factor Tcf (Korinek et al., 1998). Tcf is involved in activating transcription of a number of important genes including *c-Myc*, deletion of which leads to ablation of crypts in the mouse intestinal epithelium (Muncan et al., 2006). Concomitant deletion of *c-Myc* with *Apc* rescues the *Apc* 'crypt progenitor' phenotype highlighting its absolute requirement for development of the Wnt driven phenotype (Sansom et al., 2007). Furthermore, deletion of Wnt target genes *EphB2* and *EphB3* results in mislocalisation of paneth cells from their position at the bottom of the crypts, demonstrating requirement of Wnt signalling in correct migration and localisation of differentiated cell types (Batlle et al., 2002). These studies all highlight the importance of Wnt signalling in proliferation and differentiation and hence, appropriate control of Wnt signalling is required in the stem cell compartment and the stem cell niche, to maintain normal development and homeostasis. An extensive investigation of Wnt agonists and antagonists by in situ hybridisation techniques revealed a gradient of Wnt activity throughout the crypt-villus axis. Cells at the base of the crypt, where the stem cells reside, were shown to maintain a high level of Wnt activation whilst progenitors and differentiated cells migrating up the villus had no Wnt activation (Gregorieff et al., 2005). This discrete pattern of Wnt activation is regulated by a number of signalling pathways including those mentioned below to together maintain intestinal homeostasis.

1.3.2 The Hedgehog signalling pathway

Hedgehog signalling is a highly conserved signalling cascade, essential for embryonic development as well as differentiation, proliferation and maintenance of various adult tissues. Three Hedgehog genes exist in vertebrates which encode for three highly homologous ligands: Sonic Hedgehog (Shh), Indian Hedgehog (Ihh) and Desert Hedgehog (Dhh) (Echelard et al., 1993). These are cleaved proteins released by Dispatched (Disp) from the cell membrane where they bind to Patched (Ptch), a 12-transmembrane receptor (Marigo et al., 1996). In the absence of Hh proteins, Ptch inhibits Hedgehog signalling by inhibiting activation of a 7-transmembrane receptor, Smoothened (Smo). In the presence of Hh, inhibition on Smo is released and in turn, allows intracellular signal transduction via the Glioblastoma (Gli) family of

zinc finger transcription factors, Gli1, Gli2 and Gli3 (Ruiz i Altaba, 1999). These are able to translocate into the nucleus where they regulate target gene transcription of the Hedgehog pathway (summarised in figure 1.3).

Indian Hh is the primary Hedgehog protein expressed in differentiated cells of the small intestine, and analysis of Hedgehog targets *Ptch1* and *Gli1* by in situ hybridization techniques revealed that Hedgehog signals exclusively in a paracrine fashion from epithelial to mesenchymal cells (van Dop et al., 2010). This in return has highlighted that Hedgehog responsive cells consist of smooth muscle precursor and differentiated cells, myofibroblast-like cells and pericytes. A variety of studies have highlighted the role of Hedgehog signalling in regulating homeostasis of intestinal mesenchymal cells using transgenic mice. An increase in Hedgehog signalling via loss of *Ptch*, driven by the epithelial specific promoter *VillinCre*, led to an increase in the smooth muscle cell marker smooth muscle actin (α -Sma) positive cells in the mesenchyme (Zacharias et al., 2011). Additionally, overexpression of *Ihh* also by the *Villin* promoter resulted in an increase in smooth muscle precursors, differentiated smooth muscle cells as well as myofibroblast-like cells (van Dop et al., 2009). In another study by van Dop et al, the authors noted that deletion of *Ihh* from the intestinal epithelium resulted in a proliferative response mediated by increased Wnt signalling and loss of BMP signalling from the villus and loss of activin from the crypts. They also observed that prolonged loss of *Ihh* resulted in complete loss of smooth muscle precursor cells as well as complete loss of villus core support structure. Similarly, inhibition of Hedgehog signalling by overexpression of hedgehog-interacting protein (Hhip), leads to absence of villi and a highly proliferative crypt-like intestine epithelium with activated Wnt signalling and a lack of differentiated cells (Madison et al., 2005). Therefore, the Hedgehog signalling pathway is crucial for formation of villi (through epithelial to mesenchymal signalling in the intervillus regions), restricting proliferation in the intervillus region as well as the crypt, and essential for maintaining spacing between crypts in the lamina propria. Taken together, it can be hypothesised that Hedgehog signalling acts from the epithelium to the mesenchyme as an inhibitor of Wnt signalling through upregulation of BMPs (described below in section 1.3.3) and may contribute to the tight control of Wnt activation in the normal intestinal epithelium.

1.3.3 The TFG β /BMP signalling pathway

The Bone Morphogenetic Protein (BMP) pathway forms a large subgroup within the Transforming Growth Factor β (TFG β) superfamily. Members of this family signal through a common mechanism in which the ligands bind to a complex of type 1 and type 2

transmembrane serine-threonine kinase receptors. This results in phosphorylation of the cytoplasmic domain of the type 1 receptor by the type 2 receptor, and leads to signal transduction via a family of proteins known as mothers against decapentaplegic, or Smads. Receptor regulated Smads (R-Smads) Smad 1, Smad 5 and Smad 8 are recruited to the receptor where they are activated by phosphorylation and in turn, able to complex with the common Smad (co-Smad), Smad 4. This association results in nuclear translocation of the complex where it interacts with co-activators and co-repressors of transcription to modulate target gene expression (summarised in figure 1.3) (Massagué, 1998).

The BMP pathway was initially implicated in the initiation of CRC when inactivating mutations in BMP receptor type 1A (BMPR1A) and Smad4 were found in the majority of patients with Juvenile Polyposis Syndrome (JPS) (Howe et al., 1998, Zhou et al., 2001). JPS is a rare autosomal hamartoma syndrome in which patients can develop between 50-200 polyps which display gross chronic inflammation and expanded mesenchymal stroma (Roth and Helwig, 1963). Investigation of various alterations of TGF β /BMP signalling in the mouse intestine has generated a number of gastrointestinal phenotypes. Inhibition of BMP signalling in the villus by ectopic expression of Noggin (a secreted BMP inhibitor) led to *de novo* crypt formation, a JPS resembling phenotype and late forming adenomas (Haramis et al., 2004). Deletion of the *Bmpr1a* gene driven by an interferon-inducible promoter *Mx1Cre* (acts in the epithelium and the underlying stroma) also led to development of hamartomatous polyps as well as an expanded proliferative compartment in the intestine (He et al., 2004b). Deletion of *Bmpr1a* in the intestine driven by the epithelial-specific promoter *VillinCre* was not sufficient for the *de novo* crypt phenotype associated with JPS, but did lead to hyperproliferation of crypts and impaired terminal differentiation of cells from secretory lineages. Furthermore, stromal specific deletion of BMP receptor type 2 (*Bmpr2*) lead to development of hamartomas (Beppu et al., 2008) and T-cell specific deletion of Smad4 resulted in development of hamartomas which further developed into invasive carcinoma (Kim et al., 2006). Together, the studies outlined above highlight the importance of BMP signalling in the stroma and immune cells, and implicate a role in maintaining intestinal homeostasis.

The BMP signalling pathway has a well defined role of establishing the crypt-villus axis in the intestine. BMP ligands, receptors and Smad proteins are found to be expressed in mesenchymal and epithelial cells whereas BMP antagonists are only found to be expressed in the mesenchyme (Li et al., 2007). Additionally, phosphorylated Smads 1, 5 and 8 can only be visualised in the nuclei of villus epithelial cells indicating BMP signals from the mesenchyme in

a paracrine fashion where mature epithelial cells are the main target (Haramis et al., 2004, He et al., 2004b). BMPs are also known to play an important role in controlling the proliferative compartment. Here, BMPs are found to directly inhibit Wnt activated and β -catenin driven proliferation, via intracellular mechanisms mediated by Pten, a negative regulator of the PI3K pathway (Tian et al., 2005). Additionally, BMP signalling has been shown to be required for full maturation of secretory lineages *in vivo*, an important function of the Notch signalling pathway (described below in section 1.3.4). *Bmpr1a* mutant mice were deficient in enteroendocrine cells, had immature-appearing paneth cells and goblet cell granules as well as reduced expression of secretory lineage gene expression, but did not affect absorptive cell maturation (Auclair et al., 2007). Taken together, these functions of BMP signalling imply an important role for BMP signalling in the lamina propria in regulating proliferation and lineage allocation in the intestine.

1.3.4 The Notch signalling pathway

The Notch signalling pathway, initially characterized in the 1980s plays a crucial role in regulating the balance between cell proliferation, differentiation, spatial patterning and apoptosis in a variety of tissues. Mammals possess four Notch genes, each of which encode a heterodimeric transmembrane receptor (Notch 1-4) with individual extracellular and cytoplasmic characteristics. Activation of Notch receptors by any one of five ligands (Delta like (Dll) 1, 3 and 4 and Jagged (Jag) 1 and 2) present on adjacent cells leads to proteolytic cleavage of the Notch intracellular domain (Ncd) by γ -secretases and metalloproteases into the cytoplasm. Ncd is then able to translocate into the nucleus where it binds to the transcription factor CBK1/RBP-Jk/Suppressor of Hairless/LAG-1 (Csl) to activate transcription of *Hes* (1, 5 and 7), *Hey* (1, 2) and *Heyl* genes, encoding basic helix-loop-helix/orange domain transcriptional repressors (summarised in figure 1.3) (Radtke and Raj, 2003).

Notch signalling in the intestine is restricted to the crypt region and to a lesser extent, the surrounding mesenchyme (Schröder and Gossler, 2002). The pathway governs cell fate in the intestinal epithelium by regulating differentiation predominantly between absorptive and secretory lineages. Overexpression of Ncd and hence aberrant activation of Notch signalling in the mouse intestinal epithelium, resulted in a reduced number of secretory cells (Fre et al., 2005). Conversely, inhibition of the Notch pathway, either by deletion of the transcription factor Csl or inhibition of γ -secretases leads to an increase in the number of differentiated secretory cells (Fre et al., 2005, van Es et al., 2005). Notch is primarily expressed in the intestinal crypt and is thought to maintain the undifferentiated state by upregulation of *Hes1*

which is also only expressed in crypts. Animals deficient in Hes1 die perinatally due to neurological abnormalities. However, the developing intestines showed an increase in secretory cells at the expense of absorptive enterocytes (Jensen et al., 2000). Furthermore mice deficient in *Math1*, a target gene of Hes1 mediated repression, also have increased secretory goblet cells and reduced enteroendocrine cells (VanDussen and Samuelson, 2010). In accordance with previous data, a recent study in which Notch ligands Delta like (Dll) 1 and 4 were deleted in the mouse intestinal epithelium resulted in an increase in secretory cell types. Interestingly however, unlike previous studies, mice died rapidly after loss of Dll1 and Dll4 due to crypt loss and ablation of the stem cell population. Together, these observations suggest that cells expressing Notch ligands are committed to a secretory cell fate and activate Notch signalling in their neighbouring cells in order to prevent their commitment to a secretory cell fate also. These observations also highlight the role of Notch signalling in maintaining the progenitor phenotype of cells in the crypt as well as stem cell maintenance, most likely through co-operation with the Wnt pathway (Peignon et al., 2011). Additional data to support this was recently reported in a study which showed Hath1 (the *Drosophila Melanogaster* homologue of Math1) expression is not only regulated by Notch, but also by the Wnt signalling pathway. This study showed that Math1 can be targeted for ubiquitination and subsequent proteosomal degradation by Gsk3- β when Wnt signalling is activated as opposed to targeting β -catenin for degradation in the absence of Wnt signalling (Tsuchiya et al., 2007). Moreover, other studies indicate Notch ligands Hes1 and Jag1 are also regulated by Wnt/ β -catenin signalling, further highlighting the co-ordination between Notch and Wnt signalling in the maintenance of differentiation and homeostasis in the intestine (Rodilla et al., 2009).

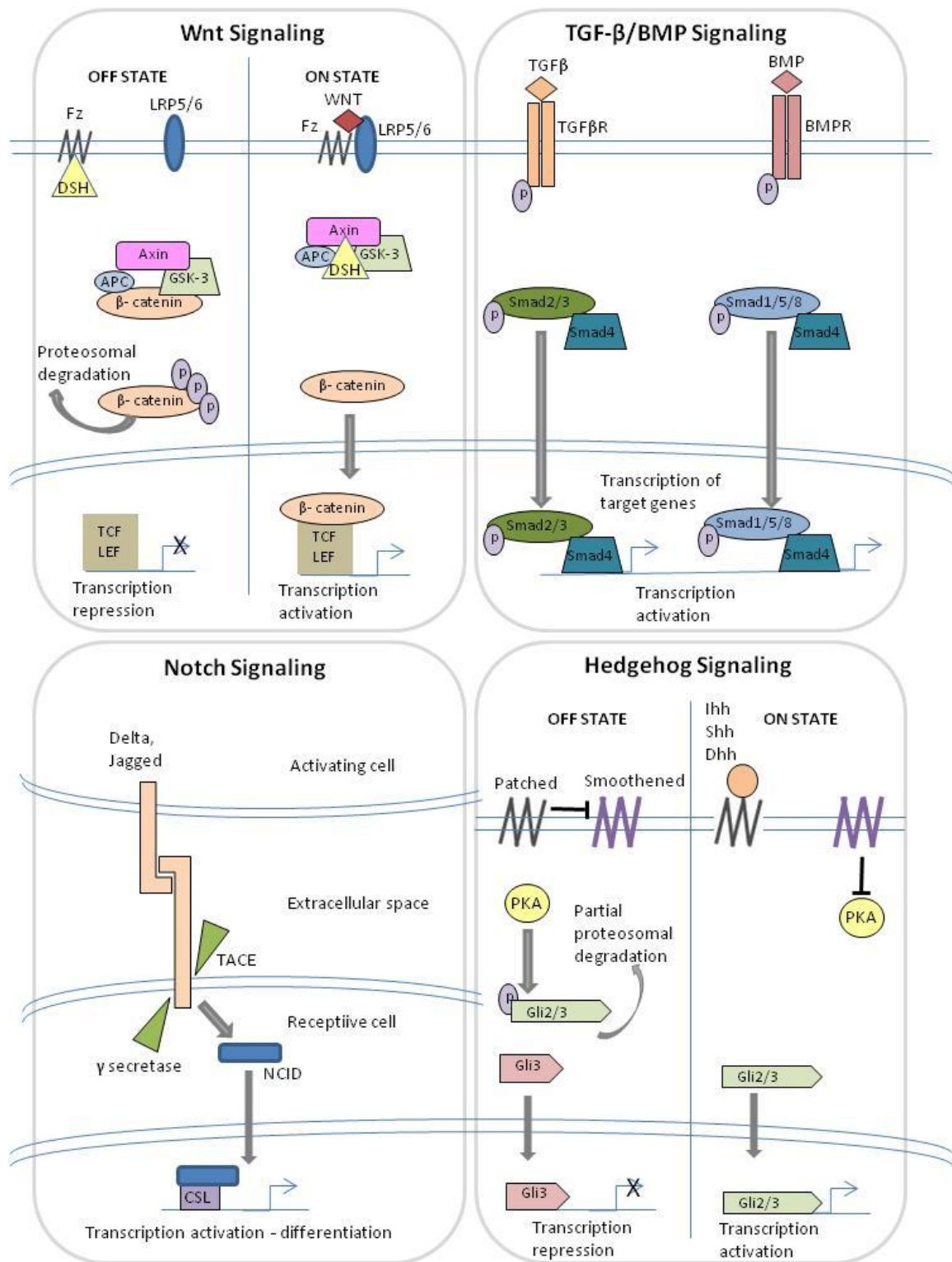


Figure 1.3 Schematic representations of four main signalling pathways which regulate small intestinal homeostasis

Whilst Wnt signalling is crucial for regulating proliferation, the TGF-β/BMP and Hedgehog signalling pathways regulate Wnt pathway activation. Notch signalling influences differentiation of intestinal cell types and maintains an immature state in the crypt through high levels of Notch activity.

1.3.5 Colorectal Cancer stem cells

The identity of the cancer cell of origin and the mechanism by which a tumour is propagated has been a widely contentious issue in the field. This is because it has major implications on multiple aspects of cancer biology, including early cancer detection and prevention, therapeutic target discovery, drug resistance, as well as metastasis (Wicha et al., 2006). The original observations from tumour histology of heterogeneity in tumours alluded to a model whereby any cell type including stem cells, progenitors and early differentiated cells could be the cancer cell of origin (Little and Wright, 2003). It was also assumed that all cells had equal capacity to propagate the tumour by aberrantly proliferating. This model, currently termed the stochastic model was used to explain tumour heterogeneity as a consequence of genomic instability of tumour cells and microenvironmental factors affecting the tumour (Lobo et al., 2007). Therefore from the stochastic model, obliteration of all cancer cells is required for successful treatment as any neoplastic cell can hypothetically propagate the tumour.

Alternatively, substantial evidence for the existence of a discrete population of tumour cells capable of self-renewal and differentiation of multiple lineages has recently gained momentum. This theory is known as the cancer stem cell model (or the hierarchical model) and is now the more widely accepted notion used to explain the cancer cell of origin, tumour heterogeneity as well as tumour progression. Due to their long-living, self-renewing and proliferative capacity, stem cells are favourable contenders for transformation into cell of origin for intestinal cancer. In this model, tumour cells maintain a hierarchical organisation whereby a population of cells (cancer stem cells) at the top of the hierarchy, are responsible for renewing cells. They can give rise to further cancer stem cells, progenitor cells with proliferative capacity as well as aberrantly differentiated cells with no proliferative capacity (Vries et al., 2010). Clinically, this implies that therapies targeting the cancer stem cells will eradicate the tumour whereas those targeting the bulk tumour cells would be less successful, resulting in the cancer stem cells giving rise to more tumour cells and causing recurrence of the disease (He et al., 2009). However it is likely that selective killing of CSC within the tumour may create an opening for non-stem cell pools to revert to stem cell-like cells to help revive tumour growth. In this case, targeting CSCs and bulk tumour cells which provide a supporting microenvironment may be required for complete tumour eradication.

There have been considerable efforts to identify the pools of cancer stem cells in order to isolate and confirm their ability to initiate tumourigenesis as well as develop therapeutics that could potentially target these cells. The first cell surface marker to identify intestinal cancer

stem cells was CD133, also known as Prominin1. Identified in cells with a high proliferative capacity, CD133+ cells were found to be 200 fold enriched for tumour-initiating cells compared to CD133- cells as deduced upon transplantation into non-obese diabetic/severe combined immune deficiency (NOD/SCID) mice (O'Brien et al., 2007). Similarly, high expression of epithelial cell adhesion molecule (EpCAM) and CD44 were also identified as markers of tumour-initiating cells which when transplanted, formed lesions morphologically similar to the original human lesion (Dalerba et al., 2007). Other intestinal cancer stem cell markers include CD166, CD29, CD24 and Lgr5, based on their expression in CD133+ cultures (Vermeulen et al., 2008, Dalerba et al., 2007). Confirmation of these markers was achieved from transplantation of cell surface marker positive cells into immune-compromised mice, indicating CD133+/CD24+ and EpCAM high/CD44+/CD166+ populations to represent tumour initiating populations (Vermeulen et al., 2008, Dalerba et al., 2007). Previously used to isolate hematopoietic precursors, Aldehyde Dehydrogenase 1 (ALDH1) has also been shown to mark human CRC stem cells. Huang and colleagues isolated ALDH1+ CRC cells based on their enzymatic activity and showed they were capable of forming tumours when injected into NOD/SCID mice, whereas ALDH1- cells did not (Huang et al., 2009a). As ALDH1 functions as a detoxification enzyme (Riveros-Rosas et al., 1997), it is hypothesised that this could act to protect CSCs from oxidative insult, permitting longevity and increased proliferative capacity (Miyamoto and Rosenberg, 2011).

Identification of these various cell surface markers allowed Barker and colleagues, and Zhu and colleagues to formally provide evidence for the small intestinal stem cell as the cell of origin for intestinal adenomas. These studies utilised conditional transgenic techniques to activate the Wnt pathway by loss of the tumour suppressor Apc in Lgr5 or CD133 expressing cells in the intestine. This led to efficient tumour formation which was not the case when Apc was lost in progenitor or differentiated cells (Zhu et al., 2009, Barker et al., 2009). Additionally, Schepers et al used a Confetti Cre-reporter allele to demonstrate that Lgr5+ cancer stem cells are able to fuel growth of established intestinal adenomas and give rise to additional Lgr5+ cells as well as other adenoma cell types (Schepers et al., 2012). Although it remains to be determined whether targeting Lgr5/CD133 expressing cells would be capable of causing tumour progression or chemo-refraction, the use of *in vivo* mouse models to investigate CSCs raise less caveats than those which utilise sorting of elusive cell surface markers in human CRCs and serial transplantations of these cells into immunodeficient mice. These caveats include extended culture of human cancer cells, transplantation of cells into foreign sites in immune-deficient mice, addition of multiple cocktails of growth factors and absence of any

natural tumour-host interactions. Although these experiments do provide valuable information on long term self-renewal of the cells, they fail to reflect the true physiological fate of cells in their natural environments.

Additional evidence for the CSC hypothesis has recently been provided by Driessen and colleagues, utilising mouse models of benign papillomas and squamous skin carcinoma, and Chen and colleagues, using a mouse model of glioblastoma. Driessens and colleagues utilised genetic lineage tracing experiments to analyse clonal expansion in an established mouse model of benign papillomas. This study reported the presence of two distinct proliferative compartments, one which terminally differentiated, seldom cycled and had a limited proliferative potential and another with the capacity to persist long term, actively cycled and possessed more stem-cell like characteristics, reminiscent of the hierarchy found in normal tissue. Furthermore, the authors assessed similar features in invasive squamous cell carcinomas and found clonal expansion of a single proliferative population with reduced ability to undergo terminal differentiation. Together, these data are consistent with the CSC paradigm and highlight the differing hierarchy of tumour growth present in benign and invasive cancers (Driessens et al., 2012). Chen and colleagues also provided compelling evidence for the CSC hypothesis. In this study, the authors challenged murine glioblastomas with the standard cytotoxic temozolomide and found a small population of cells with similar properties to CSCs responsible for long term tumour re-growth through the production of highly proliferative cells. Additionally, the study found genetic targeting of glioblastoma CSCs together with cytotoxics for the bulk tumour cells significantly reduced growth of the established tumours, showing proof of concept of targeting CSC *in vivo* (Chen et al., 2012a). Although these studies provide strong evidence for the CSC hypothesis, a number of challenges within the area remain, including determining mechanisms involved in tumour re-growth, the influence of external environment on tumour growth and progression and finally, identification of novel therapeutics which target these increasingly problematic cells.

1.4 The genetic model of colorectal cancer progression

Although tumourigenesis has long been thought a multistep process, the identification of key molecular events which underlie initiation and progression of tumourigenesis are not only vital for our understanding of tumourigenesis but are also imperative for the development of novel targeted therapeutics. The genetic model of CRC progression, first proposed over 20 years ago by Fearon and Vogelstein following a comprehensive review of available histopathological and genetic data, is currently coined the 'classical model' and is remarkably still valid today. Fearon

and Vogelstein proposed that the accumulation of multiple mutations leads to progression of a tumour from a dysplastic epithelium, to a benign adenoma through to metastatic carcinoma. Furthermore, they proposed that although the mutations often occur in a preferred sequence, it is the total accumulations of mutations rather than the order in which they accumulate that is responsible for the biological properties of a tumour (Fearon and Vogelstein, 1990). The model describes mutations in the *APC* gene as the initiating mutation of CRC, followed by subsequent mutations in Kirsten rat sarcoma viral oncogene homologue (*KRAS*), allelic loss of the 18q locus, and mutations in *p53* which contribute to development of malignant disease (figure 1.4).

As described previously, the Apc protein plays an important role in mediating the Wnt signalling pathway and is often regarded as the gatekeeper mutation, due to its central role in maintaining proliferation in the normal intestine (Powell et al., 1992, Kinzler and Vogelstein, 1996). Understanding the molecular pathogenesis of the predisposition syndrome FAP where germline mutations in Apc resulted in hundreds of adenomas also implicated a role for Apc in initiation of CRC. Here, Apc mutations are not sufficient enough to cause progression of lesions and rather accumulations of other mutations leads to metastatic disease. Recently, the Cancer Genome Atlas Network identified altered Wnt signalling in 93% of all cases, with APC found to be inactivated in approximately 80% of cases, as well as CTNNB1 (which encodes β -catenin) mutations in up to 7% and finally AXIN2 mutations in up to 23% of cases (Network, 2012). This highlights the commonality of Wnt pathway mutations in colorectal tumourigenesis and implicates a role in the initiation of CRC. Additionally, APC loss is associated with Chromosomal instability (CIN), a process which increases chromosome rearrangements and hence promotes accumulation of further mutations. Fearon and Vogelstein hypothesised this as a mechanism to accumulate the 7 genetic alterations required for development and progression of tumourigenesis (loss of both alleles of 3 tumour suppressors and activation of 1 oncogene), a process which would normally take more than a lifetime given the mutation rates of the normal intestinal epithelium (Fodde et al., 2001).

The acquisition of activating mutations in the *RAS* oncogene is regarded as the next step for adenoma progression. Fearon and Vogelstein noted that RAS mutations were more prevalent in larger adenomas and carcinomas as opposed to small adenomas indicating a role in tumour progression (Vogelstein et al., 1988). As further described in section 1.5.2, Kirsten-RAS (*KRAS*) is the RAS homologue most commonly mutated in CRC, and is a downstream mediator of the Mitogen activated protein kinase/Extracellular regulated MAP kinase (MAPK/ERK) pathway.

Manipulation of Apc and Kras in the murine intestine confirmed a role for Kras in tumour progression as mice developed more invasive intestinal lesions, and had a significantly reduced survival (Janssen et al., 2006, Sansom et al., 2006). Genomic analyses have indicted activation of KRAS in approximately 40% of CRC cases, and have also indicated a significantly higher frequency of mutations in Duke's stage C tumours, confirming its association with tumour progression (Network, 2012, Smith et al., 2002).

Fearon and Vogelstein also reported loss of the long arm of chromosome 18 in 70% of carcinomas and 50% of late adenomas (Vogelstein et al., 1988). This region was subsequently mapped and the tumour suppressor involved was termed Deleted in colorectal cancer (DCC) (Fearon et al., 1990). Despite its potential role in tumour progression, loss of Dcc failed to predispose mice to CRC and failed to promote tumour progression in Apc^{min} mice, indicating the role of Dcc currently remains unknown (Fazeli et al., 1997). The lack of phenotype observed by DCC mutants in the mouse may be attributed to the involvement of other genes at the 18q region, namely *SMAD2* or *SMAD4*. As previously described, both mediate downstream signalling of the TGF- β /BMP pathway and are essential for maintenance of intestinal homeostasis through epithelial to mesenchymal signalling (section 1.3.3). Recent genomic analysis revealed the TGF- β signalling pathway to be altered in 27% of non-hypermuted and 87% of hypermutated tumours, including mutations in Smad4 (20%) and Smad2 (13%) (Network, 2012) and establishing a major role for the pathway in colorectal tumourigenesis.

Finally, Fearon and Vogelstein identified loss of the short arm of chromosome 17 as the final step for development of malignant disease. This region, lost in 75% of colorectal carcinomas, was mapped to the TP53 locus which encodes for a potent tumour suppressor, protein 53 (p53) (Vogelstein et al., 1988). Furthermore, concomitant with loss of 17p, point mutations in the wild-type p53 gene have also been implicated in colorectal, breast, brain and bladder cancers where it was strongly associated with metastatic disease and poor prognosis (Iacopetta et al., 2006). Elegant evaluation of p53 using mouse models of CRC revealed loss of p53 had no effect on tumourigenesis or tumour progression; however mutant p53 promoted progression of Apc mutant colorectal tumours implicating the type of p53 mutation greatly impacts tumour biology (Clarke et al., 1995, Muller et al., 2009).

Along with the Wnt, MAPK/ERK, TGF- β and p53 signalling pathways, the Phosphoinositide 3-kinase (PI3K) pathway has also been implicated in colorectal tumourigenesis. As described in section 1.5.3, a number of elements along the pathway are mutated in CRC. A recent genomic

study of colorectal tumours found the *PIK3CA* gene, which encodes the p110 α protein- the catalytic subunit of PI3K, to be a 'mountain' in the cancer genome landscape, together with APC, KRAS and TP53 (Wood et al., 2007). The implication from this study is that mutations in the PI3K pathway are likely to be 'drivers' of neoplastic processes rather than 'passengers' that provide no selective advantage to the tumour. This has been evidenced by a number of studies which implicate the pathway in mediating progression of tumours and poor prognosis (Yang et al., 2013). Activation of the PI3K pathway by loss of the tumour suppressor protein Phosphatase and tensin homolog (Pten) has been shown to promote invasion of Apc heterozygous intestinal tumours and also to synergise with oncogenic Kras in the small intestine to induce metastasis *in vivo* (Marsh et al., 2008, Davies et al., *in press*). The identification of various genetic events which underlie pathogenesis of CRC has not only helped our understanding of the disease but has also highlighted some credible therapeutic targets.

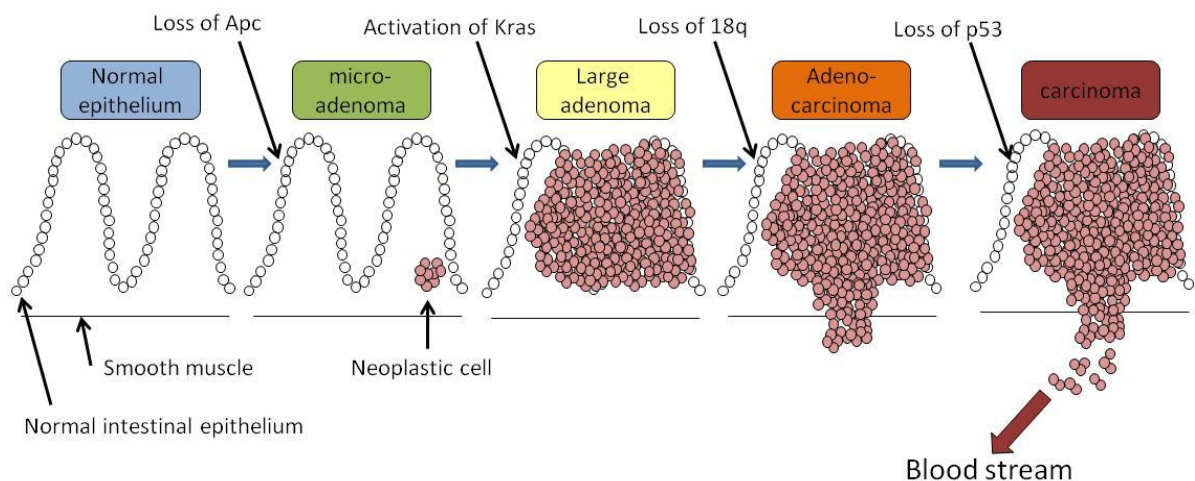


Figure 1.4 Schematic outlining Fearon and Vogelstein model of colorectal cancer progression

Fearon and Vogelstein proposed that accumulation of outlined mutations leads to progression of a benign lesion to metastatic carcinoma. Here, mutations the tumour suppressor *APC* are regarded as the initiating mutation of colorectal cancer, whilst mutations activating the oncogene *KRAS* and allelic loss of the 18q locus lead to progression of a tumour. Finally, mutations in the tumour suppressor protein *p53* are associated with metastatic disease.

1.5 Novel targeted therapeutic strategies in pre-clinical and clinical development for CRC

The notion of stratified medicine whereby the molecular definition of a tumour determines the choice of therapeutic strategy has been revolutionised by extensive analysis of molecular events underlying cancer development. Additionally, targeting patients on the basis of distinctive biological characteristics will identify enriched subpopulations that respond differently to treatment, leading to overall better treatment of cancer.

1.5.1 Targeting developmental pathways and cancer stem cells: Wnt, Notch and Hedgehog pathways

Since aberrant Wnt signalling is implicated in sporadic, familial and hereditary forms of CRC as well as FAP, there has been extensive interest in developing drugs which target the signalling cascade. Due to the complexity of Wnt signalling (discussed previously in section 1.3.1), intervention can occur at multiple levels including ligand expression, receptor-ligand interactions, as well as promote β -catenin degradation and disrupt Tcf/ β -catenin interactions in the nucleus (Barker and Clevers, 2006). Human cancers with or without mutations in APC, AXIN or β -catenin may activate Wnt signalling by increasing expression of Wnt ligands or Fz receptors (Rhee et al., 2002, He et al., 2005a, He et al., 2005b). He and colleagues recently developed a monoclonal antibody against Wnt-1 which has since been shown to effectively block Wnt signalling, halt proliferation and induced apoptosis in a number of human cancer cell lines including head and neck, non-small-cell lung, breast, mesothelioma and sarcoma cells (He et al., 2004a). Furthermore, the Wnt-1 antibody also induced apoptosis in colon cancer cells which had downstream activating mutations, most likely attributed to the rarity of null mutations (He et al., 2005b). Although encouraging, these preliminary results need further validation in animal models to determine true *in vivo* efficacy before further clinical development. Alternatively, a monoclonal antibody against sclerostin, a protein that inhibits the LRP5/6 receptors is currently undergoing clinical evaluation for osteoporosis (produced by Amgen) and may be an attractive therapeutic strategy if found to be tolerated well in patients (Rey and Ellies, 2010).

Other strategies employed to inhibit Wnt signalling focus on targeting β -catenin for degradation or disrupting Tcf/ β -catenin interactions in the nucleus. Two recent studies independently highlighted the role of poly-ADP-ribosylating enzymes tankyrase 1 and 2 (Tnks) in promoting degradation of Axin2. Enzymatic inhibition of Tnks by XAV-939 (Novartis) was able to stabilise Axin2 and promote degradation of β -catenin (Huang et al., 2009b, Chen et al.,

2009) in Apc mutant cells, and may indeed hold some promise for anti-cancer therapy. Alternatively, targeting nuclear TCF/ β -catenin interactions may yield more fruitful effects. A recent screen conducted by Emami and colleagues identified a number of TCF/ β -catenin inhibitors including the lead compound ICG-001, which specifically inhibits the co-activator CREB binding protein (CBP). The compound has since been validated *in vitro* where it has been shown to preferentially induces apoptosis in colon cancer cells whilst sparing normal colon cells, and has also been assessed *in vivo* in human xenografts and the APC^{min} mouse model of human FAP (Emami et al., 2004), showing some early promise.

Despite the growing pharmaceutical interest and efforts into developing efficacious Wnt pathway inhibitors, a number of drugs already in the market, as well as many natural compounds, have been found to directly or indirectly target the Wnt pathway. These include Non-steroidal anti-inflammatory drugs (NSAIDs) such as aspirin and sulindac, both of which have chemopreventive effects by targeting cyclooxygenase (COX) enzymes which mediate Wnt pathway activation via Prostaglandin induced β -catenin degradation (Dihlmann et al., 2001, Boon et al., 2004). However, long term use of NSAIDs such as aspirin, can lead to severe intestinal bleeding and kidney damage. This has resulted in the development of novel NSAIDs which are hypothesised to have increased anti-tumour activity and limited toxic side effects (Barker and Clevers, 2006). Nitric Oxide-donating aspirin (NO-ASA) is an example of a safer, more effective NSAID that has been shown to reduce polyp formation in APC^{min} mice and reduce Wnt signalling in colon cancer cell lines by disrupting TCF/ β -catenin interactions (Williams et al., 2004, Nath et al., 2003). The Vitamin derivative retinoid, has also been used for pre-clinical therapy and chemoprevention whilst Vitamin A has been used against acute promyelocytic leukemia (APL), and active forms of Vitamin D have been shown to be chemopreventative in animal models of colorectal and breast cancers (Takahashi-Yanaga and Kahn, 2010, Pálmer et al., 2001). Various mechanisms have been proposed for the anti-tumour capabilities of vitamin derivatives including a study by Jiang et al, and Pendás-Franco et al, who evidenced vitamin A and D induced activation of Wnt/ β -catenin inhibitory proteins Disabled-2 (Dab2) and Dickkopf 1 and 4 (Dkk1, Dkk4) (Jiang et al., 2008, Pendás-Franco et al., 2008). Additionally polyphenols, a chemical group found in plants and include compounds such as quercetin, curcumin and resveratrol, have all been implicated as Wnt inhibitors. Resveratrol, a compound extracted from grape skin and wine has been shown to reduce Wnt signalling and also CD133 expression in colonic epithelium when evaluated in a CRC prevention trial as a dietary supplement. Subsequently, this is currently under phase II clinical evaluation (Berge et al., 2011, Martinez et al., 2010). Although novel Wnt inhibitors have enormous

potential therapeutically, the Wnt pathway is critical to normal somatic stem cell maintenance and tissue homeostasis and therefore thorough evaluation will be required prior to integration with existing cancer treatments.

Alternatively, the Hedgehog and Notch signalling pathways, also implicated in maintenance of cancer stem cells, may present as attractive therapeutic targets. The identity of cyclopamine, a naturally occurring hedgehog inhibitor found in *Veratrum Californicum*, has previously been utilised as an anti-cancer agent (Cooper et al., 1998). Despite potent anti-tumour activity *in vitro* and *in vivo*, cyclopamine was found to be highly insoluble and toxic. This led to the development of further compound screens to identify potent analogues (Teglund and Toftgård, 2010). Currently, the majority of Hedgehog inhibitors in pre-clinical and clinical evaluation from screening processes are Smoothed inhibitors. As described previously, Smoothed is a transmembrane receptor which is activated by a cognate transmembrane receptor Patched (PTCH), upon Hedgehog ligand binding. The smoothed inhibitor GDC-0449 (vismodegib, Genentech) demonstrated potent single agent activity in patients with *PTCH1* mutant medulloblastoma and basal cell carcinoma (BCC) (Von Hoff et al., 2009), and subsequently resulted in FDA approval (in 2012) as the first agent approved for metastatic and inoperable locally advanced BCC. Interestingly, although mutations in Hedgehog signalling occur much less frequently in human malignancies of other origins including colorectal, ovarian, prostate and pancreatic cancer, *in vitro* studies have shown a lack of correlation between hedgehog pathway activation and response to pathway inhibitors, suggesting that hedgehog inhibition may be beneficial for other tumour settings (Yauch et al., 2008). This is thought to be attributed to the role of hedgehog signalling in the mesenchyme and the tumour microenvironment i.e. tumour stroma. Evidence for this was formally provided from a genetically engineered mouse model of pancreatic cancer where smoothed inhibition resulted in enhanced delivery and response to chemotherapeutics by depleting tumour associated stromal tissue (Olive et al., 2009). Promisingly, the lead Smoothed inhibitor vismodegib is currently in Phase I/II evaluation in gastrointestinal and pancreatic malignancies.

The Notch signalling cascade has been implicated in maintenance of cancer stem cells and chemoresistance in a number of human malignancies. Furthermore, genetic alterations that implicate the Notch pathway have been detected in some cancers, in particular, T-cell acute lymphoblastic leukemia (T-ALL) in which 50% of cases are attributable to chromosomal translocations that activate Notch1 (Weng et al., 2004). The Notch pathway is also activated in CRC, where upregulation of NOTCH-1, JAGGED-1 and JAGGED-2 ligands have previously

observed in human intestinal adenomas, implicating the pathway in early stages of tumour growth (Reedijk et al., 2008). Furthermore, expression of NOTCH-1 was highest in liver metastases suggesting its requirement in tumour progression (Meng et al., 2009). Chemotherapeutics including oxaliplatin and 5-fluorouracil have also been shown to indirectly induce NICD and HES-1 expression through increased γ -secretase activity, suggesting notch inhibition may act as a potent chemo-sensitizer (Meng et al., 2009). The majority of Notch pathway inhibitors are γ -secretase inhibitors (GSIs) which block proteolytic cleavage of the Notch receptor and NICD (described previously in 1.3.4). GSIs were initially developed to treat or prevent Alzheimer's disease however significant toxicity evidenced by gastrointestinal bleeding and diarrhoea, observed in animal experiments and early human trials, ceased further development and forced development of less cytotoxic agents (Searfoss et al., 2003). Various novel agents are currently under clinical evaluation, including the third generation GSI-R04929097, currently in phase I evaluation in combination with the anti-EGFR agent cetuximab and in phase II evaluation as a single agent for third-line treatment of metastatic CRC. Furthermore, oxaliplatin-induced activation of Notch signalling was reduced by simultaneous GSI treatment and resulted in an increased anti-tumour effect, indicating promising potential of targeting the Notch signalling pathway (Meng et al., 2009).

1.5.2 Mitogen-Activated Protein Kinase Pathway (MAPK/ERK) pathway

The MAPK/ERK pathway is stimulated by Receptor Tyrosine Kinases (RTK), Integrins and influx of calcium ions. Downstream of RTKs such as EGFR, are RAS proteins which belong to a larger family of small guanosine-5'-triphosphate binding proteins (GTPases) (Schubbert et al., 2007). This includes HRAS, KRAS and NRAS, all of which are crucial in mediating intracellular responses to extracellular stimuli, such as growth factor signalling. RAS is often localised to the membrane by farnesylation, a process that adds a 15-carbon isopropene chain to the C-terminal CAAX (Downward, 2003, Sebti and Der, 2003). Once membrane bound, activation of the Growth-factor receptor binding protein 2 (GRB2) leads to subsequent activation of Sevenless homolog (SOS), which in turn leads to full activation of RAS by facilitating dissociation of GDP and binding of GTP to RAS. Immediately downstream RAS are RAF proteins (A-RAF, B-RAF and C-RAF) which are serine/threonine protein kinases, and whose phosphorylation leads to further downstream activation of Mitogen Activated Kinase 1/2 (MEK1/2). These in turn act as catalytic substrates for extracellular signal-related kinase 1/2 (ERK1/2) (Figure 1.5). Phosphorylation of ERK leads to nuclear translocation where key cell

cycle regulators are targeted including c-jun and cyclin D, as well as MAPK-interacting kinases (MNK1 AND MNK2), stress activated kinases (MSK1and MSK2) and various transcription factors (Maekawa et al., 2002, Roux et al., 2004, Ledwith et al., 1990). All of these targets are pivotal in regulating various cellular processes including proliferation, survival, apoptosis and migration.

KRAS has been implicated in the oncogenesis of many tumour types including non-small-cell lung, pancreatic, papillary and colon cancer (Sebolt-Leopold and Herrera, 2004), and is the most commonly mutated protein in the MAPK pathway. Approximately 40% of CRCs present with mutations in *KRAS*, the majority of which occur in codon 12 and 13 (Bos et al., 1987, Smith et al., 2002). These mutations often involve glycine-to-valine substitutions at the catalytic sites of amino acids which subsequently lead to loss of GTPase activity and therefore continuous binding of GTP to RAS (Yokota, 2012). Importantly, retrospective studies have found mutations in *KRAS* to be the key negative predictor for response to anti-EGFR antibodies for CRC, and currently patients are screened prior to cetuximab treatment to ensure absence of *KRAS* mutations (Karapetis et al., 2008). The MAPK pathway is also activated following mutations in B-RAF, most of which occur at the V600E kinase domain. This mutation involves a valine-to-glutamic acid substitution in the kinase activation loop resulting in constitutive activation of B-RAF (Ikenoue et al., 2003). The V600E mutation occurs in approximately 15% of CRCs and is also a negative predictor of anti-EGFR therapy. Subsequently, although mutations activating *KRAS* and B-RAF are mutually exclusive (Rajagopalan et al., 2002), together can identify up to 55% of non-responders to anti-EGFR therapy. This also highlights a large population of patients that could potentially benefit from agents targeting the MAPK pathway downstream of EGFR.

Efforts to target the MAPK pathway have yielded agents targeting RAS and RAF proteins, but more fruitfully, MEK1/2. As RAS requires membrane localisation via farnesylation, much effort and early promise focused on inhibiting this process with selective farnesyltransferase inhibitors (FTIs) with hope to target a number of malignancies with *KRAS* mutations. Several compounds entered clinical trials including R115777 (Tipifarnib, Zanestra), however concerns developed when higher concentrations of FTIs were required to inhibit oncogenic *KRAS*, in comparison with wild-type RAS or oncogenic HRAS (End et al., 2001). Furthermore, disappointing results from trials in *KRAS* mutant pancreatic cancers provided further evidence against the use of FTIs. Here, the lack of response in *KRAS* mutant tumours was thought to be

attributable to geranylation, an alternative activating mechanism adopted by KRAS mutant tumours to ensure membrane localisation (Berge et al., 2011).

Much interest into inhibiting RAF proteins stemmed from the discovery of the protein functioning as an effector downstream RAS. Additionally, oncogenic B-RAF mutations are present in a number human malignancies including melanoma, ovarian, thyroid and colon cancers (Davies et al., 2002, Singer et al., 2003, Cohen et al., 2003). Hence there are a number of promising BRAF inhibitors at various stages of clinical development, including PLX4032 (Vemurafenib, Plexxicon) and XL281 (Excelelexis), both of which target the V600E mutant form, and are proving well tolerated with mild toxicities in patients with a number of malignancies including colorectal cancer (Falchook et al., 2012) Despite this, a number of pre-clinical studies have recently reported compensatory activation of MAPK signalling through negative feedback loops activating EGFR in B-raf mutant tumours, in response to selective B-raf inhibition (Prahallad et al., 2012, Corcoran et al., 2012). Nevertheless, these studies show B-raf inhibition is well tolerated and suggest combination therapy with EGFR inhibitors could be beneficial for this patient population.

As most mutations activating MAPK signalling occur in RAS or RAF proteins, targeting the pathway immediately downstream these effectors in an attractive strategy. This has led to the development of inhibitors targeting MEK1/2, dual specificity kinases which phosphorylate ERK1 and ERK2 at Threonine 202/Tyrosine 204 and Threonine185/Tyrosine187 respectively (Haystead et al., 1992). The high degree of homology between the MEK1 and MEK2 is promising for a small molecule inhibitor to potently target both kinases. Early MEK inhibitors, including CI-1040 and PD0325901, showed some promise *in vivo* in terms of inhibiting colon tumour growth, however were soon abandoned due to lack of efficacy during phase II trials (Allen et al., 2003, Rinehart et al., 2004). Nevertheless, target validation studies showed effective inhibition of ERK signalling, and the observation that these compounds were well tolerated in patients, spurred further pharmaceutical development of MEK inhibitors (Sebolt-Leopold and Herrera, 2004). Furthermore, structural analysis of MEK inhibitors identified these to be non-competitive and to avoid perturbation of the ATP binding site, indicating selectivity of targeting MEK kinases only (Sebolt-Leopold and Herrera, 2004). Currently, third generation MEK inhibitors are in clinical development and are showing promise in combination with other targeted agents as well as standard chemotherapy. These include AZD6244 (selumetinib, Astra Zeneca), GSK1120212 (GSK) and MEK162 (Novartis Pharmaceuticals) and are currently undergoing extensive pre-clinical evaluation for a number of different human malignancies.

1.5.3 Phosphoinositide-3-kinase (PI3K) pathway

The PI3K pathway is one of the most frequently deregulated pathways in cancer. Similarly to the MAPK pathway, downstream signalling is activated by RTKs, integrins and cytokine receptors but also indirectly by KRAS which activates the catalytic p110 subunit of the PI3K protein (Engelman, 2009, Kurosu et al., 1997). PI3Ks are heterodimers made up of a regulatory subunit (p85 α , p55 α , p50 α , p85 β , p55 γ) and a catalytic subunit (p110 α , p110 β , p110 δ). The main function of PI3Ks is to phosphorylate the 3'-hydroxyl group of phosphatidylinositol 4,5-bisphosphate (PI[4,5]P₂ or PIP₂) to phosphatidylinositol 3,4,5-triphosphate (PI[3,4,5]P₃ or PIP₃). The 3'-phosphatase PTEN dephosphorylates PIP₃ terminating PI3K signalling. Accumulation of PIP₃ however acts as a crucial secondary messenger and recruits AKT to the membrane where it is phosphorylated and activated by phosphoinositide-dependent protein kinase 1 (PDK1) at threonine 308 (in the activation loop of AKT) and by mechanistic target of rapamycin complex 2 (mTORC2) at serine 473 (in a hydrophobic motif of AKT) to fully activate the protein kinase (Figure 1.5) (Engelman, 2009). AKT is then able to phosphorylate several cellular proteins (shown in figure 1.5) and regulate important processes including proliferation, cell survival, protein synthesis and glucose metabolism (Engelman et al., 2006).

All of the major elements of the PI3K pathway, from receptor to protein kinase, have been found to be altered in an extensive range of human malignancies. The *PIK3CA* gene which encodes the p110 α catalytic subunit is mutated in 14% of CRC as well as breast, endometrial, urinary and ovarian cancer (www.sanger.ac.uk/genetics/CPG/cosmic). Mutations in this gene cluster in two conserved regions which encode the kinase and helical domains that confer constitutive kinase activity (Yuan and Cantley, 2008). The antagonist of the PI3K pathway, the phosphatase and tensin homologue (*PTEN*), is often mutated or lost in both heritable and spontaneous cancers. Germline mutations of this gene are associated with hamartoma tumour syndromes (Blumenthal and Dennis, 2008) whereas sporadic mutations are associated with 9% CRCs as well as endometrial, skin, prostate and breast cancers (Salmena et al., 2008). More recently, somatic mutations in *AKT* have been identified in 6% of CRCs as well as ovarian and breast cancers (Carpten et al., 2007) and amplifications of the gene have been identified in pancreatic, ovarian and head and neck cancers (Engelman et al., 2006).

With a number of elements in the complex PI3K pathway found to be altered in human cancers, an increasing number of strategies are available to target this pathway. The four main classes of inhibitors currently in clinical development include dual PI3K/mTOR inhibitors, isoform-specific and pan PI3K inhibitors, AKT inhibitors as well as mTOR inhibitors. Several

small molecules target both PI3K and the PI3K related kinase (PKK) mTOR as they share similar ATP-binding site structures (Garcia-Echeverria and Sellers, 2008). These inhibitors target all isoforms of the p110 subunit as well as both mTORC1 and mTORC2 and offer the advantage of complete signalling shutdown. There are currently a number of compounds in Phase I/II clinical trials producing promising results, including NVP-BEZ235 and NVP-BGT226 (Novartis Pharmaceuticals) as well as XL765 (Exelixis) and SF1126 (Semafore).

One concern however is that PI3K targeted therapy could mediate insulin resistance in insulin sensitive tissues given the role of the pathway in insulin signalling and glucose metabolism. It is thought that isoform-specific or pan-PI3K inhibitors may provide the solution as selective but transient target inhibition may be better tolerated and more effective clinically (Engelman, 2009). Pan-PI3K inhibitors currently in phase I/II clinical development include XL147 (Exelixis) for endometrial cancers, GDC0941 (Genentech) for metastatic breast cancer as well as BKM120 (Novartis) for a variety of solid tumours. A number of studies have highlighted the importance of individual isoforms in a subset of malignancies for example, p110 α was found to be crucial for breast cancers with ERBB2 amplifications (Torbett et al., 2008) and p110 β in PTEN deficient cancers (Jia et al., 2008). Indeed these highlight a specific group which may benefit from isoform specific inhibitors, but there is a concern that other isoforms may simply compensate for the targeted isoform. Nevertheless, these inhibitors hold potential for further development predominantly in combination with other targeted therapeutics including MAPK inhibitors.

Given the central role of AKT in the PI3K pathway, a number of pharmaceutical companies have developed allosteric and non-catalytic site inhibitors of the kinase. Allosteric inhibitors prevent recruitment of AKT to the membrane by interfering with binding of the crucial PH domain of the kinase to phosphoinositides involved in phosphorylation of AKT (She et al., 2008). Alternatively, inhibitors may not affect phosphorylation of AKT and may instead prevent phosphorylation of AKT substrates including AKT substrate 1 (AKT1/PRAS40), glycogen synthase kinase 3 (GSK3) and forkhead box transcription factors (Engelman, 2009). One agent in particular Perifosine (Keryx), showed early promise with an overall response rate of 20% vs. 7%, and mild toxicity, when combined with capecitabine in phase I trials, and is currently in phase III trials with capecitabine (Bendell et al., 2011). As one of the major downstream effectors of AKT, mTORC1 is an attractive therapeutic target as it integrates growth factor signalling with energy sensing and other cellular processes such as protein synthesis. mTOR was originally identified as the target of a molecule known as rapamycin, a

potent anti-proliferative agent (Laplane and Sabatini, 2012). Despite the anti-tumour activity of rapamycin, it was found to primarily target mTORC1 and the presence of multiple feedback loops in the mTOR pathway (mainly through mTORC2 phosphorylating AKT at serine 473), limited the therapeutic efficacy of it (Harrington et al., 2005, O'Reilly et al., 2006). This provided the rationale for targeting both mTORC1 and mTORC2 to improve the impact on cancer cells. Several compounds have been developed including AZD8055 (Astra Zeneca) an ATP-competitive inhibitors of mTOR as well as OSI-027N and OXA-01 (Astellas Pharma Inc). The later compounds function by preventing phosphorylation of effectors downstream mTORC1 and mTORC2 to impair growth and proliferation better than rapamycin (Falcon et al., 2011). Despite this, there are concerns that inhibition of phosphorylation of AKT at serine 473 is not sufficient enough to completely inhibit AKT signalling (Jacinto et al., 2006). Nevertheless, targeting PI3K signalling holds great promise for the treatment of cancer given the high prevalence of mutations activating this signalling cascade in human cancers.

Whilst targeting the MAPK and PI3K signalling pathways independently may be clinically beneficial in some settings, concurrent pathway activation frequently occurs in cancer and in CRC, a third of all cases present with *KRAS* and PI3K pathway mutations (Cancer Genome Atlas Network, 2012). This may be due to the extensive cross-talk between the two pathways as well as convergence on at least two downstream targets, mTORC1 and the BH3 family of proteins, namely BCL-2-associated antagonist of cell death (BAD) and BCL-2-interacting mediator of cell death (BIM), which regulate cell growth and apoptosis respectively (Figure 1.5) (Engelman, 2009). Extensive evidence of pathway regulation is also evident, indicating a highly complex system of interactions. Whilst *KRAS* is known to lead to activation of the PI3K pathway through direct interactions with the p110 subunit (Kodaki et al., 1994), ERK and its kinase substrate p90RSK also inhibit GSK3 function, a negative regulator of the PI3K antagonist PTEN, subsequently resulting in reduced PI3K signalling (Cohen and Frame, 2001, Al-Khouri et al., 2005). Furthermore, regulation of PI3K signaling can positively or negatively influence MAPK signalling. Here, PIP₃ accumulation can recruit the Grb-2 associated binding partner (GAB), IRS and Grb7 scaffold proteins which following subsequent phosphorylations, can interact with a number of molecules including ERK to mediate MAPK signalling (Wöhrle et al., 2009). Also, PIP₃ can stimulate PAK signalling which is crucial for phosphorylation of the MAPK effector RAF at Serine 388, which is essential for full activation of RAF (Chaudhary et al., 2000, Xiang et al., 2002). PI3K signalling can also influence MAPK effectors downstream AKT through mTOR and p70RSK proteins (Kiyatkin et al., 2006). These are able to negatively regulate GAB and IRS proteins which result in reduced tyrosine phosphorylations at the receptor and

subsequently impair ability to sustain and amplify ERK phosphorylations. Despite this, AKT can also positively regulate MAPK signalling, through multiple protein phosphatases (MKPs). Suppression of GSK-3 by AKT results in downregulation of MKPs which subsequently prevent inactivation of phosphorylated ERK (Aksamitiene et al., 2010). Together these interactions highlight the complex cross-talk between the two cascades but suggest the potential benefits of concomitant pathway inhibition, given these pathways govern crucial processes such as growth, cell survival and apoptosis in cancer cells. Subsequently, evidence for targeting both signalling pathways has been emerging from pre-clinical studies, in particular from genetically engineered mouse models (GEMMs) of lung (Engelman et al., 2008), ovarian (Kinross et al., 2011) and thyroid cancer (Miller et al., 2009) which show activation of both signalling pathways.

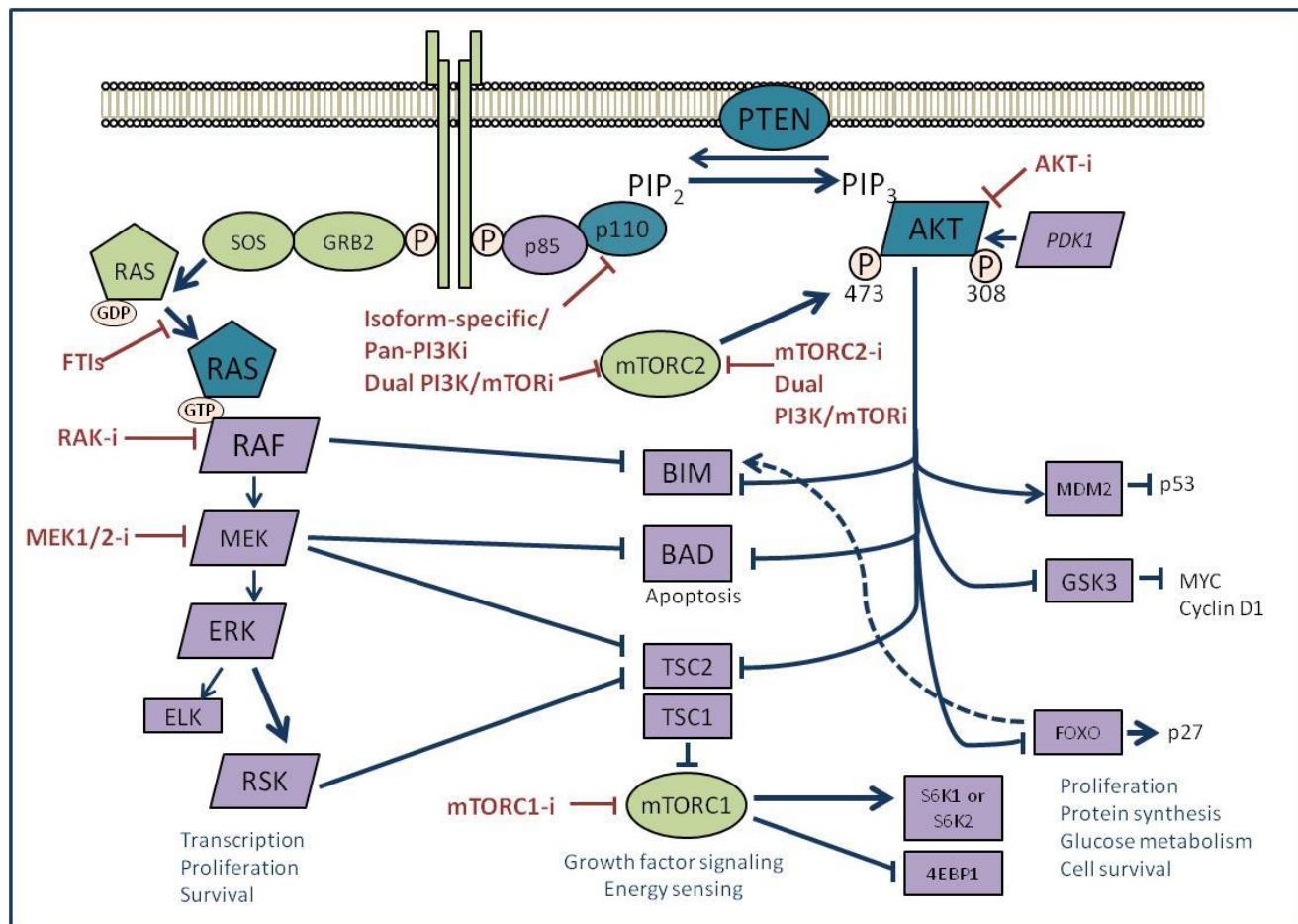


Figure 1.5 Schematic representation of the MAPK and PI3K signalling cascades (adapted from Engelman et al, 2006) and agent available to target various molecules involved in the respective signalling cascades

MAPK pathway inhibitors include farnesyltransferase inhibitors (FTIs) which prevent membrane localisation of RAS, specific RAF inhibitors (RAF-i) such as B-RAF inhibitors which target the V600E mutant form, and MEK1/2 inhibitors which as catalytic site inhibitors, prevent phosphorylation and activation of ERK. PI3K pathway inhibitors include isoform specific p110 inhibitors, pan-PI3K inhibitors, dual PI3K/mTOR inhibitors which target all isoforms of p110 as well as both mTORC1 and mTORC2, AKT inhibitors (AKT-i) which are either allosteric or catalytic site inhibitors, and finally mTOR inhibitors which inhibit individual or both complexes of mTOR.

1.5.4 Anti-cancer prodrugs

Despite the increasing number of promising avenues for developing targeted therapeutics, chemotherapy remains the backbone of cancer treatment. Many efforts are striving to improve the efficacy of standard cytotoxics and significantly decrease their toxicity. One large area of research is currently adopting the prodrug approach which via simple chemical modifications, aims to increase solubility, stability, permeability as well as reduce side effects of chemotherapy (Mahato et al., 2011). This is an attractive approach as due to poor selectivity, chemotherapy targets many rapidly proliferating cells including bone marrow, hair follicle, blood and intestinal cells leading to unpleasant side effects including hair loss, nausea, skin rashes and immunosuppression. Additionally, high doses of chemotherapy are often required for highly proliferative solid tumours leading to rapid toxicity and often discontinuation of treatment (Keefe and Bateman, 2012). Prodrugs currently represent 5-7% of all approved drugs worldwide and are becoming increasingly attractive therapeutic approaches (Ettmayer et al., 2004). Prodrugs typically are designed as biologically inert small molecules which are transformed *in vivo* to release the pharmacologically active components (Knox and Connors, 1997). They can be designed to target specific antigens, peptide transformers or enzymes overexpressed in tumour cells. The design of prodrugs is highly variable but often consists of combinations of the following components: the parent drug or a close derivative, a chemical linker, a cleavable spacer designed to release the drug in the presence of specific conditions (for example an enzyme or specific pH) and a targeting part to aid specific delivery to tumour cells (Mahato et al., 2011). An example of a successful anti-cancer prodrug is capecitabine, an oral prodrug of 5-Flurauracil (5-FU). Capecitabine is thought to be absorbed in the small intestine where it undergoes a cascade of three enzyme bioconversions to release active 5-FU, with almost 100% bioavailability and minimising systemic toxicity (Miwa et al., 1998, Walko and Lindley, 2005). In the absence of the essential enzymes required for prodrug bioconversion, numerous modes of delivering exogenous enzymes are under investigation and currently include the use of antibodies and gene vectors. Here, an antibody-enzyme complex is initially delivered to bind to tumour-specific antigens, then the inactive prodrug is administered with the aim for it to be activated *in vivo* by the localised enzyme (Sharma et al., 2005). Similarly, genes encoding a specific enzyme can also be utilised by means of a vector to deliver the gene to specific tumours (Dachs et al., 2005). These systems raise a number of caveats including immunogenicity of the enzyme/gene-antibody complex, random activation of prodrugs by unbound enzyme/gene-antibody circulating in the blood and conjugation heterogeneity, all of which are caveats which require addressing prior

to safe usage of this technology. However despite the limitations, the main advantage of these systems is the hope for limited toxicity and since a number of enzymes are overexpressed in tumours, it is anticipated this will lead to the development of potent anti-cancer agents. Overall, the prodrug approach is a novel and versatile method which could be applied to a wide range of parental molecules to improve their efficiency and limit toxicity.

1.6 *Preclinical mouse models of colorectal cancer and their value to study translational research*

1.6.1 *Genetically engineered mouse models as useful tools for translational research*

Despite the significant progresses made in understanding the molecular mechanisms required for tumourigenesis and subsequent development of novel anti-cancer drugs, for CRC, only 1 in 10 compounds successful at phase I evaluation are eventually approved by regulators (Johnston and Kaye, 2001). This is largely attributed to the drug development strategies adopted and lack of accurate guidance from preclinical studies which often leads to major failures at phase II evaluations (Robles and Varticovski, 2008). In most drug development strategies, target validation and compound discovery is initially assessed in a variety of human cancer cell lines. These are immortalized cell lines isolated and propagated from a variety of human cancers, decades ago. Although they provide a useful, rapid and inexpensive approach to identify lead compounds, they also suffer from a number of inadequacies. Cancer cell lines maintained under culture conditions may be highly susceptible to genetic drift due to genomic instability in cancer cells and this may affect reproducibility of experiments. Furthermore, *in vitro* conditions lack exposure to certain growth factors, interactions with stromal cells and the extracellular matrix, all of which may contribute to survivability of cancer cells *in vivo* (Watt and Driskell, 2010). For years, the preclinical testing of lead compounds has relied on xenotransplantation (xenograft) models. Xenotransplantation procedures usually involve a subcutaneous injection of human cancer cells into the flanks of immune-compromised mice. Here, lesions develop rapidly and are subsequently utilised to investigate the ability of compounds to reduce or halt tumour growth. Although this system addresses some of the caveats raised by *in vitro* experiments, it still does not recapitulate a number of key processes in cancer development. These including the sporadic nature of tumour formation, the native tumour microenvironment, angiogenesis required for survival, or a host immune response to tumour development, all of which contribute to the characteristics of the primary tumour and

its response to treatment. Most of these issues may be resolved by using genetically engineered mouse models (GEMM) of cancer which more accurately recapitulate many aspects of the disease. GEMMs have the potential to model cell-intrinsic and cell-extrinsic factors that drive *de novo* tumour formation and their progression to metastatic disease. Furthermore, these are useful for validating candidate genes involved in cancer development, and also provide a valuable platform for drug testing and defining mechanisms of resistance (van Miltenburg and Jonkers, 2012).

An increasing number of novel therapeutic agents have been evaluated in clinically relevant GEMMs and together, these highlight some exciting new avenues which should be explored clinically. GEMMs have been used to assess a number of novel combination treatments, for example, Engelman and colleagues showed that Kras mutant lung tumours efficiently regress in response to combined PI3K/mTOR and MEK inhibitor treatment (Engelman et al., 2008). Similarly, De Raedt and colleagues evidenced combination of HSP90 inhibitor the IPI-504 with the mTOR inhibitor rapamycin as effective treatment against Kras driven tumours (De Raedt et al., 2011). Olive and colleagues showed the benefits of adding a novel therapy to a cytotoxic to improve outcome. Here, pre-treatment of mice with a smoothened inhibitor depleted tumour stroma and increased chemotherapy delivery in a mouse model of pancreatic cancer (Olive et al., 2009). Furthermore, Singh and colleagues showed that Kras mutant non-small-cell lung cancer (NSCLC) and pancreatic adenocarcinoma mouse models mimic clinical response to EGFR and VEGF inhibitors, highlighting the use GEMMs in predicting clinical response (Singh et al., 2010). More recently, Chen and colleagues conducted a mouse 'co-clinical' trial which mirrored an ongoing human trial testing the efficacy of MEK inhibitor AZD6244 with standard of care treatment docetaxel, for patients with Kras mutant lung cancer. They demonstrated that concomitant loss of Lkb1, a potent tumour suppressor and not p53 impaired response of Kras mutant lung cancers to the combination treatment. As most patients recruited to clinical trials are stratified according to single oncogenic drivers, the study by Chen and colleagues highlighted variation within the stratified group and explored key mutations underlying this variation (Chen et al., 2012b).

Not only are GEMMs useful for identifying novel therapeutic strategies and mimicking the human situation, but they are also powerful tools for studying acquired drug resistance and may provide insights into the underlying mechanisms of this. Gilbert and Hemann showed that stromal factors released from thymic endothelial cells created a chemoresistant niche for lymphoma cell survival following chemotherapy, allowing relapse in a mouse model for

Burkitt's lymphoma (Gilbert and Hemann, 2010). Additionally, a recent study using the doxycycline-inducible oncogenic PIK3CA^{H1047R} mutant breast cancer GEMM identified Myc activation as a mechanism of resistance to PIK3CA^{H1047R} de-activation, elegantly indicating this may induce resistance to PI3K targeted therapies (Liu et al., 2011).

Despite this, genetically engineered tumour models also have their intrinsic shortcomings. Generating GEMMs with multiple driver mutations is not only time consuming and costly but transgene expression in many GEMMs often surpasses levels of proteins ever observed in patients (Lin, 2008). Furthermore not all pre-clinical studies using GEMMs have predicted clinical response in humans. For example, although Olive et al identified the hedgehog inhibitor Vismodgib to deplete stromal tissue and improve Gemcitabine delivery in a mouse pancreatic ductal adenocarcinoma model, the combination of these compounds in a human phase II clinical trial detrimentally reduced survival of patients by 6 month in comparison to the control arm of Gemcitabine only therapy (<http://www.olivelab.org/ipi-926-03.html>).

As such, an increasing number of pre-clinical studies employ the use of patient derived tumour xenograft (PDX) models. These models involve immediate transplantation of resected patient tumours into immunocompromised mice, eliminating an intermediate *in vitro* propagation step (Parmar et al., 2002, Kuperwasser et al., 2004). Furthermore, PDX models allow ongoing propagation of tumour lines within murine hosts without the compromising conditions encountered by continuous *in vitro* culturing (Jin et al., 2010). These models have been shown to remain faithful to cellular complexity and heterogeneity, tumour architecture including vasculature and supporting stromal tissue, as well as chromosomal architecture (Daniel et al., 2009). PDX models of melanoma, breast, pancreatic, ovarian, lung and colorectal cancer have been successfully established and have also been shown to display similarities to the donating patients with regards to chemotherapy response, adding credence to these models (Decaudin, 2011). Nevertheless, PDX models also have their shortcomings. The engraftment frequency and growth rate is known to vary considerably between patients perhaps suggesting dependence of some tumours on the surrounding tumour microenvironment. Other factors likely to contribute to ineffective tumour engraftment include the time inbetween resection and implantation, lack of supportive growth factors and perhaps an inhospitable site for a particular tumour type. Furthermore, these models heavily rely on patient material which may not be readily accessible (reviewed in Williams et al., 2013). Despite this, PDX models represent an exciting avenue in cancer research, particularly for translational studies as they allow direct evaluation of patient material within a laboratory setting.

1.6.2 Overview of conditional transgenesis techniques

The genetic modification techniques developed in the 1980s by Capecchi, Evans and Smithies to generate mice with targeted disruptions has indisputably revolutionised biomedical research (Evans and Kaufman, 1981, Thomas and Capecchi, 1987, Doetschman et al., 1987). Since then, numerous constitutive gene knockout mice have been generated to study gene function *in vivo*. Although this has provided some useful insights into the physiological role of many genes, a large number of genes involved in tumourigenesis are also required for normal development and hence manipulation of these results in embryonic or perinatal lethality. To circumvent this, the heterozygous form is often studied however this is frequently insufficient for tumour formation. Additionally, constitutive knockout mice display phenotypes in a number of tissues as the gene manipulation is cell autonomous and not limited to a specific tissue type and so, may mask tissue specific effects. Since then, a number of techniques have been adopted to investigate tissue specific gene manipulation and include Tet-on and Tet-off systems as well as site-specific recombination techniques (Miller, 2011).

The Tetracycline Operator (TetO) system developed by Bujard and Gossen, is a reversible method used to control temporal and spatial expression of target genes. It has two variants: the tetracycline controlled transactivator (tTA) or the Tet-off system, and the reverse-tTA (rtTA) or the Tet-on system. Here, the tTA made up of a tetracycline repressor protein (TetR) and the VP16 protein produced by Herpes Simplex Virus, is placed under control of a tissue specific promoter. The expressed protein is able to bind its target- a 19bp Tetracycline operator (TetO) sequence in a separate transgene and in doing so, allows expression of the target gene of interest downstream of the operator. Tetracycline derivatives such as doxycycline are used to antagonise this system as they are able to bind to the tTA protein and prevent it binding to the TetO sequence, therefore doxycycline addition switches off target gene expression. Alternatively, the Tet-On system utilises the rtTA which is capable of binding to TetO sequences only in the presence of doxycycline and hence the addition of doxycycline in this system initiates target gene expression (Gossen and Bujard, 1992).

Site-specific DNA recombination systems are also used to manipulate the mouse genome in a temporal and spatial manner. The Cre-loxP (causes recombination (Cre) – locus of crossover of bacteriophage P1 (loxP)) system involves addition of Cre, a DNA recombinase under the control of a chosen promoter, and loxP sites which are 34 base pair sequences from

bacteriophage P1 (Sauer and Henderson, 1988). Induction of cre recombinase activity, usually using a xenobiotic, will catalyse recombination between loxP sites and usually orientation of loxP sites determines either inversion or excision of the flanked DNA fragment. Most commonly, loxP sites flank the essential part of a gene or flank a transcription terminating stop-cassette. This will either excise the essential part of the gene and hence inactivate the gene, or, excise the transcriptional stop-cassette and activate the gene (Orban et al., 1992). This system is most commonly used to exploit inducible promoters and tissue specific promoters. Inducible promoters which are transcriptionally silent under normal physiological conditions can be activated at a given time by administration of a xenobiotic. Tissue specific promoters on the other hand are often manipulated using post-translational approaches to offer temporal control. An example of a post-translational approach most commonly used is the CreER^T transgene (Feil et al., 1997). This transgene encodes for a cre recombinase-estrogen receptor fusion protein which is only activated in the presence of the estrogen antagonist tamoxifen and not endogenous oestrogen. Tamoxifen is able to bind to the ER domain of the fusion protein and allow nuclear localisation where it is able to catalyse recombination between loxP sites. Finally, both systems can be integrated to create tighter control of inducible promoters which are commonly expressed in a number of tissues. This avoids expression of inducible promoters during development as complete cre induction would require both xenobiotic and tamoxifen administration (Kemp et al., 2004).

An alternative to the Cre-loxP system is the FLP-FRT system which works in the same manner. FLP is a recombinase extracted from yeast *saccharomyces cerevisiae* and is inserted as a transgene into the mouse genome along with FLP recognition target (FRT) sites which flank the gene of interest in the same manner as loxP sites (O'Gorman et al., 1991, Dymecki, 1996). Additionally, a FLP-ER transgene has also been developed to enable tighter control of recombination, much like the Cre-ER transgene.

In addition to temporal and spatial gene manipulation, Tet based systems and Cre-loxP systems can be integrated to include lineage-specific gene expression in mice. These systems whilst require complex breeding programs and an extensive number of transgenes integrated into one mouse, rely on promoter specificity of the Cre transgene to determine where the Tet-based system is active. Nevertheless, this system provides additional control over where the transgene is activated and the period of time for which it is activated, providing a powerful tool for lineage tracing experiments (Sun et al., 2007).

1.6.3 Modelling colorectal cancer in the mouse

Before the advent of conditional transgenesis techniques, much of cancer research relied upon chemical mutagenesis screens to cause random disruptions in the mouse genome which then randomly gave rise to tumours. From this, emerged the first mouse model of human FAP, the Apc^{Min} mouse (Su et al., 1992). These mice have a germline mutation in the tumour suppressor *Apc*, and heterozygous mice develop numerous polyps in the small and large intestines. Although this model has proven to be widely useful in investigating various candidate cancer genes and therapeutic regimens, it is limited in its ability to model other aspects of tumourigenesis such as tumour progression and metastasis.

The availability of a number of inducible and tissue specific promoters as well as various loxP targeted tumour suppressors and oncogenes has allowed more faithful mouse models of human CRC to be developed. Most commonly, the tissue specific promoter VillinCre (el Marjou et al., 2004) and the inducible promoter AhCre (Kemp et al., 2004) are used in developing CRC GEMMs. AhCreER mediated heterozygous deletion of *Apc* and homozygous deletion of *Pten* leads to development of invasive adenocarcinoma in the small intestine (Marsh et al., 2008). Similarly, heterozygous deletion of *Apc* and oncogenic activation of *Kras* driven by VillinCreER also leads to invasive adenocarcinomas of the small intestine (Janssen et al., 2006). Furthermore, *Ink4a/Arf* deletion in the presence of oncogenic *Kras* driven by VillinCreER leads to development of metastasis (Bennecke et al., 2010). A recent study in the lab investigating the synergy between *Pten* deletion and *Kras* activation in the murine intestine found in the presence of a heterozygous *Apc* mutation, this led to rapid onset of tumourigenesis however, in the absence of *Apc*, mice developed metastatic carcinoma over a long latency (Davies EJ, *unpublished*). These models not only provide valuable tools for investigating progression of tumourigenesis but they also represent differing stages of the disease in particular metastasis which could be hugely beneficial for testing novel therapeutics.

1.7 Aims and Objectives

The main aim of this thesis was to evaluate novel therapeutic strategies for CRC utilising valid mouse models of the disease. For this, I first aimed to evaluate PI3K and MEK inhibitors for Pten and Kras mutant CRCs in 'a mouse clinic' setting to explore their clinical application and secondly, to characterise novel ProTide agents aimed to overcome 5-FU resistance in CRCs.

To address the first objective I aimed to utilise four GEMMs of CRC mutant for combinations of Apc, Pten and Kras, to investigate inhibition of the MAPK pathway through the MEK inhibitor MEK162, and inhibition of the PI3K pathway through the dual PI3K/mTOR inhibitor NVP-BEZ235 (both supplied by Novartis pharmaceuticals). The four mouse models used here represent four clinically relevant tumour genotypes for human CRC. I aimed to explore the short term anti-tumour activity of single-agent treatment at various time points following administration, in each genotype as well as early pharmacodynamic effects of agents through assessing their effect on signal transduction. I also aimed to evaluate the therapeutic potential of MEK and PI3K/mTOR inhibition by conducting long term treatment experiments to investigate the impact of continuous drug administration on survival and tumour burden of mice. Furthermore, given the extensive cross-talk between MAPK and PI3K pathways, I also aimed to investigate the therapeutic potential of combined MEK and PI3K/mTOR inhibition in the genetically differing tumour models. These investigations are described in chapters 3-6.

The second objective of this thesis addressed resistance to the most commonly used chemotherapeutic agent for CRC, 5-fluorouracil (5-FU). A key enzyme implicated in the resistance to 5-FU is Thymidylate synthase (TS). Tumours become resistant by upregulation of TS and therefore the main objective here was to develop and characterize novel ProTides, similar to prodrugs, which could potentially target the increased TS in resistant tumours and result in an increased anti-tumour activity. The ProTide compounds designed and synthesised by Prof Chris McGuigan's group (Department of Pharmacy, Cardiff University), use the anti-viral compound Brivudin (BVDU) as the parent compound. The BVDU metabolite BVdUMP is a substrate of TS however the charge of BVdUMP prevents passive entry into cells. The ProTide method temporarily masks the charge on compounds to allow entry of the compound into the cell through the addition of additional chemical groups which are subsequently cleaved upon

entry into the cell to release the active compound. The hypothesis therefore suggested ProTide agents would present with increased anti-tumour activity in TS upregulated settings. ProTides with differing structures were synthesised by collaborators and first evaluated *in vitro* in normal and TS upregulated cancer cells using cell viability and colony forming assays to identify compounds potent in cancer cells but also those more potent in TS overexpressing cells. A handful of lead compounds were then assessed *in vivo* in a short time point experiment to investigate the *in vivo* potential of agents. Two potent compounds were then selected for long term treatment in an invasive mouse model of CRC to investigate long term the effect on survival of mice. Additionally, I aimed to model upregulation of TS through long term administration of 5-FU. The aim here was to investigate the anti-tumour effects of the selected compounds in a TS upregulated tumour setting. This work is described in chapter 7.

2 Materials and Methods

2.1 Experimental Animals

2.1.1 Animal Husbandry

All experiments involving animals were carried out in accordance with national Home Office regulations (Animals (Scientific Procedures) Act 1986), under valid project and personal licences.

2.1.2 Colony Maintenance

All mice used in this thesis were of an outbred background. Mice had access to diet (Special diets service UK, PM3[E]) and fresh drinking water *ad libitum*.

2.1.3 Breeding

Adult animals of known genotypes were bred in trios consisting of one male and two females. Pups were weaned at around 4 weeks of age and ear biopsies were taken for identification and genotyping purposes. All mice were genotyped to determine the correct alleles were present before being used for experimental or breeding purposes.

2.1.4 Genetic Mouse Models

A number of transgenic mouse models were used for this study (origin of alleles used is outlined in table 2.1 below). Two Cre recombinase transgenes were used in this study, *VillinCre*, which is expressed in the intestinal epithelium, and *AhCre*, which is also expressed in the intestinal epithelium as well as the liver and skin. Both Cre recombinase transgenes are fused to a mutated estrogen receptor protein. This ensures that the Cre recombinase protein will only translocate to the nucleus in the presence of tamoxifen. Mice bearing the Cre recombinase transgene were crossed with mice bearing one or more targeted alleles including *Apc*, *Pten* and an oncogenic *Kras* knock in allele. Fig 2.1 is a schematic representation of how gene knock-in and knockout was controlled.

Transgene	Transgene details
<i>AhCreER</i> (Ireland H et al., 2004)	Intestinal epithelium, liver and skin cells
<i>VillinCre ER</i> (El Marjou et al., 2004)	Intestinal epithelium
LoxP targeted <i>Apc</i> allele (Shibata et al., 1997)	Endogenous <i>Apc</i> allele bearing loxP sites flanking exon 14
LoxP targeted <i>Pten</i> allele (Suzuki et al., 2001)	Endogenous <i>Pten</i> allele bearing loxP sites flanking exons 4 and 5
<i>Kras</i> knock-in (Guerra et al., 2003)	Mutated (G12V) <i>Kras</i> allele bearing loxP sites flanking a transcriptional stop cassette in the 5'UTR replacing the endogenous allele

Table 2-1 Outline of transgenic mice used in this thesis

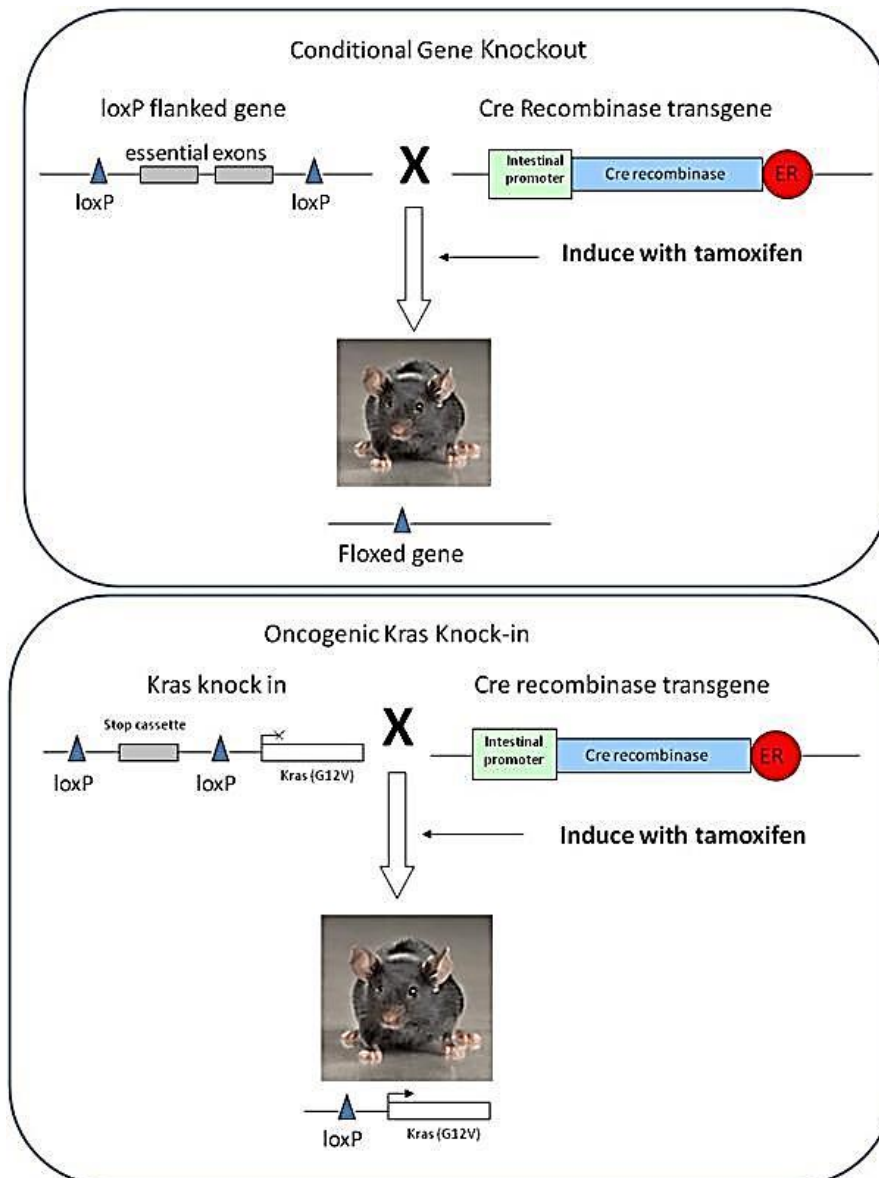


Figure 2.1 Schematic representation of transgenic mouse techniques used in this thesis

Mice that bore loxP flanked genes and the Cre recombinase transgene were generated for experimental use. Conditional knockout mice such as Apc and Pten had the endogenous allele replaced by one which contained loxP sites flanking essential exons of the gene. When activated, Cre recombinase recombined DNA at loxP sites causing deletion of essential exons simulating gene knockout. For conditional knock-in mice such as the oncogenic Kras knock-in mouse, one endogenous allele is replaced with an oncogenic version whereby in this case Glycine is replaced with Valine at codon 12 resulting in a missense mutation. A transcriptional stop cassette flanked by loxP sites is inserted upstream this gene. Activation of Cre recombinase causes recombination between loxP sites resulting in deletion of the transcriptional stop cassette and expression of the oncogenic Kras allele.

2.2 Experimental Procedures

2.2.1 Ear Biopsies

Ear biopsies were taken using a 2mm ear punch (Harvard Apparatus) from individual mice and used for identification purposes as well as DNA genotyping of individual mice.

2.2.2 Administration of Tamoxifen

Animals expressing *Villin*Cre-Estrogen Receptor (*Vi*CreER) fusion protein were induced by Tamoxifen treatment. Corn oil (Sigma Aldrich) was heated to 80°C in a water bath and powdered Tamoxifen (Sigma Aldrich) was added to give a concentration of 10mg/ml. The solution was further heated until the Tamoxifen had dissolved and was kept at this temperature until just prior to administration. A dose of 80mg/kg was administered by intra-peritoneal (i.p) injection to each animal, once daily for four consecutive days.

2.2.3 Administration of beta-Naphthoflavone and Tamoxifen

Animals expressing the AhCreER transgene were induced by Tamoxifen dissolved in beta-naphthoflavone (β NF, Sigma Aldrich). Initially, to make up β NF, corn oil was heated to 99°C in a water bath and powder β NF was added to give a concentration of 10mg/ml. The solution was further heated until the β NF had dissolved completely. Aliquots were frozen in small amber glass bottles at -20°C and defrosted as required. The β NF solution was defrosted and heated to 80°C in a water bath to which powdered Tamoxifen was added to give a concentration of 10mg/ml. A dose of 80mg/kg was administered by i.p injection to each animal, once daily for four consecutive days.

2.2.4 Treatment strategy for NVP-BEZ235 and MEK162

To investigate the therapeutic potential of PI3K/mTOR and MAPK inhibition in the various mouse models, two main methods were utilised.

- 1) To assess the early pharmacodynamic effects of respective drugs, mice were exposed to respective inhibitors for a series of time point (4, 8 or 24 hours were used, $n \geq 3$ mice). This would provide valuable insight into immediate anti-tumour effect drug administration had on various tumour types.
- 2) To investigate the long term therapeutic potential of respective inhibitors, a time point was chosen to start continuous treatment when mice were known to have a

significant tumour burden to avoid prophylaxis treatment. Treatment was continued (as specified for each cohort) until a defined end point.

The schematic in figure 2.2 describes acute and chronic treatment regimens used in this study and table 2.2 outline details for chronic treatment regimens for individual mouse models.

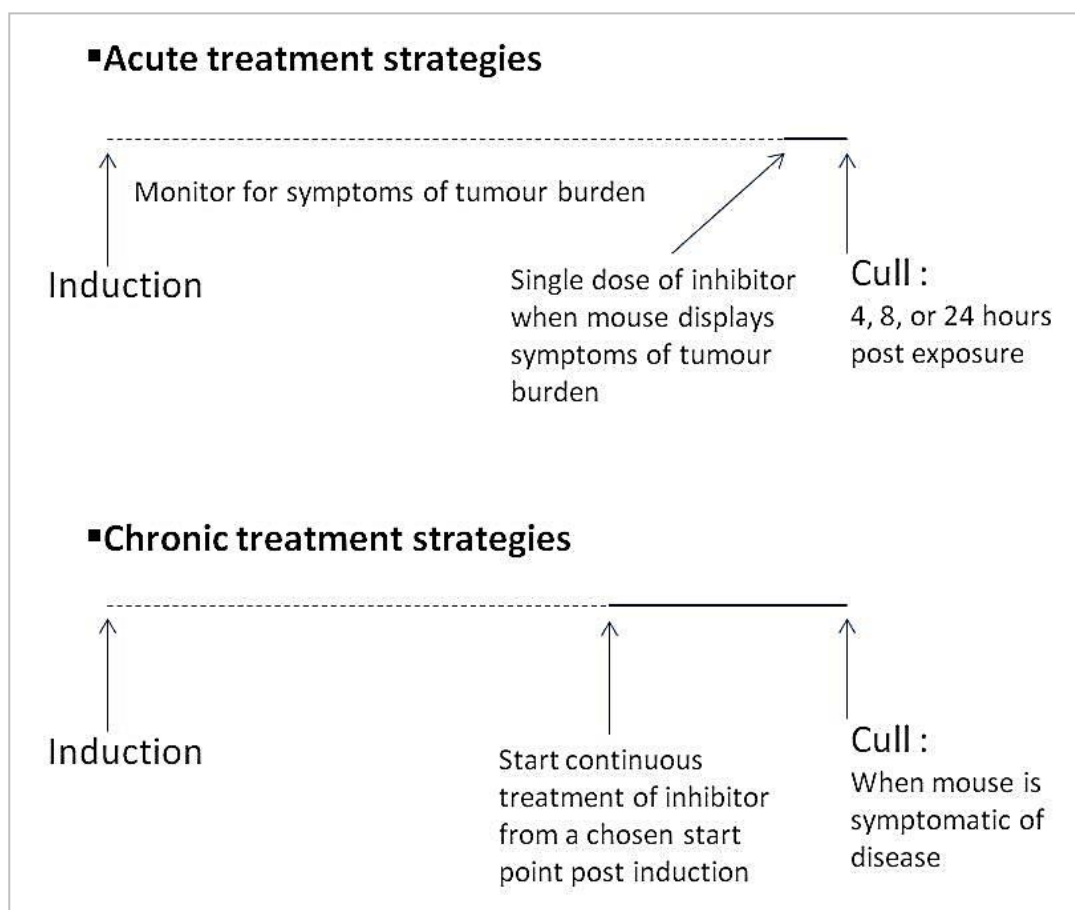


Figure 2.2 Schematic description of treatment regimens used in this thesis

Outline of treatment regimens used to investigate therapeutic potential of inhibitors. For investigation of immediate anti-tumour and pharmacodynamic effects of inhibitors, an acute treatment strategy was used (as outlined in section 2.2.4). To determine whether continuous treatment improved survival of mice, a chronic treatment strategy was undertaken whereby mice were started on daily treatment at a chosen start point following induction (as outlined in table 2.2)

Mouse model	Median survival (days post induction)	Chronic treatment start point (days post induction)
<i>VillinCreER Apc^{f/+}</i>	270	220
<i>AhCreER Apc^{f/+} Pten^{f/f}</i>	100	77
<i>VillinCreER Apc^{f/+} Kras^{LSL/+}</i>	153	100
<i>VillinCreER Apc^{f/+} Pten^{f/f} Kras^{LSL/+}</i>	41	22

Table 2-2 Outline of chronic treatment start points for each mouse model used in this study

2.2.4.1 Short term administration of compounds

Mice which presented with symptoms of intestinal tumour burden, indicated by pale feet, bloating or rectal bleeding were exposed to a single dose of 35mg/kg NVP-BEZ235 or 30mg/kg MEK162 by oral gavage and were culled at either 4, 8 or 24 hour time points following drug administration.

For short term combination studies 3 differing treatment strategies were employed:

1. Combo 1: mice were exposed to 35mg/kg NVP-BEZ235 first followed by 30mg/kg MEK162 1 hour after, and culled 4 hours following last drug administration.
2. Combo 2: mice were exposed to 30mg/kg MEK162 first followed by 35mg/kg NVP-BEZ235 1 hour after, and culled either 4 or 24 hours following last drug administration.
3. Combo 3: mice were exposed to 35mg/kg NVP-BEZ235 followed immediately by 30mg/kg MEK162 and culled 4 hours following drug administration.

2.2.4.2 Long term administration of NVP-BEZ235

NVP-BEZ235 (Novartis Pharmaceuticals) was resuspended in 0.5% Methyl cellulose (MC, Sigma Aldrich) and vortexed to form a milky solution. The solution was then administered at 35mg/kg once daily (O-D) or twice-daily (T-D) by oral gavage (Harvard apparatus) according to cohorts.

2.2.4.3 Long term administration of MEK162

MEK162 (Novartis Pharmaceuticals) was suspended in 1% Carboxy-methyl cellulose (CMC, Sigma Aldrich) in 0.5% Tween⁸⁰ (Sigma Aldrich) and vortexed to form a translucent solution. The solution was then administered at a dose of 30mg/kg once daily (O-D) or twice-daily (T-D) by oral gavage (Harvard Apparatus) according to cohorts.

2.2.4.4 Long term administration of Combination

NVP-BEZ235 and MEK162 were prepared as outlined above in section 2.2.4.2 and 2.2.4.3 respectively. The NVP-BEZ235 solution was administered at 35mg/kg first followed by MEK162 administered an hour later at 30mg/kg once-daily or twice-daily according to cohorts.

2.2.4.5 Vehicle treatment for NVP-BEZ235 and MEK162

Controls of 0.5% MC (Sigma Aldrich) were administered by oral gavage (Harvard Apparatus) according to the volume administered for the drug counterpart.

2.2.5 Treatment strategy for BVDU ProTide compounds

2.2.5.1 Short term administration of selected compounds

Selected ProTides and Thymectacin (synthesised by Stephanie Rats and Sahar Kandil, Cardiff University) were dissolved in a 50:40:10 [w/w/w] PEG300 (Sigma Aldrich):Ethanol:Tween 80 (Sigma Aldrich) solution to give a 50mg/ml stock solution, which was stored at 4°C. For administration of 50mg/kg, the stock was diluted 1/20 in 1X Phosphate Buffered Solution (PBS, Invitrogen). AhCreER Apc^{f/+} Pten^{f/f} mice aged 85 days post induction were administered at 500µl/25g mouse by oral gavage (Harvard Apparatus) once daily for 4 days (n=4 mice per cohort). Mice were sacrificed 6 hours after the final dose and were also administered BrdU 2 hours prior to culling as described in section 2.2.6.

2.2.5.2 Long term administration of selected compounds

CFP472, CFP3172 and Thymectacin (synthesised by Sahar Kandil, Cardiff University) were prepared as outlined above to form a stock of 75mg/ml, which was stored at 4°C for 5 days. The stock was then diluted and administered as outlined above. AhCreER Apc^{f/+} Pten^{f/f} mice aged 77 days post induction were treated daily until a survival end point (n=15 mice per cohort).

2.2.6 Administration of BrdU

Where indicated, mice received an excessive dose of 5-Bromo-2-deoxyuridine (BrdU, Amersham Biosciences) in order to label cells in the S-phase of the cell cycle. Mice received 10ml/kg BrdU by i.p injection 2 hours prior to culling.

2.3 Polymerase Chain Reaction (PCR) genotyping

2.3.1 DNA extraction from ear biopsies

Mouse ear biopsies were collected after weaning and stored at -20°C for DNA extraction. The tissue was digested in 250µl lysis buffer (Purgene) containing 0.4mg/ml Proteinase K (Roche), overnight at 37°C with agitation. Protein was then precipitated by addition of protein precipitation solution (Purgene). The solution was mixed by inversion and protein and any remaining debris was pelleted by centrifugation at 14000 x g for 10 minutes. The supernatant was added to 250µl isopropanol to precipitate the DNA. The mixture was then inverted and centrifuged at 14000 x g for 15 minutes to pellet the DNA. The supernatant was discarded and the pellet was allowed to air dry for 2 hours before resuspending in 250µl of PCR grade water (Sigma Aldrich).

2.3.2 Generic PCR genotyping protocol

PCR reactions were carried out to detect the presence of loxP sites in targeted alleles. The PCR primers used in each reaction were designed using the web based program Primer 3. Reactions were carried out on 96 well PCR plates (Greiner Bio-One). 2.5µl of genomic DNA (gDNA) extracted from individual ear biopsies or control PCR grade water was pipetted into individual wells, and a PCR master mix containing PCR grade water (Sigma Aldrich), magnesium chloride (Promega), dNTPs (25mM dATP, dTTP, dCTP, dGTP (Bioline)), DNA polymerase (either Dream Taq (Fermentas) or GO taq (Promega)), PCR buffer (Promega) and gene specific primers (Sigma Genosys) were added to each well to make a final volume of 50µl (primer sequences and reaction mixtures for each PCR are outlined in table 2.3). The 96 well plates were then sealed with aluminium foil seals (Greiner Bio-One), and air bubbles were eliminated by tapping the sealed wells of the plate on a hard surface. The reactions were run in a GS4 thermocycler (G storm), individual reaction cycling times are described in table 2.4.

2.3.3 Visualisation of PCR products

PCR reaction products were visualised by gel electrophoresis. 2% agarose gels were made by dissolving agarose (Eurogentech) 2% [w/v] in 1X Tris Borate EDTA (TBE) buffer (Sigma Aldrich) and heated in a microwave until boiling. Once boiling, the gel solution was quickly cooled under a running tap and 14µl of Safe View (NBS biological) was added per 400ml of gel solution (Safe View is a nucleic acid stain which allows visualisation of DNA as it binds to DNA and fluoresces under UV light). The gel was then poured into clean moulds (Bio-Rad) and combs were placed to create wells. Once set, the gels were placed into gel electrophoresis tanks (with their moulds to prevent slippage) and covered with 1X TBE (Sigma Aldrich), Safe View (NBS Biologicals) was also added to the buffer. 5µl of loading dye (50% Glycerol (Sigma Aldrich), 50% ultrapure dH₂O, 0.1% [w/v] bromophenol blue (Sigma Aldrich)) was added to each PCR product sample, mixed by pipetting and then added to individual wells. A molecular weight marker was added to one well to ensure correct PCR product size. The gel was then run at 120V for approximately 30 minutes. Following this, PCR products were visualised using a GelDoc UV Transilluminator (Bio-Rad) and images were captured using GelDoc software (Bio-Rad). PCR product sizes are outlined in table 2.5.

DNA extraction, PCR and visualisation of PCR products by gel electrophoresis was repeated for all experimental animals once dissected to re-confirm original PCR genotyping.

Gene	Forward primer sequence (5'-3')	Reverse primer sequence (5'-3')
Cre specific	TGACCGTACACAAAATTTG	ATTGCCCCTGTTTCACTATC
Apc-loxP	GTTCTGTATCATGGAAAGATAGGTGGTC	CACTCAAAACGCTTTTGAGGGTTGATTC
Pten-loxP	CTCCTCTACTCCATTCTTCCC	ACTCCCACCAATGAACAAAC
Kras-loxP-stop	AGGGTAGGTGTTGGGATAGC	CTGAGTCATTTTCAGCAGGC

Table 2-3 Primer sequences used for gene specific PCRs

	Cre specific	Apc-loxP	Pten-loxP	Kras-loxP-stop
PCR reaction Mix				
gDNA	2.5µl	2.5µl	2.5µl	2.5µl
PCR grade water	31.7µl	31.7µl	31.7µl	31.7µl
GO Taq PCR buffer	10µl	10µl	10µl	10µl
1.5mM MgCl₂	5µl	5µl	5µl	5µl
dNTPs	0.4µl	0.4µl	0.4µl	0.4µl
Primer 1 (100mM)	0.1µl	0.1µl	0.1µl	0.1µl
Primer 2 (100mM)	0.1µl	0.1µl	0.1µl	0.1µl
Taq DNA polymerase	0.2µl	0.2µl	0.2µl	0.2µl
Brand of Taq polymerase	GO Taq	Dream Taq	Dream Taq	Dream Taq
PCR cycling conditions				
Initial denaturation	3 min, 94°C	3 min, 94°C	3 min, 94°C	3 min, 94°C
Cycle number	30 at:	30 at:	35 at:	30 at:
Step 1: denaturation	30 sec, 95°C	30 sec, 95°C	1 min, 94°C	1 min, 94°C
Step 2: annealing	30 sec, 55°C	30 sec, 60°C	1 min, 58°C	1 min, 60°C
Step 3: extension	1 min, 72°C	1 min, 72°C	1 min, 72°C	1 min, 72°C
Final extension	5 min, 72°C	5 min, 72°C	5 min, 72°C	5 min, 72°C
	Hold at 15°C	Hold at 15°C	Hold at 15°C	Hold at 15°C

Table 2-4 Outline of PCR reaction mixtures, cycling conditions

PCR product size (bp)	Cre specific	Apc-loxP	Pten-loxP	Kras-stop-loxP
Wild-type		266	228	403
Targeted transgene	1000	315	335	621

Table 2-5 Outline of PCR product sizes

2.4 Tissue sample preparation

All tissues were dissected immediately after animal sacrifice to avoid degradation of RNA, protein and phospho-proteins.

2.4.1 Dissection of Organs

Mice were culled by cervical dislocation and placed on their backs. 70% ethanol was sprayed over the abdomen and the abdominal cavity was opened first by cutting through the skin and then through the muscle wall. The stomach and intestines were first dissected out (below, section 2.4.2), the stomach was opened longitudinally and contents removed prior to fixing. The kidneys, liver, spleen, pancreas and a small section of the abdominal skin were then dissected out and fixed along with the stomach (described in section 2.5).

2.4.2 Dissection of intestines

The intestines were first removed along with the stomach. The attachment between the stomach and the oesophagus was cut and the stomach was gently pulled out of the mouse taking along the intestines carefully removing all attached mesentery. Once the whole intestine was removed, the stomach was cut at the ileal-caecal junction and the caecum was cut from the small intestine and the colon. The contents of the small intestine and colon were removed by flushing with cold water and fixed as described in section 2.5. Prior to fixing and if required, the intestines were opened longitudinally and small intestine tumours, a small section of normal small intestine, colon polyps and a section of normal colon were dissected out and immediately placed into clean microtubes and quickly snap frozen in liquid nitrogen for either protein or RNA extraction.

2.5 Fixation of tissues

2.5.1 Formalin fixation

Most tissues dissected were 'quick fixed' in 10% neutral buffered formalin (Sigma Aldrich) for 24 hours, as majority of commercially available antibodies for immunohistochemistry analysis work well with formalin fixed tissues. This included the liver, pancreas, spleen, kidneys and stomach as well as the intestines which after flushing with water, were cut into 10cm lengths, opened longitudinally and rolled into 'swiss rolls' secured with needles. This allowed end-on sectioning of the intestine.

2.5.2 Methacarn fixation of intestines

To allow analysis of total macroscopic tumour number and size, a methacarn solution (a 4:2:1 ratio of methanol, chloroform and glacial acetic acid) was used for fixation. Once flushed with cold water, the small intestine and colon were opened longitudinally on blotting paper and placed into a methacarn bath overnight. Tumour number and size were accurately measured using a ruler before rolling the intestines into 'swiss rolls' and placing into 70% ethanol.

2.5.3 Processing of fixed tissue

After fixation for 24 hours, all tissues were removed from fixative solutions, placed in a cassette (Fisher) and processed using an automatic processor (Leica TP1050). This involved dehydrating the samples through increasing gradient of alcohols (70% ethanol for 1 hour, 95% ethanol for 1 hour, 2x 100% ethanol for 1 hour 30 minutes, 100% ethanol for 2 hours) and finally soaking in xylene (2x xylene for 2 hours). The tissues were then placed in liquid paraffin for 1 hour, then again twice for 2 hours. Finally, the tissue samples were removed from their cassettes and embedded in paraffin wax by hand and allowed to harden.

2.5.4 Sectioning of fixed tissue

Paraffin embedded tissues were cut into 5µm sections using a microtome (Leica RM2135), placed onto Poly-L-Lysine (PLL) coated slides and baked at 58°C for 24 hours. The sections were then used either for Haemotoxylin and Eosin (H&E) staining (described in section 2.6.4) or immunohistochemistry (IHC)(described in section 2.6.3).

2.6 Histological Analysis

2.6.1 Preparation of sections for staining or IHC

Paraffin embedded tissue sections on PLL coated slides were first de-waxed by placing in two consecutive baths of xylene for 5 minutes each. The sections devoid of paraffin were rehydrated down a gradient of alcohol baths (2x 100% ethanol, 95% ethanol, 70% ethanol) for 2 minutes each and then placed in a bath of distilled water in preparation for staining or IHC.

2.6.2 Immunohistochemistry (IHC)

IHC was used to visualise the presence and localisation of various proteins on tissue sections. A generic IHC protocol is outlined in below in section 2.6.3 and specific conditions and antibody dilutions are detailed in table 2.6

2.6.3 Generic IHC protocol

2.6.3.1 Preparation of sections for IHC

Paraffin embedded tissue sections on PLL coated slides were de-waxed and rehydrated as previously described in section 2.5.3.

2.6.3.2 Antigen retrieval

The antigen retrieval step was carried out to break cross-linking bonds formed between proteins during fixation and therefore unmask hidden antigens. This typically involved heating the tissue section slides in 1X citrate buffer (10X Sodium citrate, pH6, Thermo Scientific), either in a microwave, a pressure cooker or a water bath. After boiling, the slides were allowed to cool in solution for up to 1 hour before washing in distilled water.

2.6.3.3 Blocking of endogenous peroxidases

The antibody visualisation system used here involves an enzymatic reaction of 3,3'-diaminobenzidine (DAB) catalysed by horse radish peroxidase (HRP). Therefore, to avoid non-specific enzymatic action of endogenous peroxidases present in the tissue sample, a peroxidase block was utilised. Slides were incubated in a 3% hydrogen peroxide solution (30% stock, Sigma Aldrich) for 15 minutes at room temperature which irreversibly inactivates endogenous peroxidases. Slides were then washed in distilled water and then in wash buffer, each for 5 minutes.

2.6.3.4 Blocking of non-specific antibody binding

Non-specific binding of antibodies was blocked by incubating tissue sections with serum from a different animal to which the primary antibody used was raised in. A hydrophobic barrier pen was used to outline the tissue section on the PLL coated slides. Serum was then diluted in wash buffer to a known concentration which sufficiently prevents non-specific antibody binding and tissue sections were then incubated in serum block for an optimised period of time in a humidified slide chamber. Serum block was removed and tissue sections were incubated with primary antibody without washing.

2.6.3.5 Primary antibody incubation

Tissue sections were incubated with primary antibody diluted in blocking serum (same concentration of serum in wash buffer used for blocking) at working concentrations (described in table 2.6). Incubation was carried out either for 1 hour at room temperature or overnight at 4°C, in a humidified slide chamber. After incubation, slides were washed three times in wash buffer to remove residual unbound primary antibody.

2.6.3.6 Secondary antibody incubation

Tissue sections were then incubated with secondary antibody, typically a 1/200 dilution in normal serum diluted in wash buffer. The secondary antibody used, was raised in the same animal in which the primary antibody was raised in to ensure specific binding only to the antigen of interest. Secondary antibodies were typically incubated for 30 minutes in a humidified slide chamber. The slides were then washed three times in wash buffer.

Most secondary antibodies used were biotinylated, and therefore an additional signal amplification step was required to allow HRP binding to the secondary antibody. Other protocols required use of the Envision plus kit (DAKO) in which tissue sections were incubated in a pre-diluted secondary antibody conjugated to HRP, in which case a signal amplification step was not required and antibody binding could be immediately visualised after washing off excess secondary antibody (signal detected described in section 2.6.3.7)

2.6.3.7 Signal amplification

Signal amplification was required for biotinylated secondary antibodies. This involved formation of a complex called avidin, which was bound to the HRP, using the Vectastain Avidin-Biotin Complex (ABC) kit (Vector labs). The ABC reagent was prepared following manufacturer's instructions in wash buffer 30 minutes prior to use to allow structure formation. Tissue sections were then incubated in the ABC reagent for 30 minutes at room temperature in a humidified slide chamber before being washed three times in wash buffer. Sections were then ready for signal detection.

2.6.3.8 Detection of signal

The antigen of interest was visualised by the production of a coloured stain. This was produced as a result of a substrate-enzyme reaction. The substrate used here was 3'3-

diaminebenzidine (DAB) which was catalysed by the HRP enzyme bound to the secondary-primary antibody complex to produce a brown coloured stain. The DAB reagents (DAKO) were prepared by following manufacturer's directions just prior to incubation. Tissue sections were incubated with DAB reagents for 2-10 minutes at room temperature. Excess DAB reagent was removed by washing tissue sections in distilled water.

2.6.3.9 Counterstaining and cover slip mounting

Tissue sections were incubated in Mayer's Haemalum (R. A. Lamb) for 1 minute to stain nuclei and then washed under a running tap for 5 minutes. The slides were then dehydrated through an increasing gradient of alcohols (1X 70% ethanol, 1X 95% ethanol, 2X 100% ethanol) for 2 minutes each and finally cleared in 2X xylene baths for 5 minutes each. Slides were removed from xylene, mounted in DPX medium (R. A. Lamb) and an appropriate sized cover slip as placed on the tissue section before being left to air dry in a fume hood.

Primary antibody	Manufacturer	Antigen retrieval conditions	Non-specific signal block	Wash buffer	Primary antibody conditions	Secondary antibody	Signal amplification step
Anti-BrdU	BD Biosciences #347580	20mins, 100°C water bath	Peroxidase: envision +block (DAKO) 20mins Serum: 1%BSA 1hr both at RT	PBS 3X 5min washes	1:150 in 1% BSA for 1hr at RT	Envision+ HRP-conjugated anti-mouse (DAKO) 30mins at RT	N/A
Anti-Cleaved caspase 3 (Asp175)	Cell Signaling Technology #9661	15mins at pressure using pressure cooker	Peroxidase: 3% H ₂ O ₂ 10mins Serum: 5% NGS 1hr both at RT	TBS/T 3X 5min washes	1:200 in 5%NGS for 48hrs at 4°C	Biotinylated anti-rabbit 1:200 (Vector Labs) 30mins at RT	ABC kit (Vector Labs)
Anti-phospho Akt (Ser473) XP	Cell Signaling Technology #4060	30mins, 100°C water bath	Peroxidase: 3 H ₂ O ₂ 10mins Serum: 5% NGS 1hr Both at RT	TBS/T 3X 5min washes	1:50 in 5%NGS O/N at 4°C	Biotinylated anti-rabbit 1:200 (Vector Labs) 30mins at RT	ABC kit (Vector Labs)
Anti-phospho44/42 MAPK (phospho-ERK1/2) (Thr202/Tyr204)	Cell Signaling Technology #4376	15mins in boiling bath microwave	Peroxidase: 1.5 H ₂ O ₂ 10mins Serum: 10% NGS 1hr both at RT	TBS/T 3X 5min washes	1:75 in 10%NGS O/N at 4°C	Biotinylated anti-rabbit 1:200 (Vector Labs) 30mins at RT	ABC kit (Vector Labs)
Anti-phospho ribosomal protein S6	Cell Signaling Technology	15mins in boiling bath microwave	Peroxidase: 3 H ₂ O ₂ 10mins Serum: 10% NGS 45 mins Both at RT	TBS/T 3X 5min washes	1:100 in 10%NGS O/N at 4°C	Biotinylated anti-rabbit 1:200 (Vector Labs) 30mins at RT	ABC kit (Vector Labs)

Table 2-6 Outline of antibodies and conditions for immunohistochemistry (IHC)

Key: BSA – Bovine Serum Albumin, RT – Room temperature, PBS – Phosphate buffered solution, NGS – Normal goat serum, TBS/T – Tris buffered solution with 0.1% Tween, O/N – Over night.

2.6.4 Haematoxylin and Eosin (H&E) stain

Tissue sections were stained with haematoxylin to mark nuclei and eosin to stain the cytoplasm of cells in order to visualise tissue sections for phenotypic analysis. Paraffin embedded tissue sections on PLL coated slides were de-waxed and rehydrated as previously described. The sections were then stained by immersing in a bath of Mayer's Haemalum (R. A. Lamb) for 45 seconds and then, washed under a running tap for 5 minutes, followed by counter staining in an aqueous solution of 1% Eosin (R. A. Lamb) for 5 minutes, and finally washing under a running tap water for 30 seconds. The tissue sections were then ready to be dehydrated, cleared and mounted as described previously.

2.7 Scoring

Scoring was undertaken to reveal potential anti-tumour activity of therapeutics assessed. Typically, five random fields per tumour were assessed, also counting the total number of cells per field to accurately assess the percentage per total number of cells. All tumours present and at least three biological replicates per cohort were assessed.

2.7.1 Apoptosis and mitosis scoring

H&E stained sections were used to assess the number of apoptotic bodies and mitotic figures present in vehicle and drug treated tissue.

2.7.2 BrdU Scoring

Animals were administered a pulse of BrdU as described in section 2.2.6. The incorporation was visualised by IHC (section 2.6.3) and positive cells were counted as above.

2.7.3 Cleaved caspase 3 scoring

Cleaved caspase 3 IHC was performed on tissue sections as described in section 2.6.3 and positive staining was scored as detailed above.

2.7.4 Tumour severity grading

Tumour grading was carried out on long term drug and vehicle treated cohorts. Multiple H&E stained sections of swiss-rolled intestines per mouse were examined under the microscope. The number of lesions and severity of tumour invasiveness was assessed according to criterion outlined in table 2.7 and figures 2.3 and 2.4 below. All mice assigned to the various drug and vehicle cohorts were examined.

Tumour stage	Description
microadenoma (mAd)	Small lesions, often observed within the villi
adenoma (Ad)	Larger lesions that do not invade into the underlying submucosa
Early invasive adenocarcinoma (EIA)	Tumour displaying evidence on invasion into the underlying submucosa but does not infiltrate the smooth muscle of the intestine
Advanced invasive adenocarcinoma (AIA)	Tumour displaying evidence on invasion through the smooth muscle layer and local invasion in the peritoneum

Table 2-7 Scoring system used for grade severity of lesions

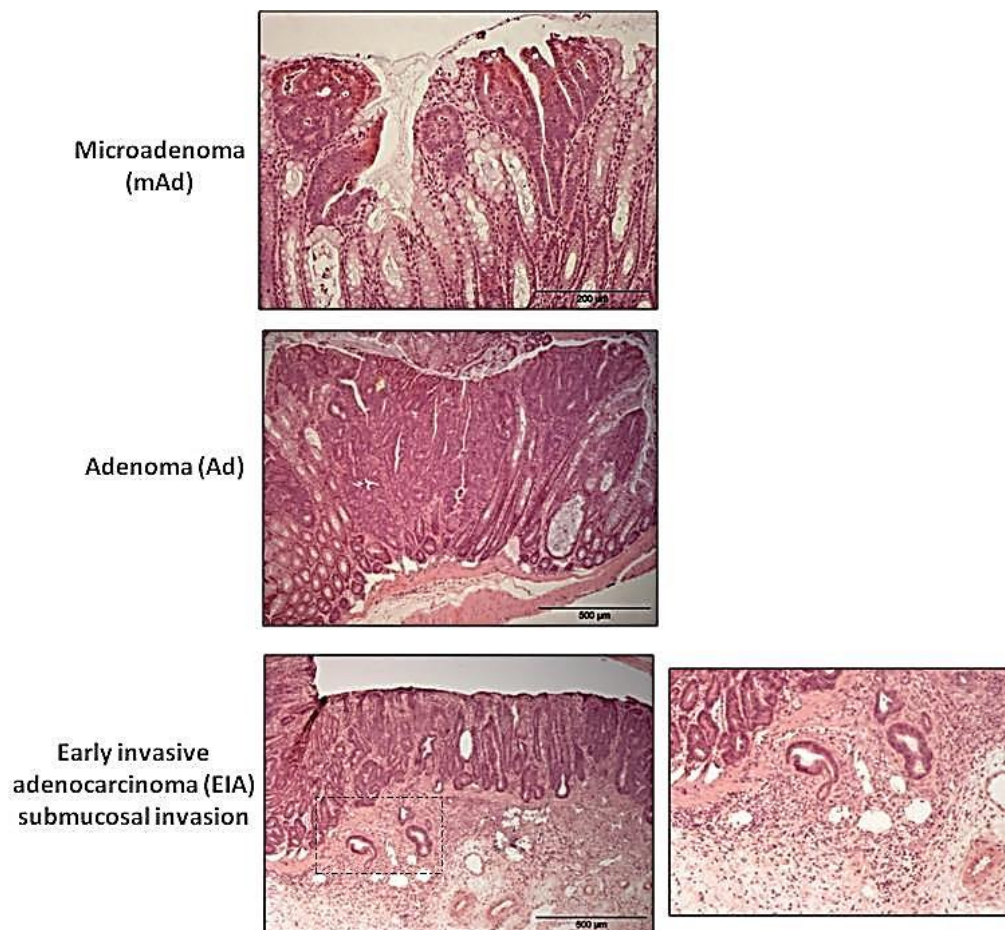


Figure 2.3 Stages of colon tumour progression

H&E stained sections of the whole colon were examined for the level of progression of each tumour. This was staged according to the criteria on table 2.7

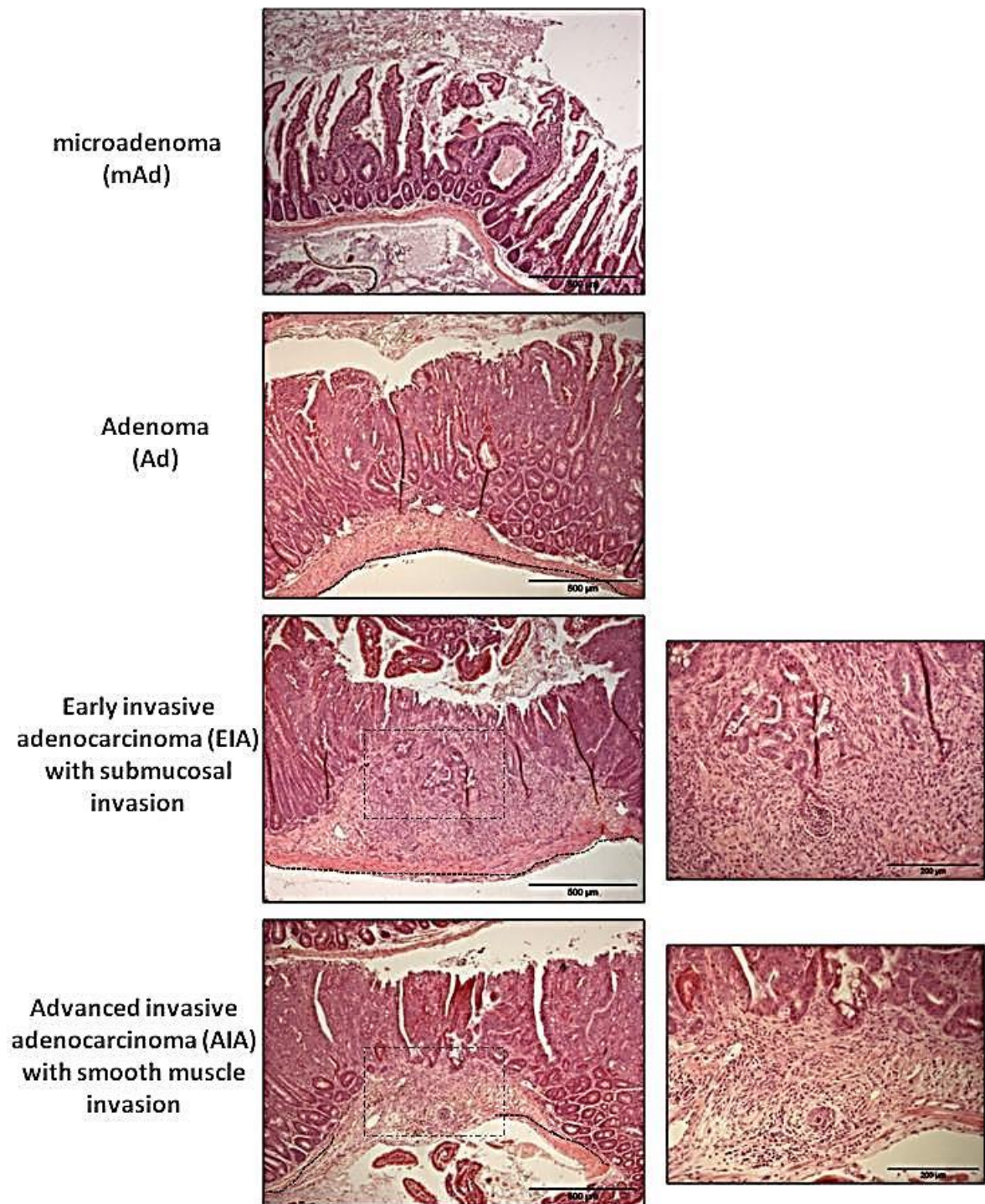


Figure 2.4 Stages of intestinal tumour progression

H&E stained sections of the whole small intestine were examined for the level of progression of each tumour. This was staged according to the criteria on table 2.7. (Dashed lines follow the smooth muscle wall to demonstrate invasion through the muscle wall)

2.8 Protein Extraction and Western Blot Analysis

Protein was extracted from tumour samples which were snap frozen during dissection in liquid nitrogen and stored at -80°C prior to protein extraction.

2.8.1 Protein extraction

Tumours were removed from frozen storage and placed in dry ice to keep frozen. 200µl of lysis buffer (20mM Tris-HCl pH8.0, 2mM EDTA pH8.0, 0.5% [v/v] NP-40 (Sigma Aldrich)) containing protease inhibitors (Complete mini protease inhibitor tablets, one per 5ml lysis buffer (Roche)), and phosphatase inhibitors (25mM sodium beta-glycerophosphate (Calbiochem), 100mM sodium fluoride (Sigma Aldrich), 20nM Calyculin A from *Discodermia calyx* (Sigma Aldrich) and 10mM sodium pyrophosphate (Sigma Aldrich)) was added to homogenising lysing matrix D tubes (MP Biomedicals) and kept cold on ice. Individual tumours were carefully placed into individual homogeniser tubes containing lysis buffer and extra care was taken to ensure samples do not defrost during the process. Whilst the tumour defrosted, cells were homogenised using a Precellys 24 Homogeniser (Bertin Technologies) at 6000 RPM for 2 cycles of 45 seconds. The samples were then further lysed by shear action by passing sample through a 21 or 23 gauge needle 10 times. The samples were then transferred to clean microtubes and centrifuged at 10000 x g for 10 minutes at 4°C. Centrifugation allowed formation of a pellet of insoluble material. The supernatant was removed and aliquoted before snap freezing in liquid nitrogen and storing at -80°C.

2.8.2 Determination of protein concentration

An aliquot of each protein sample extracted was used for protein quantification using the Bicinchoninic Acid (BCA) method. The BCA method uses the biuret reaction in which Cu²⁺ ions are reduced to Cu¹⁺ ions to produce a purple colour. The extent to which the copper ions are reduced can be quantified by colourimetric detection in a linear fashion as the BCA reagent strongly absorbs light at 562nm. Reactions were conducted in colourless, flat bottom 96 well plates (Greiner Bio-One). Each protein sample was measured in duplicate, 2µl was added to 198µl 1X Phosphate Buffer Solution (PBS) (10X stock, Invitrogen), mixed and serially diluted twice to produce three concentrations (1/100, 1/200 and 1/400) in a final volume of 100µl. A standard curve was created using Bovine Serum Albumin (BSA) diluted from a stock of 2mg/ml to 100mg/ml in lysis buffer. The diluted BSA was further diluted in PBS to generate a concentration range of 5µg/ml to 35µg/ml. BCA reagents were made up following manufacturer's instructions (Pierce), 100µl was added to each sample and mixed by pipetting.

The plate was sealed using a foil lid and incubated at 37°C for 1 hour with slight agitation or overnight at room temperature. The absorbance of each sample was read using a plate reading spectrophotometer ELx800 (Biotek), at the nearest wavelength to the optimum (562nm) at 590nm. Concentrations of each diluted sample were calculated using the standard curve.

2.8.3 Preparation of protein samples for western blot analysis

Protein samples were removed from -80°C storage and defrosted on ice. 30µg of protein from each sample was made up to 15µl with extraction buffer and a further 15µl of Laemmli buffer (Sigma Aldrich) was added. The samples were heated at 95°C for 10 minutes to denature proteins and then quenched on ice. Samples were briefly centrifuged prior to loading into wells.

2.8.4 Casting of polyacrylamide gels

The Mini-Protean III (Bio-Rad) gel casting apparatus was used to prepare 1.5mm thick polyacrylamide gels. Glass plates were rinsed with distilled water, cleaned with 70% ethanol, dried and assembled into the casting apparatus. Extra care was taken to ensure all seals were tight at the bottom of the glass plates. Gel solutions were made up to produce 10% resolving gel and 5% stacking gel without the addition of TEMED (recipes for resolving and stacking gel outlined on table 2.7). TEMED was first added to the resolving gel solution (in the fume hood), quickly mixed and poured into the glass plates, leaving approximately 2cm on top for the stacking gel. 1ml of distilled water was placed on top of the resolving gel solution to ensure the surface of the gel was flat and the gel was left to set. The remaining resolving gel solution was used to determine when the gel was set. Once set (approximately 30 minutes), the water was poured off onto tissue paper. TEMED was then added to the stacking gel solution, mixed thoroughly and pipetted onto the resolving gel up to the top of the glass plates and an appropriate comb inserted between the glass plates to create wells. Once set, the combs were removed and gel plates were placed into sodium dodecyl sulphate-polyacrylamide gel electrophoresis (SDS-PAGE) apparatus. Running buffer was added into the tank to create a buffer dam for the electric current to pass through and wells were flushed with running buffer to remove excess gel.

10% resolving polyacrylamide gel (2 gels)	5% stacking polyacrylamide gel (2 gels)
6.8ml Ultrapure double deionised H ₂ O 8.4ml 30% acrylamide/bisacrylamide (Sigma Aldrich) 9.4ml 1M Tris-HCL pH8.8 250µl 10% [w/v] Sodium Dodecyl Sulphate (SDS, Sigma Aldrich) 72µl 25% [w/v] Ammonium persulphate (APS, Sigma Aldrich) 13.2µl N,N,N',N'-teramethylethylenediamine (TEMED, Sigma Aldrich)	6.9ml Ultrapure double deionised H ₂ O 1.7ml 30% acrylamide/bisacrylamide (Sigma Aldrich) 1.3ml 1M Tris-HCL pH8.8 100µl 10% [w/v] Sodium Dodecyl Sulphate (SDS, Sigma Aldrich) 66µl 25% [w/v] Ammonium persulphate (APS, Sigma Aldrich) 13.2µl N,N,N',N'-teramethylethylenediamine (TEMED, Sigma Aldrich)

Table 2-8 Recipes for resolving and stacking gels

5X Running buffer (1L)	1X Transfer buffer (1L)	1X Stripping buffer (1L)
950ml distilled H ₂ O 15.1g Tris base (Fisher Scientific) 94g Glycine (Fisher Scientific) 50ml 10% [w/v] Sodium Dodecyl Sulphate (SDS, Sigma Aldrich)	800ml distilled H ₂ O 200ml Methanol (Fisher Scientific) 2.9g Tris base (Fisher Scientific) 14.5g Gycine (Fisher Scientific)	60ml Tris 1M pH 6.8 20g Sodium Dodecyl Sulphate (SDS, Sigma Aldrich) Make up to 1L Prior to use: add 350µl β-mercapthoethanol (Sigma Aldrich) to 50ml stripping buffer

Table 2-9 Recipes for buffers used during SDS-PAGE

2.8.5 SDS-PAGE

Once the apparatus was set up, 6µl of pre-stained full-range Rainbow molecular weight ladder (GE Healthcare) was added to the first well. Prepared protein samples (as described above in section 2.8.3) were loaded into individual wells and the gels were run at 130-200V, until the dye reached the end of the gel.

2.8.6 Protein transfer to nitrocellulose membrane

After proteins had separated in the polyacrylamide gel, the gels were removed from the SDS-PAGE tank and from the glass plates, and placed into transfer buffer before removal of the stacking gel. Amersham Hybond-ECL nitrocellulose membrane (GE Healthcare) was cut to size and also placed in transfer buffer until assembly of 'transfer sandwiches'. The gel and membrane were 'sandwiched' between two sheets of 3MM blotting paper (cut to size) on each side, as well as one piece of sponge either side (all pre-soaked in transfer buffer). Extra care was taken to ensure no air bubbles were present in between the polyacrylamide gel and the nitrocellulose membrane, as these prevent the transfer of proteins to the membrane. The 'sandwich' was placed into plastic transfer supports before being placed into the transfer tank, orientated so that the current runs through the gel towards the nitrocellulose membrane (- to +) to transfer negatively charged proteins to the nitrocellulose membrane. 1L of transfer buffer was added to the tank, which was then placed into an ice bucket and allowed to run at 100V for 1 hour. After transfer, the nitrocellulose membrane was carefully removed from the sandwich and placed in wash buffer, 1X TBS/T (Tris Buffered Saline with 0.1%Tween (10X stock, Cell signalling Technology)) in a clean container.

2.8.7 Primary and Secondary antibody probing on nitrocellulose membrane

The nitrocellulose membrane was blocked in 5% [w/v] non-fat dry milk (Marvel) in TBS/T for 1 hour at room temperature with slight agitation to prevent non-specific antibody binding. The membrane was then washed once in wash buffer before addition of the primary antibody diluted either in 5% non-fat dry milk or 5% Bovine Serum from Albumin (BSA) in TBS/T. The primary antibody was incubated either overnight at 4°C or 1 hour at room temperature, both with gentle agitation. The membranes were then washed three times for 5 minutes in wash buffer before incubation with HRP-linked secondary antibody diluted in 5% non-fat dry milk in TBS/T for 1 hour at room temperature with gentle agitation. The secondary antibody used was raised in the same animal as the primary antibody and was typically diluted 1/2000. The membrane was then washed three times for 5 minutes with wash buffer prior to signal detection

2.8.8 Signal detection

The electrochemiluminescence (ECL) reagent kit (GE Healthcare) was used for detection of antibody signal. The reagents utilise a chemifluorescent reaction catalysed by HRP exposed to X-ray film. The ECL reagents were prepared according to manufacturer's instructions just before

use. The ECL reagent was added to membranes and incubated according to manufacturer's instructions before draining excess solution and placing membranes into a light-proof cassette. The cassette was then taken to the dark room where under safelight conditions, X-ray film (Fujifilm Super RX, blue background) was exposed and processed using an automatic processor (Xograph Compact X4 automatic X-ray film processor). A number of X-rays were exposed at varying times to ensure clear images were generated. The films were then placed on top of the membranes and molecular weight ladder was used to confirm presence of correct protein band size.

2.8.9 Confirmation of equal loading

Membranes were then washed to remove excess ECL reagents before re-probing with an antibody for β -actin (conditions in table 2.9), a house keeping gene often used to confirm equal loading of proteins. Often for phosphorylated proteins, in order to confirm the difference in phosphorylated proteins was not due to a higher or lower abundance of the unphosphorylated protein, samples from one stock solution were often run on two separate gels which were simultaneously transferred and incubated with either the phosphorylated or the total protein. Alternatively, membranes were stripped of bound antibody, using a stripping buffer (described in table 2.8) to re-probe at the same region. For this, each membrane was incubated in 50mls of stripping buffer with 350 μ l β -mercapthoethanol at 55°C for 30 mins. Following this, membranes were washed in wash buffer and then subjected to normal protocols for antibody probing as outlined in section 2.8.7.

2.8.10 Densitometry Analysis

For densitometry analysis, protein bands were quantified by measuring the intensity of bands on images of western blots, using Image J software. The quantity of protein was determined relative to the loading control (β -actin) and represented as relative to control samples.

	phospho-Akt473	phospho-Akt308	Total Akt	phospho-Erk	Total Erk	phospho-S6 Ribosomal Protein	phospho-4EBP1	P110 α	β -actin
Manufacturer Catalogue #	Cell signaling Technology 4060	Cell signaling Technology 13038	Cell signaling Technology 4685	Cell signaling Technology 4377	Cell signaling Technology 4695	Cell signaling Technology 4856	Cell signaling Technology 2855	Cell signaling Technology 4249	Sigma Aldrich A5441
Block	5% TTM/ TBS/T	5% TTM/ TBS/T	5% TTM/ TBS/T	5% TTM/ TBS/T	5% TTM/ TBS/T	5% TTM/ TBS/T	5% TTM/ TBS/T	5% TTM/ TBS/T	5% TTM/ TBS/T
Primary antibody dilution Conditions	1:1000 in 5%BSA/ TBST O/N at 4°C	1:500 in 5%BSA/ TBST O/N at 4°C	1:1000 in 5%BSA/ TBST O/N at 4°C	1:1000 in 5%BSA/ TBST O/N at 4°C	1:1000 in 5%BSA/ TBST O/N at 4°C	1:500 in 5%BSA/ TBST O/N at 4°C	1:500 in 5%BSA/ TBST O/N at 4°C	1:500 in 5%BSA/ TBST O/N at 4°C	1:4000 in 5%TTM/ TBST 1hr at RT
Secondary antibody dilution Conditions	Anti-rabbit 1:2000 1hr at RT	Anti-rabbit 1:2000 1hr at RT	Anti-rabbit 1:2000 1hr at RT	Anti-rabbit 1:2000 1hr at RT	Anti-rabbit 1:2000 1hr at RT	Anti-rabbit 1:2000 1hr at RT	Anti-rabbit 1:2000 1hr at RT	Anti-rabbit 1:2000 1hr at RT	Anti-mouse 1:2000 1hr at RT
Signal detection	ECL	ECL	ECL	ECL	ECL	ECL	ECL	ECL	ECL

Table 2-10 Outline of antibodies and conditions for protein analysis Key: TTM – Non-fat dry milk, TBS/T – Tris buffered solution with 0.1% Tween, BSA – Bovine Serum Albumin, RT – Room temperature, O/N – Over night, ECL - Electrochemiluminescence.

2.9 Maintenance and culture of cells

2.9.1 Experimental cell lines

The MCF7 cell line is a human breast cancer cell line (obtained from Prof Jan Balzarini, Rega Institute, Netherlands) isolated from an invasive breast ductal carcinoma by the Michigan Cancer Foundation in 1970. The MCFTDX cell line (also obtained from Prof Jan Balzarini, Rega Institute, Netherlands) is a stable Tomudex resistant cell line created by continuous exposure to 2 μ M Tomudex by Patrick Johnston and colleagues in 1995.

2.9.2 Maintenance of cell lines

Both MCF and MCFTDX cell lines were cultured in Dulbecco's Modified Eagle Medium (DMEM, Invitrogen) supplemented with 10% [v/v] Fetal Bovine Serum (FBS, Sigma Aldrich), 1% [v/v] Hepes buffer (Invitrogen), 2mM L-glutamine (Invitrogen) and 50 units/ml penicillin-streptomycin (Invitrogen).

Cell lines were maintained in a sterile, humidified 37°C incubator and CO₂ levels were maintained at 5%. Both cell lines were routinely cultured in T25 tissue culture flasks (Corning Ltd). Cells were passaged when they reached confluency of 80-90% on a split ratio of 1/6-1/12. For cell passaging, all media was removed, cells were washed in sterile 1X Phosphate-Buffered solution (PBS, Invitrogen) and incubated in 0.05% Trypsin/EDTA (Invitrogen) (normally 2mls of trypsin/T25 flask) for 5 minutes at 37°C. Cells were then checked under the microscope to ensure detachment before being diluted in culture medium to the appropriate splitting ratio and transferred to a clean flask. Cell lines were not split for more than 25 recorded passages.

2.9.3 Long term cell storage

Cells were routinely frozen and cryo-stored in order to have sufficient aliquots of cell lines with low passage numbers. Confluent T75 flasks (Corning Ltd) of cells were detached by trypsin resuspended in 10mls of culture medium and transferred to a clean 15ml falcon tube. Cells were then pelleted by centrifugation at 1100rpm for 3 minutes. The cells were then resuspended in 10mls of freezing medium (culture medium with 10% [v/v] dimethyl sulfoxide (DMSO, Sigma Aldrich)) and aliquoted into 1ml cryo-tubes (Nunc). The tubes were placed in a freezing container filled with iso-propanol to facilitate slow freezing at -80°C overnight. Cryo-tubes containing cells were then transferred into liquid nitrogen storage.

When required, cells were retrieved from liquid nitrogen storage and kept on dry ice until prior to defrosting. Cells were quickly defrosted in a 37°C water bath and immediately resuspended

into 10mls of culture medium in a 15ml falcon tube and pelleted by centrifugation at 1100rpm for 3 minutes. The pellet was then resuspended in 7mls of culture medium and cultured in T25 flasks.

2.9.4 Collection of cells for RNA extraction

For RNA extraction, media from confluent T25 flasks of cells was removed and cells were washed twice with sterile 1X PBS (Invitrogen). 5mls of PBS was then added to each flask and cells were scraped off the surface of the plate with a cell scraper (Nunc). The cell solution was then transferred into a clean 15ml falcon tube and cells were pelleted by centrifugation at 1100rpm for 3 minutes. The supernatant was discarded and the pellet was immediately snap frozen in liquid nitrogen and stored at -80°C.

2.9.5 Cell Titer Blue cell viability assay

To assess the anti-cancer activity of BVDU ProTides in MCF7 and MCFTDX cell lines, the Cell Titer Blue cell viability assay was used. T25 flasks of 50% confluent MCF7 and MCFTDX cells were incubated with 0.05% trypsin-EDTA (Invitrogen) to detach cells as previously described. Cells were then transferred into clean 15ml falcon tubes and pelleted by centrifugation at 1100rpm for 3 minutes. The pellet was resuspended in 1ml of culture media and dissociated to ensure a single cell suspension was achieved. Cells were then counted utilising a haemocytometer cell counting chamber (Thermo Scientific) three times, and the average calculated. The total number of cells per ml could then be calculated by multiplying the average number of cells per square by 10^4 . Both MCF7 and MCFTDX cells were then seeded at a density of 5000 cells per 100 μ l into flat bottomed clear 96 well plates (Corning Ltd).

After 24 hours at 37°C with 5% CO₂, cells were treated with decreasing concentrations of individual ProTide compounds (using an initial stock of 25mM in DMSO (Sigma Aldrich)) in 6 well repeats. Concentrations used ranged between 250 μ M and 0.25 μ M. DMSO only controls as well as equivalent Thymectacin and BVDU concentrations were used to compare each ProTide compound tested. Cells were incubated with compounds for 72 hours at 37°C with 5% CO₂.

Following 72 hours of incubation, the viability of cells was determined using Cell Titer Blue (Promega), a reagent which allows measurement of cell metabolic activity. Viable cells which are metabolically active will have the ability to convert resazurin (the indicator dye used in this assay) into resofurin, a highly fluorescent product. Viability of cells is then determined by measuring fluorescent levels after incubation with the substrate. Prior to use, the Cell Titer Blue reagent was thawed at room temperature. Once thawed, 20 μ l was added per well and

incubated at 37°C with 5% CO₂ for 1 hour. The fluorescence was then measured at the excitation/emission wavelength of 560/590nm on a Flurostar Optima plate reader (BMG Labtech). The percentage of viable cells was then calculated relative to DMSO controls and plotted against concentration to determine the half maximal Inhibition Concentration (IC₅₀).

2.9.6 Colony forming assay

For colony forming assays, MCF7 and MCFTDX cells were detached and dissociated from T25 flasks as previously described in section 2.9.2 and seeded in clear, flat bottomed 6 well plates at a density of 6000 cells per well. After 24 hours at 37°C with 5% CO₂, cells were treated in duplicates with decreasing concentrations of ProTides, Thymectacin or DMSO controls. Concentrations used ranged from 150µM to 5µM. Cells were incubated with drugs for 72 hours at 37°C with 5% CO₂ after which fresh culture media was added and subsequently changed every 3 days. Colonies were left to grow for 14 days after which they were fixed with a 1:1 methanol:acetone solution for a few seconds. Cells were then air dried, rinsed with distilled water and finally stained with Giemsa Stain (Sigma Aldrich) diluted 1/10 in distilled H₂O for 1 minute. Excess stain was rinsed off with distilled water and allowed to dry.

2.10 RNA extraction and Gene expression analysis

2.10.1 RNA isolation and quantification

RNA was isolated from MCF7 and MCF7-TDX cell lysates (preparation detailed in section 2.9.4) as well as normal intestine and tumour tissue snap frozen in liquid nitrogen during dissection. The samples were stored at -80°C prior to RNA extraction

2.10.2 Homogenisation of cells

Cell lysates were added to 1ml Trizol (Invitrogen) in homogenising lysing matrix D tubes (MP Biomedicals). Normal small intestine and tumours were removed from storage and placed on dry ice to prevent defrosting. Whilst still frozen, tissue was carefully placed in 1ml Trizol in homogenising lysing matrix D tubes (MP Biomedicals). The samples were all homogenised from frozen using a Precellys 24 homogeniser (Bertin Technologies) at 6000 RPM for 2 cycles of 45 seconds.

2.10.3 RNA extraction and purification

All samples were kept on ice during RNA isolation. After homogenisation, the solution was centrifuged at 10 000 x g for 10 minutes to pellet insoluble material. The supernatant was then transferred to RNase/DNase free 1.5ml microcentrifuge tubes before adding 200µl of chloroform to each sample. The samples were shaken vigorously by hand before being incubated at room temperature for 3 minutes. The samples were then centrifuged at 10 000 x g for 15 minutes 4°C to separate the aqueous phase from the organic phase. 400µl of the aqueous phase was transferred to clean microcentrifuge tubes and an equal volume of isopropanol was added and mixed to precipitate the RNA. The RNeasy Minikit (Qiagen) was then used to isolate and purify the RNA. The RNA containing solution was added to RNeasy mini spin columns and centrifuged at 10 000 x g for 30 seconds at 4°C and the filtrate discarded. The RNA in the column was consecutively washed by adding 500µl RPE buffer containing ethanol (RNeasy Mini kit, Qiagen) once at 10 000 x g for 30 seconds at 4°C and filtrate discarded, and again at 10 000 x g for 2 minutes at 4°C and filtrate discarded. The column was centrifuged without RPE buffer at 10 000 x g for 1 minute at 4°C to ensure elimination of wash buffer. The column was then incubated with 50µl of RNase-free H₂O (RNeasy Mini kit, Qiagen) for 3 minutes on ice, placed in clean RNase/DNase free 1.5ml microcentrifuge tubes and centrifuged at 10 000 x g for 1 minute at 4°C to elute the RNA. The RNA was finally quantified in a 1µl sample using a NanoDrop 1000 (Thermo Scientific), and treated to eliminate from DNase contamination.

2.10.4 DNase treatment

The TURBO DNA-free kit (Applied Biosystems) was used to eliminate DNase contamination from the RNA sample. 0.1 volume 10X Turbo DNase buffer and 1µl Turbo DNase was added to the RNA sample, gently mixed and incubated at 37°C for 20-30 minutes. 0.1 volume DNase Inactivation Reagent was added to the RNA samples and incubated for 5 minutes at room temperature with occasional mixing. The samples were then centrifuged at 10 000 X g for 1.5 minutes, the supernatant transferred to a clean eppendorf and the RNA concentration quantified again in a 1µl sample using a NanoDrop 1000 (Thermo Scientific).

2.10.5 cDNA synthesis

cDNA was synthesised from 1µg of RNA using Superscript II reverse transcriptase (Invitrogen). First, random hexamers (Promega) were annealed to the RNA. For this, 1µg of RNA was pipetted into strip tubes (Greiner Bio-One), 5µl of random hexamers (Promega) was added to each sample and the volume was made up to 20µl with RNase free dH₂O. The samples were

incubated in a PTC-100 Thermocycler (MJ Research) at 70°C for 10 minutes followed by 25°C for 10 minutes. The samples were then held at 4°C whilst a further 20µl of reverse transcriptase enzyme mix was added to each sample (outlined in table 2.11). Reverse transcription was carried out under the following conditions: 25°C for 10 minutes, 37°C for 45 minutes, 42°C for 45 minutes and finally 70°C for 15 minutes. After completion of cDNA synthesis, 160µl of RNase free dH₂O was added to each sample to dilute the cDNA.

Q-PCR enzyme mix (per sample)	
5X first strand buffer	8µl
DDT	4µl
dNTPs	0.8µl
Superscript II	1µl
Ultrapure double deionised H ₂ O	6.2µl

Table 2.11 Recipe for qRT-PCR mix

2.10.6 Design of quantitative real-time (qRT) PCR primers

Primer sets for qRT-PCR reactions were designed across exon boundaries to avoid amplification of genomic DNA and designed to ensure a resulting product between 100-200 bp in size. The Primer3 web-based design program was used for this (<http://frodo.wi.mit.edu/>), checked using the BLAST engine against the Ensembl database (<http://www.ensembl.org/Multi/blastview>) for mis-priming and subsequently synthesised by Sigma Genosys. Primer sequences used can be found in Table 2.10.

Gene	Forward Primer Sequence	Reverse Primer Sequence	Product size
β-actin	TGTTACCAACTGGGACGACA	GGGGTGTGAAGGTC TCAA	166
thymidylate synthase	ATCATCATGTGTGCCTGGAA	GCATAGCTGGCAATGTTGAA	164

Table 2-11 Outline of primer sequences used for qRT-PCR analysis

2.10.7 Syber green gene expression analysis

All qRT-PCR reactions were run on the StepOnePlus real-time PCR system. Each reaction was performed in triplicate, with a minimum of three biological replicates and samples devoid of cDNA controls were used to ensure no contaminants of genomic DNA were present in cDNA samples. Typically, the housekeeping gene β -actin was simultaneously run during each experiment as the reference gene.

Reactions were run utilising the DyNAmo HS SYBR Green qPCR kit (Finnzymes) according to manufacturer's instructions. For this, equal quantities of forward and reverse primers were mixed (10mM final concentration per reaction). For all reactions, 4 μ l of cDNA was loaded per well into a thin wall 96 well PCR plate (Applied Biosystems) and 16 μ l of master mix containing both primers, was subsequently added. Plates were sealed using optically clear sealing film (Applied Biosystems), centrifuged and run using the following cycling conditions: 95°C for 10 minutes, followed by 40 cycles of 95°C for 15 seconds, 60°C for 30 seconds, 72°C for 30 seconds. To ensure a single product was amplified, a melt curve was run after cycling from 60°C to 95°C with a 0.3°C increment.

2.10.8 Analysis of qRT-PCR data

The data from each qRT-PCR run was automatically collected using StepOne software (Applied Biosystems). The data was examined prior to analysis to ensure amplification of one fluorescent product, the fluorescence vs cycle plots for each triplicate were comparable and there was no fluorescent product in the (no) cDNA controls. Differences between target gene expression between each cohort was assessed by comparing the changes in the number of cycles required for the fluorescent product to reach exponential phase, i.e. the higher the abundance of target gene, the lower the cycles required for the level of fluorescence to reach the exponential phase. Fluorescence vs. cycle number plots were generated and the threshold for the exponential phase was set automatically by software. Cycle times (C_T) and differences in cycle times (ΔC_T) values were calculated and normalised to β -actin control values. The $\Delta\Delta C_T$ was then calculated for each experimental sample (normalised to the average of control groups). Subsequently fold change differences were calculated using the equation $2^{(-x)}$ whereby x represents the $\Delta\Delta C_T$ values.

2.11 Data Analysis and Statistical analysis

2.11.1 Mann Whitney U test

The Mann Whitney U two-tailed test was conducted to detect statistical differences between most non-parametric data sets and was conducted using Minitab statistics package. A significant difference between data sets was accepted given p values were less than or equal to (\leq) 0.05. For analysis of acute drug time points, analysis was conducted on individual tumours, at least 4 tumours from 3 or more mice, whereas for chronic treatment analyses, n denotes the number of mice per cohort. To detect statistical differences between densitometry analyses, the Mann Whitney U one-tailed test was utilised as only three data points were available. A significant difference between data sets was accepted given p values were less than or equal to (\leq) 0.05.

2.11.2 Kaplan Meier survival analysis

Survival curves were generated using SPSS statistical software. Statistical analysis was conducted using Minitab statistics package using the Log-Rank method and the wilcoxon test for significance. A significant difference between data sets was accepted given p values \leq 0.05.

3 *Evaluating MEK and PI3K/mTOR inhibition in the Wnt activated, Apc^{f/+} tumour model*

3.1 *Introduction*

Mutations in the *APC* gene which encodes for the Adenomatous polyposis coli tumour suppressor protein is recognised as the key initial event in the development of sporadic CRC, with mutations occurring in up to 80% of cases (Wood et al., 2007). Furthermore, germline mutations in *APC* characterise Familial Adenomatous Polyposis (FAP), an autosomal syndrome characterised by hundreds of colorectal lesions (Kinzler and Vogelstein, 1996). *In vivo* models of *Apc* mutant CRC are therefore highly relevant and have proved particularly useful in characterising the role of other tumour suppressor proteins and oncogenes in tumourigenesis, as well as the effect of novel therapeutic strategies on tumour development. The models utilised for this include the multiple intestinal neoplasia (Min) or *Apc*^{min/+} mouse model, initially generated by random mutagenesis using N-ethyl-N-nitrosourea (ENU), this model carries a transversion at codon 850 causing truncation of one copy of the gene and requires loss of heterozygosity for development of benign intestinal lesions (Su et al., 1992). Additionally, other studies have used heterozygous deletion of the *Apc*^{580s} allele driven by intestinal specific AhCre or VillinCre recombinase transgene to mimic spontaneous tumour formation over a long latency (Sansom et al., 2006, Davies et al., *in press*, Janssen et al., 2006). Tumours which develop in these models are often benign adenomas as *Apc* mutations are associated with initiation of tumourigenesis and accumulation of further mutations are required for progression of disease (Fearon and Vogelstein, 1990). Nevertheless, these can be useful tools to investigate novel therapeutic strategies for the early disease setting.

Since its identification, aberrant activation of the Epidermal growth factor receptor (EGFR) has been associated with numerous cancer phenotypes including cellular proliferation, migration, metastasis, angiogenesis as well as escape from apoptosis (Gschwind et al., 2004). Binding of ligands to the extracellular receptor domain leads to activation of internal tyrosine kinase domains, which following a number of autophosphorylations at tyrosine residues, serve as binding sites for several adaptor proteins (Zhang et al., 2006). This includes GRB2, which leads to activation of RAS-RAF-ERK signalling and p85 which together with p110, activates PI3K/AKT signalling (Hynes and Lane, 2005). The observation that EGFR is often overexpressed in CRC warranted investigation of its therapeutic targeting in CRC (Resnick et al., 2004). Despite the

availability of numerous EGFR antagonists including cetuximab and panitumumab, and exhaustive investigation of these for therapeutic intervention, patients with CRC often display no or modest benefits, and subsequently develop resistance to treatment through up-regulation of MAPK or PI3K signalling (Benvenuti et al., 2007, Di Nicolantonio et al., 2008). Furthermore, extensive retrospective analyses have identified mutations in *KRAS*, *B-RAF* and those activating the PI3K pathway such as *PTEN*, to predict non-response to anti-EGFR therapies (Lièvre et al., 2008, Frattini et al., 2007, Perrone et al., 2009, Bardelli and Siena, 2010). Given these findings, targeting of MAPK and PI3K signalling downstream the pathway appears a more rational therapeutic strategy for wild-type tumours.

In this chapter, I aimed to investigate the therapeutic potential of MAPK and PI3K inhibition in a mouse model of CRC mutant for the tumour suppressor protein *Apc*¹. Here, heterozygous deletion of *Apc* is driven by the VillinCreER transgene and results in small intestinal and colonic tumours over a long latency. To antagonise the MAPK and PI3K pathways, I used the MEK1/2 inhibitor MEK162 and the dual PI3K/mTOR inhibitor NVP-BEZ235, respectively (both provided by Novartis Pharmaceuticals). For these investigations, I employed two main strategies. Firstly, tumour bearing VillinCreER *Apc*^{f/+} (referred to as *Apc*^{f/+} here forth) mice were administered a single dose of MEK162 or NVP-BEZ235 and harvested 4 hours later to evaluate the immediate pharmacodynamic and anti-tumour effects. Secondly, to evaluate the therapeutic potential of each treatment, *Apc*^{f/+} mice were continuously administered treatment, from a chosen time point post induction until a survival end point (i.e when mice were symptomatic of disease) or the experimental end point of 500 days post induction. These later experiments were conducted to investigate the effect of treatment on survival of mice as well as tumour burden.

Additionally in this chapter, I assessed activation status of MAPK and PI3K signalling in other transgenic mouse models of CRC mutant for the oncogene *Kras* and the tumour suppressor protein *Pten*, which are crucial for mediating MAPK and PI3K signalling respectively.

3.2 Results

3.2.1 *Mek inhibitor MEK162 elicits no anti-tumour effect on *Apc*^{f/+} colon polyps however, in small intestinal tumours increases proliferation and apoptosis*

To investigate the immediate anti-tumour and pharmacodynamic effects of MEK162 in *Apc*^{f/+} tumours, 10 week old *Apc*^{f/+} mice were induced and monitored until symptomatic of disease (pale feet, bloating, blood in faeces, etc.). Mice were then administered a single dose of either

¹ Some data analysis presented in this chapter was conducted by Tanya Davies under my supervision

0.5% Methylcellulose (MC, Vehicle) or 30mg/kg MEK162 and harvested 4 hours later. Additionally, an excessive dose of BrdU was administered 2 hours prior to culling to label cells in S phase of the cell cycle. Dissection was conducted as previously described (methods section 2.4.2) whereby the intestines were rolled into 'swiss-roll' like structures and quick fixed in formalin, in preparation for H&E staining and IHC.

Following exposure to a single dose of MEK162, the immediate anti-tumour effects were first evaluated through scoring of histological mitosis and apoptosis from H&E stained sections of $Apc^{f/+}$ colonic and small intestinal tumours (SITs). Scoring of mitotic figures in colon tumours and SITs revealed no significant alterations in MEK162 treated cohorts in comparison with vehicle controls (veh colon = 0.22 ± 0.11 , MEK162 colon = 0.19 ± 0.12 , p value = 0.583, veh SIT = 0.18 ± 0.064 , MEK162 SIT = 0.26 ± 0.15 , p value = 0.298, $n \geq 4$ tumours, 3 mice, Mann Whitney U test) (Figure 3.1 A). Additionally, quantification of apoptotic bodies in colon polyps and SITs revealed no significant alterations in MEK162 treated samples (veh colon = 0.77 ± 0.31 , MEK162 colon = 0.72 ± 0.32 , p value = 0.815, veh SIT = 0.32 ± 0.25 , MEK162 SIT = 0.34 ± 0.27 , p value = 0.930 $n \geq 4$ tumours, 3 mice, Mann Whitney U test) (Figure 3.1 B) indicating no immediate anti-tumour effects.

To further evaluate the immediate effects of MEK162 in $Apc^{f/+}$ tumours, IHC for BrdU and cleaved caspase 3 were carried out and scored. Quantification of BrdU positive cells revealed no significant alterations in colon polyps or SITs, in keeping with scoring of mitosis (veh colon = 16.1 ± 7.1 , MEK162 colon = 17.3 ± 5.9 , p value = 0.954, veh SIT = 24.5 ± 16.1 , MEK162 SIT = 21.8 ± 10.9 , p value = 0.911, $n \geq 4$ tumours, 3 mice, Mann Whitney U test) (Figure 3.2 A). Scoring of cleaved caspase 3 staining also revealed no significant alterations in colon polyps, in corroboration with previous scoring of histological apoptosis, however did reveal a significant increase in cleaved caspase 3 staining in SITs 4 hours post exposure to MEK162 (veh colon = 0.47 ± 0.38 , MEK162 colon = 0.31 ± 0.33 , p value = 0.378, veh SIT = 0.89 ± 0.59 , MEK162 SIT = 2.42 ± 1.54 , p value = 0.034, $n \geq 4$ tumours, 3 mice, Mann Whitney U test) (Figure 3.2 B).

In summary, the above observations indicate that MEK162 had no significant anti-tumour effect on $Apc^{f/+}$ colon tumours at the 4 hour time point investigated as no alterations in proliferation or apoptosis were detected. $Apc^{f/+}$ SITs appeared moderately sensitive to MEK162 as a significant pro-apoptotic effect was detected 4 hours post exposure, indicating some favourable anti-tumour effects.

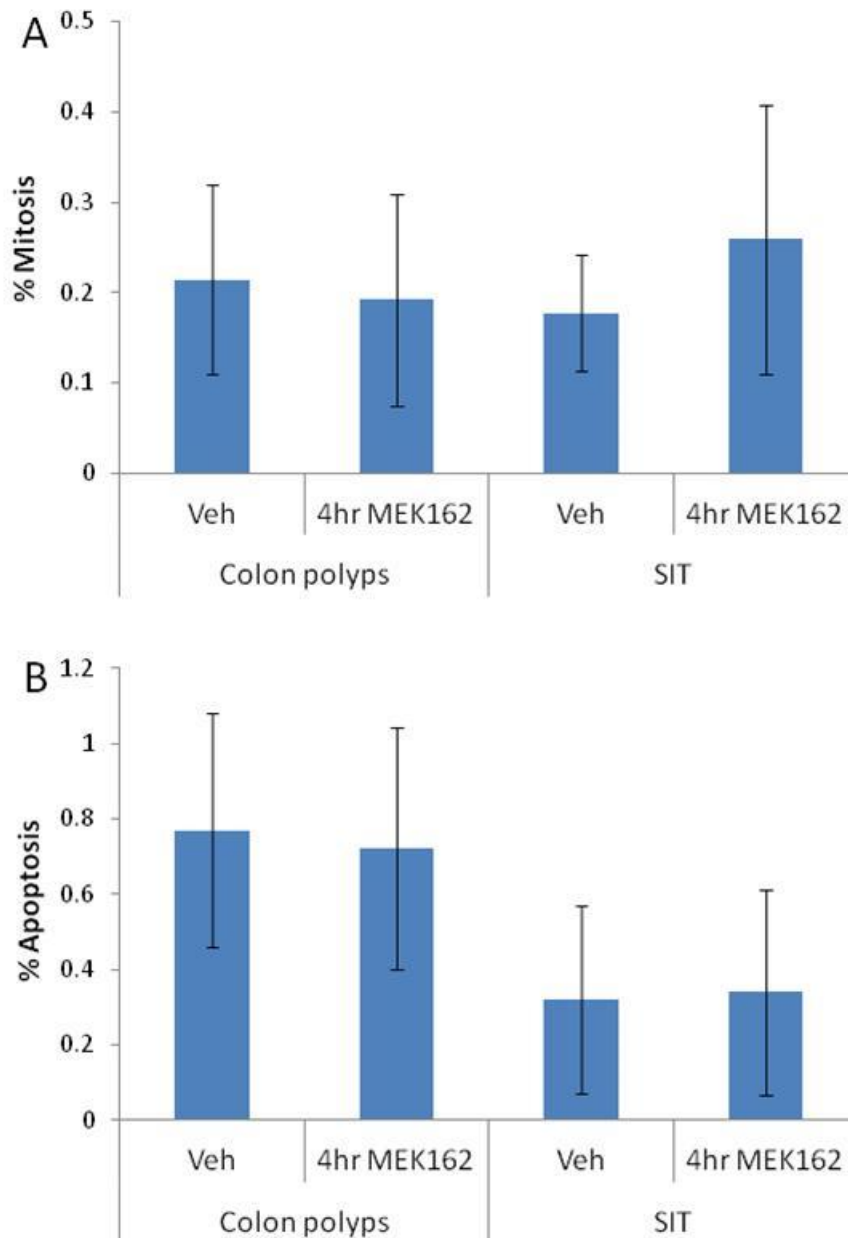


Figure 3.1 The anti-tumour effects of MEK162, characterised by scoring of histological mitosis and apoptosis in $Apc^{f/+}$ colon polyps and small intestine tumours (SITs), 4 hours post exposure

Scoring of mitotic figures **(A)** and apoptotic bodies **(B)** revealed a single dose of 30mg/kg MEK162 had no effect on colon polyps or SITs, although MEK162 led to a trend towards increased mitoses in SITs 4 hours after exposure. (p value ≥ 0.05 , $n \geq 4$ tumours, 3 mice, Mann Whitney U test). Error bars represent standard deviation

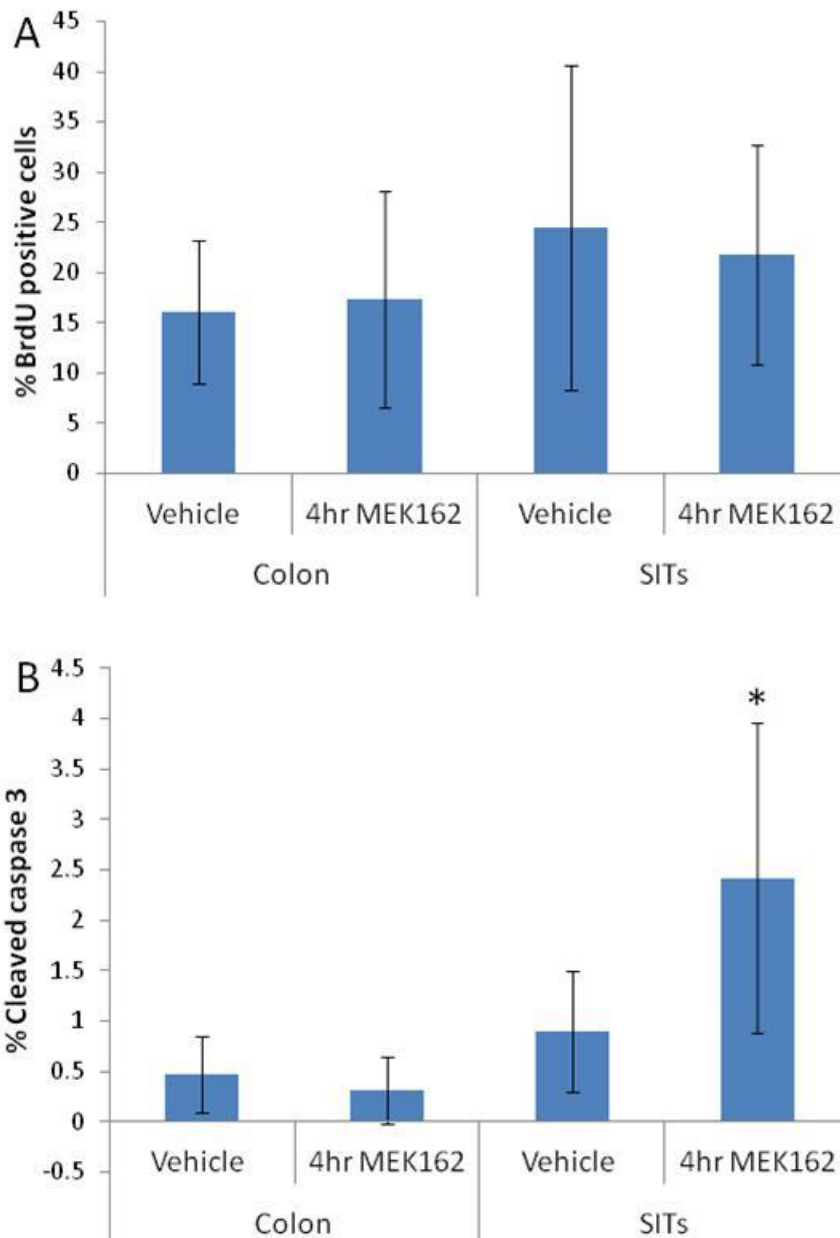


Figure 3.2 MEK162 has no effect on BrdU positive cells in $Apc^{f/+}$ colon polyps or small intestine tumours (SITs) but increased cleaved caspase 3 in SITs only

Quantification of IHC for BrdU and cleaved caspase 3 revealed a single dose of MEK162 at 30mg/kg had no effect on BrdU positive cells in colon polyps or SITs. Additionally, MEK162 had no effect on cleaved caspase 3 scoring in colon polyps, but did significantly increase cleaved caspase 3 levels in SITs 4 hours post exposure (*p value ≤ 0.05 , $n \geq 4$ tumours, 3 mice, Mann Whitney U test). Error bars represent standard deviation.

3.2.2 MEK162 reduces MAPK signalling through pERK and also reduces PI3K signalling

To investigate whether MEK162 lead to inhibition of MAPK signalling in *Apc^{f/+}* tumours, IHC against the phosphorylated and hence activated form of the MAPK effector protein ERK was carried out (Figure 3.3, 3.4). Immunostaining revealed a reduction in nuclear staining of pERK in colon polyps post exposure to MEK162 and a reduction in nuclear and cytoplasmic pERK staining in SITs, in comparison with vehicle treated tumours. These findings suggest that exposure to MEK162 for 4 hours is sufficient to inhibit MAPK signalling through pERK in *Apc^{f/+}* tumours and specifically in SITs, this may translate to biological activity, as an increase in apoptosis by cleaved caspase 3 staining was detected.

Given the close association and convergence between MAPK signalling through RAS-RAF-ERK and PI3K signalling through AKT and mTOR (Ma et al., 2007, Ma et al., 2005), the effects of MEK inhibition on the PI3K pathway was also assessed to determine whether this resulted in compensatory activation of PI3K signalling. For this, immunostaining of the phosphorylated form of AKT (pAKT) the PI3K signalling effector, and phosphorylated S6-ribosomal protein (pS6RP) which transduces signals downstream of mTOR were carried out (Figure 3.3, 3.4). Surprisingly, a reduction in membrane and cytoplasmic pAKT staining (Ser473) as well as a marked reduction in membrane, cytoplasmic and nuclear staining of pS6RP was observed in MEK162 treated colon polyps, indicating inhibition of PI3K signalling. Interestingly, a reduction in the cytoplasmic and nuclear staining of pAKT was also detected in SITs, however no alterations in pS6RP immunostaining were detected here. These observations again reflect differential sensitivities of colon polyps and SITs to MEK162; however surprisingly suggest activation of mechanisms to also inhibit PI3K signalling.

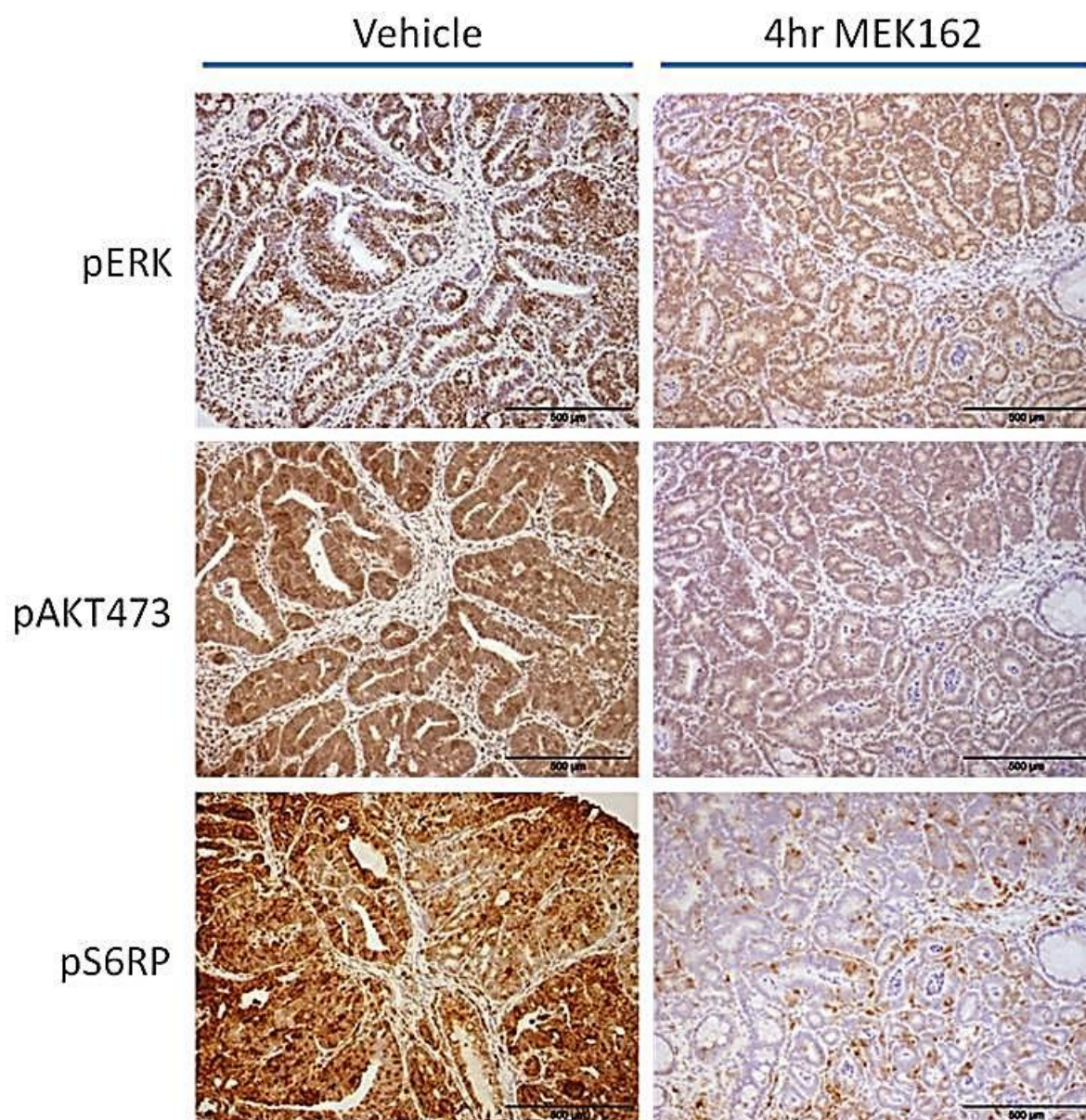


Figure 3.3 IHC reveals MEK162 reduces MAPK and PI3K signalling in colon polyps 4 hours post exposure

IHC for pERK, pAKT at Ser473 and pS6RP was carried out in MEK162 treated and control colon polyp samples. A reduction in nuclear and cytoplasmic pERK immunostaining reveals inhibition of MAPK signalling downstream MEK. Additionally, Immunostaining for pAKT473 and pS6RP appears reduced indicating inhibition of parallel PI3K/mTOR signalling pathway.

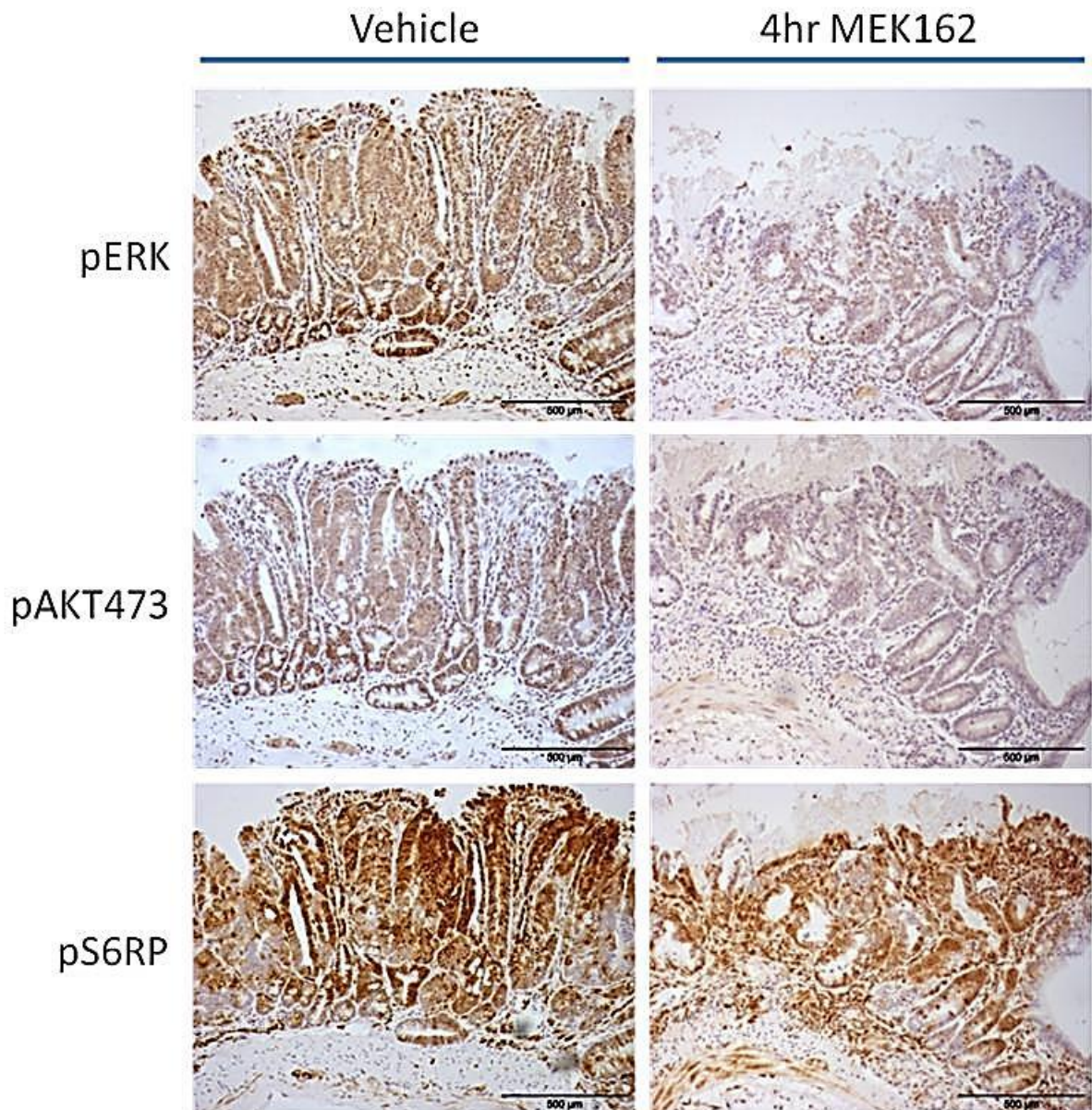


Figure 3.4 IHC for pERK, pAKT473 and pS6RP in small intestinal tumours (SITs) 4 hrs following a single dose of MEK162

Immunostaining for pERK in SITs following a single dose of 30mg/kg MEK162 reveals reduced levels of cytoplasmic and nuclear pERK, indicating inhibition of MAPK signalling. IHC showed reduced immunostaining for pAKT at Ser473 but not for pS6RP indicating partial PI3K pathway inhibition.

3.2.3 Continuous MEK162 treatment increases longevity of $Apc^{f/+}$ mice

To further evaluate the therapeutic potential of MEK162 in $Apc^{f/+}$ mice, a long term treatment experiment was undertaken in tumour bearing mice to determine the effect of treatment on overall survival and tumour burden of mice. For this, $Apc^{f/+}$ mice were induced and aged to allow for tumour development. Given the long tumour latency period in $Apc^{f/+}$ mice (Figure 3.5), 220 days post induction was chosen as an appropriate intervention start point. At this point, mice were randomly selected to either receive 30mg/kg MEK162 twice-daily (n=10 mice) or 0.5% MC twice daily (n=5 mice) by oral gavage. To increase the number of mice in the control cohort, untreated mice which were monitored until symptomatic of disease and subsequently administered a short term dose of treatment were also used for survival analyses. Mice were treated daily until a survival end point (anaemia, bloating and $\geq 10\%$ loss of body weight) or the experimental end point of 500 days post induction.

Continuous daily treatment of MEK162 in $Apc^{f/+}$ mice was found to be well tolerated and significantly increased longevity of mice (median survival of MEK162 mice = 401 vs vehicle = 270, p value = 0.011 Log-Rank and p value = 0.007 Wilcoxon test, $n \geq 9$ per cohort) (Figure 3.5). This indicates that whilst MEK162 in the immediate setting displayed only modest anti-tumour activity, chronic administration is beneficial in $Apc^{f/+}$ tumour bearing mice. Further evaluation of tumour burden following MEK162 treatment is described in section 3.2.7.

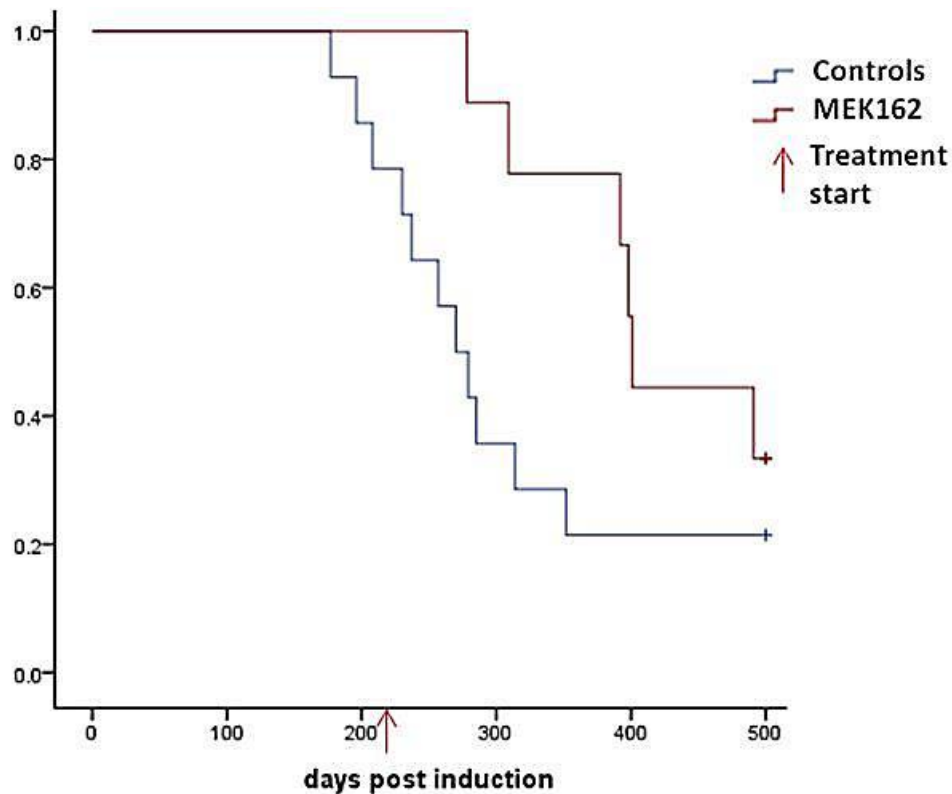


Figure 3.5 Kaplan Meier survival analysis of $Apc^{f/+}$ mice on twice daily 30mg/kg MEK162 and vehicle controls from 220 days post induction

$Apc^{f/+}$ mice were induced and aged to 220 days post induction, at which point mice were randomised to receive either 0.5% Methyl cellulose (or remained untreated, controls) or 30mg/kg MEK162 twice daily by oral gavage, either until a survival end point or an experimental end point of 500 days post induction. Continuous MEK162 treatment was found to significantly increase median survival of mice from 270 days post induction to 401 days post induction (p value ≤ 0.001 , $n \geq 8$ mice per cohort, Log-Rank and Wilcoxon test).

3.2.4 The acute effects of NVP-BEZ235 in $Apc^{f/+}$ colon polyps and SITs

As described previously, EGFR mediates growth signals not only through the MAPK signalling cascade, but also through PI3K/AKT/mTOR signalling. To elucidate the therapeutic potential of inhibiting the later signalling pathway in $Apc^{f/+}$ tumours, the biological effects of the dual PI3K/mTOR inhibitor NVP-BEZ235 were first evaluated in a short term setting. Similarly to section 3.2.1, $Apc^{f/+}$ mice were induced and aged to allowed for symptoms of tumour burden to develop, at which point they received a single dose of 35mg/kg NVP-BEZ235 and were culled 4 hours after, as previously described methods 2.4.2. Additionally, a dose of BrdU was administered 2 hours prior to culling to label cells in S phase of the cell cycle. Vehicle controls for this experiment are identical to those used previously in section 3.2.1.

The immediate anti-tumour activity of NVP-BEZ235 in $Apc^{f/+}$ mice was initially evaluated by examination of H&E stained sections of colon polyps and SITs for histological mitosis and apoptosis. Quantification of mitotic figures in $Apc^{f/+}$ colon polyps revealed no significant alterations 4 hours post exposure to NVP-BEZ235 (veh colon = 0.22 ± 0.11 , NVP-BEZ235 colon = 0.21 ± 0.10 , p value = 0.866, $n \geq 4$ tumours, 3 mice Mann Whitney U test) (Figure 3.6 A). Similarly, no significant effect on mitosis was detected in SITs following NVP-BEZ235 (veh SIT = 0.18 ± 0.064 , NVP-BEZ235 SIT = 0.23 ± 0.17 , p value = 0.621, $n \geq 4$ tumours, 3 mice Mann Whitney U test) (Figure 3.6 A). Scoring of histological apoptosis revealed no statistical differences, although a trend towards reduced apoptosis in colon polyps exposed to NVP-BEZ235 compared to vehicle controls was observed (veh colon = 0.77 ± 0.31 , NVP-BEZ235 colon = 0.57 ± 0.35 , p value = 0.0585, $n \geq 4$ tumours, 3 mice, Mann Whitney U test) (Figure 3.6 B). In contrast however, a significant increase in apoptosis was observed in SITs 4 hours post exposure to NVP-BEZ235, indicating anti-tumour activity in $Apc^{f/+}$ mice (veh SIT = 0.32 ± 0.25 , NVP-BEZ235 SIT = 0.55 ± 0.4 , p value = 0.0307, $n \geq 4$ tumours, 3 mice, Mann Whitney U test) (Figure 3.6 B).

Additionally to scoring of histological mitosis and apoptosis, IHC against the proliferation marker BrdU and the apoptosis marker cleaved caspase 3 were carried out and quantified to further characterise the anti-tumour activity of NVP-BEZ235 in $Apc^{f/+}$ tumours. Scoring of BrdU positive cells revealed no significant alterations in colon polyps or SITs exposed to NVP-BEZ235 in comparison to vehicle treated tumours, supporting mitosis scoring (veh colon = 16.1 ± 7.1 , NVP-BEZ235 colon = 17.0 ± 5.9 , p value = 0.493, veh SIT = 24.5 ± 16.1 , NVP-BEZ235 SIT = 22.9 ± 8.5 , p value = 0.609, $n \geq 4$ tumours, 3 mice Mann Whitney U test) (Figure 3.7 A). Scoring of cleaved caspase 3 staining in colon polyps exposed to NVP-BEZ235 also revealed no significant

alterations (veh colon = 0.47 ± 0.38 , NVP-BEZ235 colon = 0.38 ± 0.35 , p value = 0.178, $n \geq 4$ tumours, 3 mice, Mann Whitney U test) (Figure 3.7 B). Interestingly however, a significant reduction in the number of cleaved caspase 3 bodies was scored in SITs exposed to NVP-BEZ235 indicating an anti-apoptotic effect (veh SIT = 0.89 ± 0.59 , NVP-BEZ235 SIT = 0.44 ± 0.46 , p value = 0.0293, $n \geq 4$ tumours, 3 mice, Mann Whitney U test) (Figure 3.7 B).

In summary, characterisation of proliferation and cell death in $Apc^{f/+}$ tumours post exposure to NVP-BEZ235 revealed differences in sensitivities in colon polyps and SITs, as detected previously with MEK162 treatment. NVP-BEZ235 failed to induce any favourable anti-tumour effects in colon polyps at the 4 hour time point, but did induced both pro and anti-apoptotic effects in SITs. To further characterise the immediate effects of NVP-BEZ235, PI3K signalling was next evaluated post exposure to NVP-BEZ235, as described below.

3.2.5 NVP-BEZ235 preferentially reduces signalling downstream mTOR and not PI3K

To determine target inhibition in $Apc^{f/+}$ tumours following NVP-BEZ235 administration, IHC for pAKT at Ser473 and pS6RP were carried out to determine inhibition of signalling downstream PI3K and mTOR. Immunostaining of colon polyps exposed to NVP-BEZ235 revealed no obvious difference in pAKT473 staining however, a marked reduction in membrane, cytoplasmic and nuclear staining of pS6RP at the 4 hour time point (Figure 3.8). Interestingly, these observations were also notable in SITs, in comparison with vehicle treated tumours (Figure 3.9). Downstream of PI3K, mTOR exists in two complex forms - mTOR complex 1 (mTORC1) which controls regulation of pS6RP, and mTOR complex 2 (mTORC2) which regulates activation of pAKT at Ser473 (Jacinto et al., 2006). Observations here indicate that in $Apc^{f/+}$ NVP-BEZ235 may preferentially inhibit mTORC1 rather than mTORC2 in $Apc^{f/+}$ tumours.

Furthermore, to determine the effect of NVP-BEZ235 on closely associated MAPK signalling, IHC for pERK was carried out. Immunostaining for pERK in colon polyps and SITs revealed no obvious alterations indicating NVP-BEZ235 had no compensatory effects on MAPK signalling at the 4 hour time point investigated (Figure 3.8, 3.9).

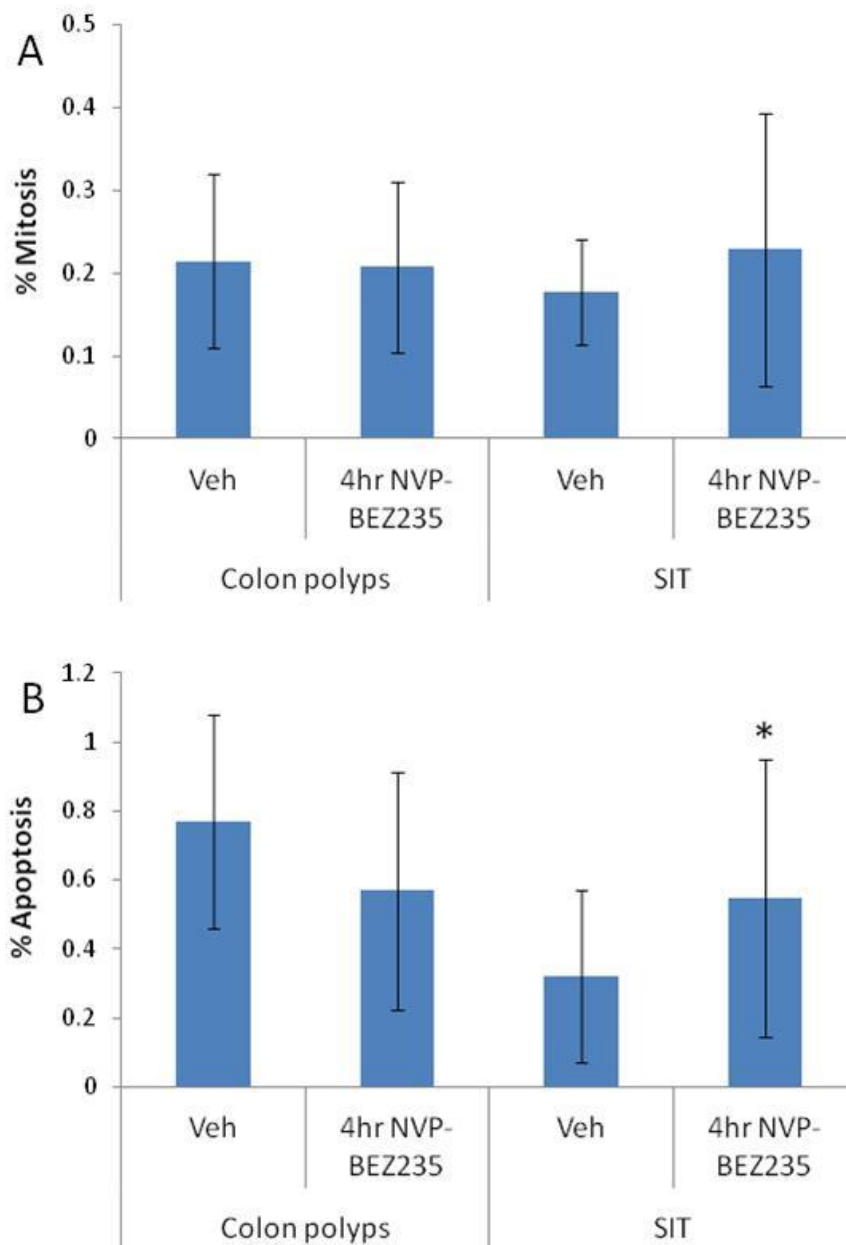


Figure 3.6 The anti-tumour effects of NVP-BEZ235, determined by scoring of histological mitosis and apoptosis in $Apc^{f/+}$ colon polyps and small intestine tumours (SITs) at a 4 hour time point following exposure

Scoring of mitotic figures **(A)** and apoptotic bodies **(B)** 4 hours following a single dose of 35mg/kg NVP-BEZ235 reveals no significant alterations in colon polyps or SITs however, did reveal a significant increase in apoptosis in SITs, in comparison with vehicle controls (*p value ≤ 0.05 , $n \geq 4$ tumours, 3 mice, Mann Whitney U test). Error bars represent standard deviation.

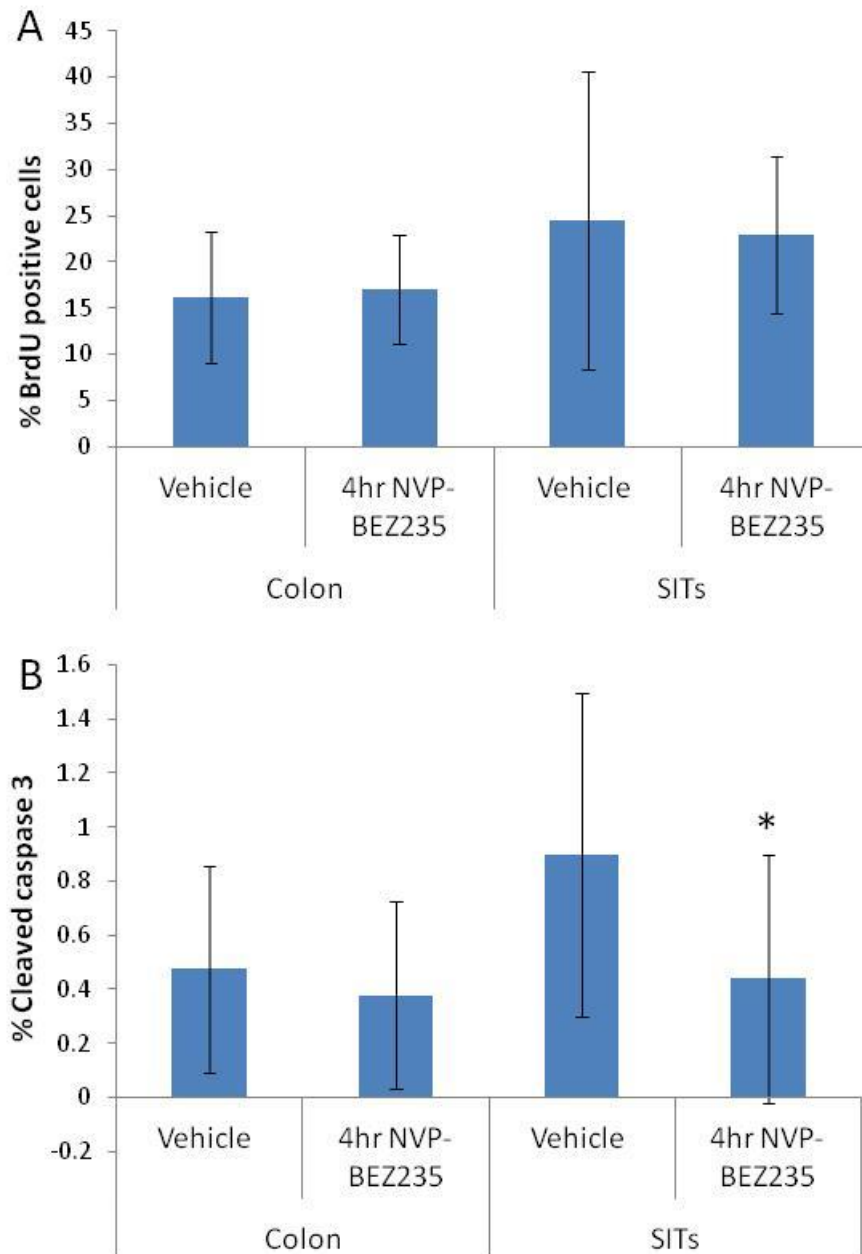


Figure 3.7 BrdU scoring revealed no significant alterations following NVP-BEZ235 treatment, cleaved caspase 3 scoring showed no significant differences in colon polyps but a significant reduction in small intestine tumours (SITs)

Scoring of IHC for BrdU positive cells **(A)** and cleaved caspase 3 staining **(B)** 4 hours following a single dose of 35mg/kg NVP-BEZ235 reveals no significant alterations in colon polyps. Similarly, no significant alterations were detected in SITs with BrdU scoring however, NVP-BEZ235 led to a significant reduction in cleaved caspase 3 staining (*p value ≤ 0.05 , $n \geq 4$ tumours, 3 mice, Mann Whitney U test). Error bars represent standard deviation.

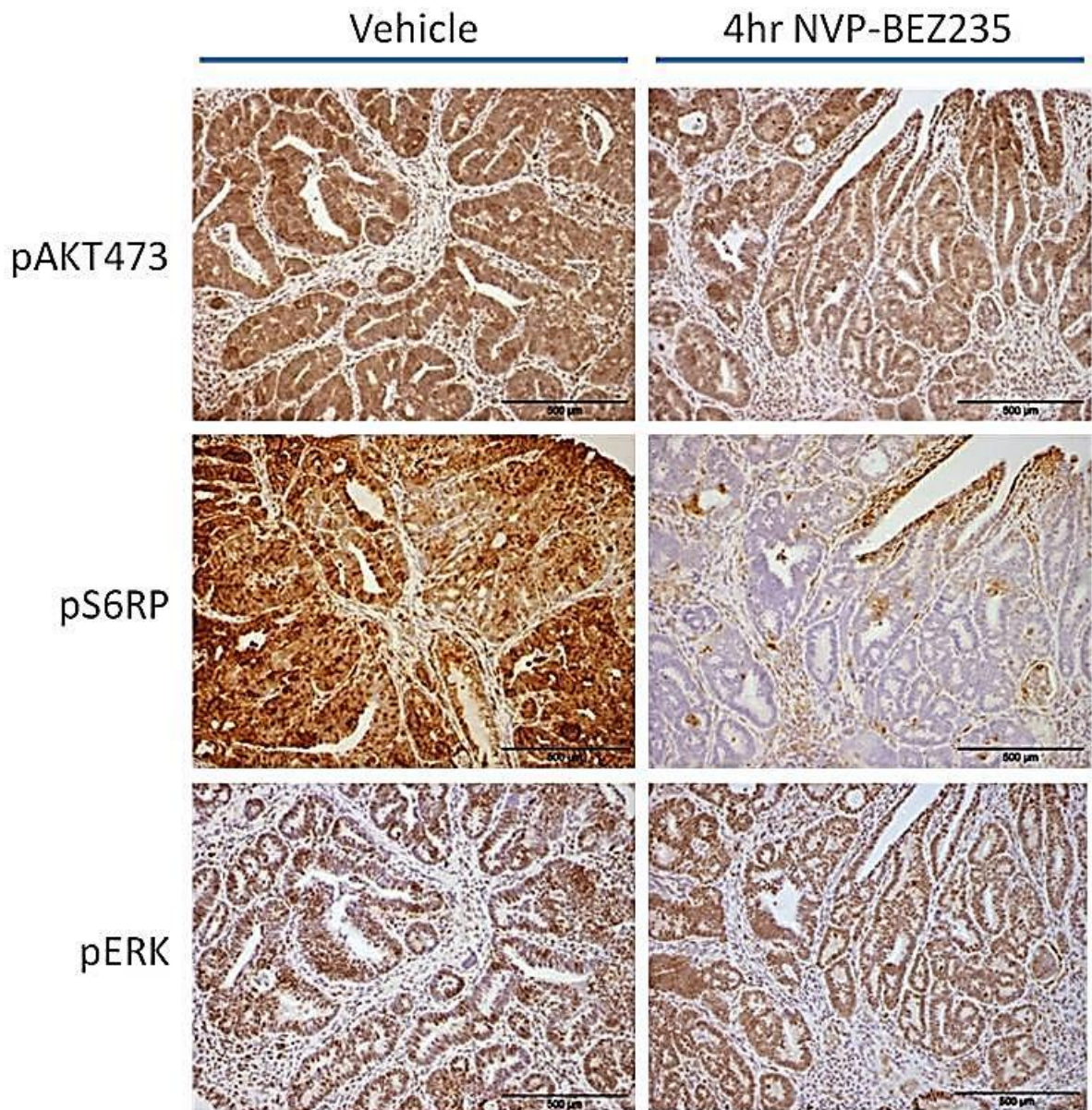


Figure 3.8 Immunostaining for PI3K pathway effectors reveals a reduction in levels of pS6RP only and no effect on MAPK signalling in colon polyps, in response to NVP-BEZ235

IHC for effectors of PI3K/mTOR signalling revealed no notable alterations in pAKT immunostaining at Ser473, however did reveal a reduction in pS6RP staining indicating inhibition downstream AKT signalling at mTORC1 in colon polyps, 4 hours following a single dose of 35mg/kg NVP-BEZ235. Additionally, IHC for pERK was conducted to detect changes in MAPK signalling but revealed no notable changes.

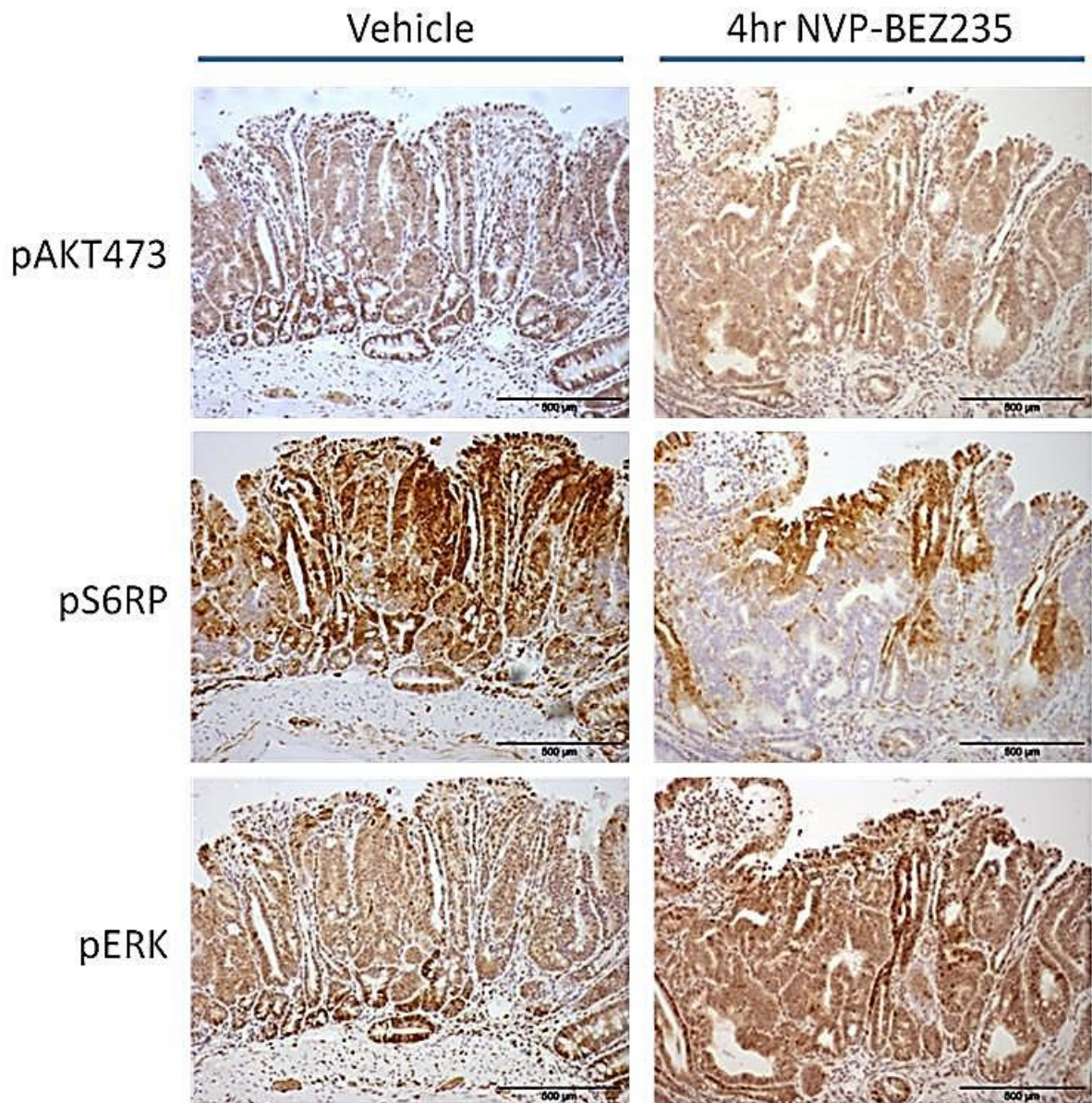


Figure 3.9 IHC for PI3K pathway and MAPK pathway effectors in small intestine tumours (SITs) 4 hours post exposure to NVP-BEZ235

Similar to $Apc^{f/+}$ colon polyps, immunostaining for pAKT at Ser473 revealed no notable differences in $Apc^{f/+}$ SITs exposed to a single dose of NVP-BEZ235 at 35mg/kg. Despite this, reduced pS6RP immunostaining was notable indicating inhibition of signalling downstream AKT in response to NVP-BEZ235. IHC for pERK revealed no alterations and hence no effect on MAPK signalling following NVP-BEZ235 exposure.

3.2.6 NVP-BEZ235 significantly increases survival of $Apc^{f/+}$ mice

Following from the short term evaluation of NVP-BEZ235 in $Apc^{f/+}$ mice, the effects of long term NVP-BEZ235 treatment were assessed through a chronic exposure experiment, similar to that in described section 3.2.3. This would examine the effects of continuous pathway inhibition on survival and tumour burden of $Apc^{f/+}$ mice. For this, a cohort of mice (n=10) were appropriately induced and aged to 220 days post induction from which point they received 35mg/kg NVP-BEZ235 twice daily by oral gavage until a survival end point (anaemia, bloating and $\geq 10\%$ loss of body weight) or until the experimental end point of 500 days post induction. Controls used for this experiment are those described previously in section 3.2.3.

Chronic NVP-BEZ235 administration was well tolerated (indicated by monitoring of body weight) by $Apc^{f/+}$ mice and Kaplan-Meier survival analysis revealed treatment significantly increased longevity of mice (median survival of NVP-BEZ235 treated mice = 371 vs vehicle = 270, $n \geq 10$ per cohort, p value = 0.018 for Log-Rank and p value = 0.049 for Wilcoxon test) (Figure 3.10). These findings indicate that chronic NVP-BEZ235 treatment is beneficial for $Apc^{f/+}$ mice, despite the lack of favourable anti-tumour activity detected from acute NVP-BEZ235 treatment. Interestingly, although the median survival of $Apc^{f/+}$ mice on MEK162 treatment is approximately 30 days longer than the NVP-BEZ235 cohort, this was not statistically more beneficial (median survival of NVP-BEZ235 mice = 371, MEK162 mice = 401, p value = 0.926 Log-Rank and p value = 0.534 Wilcoxon test), indicating equipotent effects. The effects of both chronic treatments on tumour burden at death are evaluated in section 3.2.7.

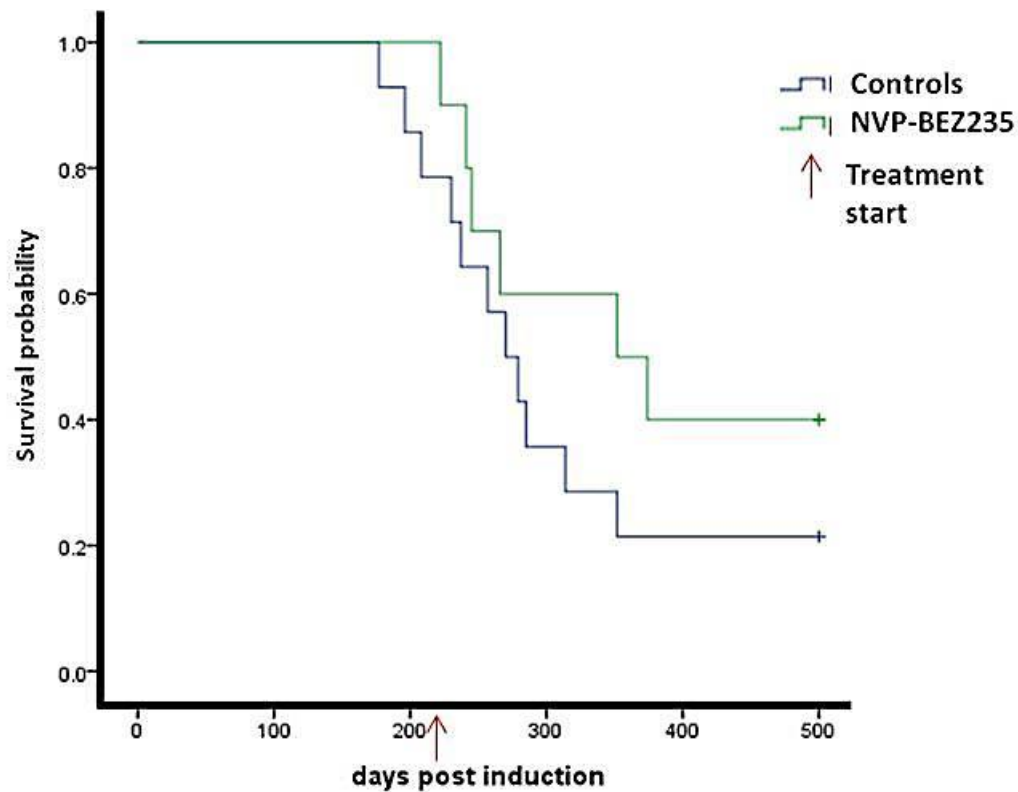


Figure 3.10 Kaplan Meier survival analysis of $Apc^{f/+}$ mice on twice daily 35mg/kg NVP-BEZ235 and vehicle controls from 220 days post induction

A cohort of 10 $Apc^{f/+}$ mice were induced and aged to 220 days post induction, at which point they received 35mg/kg NVP-BEZ235 twice daily by oral gavage either until a survival end point or the experimental end point of 500 days post induction. Continuous NVP-BEZ235 treatment was found to increase survival of mice from a median of 270 days post induction to 371 days post induction (p value ≤ 0.001 , $n \geq 8$ mice per cohort, Log-Rank and Wilcoxon test).

3.2.7 Analysis of tumour burden in *Apc^{f/+}* mice on various treatments

To investigate the effects of long term treatments on tumour burden, a number of parameters of tumour burden were assessed in comparison with the vehicle treated cohort. These parameters include the total number of tumours present at death, as scored from H&E stained sections of colon and small intestine tissues. For each sample, 3 H&E stained sections were scored and subsequently averaged per mouse, and then per cohort. Secondly, macroscopic tumours were measured from methacarn fixed colon and small intestine tissues and the total tumour area (mm²) was calculated per mouse in each cohort. Finally, tumours were staged according to severity and invasive features, as outlined previously in methods section 2.7.4, to determine whether treatment had any effect on tumour progression.

In the colon, neither MEK162 nor NVP-BEZ235 treatment significantly altered the total number of tumours present per mouse (median number of tumours: vehicle = 3, MEK162 = 3, p value = 0.784, NVP-BEZ235 = 3, p value = 0.947, n_≥4, Mann Whitney U test) (Figure 3.11 A). Additionally, both long term treatments had no significant effect on the total colon tumour area in *Apc^{f/+}* mice (median tumour area: vehicle = 71.5, MEK162 = 29.9, p value = 0.194, NVP-BEZ235 = 42.4, p value = 0.111, n_≥4, Mann Whitney U test) (Figure 3.11 B). Colon tumours were also staged according to severity and revealed presence of benign microadenoma or adenoma lesions only. Scoring here identified no significant alterations in the proportions of microadenomas and adenomas present in both MEK162 and NVP-BEZ235 treated cohorts (Proportion mAds: vehicle = 0.45, MEK162 = 0.69 p value = 0.055, NVP-BEZ235 = 0.47 p value = 0.316; proportion of Ads: vehicle = 0.55, MEK162 = 0.55 p value = 0.055, NVP-BEZ235 = 0.53 p value = 0.32, n_≥4, Mann Whitney U test) (Figure 3.11 C). Therefore, as analysis of colon tumour burden at the end of MEK162 and NVP-BEZ235 treatment revealed no significant differences in comparison with the vehicle treated cohort, it can be hypothesised that both treatments delay tumour growth given the increased survival of mice.

Analysis of tumours in the small intestine revealed both MEK162 and NVP-BEZ235 treatment also had no significant effect on the total number of small intestinal lesions present in *Apc^{f/+}* mice at death (median tumour number: vehicle = 3, MEK162 = 4, p value = 0.523, NVP-BEZ235 = 6, p value = 0.540, n_≥4, Mann Whitney U test) (Figure 3.12 A). Analysis of total small intestine tumour area revealed no significant difference with MEK162 treatment but interestingly, revealed a trend towards reduced tumour area in NVP-BEZ235 treated mice (median tumour area: vehicle = 51.1, MEK162 = 50.7, p value = 1.00, NVP-BEZ235 = 0.92, p value = 0.462) (Figure 3.12 A). The paradoxical trend for increased number of lesions but

reduced tumour size in NVP-BEZ235 treated mice may be explained by staging of tumour severity (Figure 3.12 C). This revealed a significant increase in the proportion of microadenomas present at death and a reduction in the proportion of adenomas (proportion of mAds: vehicle = 0.24, NVP-BEZ235 = 0.88 p value = 0.0085; proportion of Ads: vehicle = 0.47, NVP-BEZ235 = 0.08 p value = 0.0085; proportion of EIAs: vehicle = 0.24, NVP-BEZ235 = 0.02 p value = 0.35; proportion of AIAs: vehicle = 0.06, NVP-BEZ235 = 0.04 p value = 0.865, $n \geq 4$, Mann Whitney U test). As microadenomas are not visible macroscopically, this may explain the trends for increased number of lesions scored from H&E stained slides but the reduced overall SIT area in these mice. These later observations indicate that NVP-BEZ235 treatment may halt tumour progression in the small intestine of $Apc^{f/+}$ mice. Assessment of tumour severity in MEK162 treated $Apc^{f/+}$ mice revealed no statistically significant alterations however did indicate an increasing trend for more invasive lesions, in particular those characterised by invasion through the muscle wall of (mAds: vehicle = 0.24, MEK162 = 0.31 p value = 0.915; proportion of Ads: vehicle = 0.47, MEK162 = 0.36 p value = 0.3374; proportion of EIAs: vehicle = 0.24, MEK162 = 0.11 p value = 0.915; proportion of AIAs: vehicle = 0.06, MEK162 = 0.21 p value = 0.393, $n \geq 4$, Mann Whitney U test) (Figure 3.12 C).

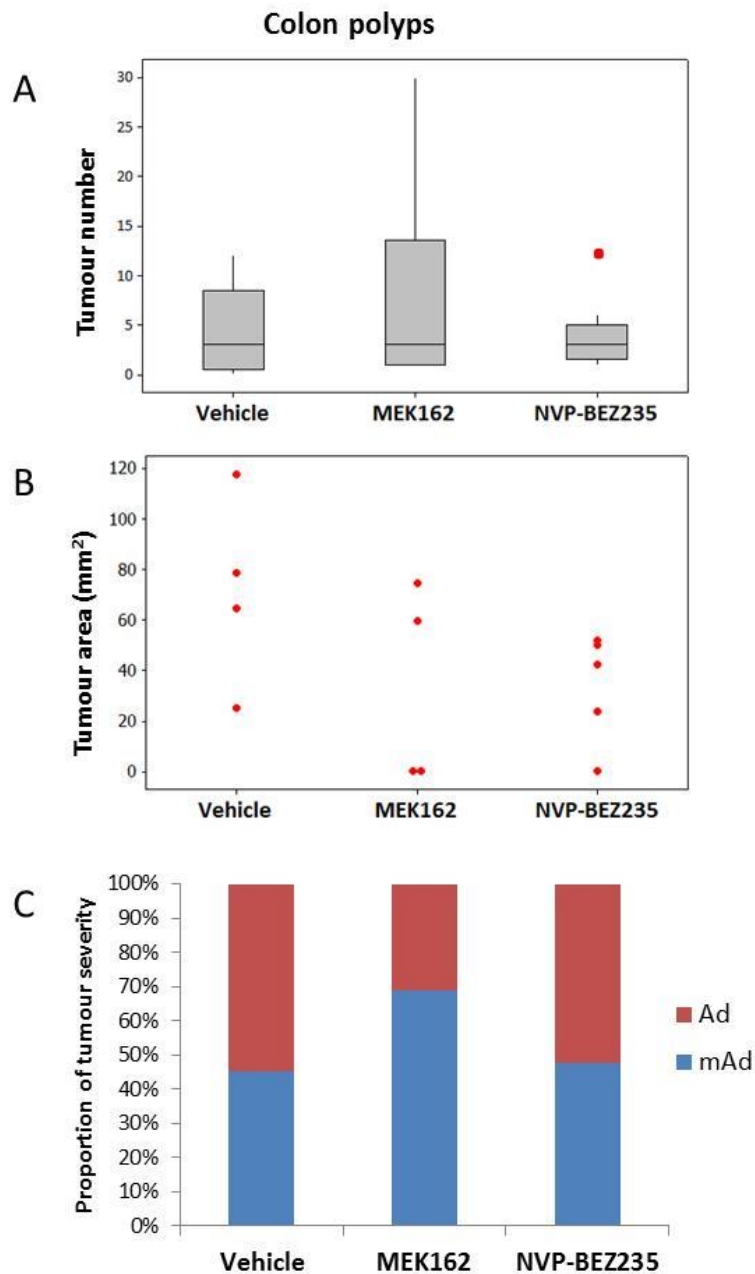


Figure 3.11 Analysis of colon tumour burden in $Apc^{f/+}$ mice on various treatments.

(A) Boxplot showing number of colon tumours present at death, as scored from H&E stained sections of colon tissue. No differences were detected in either MEK162 or NVP-BEZ235 treated cohorts (• indicates outlier). **(B)** Dot plot showing total tumour area per mouse, as scored from methacarn fixed tissue, post dissection. No significant alterations were detected here, although MEK162 and NVP-BEZ235 treatment trended to reduce total tumour area. **(C)** Key: mAd = microadenoma, Ad = Adenoma. No significant alterations were detected from staging of tumour severity according to invasiveness (all p values ≥ 0.05 , $n \geq 4$, Mann Whitney U test).

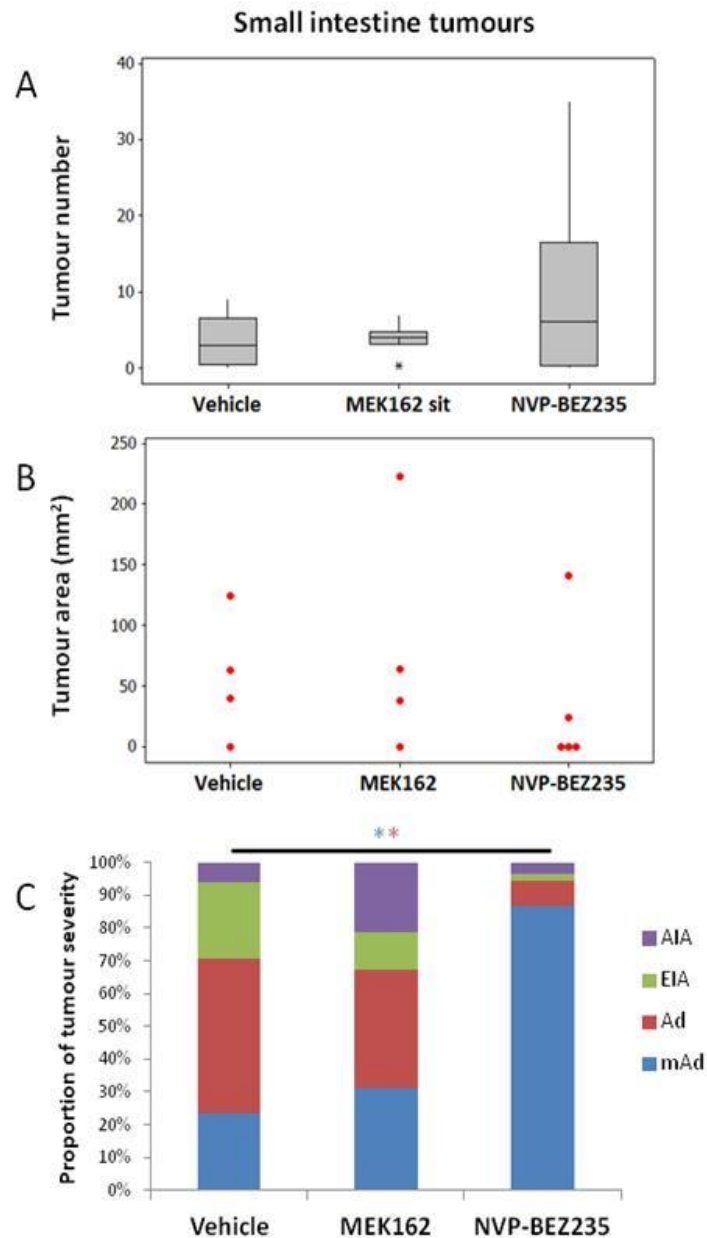


Figure 3.12 Analysis of small intestinal tumour (SIT) burden in *Apc^{f/+}* mice on various treatments.

(A) Boxplot showing number of SITs present at death, as scored from H&E stained sections of tissue samples. No differences were detected in either MEK162 or NVP-BEZ235 treated cohorts, although a trend towards increased number of tumours was observed in NVP-BEZ235 treated cohorts **(B)** Dot plot showing total tumour area per mouse, as scored from methacarn fixed tissue, post dissection. No significant alterations were detected in either treated cohorts **(C)** Key: mAd = microadenoma, Ad = Adenoma, EIA = early invasive adenocarcinoma, AIA = Advanced invasive adenocarcinoma. No significant alterations were detected from staging of tumour severity according to invasiveness in MEK162 treated mice. A significant increase in the proportion of mAds and a significant reduction in Ads was detected in NVP-BEZ235 treated mice (* p value ≤ 0.05 , $n \geq 4$, Mann Whitney U test).

3.2.8 Comparison of MAPK and PI3K activation in colonic and small intestinal tumours in alternative models of intestinal cancer

Despite the validity of the $Apc^{f/+}$ tumour model to assess MEK and PI3K/mTOR inhibition in this chapter, tumours harbouring specific mutations in oncogenes or tumour suppressor proteins resulting in activation of these pathways may be more sensitive to anti-MEK and anti-PI3K targeted agents. Recent studies within the Clarke lab have investigated the effect of oncogenic Kras and loss of the tumour suppressor protein Pten independently and also concurrently, on Apc driven tumourigenesis (Sansom et al., 2006, Marsh et al., 2008, Davies et al., *in press*). Here, Marsh et al showed that homozygous loss of the Pten allele accelerated Apc driven tumourigenesis through increased activation of pAKT (Marsh et al., 2008). The study by Davies et al supported previous findings of oncogenic Kras in accelerating Apc driven intestinal tumour development (Sansom et al., 2006, Janssen et al., 2006), but also found that concomitant deletion of Pten further accelerated tumourigenesis and shortened survival of mice compared to Apc Pten and Apc Kras controls (Davies et al., *in press*).

To confirm activation status of corresponding signalling pathways in the tumour models described above, cohorts of $Apc^{f/+}$, $Apc^{f/+}$ Kras^{LSL/+}, $Apc^{f/+}$ Pten^{f/f} and $Apc^{f/+}$ Pten^{f/f} Kras^{LSL/+} mice were generated. $Apc^{f/+}$, $Apc^{f/+}$ Kras^{LSL/+} and $Apc^{f/+}$ Pten^{f/f} Kras^{LSL/+} manipulations are driven by the VillinCreER transgene whereas the $Apc^{f/+}$ Pten^{f/f} deletions were driven by the AhCreER transgene. Cohorts of n=3 mice were induced and monitored for symptoms of tumour burden to develop (anaemia, bloating and blood in faeces). Upon development of these symptoms, mice were culled and dissected as described previously (methods section 2.4.2). Specifically tumours from the colon where appropriate, and the small intestine were snap frozen in liquid nitrogen in preparation for protein extraction and subsequent western blot analysis. For $Apc^{f/+}$ and $Apc^{f/+}$ Kras^{LSL/+} colon and SITs, lysates from 3 tumours were pooled (per well) whereas for $Apc^{f/+}$ Pten^{f/f} and $Apc^{f/+}$ Pten^{f/f} Kras^{LSL/+} SITs, 6 tumours lysates were pooled for western blot analysis of MAPK and PI3K pathway components. Antibodies against pERK, pAKT (at both Ser473 and Thr308) and pS6RP were used to investigate activation of MAPK and PI3K/mTOR pathways respectively. Immunoblotting for pERK revealed an increase in $Apc^{f/+}$ Kras^{LSL/+} colon polyps and SITs, indicating activation of MAPK signalling (Figure 3.13). Interestingly, MAPK signalling through pERK was found to be more activated in colonic tumours in comparison to SITs. Surprisingly, levels of pERK in $Apc^{f/+}$ Pten^{f/f} SITs were found to be elevated compared to controls and $Apc^{f/+}$ Kras^{LSL/+} tumours, but $Apc^{f/+}$ Pten^{f/f} Kras^{LSL/+} SITs did not show activation of pERK despite mutational activation of Kras (Figure 3.13). These findings corroborate previous

findings by IHC as reported by Davies et al (Davies et al., *in press*). Immunoblotting for pAKT473 and pAKT308 revealed activation of PI3K signalling in $Apc^{f/+} Kras^{LSL/+}$ colon polyps, but not in SITs (Figure 3.13). Both $Apc^{f/+} Pten^{f/f}$ and $Apc^{f/+} Pten^{f/f} Kras^{LSL/+}$ SITs show increased levels of pAKT473 and pAKT308 compared to $Apc^{f/+}$ and $Apc^{f/+} Kras^{LSL/+}$ controls however interestingly, oncogenic activation of Kras does not result in hyperactivation of PI3K signalling in $Apc^{f/+} Pten^{f/f}$ SITs despite the observation that Kras activation increases PI3K signalling in mutant colon polyps (Figure 3.13). To further investigate signalling downstream PI3K and AKT at mTOR, levels of pS6RP were probed in colon tumour and SIT lysates. In keeping with activation of PI3K signalling in $Apc^{f/+} Kras^{LSL/+}$ colon polyps, levels of pS6RP were found to be increased here. Surprisingly, no alterations in pS6RP levels were found in $Apc^{f/+} Kras^{LSL/+}$, $Apc^{f/+} Pten^{f/f}$ or $Apc^{f/+} Pten^{f/f} Kras^{LSL/+}$ in comparison with $Apc^{f/+}$ SITs (Figure 3.13), indicating perhaps co-operation between MAPK and PI3K signalling at mTORC1.

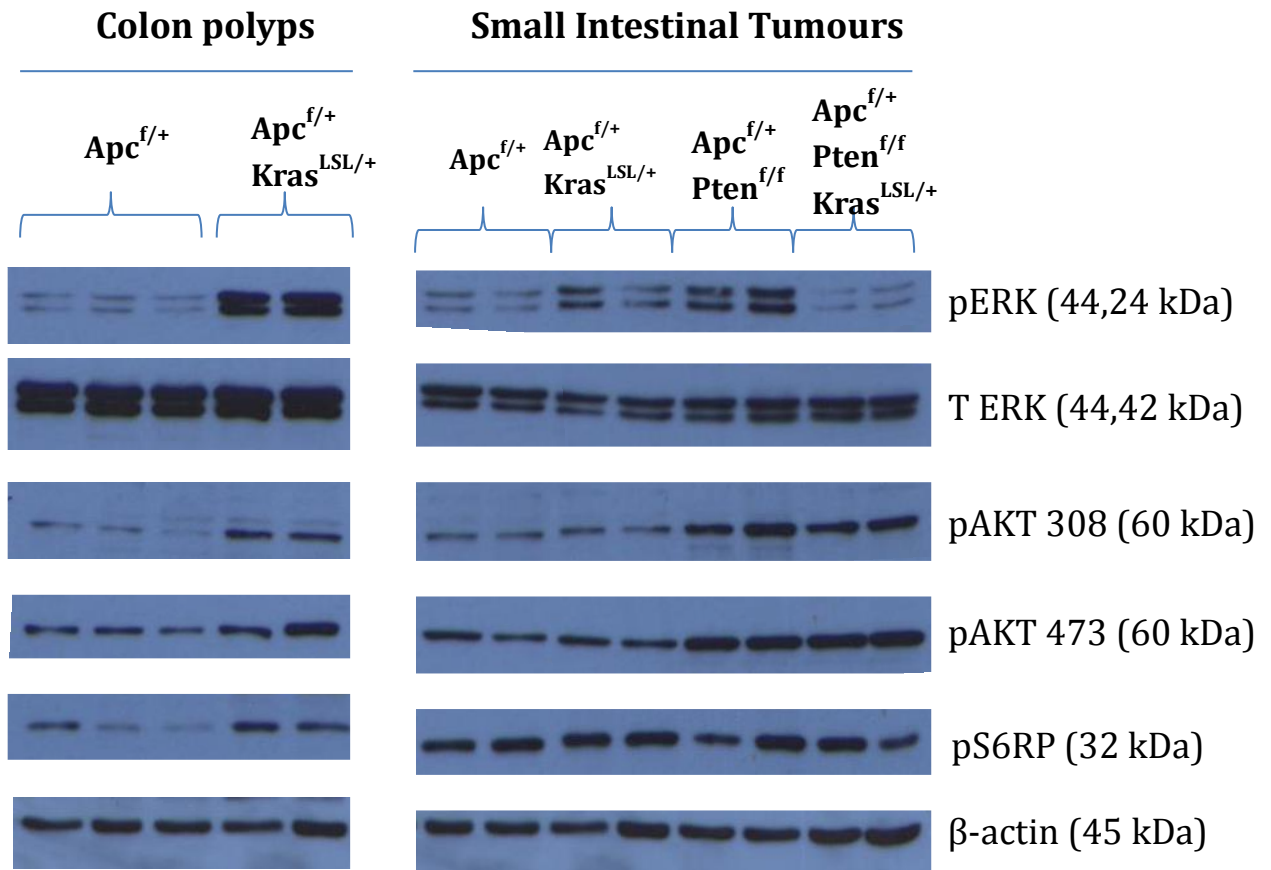


Figure 3.13 Western blot analysis indicating activation of PI3K and MAPK signalling in additional models of intestinal cancer

Pooled colon tumour and small intestine tumour (SIT) lysates (n=3-6 tumours from n=3 mice) from $Apc^{f/+}$, $Apc^{f/+} Kras^{LSL/+}$, $Apc^{f/+} Pten^{f/f}$ and $Apc^{f/+} Kras^{LSL/+} Pten^{f/f}$ mouse models were subjected to western blot analysis and subsequent immunoblotting with the MAPK effector pERK and the PI3K pathway effectors pAKT473, pAKT308 and pS6RP. $Apc^{f/+} Kras^{LSL/+}$ colon tumours display strong activation of MAPK and PI3K signalling whereas interestingly, $Apc^{f/+} Kras^{LSL/+}$ SITs only show mild activation of MAPK signalling, in comparison with $Apc^{f/+}$ controls. $Apc^{f/+} Pten^{f/f}$ and $Apc^{f/+} Kras^{LSL/+} Pten^{f/f}$ SITs both display activation of PI3K signalling in comparison with $Apc^{f/+}$ and $Apc^{f/+} Kras^{LSL/+}$ controls however surprisingly, $Apc^{f/+} Pten^{f/f}$ and not $Apc^{f/+} Kras^{LSL/+} Pten^{f/f}$ SITs show increased MAPK signalling.

3.3 Discussion

3.3.1 MEK inhibition by MEK162 increases survival of *Apc^{f/+}* mice and results in tumour growth stasis

Given that overexpression of EGFR is observed in a number of human malignancies including CRC (Ciardiello et al., 1991), drug development strategies and pre-clinical research have justifiably focused extensive efforts to target this receptor in order to inhibit downstream signalling. EGFR mediates aberrant pro-survival and anti-apoptotic signalling in cancer cells through a number of signalling pathways including the MAPK and PI3K cascades (Zwick et al., 1999). Despite the early promise of anti-EGFR antagonists including cetuximab and panitumumab for CRC, and gefitinib and irressa for non-small-cell-lung carcinoma, it quickly became apparent that pre-existing mutations activating MAPK and PI3K signalling predicted non-response to anti-EGFR therapies (Lièvre et al., 2008, Frattini et al., 2007, Perrone et al., 2009). Tumours determined wild-type for *KRAS*, *B-RAF*, *PIK3CA* or *PTEN* have also been shown to acquire mutations in these proteins resulting in resistance to anti-EGFR antagonists (Benvenuti et al., 2007, Di Nicolantonio et al., 2008, Diaz et al., 2012). Other mechanisms of resistance include strong activation of cognate receptors, including HER2, HER3 and cMET (Wheeler et al., 2008), and whilst targeting these with multiple anti-HER agents may be a rational therapeutic strategy, it was hypothesised that inhibition of signalling downstream EGFR, namely MEK inhibition for MAPK signalling and PI3K/mTOR inhibition for PI3K signalling, may also be an attractive therapeutic strategies for *KRAS* and PI3K pathway wild-type CRCs. To address these hypotheses in this chapter, I utilised the *Apc^{f/+}* tumour model driven by the intestinal specific transgene VillinCreER where induction with tamoxifen, results in formation of lesions within the small intestine and colon over a long latency. Two approaches were taken for investigations in this chapter. Firstly, to determine the immediate anti-tumour effects of MEK (MEK162) or PI3K/mTOR (NVP-BEZ235) inhibitors, aged mice presenting with symptoms of tumour burden were administered a single dose and culled 4 hours later. Alternatively, to address whether these agents provide any benefits to survival of *Apc^{f/+}* mice, a chronic treatment strategy was undertaken whereby mice received daily treatment from a chosen intervention start point, until a survival end point or the experimental end point of 500 days.

The therapeutic effects of MEK inhibition by MEK162 were first assessed to determine whether as hypothesised, this would be beneficial for *Apc^{f/+}* tumours. From acute treatment of MEK162, *Apc^{f/+}* SITs appear more sensitive to MEK162 than colon polyps, as at 4 hours post treatment, MEK162 resulted in a pro-apoptotic effect, whereas no discernible anti-tumour

effects were detected in colon polyps from the same animals (Figure 3.1, 3.2). Although these findings indicate MEK162 treatment did have an effect on tumours, investigation of additional time points following treatment, for example 8, 12 or 24 hours, could provide more insightful information regarding the anti-tumour effects of MEK162 in $Apc^{f/+}$ tumours over an extended period of time.

Despite the lack of favourable anti-tumour activity in $Apc^{f/+}$ colon polyps and the modest effects on SITs, IHC performed for pERK in colon polyps and SITs exposed to MEK162 revealed a marked reduction in immunostaining, indicating target inhibition (Figure 3.3, 3.4). Given the cross-talk between MAPK and PI3K/mTOR signalling (Ma et al., 2007, Ma et al., 2005), activation status of the later was also assessed post MEK162 administration. In doing so, a reduction in pAKT and pS6RP immunostaining was noted in colon polyps and SITs, indicating inhibition of the PI3K/mTOR axis also (Figure 3.3, 3.4). Although the changes in PI3K signalling detected here by immunostaining do require further confirmation and quantification by western blot analysis. The reduction in PI3K/mTOR signalling mediated by MEK inhibition may be attributable to a number of factors including p90 ribosomal S6 kinases (RSK1-4) which have previously been reported to mediate signals downstream pERK (Sturgill et al., 1988). These serine/threonine kinases regulate a number of cellular processes including proliferation, survival and growth through phosphorylation of a number of diverse substrates (Romeo et al., 2012). Interestingly, the RSK consensus phosphorylation motif is shared by other kinases including AKT and S6 kinase 1 (S6K1) (Romeo et al., 2012). Substrates targeted by AKT including TSC2, Bad, GSK3, p27 and S6RP are also phosphorylated by RSKs (Roux et al., 2004, Shimamura et al., 2000, Torres et al., 1999, Roux et al., 2007) and may account for the MEK162 mediated reduction in pS6RP levels observed in $Apc^{f/+}$ colon and SITs. Additionally, RSK1/2 protein kinases have been shown to phosphorylate Raptor, the key component of the rapamycin-sensitive mTOR complex – mTORC1 which is known to control phosphorylation of S6RP through S6K1 (Park et al., 2002). Although the reduction of pS6RP immunostaining may be explained by the interactions between ERK and mTORC1, the mechanism for reduced immunostaining of pAKT473 remain to be elucidated. Furthermore, the regulation of mTORC2 which is responsible for the phosphorylation of AKT at Ser473 is currently unknown however, it has been hypothesised that mTORC2 responds to growth signals mediated through receptor tyrosine kinase receptors and that this could lead to reduced pAKT473 staining in $Apc^{f/+}$ tumours following MEK inhibition (Oh and Jacinto, 2011).

Nevertheless, the therapeutic benefits of MEK inhibition in $Apc^{f/+}$ mice determined through continuous administration of MEK162, substantially increased median survival of $Apc^{f/+}$ mice from 270 to 401 days post induction (Figure 3.5). The favourable effects in this case may be attributable to inhibition of MAPK signalling but also to inhibition of PI3K and mTOR inhibition. Additionally, although analysis of tumour burden in $Apc^{f/+}$ mice post MEK162 treatment revealed no significant alterations in either total tumour number, area nor severity of tumours in either colon polyps or SITs, these findings suggest chronic MEK162 resulted in tumour growth stasis (Figure 3.11, 3.12). Importantly, these findings corroborate a number of previous studies which promote suppression of MAPK signalling as a rational therapeutic strategy for CRC. Sebolt-Leopold et al evaluated the MEK inhibitor PD-184352 in a number of tumour models including two xenograft models of CRC and similarly reported growth inhibition following 2 weeks of twice-daily treatment (Sebolt-Leopold et al., 1999). Yeh et al. also investigated MEK inhibition with AZD6244 in the HT-29 CRC xenograft model and found this to result in growth inhibition (Yeh et al., 2007). Furthermore, Lee and colleagues investigating the role of ERK activation in intestinal tumourigenesis of $Apc^{min/+}$ mice found that treatment with MEK inhibitor PD0325901 from 10 weeks of age resulted in 100% survival whereas all vehicle treated animals succumbed to disease by 27 weeks of age, suggesting treatment inhibits tumour growth (Lee et al., 2010). Together, these investigations support the hypothesis for MAPK inhibition as a rational therapeutic strategy for CRC.

3.3.2 NVP-BEZ235 treatment in $Apc^{f/+}$ mice also increases longevity of mice and prevents tumour progression

The therapeutic effects of the dual PI3K/mTOR inhibitor NVP-BEZ235 were next assessed in the $Apc^{f/+}$ tumour model to evaluate this as a rational therapeutic strategy for this tumour subgroup. As with MEK162 experiments, the initial effects of NVP-BEZ235 were characterised 4 hours after a single dose, in this case 35mg/kg of NVP-BEZ235. Characterisation of anti-tumour effects i.e. proliferative and apoptotic effects in colon polyps and SITs post treatment revealed no significant alterations in colon polyps in comparison with vehicle controls, but contrasting effects with regards to apoptotic signalling in SITs (Figure 3.6, 3.7). Here, a significant increase in apoptotic bodies was scored from H&E stained sections but a significant reduction in cleaved caspase 3 staining was scored from IHC, with no effect on proliferation (Figure 3.6, 3.7). Although contrasting, scoring of both histological apoptosis and cleaved caspase 3 are relevant indicators of apoptosis, cleaved caspase 3 as an earlier indicator whilst histological apoptosis is often regarded as later marker of apoptotic signalling. Investigation of

alternative time points post NVP-BEZ235 treatment for example, 2, 8, 12 or 24 hours in $Apc^{f/+}$ tumours may provide further insightful information regarding the immediate effects of NVP-BEZ235 on apoptotic signalling, as well as proliferation. Previous findings by Maira et al. suggest that NVP-BEZ235 does result in reduced cell proliferation in colorectal cancer cell lines, however this did not amount to a decline in cell viability as no difference in total cell number was observed (Maira et al., 2008). Despite this, Haagensen et al found NVP-BEZ235 to be cytotoxic to HCT116 and HT29 colorectal cancer cell lines (Haagensen et al., 2012), indicating that the effects of NVP-BEZ235 may be context dependent.

Further to the effects of NVP-BEZ235 on biological processes in tumours, the effect on PI3K signal transduction was evaluated by IHC for pAKT (Ser473) and pS6RP to assess target inhibition. Interestingly, reduction in pS6RP was observed in both colon polyps and SITs following NVP-BEZ235 administration, but no notable effects on pAKT473 immunostaining (Figure 3.8, 3.9). These findings suggest that at a 4 hour time point, $Apc^{f/+}$ tumours are more sensitive to mTORC1 inhibition, which results in reduction of pS6RP rather than mTORC2 which mediates phosphorylation of pAKT at Ser473. A study by Roper et al. corroborates these findings where by treatment of DLD-1, HCT116 and SW480 colorectal cancer cell lines with NVP-BEZ235 resulted in more transient inhibition of pAKT but sustained inhibition of pS6RP (Roper et al., 2011). This was also the case in a study by Haagensen et al. in which HT29 and HCT116 cell lines were used to evaluate the effects of NVP-BEZ235. Here, NVP-BEZ235 reduced levels of pS6RP and p4EBP1, downstream of mTORC1, more effectively than pAKT (Haagensen et al., 2012). Together these data suggest reduced sensitivity to NVP-BEZ235 mediated PI3K and mTOR inhibition. Moreover, these findings are consistent with the view of Maira et al, who noted that Pten-null cell lines may be more susceptible to the effects of NVP-BEZ235 in comparison with controls (Maira et al., 2009).

Additionally to the acute investigations of NVP-BEZ235, the therapeutic potential of PI3K/mTOR inhibition was assessed in a chronic treatment experiment in $Apc^{f/+}$ animals, from 220 days post induction. Continuous administration of NVP-BEZ235 significantly prolonged survival of mice indicating this as an effective treatment option for this subgroup of tumours (Figure 3.10). Interestingly, although long term treatment of MEK162 resulted in a longer median survival, this was not statistically more beneficial than chronic NVP-BEZ235 exposure in $Apc^{f/+}$ mice. These findings suggest equal dependence of $Apc^{f/+}$ tumours on MAPK and PI3K signalling and also propose combinatorial use of these targeted agents may provide further therapeutic benefits. Furthermore, although analysis of tumour burden yielded no significant

alterations in terms of total tumour number, tumour area or tumour severity in colon polyps (Figure 3.11), NVP-BEZ235 appeared to halt tumour progression in the small intestine (Figure 3.12). This was characterised by a significant increase in the proportion of single crypt lesions or microadenomas, and a reduction in the proportion benign adenomas. Together, these data indicate beneficial therapeutic effects of NVP-BEZ235 in $Apc^{f/+}$ mice. Previously, evaluation of NVP-BEZ235 in the adenovirus-inducible Cre recombinase model of Apc mutant colorectal cancer showed effective regression of colonic tumours as measured through consecutive colonoscopies (Roper et al., 2011). Together, these findings provide strong evidence for NVP-BEZ235 as a rational therapeutic strategy for PI3K pathway and KRAS wild-type tumours.

3.4 Summary

To summarise, MAPK targeting through the MEK inhibitor MEK162 in tumour bearing $Apc^{f/+}$ mice significantly prolonged longevity of mice despite lack of immediate anti-tumour activity detected at a 4 hour time point. Similarly, the dual PI3K/mTOR inhibitor NVP-BEZ235 equipotently increased survival of $Apc^{f/+}$ mice indicating equivalent dependence of $Apc^{f/+}$ tumours on both signalling cascades. Together, these findings evidence therapeutic targeting of MAPK and PI3K pathways as beneficial therapeutic strategies, but also suggest that in combination, MEK162 and NVP-BEZ235 may together provide further therapeutic benefit.

3.5 Further work

3.5.1 Further investigation of anti-tumour effects of MEK162 and NVP-BEZ235 in $Apc^{f/+}$ mice

In this chapter, the immediate anti-tumour and pharmacodynamic effects of MEK162 and NVP-BEZ235 were only assessed at a 4 hour time point post drug administration. As only mild pro-apoptotic effects were detected in tumours at this time point, additional shorter and longer time points for example, 2, 8, 12 or 24 hours post treatment may provide additional information regarding anti-tumour effects of MEK162 and NVP-BEZ235 in this setting. Furthermore, the effects of MEK162 and NVP-BEZ235 on MAPK and PI3K signalling by western blot analysis would provide quantitative data into the duration of pathway inhibition and hence create a profile of drug activity in $Apc^{f/+}$ tumours.

3.5.2 Acute and chronic combination therapy in $Apc^{f/+}$ mice

As described previously, both MEK and PI3K/mTOR inhibition through MEK162 and NVP-BEZ235 equally increased longevity of $Apc^{f/+}$ mice. This suggests combinatorial therapy may

provide further benefits in increasing longevity. Initially, the anti-tumour and pharmacodynamic effects of combination therapy would be assessed at short time points (4, 8, 24 hours) to ensure inhibition of both pathways as well as favourable anti-tumour effects. Following this, an appropriate dosing regimen would be required to ensure tolerability (as determined by weight loss). Nevertheless, given the benefits of single-agent therapy, I hypothesise the combination therapy to provide further therapeutic benefits for $Apc^{f/+}$ mice.

3.5.3 MEK and PI3K/mTOR inhibition in MAPK and PI3K-activated tumour settings

Despite the validity of the $Apc^{f/+}$ model to evaluate MEK and PI3K/mTOR inhibition as therapeutic strategies for MAPK and PI3K wild-type colorectal cancer, these types of lesions are often associated with early stage disease which are often effectively treated with adjuvant or neo-adjuvant chemotherapy and tumour resection. Colorectal cancer is often detected at late stages, due to mild symptoms, and often these lesions have accumulated further mutations, including those in the *KRAS* oncogene and those in genes activating the PI3K pathway- such as *PTEN* and *PIK3CA*. Therefore, it is hypothesised that MEK and PI3K/mTOR inhibition may be more beneficial in lesions presenting with mutations activating these. In this chapter, I assessed activation of MAPK and PI3K signalling in three models mutant for *Kras* and *Pten* and confirmed activation of associated signalling pathways. Following this, in chapters 4-6 I explored therapeutic targeting of MEK through MEK162 and PI3K/mTOR through NVP-BEZ235 as monotherapies and in combination to evaluate these as rational therapeutic strategies for *Kras* and *Pten* mutant intestinal tumour models.

4 *Investigating PI3K/mTOR inhibition and MEK inhibition in the $Apc^{f/+}$ $Pten^{f/f}$ colorectal cancer mouse model*

4.1 *Introduction*

Findings in chapter 3 indicate that targeting PI3K and mTOR in the absence of mutational activation of the pathway results in a significant survival benefit. Nevertheless, the rationale behind pathway-specific inhibitors is that these would be more effective for tumours with specific mutations which lead to activation of the respective pathway. Alterations in the PI3K pathway occur in a wide range of human malignancies and are often associated with progression of disease and metastasis, as well as poor prognosis for patients (Parsons et al., 2005). Mutations in the PI3K pathway are known to occur at every major node including the receptor tyrosine kinases upstream PI3K, the p110 α subunit of PI3K, the negative regulator PTEN, and at the downstream kinase AKT (Engelman, 2009). Furthermore, in the clinical setting, mutations in the PIK3CA gene (which encodes the p110 α subunit) or PTEN loss are consistently associated with lack of response to anti-EGFR therapies, for example cetuximab and panitumumab which are both approved for third-line use of metastatic CRC (Bardelli and Siena, 2010). Together, this has led to a surge in the assessment of pharmacological inhibitors of the PI3K pathway specifically targeting tumours which present with pathway mutations as a stratified treatment strategy.

Several pre-clinical studies have reported efficacy of a number of novel inhibitors of the PI3K/mTOR pathway in a range of human colorectal cancer cell lines. Herlund et al. evaluated the dual PI3K/mTOR inhibitor NVP-BE2235 in a 3D colon carcinoma model and found this to potently inhibit cell proliferation and induce apoptosis in cancer cells, and also after prolonged use of cytotoxics (Hernlund et al., 2012). Furthermore, Blaser et al. reported NVP-BE2235 and a novel ATP-competitive inhibitor of mTOR PP242 (Merck) were more effective than the allosteric mTOR inhibitor rapamycin at reducing growth and proliferation of colon cancer cells and xenografts (Blaser et al., 2012). In addition, Mueller et al. showed that NVP-BE2235 and the novel pan-PI3K inhibitor BKM120 had an increased pro-apoptotic effect in colon cancer cell lines with PI3KCA mutations (Mueller et al., 2012). These studies all highlight the benefits of targeting the PI3K pathway and suggest further development of these in human clinical trials.

However, although cancer cell lines are valuable tools for quickly determining anti-tumour activity and evaluating the pharmacodynamics of novel agents, given that the main aim of pathway-targeted agents is to specifically target oncogenic proteins driving tumourigenesis, many studies crucially fail to evaluate mutation status of the PI3K pathway in the cancer cell lines used (Haagensen et al., 2012, Balmano et al., 2009).

In this chapter, I first evaluate the dual PI3K and mTOR inhibitor NVP-BEZ235 in an autochthonous mouse model of colorectal cancer mutant for the tumour suppressor Pten. Here, AhCreER driven homozygous deletion of Pten and heterozygous deletion of Apc within the intestinal epithelium leads to invasive adenocarcinoma driven by activation of Akt.

Mutations in the PI3K pathway have previously been shown to predict non-response to MEK mediated inhibition of the MAPK pathway (Balmano et al., 2009, Chen et al., 2012b, Dry et al., 2010). However, a number of studies have recently reported that combined PI3K and MEK targeting results in synergistic pro-apoptotic effects in human colon cancer cell lines and xenografts (Haagensen et al., 2012, Migliardi et al., 2012). To further investigate this, I will also evaluate MEK inhibition using MEK162 as a single agent and also in combination with NVP-BEZ235 in this Pten deficient tumour model.

To evaluate the therapeutic potential of PI3K/mTOR, MEK and combined inhibition in the Pten deficient setting, I employed two main strategies. First, tumour-bearing AhCreER $Apc^{f/+}$ $Pten^{f/f}$ (referred to as $Apc^{f/+}$ $Pten^{f/f}$ hereon in) mice were administered a single dose of each treatment and culled 4, 8 or 24 hour time points post exposure to evaluate early pharmacodynamic and anti-tumour effects. Secondly, to investigate the long term effects of each treatment, tumour bearing mice were started on treatment at a defined time point following induction and treated daily to a survival end point i.e. when mice were symptomatic of disease, to investigate the effect of treatment on survival and tumour burden of $Apc^{f/+}$ $Pten^{f/f}$ mice.

4.2 Results

4.2.1 *NVP-BEZ235 reduces proliferation, induces apoptosis and leads to inhibition of the PI3K and mTOR signalling cascade in $Apc^{f/+}$ $Pten^{f/f}$ tumours*

For short term experiments, 10 week old $Apc^{f/+}$ $Pten^{f/f}$ mice were induced and monitored until symptomatic of disease (pale feet, bloating and blood in faeces). Mice ($n \geq 3$ per cohort) were then administered a single dose of 0.5% Methyl Cellulose (MC, Vehicle) and culled 4 hours later, or 35mg/kg NVP-BEZ235 and culled either 4, 8 or 24 hours later. Additionally, BrdU was administered to mice 2 hours prior to culling to label cells undergoing S phase of the cell cycle.

At dissection small intestinal tumours (SITs) were quickly dissected and snap frozen in liquid nitrogen for protein extraction, and the small intestine was 'swiss-rolled' and fixed in formalin in preparation for H&E staining and IHC (methods section 2.4.2).

To characterise the immediate anti-tumour activity of NVP-BEZ235 in $Apc^{f/+}$ $Pten^{f/f}$ tumours, histological mitosis and apoptosis was scored in SITs from H&E stained slides. Quantification of mitotic figures (Figure 4.1 A), revealed no significant alterations at 4, 8 or 24 hours after a single dose of NVP-BEZ235, compared to vehicle (4hr NVP-BEZ235 = 0.548 ± 0.363 , vehicle = 0.407 ± 0.318 , p value = 0.198, $n \geq 15$ tumours, 4 mice Mann Whitney U test). (8hr NVP-BEZ235 = 0.311 ± 0.212 , 24hr NVP-BEZ235 = 0.269 ± 0.303 , vehicle = 0.407 ± 0.318 , p value = 0.6004 for 8hr NVP-BEZ235 and p value = 0.0844 for 24hr NVP-BEZ235, $n \geq 15$ tumours, 4 mice, Mann Whitney U test). Similarly, scoring of apoptotic bodies in small intestine tumours indicated no significant alterations 4, 8 and 24 hours after a single dose of NVP-BEZ235 treatment compared to vehicle treated tumours (4hr NVP-BEZ235 = 1.871 ± 1.570 , 8hr NVP-BEZ235 = 1.2711 ± 0.766 , 24hr NVP-BEZ235 = 1.409 ± 0.655 , vehicle = 1.802 ± 1.123 , p value = 0.951 for 4hr NVP-BEZ235, p value = 0.295 for 8hr NVP-BEZ235, p value = 0.399 for 24hr NVP-BEZ235, $n \geq 15$ tumours, 4 mice, Mann Whitney U test) (Figure 4.1 B).

In order to further characterise the biological effects immediately after a single dose of NVP-BEZ235, IHC against BrdU and cleaved caspase 3 was carried out and scored (Figure 4.2 A, B). Quantification of BrdU staining revealed a significant decrease in number of BrdU positive tumour cells 4 and 8 hours post NVP-BEZ235 treatment (4hr NVP-BEZ235 = 14.877 ± 4.053 , 8hr NVP-BEZ235 = 9.629 ± 3.105 , vehicle = 30.7 ± 9.761 , p value < 0.000 for 4hr NVP-BEZ235, p value = 0.0004 for 8hr NVP-BEZ235, $n \geq 15$ tumours, 4 mice, Mann Whitney U test), indicating a reduction in the number of cells in S phase of the cell cycle. The number of BrdU positive cells 24 hours after NVP-BEZ235 was not altered in comparison with vehicle cohorts (24hr NVP-BEZ235 = 25.729 ± 10.341 , vehicle = 30.7 ± 9.761 , p value = 0.125, $n \geq 15$ tumours, 4 mice, Mann Whitney U test) indicating that NVP-BEZ235 initially induces a reduction in the number of cells in S phase of the cell cycle, however this returns to normal physiological levels between 8 and 24 hours after administration (Figure 4.2 A).

Quantification of cleaved caspase 3 staining revealed a significant increase 4 hours post NVP-BEZ235 exposure, (4hr NVP-BEZ235 = 5.631 ± 2.436 , vehicle = 3.046 ± 2.298 , p value = 0.0002 $n \geq 15$ tumours, 4 mice, Mann Whitney U test) indicating an immediate pro-apoptotic effect. Cleaved caspase 3 scoring in SITs at further 8 and 24 hour time points following NVP-BEZ235 treatment revealed a trend towards a reduction in cleaved caspase 3 at 8 hours and a

significant reduction at 24 hours (8hr NVP-BEZ235 = 2.247 ± 0.801 , 24hr NVP-BEZ235 = 1.149 ± 0.635 , vehicle = 3.046 ± 2.297 , p value = 0.544 for 8hr NVP-BEZ235, p value = 0.037 for 24hr NVP-BEZ235, $n \geq 15$ tumours, 4 mice, Mann Whitney U test), perhaps suggesting activation of compensatory mechanisms to reduce the increased apoptosis at 4 hours (Figure 4.2 B).

To investigate whether the early anti-tumour effects of NVP-BEZ235 described above correspond to pathway inhibition, SIT lysates were subjected to western blot analysis (Figure 4.3 A-C). Protein extracted from 6 small intestinal tumours from $n=3$ mice harvested 4, 8 and 24 hours after a single dose of NVP-BEZ235, or 4 hours after vehicle treatment were pooled for analysis. Antibodies for the phosphorylated forms (and hence activated form) of AKT at Thr308 and Ser473 were probed to assess activation of PI3K signalling through PDK1 and mTORC2 respectively. Additionally, phospho S6 ribosomal protein (S6RP) at Ser235/236 and phospho 4EBP1 at Thr37/46 were also probed to investigate pathway activation status downstream of mTORC1. Western blotting and densitometry analysis revealed complete inhibition of the PI3K and mTOR signalling axis 4 hours after a single dose of NVP-BEZ235. This is evidenced through complete reduction in the abundance of pAKT at Ser473 and Thr308, as well as pS6RP and p4EBP1 (Figure 4.3, Table 4.1). Western blotting also revealed this inhibition is predominantly relieved by 8 hours post NVP-BEZ235 as tumours harvested 8 and 24 hours post NVP-BEZ235 administration show no obvious reduction in pathway effectors compared to vehicle controls. Interestingly, densitometry analysis revealed a significant 50% increase in abundance of pAKT Thr308, 8 hours post treatment (Figure 4.3, Table 4.2) and a trend towards reduced levels of p4EBP1 at 24 hours post treatment. These later changes suggest activation of a negative feedback loop activated by tumours in response to PI3K/mTOR pathway inhibition and may reflect a mechanism of rebalancing cell signalling to basal levels.

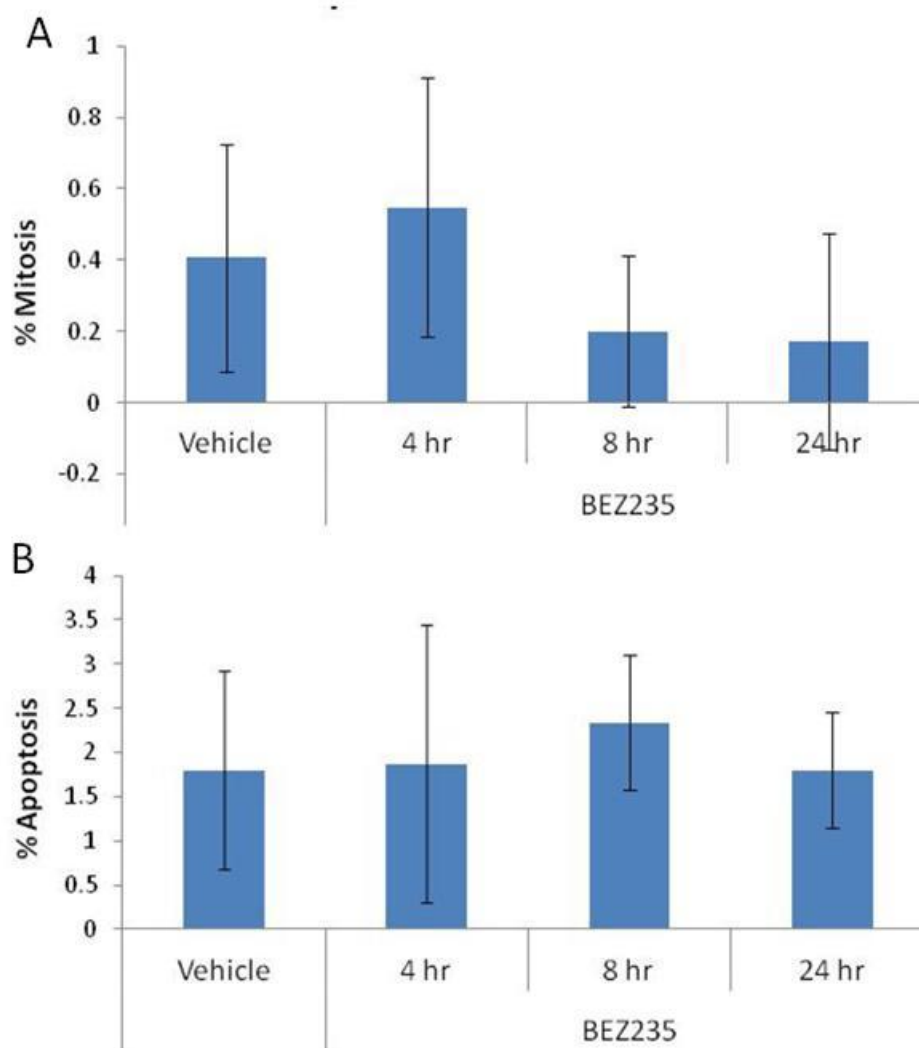


Figure 4.1 NVP-BEZ235 does not alter levels of mitosis and apoptosis in $Apc^{f/+} Pten^{f/f}$ small intestine tumours

Scoring of mitotic figures **(A)** and apoptotic bodies **(B)** revealed no significant alterations 4, 8 or 24hrs after a single dose of 35mg/kg NVP-BEZ235 compared to vehicle (0.5% MC) however, there appears to be a trend towards a reduction in the number of mitotic figures 8 and 24hrs post NVP-BEZ235 exposure (p value ≥ 0.05 , $n \geq 15$ tumours, 4 mice, Mann Whitney U test). Error bars represent standard deviation.

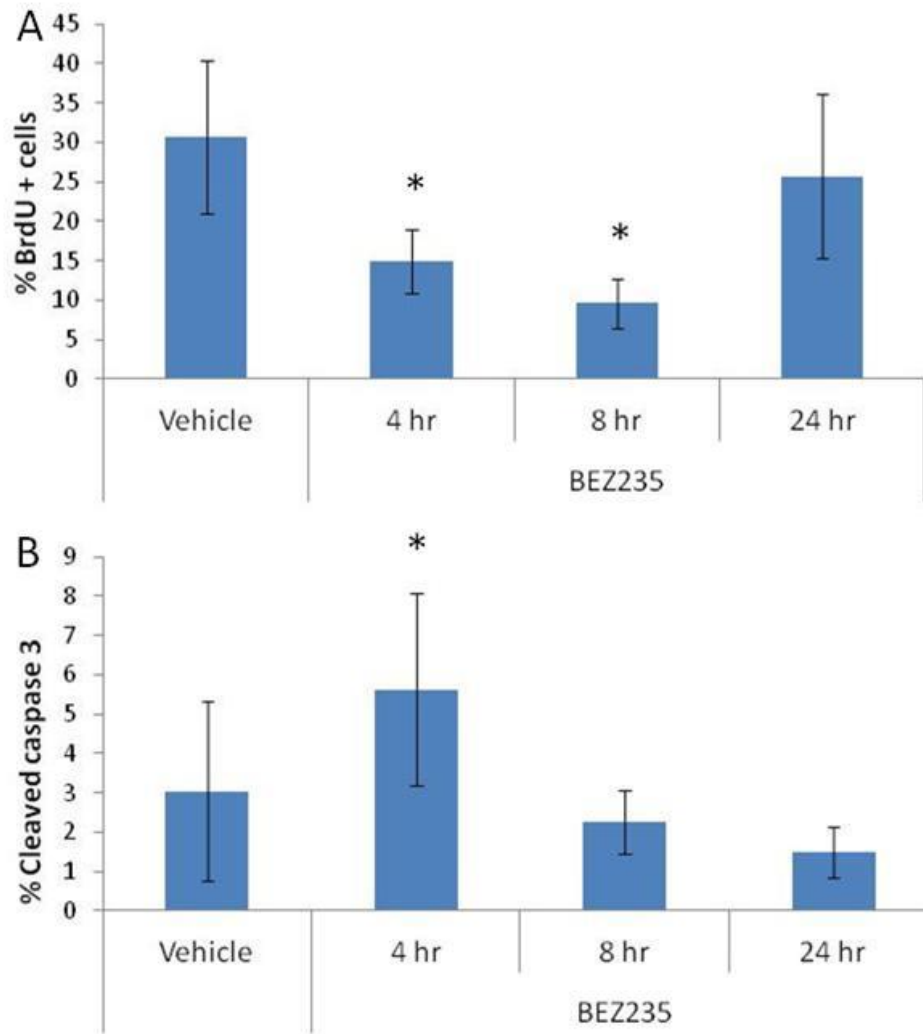


Figure 4.2 NVP-BEZ235 reduces the number of cycling cells and induces apoptosis through cleaved caspase 3 in $Apc^{f/+}$ $Pten^{f/f}$ small intestine tumours (SITs)

IHC against the proliferation marker BrdU and the apoptotic marker cleaved caspase 3 were carried out and quantified. **(A)** Scoring revealed a significant reduction in the number of BrdU positive cells 4 and 8 hours after exposure to NVP-BEZ235 indicating less cells going through the cell cycle (p value ≤ 0.0001 for 4hr, p value = 0.0004 for 8hr, $n \geq 3$, Mann Whitney U test) as well as a pro-apoptotic increase in cleaved caspase 3 staining 4 hours after exposure **(B)** (p value = 0.0002, $n \geq 3$, Mann Whitney U test). The initial anti-proliferative effect appears to return to baseline levels between 8 and 24 hours post exposure whereas cleaved caspase 3 levels appear to further decrease 8 and 24 hours post exposure (p value ≥ 0.05 , $n \geq 15$ tumours, 4 mice, Mann Whitney U test). Error bars indicate standard deviation.

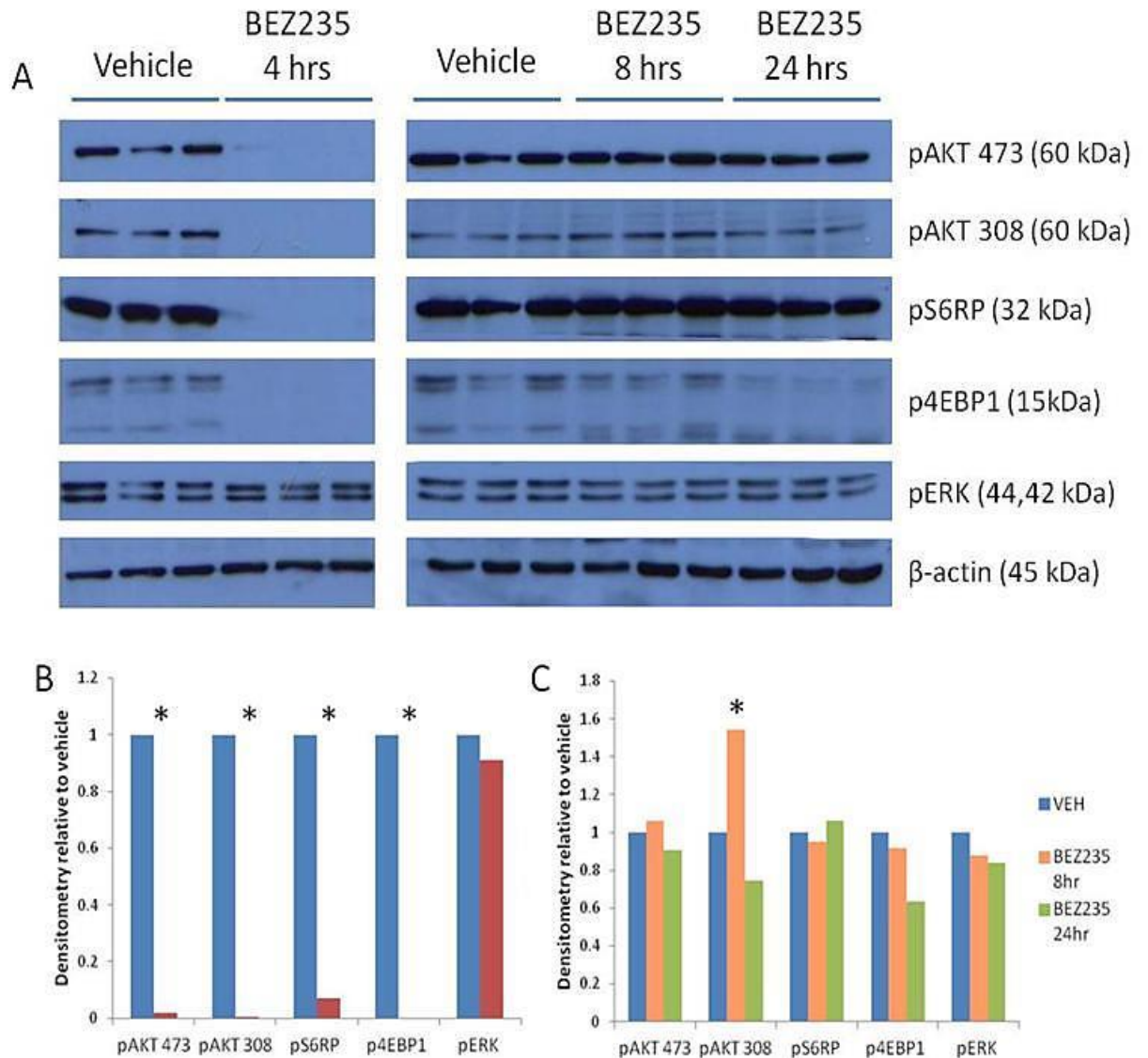


Figure 4.3 NVP-BEZ235 reduces PI3K and mTOR signalling in *Apc^{f/+} Pten^{f/f}* small intestine tumours (SITs) 4 hours post exposure

(A) 6 SIT lysates pooled from n=3 mice exposed to NVP-BEZ235 for varying time points were subjected to western blot analysis. Effectors of the PI3K and mTOR signalling pathways were probed and this revealed marked reduction of PI3K and mTOR signalling 4 hours post exposure. Signalling mostly appeared to return to basal levels by 8 hours post exposure. Additionally, the MAPK pathway effector pERK was probed to assess activation of this pathway, no significant alterations were present here. **(B + C)** Densitometry was carried out to quantify differences observed from immunoblotting. These are normalised to β-actin as loading control and represented as relative to vehicle controls (*p value = 0.0404, n=3, Mann Whitney U test).

	Vehicle	4 hours post NVP-BEZ235 (p value)
pAKT473	6804 ± 1921.9	131.7 ± 224.6 (0.0404)
pAKT308	4770.1 ± 790.3	13.0 ± 22.5 (0.0404)
pS6RP	12287.0 ± 92.6	863.6 ± 110.0 (0.0404)
p4EBP1	1317.4 ± 1059.3	5.2 ± 1.3 (0.0404)
pERK	10821.0 ± 3706.3	9873 ± 984.9 (0.5)

Table 4-1 Raw densitometry values from western blot analysis of pooled $Apc^{f/+}$ $Pten^{f/f}$ SITs 4 hours post exposure to NVP-BEZ235, n=3, One-tailed Mann Whitney U test was used for statistical analysis

	Vehicle	8 hours post NVP-BEZ235 (p value)	24 hours post NVP-BEZ235 (p value)
pAKT473	9273.1 ± 1866.7	9826.7 ± 400.2 (0.3313)	8416.0 ± 963.9 (0.5)
pAKT308	2933.2 ± 407.8	4526.0 ± 605.9 (0.0404)	2188.3 ± 417.4 (0.095)
pS6RP	10963.3 ± 696.8	10430.6 ± 922.9 (0.1914)	11640.6 ± 112.4 (0.5)
p4EBP1	10904.6 ± 4570.9	10944.3 ± 922.9 (0.5)	11640.6 ± 112.4 (0.095)
pERK	12500.5 ± 908.6	10972 ± 822.4 (0.095)	10483.2 ± 2599.4 (0.5)

Table 4-2 Raw densitometry values from western blot analysis of pooled $Apc^{f/+}$ $Pten^{f/f}$ SITs 8 and 24 hours post exposure to NVP-BEZ235, n=3, One-tailed Mann Whitney U test was used for statistical analysis

Additionally to investigating the effect of NVP-BEZ235 on PI3K and mTOR signalling, activation of the MAPK pathway through pERK was also assessed. Both pathways are known to converge at a number of downstream effectors and AKT is also known to lead to activation of MAPK signalling through RAF1 (Zimmermann and Moelling, 1999), upstream of MEK and downstream of RAS in the MAPK signalling cascade. Immunoblotting and subsequent densitometry analysis for pERK at Thr202/Tyr204 revealed no significant changes at either 4, 8 or 24 hours after exposure to NVP-BEZ235 in comparison to vehicle treated tumours (Figure 4.3, Table 4.1 and table 4.2), indicating no effect on MAPK signalling through phospho ERK in response to PI3K/mTOR inhibition by NVP-BEZ235.

In summary, acute NVP-BEZ235 exposure in Pten deficient SITs lead to effective inhibition of downstream pathway effectors (Figure 4.4). As PI3K signalling is known to be crucial for survival and apoptosis, the reduction in signalling may be responsible for the reduced proliferation and increased apoptosis in tumours as detected by BrdU and cleaved caspase 3 quantification.

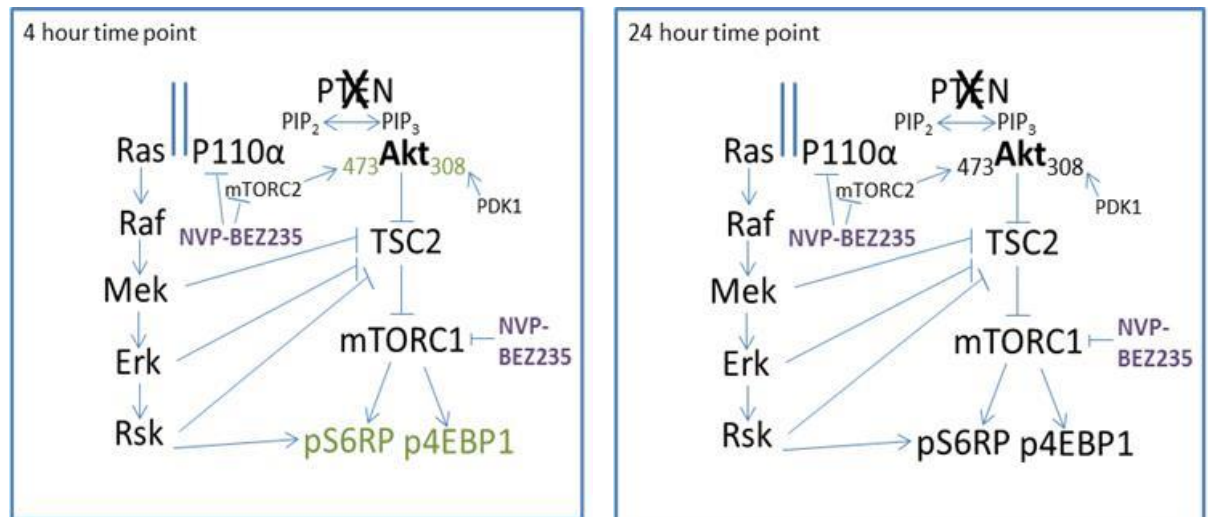


Figure 4.4 Schematic showing the effects of NVP-BEZ235 on PI3K/mTOR and MAPK pathway components as detected through western blot analysis (Green denotes a reduction in protein levels).

At 4 hours post exposure, NVP-BEZ235 leads to a reduction in levels of pAKT at Ser473 and Thr308, pS6RP and p4EBP1 whereas at 24 hours post exposure, NVP-BEZ235 has no significant effect on PI3K/mTOR or MAPK signalling.

4.2.2 Long term PI3K/mTOR inhibition through NVP-BEZ235 leads to a significant increase in survival of $Apc^{f/+}$ $Pten^{f/f}$ mice

To investigate the therapeutic potential of PI3K/mTOR inhibition in this $Pten$ deficient tumour model, a chronic treatment experiment was conducted to determine the effect firstly upon longevity of mice, but also intestinal tumour burden (section 4.2.7). For this, 10 week old $Apc^{f/+}$ $Pten^{f/f}$ mice were induced and allowed to establish disease over an 11 week period (77 days). Given that the majority of these mice become symptomatic of disease immediately after 11 weeks, a 77 days post induction (dpi) time point was chosen as an appropriate intervention start point. Mice ($n \geq 15$ per cohort) were randomised to receive either 0.5% MC (Vehicle) or 35mg/kg NVP-BEZ235 twice daily (weekdays only) by oral gavage until a survival end point (anaemia, bloating, $\geq 10\%$ loss of body weight).

Continuous twice daily treatment of NVP-BEZ235 in $Apc^{f/+}$ $Pten^{f/f}$ mice was well tolerated and led to a significant increase in survival of mice (median survival NVP-BEZ235 mice = 266 dpi, median survival Vehicle mice = 99 dpi, p value ≤ 0.001 , $n \geq 15$, Log-Rank and wilcoxon test) (Figure 4.5) indicating this as a beneficial therapeutic strategy for $Apc^{f/+}$ $Pten^{f/f}$ mice. Analysis of tumour burden at death following chronic NVP-BEZ235 treatment was also conducted (section 4.2.7) to further evaluate the effects of treatment.

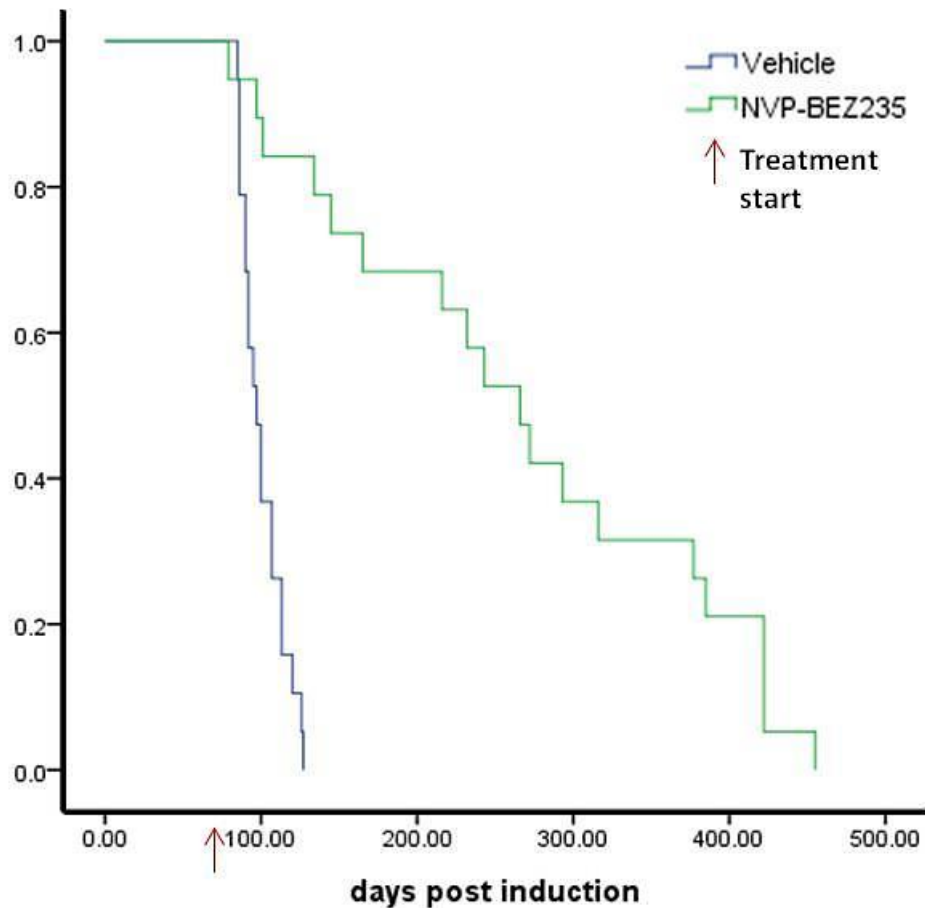


Figure 4.5 Kaplan-Meier survival analysis of $Apc^{f/+}$ $Pten^{f/f}$ mice on NVP-BEZ235 compared to vehicle controls

$Apc^{f/+}$ $Pten^{f/f}$ mice were induced and aged to 77 days post induction, at which point mice were randomised to receive either 0.5% Methyl cellulose (Vehicle control) or 35mg/kg NVP-BEZ235 twice-daily by oral gavage until a survival end point. Continuous NVP-BEZ235 treatment was found to increase survival of mice from 99 days (vehicle controls) to a median of 266 days post induction (p value ≤ 0.001 , $n \geq 15$ mice per cohort, Log-Rank and wilcoxon test).

4.2.3 Acute MEK inhibition through MEK162 reduces MAPK signaling and cellular proliferation in $Apc^{f/+}$ $Pten^{f/f}$ tumours, but reduces apoptosis and increases PI3K signalling

Similarly to section 4.2, mice for short term experiments were induced and aged to allow for development of intestinal tumours. Mice symptomatic of disease were subsequently administered with a single dose of 30mg/kg MEK162 and harvested either 4 or 24 hours later as described previously (section 2.4.2). Mice were also administered BrdU 2 hours prior to culling. Vehicle controls for this experiment are identical to those used in section 4.2.

To investigate the immediate anti-tumour activity of MEK162 in $Apc^{f/+}$ $Pten^{f/f}$ tumours, mitotic figures and apoptotic bodies were scored in SITs from H&E stained slides (Figure 4.6 A, B). Quantification of mitotic figures revealed no significant alterations at either 4 or 24 hours post exposure to MEK162 (4hr MEK162 = 0.372 ± 0.137 , 24hr MEK162 = 0.417 ± 0.271 , veh = 0.407 ± 0.318 , p value = 0.884 for 4hr MEK162 and p value = 0.774 for 24hr MEK162, $n \geq 15$ tumours, 4 mice, Mann Whitney U test). However, scoring of apoptosis revealed a significant reduction in the number apoptotic bodies at both 4 and 24 hours following MEK162 exposure (4hr MEK162 = 0.645 ± 0.546 , 24hr MEK162 = 0.8 ± 0.675 , veh = 1.802 ± 1.123 , p value = 0.0036 for 4hr MEK162 and p value = 0.0072 for 24hr MEK162 $n \geq 15$ tumours, 4 mice, Mann Whitney U test)

Furthermore, IHC for BrdU and cleaved caspase 3 was carried out and scored to further evaluate the anti-tumour effects of MEK162 (Figure 4.7 A,B). Scoring revealed a significant reduction in BrdU positive cells at both 4 and 24 hour time points post MEK162 exposure (4hr MEK162 = 17.65 ± 4.82 , 24hr MEK162 = 15.614 ± 8.64 , veh = 30.7 ± 9.761 , p value = 0.0003 for 4hr MEK162 and 0.001 for 24hr MEK162, $n \geq 15$ tumours, 4 mice, Mann Whitney U test) indicating an anti-proliferative reduction in cells undergoing S phase of the cell cycle. Quantification of cleaved caspase 3 bodies revealed no significant changes at both 4 and 24 hours post MEK162 (4hr MEK = 2.76 ± 1.68 , 24hr MEK = 4.036 ± 2.81 , Veh = 3.046 ± 2.29 , p value ≥ 0.05 , $n \geq 15$ tumours, 4 mice, Mann Whitney U test) (Figure 4.7 B).

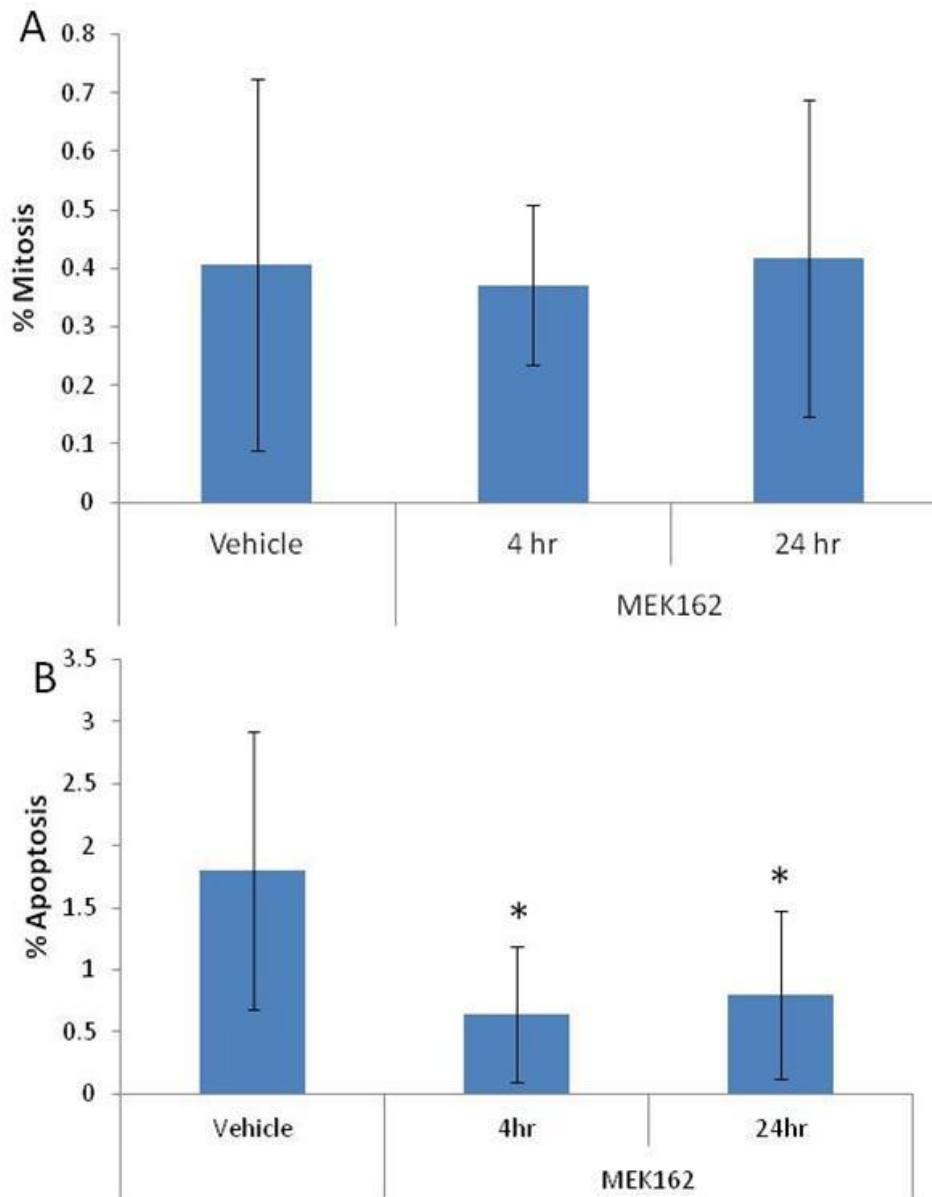


Figure 4.6 MEK162 resulted in a reduction of apoptotic bodies in $Apc^{f/+} Pten^{f/f}$ small intestine tumours (SITs)

Scoring of mitotic figures **(A)** and apoptotic bodies **(B)** by H&E examination revealed no significant alterations in the number of mitotic figures present, however revealed a significant reduction in the number apoptotic bodies 4 and 24 hours after a single dose of 30mg/kg MEK162 (p value = 0.0036 for 4hr and p value = 0.0072 for 24hr, $n \geq 15$ tumours, 4 mice, Mann Whitney U test). Error bars represent standard deviation.

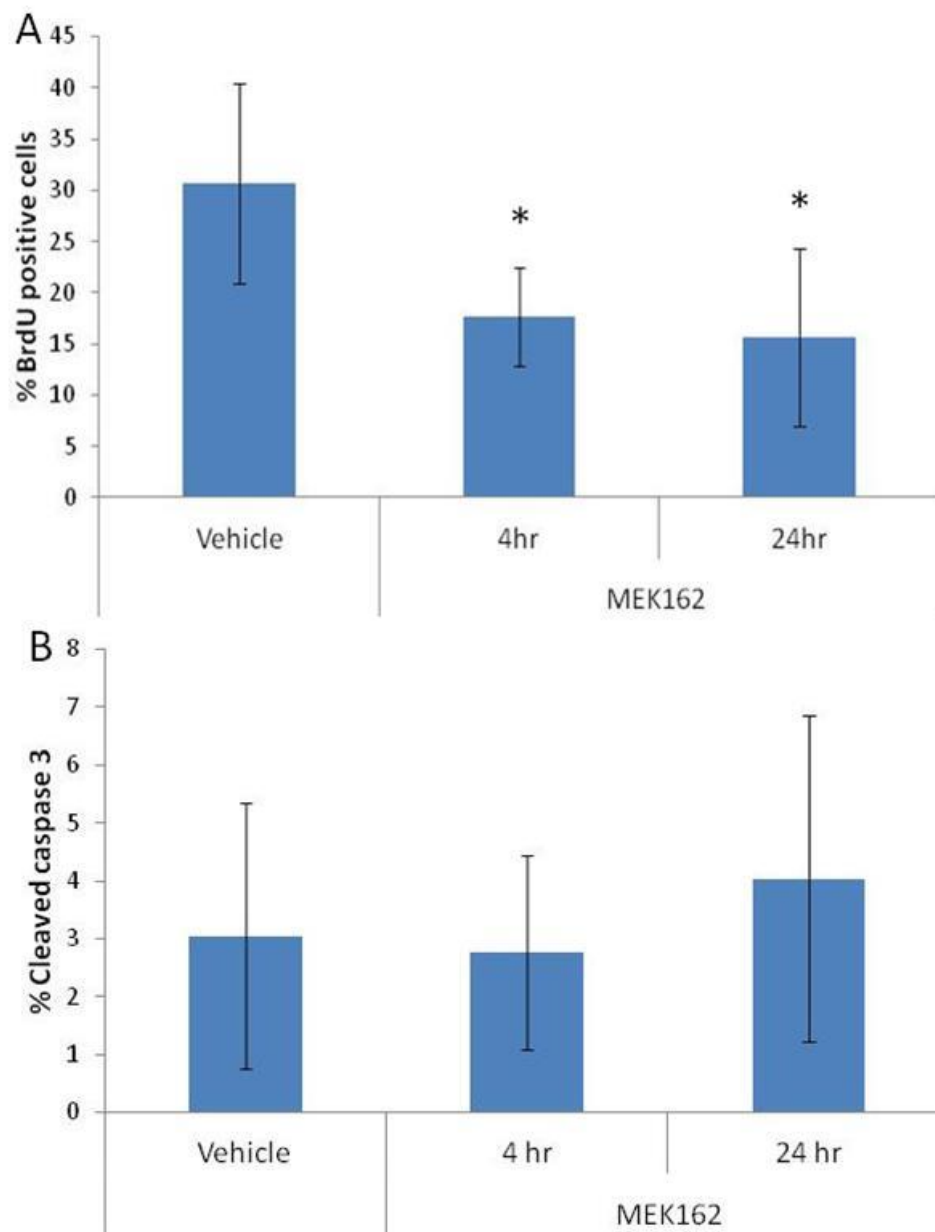


Figure 4.7 MEK162 lead to a reduction in the number of BrdU positive cells however, no alterations in cleaved caspase 3 were detected in *Apc^{f/+} Pten^{f/f}* small intestine tumours (SITs)

Quantification of IHC against the proliferation marker BrdU **(A)** and the apoptotic marker cleaved caspase 3 **(B)** revealed a significant reduction in BrdU positive cells 4 and 24 hours after a single dose of 30mg/kg MEK162 indicating less cells undergoing the cell cycle (p value = 0.0003 for 4hrs and p value = 0.001 for 24hr, $n \geq 3$, Mann Whitney U test) however, no alterations were observed with regards to cleaved caspase 3 staining (p value ≥ 0.05 , $n \geq 15$ tumours, 4 mice, Mann Whitney U test). Error bars indicate standard deviation.

Mutations of the PI3K pathway have previously proved to be inherently impervious to MEK inhibition in other models of human cancer (Balmanno et al., 2009, Chen et al., 2012b, Dry et al., 2010). To evaluate the immediate pharmacodynamic effects of MEK162 in this Pten deficient and hence PI3K activated intestinal tumour setting, protein extracted from 6 SITs (from n=3 mice per cohort) were pooled and subjected to western blot analysis. Immunoblotting for pERK (Thr 202/Tyr204) revealed a marked reduction at 4 and 24 hours post MEK162 exposure, indicating prolonged target inhibition in the Pten deficient tumour setting (Figure 4.8 A-C, Table 4.3, Table 4.4).

	Vehicle	4 hours post MEK162 (p value)
pERK	10821.0 ± 3706.3	2961.3 ± 1120.1 (0.0404)
pAKT473	6804.6 ± 192.9	6393.7 ± 545.1 (0.3313)
pAKT308	4770.1 ± 790.3	2907.8 ± 982.2 (0.0404)
pS6RP	12287.0 ± 942.6	9954 ± 1462 (0.0404)
p4EBP1	13174 ± 1059.3	15543 ± 2254.5 (0.0952)

Table 4-3 Outline of raw densitometry values from western blot analysis of pooled Apc^{f/+} Pten^{f/f} SITs 4 hours post exposure to MEK162, n=3, One-tailed Mann Whitney U test was used for statistical analysis

	Vehicle	24 hours post MEK162 (p value)
pERK	15657.0 ± 805.8	1451.5 ± 197.1 (0.0404)
pAKT473	5420.1 ± 385.9	8678.3 ± 596.0 (0.0404)
pAKT308	2754.0 ± 105.9	5483.5 ± 371.9 (0.0404)
pS6RP	15479.0 ± 1066.3	7776.3 ± 2165.8 (0.0404)
p4EBP1	7954.1 ± 618.5	43.3 ± 75.0 (0.0404)
p110	818.8 ± 246.8	4399.2 ± 560.1 (0.0404)

Table 4-4 Outline of raw densitometry values from western blot analysis of pooled Apc^{f/+} Pten^{f/f} SITs 24 hours post exposure to MEK162, n=3, One-tailed Mann Whitney U test was used for statistical analysis

Given the extensive cross-talk between both pathways, the immediate effect of MEK inhibition on PI3K and mTOR signalling was explored through western blot analysis of antibodies against pAKT, pS6RP and p4EBP1 were probed. Subsequent densitometry analysis revealed no significant difference in pAKT473 or p4EBP1 abundance, but did show a significant reduction in pAKT308 and pS6RP abundance 4 hours post MEK inhibition, indicating partial inhibition of PI3K and mTOR signalling (Figure 4.8, Table 4.3). Together, these changes to PI3K signalling are surprising but highlight immediate modulation of the closely associated signalling cascades. Furthermore, western blotting of tumour samples from mice harvested 24 hours after MEK162 exposure revealed additional modulation of PI3K signalling. Here, densitometry analysis revealed a significant increase in both pAKT 473 and 308 abundance but a significant reduction in levels of pS6RP and p4EBP1 (Figure 4.8, Table 4.4). The changes in PI3K signalling triggered through acute MEK inhibition may be attributable to convergence of both signalling cascades at mTOR or alternatively, activation of receptor tyrosine kinases through a feedback mechanism downstream of pERK may be responsible for activation of PI3K signalling. To further evaluate whether this was the case, western blotting of p110 α was conducted. Interestingly, western blotting revealed a significant increase in p110 α abundance 24 hours post MEK162 administration, correlating the increase in pAKT 473 and 308 abundance observed at this time point (Figure 4.9, table 4.4).

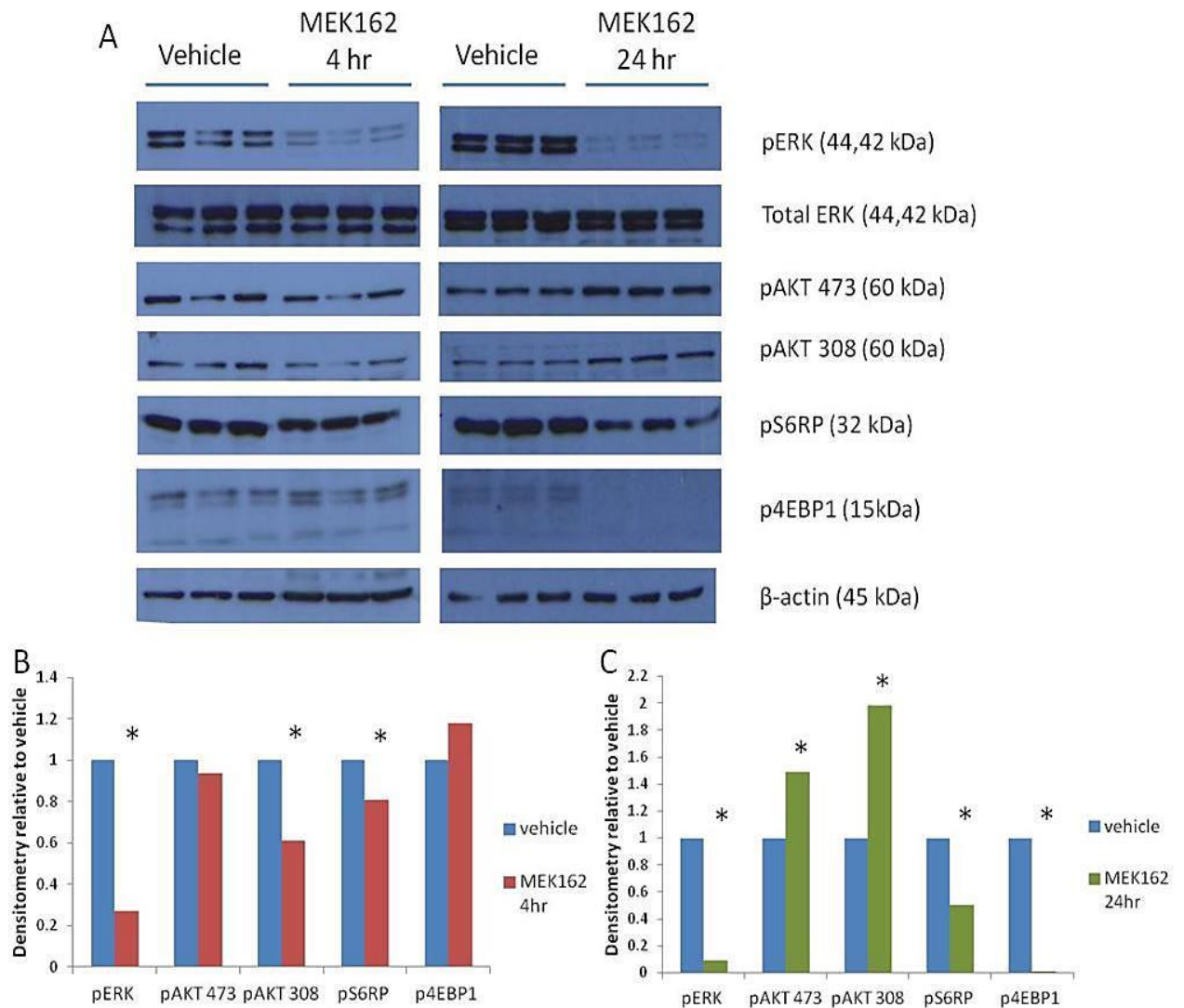


Figure 4.8 MEK162 leads to inhibition of MAPK signalling through pERK in $Apc^{f/+}$ $Pten^{f/f}$ small intestine tumours (SITs), however leads to differential modulation of PI3K and mTOR signalling

(A) 6 SITs pooled from $n=3$ mice exposed to MEK162 for either 4 or 24 hours were subjected to western blot analysis. Immunoblotting revealed a reduction in pERK abundance compared to vehicle controls indicating inhibition of MAPK signalling. Effectors of PI3K and mTOR signalling were also probed to investigate cross-talk of pathways. PI3K/mTOR signalling was found to be predominantly reduced at 4 hours, however PI3K signalling (through pAKT) was found to be increased after 24 hours but mTOR signalling (through pS6RP and p4EBP1) was found to be reduced. (B + C) Densitometry was carried out to quantify differences observed from immunoblotting. These are normalised to β -actin as loading control and represented relative to vehicle controls (* p value = 0.0404, $n=3$, Mann Whitney U test).

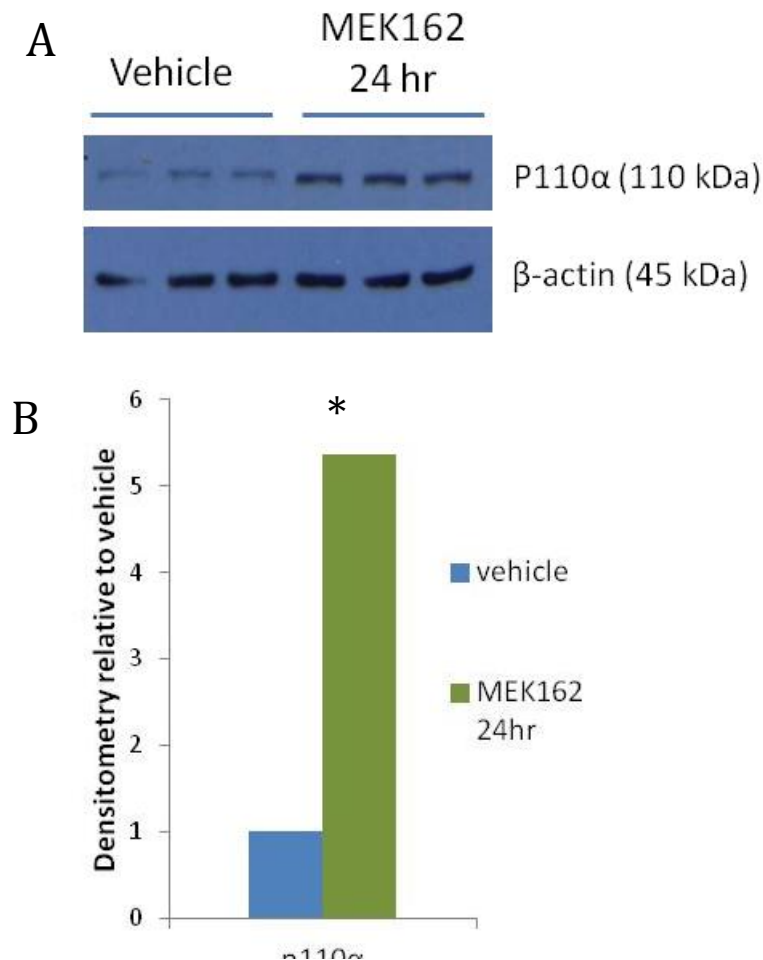


Figure 4.9 MEK162 leads to a significant increase in p110α 24 hours post exposure in *Apc^{f/+}* *Pten^{f/f}* small intestine tumours (SITs)

(A) Pooled SITs from mice culled 24 hours after exposure to MEK162 were subjected to western blotting and probed for p110α. Immunoblotting and subsequent densitometry analysis, (B) revealed a significant increase in p110α abundance. For densitometry, p110α bands were normalised to β-actin as loading control and represented relative to vehicle controls (*p value = 0.0404, n=3, Mann Whitney U test).

In summary, the immediate consequences of MEK162 in $Apc^{f/+}$ $Pten^{f/f}$ SITs involved prolonged inhibition of MAPK signalling through pERK which may be responsible for the anti-proliferative effects observed by BrdU scoring. Interestingly however, MEK162 also led to modulation of PI3K and mTOR signalling further evidencing cross-talk between the two pathways. Here, an initial reduction in PI3K and mTOR signalling was observed at 4 hours post MEK162 exposure however at 24 hours, MEK162 leads to activation of p110 α and AKT signalling but a significant reduction in levels of the mTORC1 effectors pS6RP and p4EBP1.

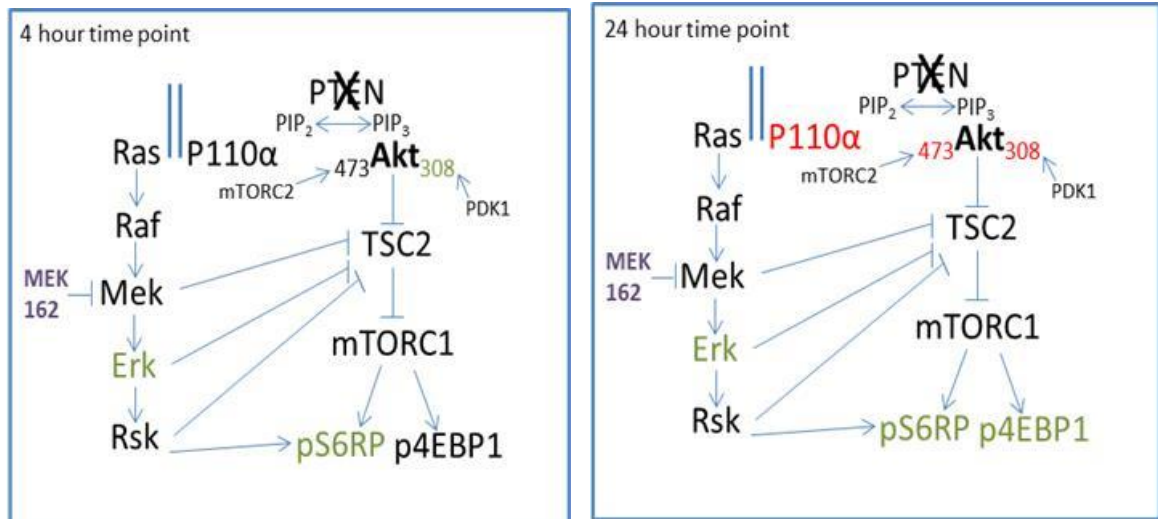


Figure 4.10 Schematic showing the effects of MEK162 on PI3K/mTOR and MAPK pathway components as detected by western blot analysis (Green denotes a reduction and red denotes an increase in protein levels).

At 4 hours post exposure, MEK162 leads to a reduction in levels of pERK, pAKT at Thr308 and pS6RP. At 24 hours post exposure, MEK162 reduced levels of pERK, pS6RP and p4EBP1 but led to increased levels of p110 α and pAKT at Ser473 and Thr308.

4.2.4 Chronic Mek162 treatment has no effect on longevity of $Apc^{f/+}$ $Pten^{f/f}$ mice

Similarly to section 4.2.2, 10 week old $Apc^{f/+}$ $Pten^{f/f}$ mice were induced and aged to 77 dpi for long term treatment with MEK162. A cohort of 13 mice received 30mg/kg twice daily (weekdays only) by oral gavage until a survival end point (anaemia, bloating, $\geq 10\%$ loss of body weight). Vehicle controls for this experiment are identical to those used in section 4.2.2.

Chronic twice daily treatment of MEK162 although well tolerated (determined by body weight) in $Apc^{f/+}$ $Pten^{f/f}$ mice, had no advantageous effect on median survival of mice (median survival of MEK162 mice = 101dpi, vehicle mice = 99dpi, $n \geq 13$, log rank p value = 0.224 and Wilcoxon p

value = 0.529) (Figure 4.11). Therefore, despite the immediate reduction in MAPK signalling, $Apc^{f/+}$ $Pten^{f/f}$ mice are unresponsive to long term MEK inhibition potentially due to immediate compensatory modulation of the PI3K signalling cascade.

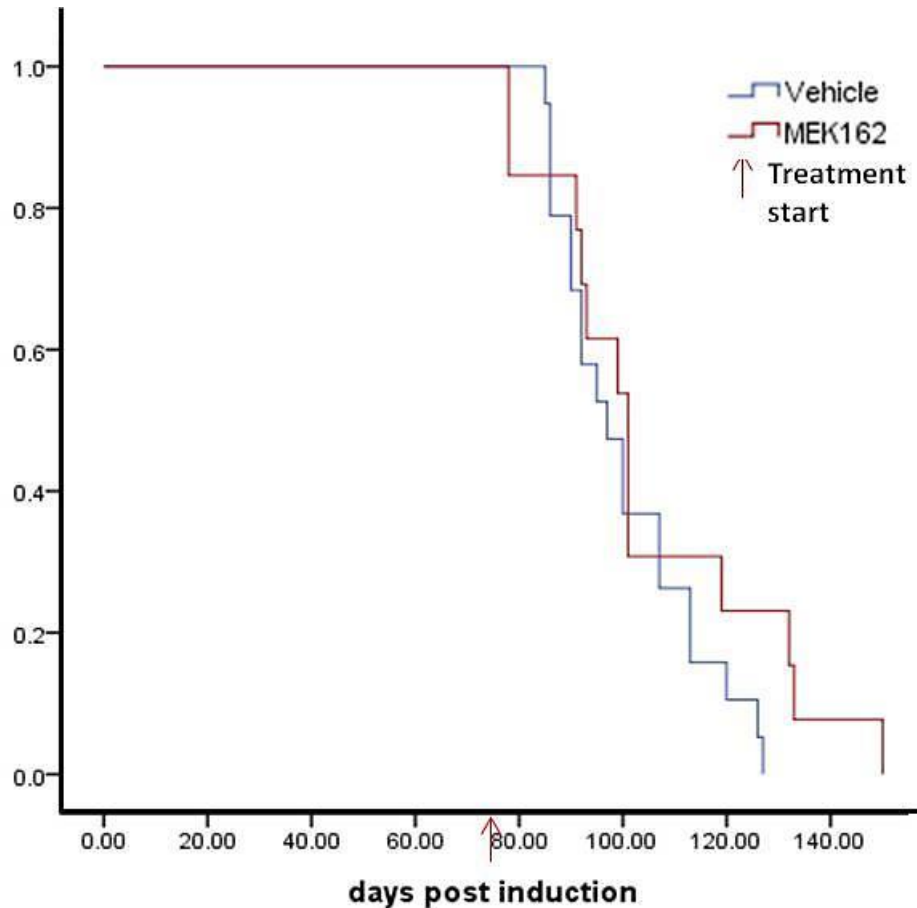


Figure 4.11 Kaplan-Meier survival analysis of $Apc^{f/+}$ $Pten^{f/f}$ mice on MEK162 compared to vehicle controls

$Apc^{f/+}$ $Pten^{f/f}$ mice were induced and aged to 77 days post induction, at which point mice were randomised to receive either 0.5% Methyl cellulose (Vehicle control) or 30mg/kg MEK162 twice-daily by oral gavage until a survival end point. Continuous MEK162 treatment was found to have no benefit on survival of mice (p value = 0.224 Log-Rank, p value = 0.529 Wilcoxon test, $n \geq 13$ mice per cohort).

4.2.5 The sequence of NVP-BEZ235 and MEK162 administration is crucial for combined inhibition of PI3K and MAPK signalling in $Apc^{f/+}$ $Pten^{f/f}$ mice

Given the effectiveness of long term PI3K/mTOR inhibition in this $Pten$ deficient tumour model, and the lack of response to chronic MEK inhibition, combined PI3K and MEK inhibition

was then investigated to determine whether the effects of chronic single agent NVP-BEZ235 could be improved upon. First however, it was crucial to determine the most effective manner of administering the combination therapy. Three differing dosing strategies were chosen (as outlined below, Table 4.5) and investigated in a short term setting to help identify the most effective strategy for administering the combination in the long term setting. A cohort of $n \geq 3$ mice were administered with each strategy and harvested 4 hours after the final dose. The dosing strategies chosen differ in the order of inhibitors administered. Combination strategy 1 (Combo 1) involved administration of MEK162 1 hour prior to NVP-BEZ235 whereas combination strategy 2 (Combo 2) involved administration of MEK162 1 hour following NVP-BEZ235 treatment. The 1 hour time gap in between treatments was initially chosen to reduce the stress of oral gavage however to eliminate any effect this may have had on tumours, both inhibitors were also administered simultaneously in combination strategy 3 (Combo 3). Mice were also administered with a dose of BrdU 2 hours prior to culling and were dissected as previously described in section 4.2. Vehicle controls for short term combination experiments are identical to those described previously in section 4.2.

<i>Strategy</i>	<i>Dosing schedule</i>
Combo 1	30mg/kg MEK162 followed by 35mg/kg NVP-BEZ235 1hr later
Combo 2	35mg/kg NVP-BEZ235 followed by 30mg/kg MEK162 1hr later
Combo 3	35mg/kg NVP-BEZ235 and 30mg/kg MEK162 at the same time

Table 4-5 Outline of combination dosing strategies utilised for short term pharmacodynamic and anti-tumour evaluations

To elucidate the immediate anti-tumour effect of each combination strategy, histological mitosis and apoptosis was scored from H&E stained slides (Figure 4.12) and also, IHC for brdU and cleaved caspase 3 was carried out and quantified (Figure 4.13). Scoring of mitotic figures in the Pten deficient SITs revealed no significant alterations following exposure to any of the three combinations in comparison to vehicle controls (4hr veh = 0.407 ± 0.318 , combo 1 = 0.347 ± 0.16 , combo 2 = 0.138 ± 0.239 , combo 3 = 0.393 ± 0.417 , combo 1 p value = 0.897, combo 2 p value = 0.144, combo 3 p value = 0.778, $n \geq 8$ tumours, 4 mice, Mann Whitney U test). Quantification of apoptotic bodies revealed a significant increase in histological apoptosis only after exposure to combo 2 (4hr veh = 1.802 ± 1.123 , combo 1 = 1.85 ± 1.141 , combo 2 = 4.77 ± 0.406 , combo 3 = 2.365 ± 1.102 , combo 1 p value = 0.927, combo 2 p value = 0.0058, combo 3 p value = 0.218, $n \geq 8$ tumours, 4 mice, Mann Whitney U test) (Figure 4.12).

IHC for BrdU and cleaved caspase 3 was carried out and quantified to further evaluate the immediate anti-tumour activity of the three combination strategies. Scoring of BrdU positive cells showed a significant reduction in positive cells following combo 1 and 2 but not with combo 3 (Veh = 30.7 ± 9.76 combo 1 = 13.65 ± 6.18 , combo 2 = 10.45 ± 3.32 , combo 3 = 26.93 ± 5.02 , both p value ≤ 0.05 , $n \geq 8$ tumours, 4 mice, Mann Whitney U test). Quantification of cleaved caspase 3 revealed a significant increase in staining in SITs exposed to all three combination strategies (4hr veh = 3.046 ± 2.297 , combo 1 = 4.06 ± 1.38 , combo 2 = 4.4 ± 1.702 , combo 3 = 9.567 ± 2.351 , combo 1 p value = 0.0305, combo 2 p value = 0.0033, combo 3 p value = 0.0009, $n \geq 8$ tumours, 4 mice, Mann Whitney U test) compared to vehicle treated tumours, although the levels of cleaved caspase 3 was higher in combo 3 treated tumours than combo 1 and 2 (Figure 4.13).

As described previously, exposure to NVP-BEZ235 led to inhibition of a number of components along the PI3K/mTOR signalling cascade and similarly, exposure to MEK162 led to a reduction in MAPK signalling evidenced through a reduction in pERK. To determine whether combination of NVP-BEZ235 and MEK162 led to simultaneous inhibition of PI3K/mTOR and MAPK signalling in *Apc^{f/+} Pten^{f/f}* tumours, SITs harvested from mice exposed to the three combination strategies (Table 4.5) were subjected to protein extraction. For western blot analysis, 6 SITs per cohort were pooled and probed for components of the PI3K/mTOR and MAPK signalling pathways to build pharmacodynamic profiles of the three combination strategies.

Surprisingly, immunoblotting for pathway components revealed notable differences between the three combination strategies with regards to pathway inhibition. Administration of MEK162 1 hour prior to NVP-BEZ235 (Combo 1) led to a reduction in levels of pERK, but differential modulation of PI3K/mTOR signalling, evidenced by partial inhibition of pAKT at Ser473 and Thr308 and p4EBP1, but complete reduction of pS6RP (Figure 4.14, Table 4.6). Interestingly, administration of NVP-BEZ235 1hr prior to MEK162 (Combo 2), led to potent inhibition of pERK and a number of PI3K pathway components including pAKT Ser473 and Thr308 and pS6RP (Figure 4.14, Table 4.7), suggesting that MEK inhibition prior to PI3K/mTOR inhibition may render *Apc^{f/+} Pten^{f/f}* tumours insensitive to PI3K/mTOR inhibition whereas MEK inhibition post PI3K/mTOR inhibition results in a cooperative effect to inhibit both pathways. To evaluate whether the differences observed between combo 1 and combo 2 with regards to pathway inhibition were due to the order of which inhibitors were administered or whether this perhaps was due to the 1 hour time in between doses, both inhibitors were administered at the same time (combo 3) and tumours were similarly evaluated for differences in pathway output. Western blotting of these tumours revealed that administration of NVP-BEZ235 and

MEK162 at the same time lead to inhibition of MAPK signalling through reduced levels of pERK, but differential inhibition of PI3K/mTOR signalling. Here, a partial reduction in pAKT Ser473 levels, no difference in levels of p4EBP1 however, a considerable reduction in pAKT Thr308 and pS6RP was detected (Figure 4.14, Table 4.7). This later finding suggests that tumours exposed to combo 3 are no longer sensitive to potent PI3K/mTOR inhibition as observed by NVP-BEZ235 alone 4 hours after a single dose and that perhaps when administered at the same time, the effects of one agent negate the effects of the other.

	Vehicle	Combo 1 (p value)
pERK	10280 ± 276	1852 ± 390 (0.0404)
pAKT473	8417 ± 798	5855 ± 460 (0.0404)
pAKT308	3461 ± 1562	2350 ± 743 (0.0404)
pS6RP	5344 ± 1022	65 ± 39 (0.0404)
p4EBP1	6614 ± 2694	2261 ± 671.9 (0.0404)

Table 4-6 Outline of raw densitometry values from western blot analysis of pooled *Apc^{f/+}* *Pten^{f/f}* SITs 4 hours post exposure to combo 1, n=3, One-tailed Mann Whitney U test was used for statistical analysis

	Vehicle	Combo 2 (p value)	Combo 3 (p value)
pERK	12689 ± 1257	1221 ± 352 (0.0404)	2683 ± 954 (0.0404)
pAKT473	11861 ± 197	713 ± 280 (0.0404)	9521 ± 1283 (0.0404)
pAKT308	5308 ± 574	No bands detected	2165 ± 423 (0.0404)
pS6RP	16685 ± 854	386 ± 114 (0.0404)	1818 ± 814 (0.0404)
p4EBP1	9452.9 ± 2308.1	13063.9 ± 1602.6 (0.0404)	11543.4 ± 2089.7 (0.1914)

Table 4-7 Outline of raw densitometry values from western blot analysis of pooled *Apc^{f/+}* *Pten^{f/f}* SITs 4 hours post exposure to combo 2 and combo 3, n=3, One-tailed Mann Whitney U test was used for statistical analysis

In summary, western blotting of the three combination strategies chosen show that $Apc^{f/+}$ $Pten^{f/f}$ tumours are highly sensitive to the order of which inhibitor is administered, in order to achieve simultaneous inhibition of both pathways.

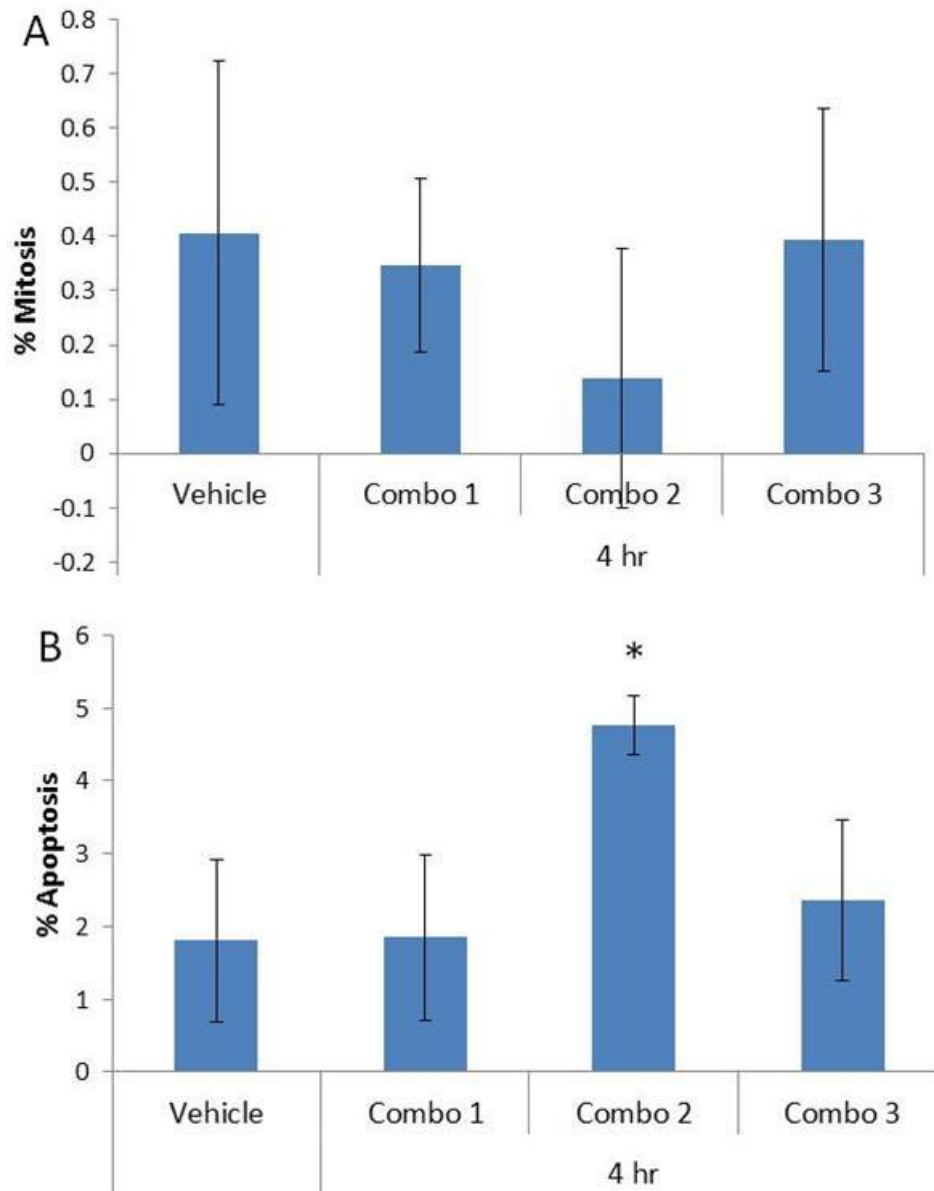


Figure 4.12 Sequencing of combination is important for anti-tumour effects in $Apc^{f/+}$ $Pten^{f/f}$ small intestine tumours (SITs)

Scoring of mitotic figures **(A)** and apoptotic bodies **(B)** revealed a trend towards reduced mitotic figures only after combo 2 administration, but a significant increase in apoptosis 4 hours after combo 2 exposure (p value ≤ 0.05 , $n \geq 8$ tumours, 4 mice, Mann Whitney U test). Error bars represent standard deviation.

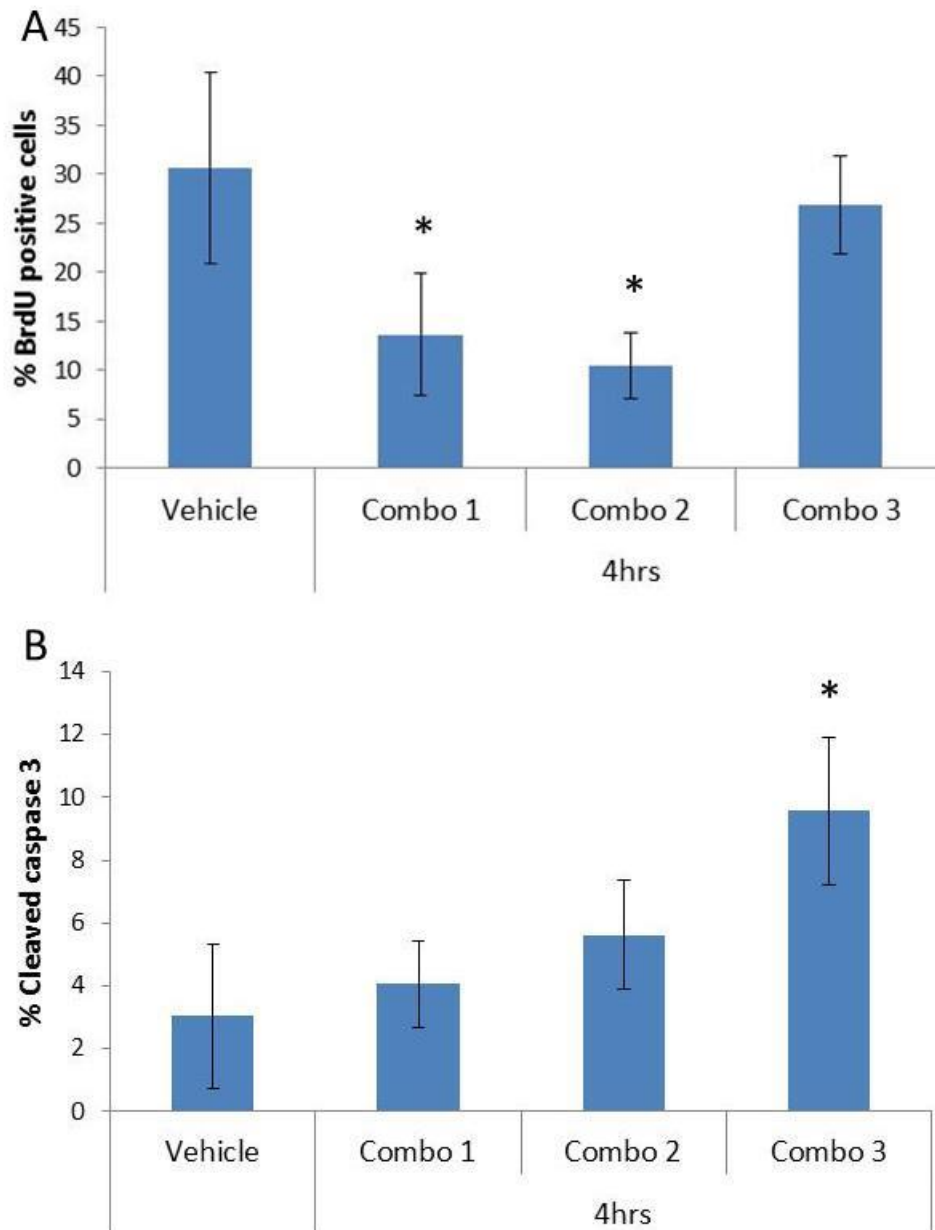


Figure 4.13 Sequencing of combination is important for anti-tumour effects in $Apc^{f/+}$ $Pten^{f/f}$ small intestine tumours

Quantification of IHC against the proliferation marker BrdU **(A)** and the apoptotic marker cleaved caspase 3 **(B)** revealed a significant reduction in BrdU positive cells 4 after combo 1 and 2, and increase in cleaved caspase 3 only after combo 3 administration. (*p value ≤ 0.05 , $n \geq 8$ tumours, 4 mice, Mann Whitney U test). A trend towards an increase in cleaved caspase 3 after combo 2 was also observed, however this was not significantly altered. Error bars indicate standard deviation.

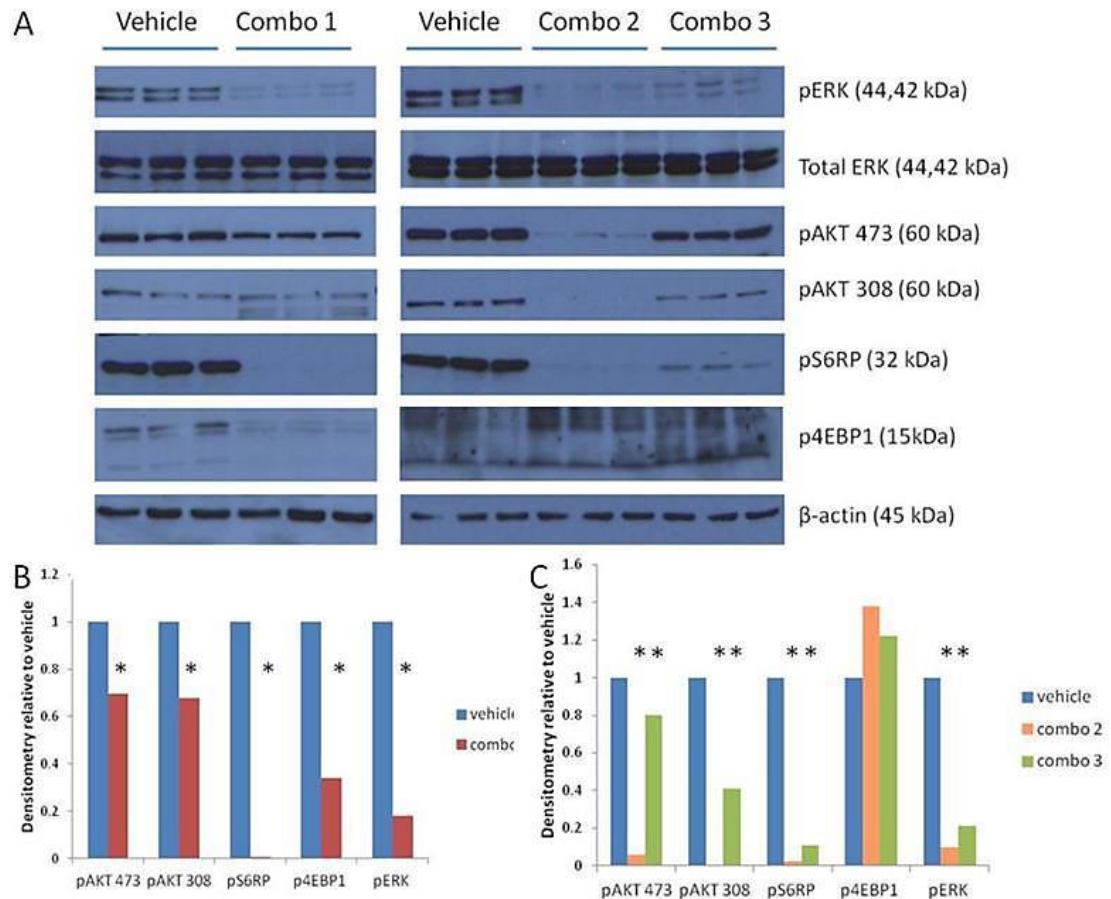


Figure 4.14 Sequencing of combination is crucial for combined inhibition of PI3K/mTOR and MAPK signalling in *Apc^{f/+} Pten^{f/f}* small intestine tumours

(A) 6 small intestine tumours pooled from $n=3$ mice exposed to the differing combination strategies were subjected to western blot analysis and probed for effectors of PI3K/mTOR and MAPK signalling. Immunoblotting revealed complete inhibition of PI3K/mTOR and MAPK signalling only with combo 2. Combo 1 and 3 led to substantial inhibition of MAPK signalling through pERK, but differential modulation of PI3K/mTOR signalling. (B + C) Densitometry was also carried out to quantify differences observed from immunoblotting. These are normalised to β -actin as loading control and represented relative to vehicle controls (* p value = 0.0404, $n=3$, Mann Whitney U test).

4.2.6 Combination strategy 2 results in prolonged inhibition of the PI3K/mTOR and MAPK signalling cascades

The preferred combination strategy identified from short term 4 hour treatments (section 4.2.5) was combo 2, given the increased anti-tumour effects and the favourable immediate pharmacodynamic effects. To investigate whether this was still the case at a 24 hour time point after a single dose of the combination, a cohort of n=4 tumour bearing $Apc^{f/+}$ $Pten^{f/f}$ mice were administered with combo 2 and culled 24 hours following the last dose. Mice were also administered a 2 hour pulse of BrdU to label cells in S phase of the cell cycle prior to culling. Mice were harvested as previously described and controls for this experiment are those used in section 4.2.

H&E stained sections of the small intestine were used to assess histological mitosis and apoptosis in tumours, and IHC for BrdU and cleaved caspase 3 were also carried out to determine the biological effects of combo 2 24 hours after exposure (Figure 4.15). Quantification of mitotic figures here revealed no significant alterations (vehicle = 0.407 ± 0.318 , 24hr combo 2 = 0.418 ± 0.271 , p value = 0.0932, n≥8 tumours, 4 mice, Mann Whitney U test) (Figure 4.15 A) however histological apoptosis was significantly reduced (vehicle = 1.802 ± 1.123 , 24hr combo 2 = 0.800 ± 0.675 , p value = 0.0243, n≥8 tumours, 4 mice, Mann Whitney U test) (Figure 4.15 B) indicating activation of a compensatory mechanism which results in reduced apoptosis following the 4-fold increase in apoptosis observed at 4 hours following combo 2 (section 4.2.5). The levels of BrdU positive cells was also significantly reduced (vehicle = 30.7 ± 9.761 , 24hr combo 2 = 23.887 ± 5.011 , p value = 0.0179, n≥8 tumours, 4 mice, Mann Whitney U test) indicating less S phase cells are present 24 hours post combo 2 treatment (Figure 4.15 C). Scoring of cleaved caspase 3 staining revealed no significant alterations (24hr vehicle = 3.046 ± 2.297 , combo 2 = 2.203 ± 1.150 , p value = 0.4365, n≥8 tumours, 4 mice, Mann Whitney U test) (Figure 4.15 D) consistent with levels 4 hours after combo 2 exposure (Figure 4.13 B).

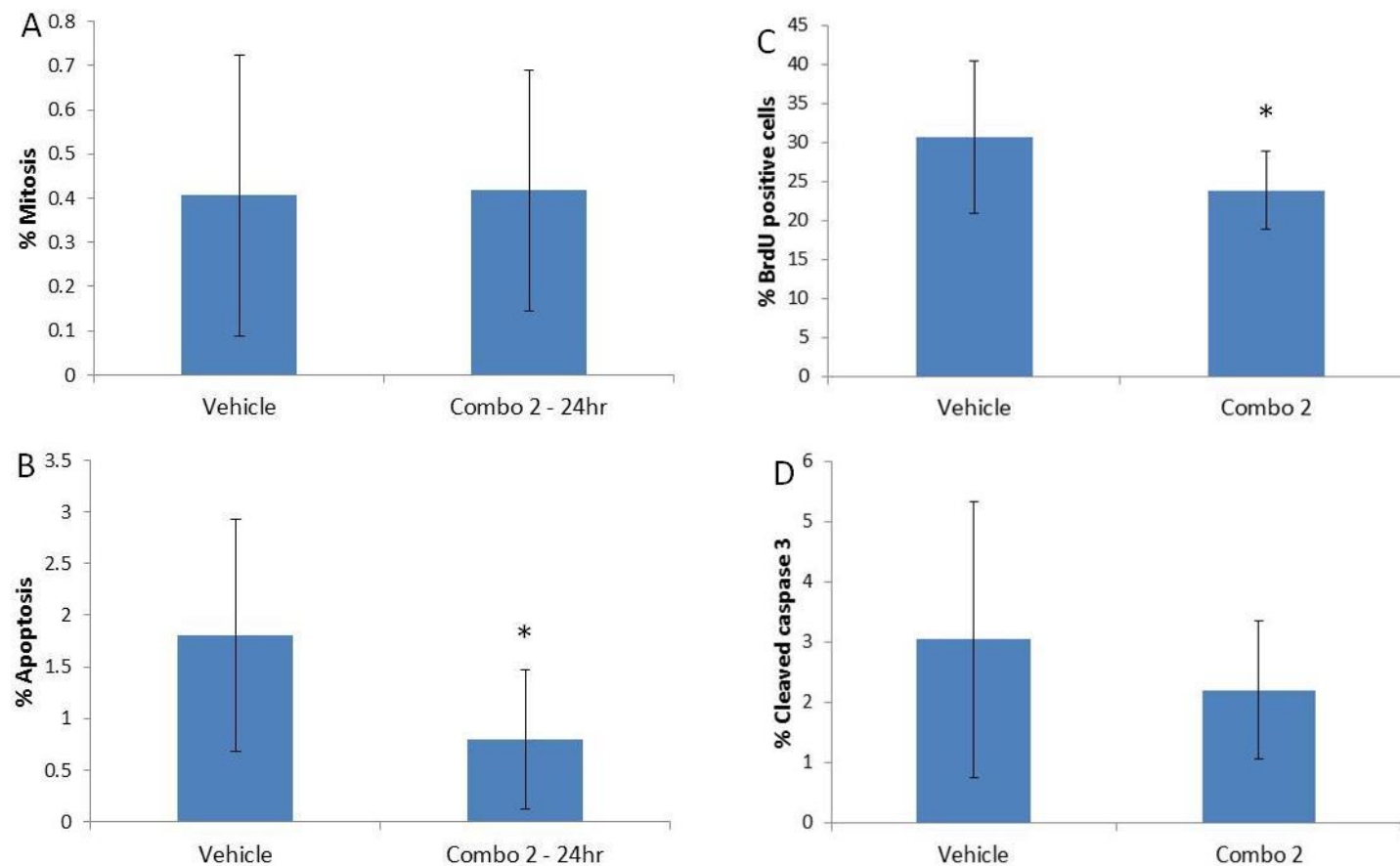


Figure 4.15 Biological effects of combo 2, 24 hours following NVP-BEZ235 exposure in *Apc^{f/+} Pten^{f/f}* small intestine tumours (SITs). Quantification of histological mitotic figures (A), apoptotic bodies (B), the proliferation marker BrdU (C) and the apoptotic marker cleaved caspase 3 (D) revealed a significant reduction in BrdU positive cells and surprisingly, a reduction in histological apoptotic bodies (*p value ≤ 0.05 , $n \geq 3$, Mann Whitney U test). Error bars represent standard deviation.

Given that PI3K/mTOR signalling was not reduced 24 hours after exposure to single agent NVP-BEZ235 and MEK162 caused significantly varied modulation of PI3K/mTOR signalling 24 hours after administration, it was important to examine the pharmacodynamic effects of combo 2 24 hours post exposure. For this, tumours harvested from mice were subjected to whole cell protein extraction and 6 SITs were pooled for western blot analysis of downstream signalling components. Western blotting and subsequent densitometry analysis revealed a significant reduction of all components of the PI3K/mTOR signalling cascade probed including, pAKT at Ser473 and Thr308, pS6RP and p4EBP1 as well as the MAPK pathway component pERK, indicating efficient and prolonged inhibition of both pathways (Figure 4.16, Table 4.8).

	Vehicle	24 hours post Combo 2 (p value)
pERK	5296 ± 457.97	393.20 ± 64.03 (0.0404)
pAKT473	3730.6 ± 303.1	134.69 ± 26.48 (0.0404)
pAKT308	1491.01 ± 254.09	No bands detected
pS6RP	4893.369 ± 428.92	No bands detected
p4EBP1	2031.21 ± 125.08,	No bands detected

Table 4-8 Outline of raw densitometry values from western blot analysis of pooled $Apc^{f/+}$ $Pten^{f/f}$ SITs 24 hours post exposure to combo 2, n=3, One-tailed Mann Whitney U test was used for statistical analysis

These results reveal combo 2 effectively delivers prolonged reduction of MAPK and PI3K/mTOR signalling in $Pten$ deficient tumours and suggests this may be more advantageous in a long term treatment setting, as explored next.

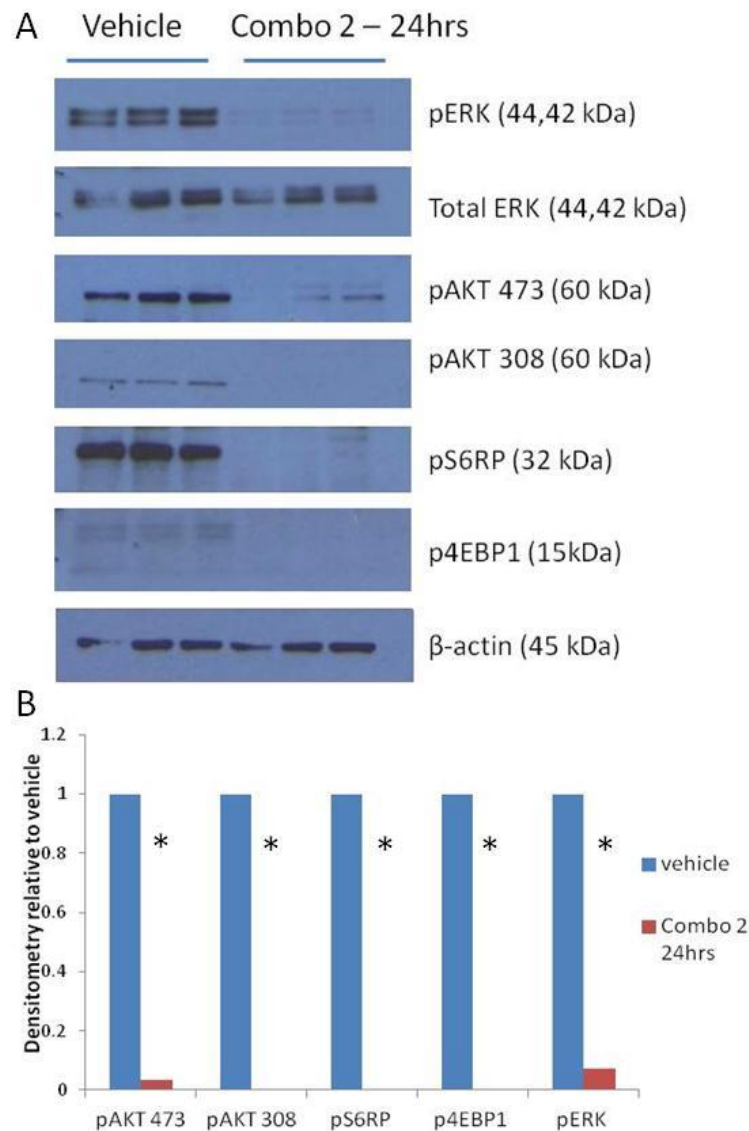


Figure 4.16 Sequencing of combination is crucial for prolonged inhibition of PI3K/mTOR and MAPK signalling in *Apc^{f/+} Pten^{f/f}* small intestine tumours (SITs)

(A) 6 SITs were pooled from n=3 mice exposed to combo 2 for 24 hours were subjected to western blot analysis and probed for effectors of PI3K/mTOR and MAPK signalling. Immunoblotting revealed substantial inhibition of both PI3K/mTOR and MAPK signalling cascades. (B) Densitometry analysis was carried out to quantify differences observed from immunoblotting. These are normalised to β -actin as loading control and represented relative to vehicle controls (*p value = 0.0404, n=3, Mann Whitney U test).

4.2.7 Combined PI3K/mTOR and MEK inhibition increases longevity of $Apc^{f/+}$ $Pten^{f/f}$ mice however it does not provide any additional benefit compared to dual PI3K/mTOR inhibition by NVP-BEZ235

Given the importance of scheduling when administering the combination of PI3K/mTOR and MEK inhibitors in $Apc^{f/+}$ $Pten^{f/f}$ mice in the short term setting, combination strategy 2 (combo 2) was chosen for the chronic treatment regimen to achieve concomitant pathway inhibition. For all single agent long term treatments, inhibitors were administered as a twice daily regimen and so to be comparative, the combination would also require twice daily dosing of both inhibitors (despite effective inhibition of pathways for 24 hours after a single dose of combo 2 – section 4.2.5 and 4.2.6). However, it was not known whether administering combo 2 twice-daily would be well tolerated by mice. To test this, a cohort of n=4 wild type mice were subjected to daily treatment of twice daily combo 2 treatment from 12 weeks of age for a 2 month (8 week) period. Mice were monitored daily and overall body weight was recorded throughout the treatment period. As shown on figure 4.17, the combo twice-daily regimen proved toxic to wild-type mice as overall body weight was shown to be dramatically reduced (approximately 20% reduced) after only 4 days of treatment. Therefore, although this regimen was initiated as an 8 week experiment, as Home Office guidelines prohibit weight loss of more than 20%, mice had to be culled prior to the experimental end point. Of the 4 mice in this cohort, 2 were culled before the experimental end point due to excess weight loss and therefore due to toxicity. Despite reaching the experiment end point, the 2 remaining mice did demonstrate fluctuations in weight – usually weight loss during weekdays whilst on treatment after which weight would increase during the weekend whilst not receiving treatment. This was a clear indication of treatment induced toxicity. Additionally, when compared to relative weights of $Apc^{f/+}$ $Pten^{f/f}$ mice on twice daily 35mg/kg NVP-BEZ235 treatment, the combo twice daily regimen was more variable and therefore a less desirable chronic treatment option.

In light of this toxicity issue, I next investigated a reduced combination dose. NVP-BEZ235 at 35mg/kg twice daily previously demonstrated efficacy in $Apc^{f/+}$ $Pten^{f/f}$ mice (Figure 4.4) and so to be comparable, this dose was kept constant. MEK162 at 30mg/kg twice daily showed no survival benefit (Figure 4.11) and so this dose was reduced to once daily administration 1 hour after the first NVP-BEZ235 dose. This reduced combination dose was administered to a cohort of 13 $Apc^{f/+}$ $Pten^{f/f}$ mice aged to 77 days post induction, as a chronic treatment experiment, to a survival end point. During the experiment, mice were closely monitored and body weights recorded. As depicted in figure 4.17, mice still showed some fluctuations in body weight;

however this was not as extreme as in the combo 2 twice-daily cohort and was well tolerated by the majority of mice.

Chronic administration of 35mg/kg NVP-BEZ235 twice daily plus 30mg/kg MEK162 once daily 1 hour after the first NVP-BEZ235 dose by oral gavage, significantly increased median survival of $Apc^{f/+}$ $Pten^{f/f}$ mice from 99 dpi to 270 dpi (Figure 4.18) (median survival combination mice = 270 dpi, median survival Vehicle mice = 99 dpi, $n \geq 15$, p value ≤ 0.001 , Log-Rank and wilcoxon test). Interestingly however, this treatment showed no significant additional benefit compared to single agent NVP-BEZ235 and in fact the two treatments resulted in comparable median survivals (median survival combination mice = 270dpi, median survival NVP-BEZ235 mice = 266dpi, $n \geq 15$, p value = 0.201 Log Rank test and p value = 0.514 Wilcoxon test). This result indicates a lack of additional synergy from the combination therapy with regards to the survival of animals, despite the favourable short term pharmacodynamic effects. Despite this, I next investigated whether the combination therapy may have had more subtle effects on tumour burden of mice at point of culling as described in section 4.2.8.

Weights of mice on treatment

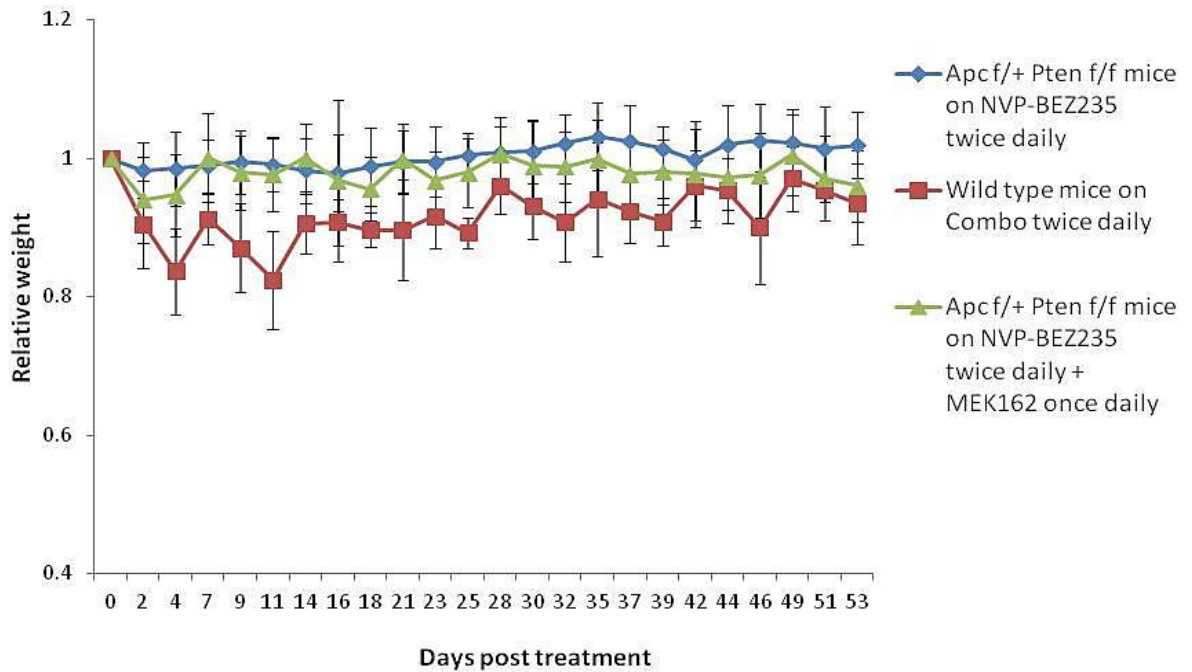


Figure 4.17 Twice-daily combo 2 administration resulted in significant weight loss in wild type mice and so a reduced combination dose, which was better tolerated, was chosen for long term treatment for the $Apc^{f/+}$ $Pten^{f/f}$ tumour model

To investigate whether administration of combo 2 twice-daily would be well tolerated by mice, n=4 wild type mice were dosed the regimen from 12 weeks of age for an 8 week period prior to usage of this combination regimen in tumour models. This led to significant fluctuations in body weight and n=2 mice were sacrificed due to severe weight loss prior to the 8 week experimental end point. Therefore, a reduced combination dose of 35mg/kg NVP-BEZ235 twice-daily plus 30mg/kg MEK162 once daily (1 hour after first NVP-BEZ235 dose) was utilised. This appeared to be better tolerated compared to twice daily combination. Single agent NVP-BEZ235 twice daily was well tolerated in $Apc^{f/+}$ $Pten^{f/f}$ mice and so was chosen as a comparison.

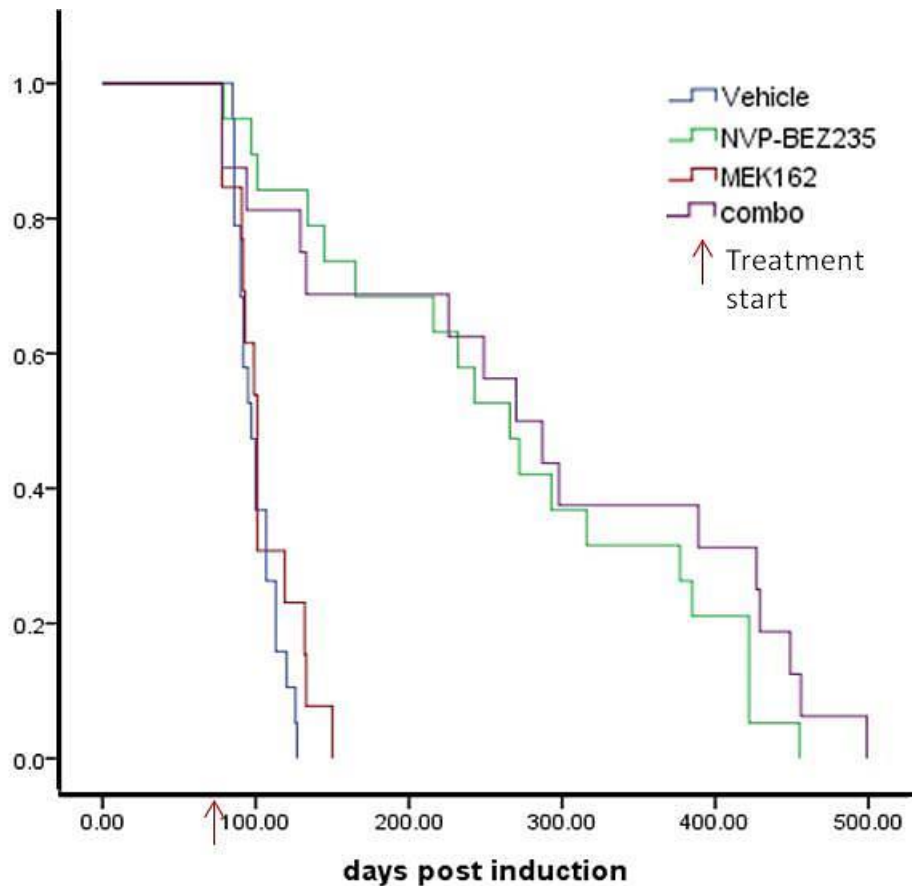


Figure 4.18 Kaplan-Meier survival analysis of $Apc^{f/+}$ $Pten^{f/f}$ mice on combination therapy compared to vehicle and single agent controls

$Apc^{f/+}$ $Pten^{f/f}$ mice were induced and aged to 77 days post induction, at which point mice were randomised to receive either 0.5% Methyl cellulose (Vehicle control) or combination (35mg/kg NVP-BEZ235 twice daily plus 30mg/kg MEK162 once daily, 1 hour after the first NVP-BEZ235 dose) by oral gavage until a survival end point. Continuous combination (combo) administration significantly increased longevity of mice from 99 days (Vehicle) to 270 days post induction (p value ≤ 0.001 Log-Rank and Wilcoxon test $n \geq 15$ mice per cohort). This was also significantly better than single agent MEK162 administration p value ≤ 0.001 Log-Rank and Wilcoxon test $n \geq 13$ mice per cohort) however, combo was not significantly different in comparison to single agent NVP-BEZ235 treatment (p value = 0.201 Log-Rank, p value = 0.514 Wilcoxon test, $n \geq 15$ mice per cohort).

4.2.8 Tumour burden analysis of $Apc^{f/+}$ $Pten^{f/f}$ mice on long term treatments

Long term treatment with single agent NVP-BEZ235 and combined NVP-BEZ235 plus MEK162 significantly increased longevity of $Apc^{f/+}$ $Pten^{f/f}$ mice compared to vehicle treated mice, whereas MEK162 failed to show any efficacy in this setting. To establish the effects of these chronic treatment strategies on tumour burden at the end of treatment, tumours were counted, measured for size and staged according to severity (methods section 2.7.4). Additionally, as intervention with the various treatment regimens was started at a chosen time point, the parameters of tumour burden outlined above were also scored in a cohort of mice culled at day 77 post induction (treatment start time) as a measure of basal levels. The number of tumours present at death for all cohorts was scored on 3 H&E stained slides of small intestine rolls per sample.

At 77dpi (start of treatment) $Apc^{f/+}$ $Pten^{f/f}$ mice possessed a median of 3 tumours per mouse whereas vehicle treated mice at death had a median of 6 lesions (Figure 4.19 A). Importantly, this shows that tumours are present at the start of treatment and although new lesions develop during the course of vehicle treatment, the number of tumours between the two cohorts was not significantly different (p value = 0.1134, $n \geq 11$, Mann Whitney U test). $Apc^{f/+}$ $Pten^{f/f}$ mice on NVP-BEZ235 treatment possessed a median of 2 tumours at time of death which is significantly reduced compared to vehicle but not to the start of treatment (p value = 0.0291 compared to vehicle, p value = 0.2857 compared start cohort), suggesting that NVP-BEZ235 may function by halting initiation of further lesions (Figure 4.19 A). Scoring of lesions in MEK162 treated mice reveal a median of 5 lesions and as expected, this is not significantly altered from the vehicle or start of treatment cohorts (p value = 0.287 for vehicle, p value = 0.325 for start, $n \geq 11$ for each cohort, Mann Whitney U test). Similarly to the NVP-BEZ235 treated cohort, long term combo 2 treated mice possessed significantly reduced tumours at death in comparison to vehicle treated mice and not in comparison to the start cohort (median number of lesions at death combo = 4, vehicle = 6, start cohort = 3, p value = 0.0362 for vehicle, p value = 0.584 for start, $n \geq 11$, Mann Whitney U test). This again suggests treatment has an effect on further tumour initiation (Figure 4.19 A). Interestingly, there is no significant difference between NVP-BEZ235 treated and combination treated mice with regards to tumour number at death, further suggesting lack of cooperation or synergy in the context of *Pten* deficient tumours (number of lesions at death: NVP-BEZ235 = 2, combo = 4 p value = 0.8183, $n \geq 11$, Mann Whitney U test).

To address whether the size of lesions was affected by treatment, macroscopic tumours were measured from methacarn fixed small intestines and the total tumour area (in mm²) was calculated per mouse in each cohort (Figure 4.19 B). *Apc^{f/+} Pten^{f/f}* mice on vehicle treatment trended to possess larger tumours at death compared to the start cohort, however this was not significantly different (start = 37.8 ± 39.38 n=13, vehicle = 53.21 ± 32.48 n = 4, p value = 0.174, Mann Whitney U test). Similarly, a trend for larger small intestinal tumours at death was observed in NVP-BEZ235 and combination treated mice compared to vehicle and the start cohort, but again this was not significant (vehicle = 53.21 ± 32.48 n = 4, NVP-BEZ235 = 81.57 ± 44.76 n = 7 and p value = 0.508, combo = 108.23 ± 81.28 n = 5 and p value = 0.2207 Mann Whitney U test), due to large variation within the cohorts. As expected, tumours in mice on long term MEK162 treatment were not significantly altered in size compared to vehicle treated or the start cohort (vehicle = 53.21 ± 32.48 n = 4, mek162 = 66.61 ± 26.2 n=4, p value = 0.665 Mann Whitney U test) (Figure 4.19 B).

Lastly, for tumour burden analysis, tumours on H&E stained sections of the small intestine were staged according to severity and invasive characteristics as described in section 2.7.4. These stages refer to microadenomas (mAd) or single crypt lesions, benign adenomas (Ad) with no signs of invasion, early invasive adenocarcinomas (EIA) identified by submucosal invasion, and advanced invasive adenocarcinomas (AIA) characterised by invasion into the muscle wall and the underlying serosa. The average number of these per cohort were calculated and displayed in figure 4.17 C as a proportion of the total number of tumours scored. This was due to a difference in the total number of tumours observed between the various treatment cohorts, as described previously (figure 4.19 B). The proportion of microadenomas observed was found to be unchanged between all groups: 17.4% in the start cohort (n=11), 19.3% in the vehicle cohort (n=15), 14.3% in NVP-BEZ235 treated mice (n=14), 17.6% in MEK162 treated mice (n=11) and 25% in combination treated mice (n=14) (p value ≥ 0.05 for all comparisons) (Figure 4.19 C). The proportion of adenomas was found to be significantly reduced in all treated cohorts in comparison with the start cohort (start = 60%, vehicle = 44% p value = 0.027, NVP-BEZ235 = 33% p value = 0.0038, MEK162 = 41% p value = 0.0086, combo = 12.5% p value = 0.0002, n≥8, Mann Whitney U test) and in combination treated mice, compared to the vehicle cohort (p value = 0.0011, n≥8, Mann Whitney U test). The proportion of EIAs is statistically unaltered in all cohorts however, a trend towards increased proportion of EIAs was notable in vehicle and MEK162 cohorts compared to the start cohort (Start cohort = 22%, vehicle = 28% p value = 0.161, NVP-BEZ235 = 20% p value = 0.954 for start cohort and p value = 0.249 for vehicle cohort, MEK162 = 31% p value = 0.158

for start cohort and p value = 0.795 for vehicle cohort, combo = 23% p value = 0.743 for start cohort and p value = 0.126 for vehicle cohort, $n \geq 8$, Mann Whitney U test). Interestingly, a significant increase in the proportions of AIAs was observed in NVP-BEZ235 and combination treated cohorts, suggesting that a larger proportion of tumours were more invasive and that the $Apc^{f/+}$ $Pten^{f/f}$ mice were able to tolerate such an increase in severity of tumours (proportions of AIAs: start = 0, vehicle = 8%, NVP-BEZ235 = 33% p value = 0.0121, MEK162 = 10% p value = 0.856, combo = 40% p value = 0.0095, $n \geq 8$, Mann Whitney U test) (Figure 4.19 C).

Interestingly at dissection, $Apc^{f/+}$ $Pten^{f/f}$ mice on NVP-BEZ235 were noted to have abnormal livers compared to vehicle treated animals, in which large macroscopic lesions were clearly identifiable. Closer pathological analysis of H&E stained sections of the liver identified the large white lesions as well differentiated hepatocellular tumours with trabeculae scanti-mitosis, mild to moderate nuclear pleomorphisms and no definite invasion of adjacent parenchyma or of intra hepatic blood vessels however, occasional tumours showed focal necrosis². Further comparisons of whole cohorts identified tumours to be present in 50% of animals exposed to chronic NVP-BEZ235 compared to none of the vehicle treated mice. Additionally, hepatocellular tumours were not identified in MEK162 mice however interestingly, only 7% of $Apc^{f/+}$ $Pten^{f/f}$ mice on combo treatment were identified to present with these tumours (Figure 4.20).

² pathological description of hepatocellular tumours was provided by Professor Geraint Williams, Cardiff University, School of Medicine

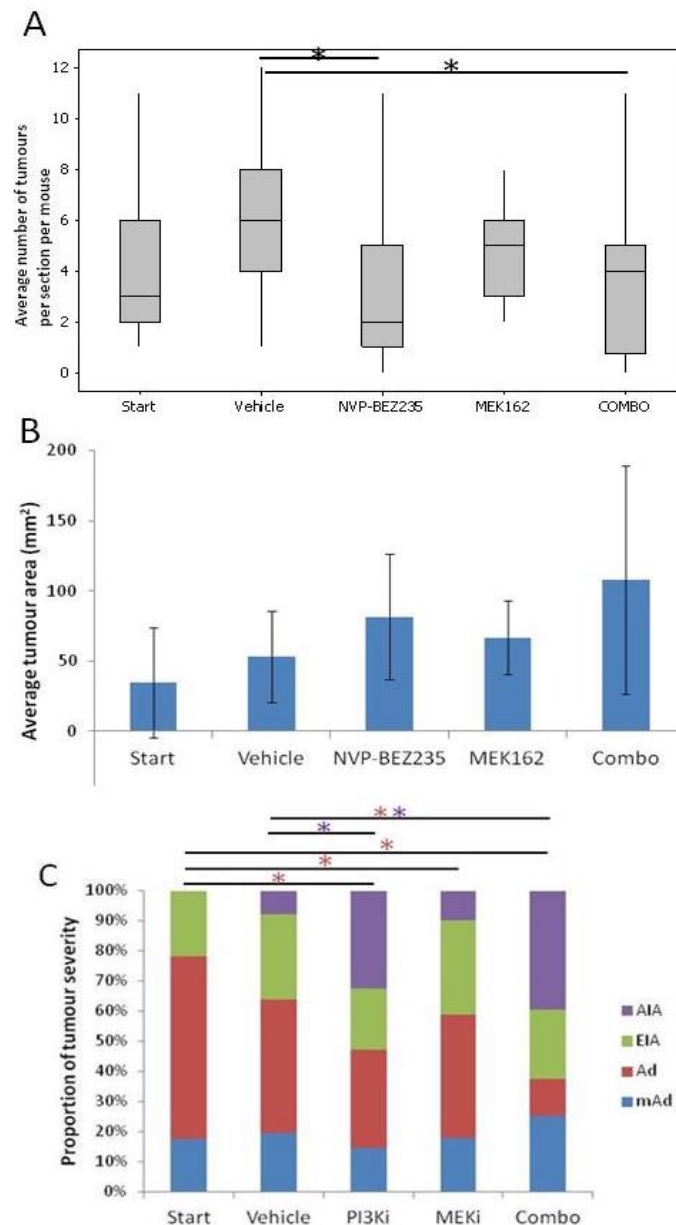


Figure 4.19 Analysis of tumour burden in $Apc^{f/+} Pten^{f/f}$ mice

(A) $Apc^{f/+} Pten^{f/f}$ mice on NVP-BEZ235 and combo had significantly less tumours at death compared to vehicle controls (p value = 0.0291 for NVP-BEZ235 and p value = 0.0362 for combo, $n \geq 11$, Mann Whitney U test). **(B)** No significant alterations were observed when comparing tumour area, however NVP-BEZ235 and combo treated mice trended to have larger tumours at death, compared to the start and vehicle treated cohorts (p value ≥ 0.05 , $n \geq 4$, Mann Whitney U test). **(C)** Key: mAd – microadenoma, Ad – adenoma, EIA – early invasive adenocarcinoma, AIA – advanced invasive adenocarcinoma. Staging of tumours at death reveals no alterations in the proportions of microadenomas across the cohorts, a significant reduction in adenomas in all treated cohorts, in comparison with the start cohort but also the proportion of adenomas was reduced in combination treated mice, compared to the vehicle cohort (*p value ≤ 0.05 , Mann Whitney U test). Additionally, although no significant differences were detected in the proportions of EIAs, the proportion of AIAs was significantly increased in NVP-BEZ235 and combo treated mice.

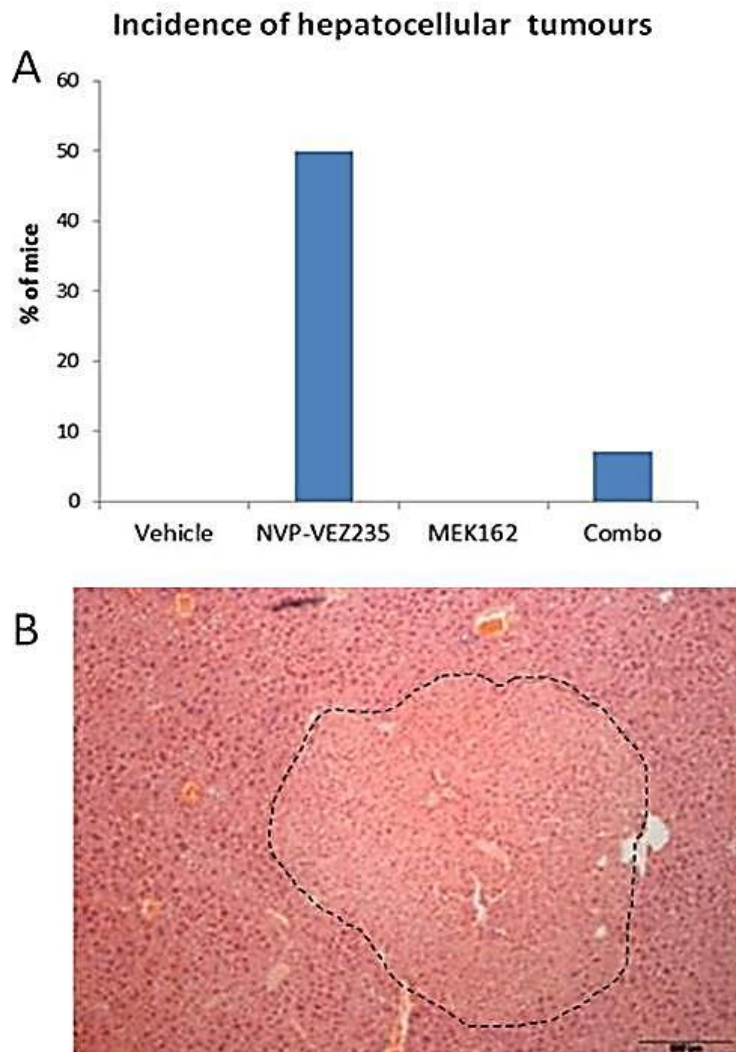


Figure 4.20 Incidence of liver tumours in $Apc^{f/+} Pten^{f/f}$ mice on long term treatment

(A) Analysis of liver tissue indicated 50% of mice on NVP-BEZ235 developed hepatocellular tumours, approximately 7% of mice on Combo had liver lesions whereas none of the mice on Vehicle or MEK162 developed HCC **(B)** H&E image of hepatocellular tumour (dashed lines used to highlight an example of a lesion).

4.3 Discussion

4.3.1 *NVP-BEZ235 leads to inhibition of PI3K and mTOR signalling whilst imposing anti-proliferative and pro-apoptotic effects in Pten deficient small intestinal tumours and long term, substantially increasing longevity of mice*

The therapeutic potential of targeting the PI3K pathway in the context of PI3K activated CRC was assessed in the AhCreER Apc^{f/+} Pten^{f/f} mouse model (Marsh et al., 2008) using the potent dual PI3K/mTOR inhibitor NVP-BEZ235. The mouse model used in this chapter is a robust and relatively quick model of invasive adenocarcinoma driven by activation of AKT and mice usually succumb to disease by 100 days post induction. Therefore, the main aim of this chapter was to inhibit the primary pathway driving tumourigenesis in this model. For all experiments described in this chapter, 10 week old mice were induced via i.p. injections of Tamoxifen and β NF and aged, either until symptomatic of disease or until the chosen treatment start point. Mice which presented with symptoms of tumour burden were also administered short term doses of NVP-BEZ235 to investigate anti-tumour and pharmacodynamic effects.

NVP-BEZ235 resulted in complete inhibition of PI3K and mTOR signalling, as observed by the reduction in levels of pAKT at Ser473 and Thr308, pS6RP and p4EBP1 4 hours after exposure (Figure 4.3). As described previously, the serine-threonine kinase AKT is a major effector of PI3K signalling and has well established roles in mediating cellular growth and survival. AKT is known to bind to accumulated PIP₃ at the plasma membrane which in turn allows PDK1 into the 'activation loop' of AKT where it is able to phosphorylate Thr308 and hence activate AKT (Alessi et al., 1997). This, in turn, is sufficient to activate a number of proteins including mTORC1 (complex 1) which mediates activation of S6RP and 4EBP1, important for a number of cellular processes including, translation of mRNAs that encode cell cycle regulators such as MYC and cyclin D1 (Rini, 2008). For full activation of AKT, phosphorylation at Ser473 in the carboxy-terminal hydrophobic motif by mTORC2 is required and is thought to lead to a number of substrate-specific phosphorylation events including phosphorylation of pro-apoptotic FOXO proteins (Guertin et al., 2006). As well as inhibition of signalling, NVP-BEZ235 in Pten deficient tumours also induced potent anti-tumour effects, evidenced by a reduction in BrdU positive cells and an increase in cleaved caspase 3 4 hours after administration (Figure 4.2). This is in accordance with previous studies which have reported the cytotoxic effects of NVP-BEZ235 in a number of cell lines (Haagensen et al., 2012, Blaser et al., 2012), and also that Pten null cell lines are particularly sensitive to the compound (Maira et al., 2008). The later

observations were further corroborated by Mueller et al., in a study which found PI3K mutated cells to be more sensitive to the effects of NVP-BEZ235 than wild-type cells (Mueller et al., 2012). These anti-tumour effects may be attributable to inhibition of signalling given the role of the PI3K cascade in promoting cellular growth and inhibition of apoptosis (Cantley, 2002).

Given that pathway inhibition and anti-tumour effects of NVP-BEZ235 were only detected 4 hours after exposure, and that the majority of these had reached basal levels by 8 and 24 hours (Figure 4.3), a twice-daily administration regimen was anticipated to lead to potent anti-tumour effects long term. Mice were randomised at 77 days post induction to receive 0.5% Methyl cellulose (MC, Vehicle) or 35mg/kg NVP-BEZ235 by oral gavage to firstly evaluate the long term therapeutic potential of PI3K/mTOR inhibition by NVP-BEZ235 and secondly to determine its effect on tumour burden. Chronic administration of NVP-BEZ235 led to a significant increase in survival of mice from a median of 99 days to 266 days post induction, clearly indicating the benefits of PI3K and mTOR inhibition in this Pten deficient tumour setting (Figure 4.5). Additionally, at death, mice possessed fewer tumours than vehicle treated mice indicating treatment prevented growth of further tumours. Despite the fact that mice bore fewer tumours, these tumours trended to be larger than vehicle treated mice and proportionally, more invasive lesions were detected. This suggests that the rate of tumour growth is reduced, however as mice survived longer, tumours at death are larger as they have had a longer period in which to grow and become invasive (Figure 4.19). Given the trend towards increased tumour area following long term NVP-BEZ235, the component of stromal tissue within the tumours was also evaluated to investigate whether treatment influenced the stromal component of tumours (data not shown). This included scoring of total stromal tissue versus epithelial tissue and evaluation of vascularisation through scoring of CD31 positive vessels. Although no significant difference was detected between vehicle and NVP-BEZ235 treated tumours in this case, the importance of drug treatment on tumour stroma is well documented within the literature. Cancer cells are known to alter their stroma and supportive environment to allow tumour progression or regression by modulating production of stroma modulating factors such as basic FGF, VEGF, PDGF, EGFR, interleukins, colony stimulating factors, etc (Mueller and Fusenig, 2004). These factors are known to disrupt tissue homeostasis in a paracrine manner and can lead to stromal reactions such as angiogenesis and inflammatory responses (Bergers and Benjamin, 2003, Coussens and Werb, 2002).

Alterations of the PI3K pathway have been implicated in tumour development and progression of human cancer for some time now, and this has rightfully led to a surge in development of inhibitors which target multiple components of the pathway. However, the evaluation of PI3K

inhibitors for PI3K mutant cancers is limited, primarily as these mutations tend to co-exist with those activating MAPK signalling for example Ras and B-raf. NVP-BEZ235 has previously been assessed in the autochthonous p110 α H1047R mouse model of lung cancer where acutely, treatment led to reduced PI3K/mTOR signalling through pAKT, pS6RP and p4EBP1 and long term, NVP-BEZ235 led to reduced 18FDG avidity measured by PET imaging, as well as reduced tumour size (Engelman et al., 2008). The evidence presented in this chapter is the first study in an autochthonous model that establishes activity against PI3K activated intestinal cancer. Together, these studies provide rationale for stratification of PI3K mutant tumours in clinical trials.

4.3.2 MEK inhibition through MEK162 reduces MAPK signalling in Pten deficient tumours, however does not increase survival of mice potentially through increased PI3K signalling

Having established that targeting PI3K signalling using the dual PI3K/mTOR inhibitor NVP-BEZ235 is beneficial in this Pten deficient mouse model of colorectal cancer, concomitant inhibition of MAPK signalling was next investigated. Prior to that however, the effects of single agent MEK inhibition was established in this model. This involved short term experiments with MEK162, to investigate pharmacodynamic and anti-tumour effects, as well as a long term therapeutic intervention study to investigate the effect on survival and tumour burden.

Interestingly, a single dose of MEK162 led to prolonged reduction in cellular proliferation observed by a reduction in BrdU positive cells, and prolonged pathway inhibition evidenced by reduction of pERK abundance in this Pten deficient setting (Figure 4.7, 4.8). This is contrary to a number of previous reports which have found mutations activating the PI3K pathway to be intrinsically resistant to MEK inhibition (Balmanno et al., 2009, Chen et al., 2012b, Dry et al., 2010). Interestingly, MEK162 initially lead to a reduction in PI3K and mTORC1 signalling evidenced through reduced pAKT308 and pS6RP at 4 hours after exposure. However, MEK162 then lead to an increase in PI3K signalling through pAKT at Ser473 and Thr308 but a reduction in mTORC1 signalling through pS6RP and p4EBP1 at 24 hours post MEK162 exposure (Figure 4.8). There are a number of mechanisms reported in the literature, by which ERK regulates PI3K/AKT signalling. Reduction of pERK through inhibition of MEK has previously shown to lead to an increase in EGF stimulated association of GAB1 which in turn was shown to increase PI3K activity and AKT signalling (Yu et al., 2002). Also, MEK inhibition has previously led to downregulation of mTORC1 signalling, therefore relieving feedback inhibition of PI3K signalling through IGFR-1R/IRS and subsequently leading to activation of PI3K signalling (Ebi et al., 2011).

Additionally, pERK has been shown to directly regulate tyrosine phosphorylation of EGFR in the context of a Ras mutation and subsequently increase signalling downstream the receptor (Wong et al., 2002). Although it remains unclear as to the mechanism through which PI3K signalling is increased in response to MEK inhibition 24 hours post exposure, the observation that p110 α was found to be increased, together with the corresponding increase in pAKT, suggests the mechanism may be any one of those highlighted above (Figure 4.9).

Additionally, the mechanism by which MEK162 administration reduces PI3K and mTOR signalling (observed at 4 hours following MEK162 exposure) is also unknown. Both pERK and one of its substrates p90RSK have been shown to phosphorylate and inhibit activity of Gsk3 (Cohen and Frame, 2001). Gsk3 functions as a negative regulator of Pten and has previously been shown to alleviate Pten inhibition and decreasing PI3K signalling (Al-Khouri et al., 2005). Despite this, complete deletion of Pten in these tumours suggests Gsk3 may not be responsible for the reduced PI3K signalling. Interestingly, similar effects were observed in Apc^{f/+} colon tumours following acute MEK162 exposure, in section 3.2.2. It was previously suggested this could be due to the alternative effects of the p90RSK downstream pERK, as was described previously in chapter 3.3.1, and may be responsible for the similar effects observed in the Pten deficient tumours in this chapter.

Nevertheless, despite the initial inhibition of MAPK signalling, long term MEK inhibition proved to be ineffective in Pten deficient tumours, in accordance with previous reports (Balmanno et al., 2009, Chen et al., 2012b, Dry et al., 2010). This is at least, with respect to survival (Figure 4.9), the end number of tumours, tumour area and tumour severity profiles (Figure 4.17). However, given a number of studies have reported synergistic effects with simultaneous PI3K/Akt and MEK/ERK inhibition (Haagensen et al., 2012, Martinelli et al., 2013), this was next investigated in the context of Pten deficient intestinal tumours.

4.3.3 Sequencing of PI3K/mTOR and MEK inhibitors is crucial for concomitant inhibition of signalling cascades

The hypothesis for combined targeting of PI3K/AKT and RAS/MEK/ERK signalling is well documented, given the close association and convergence of the two pathways (Aksamitiene et al., 2012). A number of studies have assessed this hypothesis in cell lines (Haagensen et al., 2012, Liu and Xing, 2008, Yu et al., 2008, Martinelli et al., 2013) and murine models of human cancer including a Pten null and Kras activated ovarian cancer model (Kinross et al., 2011), PIK3CA and KRAS mutant lung cancer model (Engelman et al., 2008) and in PIK3CA and KRAS activated colon, pancreatic and lung cancer xenografts (Halilovic et al., 2010). However,

evaluation of the combination therapy has been less well characterised for only Pten deficient and hence PI3K activated only tumour settings.

To evaluate combination therapy in our Pten deficient mouse model, I first performed short term pharmacodynamic and anti-tumour experiments to identify the most desirable dosing strategy. Interestingly, western blotting revealed that $Apc^{f/+}$ $Pten^{f/f}$ SITs are particularly sensitive to the scheduling of both inhibitors (Figure 4.14). Administration of NVP-BEZ235 1 hour prior to MEK162 completely inhibited PI3K/mTOR and MAPK signalling for 24 hours (Figure 4.14, 4.16), whereas MEK162 administered 1 hour prior to or at the same time as NVP-BEZ235 resulted in less effective pathway inhibition. This was surprising, particularly given modulation of PI3K and mTOR signalling observed immediately following MEK inhibition. The reasons for this are currently unclear however it may be possible that PI3K signalling was efficiently reduced within the first hour following administration of NVP-BEZ235 and so therefore, MEK inhibition simply added to this inhibition of signalling given that reduction in pAKT Thr308 and pS6RP was observed following single agent MEK inhibition 4 hours after administration (Figure 4.8).

Previous studies investigating the acute effects of combined PI3K/mTOR and MEK inhibition in CRC have predominantly evaluated effects on signalling in cancer cell lines which differ in mutation status of the PI3K pathway. Martinelli et al. reported effective inhibition of pERK and pAKT, reduced pS6RP and p4EBP1 levels, reduced cell cycle progression and increased apoptosis with combinations of the MEK inhibitor Pimasertib and PI3K inhibitor MSC 2208382, mTOR inhibitor everolimus and multi-kinase inhibitors Sorafenib and regorafenib in HT15 cancer cells (Kras and PI3KCA mutant) (Martinelli et al., 2013). Interestingly, Haagensen et al found moderate inhibition of pAKT and pERK with combinations of the dual PI3K/mTOR inhibitor NVP-BEZ235 and MEK inhibitor PD0325901 in HCT116 (Kras and PIK3CA mutant) and HT29 (B-raf and PIK3CA mutant) cell lines. The effects of this combination in comparison with combination of PI3K inhibitor GDC-0941 and MEK inhibitor PD0325901 was markedly reduced suggesting a role for additional mTOR inhibition in reducing the synergy between PI3K and MEK inhibitors. Addition of the mTOR inhibitor KU0063794 to the later combination (PI3K and MEK) provided further evidence of compromised synergy suggesting that mTOR dependent inhibition of p4EBP1 may be responsible for preventing synthesis of proteins that negatively regulate cell cycle progression, causing synergy between PI3K and MEK inhibitors to be compromised (Haagensen et al., 2012). Despite this, the authors provide no indication of which proteins may be responsible for this. The observations from acute combination studies in this chapter have not previously been reported. This may be due to differences in

compounds or experimental systems used, for example *in vivo* metabolism of the compounds in combination may affect their target inhibition ability in comparison with *in vitro* culture systems in which compounds are administered to cells much quicker. Although further evaluation of PI3K and MAPK signalling components is required to determine the distinct mechanism behind the differential effects of combined NVP-BEZ235 and MEK162 in $Apc^{f/+}$ $Pten^{f/f}$ tumours, the modulation of signalling observed here is novel and highlights the necessity of such experiments, especially when the pathways targeted are closely associated.

Despite this, when taken forward for the long term survival experiment, combination therapy failed to provide any additional benefit compared to single agent NVP-BEZ235 treatment (Figure 4.18, 4.19). Mice on long term NVP-BEZ235 and combination had similar median survivals (NVP-BEZ235 = 266 days vs combo = 270 days post induction) and the number of tumours at death were not significantly altered (NVP-BEZ235 = 2 vs combo = 4 tumours). Similarly, although there was a trend towards an increase in total tumour area, this was not significantly different (median tumour size: NVP-BEZ235 = 81.6mm^2 vs combo = 108.2mm^2) and finally, assessment of tumours revealed the profiles did not differ with regards to invasiveness (Figure 4.19).

One stark difference observed at dissection and subsequent analysis was that the incidence of HCC was dramatically reduced in mice which received long term combo compared to those of long term NVP-BEZ235 (Figure 4.20). Although the AhCreER transgene is predominantly used to drive recombination in the small intestinal epithelium, it is also known to drive recombination in a number of other tissues including the liver, fore stomach, gall bladder and prostate (Ireland et al., 2004). In the liver, AhCreER driven *Pten* loss has previously been shown to result in liver steatosis and hepatomegaly (Marsh et al, unpublished observations) and in one case, this lead to HCC. These findings corroborate previous phenotypes reported in the literature from hepatocyte specific deletion of *Pten* using a cre recombinase transgene driven by the Albumin gene (Horie et al., 2004, Stiles et al., 2004). Interestingly, the Wnt signalling pathway is also known to have a major role in development of HCC. Here, abnormal regulation of the transcription factor β -catenin appears to be a major early event in HCC development (de La Coste et al., 1998). Additionally, mutations in *Axin1* and promoter methylation of *Apc* which lead to gene inactivation are also implicated in HCC (Taniguchi et al., 2002, Yang et al., 2003) however importantly, these are not sufficient to cause HCC. The lack of HCC in compound $Apc^{f/+}$ $Pten^{f/f}$ mice is most likely due to the severe intestinal tumour phenotype, therefore it is hypothesised that mice with increased survival due to NVP-BEZ235 treatment had a longer period in which to allow development of HCC phenotypes. It was

surprising however to find that although mice on NVP-BEZ235 and combination treatments had a comparable median survivals, combination treated mice had a substantially lower incidence of HCC (7% of combo treated mice compared to 50% of NVP-BEZ235 treated mice) (Figure 4.20). These findings suggest perhaps MEK inhibition in liver cells prevented growth of tumours. Although RAS and RAF mutations are rare in HCC, the importance of MAPK signalling in HCC has previously been highlighted by preclinical studies showing that the MEK inhibitor AZD6244 displayed significant anti-tumour activity in primary HCC cells and xenografts (Huynh et al., 2007b, Huynh et al., 2007a).

4.3.4 Summary

In summary, the work described in this chapter highlights the benefits of targeting PI3K and mTOR signalling through NVP-BEZ235 for Pten deficient intestinal tumours. Furthermore, I provide evidence corroborating previous findings that mutations activating the PI3K pathway predict non-response to MEK inhibition. Finally, although combinatorial MEK and PI3K inhibition failed to provide any additional benefit for Pten deficient tumours with respect to survival of mice, work in this chapter describes novel sensitivities of Pten deficient tumours to the sequence of combination drug administration to achieve concomitant inhibition of both PI3K/mTOR and MAPK signalling pathways.

4.4 Further work

4.4.1 Mechanisms of resistance to chronic single agent NVP-BEZ235

The findings in this chapter highlight PI3K and mTOR targeting to be a beneficial therapeutic strategy for Pten deficient and hence PI3K activated intestinal tumours. Despite this, resistance to targeted agents is a common obstacle in the success of these agents and so further characterisation of $Apc^{f/+}$ $Pten^{f/f}$ tumours exposed to long term NVP-BEZ235 treatment may provide insightful observations. IHC for PI3K pathway effects together with scoring of proliferation and apoptosis could identify whether tumours were still responding to NVP-BEZ235 at death. Furthermore, this could be correlated to tumour severity to determine whether tumour progression is associated with non-response of tumours to NVP-BEZ235.

4.4.2 Further evaluation of the differential sensitivities to acute combination treatment

Investigation of the three combination strategies in $Apc^{f/+}$ $Pten^{f/f}$ tumours revealed that administration of MEK162 1 hour prior to, or at the same time as NVP-BEZ235 prevented effective inhibition of both PI3K and MAPK signalling pathways 4 hours following the final

dose. Investigation of signalling components and potential mechanisms of cross-talk at 4 hours and further time points for example 1, 2, 3, 8 or 12 hours following exposure may help identify the mechanism behind these observations.

5 *Investigating MEK inhibition and PI3K/mTOR inhibition in the $Apc^{f/+}$ $Kras^{LSL/+}$ colorectal cancer mouse model*

5.1 *Introduction*

In chapter 3, I described work indicating that MEK inhibition leads to a significant survival benefit in the absence of hyper-activated MAPK signalling through the RAS-RAF-MEK-ERK kinase cascade. This pathway is known to be crucial for mediating signals that regulate proliferation, differentiation, apoptosis and cellular growth, and is often found to be deregulated in a number of human cancers, including pancreatic, lung and ovarian cancer (Downward, 2003). The oncogene KRAS is frequently altered in cancer and in particular, is found to be mutationally activated in approximately 50% of human CRC (Bos et al., 1987). Oncogenic Kras has been implicated in the activation of PI3K signalling through direct interaction with the p110 catalytic subunit of PI3K (Kodaki et al., 1994) and MAPK signalling through subsequent phosphorylations of RAF, MEK and ERK. Thus, the notion (and confirmation of this in Kras mutant colon tumours, as observed in chapter 3) that aberrant activation of Kras results in a 'double hit' causing activation of both PI3K and MAPK signalling in cancer cells, has led to the investigation of MAPK and PI3K inhibitors as rational therapeutic strategies for Kras mutant cancers.

Several studies have evaluated inhibition of MAPK and PI3K signalling independently and concurrently in Kras mutant tumour models. Perturbation of MAPK signalling through potent MEK1/2 inhibitors, has been well characterised in the Kras driven genetically engineered mouse model for lung cancer (Engelman et al., 2008, Holt et al., 2012, Chen et al., 2012b, Simmons et al., 2012, Corcoran et al., 2013). Furthermore, these studies have also investigated combined PI3K or mTOR inhibition. The study by Engelman et al. found that addition of dual PI3K/mTOR inhibitor NVP-BEZ235 enhanced activity of the MEK inhibitor AZD6244 in this setting and similarly, Simmons et al. highlighted that addition of the dual PI3K/mTOR PF-04691502 to MEK inhibitor PD-0325901 increased target inhibition and further reduced tumour burden in the same tumour model (Engelman et al., 2008, Simmons et al., 2012). A recent study by Holt et al. found that combination of MEK inhibitor AZD6244 and mTOR inhibitor AZD0855 was well tolerated and increased anti-tumour efficacy in NSCLC xenograft models (Holt et al., 2012). Interestingly, a Kras driven GEMM for pancreatic cancer was found to be more sensitive to MEK inhibition (through AZD6244) than PI3K inhibition (through

GDC0941), but that the combination of inhibition resulted in an enhanced effect (Hofmann et al., 2012). Furthermore, Williams et al. found that the radiosensitising activity of MEK inhibitor PD0325901 was potentiated by the AKT inhibitor AP1-2 in Kras mutant pancreatic xenografts (Williams et al., 2012). For CRC however, the evaluations of MEK and PI3K inhibitors in the Kras mutant setting is mostly limited to studies in cancer cell lines and xenograft models. A recent study by Jing J et al. profiled sensitivity to the MEK inhibitor GSK1120212 in over 200 cancer cell lines and identified that RAS/RAF mutations were strong predictors of sensitivity whereas PI3K/PTEN mutations conferred cytostatic responses in CRC cell lines (Jing et al., 2012). Additionally, Tentler et al. found that Kras mutant colon cancer cell lines, xenografts and patient derived xenografts were most likely to respond to the MEK inhibitor AZD6244 (Tentler et al., 2010). Furthermore, Yeh et al. evaluated Kras as a biomarker for MEK inhibition and found mutations in Kras tend to predict response to MEK inhibition in cancer cell lines. Although the observations from studies outlined here allude to the benefits of MEK inhibition in the Kras mutant setting, the proof of principle experiment in an autochthonous mouse model has yet to be reported. Additionally, the therapeutic potential of PI3K signalling alone and concurrently with MAPK inhibition has yet to be evaluated in the Kras mutant intestinal cancer setting.

In light of these observations, in this chapter, I aimed to evaluate MEK inhibition and PI3K/mTOR inhibition as monotherapies and in combination in a clinically valid mouse model of intestinal cancer mutant for Kras. Here, the activation of the endogenously expressed G12V (glycine to valine at codon 12) mutant Kras allele and heterozygous deletion of Apc within the intestinal epithelium driven by the VillinCreER transgene leads to a reduced lifespan and progression of both colonic and small intestinal lesions (Janssen et al., 2006). Therefore, I first evaluated acute MEK inhibition by MEK16 in the resulting Kras mutant colon and small intestinal tumours (SITs) to investigate the anti-tumour and pharmacodynamic effects, followed by a long term dosing experiment to deduce the therapeutic potential of MEK inhibition for Kras mutant cancer using this autochthonous genetically engineered mouse model (GEMM).

Given the role of mutant Kras in activating PI3K signalling, I next evaluated targeting this pathway utilising the dual PI3K and mTOR inhibitor NVP-BEZ235 (Novartis Pharmaceuticals) alone and in combination with MEK162. Similarly, acute and chronic administration methods were utilised to investigate the potential *in vivo* anti-tumour and pharmacodynamic effects, and survival benefit respectively.

Similarly to chapters 3 and 4, two main strategies were employed for these investigations. Firstly, tumour bearing VillinCreER $Apc^{f/+}$ $Kras^{V12LSL/+}$ mice (hereon referred to as $Apc^{f/+}$ $Kras^{LSL/+}$ mice) were administered a single dose of MEK162, NVP-BEZ235 or a combination of both and harvested at 4 or 24 hour time points to investigate the immediate anti-tumour and pharmacodynamic effects. To evaluate the effect of treatment on survival, tumour bearing $Apc^{f/+}$ $Kras^{LSL/+}$ mice were started on daily treatment at a chosen time point either until a survival end point (when mice were symptomatic of disease defined by pale feet, anal bleeding, bloating, weight loss) or until an experimental end point of 500 days post induction. Similarly in chapter 3, a 500 days post induction time point was chosen due to the increased latency $Apc^{f/+}$ $Kras^{LSL/+}$ mice have for tumour development and subsequent death, in comparison to $Apc^{f/+}$ $Pten^{f/f}$ mice. Therefore, it was hypothesised that a 500 day window following induction was sufficient time to observe any significant survival benefit.

5.2 Results

5.2.1 *MEK162 results in a pro-apoptotic effect in $Apc^{f/+}$ $Kras^{LSL/+}$ tumours and reduces MAPK signalling through reduced phosphorylated ERK*

For all short term experiments described in this chapter, 10 week old $Apc^{f/+}$ $Kras^{LSL/+}$ mice were induced using tamoxifen (methods 2.2.2) and aged until symptomatic of disease (pale feet, bloating, blood in faeces). A cohort of $n \geq 3$ mice were then administered 0.5% MC (vehicle) and culled 4 hours after, or 30mg/kg MEK162 and harvested at either 4 or 24 hour time points. Additionally, a dose of BrdU was administered to mice 2 hours prior to culling. At dissection, colon and SITs were quickly snap frozen in liquid nitrogen and the whole colon and small intestine was 'swiss-rolled' and fixed in formalin in preparation for H&E staining and IHC, as outlined in section 2.4.

To evaluate the anti-tumour activity of MEK162 in $Apc^{f/+}$ $Kras^{LSL/+}$ colon and SITs, mitotic figures and apoptotic bodies were scored from H&E stained slides. Interestingly, quantification of mitotic figures revealed a trend towards an immediate increase in mitosis in colon polyps (4hr MEK162 polyps = 0.36 ± 0.176 , vehicle polyps = 0.199 ± 0.169 , p value = 0.072, $n \geq 8$ tumours, 3 mice, Mann Whitney U test) (Figure 5.1 A) however no significant alteration in proliferation in SITs was observed 4 hours post MEK162 exposure (4hr MEK162 SIT = 0.193 ± 0.113 , vehicle SIT = 0.258 ± 0.154 , p value = 0.672, $n \geq 5$ tumours, 3 mice, Mann Whitney U test) (Figure 5.1 A). At 24 hours post exposure, no significant alteration in mitotic figures were observed in colon polyps (24hr MEK162 polyps = 0.316 ± 0.265 , vehicle polyps = 0.199 ± 0.169 , p value = 0.508,

n≥8 tumours, 3 mice, Mann Whitney U test), or in SITs (24hr MEK162 SIT = 0.329 ± 0.222 , vehicle SIT = 0.258 ± 0.154 , p value = 0.523, n≥5 tumours, 3 mice, Mann Whitney U test) (Figure 5.1 A).

Scoring of apoptotic bodies in colon polyps and SITs following MEK162 exposure indicated an increase in apoptosis at the 4 hour time point but a reduction at 24 hours, suggesting tumours return to normal physiological levels by 24 hours following MEK162 administration (4hr MEK162 polyps = 2.67 ± 1.153 , 24hr MEK162 polyps = 0.768 ± 0.424 , vehicle polyps = 0.508 ± 0.49 , p value = 0.0014 for 4 hrs MEK162 and p value = 0.129 for 24hr MEK162; 4hr MEK162 SIT = 2.606 ± 1.723 , 24hr MEK162 SIT = 0.932 ± 0.607 , vehicle SIT = 0.522 ± 0.333 , p value = 0.001 for 4hr MEK162 and p value = 0.201 for 24 hour MEK162, n≥5 tumours, 3 mice, Mann Whitney U test) (Figure 5.1 B).

In order to further characterise anti-tumour effects following MEK162 exposure in $Apc^{f/+}$ $Kras^{LSL/+}$ lesions, IHC against BrdU and cleaved caspase 3 were carried out and scored. Quantification of BrdU positive cells revealed no significant difference in the number of BrdU positive cells in colon polyps 4 and 24 hours after MEK162 exposure (4hr MEK162 polyps = 13.45 ± 4.07 , 24hr MEK162 polyps = 13.914 ± 10.35 , vehicle polyps = 10.686 ± 7.059 , p value = 0.316 for 4hr, p value = 0.651 for 24hr, n≥8 tumours, 3 mice, Mann Whitney U test) (Figure 5.2 A), corroborating previous scoring of mitosis. BrdU scoring in SITs revealed no significant alteration in staining 4 hours post exposure to MEK162 but a significant increase in BrdU positive cells in SITs 24 hours after MEK162 (4hr MEK162 SIT = 8.848 ± 3.066 , 24hr MEK162 SIT = 24.743 ± 7.863 , vehicle SIT = 10.188 ± 5.617 , p value = 0.589 for 4hr, p value = 0.0298 for 24hr, n≥5 tumours, 3 mice, Mann Whitney U test) (Figure 5.2 A), indicating an increase in the number of cells in S phase of the cell cycle.

For further characterisation of anti-tumour effects, cleaved caspase 3 scoring was performed. This revealed an increase in staining at 4 hours post MEK162 in colon polyps, but no significant difference in SITs (4hr MEK162 polyps = 8.002 ± 4.83 , vehicle polyps = 0.977 ± 0.609 , p value = 0.0011; 4hr MEK162 SIT = 2.397 ± 0.885 , vehicle SIT = 1.792 ± 1.029 , p value = 0.159, n≥8 tumours, 3 mice, Mann Whitney U test) (Figure 5.2 B). This was also the case at 24 hours post MEK162 exposure, whereby a significant increase in cleaved caspase 3 staining was observed in colon polyps but no difference was detected in SITs (24hr MEK162 polyps = 2.875 ± 1.722 , vehicle polyps = 0.977 ± 0.609 , p value = 0.0138; 24hr MEK162 SIT = 2.656 ± 1.654 , vehicle SIT = 1.792 ± 1.029 , p value = 0.524, n≥5 tumours, 3 mice, Mann Whitney U test) (Figure 5.2 B). For the colon polyps exposed to MEK162, these observations indicate that the initial pro-

apoptotic effect observed at 4 hours post exposure may be returning to basal physiological levels by 24 hours. However, as apoptosis is still significantly increased compared to vehicle treated tumours, it can be concluded that MEK162 induces a prolonged pro-apoptotic effect in Kras mutant colon polyps. For the SITs, it is possible that a significant increase in cleaved caspase 3 staining may be observed at a time point between 4 and 24 hours as an increase in histological apoptosis was previously observed.

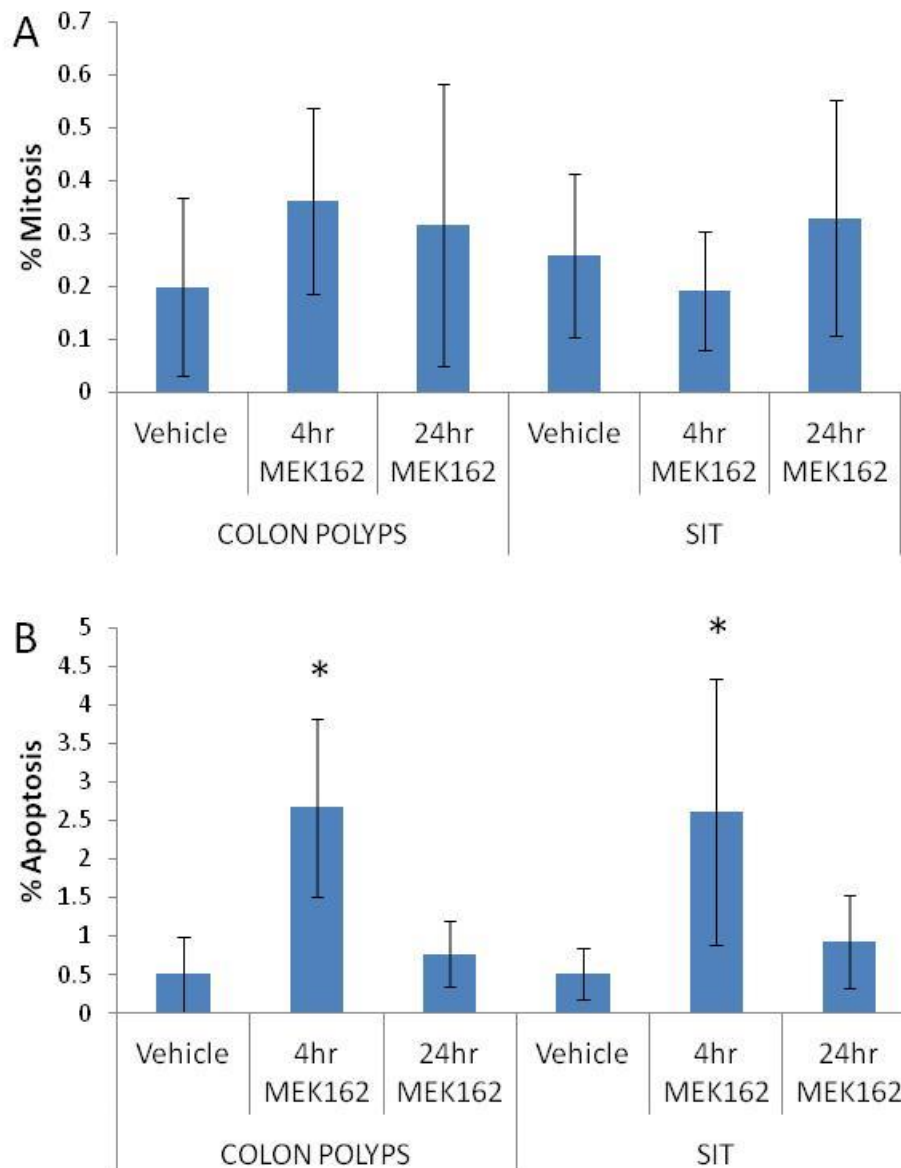


Figure 5.1 MEK162 had no effect on mitosis but increased apoptosis in $Apc^{f/+}$ $Kras^{LSL/+}$ colon polyps and small intestinal tumours (SITs)

Scoring of mitotic figures **(A)** and apoptotic bodies **(B)** in colon polyps and SITs by H&E examination revealed no significant alterations in the number of mitotic figures present, however revealed a significant increase in the number of apoptotic bodies 4 hours after a single dose of 30mg/kg MEK162 (p value = 0.0014 for 4hr polyps and p value = 0.001 for 4hr SIT, $n \geq 5$ tumours, 3 mice, Mann Whitney U test). Error bars represent standard deviation.

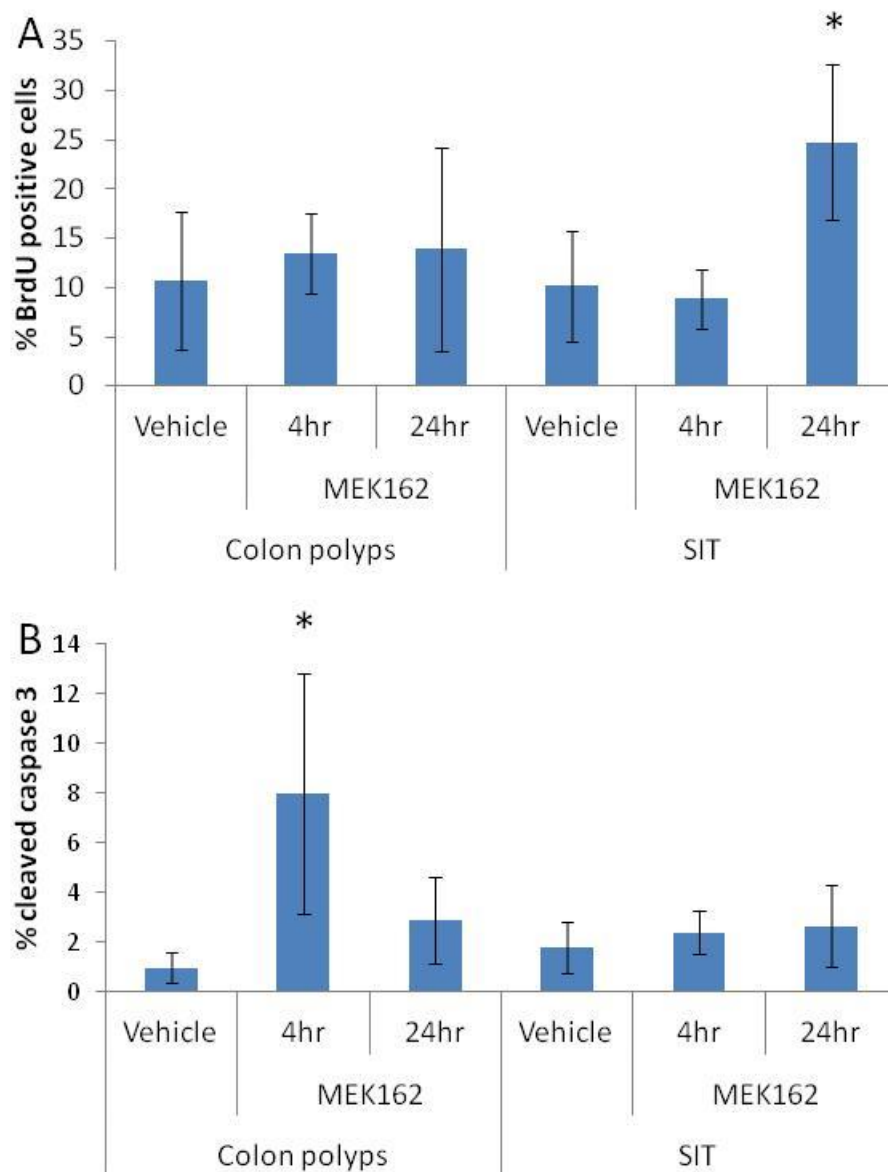


Figure 5.2 MEK162 also increased BrdU positive cells in small intestinal tumours (SITs) and cleaved caspase 3 staining in colon polyps

Scoring of IHC against BrdU **(A)** and cleaved caspase 3 **(B)** in $Apc^{f/+}$ $Kras^{LSL/+}$ colon polyps and SITs revealed a significant increase in BrdU positive cells in SIT 24 hours after MEK162 exposure. A significant increase in cleaved caspase 3 was observed 4hrs after MEK162 in colon polyps. (p value = 0.0298 for 24hr SIT BrdU and p value = 0.0011 for 4hr polyp cleaved caspase 3, $n \geq 5$ tumours, 3 mice, Mann Whitney U test). The levels of cleaved caspase 3 appears to have been reduced 24 hours after exposure, however the trend towards an increase compared to vehicle controls remains. Error bars represent standard deviation.

To investigate whether the anti-tumour effects described above correspond with pathway inhibition, colon polyps and SIT lysates were subjected to western blot analysis. Protein extracted from individual colon polyps and SITs from n=3 mice harvested 4 or 24 hours after exposure to MEK162 were compared to corresponding tumours harvested 4 hours post vehicle treatment. Activation status of the MAPK pathway was assessed utilising an antibody against the phosphorylated form (and hence activated form) of the MAPK Kinase- ERK at Thr202/Tyr204. Immunoblotting and subsequent densitometry analysis revealed a significant reduction in the levels of pERK in colon polyps 4 and 24hrs indicating prolonged inhibition (Figure 5.3, Table 5.1, Table 5.2). Here, levels of pERK were difficult to detect at 4 hours post exposure and was still reduced to approximately 50% at the 24 hour time point, indicative of prolonged but reduced inhibition of MAPK signalling. A significant reduction in levels of pERK was detected at 4 hours post exposure in SITs however no difference was observed 24 hours post exposure indicating return to basal levels by this time point (Figure 5.4, Table 5.3, Table 5.4). These observations confirm target inhibition by MEK162 in Kras mutant tumours but suggest that colon polyps may be more sensitive to the effects of MEK162 than SITs, perhaps due to increased signalling through pERK, as observed in chapter 3 section 3.2.8.

Given the convergence of MAPK and PI3K signalling at a number of downstream nodes and the role of Kras in activation of PI3K signalling, it was hypothesised that inhibition of MAPK signalling in the context of activated Kras may lead to increased activation of PI3K signalling as a compensatory mechanism. To investigate this, status of PI3K pathway signalling was assessed by western blotting. Antibodies described previously in section 4.2.1 were used to investigate complete activation of pAKT and signalling downstream of mTOR. Immunoblotting revealed an increasing trend, although not significant, in PI3K signalling through pAKT473, pAKT308 and pS6RP in colon polyps 4 hours after MEK162 exposure (Figure 5.3, Table 5.1). Interestingly, further modulation of PI3K signalling was observed at 24hrs post MEK162 exposure. Here, levels of pAKT308 were increased approximately 50%, however all other downstream effectors of PI3K signalling probed appeared reduced (Figure 5.3, Table 5.2) and may simply reflect a mechanism of rebalancing cell signalling to basal levels.

The initial effect of MEK inhibition on PI3K signalling in SITs appears to be contrasting to colon polyps. Overall, a trend towards reduced PI3K signalling at 4 hours post MEK162 was observed however a significant reduction was only detected in levels of pAKT473 (Figure 5.4, Table 5.3). No significant alteration in PI3K signalling was observed at 24 hours post exposure with the exception of pS6RP which was found to be significantly reduced (Figure 5.4, Table 5.4).

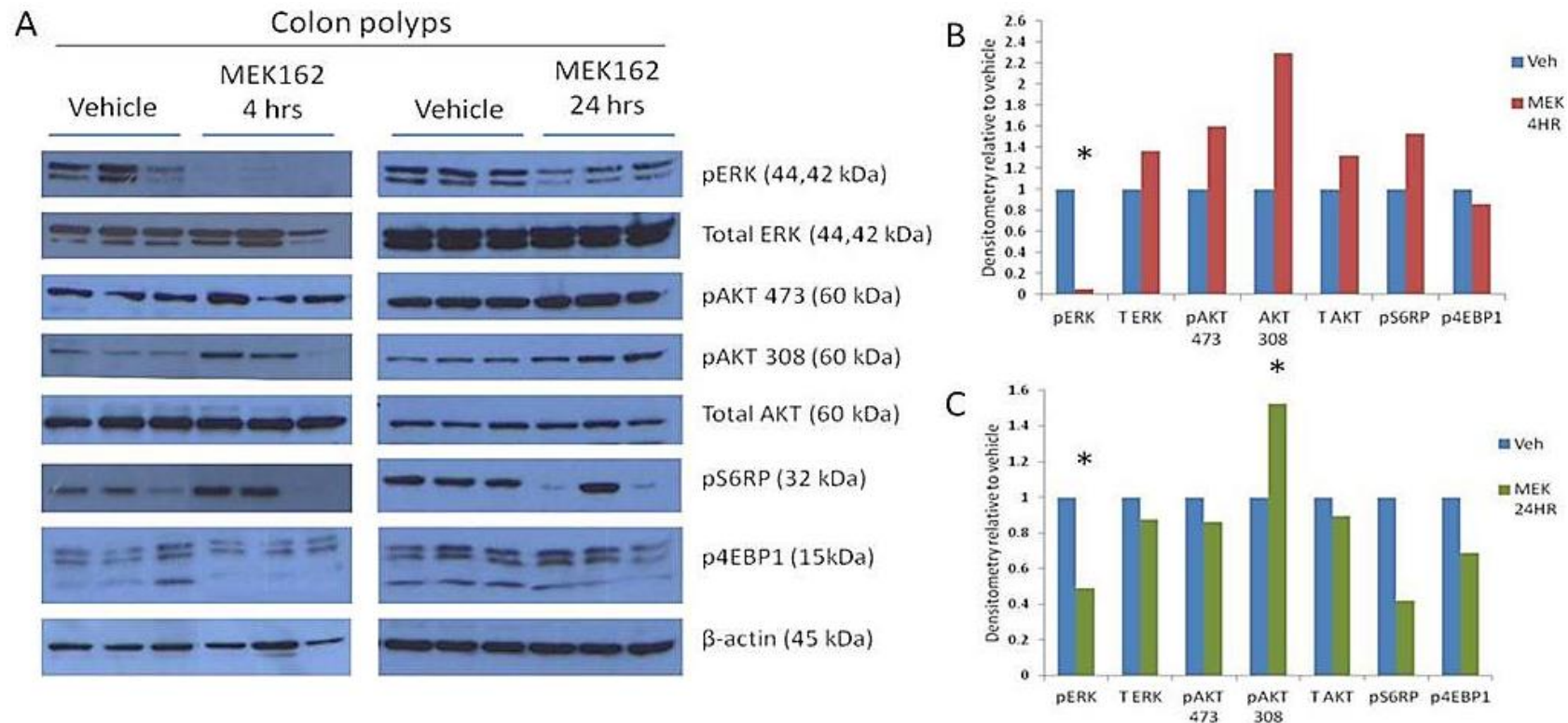


Figure 5.3 MEK162 reduces MAPK signalling in $Apc^{f/+}$ $Kras^{LSL/+}$ colon polyps , however leads to modulation of PI3K and mTOR signalling.

(A) Individual colon tumours lysates from $n=3$ mice exposed to 30mg/kg MEK162 for 4 or 24 hours were subjected to western blot analysis. Immunoblotting with the MAPK effector pERK revealed significant reduction in abundance at 4 and 24 hours after exposure. Additionally, effectors of PI3K and mTOR signalling probed revealed a trend towards increased signalling at 4 hours but a trend towards reduced signalling at 24 hours, with the exception of significantly increased pAKT308 at 24 hours post exposure. **(B + C)** Densitometry was carried out to quantify differences observed from western blotting. These are normalised to β -actin as loading control and represented as relative to vehicle controls (* p values = 0.0404, $n=3$, Mann Whitney U test).

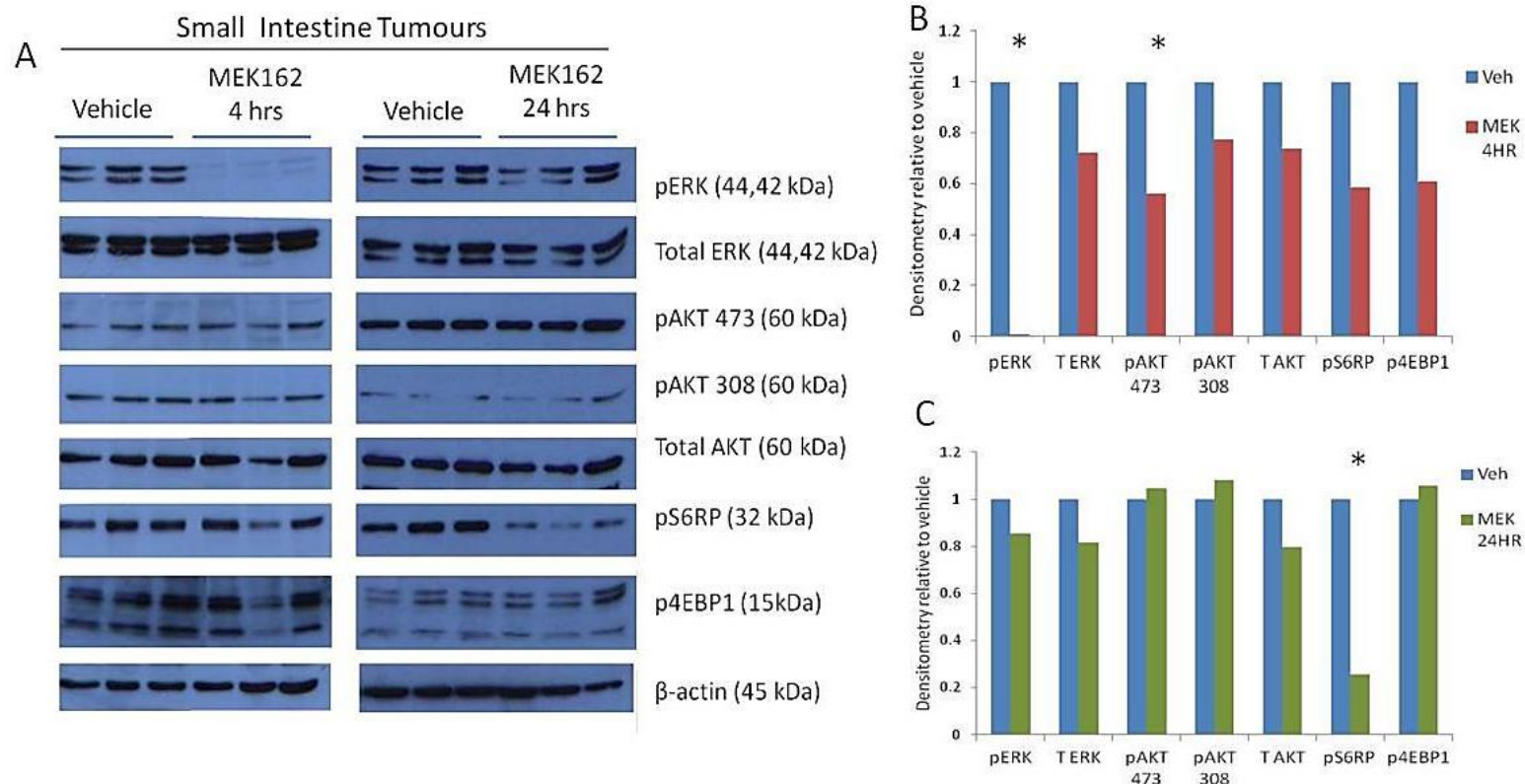


Figure 5.4 reduces MAPK signalling in $Apc^{f/+}$ $Kras^{LSL/+}$ small intestine tumours (SITs) and partial inhibition of PI3K and mTOR signalling.

(A) Individual SIT lysates from $n=3$ mice exposed to 30mg/kg MEK162 for 4 or 24 hours were subjected to western blot analysis. Western blotting for the MAPK effector pERK revealed significant reduction in abundance at 4 hours post exposure. Immunoblotting of PI3K and mTOR pathway effectors probed to investigate cross-talk of pathways revealed a significant reduction in pAKT473 4 hours post exposure and pS6RP 24 hours post exposure. **(B + C)** Densitometry was carried out to quantify differences observed from western blotting. These are normalised to β -actin as loading control and represented as relative to vehicle controls (*p value = 0.0404, $n=3$, Mann Whitney U test).

Colon polyps	Vehicle	4 hour MEK162 (p value)
pERK	4126 ± 2113	211.5 ± 184.8 (0.0404)
pAKT473	1062.2 ± 138	1362 ± 596.9 (0.3313)
pAKT308	716.9 ± 230	1496.2 ± 1217.1 (0.3313)
pS6RP	1407.2 ± 655.6	2043.4 ± 1680.8 (0.3313)
p4EBP1	3128.4 ± 630.2	2132.6 ± 177.4 (0.3313)

Table 5-1 Outline of raw densitometry values from western blot analysis of Apc^{f/+} Kras^{LSL/+} colon polyps 4 hours post exposure to MEK162, n=3, One-tailed Mann Whitney U test was used for statistical analysis

Colon polyps	Vehicle	24 hour MEK162 (p value)
pERK	4988 ± 452.4	2751.5 ± 736.9 (0.0404)
pAKT473	4421.3 ± 268.7	4314.7 ± 748.9 (0.1914)
pAKT308	1523.1 ± 114.1	2619.7 ± 593.5 (0.0404)
pS6RP	3511 ± 333.1	1634 ± 2253.4 (0.3313)
p4EBP1	6881 ± 1037	5399 ± 1942.3 (0.0952)

Table 5-2 Outline of raw densitometry values from western blot analysis of Apc^{f/+} Kras^{LSL/+} colon polyps 4 hours post exposure to MEK162, n=3, One-tailed Mann Whitney U test was used for statistical analysis

Small intestinal tumours	Vehicle	4 hour MEK162 (p value)
pERK	4101.8 ± 748	42.5 ± 14.7 (0.0404)
pAKT473	2160.7 ± 185.9	1686 ± 612.7 (0.0404)
pAKT308	525.4 ± 131.9	566.6 ± 212.7 (0.1914)
pS6RP	4015.2 ± 602.4	3221.8 ± 1407.7 (0.0952)
p4EBP1	5671.9 ± 284.7	4759 ± 2357 (0.0952)

Table 5-3 Outline of raw densitometry values from western blot analysis of Apc^{f/+} Kras^{LSL/+} SITs 4 hours post exposure to MEK162, n=3, One-tailed Mann Whitney U test was used for statistical analysis

Small intestinal tumours	Vehicle	24 hour MEK162 (p value)
pERK	4923.5 ± 195.8	4200.6 ± 2513.8 (0.0404)
pAKT473	3763 ± 212.9	3929 ± 844.9 (0.1914)
pAKT308	916.2 ± 268.7	991.8 ± 684.8 (0.1914)
pS6RP	4199 ± 445.1	1082.3 ± 370.7 (0.0404)
p4EBP1	5286 ± 828.7	5702.2 ± 1899.6 (0.0952)

Table 5-4 Outline of raw densitometry values from western blot analysis of Apc^{f/+} Kras^{LSL/+} colon polyps 24 hours post exposure to MEK162, n=3, One-tailed Mann Whitney U test was used for statistical analysis

In summary, the observations above highlight favourable anti-tumour activity of MEK162 in the Kras mutant setting, however also identify as hypothesised, activation of closely related PI3K signalling (summarised in Figure 5.5, 5.6). Nevertheless, the long term therapeutic efficacy of MEK162 in Kras mutant tumours was further probed below in section 5.2.2.

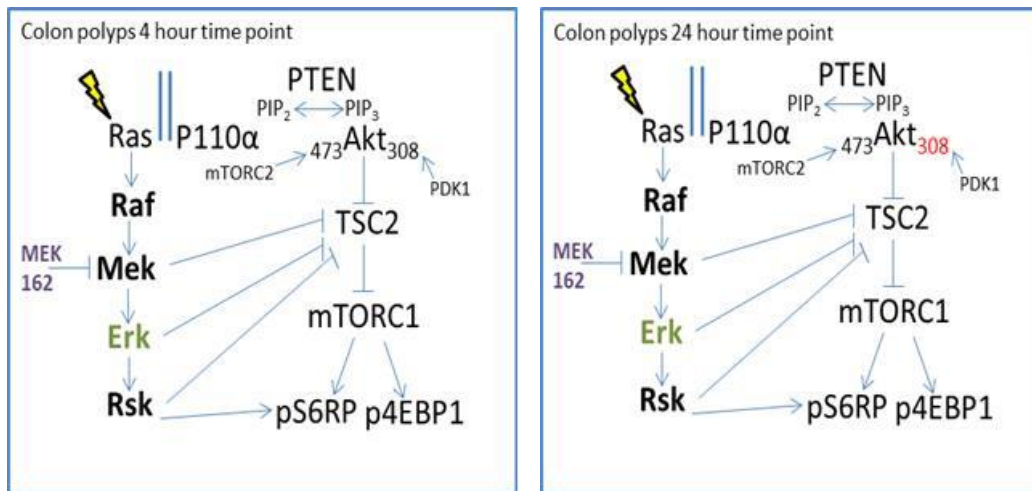


Figure 5.5 Schematic showing the effects of MEK162 on MAPK and PI3K/mTOR pathway components in $Apc^{f/+}$ $Kras^{LSL/+}$ colon polyps detected through western blot analysis (Green denotes a reduction whereas red indicates an increase)

MEK162 leads to a reduction in levels of pERK at 4 and 24 hours post exposure and significantly increases levels of pAKT at Thr308 24 hours post exposure.

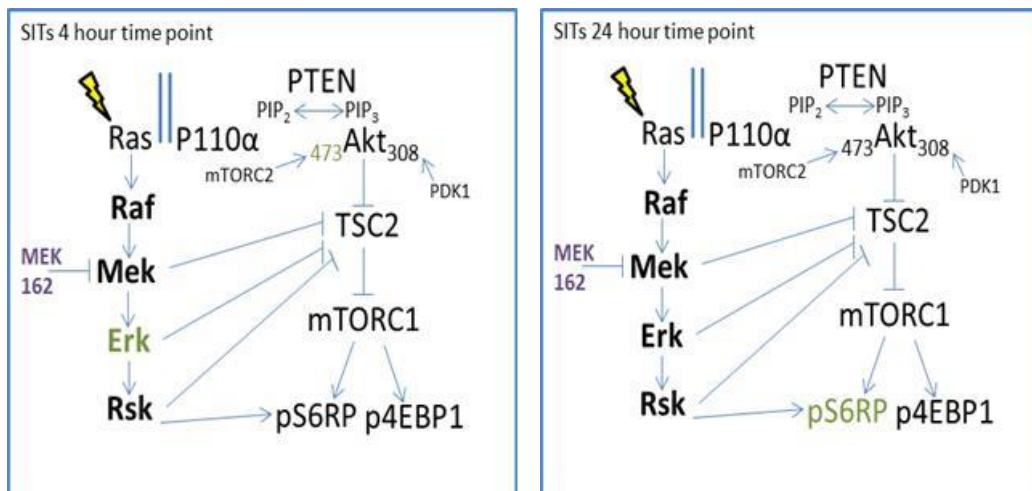


Figure 5.6 Schematic showing the effects of MEK162 on MAPK and PI3K/mTOR pathway components in $Apc^{f/+}$ $Kras^{LSL/+}$ SITs detected through western blotting (Green denotes a reduction whereas red indicates an increase).

MEK162 leads to a reduction in levels of pERK and pAKT473 at 4 hours post exposure and reduces levels of pS6RP 24 hours post exposure.

5.2.2 MEK162 increases survival of $Apc^{f/+}$ $Kras^{LSL/+}$ mice

To investigate the therapeutic potential of MEK inhibition as a rational therapeutic strategy for *Kras* mutant tumours, a chronic treatment experiment was conducted to elucidate the effect of MEK162 upon survival and also to determine the effect on intestinal tumour burden. 10 week old $Apc^{f/+}$ $Kras^{LSL/+}$ mice were induced and allowed to develop disease over approximately 14 weeks. Given that the tumour latency period of untreated mice (Davies EJ, unpublished) is between 80 and 250 days post induction, 100 days post induction was chosen as an appropriate intervention start point. Presence of tumours at this point was confirmed in a cohort of mice culled at 100 days post induction (section 5.2.8). Subsequently, mice (n=12 per cohort) were randomised to receive either 0.5% MC (vehicle) or 30mg/kg MEK162 twice daily (weekdays only) by oral gavage, until a survival end point (anaemia, bloating, $\geq 10\%$ loss of body weight) or the experimental end point of 500 days post induction.

Continuous twice daily administration of MEK162 in $Apc^{f/+}$ $Kras^{LSL/+}$ mice was well tolerated (defined by weight during treatment) and led to a significant increase in survival of mice with 2/12 mice culled at the experimental end point of 500 days (median survival MEK162 mice = 287 days vs vehicle = 153 days post induction, p value ≤ 0.0001 , n=12, Log-Rank and Wilcoxon test) (Figure 5.7), indicating this as a beneficial therapeutic strategy. To further the investigations of chronic MEK162 treatment, the effect on tumour burden was assessed as described in section 5.2.8.

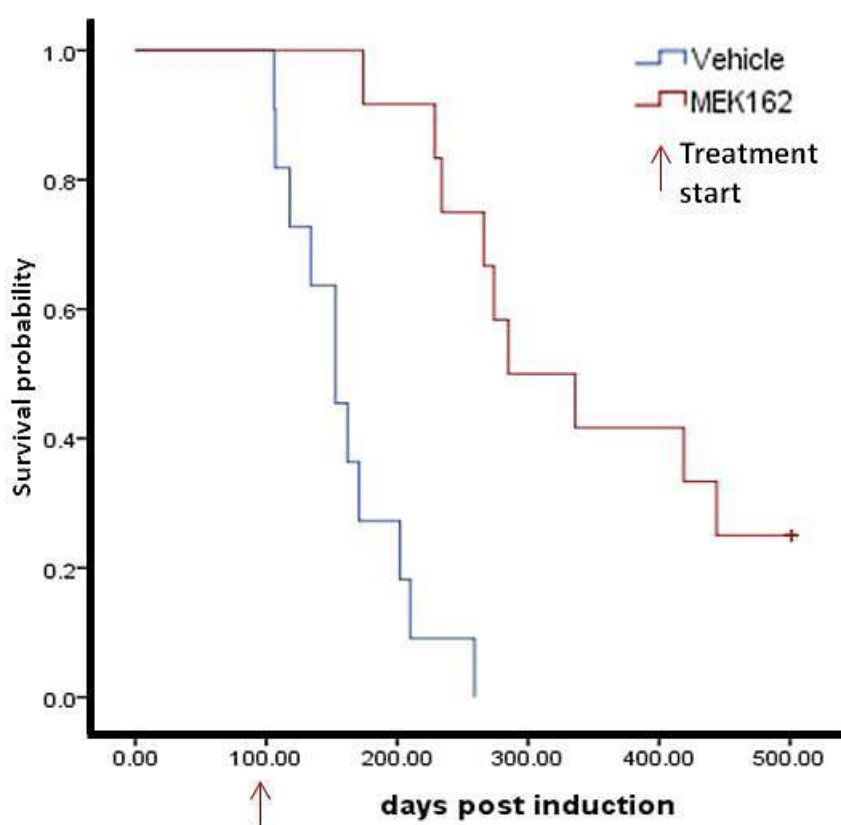


Figure 5.7 Kaplan-Meier survival analysis of $Apc^{f/+}$ $Kras^{LSL/+}$ mice receiving MEK162 compared to vehicle controls

$Apc^{f/+}$ $Kras^{LSL/+}$ mice were induced and aged to 100 days post induction, at which point mice were randomised to receive either 0.5% Methyl cellulose (Vehicle control) or 30mg/kg MEK162 twice-daily by oral gavage until a survival end point or the experimental end point of 500 days post induction. Continuous MEK162 treatment was found to significantly increase survival of mice from 153 days to 287 days post induction (p value ≤ 0.001 Log-Rank and Wilcoxon test, $n \geq 12$ mice per cohort).

5.2.3 NVP-BEZ235 increases apoptosis in *Kras* mutant tumours and significantly reduces signalling downstream PI3K and mTOR

Given that oncogenic *Kras* also impinges on the PI3K signalling cascade, I next investigated the short term effects of pathway inhibition through the dual PI3K/mTOR inhibitor to ascertain whether this results in any favourable anti-tumour effects. Similarly to section 5.2.1, the initial effects of NVP-BEZ235 were assessed through short term exposure experiments. Mice were induced and aged to allow for symptoms of intestinal tumour burden. Subsequently, mice

were administered a single dose of 35mg/kg NVP-BEZ235 and culled either 4 or 24 hours post exposure as described previously (cohort of $n \geq 3$ mice). Mice also received a dose of BrdU 2 hours prior to killing. Vehicle treated controls for this experiment are identical to those used in section 5.2.1.

To investigate the immediate anti-tumour activity of NVP-BEZ235 in $Apc^{f/+}$ $Kras^{LSL/+}$ tumours, the levels of mitosis and apoptosis were quantified by examination of H&E stained slides and IHC for BrdU and cleaved caspase 3. Quantification of mitotic figures revealed no significant alterations at either 4 or 24 hours post exposure to NVP-BEZ235 in either colon polyps or SITs (Colon polyps: 4hr veh = 0.198 ± 0.169 , 4hr NVP-BEZ235 = 0.213 ± 0.193 , 24hr NVP-BEZ235 = 0.432 ± 0.284 , p value = 0.973 for 4hr NVP-BEZ235, p value = 0.059 for 24hr NVP-BEZ235, $n \geq 9$ tumours, 4 mice, Mann Whitney U test) (SITs: 4hr veh = 0.258 ± 0.154 , 4hr NVP-BEZ235 = 0.346 ± 0.239 , 24hr NVP-BEZ235 = 0.345 ± 0.416 , p value = 0.672 for 4hr NVP-BEZ235, p value = 0.289 for 24hr NVP-BEZ235, $n \geq 6$ tumours, 4 mice, Mann Whitney U test) (Figure 5.8 A). However, a trend towards an increase in mitotic figures was observed 24 hours post exposure in colon polyps. Scoring of apoptotic bodies here revealed a significant increase 4 hours post exposure in both colon polyps and SITs (Colon polyps: 4hr veh = 0.508 ± 0.490 , 4hr NVP-BEZ235 = 1.84 ± 1.823 , p value = 0.0103, SITs: 4hr veh = 0.522 ± 0.33 , 4hr NVP-BEZ235 = 1.75 ± 0.679 , p value = 0.003, $n \geq 6$ tumours, 4 mice, Mann Whitney U test) (Figure 5.8 B). The initial increase at 4 hours was reduced by 24 hours, indicating a transient effect on apoptosis (Colon polyps: 4hr veh = 0.508 ± 0.490 , 24hr NVP-BEZ235 = 0.558 ± 0.362 , p value = 0.693, SITs: 4hr veh = 0.522 ± 0.33 , 24hr NVP-BEZ235 = 0.814 ± 0.416 , p value = 0.0903, $n \geq 6$ tumours, 4 mice, Mann Whitney U test).

Additionally, the anti-tumour properties of NVP-BEZ235 were further characterised through BrdU and cleaved caspase 3 scoring. Consistent with the histological characterisation of mitosis, the number of BrdU positive cells was unaltered in both colon polyps and SITs at 4 and 24 hour time points post exposure (Colon polyps: 4hr veh = 10.686 ± 7.059 , 4hr NVP-BEZ235 = 6.757 ± 2.316 , 24hr NVP-BEZ235 = 12.896 ± 4.716 , p value = 0.374 for 4hr NVP-BEZ235, p value = 0.339 for 24hr NVP-BEZ235, $n \geq 9$ tumours, 4 mice, Mann Whitney U test) (SITs: 4hr veh = 10.19 ± 5.62 , 4hr NVP-BEZ235 = 17.71 ± 7.29 , 24hr NVP-BEZ235 = 12.31 ± 3.32 , p value = 0.1939 for 4hr NVP-BEZ235, p value = 0.713 for 24hr NVP-BEZ235, $n \geq 6$ tumours, 4 mice, Mann Whitney U test) (Figure 5.9 A). Quantification of active caspase in *Kras* mutant tumours conducted through cleaved caspase 3 scoring revealed a significant increase in staining 4 and 24 hours post NVP-BEZ235 exposure in colon polyps and a significant increase in staining at 24

hours post exposure in SITs (Colon polyps: 4hr veh = 0.977 ± 0.609 , 4hr NVP-BEZ235 = 1.927 ± 1.059 , 24hr NVP-BEZ235 = 2.00 ± 1.37 , p value = 0.0433 for 4hr NVP-BEZ235, p value = 0.0485 for 24hr NVP-BEZ235, $n \geq 9$ tumours, 4 mice, Mann Whitney U test) (SITs: 4hr veh = 1.79 ± 1.028 , 4hr NVP-BEZ235 = 3.05 ± 1.69 , 24hr NVP-BEZ235 = 2.99 ± 0.803 , p value = 0.1599 for 4hr NVP-BEZ235, p value = 0.0472 for 24hr NVP-BEZ235, $n \geq 6$ tumours, 4 mice, Mann Whitney U test) (Figure 5.9 B). These later findings corroborate previous analysis of histological apoptosis and highlight prolonged pro-apoptotic effects of NVP-BEZ235.

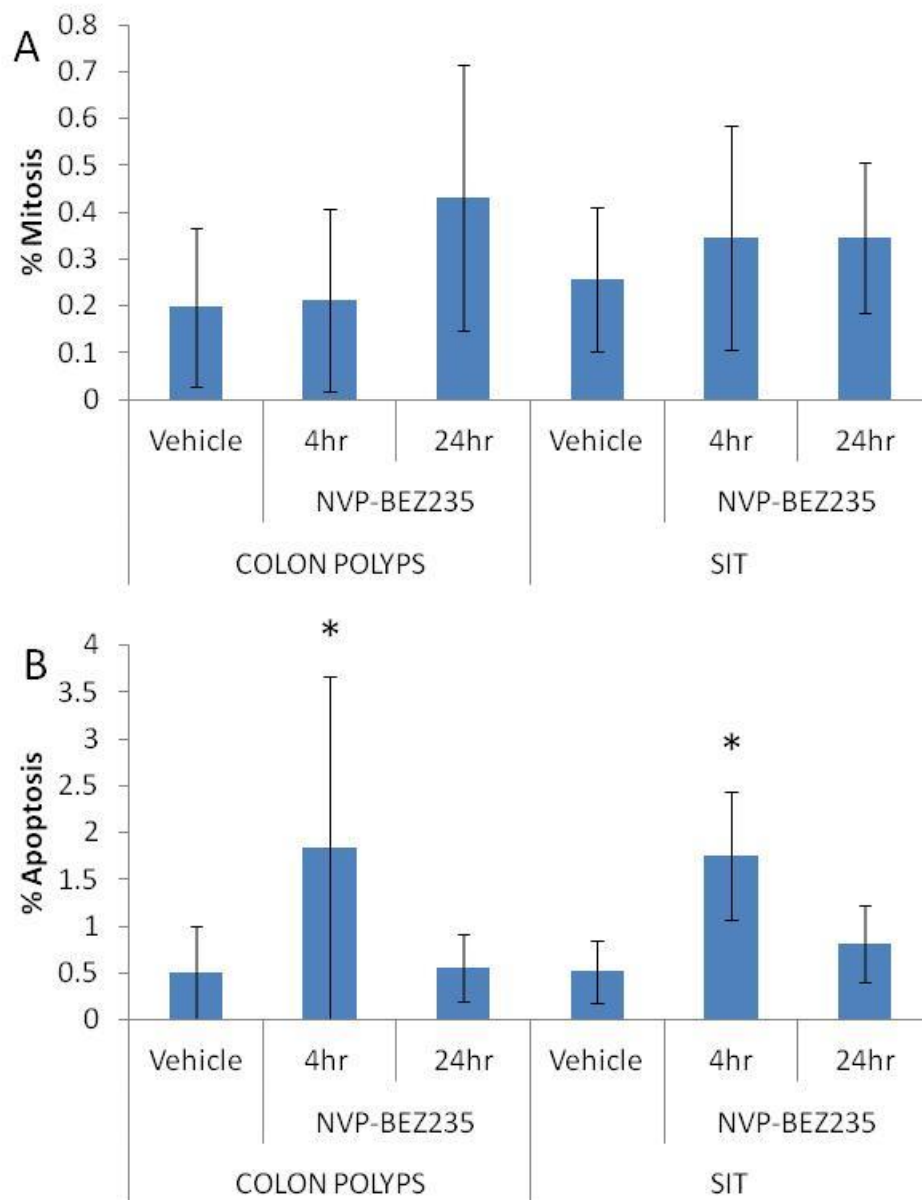


Figure 5.8 NVP-BEZ235 significantly increases apoptosis in $Apc^{f/+}$ $Kras^{LSL/+}$ colon polyps and small intestine tumours (SITs), but elicits no significant anti-proliferative effects.

(A) Quantification of mitotic figures and apoptotic bodies **(B)** in colon polyps and SITs of mice exposed to a single dose of 35mg/kg NVP-BEZ235. Scoring revealed a trend towards an increase in mitosis 4 and 24 hours after exposure and a significant increase in apoptotic bodies in both polyps and SITs, 4 hours post administration (p value = 0.0103 for 4hr polyps apoptosis, p value = 0.003 for 4hr SIT apoptosis, $n \geq 6$ tumours, 4 mice, Mann Whitney U test). The initial apoptotic effects appear reduced to baseline levels between 4 and 24 hours after exposure to NVP-BEZ235. Error bars represent standard deviation

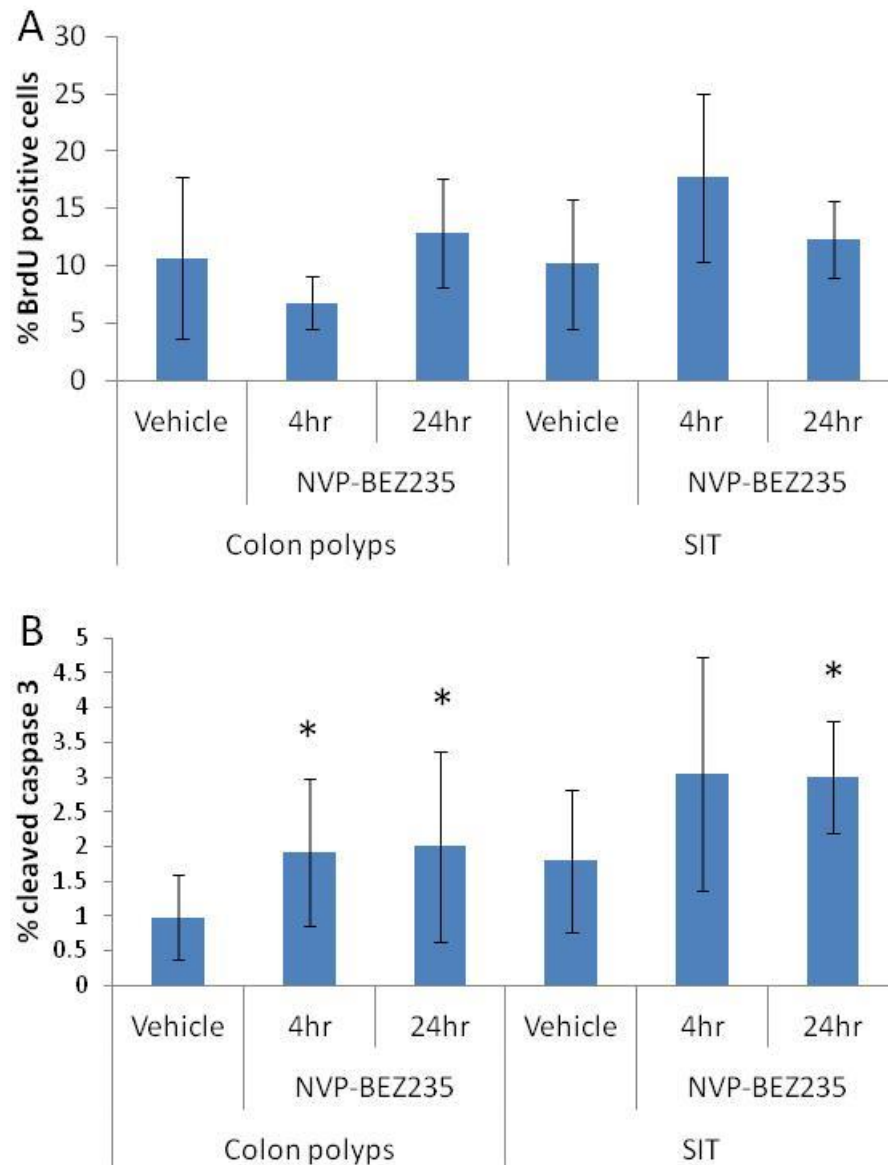


Figure 5.9 Further anti-tumour evaluation of NVP-BEZ235 revealed an increased pro-apoptotic effect in $Apc^{f/+}$ $Kras^{LSL/+}$ colon polyps and small intestine tumours (SITs)

To further evaluate the anti-tumour properties of NVP-BEZ235 in $Apc^{f/+}$ $Kras^{LSL/+}$ intestinal lesions, IHC against BrdU (**A**) and cleaved caspase 3 (**B**) were carried out and scored. Scoring of BrdU positive cells revealed no significant alterations at either 4 or 24 hours in colon polyps or SITs following exposure to NVP-BEZ235. Cleaved caspase 3 scoring was increased in colon polyps at both 4 and 24 hour time points, and at 24 hours in SITs (colon polyps: p value = 0.0433 for 4hr, and p value = 0.0485 for 24hr; SITs: p value = 0.159 for 4hr, p value = 0.0472 for 24hr, $n \geq 6$ tumours, 4 mice, Mann Whitney U test). Error bars represent standard deviation

To explore the immediate effects of NVP-BEZ235 on PI3K and mTOR signalling in $Apc^{f/+} Kras^{LSL/+}$ tumours, proteins extracted from individual colon polyps and SITs harvested from mice (n=3) at 4 and 24 hour time points post exposure to NVP-BEZ235, were subjected to western blot analysis. Immunoblotting and subsequent densitometry analysis of colon polyp samples with antibodies against the downstream PI3K targets, revealed a significant reduction in levels of pAKT473, pS6RP and p4EBP1 and a trend towards reduced pAKT308, 4 hours following exposure to NVP-BEZ235 (Figure 5.10, Table 5.5). A trend towards reduced PI3K signalling was still evident at 24 hours post exposure with a significant reduction in pAKT473, indicating prolonged inhibition of PI3K signalling (Figure 5.10, Table 5.6).

Colon polyps	Vehicle	4 hour NVP-BEZ235 (p value)
pAKT473	1062.2 ± 137.8	460.8 ± 204.6 (0.0404)
pAKT308	716.9 ± 230	443.6 ± 400.1 (0.3313)
pS6RP	1407.2 ± 655.6	91.4 ± 66.1 (0.0404)
p4EBP1	3128.4 ± 630.2	3128.4 ± 630 (0.0404)
pERK	4125.7 ± 2118	4113 ± 1139.2 (0.5)

Table 5-5 Outline of raw densitometry values from western blot analysis of $Apc^{f/+} Kras^{LSL/+}$ colon polyps 4 hours post exposure to NVP-BEZ235, n=3, One-tailed Mann Whitney U test was used for statistical analysis

Colon polyps	Vehicle	24 hour NVP-BEZ235 (p value)
pAKT473	4421.3 ± 268.7	3992.1 ± 494.8 (0.0404)
pAKT308	1523.1 ± 114.1	1162.9 ± 477.4 (0.0952)
pS6RP	3511 ± 333.1	3358.7 ± 1858.7 (0.5)
p4EBP1	6881 ± 1037	6831 ± 984.7 (0.3313)
pERK	4988 ± 452.4	6133.8 ± 588.7 (0.1914)

Table 5-6 Outline of raw densitometry values from western blot analysis of $Apc^{f/+} Kras^{LSL/+}$ colon polyps 24 hours post exposure to NVP-BEZ235, n=3, One-tailed Mann Whitney U test was used for statistical analysis

In SITs, analysis of PI3K and mTOR downstream effectors also revealed prolonged inhibition of PI3K and mTOR signalling evidenced through reduced levels of pAKT308, pS6RP and p4EBP1 4 hours post exposure and significantly reduced levels of pAKT473 and pS6RP at 24 hours post exposure (Figure 5.11, Table 5.7, Table 5.8). Together, these observations confirm target inhibition and indicate that NVP-BEZ235 induced prolonged inhibition of PI3K signalling in this Kras mutant tumour setting similar to effects of MEK inhibition.

Small intestinal tumours	Vehicle	4 hour NVP-BEZ235 (p value)
pAKT473	525.4 ± 131.9	601.6 ± 478.3 (0.3313)
pAKT308	2160.7 ± 185.9	915.6 ± 407.4 (0.0404)
pS6RP	4015.2 ± 602.4	1033.3 ± 224.1 (0.0404)
p4EBP1	5671.9 ± 284.7	267.4 ± 863.3 (0.0404)
pERK	4101.8 ± 748	4847.7 ± 621.5 (0.5)

Table 5-7 Outline of raw densitometry values from western blot analysis of Apc^{f/+} Kras^{LSL/+}

SITs 4 hours post exposure to NVP-BEZ235, n=3, One-tailed Mann Whitney U test was used for statistical analysis

Small intestinal tumours	Vehicle	24 hour NVP-BEZ235 (p value)
pAKT473	3763 ± 212.9	3290.6 ± 1176.7 (0.0404)
pAKT308	916.2 ± 268.7	1214 ± 925.9 (0.5)
pS6RP	4199 ± 445.1	2398.4 ± 1383.7 (0.0404)
p4EBP1	5286 ± 828.7	6104.9 ± 3321.3 (0.5)
pERK	4923.5 ± 195.8	6203.8 ± 738.7 (0.3313)

Table 5-8 Outline of raw densitometry values from western blot analysis of Apc^{f/+} Kras^{LSL/+} SITs

24 hours post exposure to NVP-BEZ235, n=3, One-tailed Mann Whitney U test was used for statistical analysis

Given previous observations of cross-talk between MAPK and PI3K signalling in this study and elsewhere (Ma et al., 2005, Ma et al., 2007, Turke et al., 2012, Zimmermann and Moelling, 1999), activation status of MAPK signalling was also interrogated in samples exposed to NVP-BEZ235 through western blot analysis. Immunoblotting and subsequent densitometry analysis for pERK revealed no significant alterations in either colon polyps or SITs, 4 or 24 hours after exposure to NVP-BEZ235, indicating PI3K inhibition does not affect MAPK signalling in the Kras mutant setting (Figure 5.10, Figure 5.11, table 5.5- 5.8). Overall, these investigations reflect favourable anti-tumour and pharmacodynamic effects of NVP-BEZ235 in the Kras mutant setting (summarised in Figure 5.12) and warrant further investigation to determine whether continuous NVP-BEZ235 treatment can increase survival of tumour bearing mice.

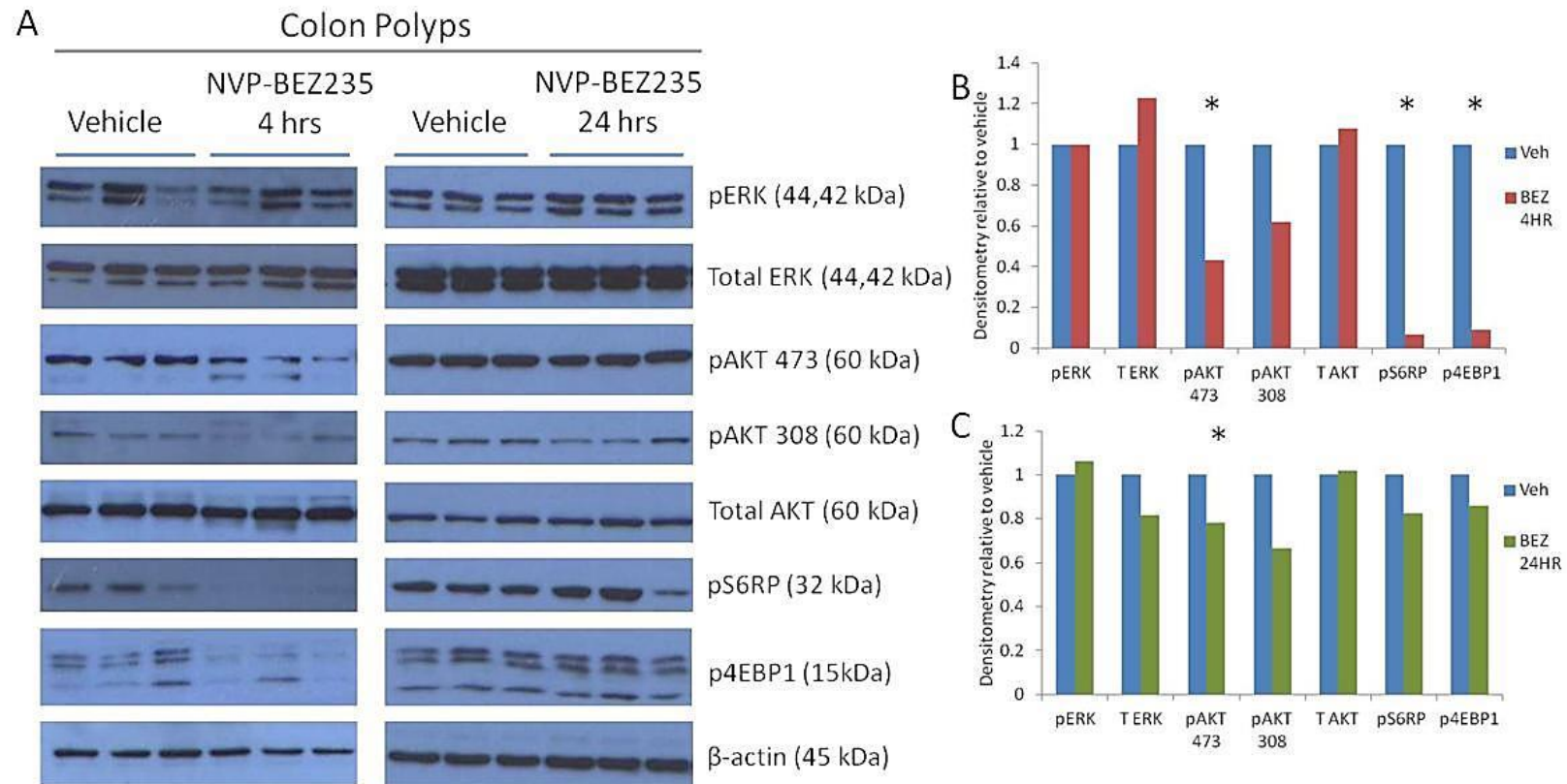


Figure 5.10 NVP-BEZ235 significantly reduces signalling downstream PI3K and mTOR in $Apc^{f/+}$ $Kras^{LSL/+}$ colon polyps

(A) Individual colon polyp lysates from $n=3$ mice exposed to 35mg/kg NVP-BEZ235 for 4 or 24 hours were analysed by western blotting. A significant reduction in PI3K and mTOR signalling through pAKT473, pS6RP and p4EBP1 was observed 4 hours after exposure and overall, a trend towards reduced signalling at 24 hours with only a significant reduction of pAKT473. Additionally, MAPK pathway status was probed using pERK but showed no alterations at 4 or 24 hours following NVP-BEZ235 exposure. **(B + C)** Densitometry was carried out to quantify differences observed from western blotting. These are normalised to β -actin as loading control and represented as relative to vehicle controls (* p value = 0.0404, $n=3$, Mann Whitney U test).

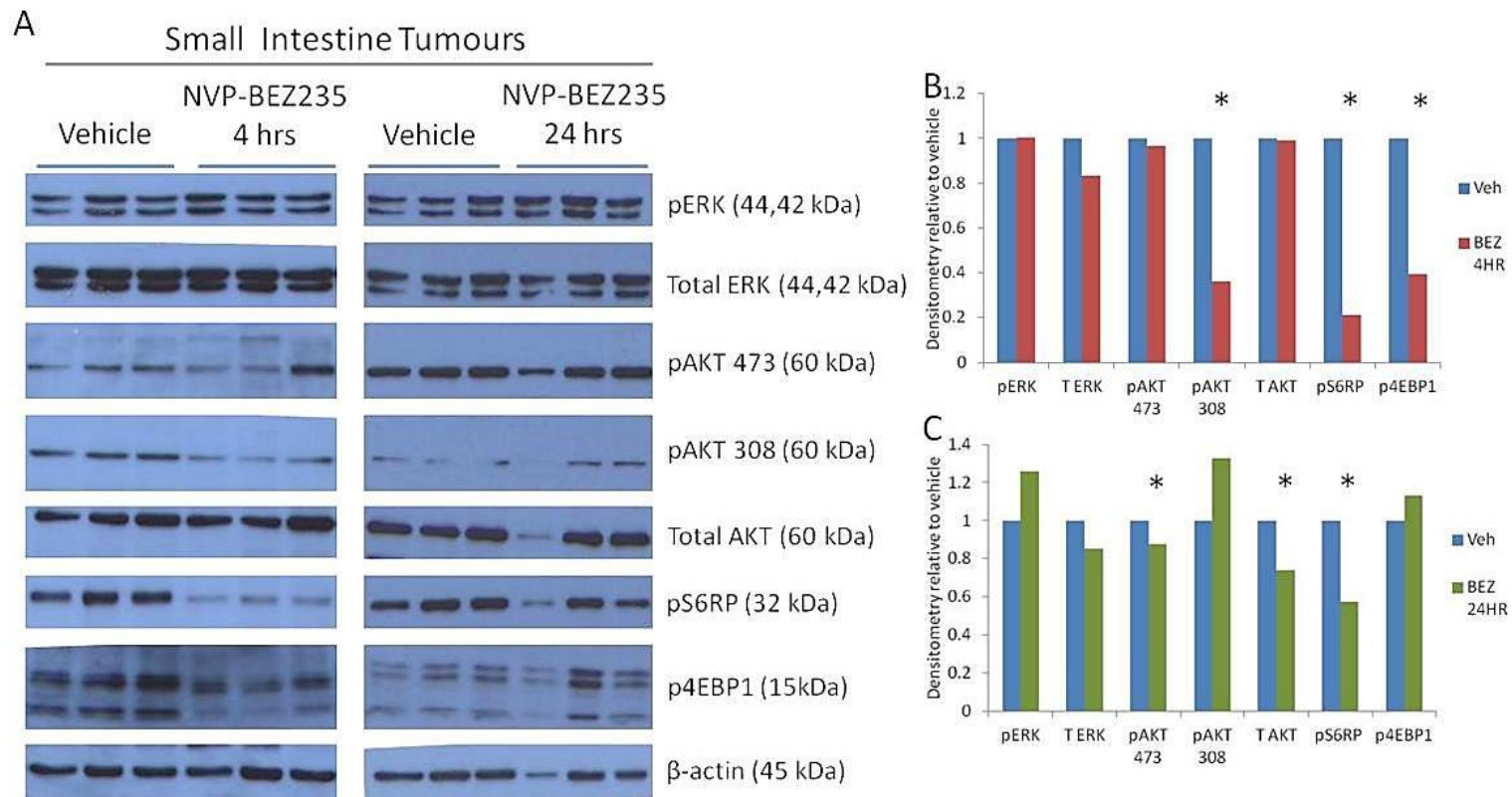


Figure 5.11 Figure 5.9 NVP-BEZ235 significantly reduces signalling downstream PI3K and mTOR in *Apc^{f/+} Kras^{LSL/+}* small intestine tumours (SITs)

(A) Analysis of individual SIT lysates from $n=3$ mice exposed to 35mg/kg NVP-BEZ235 for 4 or 24 hours by western blotting. Immunoblotting for effectors of PI3K and mTOR signalling revealed a significant reduction in pAKT308, pS6RP and p4EBP1 4 hours after exposure and pAKT473 and pS6RP 24 hours after exposure to NVP-BEZ235. To investigate the effect of NVP-BEZ235 on MAPK signalling, antibody against pERK was probed. No significant alterations in the levels of pERK were observed either 4 or 24 hours after exposure. **(B + C)** Densitometry was carried out to quantify differences observed from western blotting. These are normalised to β -actin as loading control and represented as relative to vehicle controls (* p value = 0.0404, $n=3$, Mann Whitney U test).

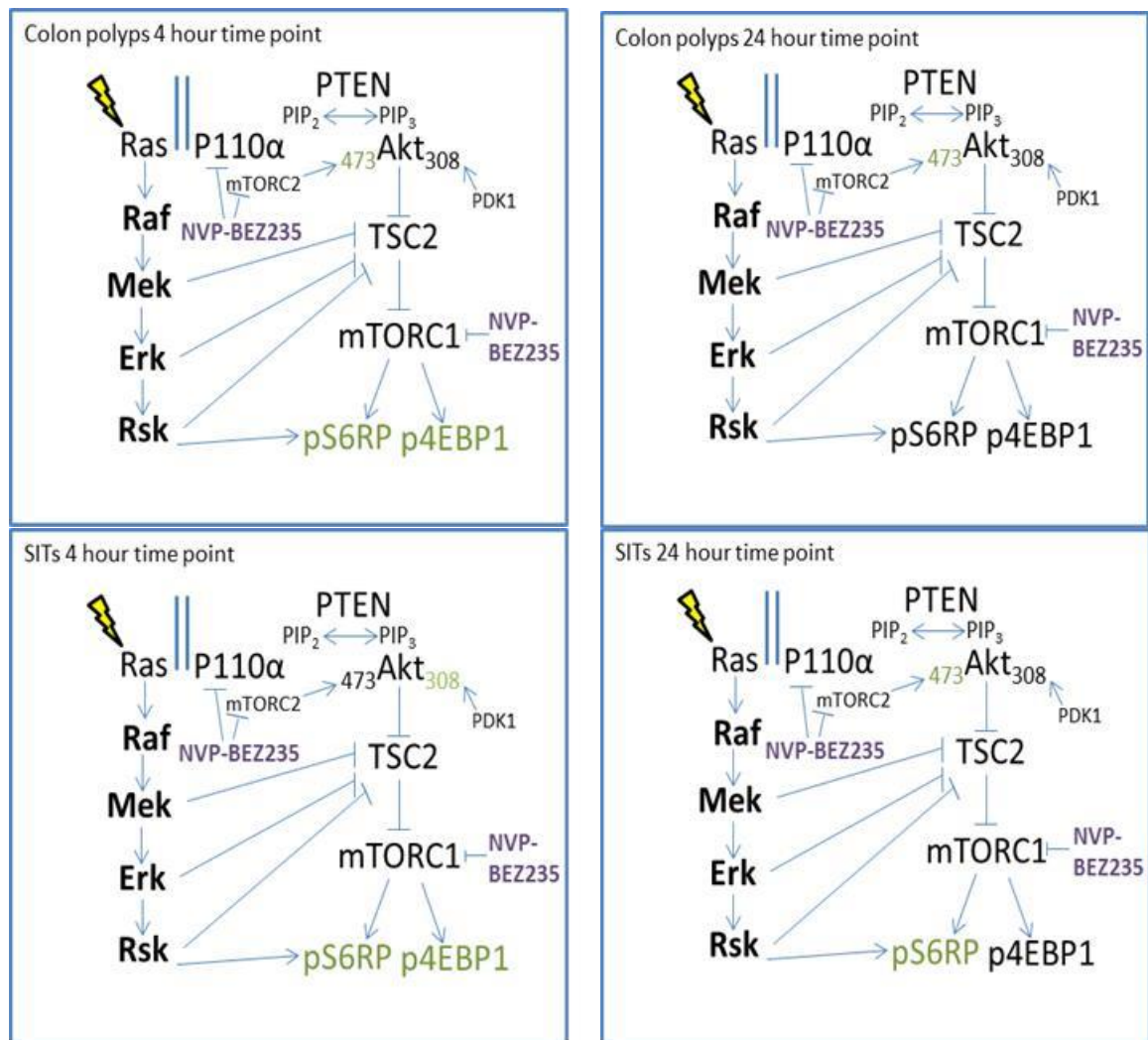


Figure 5.12 Schematic showing the effects of NVP-BEZ235 on PI3K/mTOR and MAPK pathway components in $Apc^{f/+}$ $Kras^{LSL/+}$ colon polyps and SITs detected through western blotting (Green denotes a reduction).

NVP-BEZ235 leads to a reduction in levels of PI3K pathway components and does not have any effect on MAPK signalling

5.2.4 NVP-BEZ235 significantly increases longevity of $Apc^{f/+}$ $Kras^{LSL/+}$ mice

To investigate the therapeutic potential of NVP-BEZ235 in $Apc^{f/+}$ $Kras^{LSL/+}$ mice, 10 week old mice were induced and aged to 100 days post induction at which point they started long term treatment with NVP-BEZ235. A cohort of n=12 mice received 35mg/kg NVP-BEZ235 twice daily (weekdays only) by oral gavage until a survival end point (anaemia, bloating, $\geq 10\%$ loss of body weight) or the experimental end point of 500 days post induction. Vehicle controls are identical to those used in section 5.2.2.

As with MEK162 treatment, chronic twice-daily treatment of NVP-BEZ235 was well tolerated by $Apc^{f/+}$ $Kras^{LSL/+}$ mice and significantly increased survival of mice with 2/12 mice reaching the experimental end point of 500 days (median survival of NVP-BEZ235 mice = 343 days vs vehicle = 153 days post induction, n=12 mice per cohort, p value ≤ 0.0001 for Log-Rank and Wilcoxon test) indicating a therapeutic benefit (Figure 5.13). Comparison of both chronic treatments revealed no significant difference between the two, suggesting MEK162 and NVP-BEZ235 are equipotent with regards to survival benefit, in $Apc^{f/+}$ $Kras^{LSL/+}$ mice (median survival of MEK162 mice = 287 days vs NVP-BEZ235 mice = 343 days post induction, n=12 per cohort, p value = 0.523 for Log-Rank and p value = 0.818 for Wilcoxon test).

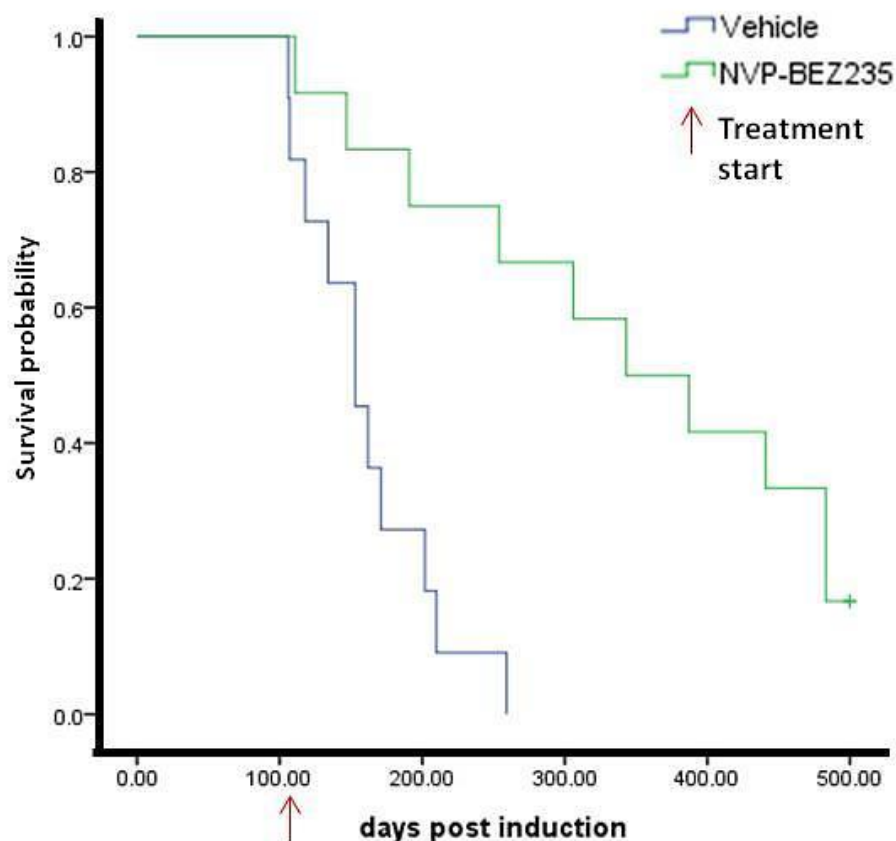


Figure 5.13 Kaplan-Meier survival analysis of $Apc^{f/+}$ $Kras^{LSL/+}$ mice receiving chronic NVP-BEZ235 treatment compared to vehicle controls

$Apc^{f/+}$ $Kras^{LSL/+}$ mice were induced and aged to 100 days post induction, at which point mice were randomised to receive either 0.5% Methyl cellulose (Vehicle control) or 35mg/kg NVP-BEZ235 twice-daily by oral gavage until a survival end point or the experimental endpoint of 500 days. Continuous NVP-BEZ235 treatment was found to significantly increase survival of mice from 153 days to 343 days post induction (p value ≤ 0.001 Log-Rank and Wilcoxon test, $n \geq 12$ mice per cohort).

5.2.5 Investigating the varied combination strategies in Kras mutant colon polyps and small intestinal tumours

Given the effectiveness of both MEK162 and NVP-BEZ235 as single agents in $Apc^{f/+}$ $Kras^{LSL/+}$ mice, it was anticipated that combined inhibition of MAPK and PI3K signalling may result in an additive benefit in this tumour model. First however, given that $Apc^{f/+}$ $Pten^{f/f}$ mice were particularly sensitive to the scheduling of the combination (section 4.2.5), the three combination strategies were also investigated in a short term setting to determine whether Kras mutant tumours were similarly sensitive to the sequence of drug delivery. The three differing dosing strategies outlined in table 4.5 were used; a cohort of $n \geq 3$ mice were administered with each strategy, and culled 4 hours following the final dose. Mice were also administered with a dose of BrdU 2 hours prior to killing, and were dissected as previously described in section 2.4. Vehicle treated controls for this experiment are identical to those described in section 5.2.1.

Firstly, to determine the anti-tumour effects of each combination strategy in Kras mutant lesions, histological mitosis and apoptosis were scored from H&E stained slides. Scoring of mitotic figures in both colon polyps and SITs revealed no significant differences between any of the combination strategies compared to vehicle controls (colon polyp samples: 4hr veh = 0.199 ± 0.169 , combo 1 = 0.405 ± 0.361 , combo 2 = 0.281 ± 0.165 , combo 3 = 0.201 ± 0.222 , p value = 0.291 for combo 1, p value = 0.329 for combo 2, p value = 0.753 for combo 3, $n \geq 8$ tumours, 4 mice; SIT samples: 4hr veh = 0.258 ± 0.154 , combo 1 = 0.283 ± 0.279 , combo 2 = 0.252 ± 0.174 , combo 3 = 0.299 ± 0.115 , p value = 0.862 for combo 1, p value = 1 for combo 2, p value = 0.721 for combo 3, $n \geq 6$ tumours, 4 mice, Mann Whitney U test) (Figure 5.14). Quantification of histological apoptosis however revealed significantly increased levels of apoptosis 4 hours following exposure to all three combination strategies, in both colon polyps and SITs indicating potent pro-apoptotic effects (colon polyp samples: 4hr veh = 0.508 ± 0.49 , combo 1 = 10.63 ± 5.51 , combo 2 = 6.53 ± 4.58 , combo 3 = 9.73 ± 5.68 , p value = 0.0011 for combo 1, p value = 0.002 for combo 2, p value = 0.0004 for combo 3, $n \geq 8$ tumours, 4 mice; SIT samples: 4hr vehicle = 0.52 ± 0.33 , combo 1 = 6.57 ± 2.44 , combo 2 = 6.94 ± 1.45 , combo 3 = 7.09 ± 4.59 , p value = 0.0015 for combo 1, p value = 0.0058 for combo 2, p value = 0.0034 for combo 3, $n \geq 6$ tumours, 4 mice, Mann Whitney U test) (Figure 5.14).

IHC for BrdU and cleaved caspase 3 were quantified to further characterise the immediate anti-tumour activity of each combination strategy. Scoring of BrdU positive cells in $Apc^{f/+}$ $Kras^{LSL/+}$ colon polyps revealed no significant alterations (4hr veh = 10.69 ± 7.06 , combo 1 =

12.58 ± 2.49, combo 2 = 14.92 ± 1.78 , combo 3 = 12.52 ± 4.23, p value = 0.377 for combo 1, p value = 0.337 for combo 2, p value = 0.331 for combo 3, n≥8 tumours, 4 mice, Mann Whitney U test) similar to mitosis scoring. Additionally in SITs, no significant effect was detected with combo 1 however a significant increase in BrdU positive cells was detected following combo 2 and 3, indicating a pro-proliferative increase in the number of cells in S phase of the cell cycle (4hr veh = 10.19 ± 5.62, combo 1 = 13.45 ± 6.59, combo 2 = 18.96 ± 2.18, combo 3 = 27.28 ± 7.45, p value = 0.3502 for combo 1, p value = 0.0304 for combo 2, p value = 0.0015, n≥6 tumours, 4 mice, Mann Whitney U test) (Figure 5.15).

Further to scoring of histological apoptosis, quantification of cleaved caspase 3 staining also revealed a significant increase in both colon polyps and SITs, in response to all three combination strategies (Colon polyps: 4hr veh = 0.978 ± 0.609, combo 1 = 17.876 ± 5.99, p value = 0.0014, combo 2 = 6.22 ± 1.91, p value = 0.142, combo 3 = 16.53 ± 6.47, p value = 0.0004, n≥ 8 tumours, 4 mice, Mann Whitney U test) (SIT: 4hr veh = 1.79 ± 1.029, combo 1 = 24.14 ± 11.33, p value = 0.0015, combo 2 = 15.73 ± 4.74, p value = 0.0107, combo 3 = 14.16 ± 9.66, p value = 0.0015, n≥ 6 tumours, 4 mice, Mann Whitney U test) (Figure 5.15). These surprisingly high levels of cleaved caspase 3 suggest long term combination treatment may be highly beneficial in killing tumour cells effectively.

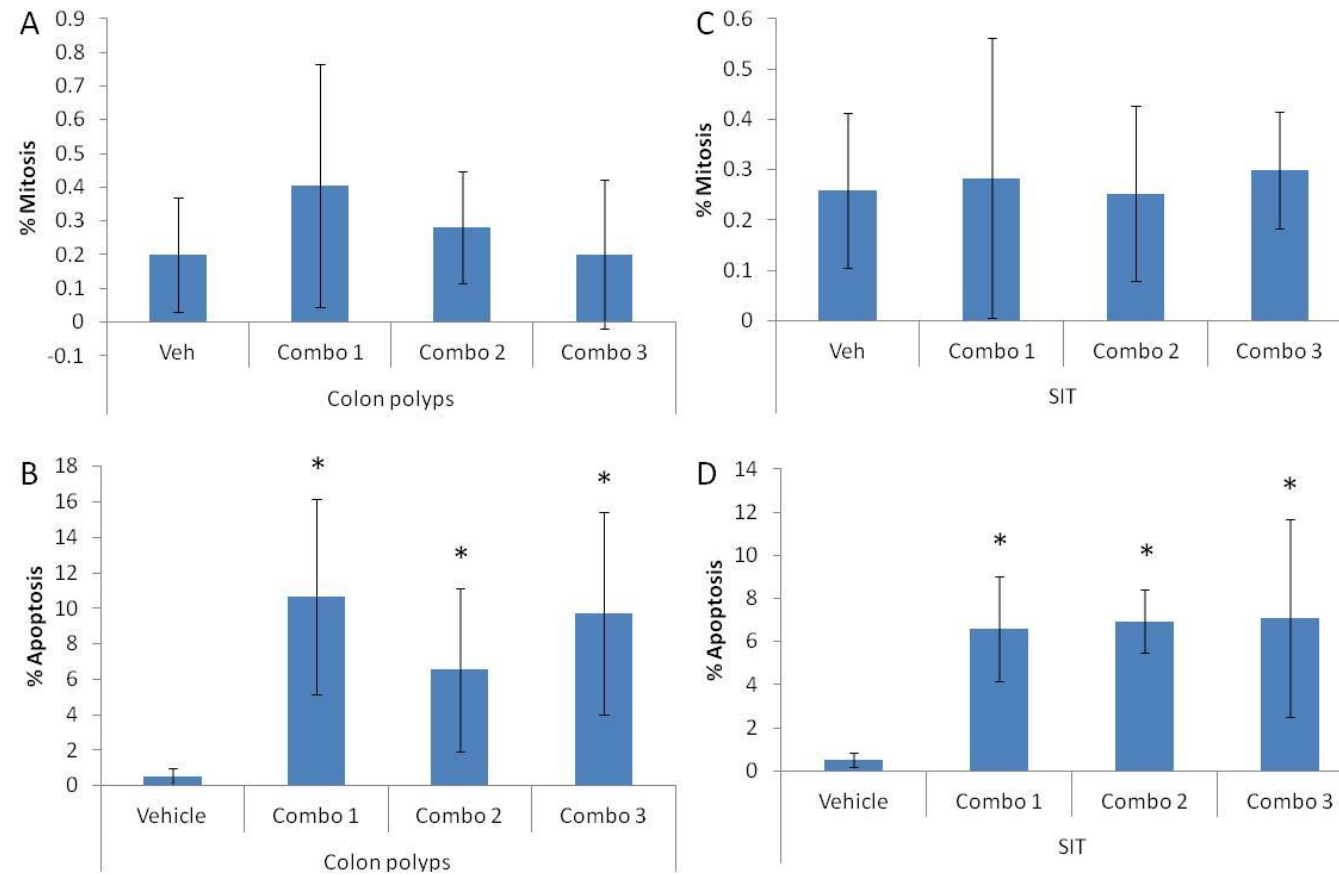


Figure 5.14 Anti-tumour effects of different combination strategies in $Apc^{f/+}$ $Kras^{LSL/+}$ colon polyps and small intestinal tumours (SITs)

Scoring of mitotic figures (**A + C**) and apoptotic bodies (**B + D**) in colon polyps and SITs by H&E examination revealed no significant alterations in the levels of mitotic figures, however did reveal increased apoptosis in colon polyps and SITs following all three combination strategies (*p value ≤ 0.05 for all, $n \geq 6$ tumours, 4 mice, Mann Whitney U test). Error bars represent standard deviation.

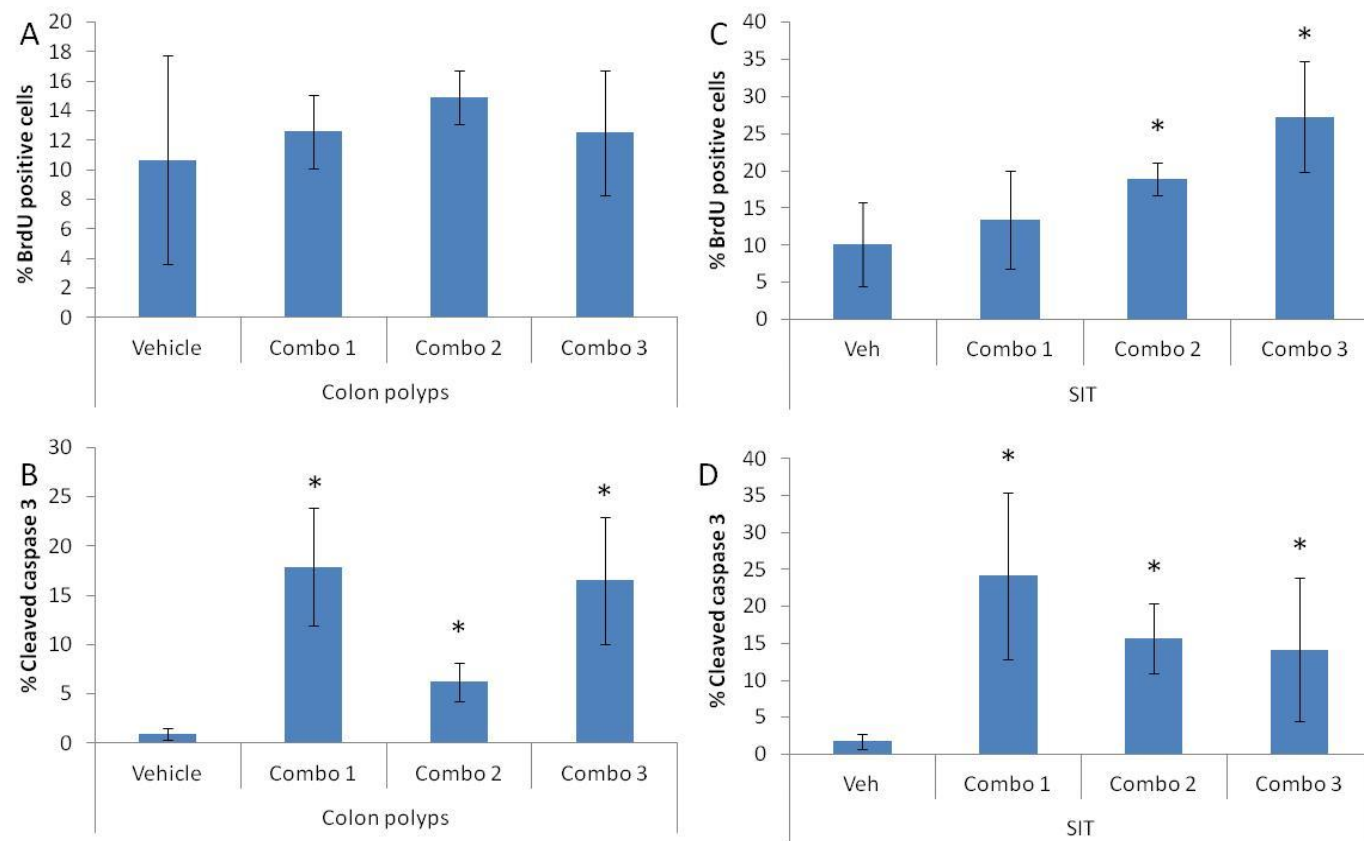


Figure 5.15 BrdU and cleaved caspase 3 scoring of three combination strategies in $Apc^{f/+} Kras^{LSL/+}$ colon polyps and small intestinal tumours (SITs)

IHC for BrdU and cleaved caspase 3 was carried out and scored in colon polyps and SITs from mice following exposure to the three different combination strategies. Scoring of BrdU (**A + C**) revealed no significant alterations in colon polyps but increased BrdU staining in SITs following combo 2 and 3. Quantification of cleaved caspase 3 staining (**B + D**) revealed increased levels following all three combination strategies in colon polyps and SITs. (*p value ≤ 0.05 for all, $n \geq 6$ tumours, 4 mice, Mann Whitney U test). Error bars represent standard deviation.

To investigate whether the anti-tumour effects of the combination strategies described above correlate with pathway inhibition, both colon polyps and SITs samples from mice exposed to the different combinations were interrogated by western blot analysis for MAPK and PI3K pathway status. Immunoblotting and subsequent densitometry analysis of individual polyp lysates (from n=3 mice) revealed a marked reduction in the levels of pERK with all three combinations, however no significant alteration in levels of either pAKT473 or pAKT308 (Figure 5.16, Table 5.9, Table 5.10). A significant reduction in levels of pS6RP was also observed with all three combinations but levels of p4EBP1 were found to be reduced only in response to combo 2 and 3 (Figure 5.16, Table 5.9, Table 5.10). Interestingly, the trends observed here with all three combination strategies suggest that addition of MEK162 to NVP-BEZ235, irrelevant of the order, eliminates the ability of NVP-BEZ235 to reduce levels of pAKT in colon polyps. The reason for this is currently unclear but may be attributable to an additive effect on levels of pAKT, whereby the increasing effects of MEK162 are negated by the reducing effects of NVP-BEZ235, as previously observed.

Colon polyps	Vehicle	Combo 1 (p value)	Vehicle	Combo 2 (p value)
pERK	5903.6 ± 308.6	355.42 ± 91.97 (0.0404)	4264 ± 1238.9	20.8 ± 18.9 (0.0404)
pAKT473	2405.1 ± 947.8	1677.1 ± 901.8 (0.1914)	2453.5 ± 69.6	3024.9 ± 256.5 (1.0)
pAKT308	1844.9 ± 254.9	2780.7 ± 96.1 (0.0404)	1663.8 ± 277.7	1694.9 ± 598.8 (0.6625)
pS6RP	2152.4 ± 1693.2	87.7 ± 59.3 (0.0404)	3570.9 ± 1445.1	1153.5 ± 472.5 (0.0404)
p4EBP1	4168.9 ± 1565.3	3268.7 ± 1218.9 (0.3313)	4189.9 ± 1565.3	1226.1 ± 682.9 (0.0404)

Table 5-9 Outline of raw densitometry values from western blot analysis of $Apc^{f/+}$ $Kras^{LSL/+}$

colon polyps 4 hours post exposure to combo 1 and combo 2, n=3, One-tailed Mann Whitney U test was used for statistical analysis

Colon polyps	Vehicle	Combo 3 (p value)
pERK	5876.9 ± 184.2	1216.1 ± 916 (0.0404)
pAKT473	4178.5 ± 702.5	3351.9 ± 195.4 (0.0952)
pAKT308	1661.1 ± 748.2	1790.1 ± 490.7 (1.0)
pS6RP	1453.9 ± 813.8	16.2 ± 20.4 (0.0404)
p4EBP1	5153.9 ± 765.2	3651.3 ± 320.9 (0.0404)

Table 5-10 Outline of raw densitometry values from western blot analysis of $Apc^{f/+}$ $Kras^{LSL/+}$ colon polyps 4 hours post exposure to combo 3, n=3, One-tailed Mann Whitney U test was used for statistical analysis

Western blot analysis of SITs from mice exposed to the varying combinations revealed a similar trend to that observed in colon polyps, with regards to pathway inhibition. A marked reduction in the levels of pERK was observed with all three combinations but no significant alterations in levels of pAKT473 or pAKT308 were observed (Figure 5.17, Table 5.11 and Table 5.12). Similarly to colon polyps, levels of pS6RP were found to be reduced with all three combinations whereas, p4EBP1 was found to be reduced with both combo 1 and combo 2 (Figure 5.17, Table 5.11 and Table 5.12). Overall in SITs, the addition of MEK162 has also diminished the ability of NVP-BEZ235 to reduce PI3K signalling through pAKT (mainly pAKT308) however in this case, the observations cannot be attributed to an additive effect because MEK162 alone did not increase levels of pAKT308 but in fact led to a significant reduction in levels of pAKT308.

SITs	Vehicle	Combo 1 (p value)	Vehicle	Combo 2 (p value)
pERK	3546.9 ± 1033.7	297.4 ± 35.9 (0.0404)	6274.9 ± 564.4	1054.7 ± 273.6 (0.0404)
pAKT473	1794.2 ± 340.2	1327.8 ± 452.6 (0.0952)	3235.7 ± 470.2	3123.6 ± 647.8 (0.0952)
pAKT308	1993.2 ± 406.9	1459.1 ± 567.4 (0.0952)	1019.7 ± 333.9	2067.2 ± 913.3 (0.1914)
pS6RP	1544.0 ± 886.9	578.3 ± 147.9 (0.0404)	1544.0 ± 886.9	134.9 ± 125.9 (0.0404)
p4EBP1	5972.1 ± 1966.8	3827.0 ± 864.7 (0.0404)	5972.1 ± 1966.8	1795.9 ± 90.8 (0.0404)

Table 5-11 Raw densitometry values from western blot analysis of Apc^{f/+} Kras^{LSL/+} SITs 4 hours post exposure to combo 1 and combo 2, n=3, One-tailed Mann Whitney U test was used for statistical analysis

SITs	Vehicle	Combo 3 (p value)
pERK	5158.9 ± 416.2	271.1 ± 159.2 (0.0404)
pAKT473	2829.9 ± 681.7	2124.4 ± 1833.9 (0.3313)
pAKT308	1711.9 ± 490.1	1249.8 ± 1061.7 (0.1914)
pS6RP	5702.2 ± 884.9	1379.4 ± 842.5 (0.0404)
p4EBP1	6585.9 ± 1256.2	4897.2 ± 3318.2 (0.1914)

Table 5-12 Raw densitometry values from western blot analysis of Apc^{f/+} Kras^{LSL/+} SITs 4 hours post exposure to combo 3, n=3, One-tailed Mann Whitney U test was used for statistical analysis

Given the above observations, analysis of the three chosen combination strategies in Kras mutant colon and SITs revealed that all three were similar in terms of their anti-tumour and pharmacodynamics effects. In light of this, combination strategy 2 which was identified as the most effective in Apc^{f/+} Pten^{f/f} tumours in chapter 4, was chosen for all further experiments to remain consistent across the different genotypes of mice evaluated in this study.

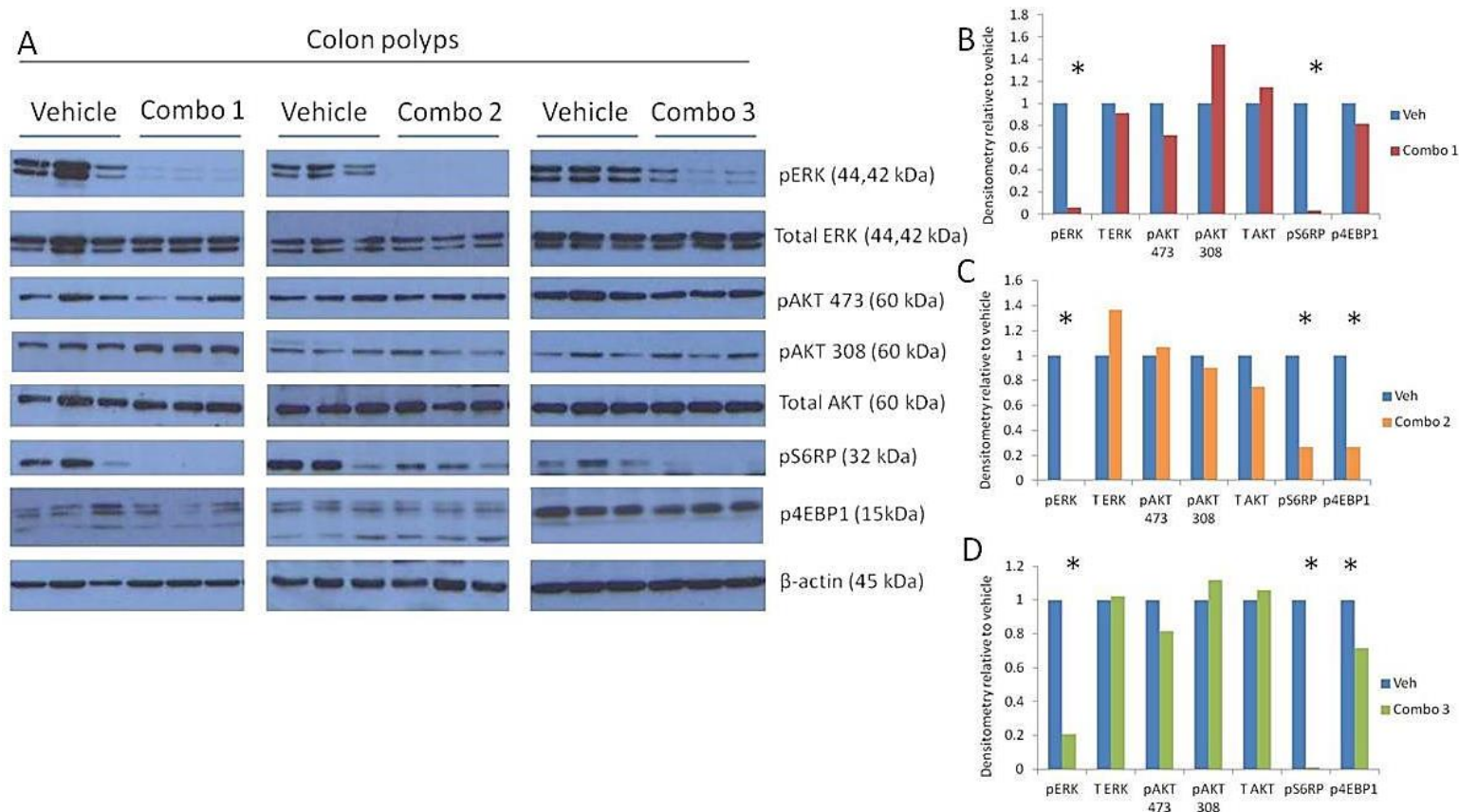


Figure 5.16 sequencing of combination has no differential effect on signalling in *Apc^{f/+} Kras^{LSL/+}* colon polyps. (A) Individual colon polyp lysates from n=3 mice exposed to the different combination strategies were analysed by western blotting for effectors of MAPK and PI3K/mTOR signalling. Significant reduction of pERK but no alterations in pAKT308 or pAKT473 was observed with all three combination strategies. Significant reduction of pS6RP an effector downstream of mTOR was also observed with all three combinations however, a significant reduction in p4EBP1 was only observed with combo 2 and 3. (B + C) Densitometry analysis was carried out to quantify differences observed from western blotting. These are normalised to β-actin as loading control and represented as relative to vehicle controls (*p values = 0.0404, n=3, Mann Whitney U test).

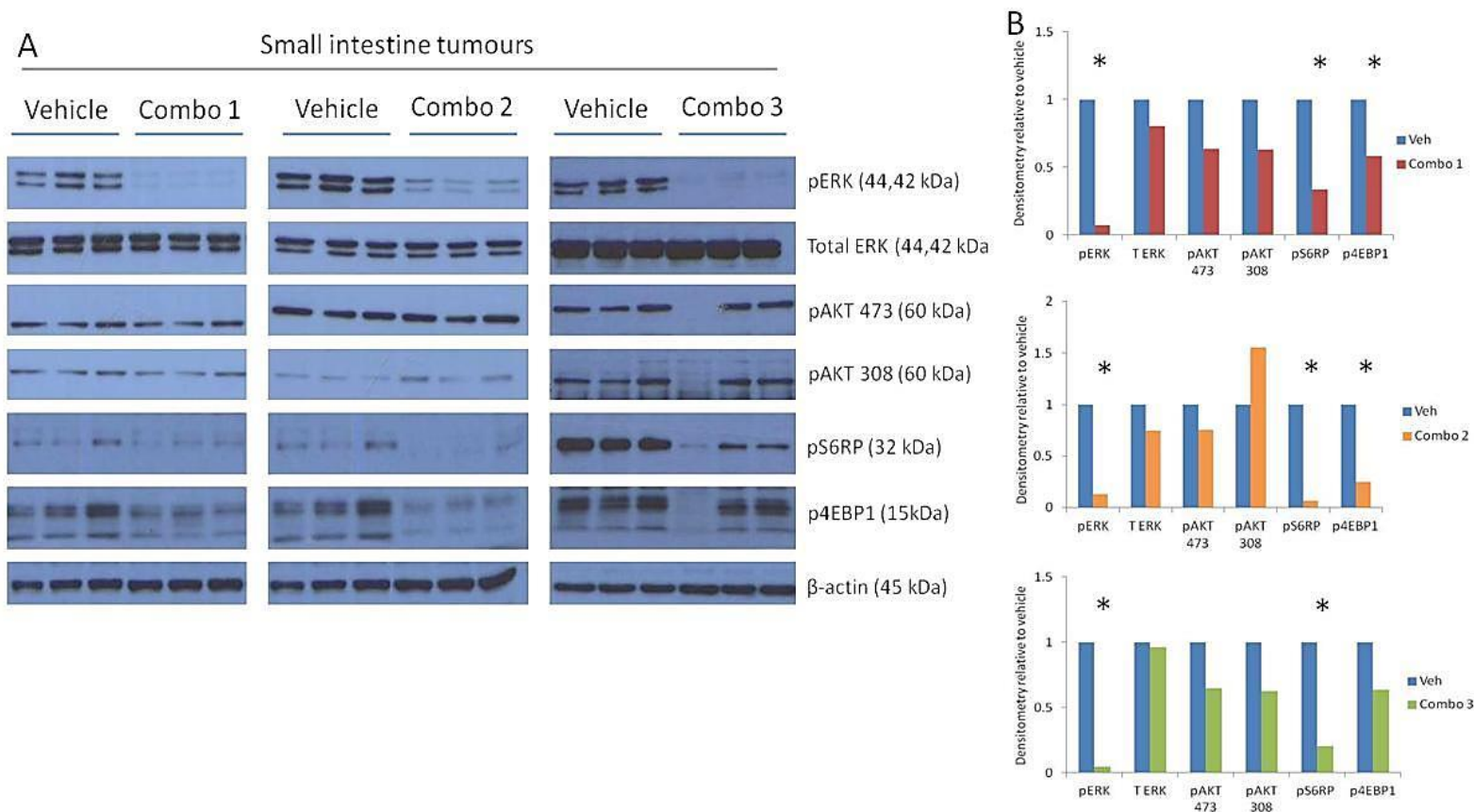


Figure 5.17 sequencing of combination has no differential effect on signalling in $Apc^{f/+} Kras^{LSL/+}$ small intestinal tumours (SITs). (A) To investigate the effects of the three combination sequences on downstream pathway signalling, individual tumour lysates from n=3 mice were analysed by immunoblotting. Similarly to colon polyps, a significant reduction in levels of pERK were observed with all three combinations and no significant reduction of pAKT308 or pAKT473 were observed. Additionally, significant reduction of pS6RP was observed with all three combination strategies, but significant reduction of p4EBP1 only with combo 1 and 2. (B + C) Densitometry analysis was carried out to quantify differences observed from western blotting. These are normalised to β -actin as loading control and represented as relative to vehicle controls (*p values = 0.0404, n=3, Mann Whitney U test).

5.2.6 Long term combination results in an additive increase in survival in $Apc^{f/+}$ $Kras^{LSL/+}$ mice

As described previously, investigation of twice-daily NVP-BEZ235 and MEK162 treatment in a short pilot experiment identified this regimen to be toxic (determined by weight loss) for wild-type mice (Figure 4.16). Therefore, the combination dose was reduced and administered as twice-daily NVP-BEZ235 but only once-daily MEK162, which was found to be well tolerated in $Apc^{f/+}$ $Pten^{f/f}$ mice and increased lifespan of mice (Figure 4.18). Given these observations, the later combination regimen was chosen for long term treatment in $Apc^{f/+}$ $Kras^{LSL/+}$ mice. A cohort of 13 mice were induced and aged to 100 days post induction at which point they were administered with 35mg/kg NVP-BEZ235 twice-daily plus 30mg/kg MEK162 once daily (1 hour after the initial dose) and monitored closely until a survival end point. Shortly after the experiment began it became apparent that this regimen was toxic for $Apc^{f/+}$ $Kras^{LSL/+}$ mice as 8/13 were culled due to substantial weight loss (weights of mice are shown on figure 5.18, survival of mice on figure 5.19). Despite this, 5/13 mice appeared to tolerate the treatment after some time and displayed a marginal survival benefit compared to vehicle controls (figure 5.19), indicating the potential benefits of combination in the absence of toxic effects.

In light of these additional toxicity issues, a second further reduced combination regimen of 35mg/kg NVP-BEZ235 once daily plus 30mg/kg MEK162 once daily (1 hour after the first dose) – combo R2, was conducted, in an effort to elucidate the potential of long term combination treatment in the *Kras* mutant tumour setting. For this, a cohort of 12 mice were induced and aged to 100 days post induction at which point they were administered with the further reduced combination treatment (as above) until a survival end point, or until the experimental end point of 500 days post induction. Additionally, controls of 35mg/kg NVP-BEZ235 as once daily and 30mg/kg MEK162 as once daily treatments were also conducted. Interestingly, reduced once daily MEK162 treatment significantly increased survival of $Apc^{f/+}$ $Kras^{LSL/+}$ mice in comparison with vehicle controls, but not in comparison to twice daily administration of MEK162 (median survivals: MEK T-D = 287 days vs MEK O-D = 286 vs veh = 153 days post induction, p values ≤ 0.0001 , Log-Rank and Wilcoxon test) (Figure 5.20), indicating that the maximal benefit with respect to survival benefit was reached with the once-daily regimen. Similarly, reduced NVP-BEZ235 to a once-daily regimen also significantly increased survival of $Apc^{f/+}$ $Kras^{LSL/+}$ mice in comparison with vehicle treated mice however, in this case, the effect on survival was found to be dose dependent as the higher dose was found to increase survival further (median survivals: NVP-BEZ235 T-D = 343 days, NVP-BEZ235 O-D = 267 days, veh = 153

days post induction, p value = 0.019, n=12 mice per cohort, Log-Rank test) (Figure 5.20). Importantly, the reduced combination treatment in $Apc^{f/+} Kras^{LSL/+}$ mice was found to be better tolerated than the first combination regimen (figure 5.18) and significantly increased longevity of $Apc^{f/+} Kras^{LSL/+}$ mice from a median of 153 days to 389 days post induction (Figure 5.20). The combination treatment here was found to be significantly better than single agent NVP-BEZ235 once-daily treatment (combo median survival = 389 vs NVP-BEZ235 median survival = 267 days post induction, p value = 0.029 for Log-Rank and p value = 0.042 for Wilcoxon test) however, not significantly better in comparison with single agent MEK162 regardless of the 100 days increase in median survival on combination treatment (MEK162 median survival = 286 days vs combo = 389 days post induction, p value = 0.374 for Log-Rank and p value = 0.279 for Wilcoxon test) (Figure 5.20). This was likely to be due to convergence of the two survival curves at 400 days post induction with both cohorts having 2/12 mice reach the experimental end point of 500 days. Nevertheless, the combination treatment resulted in an additive increase in median survival for $Apc^{f/+} Kras^{LSL/+}$ mice, potentially indicating increased therapeutic benefits here.

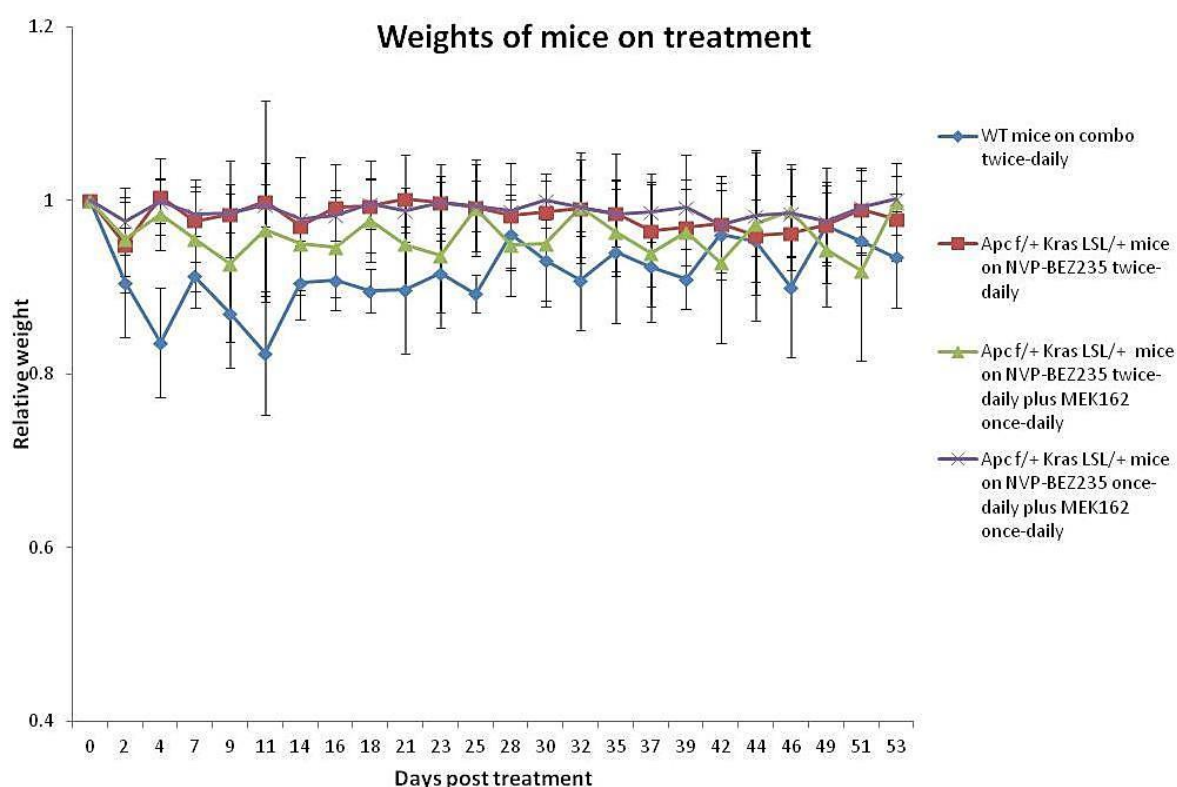


Figure 5.18 Combination treatment was found to induce toxicity in $Apc^{f/+}$ $Kras^{LSL/+}$ mice.

Previously in figure 4.15, administration of 35mg/kg NVP-BEZ235 twice-daily plus 30mg/kg MEK162 once daily was shown to be well tolerated in $Apc^{f/+}$ $Pten^{f/f}$ mice. Administration of this combination strategy in $Apc^{f/+}$ $Kras^{LSL/+}$ mice however, led to notable fluctuations in body weight, n=8/13 mice were culled due to weight loss of approximately 20% of the original body weight. A further reduced combination of 35mg/kg NVP-BEZ235 once daily plus 30mg/kg MEK162 once daily (1 hour later) was then conducted and was found to be better tolerated. Single agent NVP-BEZ235 twice daily was well tolerated in $Apc^{f/+}$ $Kras^{LSL/+}$ mice and so was chosen as a comparison. Error bars represent relative standard deviation

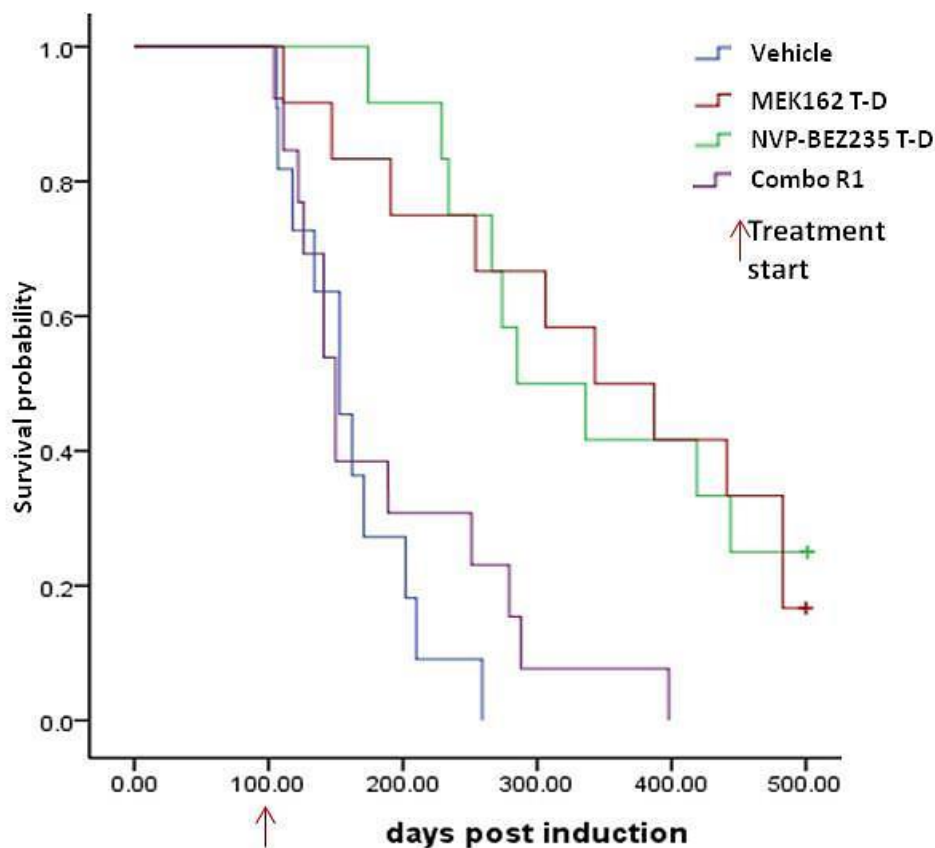


Figure 5.19 Kaplan-Meier survival analysis of $Apc^{f/+}$ $Kras^{LSL/+}$ mice receiving long term combination treatment (Combo R1) compared to single agent NVP-BEZ235, MEK162 and vehicle controls

$Apc^{f/+}$ $Kras^{LSL/+}$ mice were induced and aged to 100 days post induction, at which point mice were randomised to receive either 0.5% Methyl cellulose (Vehicle control) or 35mg/kg NVP-BEZ235 twice daily plus 30mg/kg MEK162 once daily, 1 hour after the first dose, by oral gavage, until a survival end point or the experimental endpoint of 500 days. Continuous combination treatment (Combo R1) was shown to have no significant effect on median survival of mice in comparison to vehicle controls and approximately only 40% of mice appeared to have had some survival advantage. (Median survival: combo R1 = 150 days vs vehicle = 153 days post induction, p values: Log-Rank = 0.41 and Wilcoxon test = 0.84, $n \geq 12$ mice per cohort). Interestingly, single agent MEK162 and NVP-BEZ235 are equipotent in terms of survival benefit for $Apc^{f/+}$ $Kras^{LSL/+}$ mice (Median survival: MEK162 = 287 days vs NVP-BEZ235 = 343 days post induction, p values: Log-Rank = 0.523 and Wilcoxon test = 0.878, $n \geq 12$ mice per cohort).

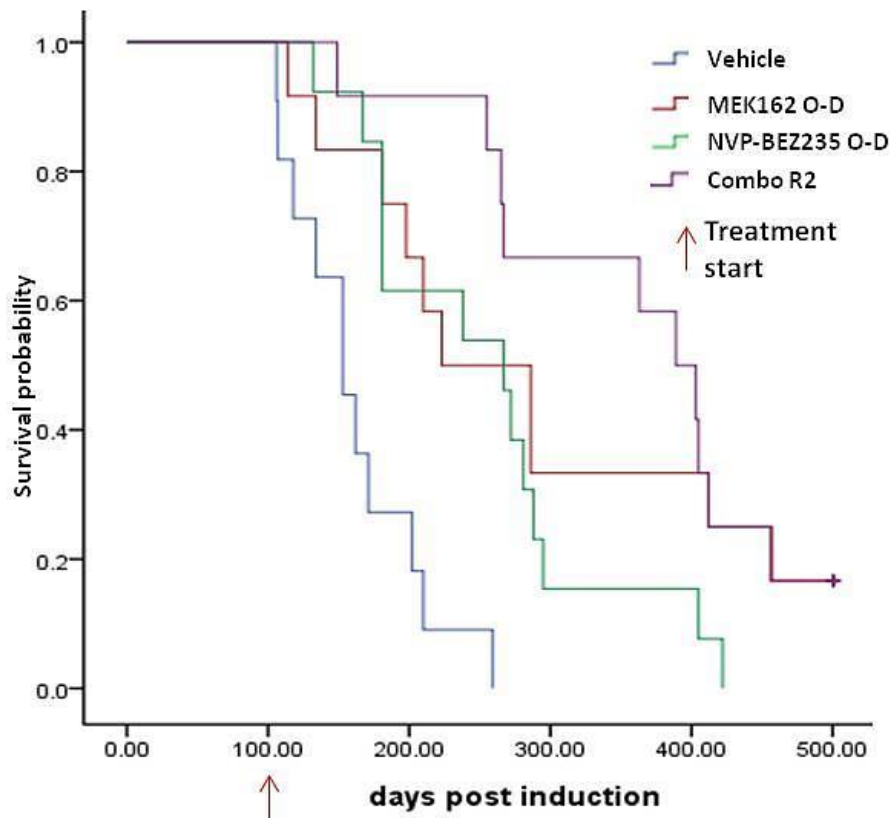


Figure 5.20 Kaplan-Meier survival analysis of $Apc^{f/+}$ $Kras^{LSL/+}$ mice receiving reduced combination treatment (Combo R2) long term compared to reduced single agent NVP-BEZ235 and MEK162, and vehicle controls

Induced and aged to 100 days post induction, $Apc^{f/+}$ $Kras^{LSL/+}$ mice were randomised to receive either 0.5% Methyl cellulose (Vehicle control), 30mg/kg MEK162 once daily, 35mg/kg NVP-BEZ235 once daily or 35mg/kg NVP-BEZ235 once daily plus 30mg/kg MEK162 once daily (1 hour after) by oral gavage, until a survival end point or the experimental endpoint of 500 days. Combo R2 treatment significantly increased survival of mice to a median of 389 days post induction, compared 153 days with vehicle controls (p values Log-Rank and Wilcoxon test ≤ 0.0001 , $n \geq 12$ mice per cohort). Interestingly, combo 2 was significantly better than reduced single agent NVP-BEZ235, but not in comparison to reduced single agent MEK162 (median survival Combo R2 = 389 days vs NVP-BEZ235 = 267 days vs MEK162 = 286 days, p values for Combo R2 vs NVP-BEZ235: Log-Rank = 0.029 and Wilcoxon = 0.042, p values for Combo R2 vs MEK162: Log-Rank = 0.374 and Wilcoxon = 0.279).

5.2.7 Analysis of tumour burden following treatment in $Apc^{f/+}$ $Kras^{LSL/+}$ mice

As well as the effect of treatment on survival of mice, the effect on tumour burden was also assessed following long term treatment. For this, tumours were counted, measured and staged according to severity (as described in methods section 2.7.4). As in section 4.2.8, these parameters of tumour burden were also assessed in a cohort of mice harvested at the treatment start point which in this case was 100 days post induction.

5.2.7.1 Analysis of tumour number following treatment in $Apc^{f/+}$ $Kras^{LSL/+}$ mice

The total number of tumours present at death was scored from H&E stained slides of colon and small intestine 'swiss rolls'. For each sample three H&E stained slides were scored blind, the average calculated per mouse and subsequently averaged per cohort. At 100 days post induction, $Apc^{f/+}$ $Kras^{LSL/+}$ mice bore a median of 16 colon lesions and 33 SITs per mouse (n=4 mice). Vehicle treated $Apc^{f/+}$ $Kras^{LSL/+}$ mice had a median of 30 colon lesions and 34 SITs (n=12 mice) at death indicating that although the number of colon polyps significantly increased between the start and vehicle cohorts, tumours were present at the start of treatment confirming treatment was not in a prophylactic setting (start = 15.5 tumours vs vehicle = 30.3 tumours, $p = 0.0223$, $n \geq 6$, Mann Whitney U test) (Figure 5.21, 5.22). The median number of colon polyps at death was significantly reduced in both MEK162 treatment cohorts (T-D and O-D) compared to vehicle controls (vehicle = 30.3 vs MEK162 T-D = 7.7, p value = 0.0064, MEK162 O-D = 13, p value = 0.0058, $n \geq 6$, Mann Whitney U test) (Figure 5.21) however, SITs were found to be reduced in MEK162 twice-daily treated mice (and not once-daily) in comparison with the start and vehicle treated cohorts (start = 32.5 veh = 34, MEK162 T-D = 12, p value = 0.050 compared to start and p value = 0.026 compared to vehicle, MEK162 O-D = 14, p value = 0.058 compared to start and p value = 0.057 compared to vehicle cohorts, $n \geq 6$, Mann Whitney U test) (Figure 5.22).

Analysis of tumours present at death following long term NVP-BE2235 treatment revealed that the median number of colon tumours at death was significantly increased with the once-daily (O-D) treatment, in comparison to with the start cohort but not in comparison with vehicle treated mice (Colon polyps: start = 15.5, vehicle = 30.3, NVP-BE2235 O-D = 39, p value = 0.037 for start and p value = 0.095 for vehicle comparisons, $n \geq 6$, Mann Whitney U test) (Figure 5.20). The number of SITs with once-daily NVP-BE2235 treatment however, was found to be increased compared to vehicle but not in comparison with the start cohort (SITs: start = 32.5, vehicle = 34, NVP-BE2235 O-D = 74, p value = 0.076 for start and p value = 0.023 for vehicle

comparison, $n \geq 6$, Mann Whitney U test) (Figure 5.22). Interestingly, no difference in the number of colon polyps or SITs was found with NVP-BEZ235 twice daily treatment in comparison with either the start or vehicle treated cohorts. (Colon polyps: start = 15.5, vehicle = 30.3, NVP-BEZ235 T-D = 26, p value = 0.089 for start and p value = 0.526 for vehicle cohort $n \geq 6$, Mann Whitney U test) (SITs: start = 32.5, vehicle = 34, NVP-BEZ235 T-D = 63, p value = 0.289 for start and p value = 0.067 for vehicle comparison, $n \geq 6$, Mann Whitney U test) (Figure 5.21, 5.22). These observations indicate that whilst twice-daily NVP-BEZ235 treatment had no effect on total tumour number, once-daily treatment resulted in increased tumour number which may reflect increased tumour burden with the increase in longevity.

The median number of colon polyps was found to be significantly reduced with both combination strategies (R1 and R2) in comparison with vehicle treated mice but not in comparison with the start cohorts, suggesting tumour growth stasis (median number of colon polyps: start = 15.5, vehicle = 30.3, combo R1 = 17.5, p value = 0.777 for start and p value = 0.026 for vehicle comparison, combo R2 = 5, p value = 0.396 for start and p value = 0.0086 for vehicle comparison, $n \geq 6$, Mann Whitney U test,) (Figure 5.21). Additionally, a trend towards reduced SITs was observed with both combo R1 and R2 although not found to be significant in comparison with either start or vehicle cohorts (start = 32.5, vehicle = 34, combo R1 = 25.8, p value = 0.808 for start and p value = 0.926 for vehicle comparison, combo R2 = 18.3, p value = 0.299 for start and p value = 0.497 for vehicle comparison, $n \geq 6$, Mann Whitney U test) (Figure 5.22). Overall, these observations are more relevant for the combo R2 treatment due to the significant increase in survival, however together they display the favourable effects of combination treatment in terms of reduced tumour numbers in $Apc^{f/+}$ $Kras^{LSL/+}$ mice.

5.2.7.2 Analysis of total tumour area following treatment in $Apc^{f/+}$ $Kras^{LSL/+}$ mice

To determine the effect of various long term treatments on total tumour area, macroscopic tumours were measured from methacarn fixed colon and small intestine tissues and the total tumour area (mm^2) was calculated per mouse, per cohort. $Apc^{f/+}$ $Kras^{LSL/+}$ mice on vehicle treatment trended to have larger colon and SITs at death compared to the start cohort however, this was not significantly altered due to large variation within the cohorts (colon start = 12.8 ± 10.1 , colon vehicle = 55.2 ± 44.7 , p value = 0.194, SIT start = 43.8 ± 51.7 , SIT vehicle = 117.4 ± 51.7 , p value = 0.112, $n \geq 6$, Mann Whitney U test) (Figure 5.21). Analysis of colon tumour area in all treatment cohorts revealed no significant alterations in comparison to the start cohort (start = 12.8 ± 10.1 , MEK162 T-D = 21.5 ± 21.7 p value = 0.817, MEK162 O-D = 68.2 ± 90.6 p value = 0.269, NVP-BEZ235 T-D = 48.2 ± 59 p value = 0.508, NVP-BEZ235 O.D = $134.8 \pm$

105.6 p value = 0.126, combo R1 = 2.98 ± 6.3 p value = 0.123, combo R2 = 40.8 ± 58.9 p value = 1.0, $n \geq 6$, Mann Whitney U test) (Figure 5.20). This was also the case in comparison to vehicle cohorts, with the exception of combo R1 treatment, after which mice presented with significantly reduced total tumour area (start = 12.8 ± 10.1 , MEK162 T-D = 21.5 ± 21.7 p value = 0.28, MEK162 O-D = 68.2 ± 90.6 p value = 0.932, NVP-BEZ235 T-D = 48.2 ± 59 p value = 0.777, NVP-BEZ235 O-D = 134.8 ± 105.6 p value = 0.35, combo R1 = 2.98 ± 6.3 p value = 0.0168, combo R2 = 40.8 ± 58.9 p value = 0.396, $n \geq 6$, Mann Whitney U test) (Figure 5.21). These observations suggest all long term treatment regimens resulted in tumour growth stasis as no reduction in tumour area was detected in comparison with the start cohort. An Interesting observation was that mice on all reduced treatments (once-daily) trended to have larger tumour areas than mice on their corresponding twice-daily treatment regimens and may indicate a dose-dependent effect.

Analysis of SIT area in all long term treated cohorts revealed no significant differences in comparison to the start cohort (start = 43.8 ± 51.7 , MEK162 T-D = 58.3 ± 34.1 p value = 0.699, MEK162 O-D = 46.1 ± 55.9 p value = 0.671, NVP-BEZ235 T-D = 9.2 ± 10.9 p value = 0.637, NVP-BEZ235 O-D = 20.7 ± 31.1 p value = 0.799, combo R1 = 1.18 ± 2.13 p value = 0.396, combo R2 = 14.7 ± 26.1 p value = 0.488, $n \geq 6$, Mann Whitney U test) (Figure 5.22). Interestingly, all treatments except for MEK162 O-D, resulted in significantly reduced total SIT area in comparison with vehicle treated cohorts, suggesting tumour growth stasis, as tumour area was comparable in most cases with the start cohort (vehicle = 117.4 ± 26.9 , MEK162 T-D = 58.3 ± 34.1 p value = 0.037, MEK162 O-D = 46.1 ± 55.9 p value = 0.107, NVP-BEZ235 T-D = 9.2 ± 10.9 p value = 0.011, NVP-BEZ235 O-D = 20.7 ± 31.1 p value = 0.0085, combo R1 = 1.18 ± 2.13 p value = 0.0069, combo R2 = 14.7 ± 26.1 p value = 0.0069, $n \geq 3$, Mann Whitney U test) (Figure 5.22).

5.2.7.3 Analysis of tumour severity following treatment in *Apc^{f/+} Kras^{LSL/+}* mice

To further characterise the effect of treatment on tumour burden in *Apc^{f/+} Kras^{LSL/+}* mice, tumours on H&E stained colon and small intestine sections were staged according to severity and invasive features to ascertain whether treatment had an effect on tumour progression. The criteria for scoring were described previously in methods section 2.7.4 and section 4.2.8. The average number of each tumour type was calculated and is displayed as a proportion of the total number of tumours, due to differences in total tumour numbers observed.

For colon tumours, the general observations indicated a significant reduction in the percentage of microadenomas and a significant increase in the percentage of adenomas

compared to the start cohort. This was the case for all single-agent long term treatments, in comparison with the start cohort but not for combination treated cohorts. Furthermore, no significant differences were detected in tumour severity profiles of mice on any of the long term treated cohorts in comparison with vehicle treated mice (microadenomas: start = 93%, vehicle = 56% p value = 0.005, MEK162 T-D = 58% p value = 0.019, MEK162 O-D = 59% p value = 0.005, NVP-BEZ235 T-D = 72% p value = 0.0339, NVP-BEZ235 O-D = 58% p value = 0.0069; adenomas: start = 7%, vehicle = 41% p value = 0.005, MEK162 T-D = 36% p value = 0.0188, MEK162 O-D = 36% p value = 0.0188, NVP-BEZ235 T-D = 26% p value = 0.0339, NVP-BEZ235 O-D = 40% p value = 0.0069, $n \geq 6$, Mann Whitney U test) (Figure 5.21). Therefore, although differences in total tumour number and area were observed as described previously, tumours in mice at death were of comparable severity indicating treatment had no effect on tumour severity.

With long term combo R1 treatment, mice displayed no differences in the proportion of microadenomas and adenomas present at death in comparison with the start cohort however, mice did present with significantly fewer adenomas and more microadenomas in comparison with vehicle treated mice, indicating that treatment here halted progression of colon tumours even though no difference in survival was observed (microadenomas: start = 93%, vehicle = 56%, combo R1 = 86% p value = 0.525 for start and p value = 0.0043 for vehicle comparison; adenomas: start = 7%, vehicle = 41%, combo R1 = 12%, p value = 0.832 for start and p value = 0.0075 for vehicle comparison, $n \geq 6$, Mann Whitney U test) (Figure 5.21). Scoring the severity of tumours following combo R2 treatment showed no statistical alterations in comparison with both start and vehicle treated cohorts providing further evidence for tumour growth stasis (microadenomas: start = 93%, vehicle = 56%, combo R2 = 70% p value = 0.299 for start and p value = 0.651 for vehicle comparison; adenomas: start = 7%, vehicle = 41%, combo R2 = 29%, p value = 0.706 for start and p value = 0.365 for vehicle comparison, $n \geq 6$, Mann Whitney U test) (Figure 5.21).

Interestingly, grading of early invasive adenocarcinomas (EIAs) (characterised by submucosal invasion) identified a small proportion of these to be present in vehicle treated mice but not in the start cohort, indicating tumour progression (3% of tumours were EIAs in vehicle treated mice). A similar proportion of EIAs was observed in all drug treated cohorts (vehicle = 3%, MEK162 T-D = 5.5% p value = 0.358, MEK162 O-D = 4.9% p value = 0.325, NVP-BEZ235 = 1.5% p value = 0.13, NVP-BEZ235 O-D = 1.6% p value = 0.111, combo R1 = 2.3% p value = 0.149, combo R2 = 1.4% p value = 0.057, $n \geq 6$, Mann Whitney U test) indicating that although some

differences in tumour number and area as described previously, overall tumours at death were of comparable severity.

Scoring of tumour severity in the small intestine revealed that the vehicle cohort at death had more invasive lesions than the start cohort indicating tumour progression between the two points. This was characterised by the presence of significantly less microadenomas and more adenomas and a trend towards increased advanced invasive (AIAs) lesions, compared to the start cohort (start mAd = 94%, vehicle mAd = 85% p value = 0.0223, start Ad = 3.4%, vehicle Ad = 12.7% p value = 0.0109, start EIA = 2%, vehicle = 1.5% p value = 1.00, start AIA = 0%, vehicle = 0.8%, n_≥6, Mann Whitney U test) (Figure 5.22).

Furthermore in the small intestine, MEK162 treated cohorts (both once-daily and twice-daily cohorts) had significantly less microadenomas compared to the start cohort and trended to have more adenomas and invasive lesion, however this was not statistically significant (microadenomas: start = 94%, vehicle = 85% MEK162 T-D = 84% p value = 0.0265 for start and p value = 0.539 for vehicle, MEK162 O-D = 83% p value = 0.0312 for start and p value = 0.569; adenomas: start = 3.4%, vehicle = 12.6% MEK162 T-D = 11.2% p value = 0.0583 for start and p value = 0.4727 for vehicle, MEK162 O-D = 13% p value = 0.078 for start and p value = 0.361 for vehicle, n_≥6, Mann Whitney U test) (Figure 5.22). In comparison with vehicle treated mice, both MEK162 treatments had no statistically significant effect on tumour severity, although the proportion of invasive lesions (EIAs and AIAs) trended to be increased with both once-daily and twice-daily treatments (EIAs; start = 2%, vehicle = 1.5% p value = 1, MEK162 T-D = 1.2% p value = 0.648 for start and p value = 0.393 for vehicle, MEK162 O-D = 3.1% p value = 0.845 for start and p value = 0.896 for vehicle comparison, n_≥6, Mann Whitney U test).

Conversely to the observations above, mice on NVP-BEZ235 (once-daily and twice-daily treatments) and both combination regimens (combo R1 and R2) possessed less adenomas and more microadenomas in the small intestine. This was statistically significant in comparison with vehicle cohorts but not in comparison with the start cohort indicating stasis of tumour growth and progression with these treatments (microadenomas: start = 94%, vehicle = 85%, NVP-BEZ235 T-D = 90% p value = 0.289 for start p value = 0.0054 for vehicle comparison, NVP-BEZ235 O-D = 95% p value = 0.396 for start and p value = 0.003 for vehicle comparison, combo R1 = 99% p value = 0.856 for start and p value = 0.0002 for vehicle comparison, combo R2 = 90% P value = 0.508 for start and p value = 0.0185 for vehicle comparison; adenomas: start = 3.4%, vehicle = 12.7%, NVP-BEZ235 T-D = 7.9% p value = 0.104 for start and p value = 0.0317 for vehicle comparison, NVP-BEZ235 O-D = 5% p value = 0.143 for start and p value = 0.0098

for vehicle comparison, combo R1 = 0.8% p value = 0.762 for start and p value = 0.0002 for vehicle comparison, combo R2 = 7.9% p value = 0.508 for start and p value = 0.0185 for vehicle comparison, $n \geq 6$, Mann Whitney U test) (Figure 5.22).

Finally, the proportion of EIAs and AIAs was also not significantly altered with either NVP-BEZ235 or combination treatments providing further evidence for stasis of tumour progression with treatment (EIAs: start = 2%, vehicle = 1.5%, NVP-BEZ235 T-D = 0.13% p value = 0.734 for start and p value = 0.597 for vehicle comparison, NVP-BEZ235 O-D = 0.4% p value = 0.508 for start and p value = 0.224 for vehicle comparison; AIAs: vehicle = 0.85%, NVP-BEZ235 T-D = 0.4% p value = 0.86, NVP-BEZ235 O-D = 0.3% p value = 0.939, combo R1 = 0.3% p value = 0.601, combo R2 = 1.3% p value = 0.928, $n \geq 6$, Mann Whitney U test) (Figure 5.22).

In summary, analysis of various parameters of tumour burden here indicate that whilst twice-daily MEK162 treatment significantly reduced the number of small intestinal and colonic lesions and reduced total tumour area in the small intestine, treatment had no effect on progression of tumours. Also, although twice-daily NVP-BEZ235 treatment in $Apc^{f/+} Kras^{LSL/+}$ mice had no effect on colon polyps with respect to the parameters of tumour burden analysed here, treatment did reduce tumour area and halts progression of lesions in the small intestine. These findings provide some insights into the importance of MAPK and PI3K pathways in $Apc^{f/+} Kras^{LSL/+}$ tumours highlighting that MAPK signalling may be more important for growth of tumours whereas PI3K signalling may be more crucial for progression of tumours. Furthermore, tumour burden analyses in the combination treated cohorts corroborate these hypotheses as treatment resulted in fewer colon lesions. Also in the small intestine, reduced total tumour area was coupled with less invasive lesions in comparison with vehicle treated cohorts.

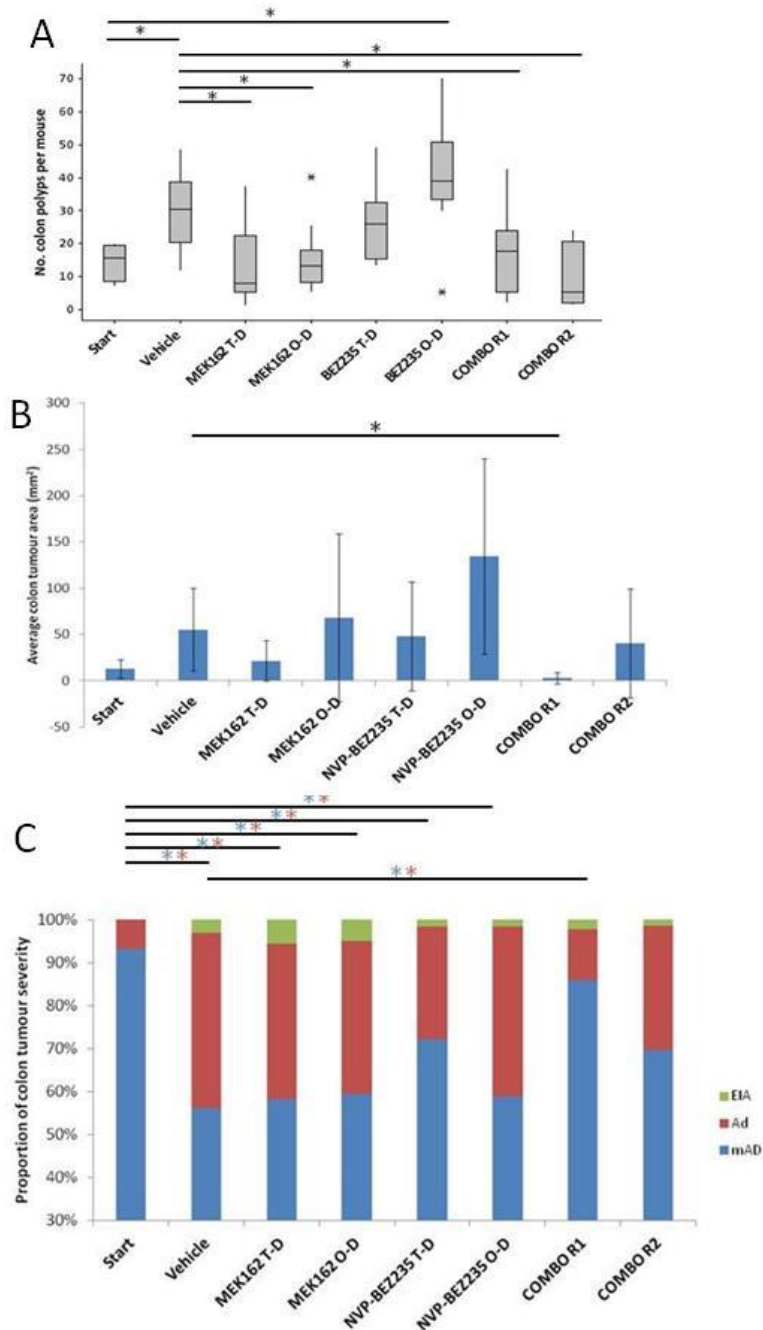


Figure 5.21 Colon tumour burden analysis of $Apc^{f/+} Kras^{LSL/+}$ mice on all long term treatments.

(A) $Apc^{f/+} Kras^{LSL/+}$ mice on vehicle had significantly more colon tumours at death compared to a cohort of mice culled at the treatment start point. Mice on MEK162 T-D and O-D and combo R1 and R2 had significantly reduced tumours compared to vehicle treated mice, **(B)** In terms of tumour area, only $Apc^{f/+} Kras^{LSL/+}$ mice on combination treatment which resulted in toxicity (combo R1) had significantly reduced total tumour area at death, **(C)** Key: mAd – microadenoma, Ad – adenoma, EIA – early invasive adenocarcinoma, AIA – advanced invasive adenocarcinoma. The proportion of mAds were found to be significantly reduced and adenomas were found to be significantly increased with all single-agent treatments in comparison to the start cohort. The opposite pattern was found with combo R1 treatment compared to vehicle cohorts (* p value ≤ 0.05 , $n \geq 6$, Mann Whitney U test).

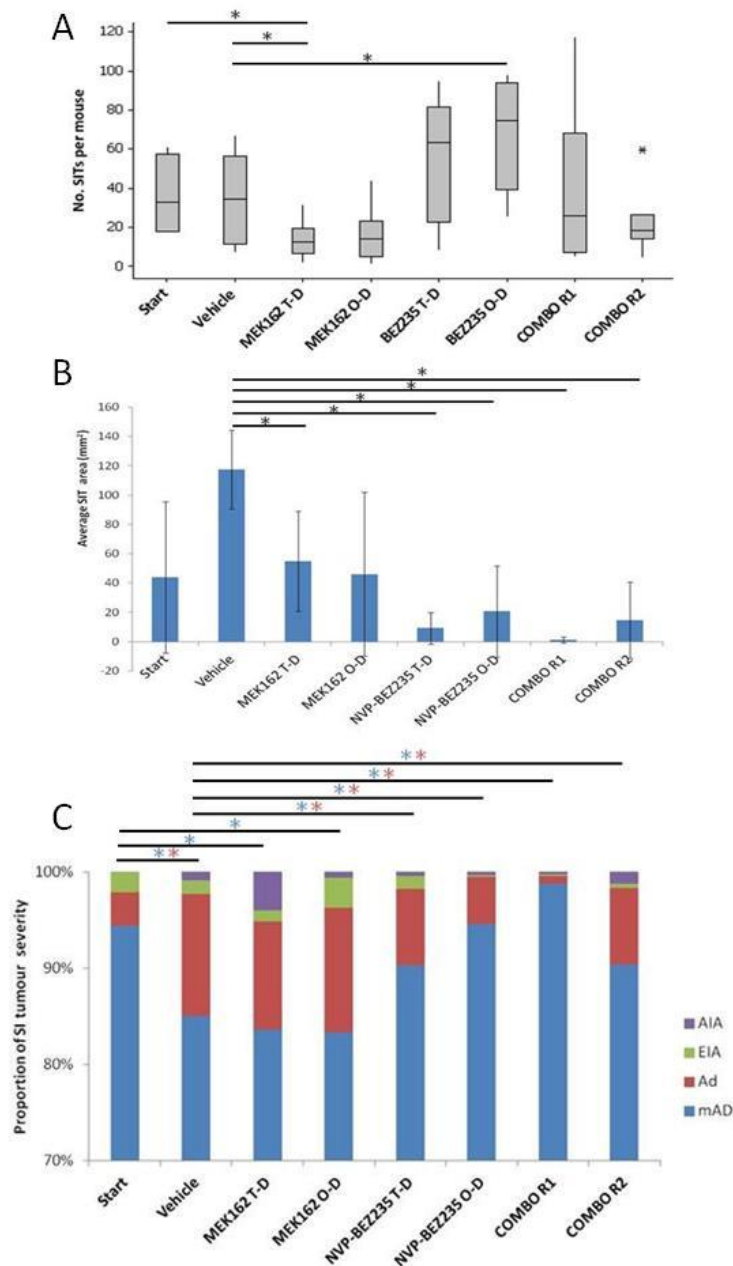


Figure 5.22 Small intestinal tumour burden analysis of $Apc^{f/+} Kras^{LSL/+}$ mice on all long term treatments

(A) $Apc^{f/+} Kras^{LSL/+}$ mice on MEK162 T-D have significantly reduced tumours compared to the start cohort and vehicle treated mice, whereas mice on NVP-BEZ235 O-D had significantly more tumours at death compared to vehicle treated mice. **(B)** Assessment of tumour area following fixation revealed mice on all treatment cohorts except those on MEK162 O-D had significantly reduced tumour area compared to vehicle cohorts. **(C)** Key: mAd – microadenoma, Ad – adenoma, EIA – early invasive adenocarcinoma, AIA – advanced invasive adenocarcinoma. Mice on vehicle and both MEK162 treatments had significantly less mAds than the start cohort but only vehicle mice had significantly more Ads compared to the start cohort. Mice on MEK162 O-D, NVP-BEZ235 T-D and O-D, Combo R1 and mice on combo R2 had significantly altered mAds and Ads compared to vehicle treated mice. (* p value ≤ 0.05 , $n \geq 6$, Mann Whitney U test)

5.3 Discussion

5.3.1 *MEK inhibition lead to increased PI3K signalling in Kras mutant tumours, however still increases survival of $Apc^{f/+}$ $Kras^{LSL/+}$ mice*

The oncogene KRAS is one of the most frequently altered genes in human cancer and leads to aberrant activation of MAPK and PI3K signalling, both of which are crucial for a myriad of processes that regulate cancer cell survival (Sebolt-Leopold and Herrera, 2004, Engelman, 2009). This has subsequently led to a surge in the development of targeted agents for these signalling pathways, and their investigation in KRAS mutant tumour settings as a stratified treatment approach. The main objective of this chapter was to investigate the therapeutic potential of targeting MAPK and PI3K signalling using a robust and clinically relevant model of CRC, driven by activation of oncogenic Kras. Here, concurrent heterozygous deletion of Apc and activation of oncogenic Kras (Janssen et al., 2006) leads to tumour progression driven by activation of ERK, a downstream effector in the RAS-RAF-MEK kinase cascade, and AKT, a downstream effector of PI3K signalling. Activation of these mutations driven by the intestinal specific VillinCreER recombinase transgene causes mice to succumb to disease by approximately 150 days post induction, at which point they present with lesions in both the colon and small intestine (Davies et al., *in press*, Janssen et al., 2006). For all experiments described in this chapter, 10 week old mice were induced by i.p. injections of Tamoxifen and aged. Mice were either aged until the chosen treatment start point of 100 days, or until they presented with symptoms of disease, at which point they received a single dose of treatment and were culled at defined short term time points to investigate the immediate anti-tumour and pharmacodynamic effects of treatment.

Firstly, the effects of targeting the MAPK pathway using the MEK1/2 inhibitor MEK162 were assessed acutely and chronically in the Kras mutant tumour model to ascertain whether this could be beneficial therapeutically against Kras mutant CRC, as hypothesised. In colon polyps, acute MEK162 administration resulted in inhibition of phosphorylated ERK, the MAPK effector directly downstream MEK1/2. Here, levels of pERK were found to be reduced at both 4 and 24 hour time points; however inhibition was less marked at 24 hours indicating reduced pathway inhibition (Figure 5.3). Western blot analysis also showed that SITs were less sensitive to MEK inhibition as pERK levels were only found to be reduced at 4 hours post exposure and not at the 24 hour time point (Figure 5.4). As described previously, phosphorylated and hence activated ERK1/2 acts as a catalyst for one branch of MAPK signalling where it is responsible for a number of cellular processes including proliferation, differentiation, survival and

apoptosis (Johnson and Lapadat, 2002). These functions are mediated in the cytoplasm or once translocated to the nucleus through direct interactions with transcriptional repressors or transcription factors of target genes including Fos, Myc and Jun (Murphy et al., 2004). As well as repressing signalling, MEK162 increased apoptosis in both colon polyps and SITs 4 hours following exposure with no discernable effect on mitosis, suggesting reduced cell number (Figure 5.1, 5.2). Concordantly, scoring of BrdU positive cells in tumours post MEK162 exposure revealed no gross alterations at the 4 hour time point however, an increase in the number of BrdU positive cells was detected in SITs 24 hours post exposure to MEK162 (Figure 5.2). The reasons for this are unclear, however may be attributable to a compensatory mechanism to overcome the initial increase in apoptosis or may reflect cells stuck in S phase of the cell cycle.

Recently, a number of studies investigating the consequences of MEK inhibition in cancer cell lines have reported compensatory activation of the closely associated PI3K signalling pathway (Turke et al., 2012, Yuen et al., 2012). In this study, probing of PI3K pathway activity revealed differential effects in colon polyps and SIT exposed to MEK inhibition. In colon polyps, a trend towards an increase in PI3K signalling through pAKT473, pAKT308 and pS6RP was observed 4 hours post exposure to MEK162 with a significant increase in pAKT308 at 24 hours post exposure (Figure 5.3). In contrast, a reduction in PI3K signalling was observed in SITs with MEK162 exposure, evidenced through reduced levels of pAKT473 and pS6RP at 4 and 24 hours post exposure respectively (Figure 5.4). The mechanisms behind the contrasting response of tumours to MEK162 are currently unclear, however may be due to differences in basal pathway activation, as observed in chapter 3, where the MAPK and PI3K pathways were found to be increasingly activated in $Apc^{f/+} Kras^{LSL/+}$ colon polyps in comparison to SITs (Figure 3.13). The mechanism behind the compensatory activation of PI3K signalling is currently unknown but may be due to divergence of the two signalling cascades at mTOR, through direct interactions between Kras and p110 (Kodaki et al., 1994), or negative feedback loops which directly affect signalling of PI3K cascade at receptor level as identified by Turke et al and Yuen et al. As such, Turke and colleagues found that MEK inhibition led to increased PI3K signalling through hyperactivation of ERBB3, which was due to loss of inhibitory threonine phosphorylation on membrane domains of EGFR and HER2 (Turke et al., 2012). Yuen et al show that MEK inhibition lead to activation of pAKT specifically in Kras mutant and not wild-type cancer cell lines. The authors propose that MEK inhibition in Kras mutant cells is not sufficient to lead to apoptosis and hence leads to increased PI3K signalling as a feedback mechanism to protect cells from apoptosis (Yuen et al., 2012). Subsequently, combinatorial

inhibition here led to sustained inhibition of MAPK and PI3K signalling as well as an enhanced effect on apoptosis (Yuen et al., 2012).

Nevertheless, continuous treatment of MEK162 in $Apc^{f/+}$ $Kras^{LSL/+}$ mice at a dose of 30mg/kg twice-daily, led to a significant increase in survival, extending lifespan of mice from a median of 153 days to 287 days post induction (Figure 5.7). The effect on tumour burden was also favourable, indicated by a reduction in the total number of colon polyps and SITs compared to vehicle treated mice (Figure 5.21, 5.22). Furthermore, the total SIT area was significantly reduced with MEK162 treatment. Interestingly, although no significant differences were detected with regards to tumour severity, a trend towards more advanced invasive adenocarcinoma, characterised through invasion into the smooth muscle wall, was observed in SITs exposed to long term MEK162, indicating potential resistant growth (Figure 5.22 C). Previous studies evaluating MEK inhibitors for Kras mutant CRC have reported moderate effects of anti-MEK monotherapy. Migliardi et al showed the MEK inhibitor AZD6244 resulted in tumour growth stasis in Kras mutant patient-derived xenografts (Migliardi et al., 2012) and Holt et al also reported AZD6244 to result in moderate efficacy in the Calu-6 xenograft model (Holt et al., 2012). Both studies however reported increased efficacy of MEK inhibition in combination with PI3K or mTOR inhibitors, providing rationale for further evaluation of these in $Apc^{f/+}$ $Kras^{LSL/+}$ mice.

Regardless of the observations from Migliardi et al and Holt et al., the beneficial effects of chronic MEK162 treatment were also observed in the reduced dose cohort. Here, $Apc^{f/+}$ $Kras^{LSL/+}$ mice were administered MEK162 at 30mg/kg once-daily (O-D) as a control single agent arm for the reduced combination therapy (Figure 5.20). Interestingly, the survival benefit observed here was comparable to that of the twice-daily treatment cohort (mice on MEK162 once-daily had a median survival of 286 days post induction compared to 287 on twice-daily treatment). Furthermore, in terms of tumour burden, both cohorts presented with similar total tumour number, tumour area and invasiveness. Although the total tumour area of $Apc^{f/+}$ $Kras^{LSL/+}$ mice on MEK162 once-daily treatment trended to be increased, fewer advanced invasive lesions (muscle wall invasion) and more early invasive lesions (submucosal invasion) were present (Figure 5.22). This later observation either indicates less resistant tumour growth, or that treatment of the reduced dose did not promote tumour progression. Despite this, the fact that no dose-dependent effect was observed with regards to survival with MEK162 alludes to a maximal effect being achieved which may be a particularly favourable property of the drug for combinatorial experiments. Similar findings by Simmons et al. where a

reduced dose of the MEK inhibitor PD-0325901 at sub-MTD levels of just 1.5mg/kg showed efficacy in the Kras mutant GEM model of lung cancer (Simmons et al., 2012) corroborate findings that MEK inhibition is highly efficacious even at reduced doses.

5.3.2 *PI3K/mTOR inhibition through NVP-BEZ235 significantly increases survival of $Apc^{f/+}$ $Kras^{LSL/+}$ mice however, leads to increased tumour burden*

Given the promiscuous nature of Kras in activation of PI3K signalling, a number of previous studies have evaluated the effects of PI3K inhibition in this setting using a multitude of pre-clinical platforms (Roberts et al., 2012, Hofmann et al., 2012, Simmons et al., 2012). Assessment of this in the Kras driven model of lung cancer by Engelman and colleagues identified that although the PI3K/mTOR inhibitor NVP-BEZ235 did not shrink tumours, levels of pAKT were found to be reduced indicating that whilst PI3K may be required for Kras induced tumourigenesis, it is less critical for maintenance of tumours, in the lung cancer setting (Engelman et al., 2008). For further investigation of this in a CRC context, I examined the effects of the PI3K/mTOR inhibitor NVP-BEZ235 in an autochthonous mouse model of intestinal cancer driven by activation of oncogenic Kras. In the acute setting, NVP-BEZ235 resulted in minimal and differential inhibition of the PI3K pathway through pAKT at both threonine 308 and serine 473 phosphorylation sites in colon and small intestine lesions (Figure 5.10, 5.11). The majority of substantial alterations in signalling from NVP-BEZ235 however, were found to be downstream of mTOR. Phosphorylated-S6RP was found to be significantly reduced in colon polyps 4 hours post exposure and in SITs at both 4 and 24 hour time points (Figure 5.10, 5.11). Also downstream of mTOR, p4EBP1 was found to be significantly reduced in colon and small intestine tumours 4 hours after exposure to NVP-BEZ235 suggesting inhibition of protein synthesis (Bracho-Valdés et al., 2011). The majority of signalling effectors probed here were found to be unaltered 24 hours after exposure in colon polyps indicating the initial inhibitory effects were diminished and signalling was returned to basal levels (Figure 5.10, 5.11). It is interesting that an increase in MAPK signalling through pERK was not observed in response to the predominantly mTOR related inhibition by NVP-BEZ235 in this setting (Figure 5.10, 5.11). This has previously been reported by Carracedo et al and others, where inhibition of mTORC1 led to activation of MAPK signalling through the S6 kinase – IRS-1 – PI3K feedback loop (Carracedo et al., 2008b, Chen et al., 2010).

The favourable pharmacodynamic effects described above correspond with encouraging anti-tumour effects of NVP-BEZ235 in Kras mutant tumours. A significant increase in the levels of apoptosis observed in both colon and SITs 4 hours post NVP-BEZ235 administration, together with no alteration in the levels of mitosis potentially indicate reduced cell numbers (Figure 5.8). These results were further investigated through BrdU and cleaved caspase 3 staining and tended to corroborate findings (Figure 5.9). Also, a significant increase in cleaved caspase 3 levels was detected at 24 hours post exposure to NVP-BEZ235 indicating a sustained pro-apoptotic effect (Figure 5.9). Together, the immediate effects of NVP-BEZ235 in $Apc^{f/+}$ $Kras^{LSL/+}$ mice appear favourable and warranted further long term investigations.

For further evaluations, the effects of PI3K/mTOR inhibition by NVP-BEZ235 were evaluated in a survival setting to determine the potential of single agent as a therapeutic strategy. Here, $Apc^{f/+}$ $Kras^{LSL/+}$ mice were induced and aged to 100 days post induction at which point they were administered with 35mg/kg NVP-BEZ235 twice-daily until a survival end point or until the experimental end point of 500 days post induction. Treatment was found to significantly increase survival of $Apc^{f/+}$ $Kras^{LSL/+}$ mice from a median of 153 days to 343 days post induction demonstrating as described previously, strong dependence of Kras mutant tumours on PI3K signalling (Figure 5.13). Analysis of tumour burden showed twice-daily NVP-BEZ235 treatment had no significant effect on colon tumour number, total tumour area or tumour severity (Figure 5.21). These observations however, indicate reduced colon tumour growth rate as mice did have increased survival with drug treatment. With regards to SITs, no significant alteration in the number of lesions was scored however, the total tumour area measured was found to be reduced and tumours were characteristically less invasive compared to vehicle cohorts suggesting treatment halted SITs growth and progression of tumours (Figure 5.22).

In comparison to the MEK162 twice-daily cohort, NVP-BEZ235 treatment was not significantly more beneficial (in terms of survival) even though the median survival of mice was 76 days increased (MEK162 T-D had a median survival of 287 days whereas NVP-BEZ235 had a median survival of 343 days post induction), suggesting equipotent effects of long term pathway inhibition on survival of tumour bearing mice. Despite this, there are notable differences with regards to tumour burden when comparing both cohorts, which could possibly allude to differing roles of both signalling pathways in the initiation, maintenance and progression of tumourigenesis. From the above observations, it can be deduced that therapeutic PI3K/mTOR inhibition elicited effects by delaying the tumour growth in the colon but also by preventing tumour progression in the small intestine. In this study, MEK inhibition was found to delay

tumour growth in the colon and significantly reduce total tumour area in the small intestine suggesting a role for MAPK signalling predominantly in promoting tumour growth. Colon tumours here were found to have the same histological profile of invasive tumours but small intestine tumours trended to be more invasive which could elude to resistant tumour growth given mice survive longer on daily MEK162 treatment. From the literature, the therapeutic effects of PI3K/mTOR and MEK inhibition on tumour growth stasis or shrinkage of tumours in Kras mutant setting, appears to be tissue specific. In the Kras mutant lung cancer model, monotherapy with PI3K/mTOR and MEK inhibitors was shown to lead to tumour growth stasis, but targeting both pathways independently led to tumour shrinkage in mouse models of Kras mutant melanoma (Engelman et al., 2008, Roberts et al., 2012). Furthermore, in the pancreatic cancer setting, Kras mutant tumours were more responsive to MEK inhibition than PI3K inhibition (Hofmann et al., 2012) in this case suggesting more dependence on MAPK signalling rather than PI3K signalling.

Further investigation of NVP-BEZ235 in $Apc^{f/+}$ $Kras^{LSL/+}$ mice showed that similarly to reduced MEK162 administration, once-daily NVP-BEZ235 treatment as a control dose for combination studies, also increased survival. Mice had a median survival of 267 days post induction with treatment, compared to 153 days post induction with vehicle treatment (Figure 5.20). In contrast to the reduced MEK162 treatment however, the survival benefit with NVP-BEZ235 was found to be dose-dependent in that mice on twice daily treatment had an increased survival benefit in comparison to mice on once daily treatment. Interestingly, tumour burden analysis of mice exposed to chronic NVP-BEZ235 revealed an increasing trend in colon tumour number and area however, no difference in the profile of tumour severity was observed, suggesting that treatment resulted in augmented tumour growth rate, in contrast with the effects of twice-daily dosing (Figure 5.21). Despite this, NVP-BEZ235 treatment in the small intestine reduced tumour growth and halted tumour progression as evidenced by an increase in the number of less invasive lesions and a reduction in the number of more invasive lesions (Figure 5.22). These conflicting observations suggest that small intestinal lesions may respond better to reduced PI3K inhibition and this may be due to the reduced activation of PI3K signalling in this tumour setting, in comparison with colon polyps (as observed in chapter 3, section 3.2.8). In comparison with the reduced MEK162 dose, the effects of NVP-BEZ235 were more favourable for SIT burden however, the opposite was the case for colon tumour burden. These observations suggest that combined inhibition may provide promising effects in terms of tumour burden.

5.3.3 Combination treatment leads to an additive increase in longevity for $Apc^{f/+}$ $Kras^{LSL/+}$ mice

As described previously, the rationale for combination therapy is well documented in the literature, providing experimental evidence from both *in vitro* and *in vivo* studies (Yuen et al., 2012, Turke et al., 2012, Engelman et al., 2008, Balmano et al., 2009). In an effort to evaluate the potential of combined inhibition in our $Apc^{f/+}$ $Kras^{LSL/+}$ mouse model of intestinal cancer, I first evaluated the three combination strategies employed previously in chapter 4 to determine whether *Kras* mutant tumours are as sensitive to the schedule of drug administration as *Pten* deficient tumours were found to be (section 4.2.5). Pharmacodynamic evaluation of *Kras* mutant colon polyps and SITs exposed to the three combination strategies, by western blot analysis of effectors of MAPK and PI3K signalling, revealed no stark differences between the three combination strategies, indicating that *Kras* mutant tumours are not sensitive to the sequence of drug administration (Figure 5.16, 5.17). All three combination strategies resulted in substantial inhibition of MAPK signalling through pERK and inhibition of PI3K/mTOR signalling through pS6RP (Figure 5.16, 5.17). Combo 2 also resulted in inhibition of p4EBP1 in colon polyps whereas both combo 1 and 2 reduced abundance of p4EBP1 in SITs (Figure 5.16, 5.17). No significant alterations in the levels of pAKT were observed in either colon polyps or SITs, in response to the combination strategies suggesting that perhaps, in combination with MEK162, the ability of NVP-BEZ235 to reduce levels of pAKT is abrogated (Figure 5.16, 5.17). To determine the mechanism behind this, further investigation is required however, it is plausible that the phenotype in colon polyps is due to an additive effect of both inhibitors. As single agent MEK162 was found to increase PI3K signalling acutely and NVP-BEZ235 was found to inhibit signalling at pAKT, the phenotype resulting from combination treatment may simply reflect an additive result. Nevertheless, combination therapy does lead to inhibition of both MAPK and PI3K/mTOR signalling albeit levels of all signalling components assessed were not completely reduced. Additionally as described previously, all three combination strategies significantly increased levels of apoptosis and cleaved caspase 3 staining in both colon and SITs with no detectable effect on the level of mitosis, suggesting reduced cell number (Figure 5.14, 5.15). Therefore, to remain consistent between genotypes with regards to the long term combination treatment strategy, combo 2 was chosen as the method of administering combination therapy for long term survival experiments.

As in $Apc^{f/+}$ $Pten^{f/f}$ mice, combination therapy here first involved administration of NVP-BEZ235 twice-daily followed by MEK162 once daily (1 hour following the first dose). This however was

quickly found to be toxic for $Apc^{f/+} Kras^{LSL/+}$ mice as the majority of mice were culled due to significant weight loss (Figure 5.18, 5.19). The lack of toxicity in $Apc^{f/+} Pten^{f/f}$ mice compared to $Apc^{f/+} Kras^{LSL/+}$ mice may be attributable to a number of factors. Firstly, the experimental system employed differed between the two mouse models. The AhCreER transgene used in the $Apc^{f/+} Pten^{f/f}$ model results in lower levels of recombination within the intestine in comparison to the VillinCreER transgene used in the $Apc^{f/+} Kras^{LSL/+}$ model, due to the requirement of both a xenobiotic and tamoxifen (el Marjou et al., 2004, Kemp et al., 2004). Therefore, less intestinal cells undergo recombination resulting in mutations with the AhCreER transgene in comparison to all intestinal cells which undergo recombination with the VillinCreER transgene. A recent study investigating the effect of heterozygous loss of Apc and activation of Kras in the normal intestinal epithelium found an increased number of cells per half villus and reduced enterodendocrine and paneth cells in comparison to controls (Davies EJ, unpublished). This therefore results in less absorptive cells within the intestinal epithelium which may lead to subtle metabolic changes (Guarner and Malagelada, 2003), which when challenged could affect absorption of food and water and subsequently result in weight loss. Despite this, no gross alteration in the histological architecture of the intestine was observed with combination therapy, indicating the toxic effect may be due to additional factors. Kras function has previously been found to be dispensable in a number of adult tissues including the intestine, which was unaffected by loss of Kras (Velho and Haigis, 2011). Additional studies investigating genetic inhibition of MAPK signalling found that although $Erk^{-/-}$ mice are fertile and present with no apparent abnormalities, they do have a reduction in the number of mature thymocytes, raising concerns of potential toxicity from inhibition of signalling (Pagès et al., 1999). Despite the later observation, long term MEK inhibition was well tolerated and $Apc^{f/+} Kras^{LSL/+}$ mice displayed no signs of toxicity (detected by weight loss). Genetic experiments investigating inhibition of PI3K signalling have previously reported important roles of the signalling cascade in insulin signalling and energy sensing mediated through interactions with IRS-1 and mTOR signalling respectively (Engelman et al., 2006, Shaw, 2006). Furthermore, deletion of p110 causes lethality during embryogenesis and although Akt1 and Akt2 null mice are viable, they are smaller in size, have a shorter lifespan and are highly susceptible to apoptosis (Foukas et al., 2006, Chen et al., 2001). Nevertheless, single agent PI3K/mTOR inhibition was found to be well tolerated in Kras mutant mice, indicating the toxic effects may be due to combined inhibition and the presence of the Kras mutation. Previous studies investigating combined PI3K/mTOR and MEK inhibition have not reported any major toxicity issues however this may be due to differences in the doses administered and regimens used

for example, Kinross et al. assessed combined inhibition of PI3K/mTOR and MEK in models of ovarian cancer with PF-04691502 and PD-0325901 respectively. In this case, although the dual PI3K/mTOR inhibitor displayed some toxicity at higher doses, the combination therapy which involved reduced dose of 7.5mg/kg of the PI3K/mTOR inhibitor and 1.5mg/kg of the MEK inhibitor, was found to be well tolerated (Kinross et al., 2011). Additionally, Engelman et al investigating the combination therapy in the Kras mutant lung cancer model reported no toxic effects. Here, the dual PI3K/mTOR inhibitor NVP-BEZ235 was also used, together with MEK inhibitor AZD6244, at once daily doses of 35mg/kg and 25mg/kg respectively.

In light of the previous toxicity issues, a further reduced combination dose was assessed in $Apc^{f/+}$ $Kras^{LSL/+}$ mice which involved once daily NVP-BEZ235 at 35mg/kg plus MEK162 at 30mg/kg 1 hour following the initial dose. Interestingly, this was well tolerated by mice and no weight loss was observed indicating the toxic effects were no longer apparent. Reduced combination therapy (combo R2) increased survival of $Apc^{f/+}$ $Kras^{LSL/+}$ mice from a median of 153 days to 389 days post induction, which also indicates an additive increase in median survival compared to single agents MEK162 and NVP-BEZ235 when administered once daily (Figure 5.20). The additive effect in median survival also supports the hypothesis regarding early pharmacodynamic effects from combination therapy as an additive effect. In terms of colon tumour burden, although the number of lesions scored was significantly reduced, total tumour area and the invasive characteristics of lesions were comparable to vehicle treated mice (Figure 5.21). Interestingly in the small intestine, fewer lesions were scored and were found to be reduced in terms of total tumour area as well as proportionally, lesions were less invasive, perhaps indicating reduced tumour burden (Figure 5.22). However, there was also a trend towards an increase in the number of advanced invasive adenocarcinomas, characterised by smooth muscle invasion and may potentially reflect resistant tumour growth. The increased beneficial effect of combinatorial therapy upon survival and tumour burden has previously been corroborated in other malignancies (Engelman et al., 2008, Migliardi et al., 2012, Singh et al., 2010, Simmons et al., 2012) however, this study provides the first proof of principle evidence for combination therapy in an autochthonous mouse model of intestinal cancer driven by oncogenic Kras.

5.4 Summary

In summary, therapeutic targeting of MAPK signalling using the MEK inhibitor MEK162 in tumour bearing $Apc^{f/+}$ $Kras^{LSL/+}$ mice, significantly prolonged longevity of mice. Acutely however, tumours respond by compensatory modulation of PI3K signalling. Subsequently,

inhibition of signalling here using the dual PI3K/mTOR inhibitor NVP-BEZ235 was found to be equally beneficial for $Apc^{f/+}$ $Kras^{LSL/+}$ mice, indicating equivalent dependence of Kras mutant tumours on both signalling pathways. Together, MEK162 and NVP-BEZ235 resulted in an additive increase in survival for $Apc^{f/+}$ $Kras^{LSL/+}$ mice suggesting this as an effective therapeutic strategy for Kras mutant colorectal cancer.

5.5 Further work

5.5.1 Further investigation of mechanisms underlying the immediate response of Kras mutant tumours to combination therapy

As described previously, combined MEK162 and NVP-BEZ235 abrogated the capability of NVP-BEZ235 to reduce PI3K signalling through pAKT. I have proposed that this may be due to an additive effect as pAKT was increased immediately after MEK162 but reduced after NVP-BEZ235 which additively, results in a null effect as observed with combination therapy. This was further supported by an additive increase in survival with combination therapy however this does not identify the mechanism underlying this. It would be insightful to investigate pharmacodynamics at shorter time points after administration, for example at 1, 2 and 3 hours post exposure, to determine whether any differences in signalling can be determined which could provide the mechanism for this. Additionally, further investigation of intracellular signalling at convergence points would also provide insight into the additive interactions. This includes status of TSC2, the BH3 proteins which control apoptotic signalling BAD, BIM as well as Mcl-1. Additionally, status of negative regulators of the MAPK pathway- Dusp and Sprouty proteins, and negative regulators of PI3K signalling – IRS-1 and S6K would be informative.

5.5.2 Further investigation to toxic effects of combination in $Apc^{f/+}$ $Kras^{LSL/+}$ mice and not $Apc^{f/+}$ $Pten^{ff}$ mice

As described previously, administration of PI3K/mTOR inhibitor NVP-BEZ235 twice daily plus MEK inhibitor MEK162 in Kras mutant mice led to substantial toxicity which was not observed in the Pten deficient setting. To further investigate whether this was due to detrimental effects on normal intestinal homeostasis, scoring of proliferation and apoptosis in the crypts (and villi) of the small intestinal and colonic epithelium could be carried out. Furthermore, characterisation of the stem cell compartment and the differentiated cell types within the epithelium in combination treated cohorts, compared to single agents could identify whether normal homeostasis was altered and may help to identify the detrimental effects of this combination regimen in the Kras mutant setting.

5.5.3 *Mechanisms of resistance to combination therapy*

Given the prevalence of Kras mutations in human colorectal cancer, the lack of effective treatment for this sub-group of tumours indicates they still represent an unmet clinical need. Although this study has provided evidence for combined MEK and PI3K/mTOR inhibition as a highly effective therapeutic strategy, it remains imperative to further investigate the effect of this as a therapy, as tumours tend to evolve and develop resistance to therapy. Previously, I have hypothesised that in some cohorts where an increase in the severity of tumours is seen, this could be indicative of resistant tumour growth. To determine if this indeed is the case, immunohistochemistry for downstream effectors of both MAPK and PI3K signalling, together with scoring of proliferation and apoptosis, could be used to determine whether tumours are still responding to treatment. These two factors could then be correlated with the severity status of tumours to determine whether tumour progression is associated with resistant tumour growth.

6 Investigating PI3K/mTOR inhibition and MEK inhibition in the *Apc^{f/+} Pten^{f/f} Kras^{LSL/+}* colorectal cancer mouse model

6.1 Introduction

Work described in chapters 4 and 5 indicate that whilst inhibition of PI3K/mTOR signalling is an effective therapeutic strategy for Pten deficient tumours, combined targeting of MEK and PI3K/mTOR was most beneficial for Kras activated tumours. This is potentially due to the ‘double-hit’ effect of Kras mutations, which were shown to activate both MAPK/ERK and PI3K/AKT signalling in chapter 3. Despite characterisation of targeted agents in Pten deficient and Kras mutant independent tumour models, concomitant mutations resulting in activation of PI3K and MAPK signalling have been shown to co-exist in approximately a third of all CRC cases (Network, 2012). Additionally, sequencing analysis has identified that mutations in *APC*, *KRAS* and *PIK3CA* are the most prevalent mutations in CRC. Furthermore, these mutations are associated with aggressive disease and a poor prognosis for cancer patients (Wood et al., 2007, Ogino et al., 2009, Richman et al., 2009). Therapeutic investigation of targeted agents in models of cancer with activating mutations of PI3K signalling and concurrent Kras mutations have indicated beneficial effects in ovarian, lung and thyroid cancers (Kinross et al., 2011, Engelman et al., 2008, Miller et al., 2009). In light of these observations, I next investigated therapeutic targeting of PI3K and MAPK signalling in the context of concurrent Pten loss and Kras activation.

A recent study in the Clarke lab investigating the synergy between Pten and Kras in the context of tumourigenesis revealed that compound deletion of Pten and activation of mutant Kras within the intestinal epithelium resulted in metastatic carcinoma. Here, mice had a median survival of 344 days post induction and presented with multiple intestinal phenotypes as well as metastatic lesions in the liver, pancreas, lung and lymph node (Davies EJ, unpublished). Although this tumour model is attractive for the evaluation of novel and targeted therapeutic strategies, a number of caveats render the model impractical. These include the long latency period of tumour development, multiple intestinal phenotypes and the fact that metastasis was not observed with 100% penetrance. However, Davies et al also found synergy between Pten loss and activation of Kras in the context of activated Wnt signalling through heterozygous deletion of *Apc*. Here, although ‘hyper-activation’ of PI3K signalling was not detected by IHC (also confirmed in chapter 3 by western blot analysis), mice had a significantly

reduced lifespan of only 41 days post induction and presented with more tumours at death (Davies EJ, unpublished). Given these later observations, the therapeutic potential of PI3K/mTOR and MEK inhibition in the mouse model mutant for Apc, Pten and Kras was next investigated.

In this chapter, the therapeutic potential of PI3K/mTOR and MEK inhibition through NVP-BEZ235 and MEK162 are evaluated independently, as well as in combination, in the Pten deficient and Kras activated tumour setting. Similarly to chapters 3-5, two main strategies were employed for these investigations. For evaluation of immediate anti-tumour and pharmacodynamic effects, tumour bearing VillinCreER Apc^{f/+} Pten^{f/f} Kras^{V12LSL/+} mice (hereon in referred to as Apc^{f/+} Pten^{f/f} Kras^{LSL/+} mice) were administered a single dose of NVP-BEZ235, MEK162 or combination and harvested 4 or 24 hours following. Additionally, the effect on survival was evaluated through daily administration of single agents and combination therapy from a chosen start point until a survival end point (when mice were symptomatic of disease defined by pale feet, anal bleeding, bloating, and weight loss).

6.2 Results

6.2.1 *NVP-BEZ235 increases apoptosis in Apc^{f/+} Pten^{f/f} Kras^{LSL/+} tumours, inhibits PI3K and mTOR signalling, however also reduces MAPK signalling*

For all short term experiments described in this chapter, 10 week old Apc^{f/+} Pten^{f/f} Kras^{LSL/+} mice were induced and monitored for symptoms of tumour burden (paling feet, bloating, blood in faeces). A cohort of n≥3 mice were then administered a single dose of 0.5% Methyl cellulose (MC, vehicle) and harvested 4 hours later, or a single dose of 35mg/kg NVP-BEZ235 and harvested 4 or 24 hours later. A dose of BrdU was also administered 2 hours prior to culling. At dissection, small intestinal tumours (SITs) were immediately snap frozen in liquid nitrogen before 'swiss-rolling' the whole small intestine and fixing in formalin for H&E staining and IHC (section 2.4).

Following exposure to a single dose of NVP-BEZ235, the immediate anti-tumour effects were characterised in Apc^{f/+} Pten^{f/f} Kras^{LSL/+} SITs through assessment of histological mitosis and apoptosis from H&E stained slides. Scoring of mitotic figures revealed no significant alterations 4 or 24 hours following NVP-BEZ235 compared to vehicle controls (4hr veh = 0.283 ± 0.192, 4hr NVP-BEZ235 = 0.339 ± 0.202, p value = 0.328, 24hr NVP-BEZ235 = 0.357 ± 0.15, p value = 0.104, n≤15 tumours, 4 mice, Mann Whitney U test) (Figure 6.1 A). Quantification of apoptotic bodies from H&E stained slides revealed a significant increase in levels of apoptosis at 4 hours

but a significant reduction at 24 hours post exposure in comparison to vehicle treated controls (4hr veh = 1.00 ± 0.515 , 4hr NVP-BEZ235 = 2.281 ± 1.301 , p value = 0.0001, 24hr NVP-BEZ235 = 0.618 , p value = 0.024, $n \geq 15$ tumours, 4 mice, Mann Whitney U test) (Figure 6.1 B). The observation that an initial wave of apoptosis at 4 hours is followed by a reduction in the levels of apoptosis at 24 hours suggests transient anti-tumour effects and subsequently, activation of a compensatory mechanism to restore levels of apoptosis.

In addition to histological mitosis and apoptosis, IHC for BrdU and cleaved caspase 3 were carried out and quantified to further characterise the anti-tumour effects. Scoring of the proliferative marker BrdU revealed no significant difference at 4 hours following NVP-BEZ235 but a significant increase at the 24 hour time point (4hr veh = 13.36 ± 4.13 , 4hr NVP-BEZ235 = 15.9 ± 4.42 , p value = 0.2667, 24hr NVP-BEZ235 = 18.82 ± 4.30 , p value = 0.006, $n \geq 15$ tumours, 4 mice, Mann Whitney U test) (Figure 6.2 A). Scoring of cleaved caspase 3 staining in $Apc^{f/+}$ $Pten^{f/f}$ $Kras^{LSL/+}$ tumours identified a significant increase in staining 4 and 24 hours post exposure to NVP-BEZ235 (4hr veh = 1.22 ± 0.56 , 4hr NVP-BEZ235 = 2.46 ± 1.14 , p value = 0.0006, 24hr NVP-BEZ235 = 1.99 ± 1.097 , p value = 0.0133, $n \geq 15$ tumours, 4 mice, Mann Whitney U test), indicating a prolonged pro-apoptotic effect (Figure 6.2 B).

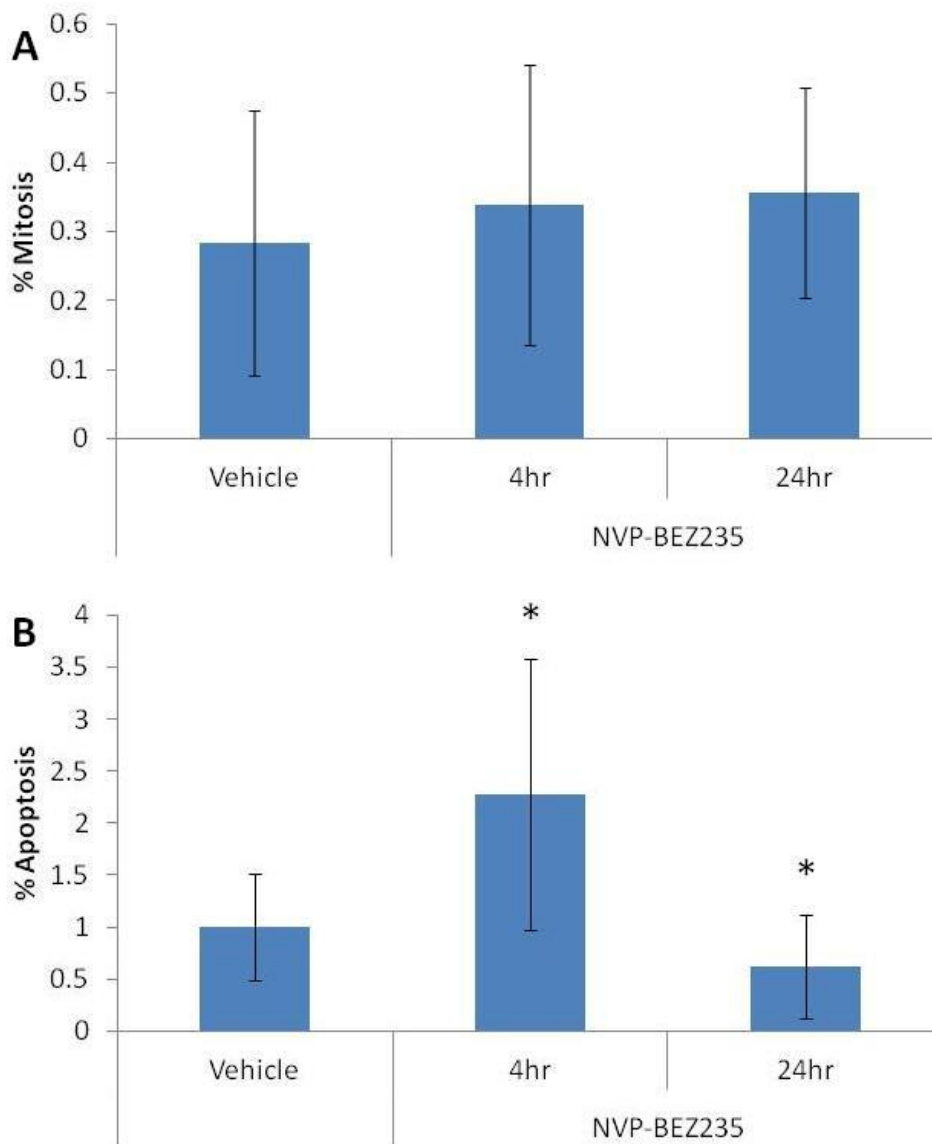


Figure 6.1 NVP-BEZ235 results in a pro-apoptotic effect in $Apc^{f/+}$ $Pten^{f/f}$ $Kras^{LSL/+}$ small intestinal tumours (SITs) 4 hours following exposure, but no effect on mitosis

Following exposure to NVP-BEZ235, scoring of mitotic figures (**A**) and apoptotic bodies (**B**) in $Apc^{f/+}$ $Pten^{f/f}$ $Kras^{LSL/+}$ tumours revealed no alterations in the levels of mitosis however, a significant increase in apoptosis 4 hours after exposure was revealed (p value = 0.0001, $n \geq 3$, Mann Whitney U test). This immediate pro-apoptotic effect was found to be significantly reduced by 24 hours post exposure (p value = 0.024, $n \geq 15$ tumours, 4 mice, Mann Whitney U test). Error bars represent standard deviation

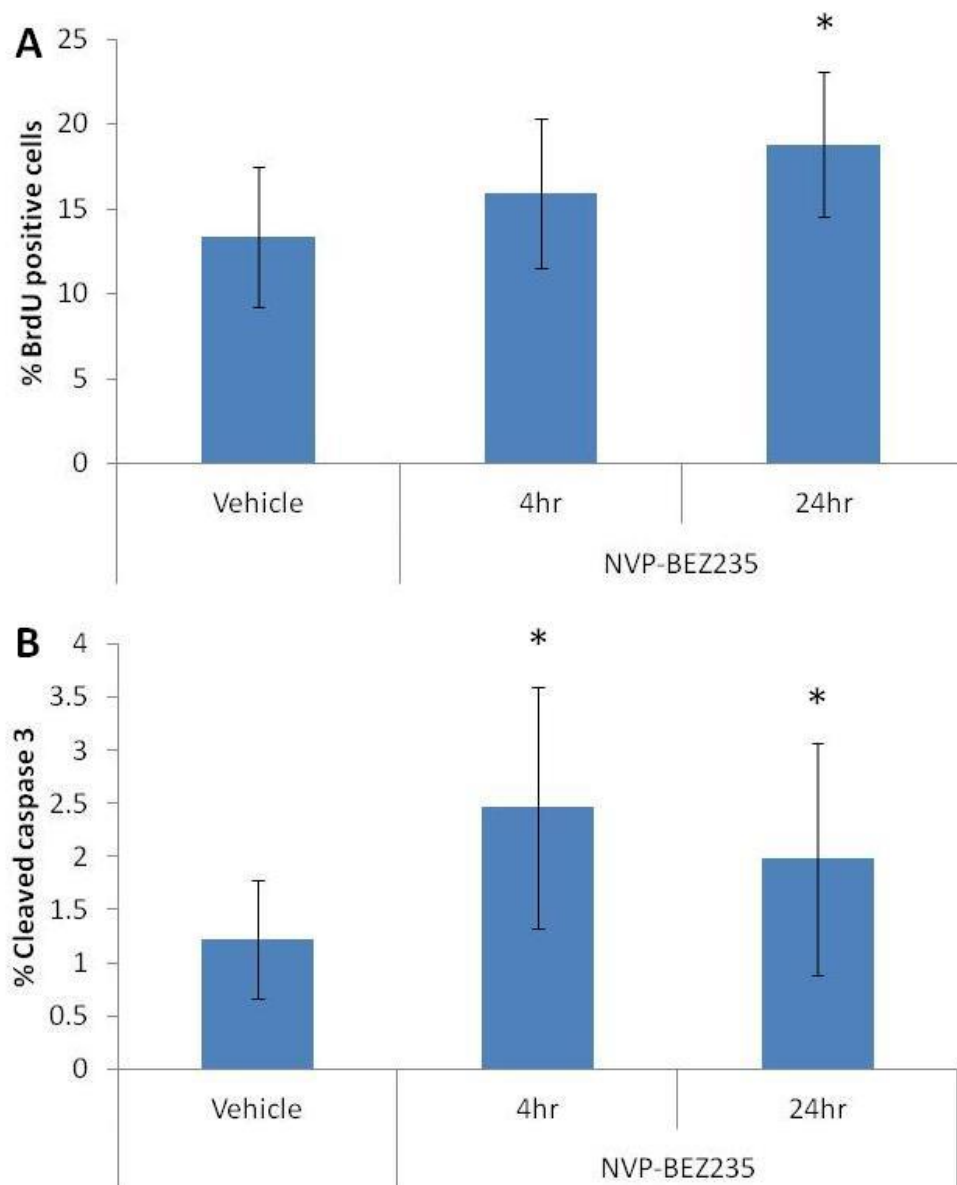


Figure 6.2 NVP-BEZ235 increases the number of cycling cells, but also increases apoptosis through cleaved caspase 3 in $Apc^{f/+}$ $Pten^{f/f}$ $Kras^{LSL/+}$ lesions

Scoring of IHCs for BrdU (**A**) and cleaved caspase 3 (**B**) revealed an anti-proliferative increase in the number of BrdU positive cells 24 hours after exposure to NVP-BEZ235, but also a pro-apoptotic increase in cleaved caspase 3 staining 4 and 24 hours after exposure (p value = 0.006 for 24hr BrdU, p value = 0.0006 for 4hr caspase and p value = 0.0133 for 24hr caspase, $n \geq 15$ tumours, 4 mice, Mann Whitney U test). Error bars represent standard deviation

To investigate the effects of NVP-BEZ235 on PI3K and mTOR signalling in $Apc^{f/+} Pten^{f/f} Kras^{LSL/+}$ tumours, western blotting was used to analyse SIT lysates. Proteins extracted from 6 SITs were pooled (per cohort) from $n=3$ mice exposed to either vehicle or NVP-BEZ235 and harvested either 4 or 24 hours following. For analysis of PI3K and mTOR signalling, antibodies against the phosphorylated (and hence activated forms) of AKT (Ser473 and Thr308) S6RP (Ser235/236) and 4EBP1 (Thr37/46) were used. Western blotting and subsequent densitometry analysis revealed subtle, yet significant reductions in the levels of pAKT473, pAKT308, and pS6RP 4 hours post exposure to NVP-BEZ235 (Figure 6.3, Table 6.1). Although not significant, a trend for reduced p4EBP1 was also notable. Signalling at 24 hours post exposure to NVP-BEZ235 was generally augmented, as evidenced though significantly increased levels of pAKT473, pAKT308, and pS6RP and a trend towards an increase in p4EBP1, and may be responsible for the reduced levels of apoptosis observed previously (Figure 6.3, Table 6.1).

	Vehicle	4hr NVP-BEZ235 (p value)	24hr NVP-BEZ235 (p value)
pAKT473	4276.9 \pm 181.2	3539.8 \pm 128.8 (0.0404)	4960 \pm 156.9 (0.0404)
pAKT308	1791.3 \pm 336.9	1003.1 \pm 80.7 (0.0404)	3073.1 \pm 608.6 (0.0404)
pS6RP	1572.9 \pm 701.9	112.4 \pm 81.9 (0.0404)	3367.9 \pm 976.0 (0.0404)
p4EBP1	4260 \pm 1633.3	3111.2 \pm 356.7 (0.1914)	4877.6 \pm 569.5 (0.3313)
pERK	6207.1 \pm 727.9	3720.9 \pm 647.9 (0.0404)	5805.6 \pm 454.2 (0.1914)

Table 6-1 Outline of raw densitometry values from western blot analysis of pooled $Apc^{f/+} Pten^{f/f} Kras^{LSL/+}$ SITs 4 and 24 hours post exposure to NVP-BEZ235 , $n=3$, One-tailed Mann Whitney U test was used for statistical analysis

Given the activation of mutant Kras in these tumours, activation status of MAPK signalling was subsequently analysed to investigate whether PI3K/mTOR inhibition led to compensatory increase in signalling through pERK. Immunoblotting and subsequent densitometry analysis revealed a surprising reduction in levels of pERK 4 hours post exposure to NVP-BEZ235 with levels returning to basal levels by 24 hours post exposure (**Figure 6.3, Table 6.1**).

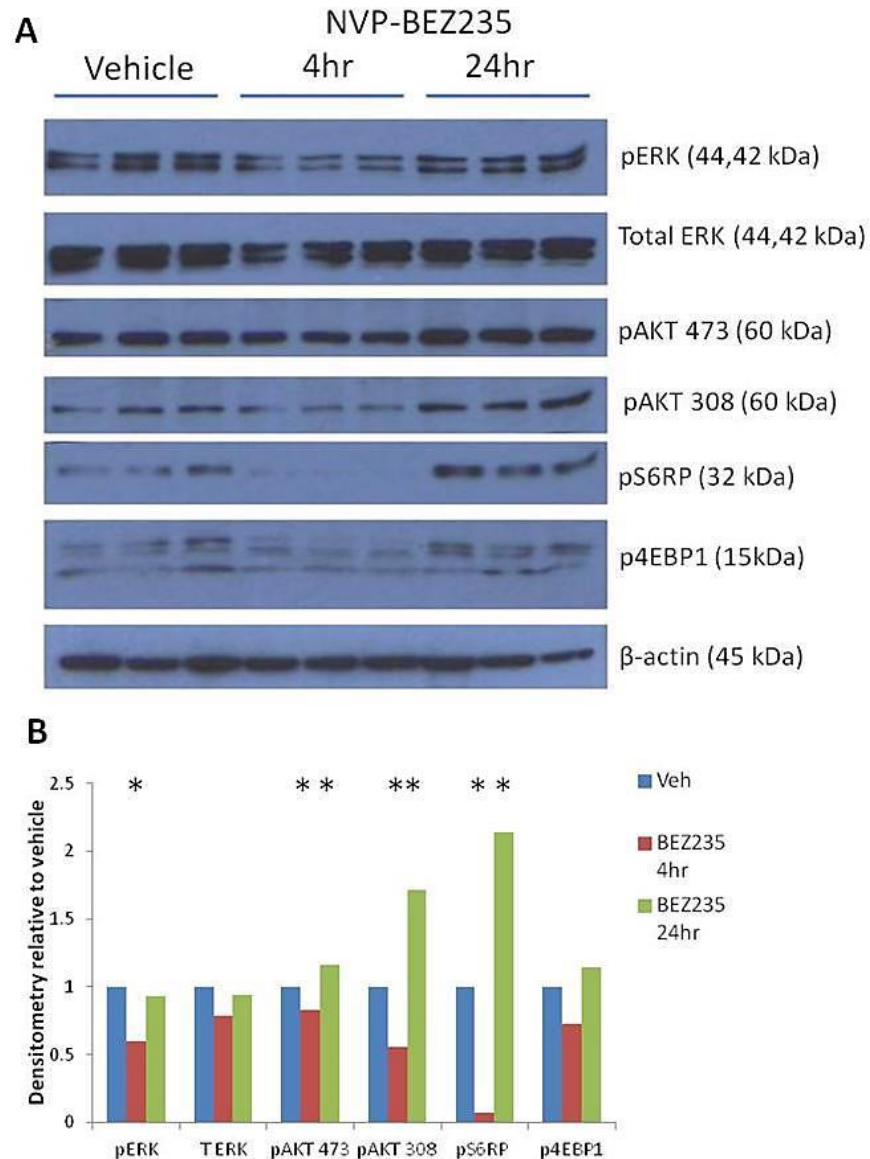


Figure 6.3 NVP-BEZ235 reduces PI3K and mTOR signalling in $Apc^{f/+} Pten^{f/f} Kras^{LSL/+}$ tumours 4 hours after exposure, however increases signalling at a 24 hour time point

(A) 6 SIT lysates pooled from $n=3$ mice exposed to NVP-BEZ235 for 4 or 24 hours were subjected to western blot analysis. Effectors of the PI3K and mTOR signalling pathways were probed and revealed marked reduction of pathway effectors 4 hours post exposure. Signalling at 24 hours post exposure was found to be significantly increased through pAKT473, pAKT308 and pS6RP. Additionally, the MAPK pathway effector pERK was probed to assess pathway activation. This revealed a significant reduction at 4 hours, but no effect at 24 hours (B). Densitometry was carried out to quantify differences observed from immunoblotting. These are normalised to β -actin as loading control and represented as relative to vehicle controls (*p value = 0.0404, $n=3$, Mann Whitney U test).

In summary, the immediate consequences of NVP-BEZ235 in $Apc^{f/+}$ $Pten^{f/f}$ $Kras^{LSL/+}$ SITs involve reduction in PI3K and mTOR signalling (summarised in Figure 1.4) and induction of apoptosis. At 24 hours however, an increase in PI3K and mTOR signalling was observed and given the role of the pathway in controlling cellular proliferation and apoptosis, this may be attributable to the increased proliferation and reduced apoptosis observed here.

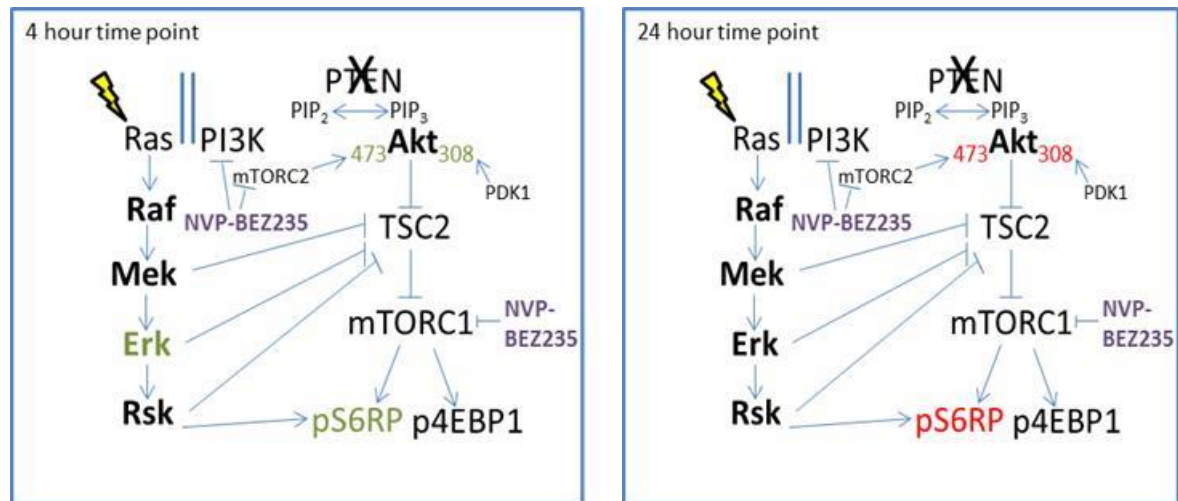


Figure 6.4 Schematic showing the effects of NVP-BEZ235 on PI3K/mTOR and MAPK pathway components as detected by western blot analysis (Green denotes a reduction whereas red indicates an increase).

At 4 hours post exposure, NVP-BEZ235 leads to a reduction in levels of pERK, pAKT at Ser473 and Thr308 and pS6RP whereas at 24 hours post exposure, NVP-BEZ235 results in increased levels of pAKT at Ser473 and Thr308 and pS6RP.

6.2.2 Chronic NVP-BEZ235 significantly increases longevity of $Apc^{f/+}$ $Pten^{f/f}$ $Kras^{LSL/+}$ mice

To investigate the therapeutic potential of PI3K and mTOR inhibition using NVP-BEZ235 in a compound *Pten* deficient and *Kras* activated tumour setting, a long term treatment experiment was conducted to assess the effect on longevity and tumour burden of mice. For this, a cohort of 13 mice per cohort were induced and aged until the chosen intervention start point. Given these mice become symptomatic of disease from 3 weeks (21 days) following induction and have a median survival of just 41 days, a time point of 22 days post induction was chosen as the intervention start point. Mice were randomised to receive either 0.5% MC (vehicle) or 35mg/kg NVP-BEZ235 twice daily (weekdays only) by oral gavage, until a survival end point (anaemia, bloating, $\geq 10\%$ loss of body weight).

Chronic NVP-BEZ235 administration in $Apc^{f/+}$ $Pten^{f/f}$ $Kras^{LSL/+}$ mice was found to be well tolerated by mice (determined by body weight) and led to a significant increase in survival of mice from 40 days to 104 days post induction ($n \geq 13$ per cohort, p value = 0.0001, Log-Rank and Wilcoxon test) (Figure 6.5). Long term NVP-BEZ235 treatment more than doubled lifespan of $Apc^{f/+}$ $Pten^{f/f}$ $Kras^{LSL/+}$ mice indicating this as a beneficial therapeutic strategy.

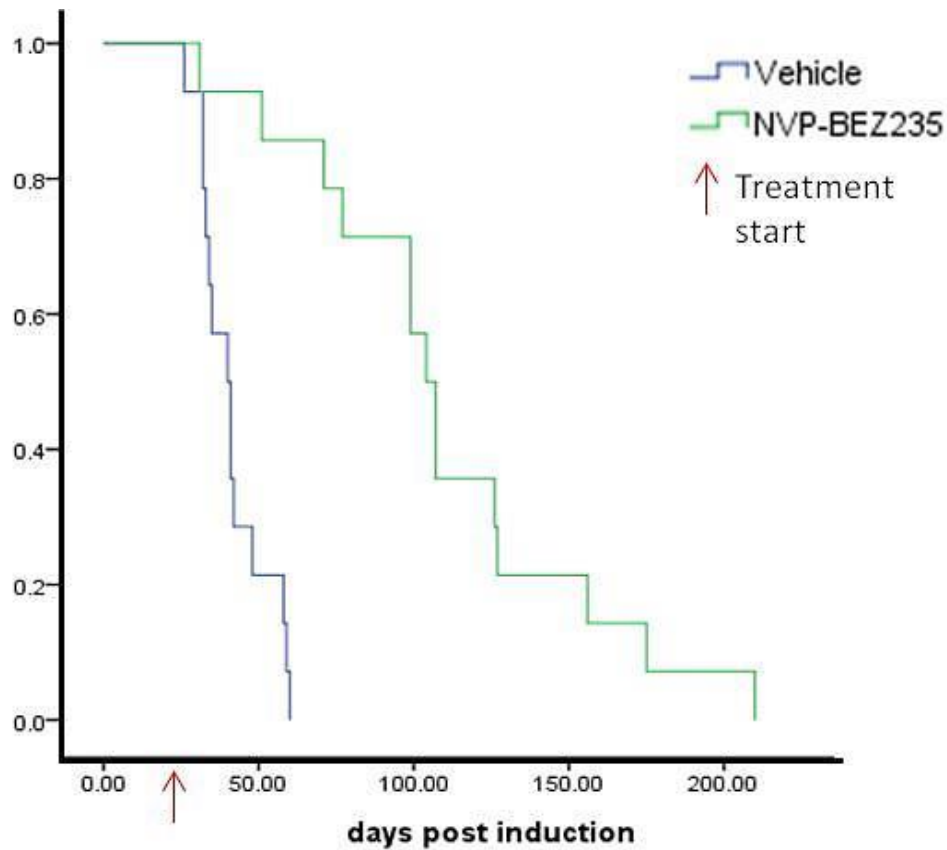


Figure 6.5 Kaplan-Meier survival analysis of $Apc^{f/+}$ $Pten^{f/f}$ $Kras^{LSL/+}$ mice on NVP-BEZ235 compared to vehicle controls

$Apc^{f/+}$ $Pten^{f/f}$ $Kras^{LSL/+}$ mice were induced and aged to 22 days post induction, at which point mice were randomised to receive either 0.5% Methyl cellulose (Vehicle control) or 35mg/kg NVP-BEZ235 twice-daily by oral gavage until a survival end point. Continuous NVP-BEZ235 treatment was found to significantly increase survival of mice from 40 days (vehicle controls) to a median of 104 days post induction (p value ≤ 0.001 , $n \geq 13$ mice per cohort, Log-Rank and wilcoxon test).

6.2.3 MEK162 increases cleaved caspase 3 in $Apc^{f/+}$ $Pten^{f/f}$ $Kras^{LSL/+}$ tumours and prolonged inhibition of MAPK signalling, however also leads to modulation of PI3K/mTOR signalling

Given that MEK inhibition induced favourable anti-tumour and pharmacodynamic effects in $Apc^{f/+}$ $Kras^{LSL/+}$ mice, I next investigated the immediate effects of MEK inhibition through MEK162 in the additional presence of Pten deletion. Similarly to section 6.2.1, for short term experiments, $Apc^{f/+}$ $Pten^{f/f}$ $Kras^{LSL/+}$ mice were induced and aged until presented with symptoms of tumour burden. Mice were then administered with a single dose of 30mg/kg MEK162 and harvested either 4 or 24 hours post exposure as described previously in methods section 2.4. Mice were also administered a dose of BrdU 2 hours prior to culling. Vehicle controls used for this experiment were previously described in section 6.2.1.

To explore the immediate anti-tumour activity of MEK162 in $Apc^{f/+}$ $Pten^{f/f}$ $Kras^{LSL/+}$ tumours, mitotic figures and apoptotic bodies were scored from H&E stained slides. Quantification of mitosis in $Apc^{f/+}$ $Pten^{f/f}$ $Kras^{LSL/+}$ SITs revealed no significant alterations at either 4 or 24 hours post exposure (4hr veh = 0.283 ± 0.192 , 4hr MEK162 = 0.439 ± 0.293 , p value = 0.0565, 24hr MEK162 = 0.288 ± 0.268 , p value = 0.494, $n \geq 15$ tumours, 4 mice, Mann Whitney U test) (Figure 6.6 A). Similarly, no significant alterations in apoptosis were observed at 4 or 24 hours post exposure to MEK162 (4hr veh = 1.00 ± 0.515 , 4hr MEK162 = 1.416 ± 0.764 , p value = 0.073, 24hr MEK162 = 0.72 ± 0.346 , p value = 0.138, $n \geq 15$ tumours, 4 mice, Mann Whitney U test) (Figure 6.6 B).

In addition to scoring of histological mitosis and apoptosis, IHC against the proliferative marker BrdU and the apoptotic marker cleaved caspase 3 was carried out and scored. Quantification of BrdU positive cells revealed a significant increase in staining 4 hours after MEK162 exposure but no significant alteration at 24 hours (4hr veh = 13.36 ± 4.134 , 4hr MEK162 = 19.57 ± 4.05 , p value = 0.0017, 24hr MEK162 = 14.96 ± 4.94 , p value = 0.521, $n \geq 15$ tumours, 4 mice, Mann Whitney U test) (Figure 6.7 A). This suggests possible compensatory activation of proliferation in response to MEK162 at 4 hours which is relieved by 24 hours. Scoring of cleaved caspase 3 staining in these samples revealed a significant increase in staining at both 4 and 24 hour time points after MEK162 exposure (4hr veh = 1.219 ± 0.56 , 4hr MEK162 = 7.028 ± 2.56 , p value ≤ 0.0001 , 24hr MEK162 = 4.12 ± 2.68 , p value = 0.0001, $n \geq 15$ tumours, 4 mice, Mann Whitney U test) (Figure 6.7 B). Although cleaved caspase 3 levels were found to be increased at both 4

and 24 hour time points, caspase 3 levels at the 4 hour time point appeared higher than at 24 hours indicating transient anti-tumour effects (Figure 6.6).

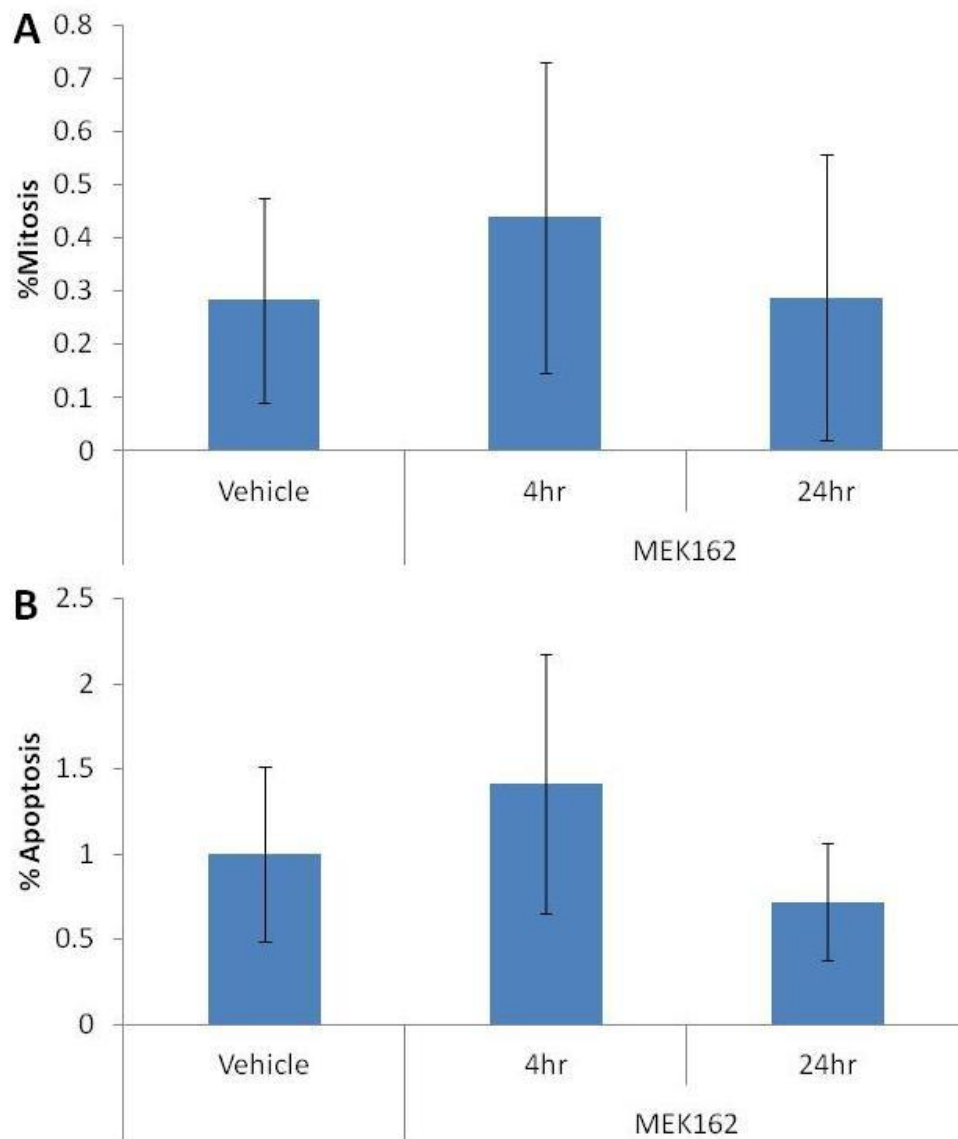


Figure 6.6 MEK162 has no effect on levels of mitosis or apoptosis in $Apc^{f/+}$ $Pten^{f/f}$ $Kras^{LSL/+}$ small intestine tumours (SITs)

Scoring of mitotic figures **(A)** and apoptotic bodies **(B)** revealed no significant alterations 4 or 24 hours after a single dose of 30mg/kg MEK162 compared to vehicle (0.5% MC) (p value \geq 0.05, $n \geq 15$ tumours, 4 mice, Mann Whitney U test). Error bars represent standard deviation.

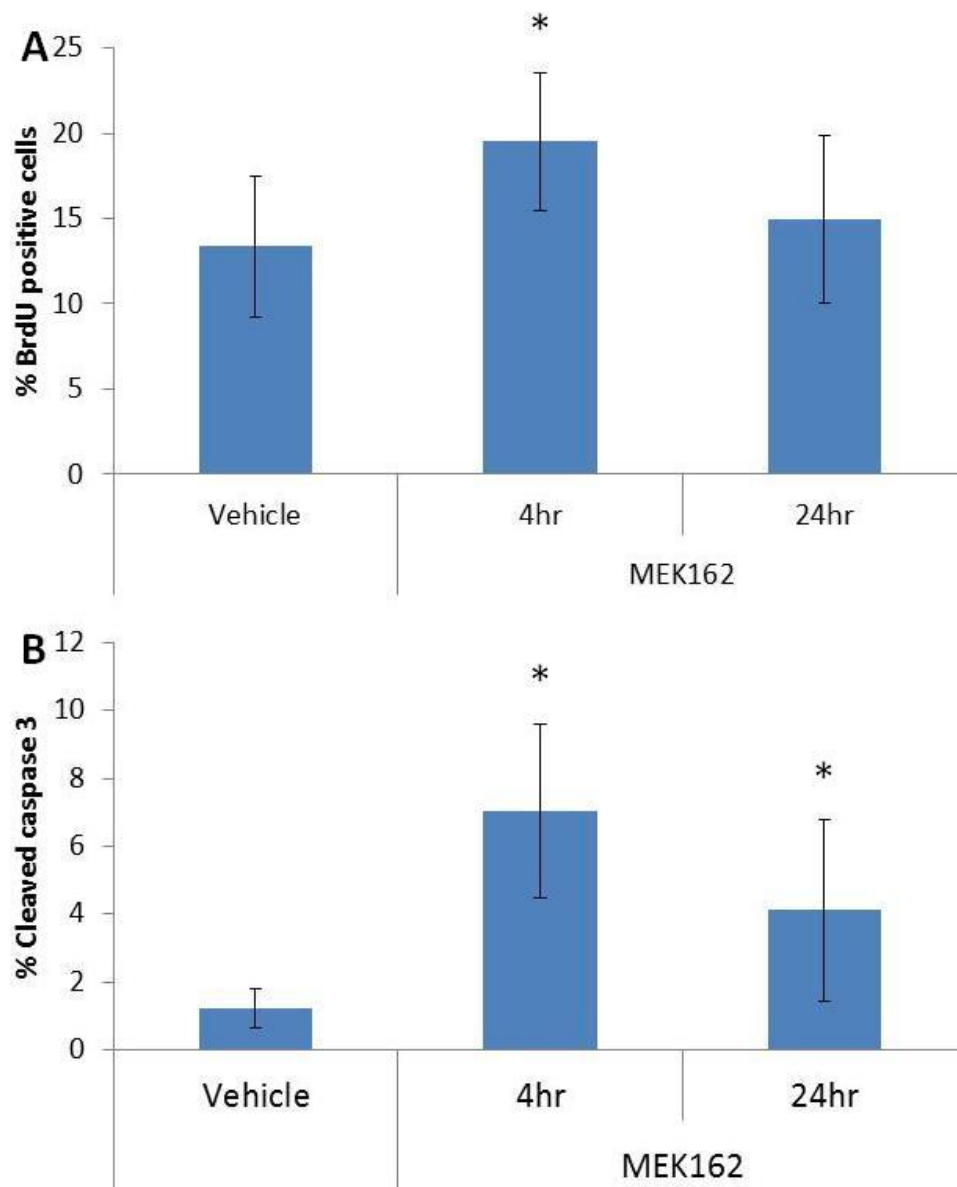


Figure 6.7 MEK162 significantly increases the number of BrdU positive cells and cleaved caspase 3 staining in $Apc^{f/+}$ $Pten^{f/f}$ $Kras^{LSL/+}$ small intestine tumours (SITs)

IHC for BrdU (**A**) and cleaved caspase 3 (**B**) was carried out and quantified. Scoring revealed a significant increase in BrdU positive cells 4 hours post exposure and a significant increase in cleaved caspase 3 staining at 4 and 24 hours following exposure to a single dose of 30mg/kg MEK162 (p value ≥ 0.05 , $n \geq 15$ tumours, 4 mice, Mann Whitney U test). Error bars represent standard deviation.

As described in studies elsewhere (Wee et al., 2009) and in chapter 4, mutations resulting in activation of PI3K signalling are inherently resistant to MEK inhibition. Wee et al showed that activated PI3K signalling renders Kras mutant tumours (which would normally be sensitive) unresponsive to MEK inhibition (Wee et al., 2009). To investigate whether this is also the case in our $Apc^{f/+}$ $Pten^{f/f}$ $Kras^{LSL/+}$ model, tumours harvested from mice 4 and 24 hours post MEK162 were analysed for effectors of MAPK and PI3K signalling. Proteins extracted from 6 SITs (from $n=3$ mice) were pooled per cohort and subjected to western blot analysis (Figure 6.8). Immunoblotting and subsequent densitometry analysis revealed prolonged inhibition of MAPK signalling evidenced through reduced pERK abundance at both 4 and 24 hour time points (Figure 6.8, Table 6.2). Interestingly, investigation of PI3K signalling in response to MEK inhibition revealed a significant reduction in signalling through pAKT473, pAKT308 and pS6RP and a trend towards reduced p4EBP1 abundance. Furthermore, analysis of signalling at the 24 hour post exposure time point revealed a trend towards increased PI3K/mTOR signalling through pAKT473 and pAKT308, with a significant increase in pS6RP and p4EBP1 (Figure 6.8, Table 6.2). As described previously, cross-talk between the MAPK and PI3K signalling cascades occurs through a number of mechanisms and these be responsible for the immediate modulations observed here. Nevertheless, the observation that acute MEK inhibition leads to reduced PI3K signalling in this model (summarised in Figure 6.9) warrants further exploration of MEK inhibition, given the increased benefit in survival following chronic PI3K/mTOR inhibition.

	Vehicle	4hr MEK162 (p value)	24hr MEK162 (p value)
pERK	5922 ± 1129	1240.2 ± 479.8 (0.0404)	706.3 ± 298.1 (0.0404)
pAKT473	4746 ± 692.6	3409.3 ± 531 (0.0404)	5156.7 ± 322 (0.1914)
pAKT308	2234.6 ± 307.2	923.7 ± 598.6 (0.0404)	2934.2 ± 551.1 (0.1914)
pS6RP	2139.1 ± 1349.3	39.8 ± 26.5 (0.0404)	4417 ± 271.8 (0.0404)
p4EBP1	2387.8 ± 494.2	832.4 ± 919.5 (0.0952)	3303.9 ± 598.5 (0.0404)

Table 6-2 Outline of raw densitometry values from western blot analysis of pooled $Apc^{f/+}$ $Pten^{f/f}$ $Kras^{LSL/+}$ SITs 4 and 24 hours post exposure to MEK162 , $n=3$, One-tailed Mann Whitney U test was used for statistical analysis

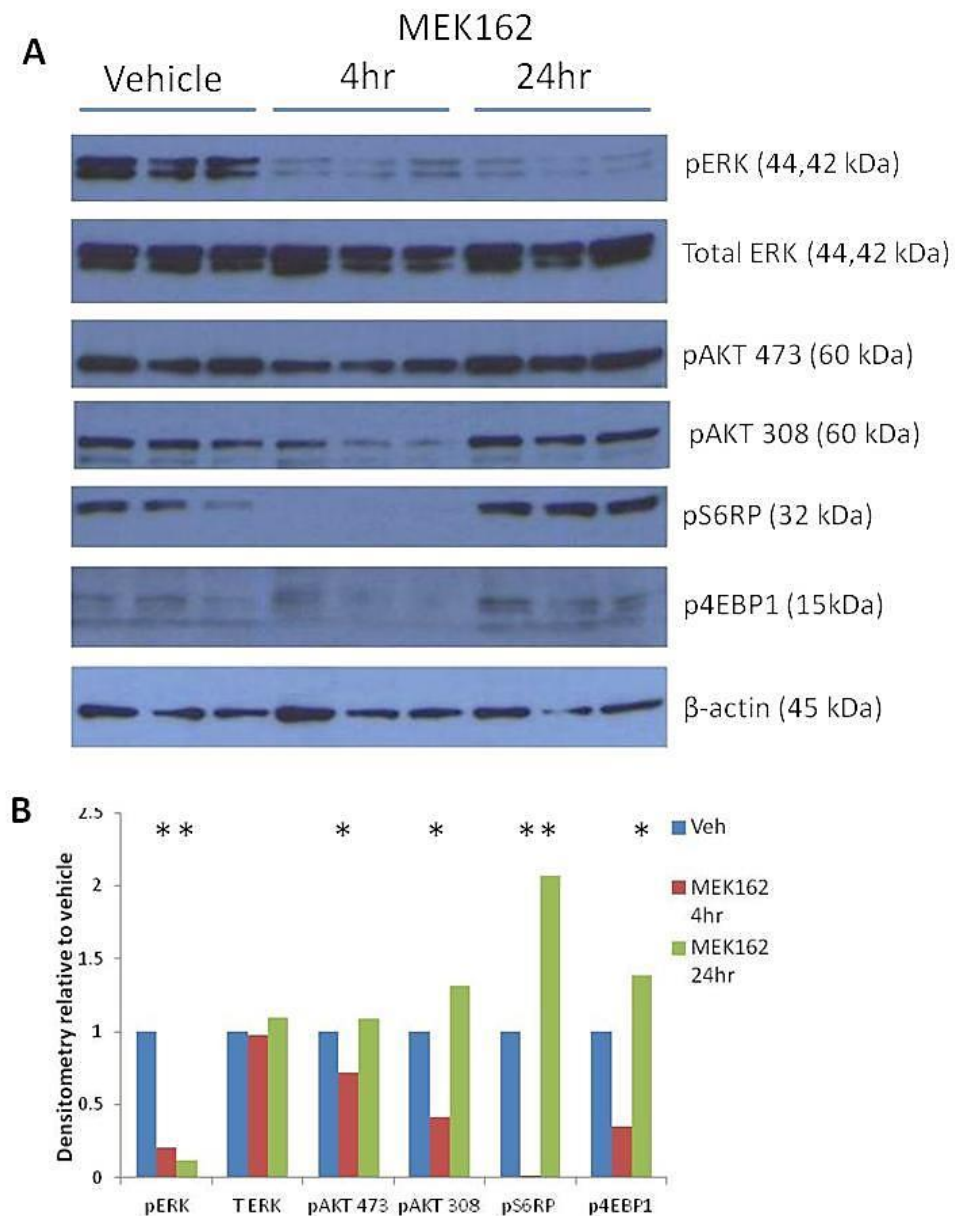


Figure 6.8 MEK162 induced prolonged inhibition of MAPK signalling in $Apc^{f/+} Pten^{f/f} Kras^{LSL/+}$ tumours and reduced PI3K signalling 4 hours after exposure, but increased levels of PI3K/mTOR signalling at the 24 hour time point

(A) 6 SIT lysates pooled from $n=3$ mice exposed to MEK162 for 4 or 24 hours were subjected to western blot analysis. Immunoblotting for the MAPK effector pERK revealed marked reduction at both 4 and 24 hour time points. Additionally, effectors of PI3K/mTOR signalling were probed to assess pathway cross-talk. This revealed inhibition of PI3K signalling 4 hours post exposure, however an increase in signalling 24 hours post exposure. (B) Densitometry was carried out to quantify differences observed from immunoblotting. These are normalised to β -actin as loading control and represented as relative to vehicle controls (* p value = 0.0404, $n=3$, Mann Whitney U test).

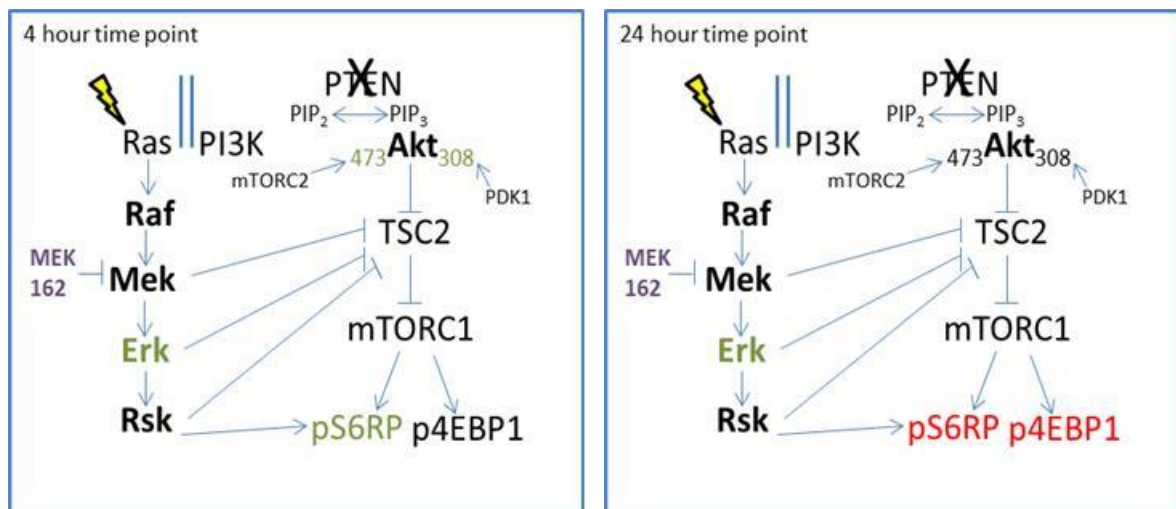


Figure 6.9 Schematic showing the effects of MEK162 on MAPK and PI3K/mTOR pathway components as detected by western blot analysis (Green denotes a reduction whereas red indicates an increase).

At 4 hours post exposure, MEK162 leads to a reduction in levels of pERK, pAKT at Ser473 and Thr308 and pS6RP whereas at 24 hours post exposure, MEK162 still reduces levels of pERK however also results in increased levels of pS6RP and p4EBP1.

6.2.4 Chronic MEK162 has no beneficial effect on survival of $Apc^{f/+}$ $Pten^{f/f}$ $Kras^{LSL/+}$ mice

For chronic MEK162 treatment, a cohort of 10 week old $Apc^{f/+}$ $Pten^{f/f}$ $Kras^{LSL/+}$ mice were induced and aged as described in section 6.2.2, to 22 days post induction. At this point mice received 30mg/kg MEK162 twice-daily (week days only) by oral gavage, until a survival end point. Vehicle controls for this experiment were also previously described in section 6.2.2.

Chronic administration with MEK162 was found to be well tolerated in $Apc^{f/+}$ $Pten^{f/f}$ $Kras^{LSL/+}$ mice, however treatment did not have any beneficial effect on survival of mice (median survival of MEK162 mice = 36 days vs vehicle mice = 40, $n \geq 13$ mice per cohort, p value = 0.547 for Log-Rank and p value = 0.937 for Wilcoxon test) (Figure 6.10). Therefore, despite the favourable anti-tumour and pharmacodynamic modulating of PI3K signalling by MEK162, mice with tumours deficient for Pten and activation of Kras were not sensitive to long term MEK162 treatment.

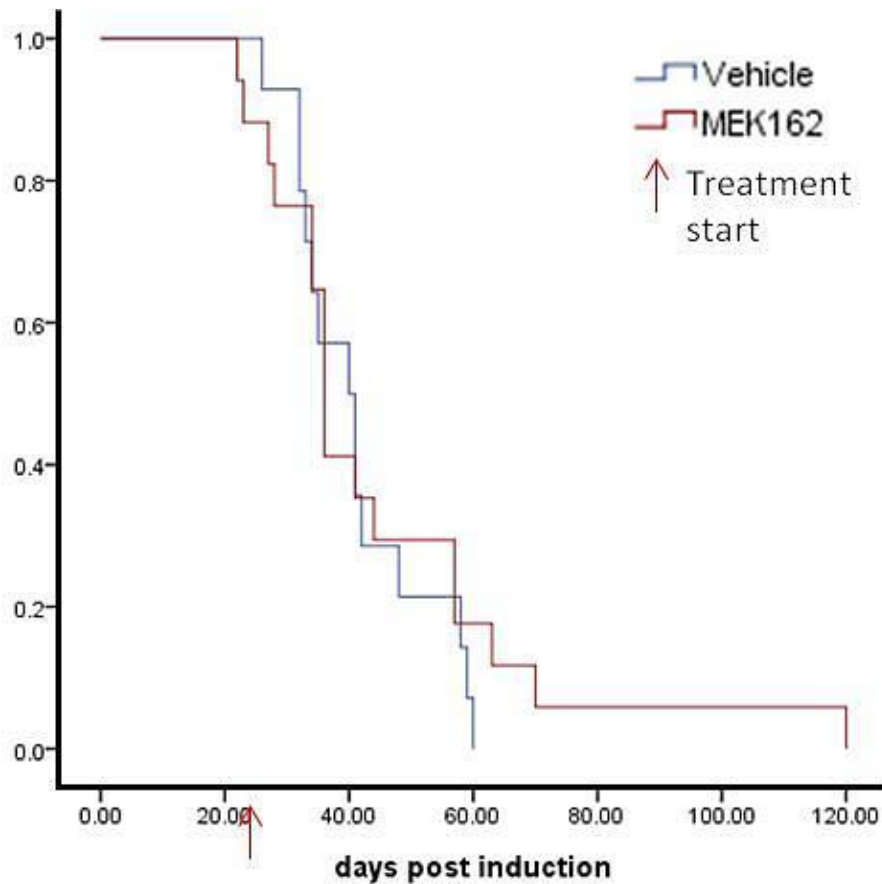


Figure 6.10 Kaplan-Meier survival analysis of $Apc^{f/+}$ $Pten^{f/f}$ $Kras^{LSL/+}$ mice on MEK162 compared to vehicle controls

$Apc^{f/+}$ $Pten^{f/f}$ $Kras^{LSL/+}$ mice were induced and aged to 22 days post induction, at which point mice received 30mg/kg MEK162 twice-daily by oral gavage until a survival end point. Continuous MEK162 treatment was found to have no significant effect on survival of mice compared to vehicle controls (Median survival: MEK = 36 days vs veh = 40 days post induction, p values: Log-Rank = 0.547 and wilcoxon test = 0.937 $n \geq 13$ mice per cohort).

6.2.5 Investigation of short term combination treatment in $Apc^{f/+}$ $Pten^{f/f}$ $Kras^{LSL/+}$ tumours

As PI3K/mTOR inhibition significantly increased survival of $Apc^{f/+}$ $Pten^{f/f}$ $Kras^{LSL/+}$ mice, but MEK inhibition failed to show any benefit on longevity, combined inhibition of PI3K/mTOR and MAPK signalling was next investigated to determine whether longevity of mice could be further improved upon. As with chapters 4 and 5, the three combination strategies were initially investigated to determine whether tumours are sensitive to the order of drug administration, as was observed with $Apc^{f/+}$ $Pten^{f/f}$ tumours (section 4.2.5), or not so, as observed with $Apc^{f/+}$ $Kras^{LSL/+}$ tumours (section 5.2.5).

Similarly to previous short term experiments, mice were induced and aged until symptomatic of tumour burden. A cohort of $n \geq 3$ mice were administered with the three differing combination strategies (outline in Table 4.5) and harvested 4 hours after the final dose. A dose of BrdU was also administered 2 hours prior to culling and mice were dissected and tissues were prepared as previously described in methods section 2.4. Vehicle controls used here were also described earlier in section 6.2.1.

To explore the immediate anti-tumour activity of the three differing combination strategies, histological mitosis and apoptosis was scored from H&E stained sections of SITs. Furthermore, IHC for BrdU and cleaved caspase 3 was carried out and quantified to further inform on the anti-tumour effects of the combination strategies. Scoring of mitotic figures revealed no significant alterations after exposure to any of the three combinations compared to vehicle controls (4hr veh = 0.283 ± 0.192 , combo 1 = 0.305 ± 0.265 , p value = 0.99, combo 2 = 0.391 ± 0.258 , p value = 0.199, combo 3 = 0.2733 ± 0.209 , p value = 0.766, $n \geq 15$ tumours, 4 mice, Mann Whitney U test) (Figure 6.11 A). Quantification of histological apoptosis in $Apc^{f/+}$ $Pten^{f/f}$ $Kras^{LSL/+}$ SITs identified significant increase in levels in response to all three combination strategies (4hr veh = 1.00 ± 0.575 , combo 1 = 3.272 , p value = 0.0002, combo 2 = 4.146 ± 2.045 , p value ≤ 0.0001 , combo 3 = 1.919 ± 0.951 , p value = 0.0022, $n \geq 15$ tumours, 4 mice, Mann Whitney U test) (Figure 6.11 B).

To further evaluate the anti-tumour properties of combination treatment, IHC for BrdU and cleaved caspase 3 were scored. Quantification of BrdU surprisingly revealed a significant increase in the number of positive cells scored after all three combination strategies (4hr veh = 13.36 ± 4.13 , combo 1 = 33.48 ± 9.61 , p value = 0.0001, combo 2 = 27.03 , p value = 0.0004, combo 3 = 20.05 ± 7.47 , p value = 0.0452, $n \geq 15$ tumours, 4 mice, Mann Whitney U test) (Figure 6.12 A), possibly indicative of compensatory actions which lead to increased proliferation in

response to treatment. Despite this, quantification of cleaved caspase 3 staining here revealed an increase in staining in samples from all three combination strategies (4hr veh = 1.22 ± 0.56 , combo 1 = 11.86 ± 9.48 , p value ≤ 0.0001 , combo 2 = 7.42 ± 4.06 , p value = 0.0002, combo 3 = 10.31 ± 4.86 , p value ≤ 0.0001 , $n \geq 15$ tumours, 4 mice, Mann Whitney U test), corroborating the scoring of histological apoptosis (Figure 6.12 C).

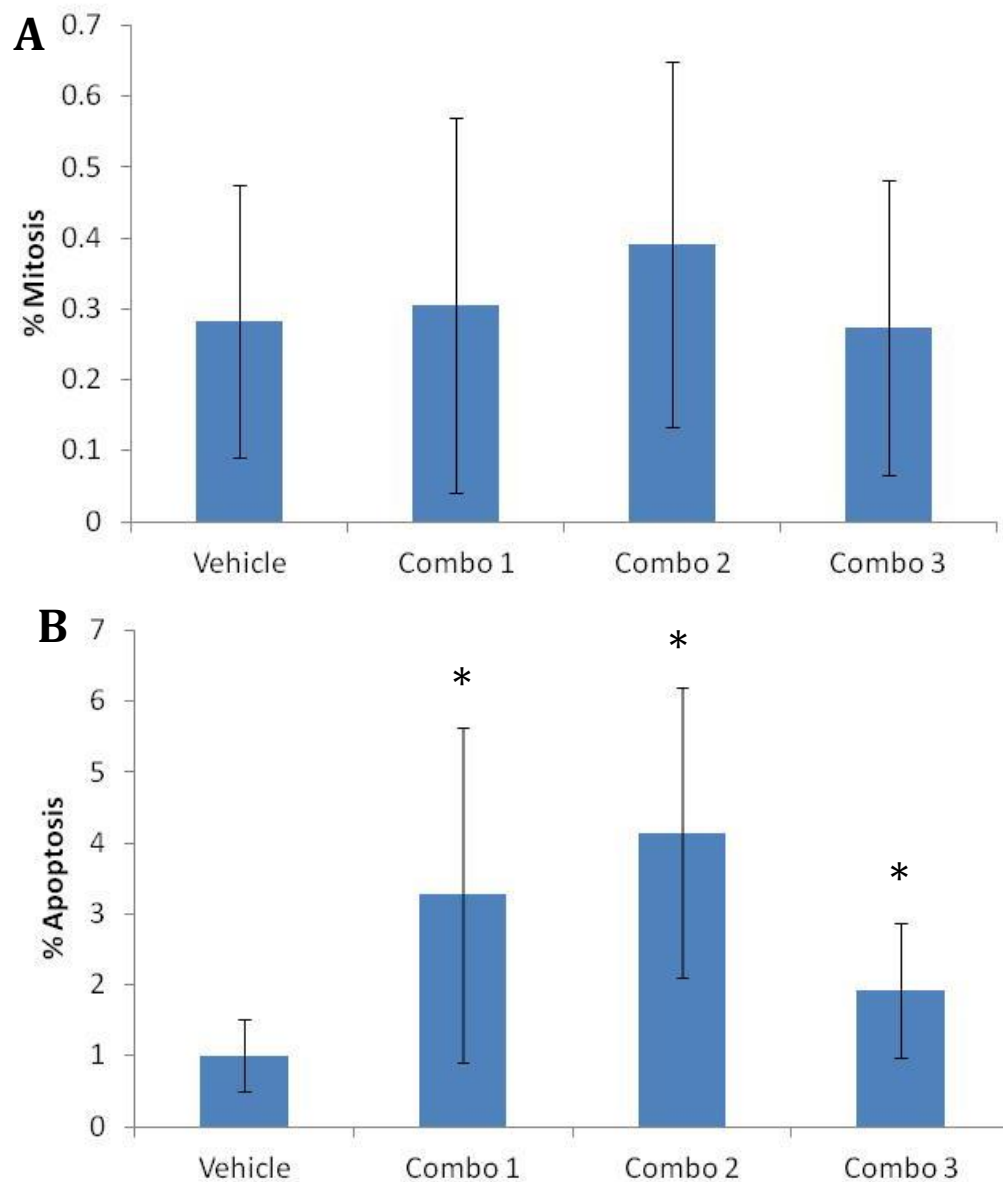


Figure 6.11 All three combination strategies resulted in a pro-apoptotic effect in

***Apc^{f/+} Pten^{f/f} Kras^{LSL/+}* but no effect on proliferation**

tions in

mitosis however, all three combinations significantly increased apoptosis, compared to vehicle controls (p value ≤ 0.05, n ≥ 15 tumours, 4 mice, Mann Whitney U test). Error bars represent standard deviation.

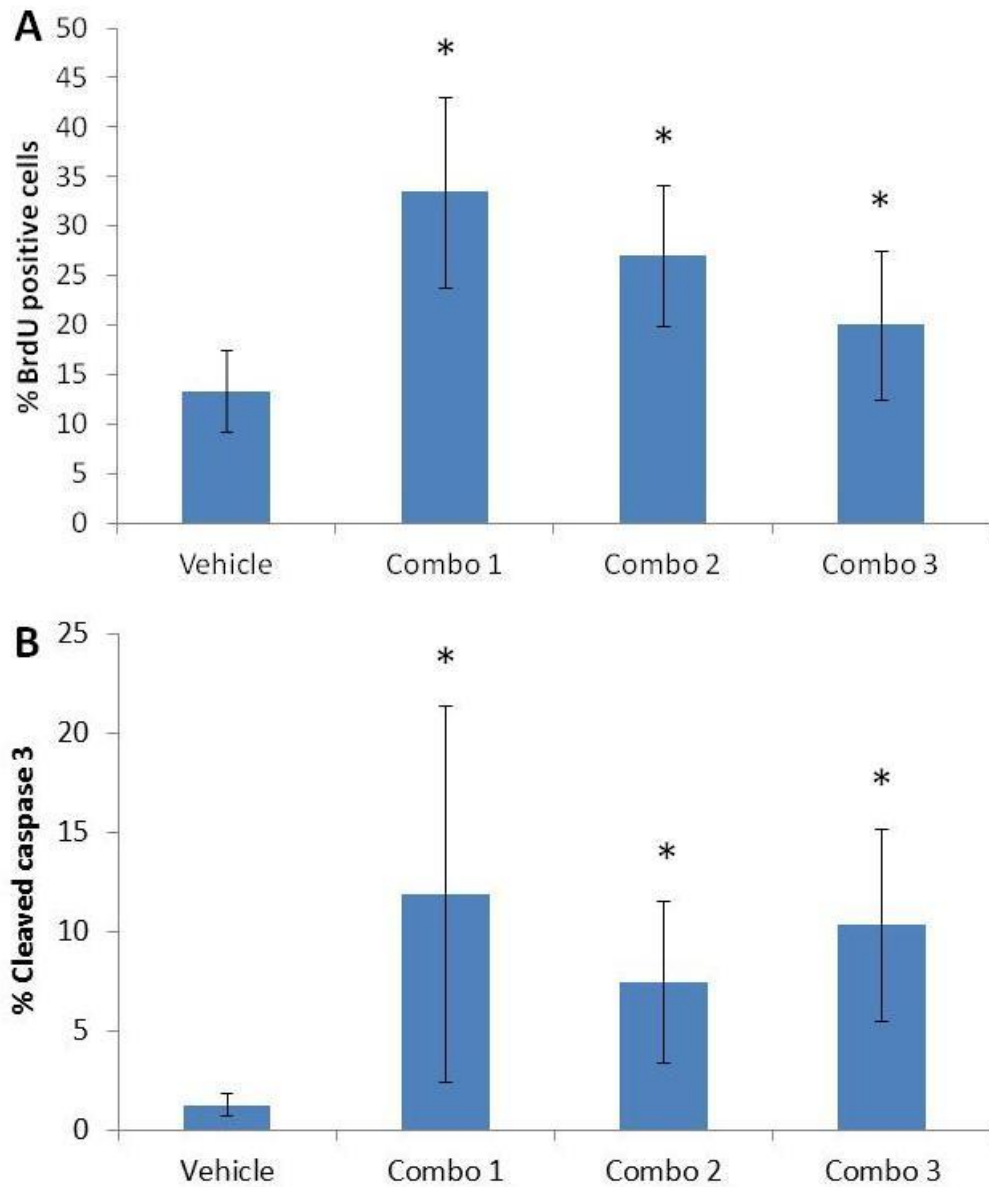


Figure 6.12 All combination strategies increased BrdU positive cells and cleaved caspase 3 staining in $Apc^{f/+}$ $Pten^{f/f}$ $Kras^{LSL/+}$ tumours

Scoring of BrdU (**A**) and cleaved caspase 3 (**B**) staining from IHCs revealed a significant increase in BrdU positive cells and cleaved caspase 3 (p value ≤ 0.05 , $n \geq 15$ tumours, 4 mice, Mann Whitney U test). Error bars represent standard deviation.

To determine the short term pharmacodynamic effects of the three differing combination strategies, tumours harvested from $Apc^{f/+}$ $Pten^{f/f}$ $Kras^{LSL/+}$ mice exposed to the combination strategies were subjected to western blot analysis. For each cohort, protein extracted from 6 SITs were pooled (from $n=3$ mice) and probed for components of PI3K/mTOR and MAPK signalling pathways to build pharmacodynamic profiles for each combination strategy. Interestingly, immunoblotting for intracellular pathway components revealed subtle but notable differences between the three combination strategies on pathway inhibition (Figure 6.13, Table 6.3, Table 6.4). Whilst all three combination strategies reduced levels of pERK to levels comparable to single agent MEK162, combo 3 also significantly reduced levels of total ERK protein (Figure 6.13, Table 6.3, Table 6.4). With respect to PI3K and mTOR signalling, combo 1 reduced pAKT473 whereas only combo 2 reduced pAKT308 levels (Figure 6.13, Table 6.3, Table 6.4). Nevertheless, all three combinations reduced pS6RP levels indicating effective mTOR inhibition even though p4EBP1 was found not reduced only following combo 1.

	Vehicle	Combo 1 (p value)	Combo 2 (p value)
pERK	3599.9 ± 1925	15.8 ± 5.2 (0.0404)	17.9 ± 13.1 (0.0404)
pAKT473	3026 ± 285.5	2257.7 ± 1107.3 (0.5)	4650.3 ± 636.8 (0.952)
pAKT308	2057.2 ± 735.8	810.6 ± 686.5 (0.0404)	1566.7 ± 99.5 (0.1914)
pS6RP	5216.6 ± 1621.0	382.7 ± 169.9 (0.0404)	62.9 ± 33.9 (0.0404)
p4EBP1	3426 ± 1392.7	3863.4 ± 1852.8 (0.5)	1217.5 ± 541.2 (0.0404)

Table 6-3 Outline of raw densitometry values from western blot analysis of pooled $Apc^{f/+}$ $Pten^{f/f}$ $Kras^{LSL/+}$ SITs 4 hours post exposure to combo 1 and combo 2, $n=3$, One-tailed Mann Whitney U test was used for statistical analysis

	Vehicle	Combo 3 (p value)
pERK	4235.1 ± 2772.8	29.9 ± 12.7 (0.0404)
T ERK	7500.4 ± 395.3	5261.6 ± 243.1 (0.0404)
pAKT473	5833.4 ± 291.8	2725.6 ± 291.8 (0.0404)
pAKT308	1517.7 ± 707.2	594.3 ± 429.6 (0.1914)
pS6RP	5816.0 ± 1622.0	280.5 ± 69.6 (0.0404)
p4EBP1	3845.9 ± 3679.1	2137.9 ± 1147.8 (0.0404)

Table 6-4 Outline of raw densitometry values from western blot analysis of pooled $Apc^{f/+}$ $Pten^{f/f}$ $Kras^{LSL/+}$ SITs 4 hours post exposure to combo 3, n=3, One-tailed Mann Whitney U test was used for statistical analysis

The overall trends observed from western blotting do not clearly identify one superior strategy out of the three evaluated, in terms of complete pathway inhibition. Concomitant inhibition of pERK and pS6RP was observed with all three combinations however, some subtle differences were apparent with regards to pathway output. Both combo 1 and 3 lead to reduction of four PI3K and MAPK effectors assessed whereas combo 2 led to reduction of three components (Figure 6.13, Table 6.3, Table 6.4). In this case, it was not known whether the number of components inhibited was more significant than the observation that both signalling pathways were terminally inhibited. Nevertheless, all three strategies increased apoptotic signals, and so to remain consistent with the two previous mouse models assessed (chapter 4 and 5), combination strategy 2 was chosen for all further short term and long term experiments in this cohort.

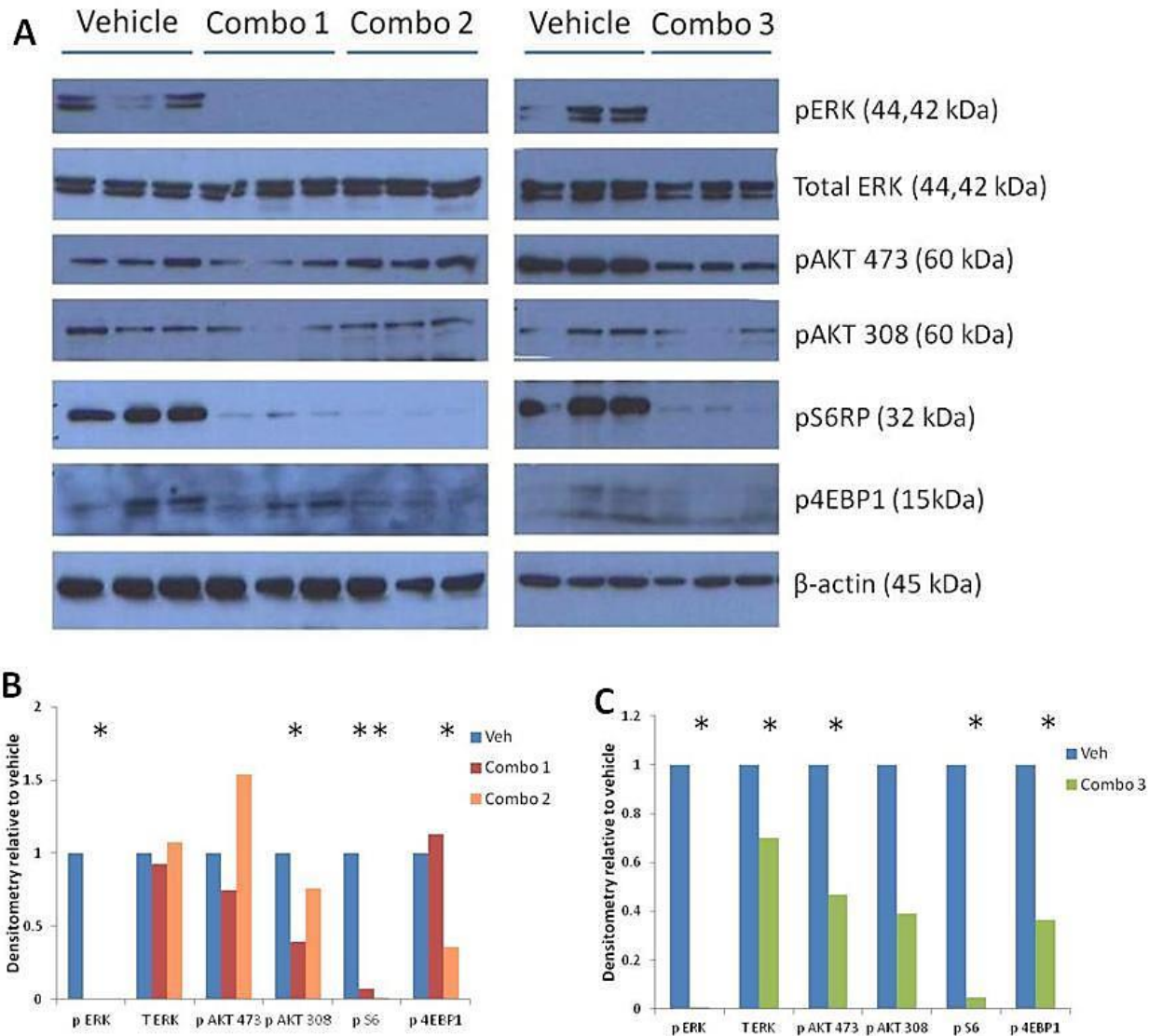


Figure 6.13 sequencing of combination results in differential inhibition of signalling downstream PI3K/mTOR and MEK in Apc^{f/+} Pten^{f/f} Kras^{LSL/+} tumours

(A) 6 SIT lysates pooled from n=3 mice exposed to the three different combination strategies were subjected to western blot analysis and probed for effectors of PI3K/mTOR and MAPK signalling. Immunoblotting revealed all three combination strategies reduced levels of pERK and pS6RP, however only combo 1 reduced levels of pAKT308 and combo 3 reduced levels of pAKT472. Both combo 2 and 3 reduced levels of p4EBP1. (B + C) Densitometry analysis was also carried out to quantify differences observed from western blotting. These are normalised to β-actin as loading control and represented as relative to vehicle controls (*p value = 0.0404, n=3, Mann Whitney U test).

6.2.6 Further analysis of combination strategy 2 in $Apc^{f/+}$ $Pten^{f/f}$ $Kras^{LSL/+}$ tumours

Combination strategy 2 where NVP-BEZ235 is administered 1 hour prior to MEK162 was chosen for all further combination experiments, and also to keep consistency between the different genotypes assessed in this thesis, to allow comparisons. To investigate whether combo 2 results in prolonged anti-tumour or favourable pharmacodynamic effects, n=4 mice were administered with combo 2 and harvested 24 hours following the final dose. Mice were also administered a pulse of BrdU 2 hours prior to culling, and were dissected as described in section 6.2.

For evaluation of anti-tumour activity, histological mitosis and apoptosis was scored from H&E stained sections of SITs and IHC for BrdU and cleaved caspase 3 was carried out and quantified to further inform on the anti-tumour effects of combo 2 24 hours post exposure (Figure 6.14). In doing so, scoring of mitotic figures revealed a significant reduction in proliferation however no significant alteration in the levels of histological apoptosis (veh mitosis = 0.283 ± 0.192 , 24hr c2 mitosis = 0.0928 ± 0.082 , p value = 0.002, veh apoptosis = 1.00 ± 0.515 , 24hr c2 apoptosis = 0.907 ± 0.681 , p value = 0.336, n \geq 3, Mann Whitney U test) (Figure 6.14 A, B), indicating an anti-proliferative effect. Furthermore, quantification of BrdU positive cells revealed no significant alterations compared to vehicle controls, but scoring of cleaved caspase 3 revealed a significant increase, indicating a pro-apoptotic effect of the combination 24 hours after administration (veh BrdU = 13.36 ± 4.13 , 24hr c2 BrdU = 13.29 ± 9.37 , p value = 0.678, veh caspase 3 = 1.22 ± 0.56 , 24hr c2 caspase 3 = 4.16 ± 2.28 , p value = 0.0025, n \geq 3, Mann Whitney U test) (Figure 6.14 C, D).

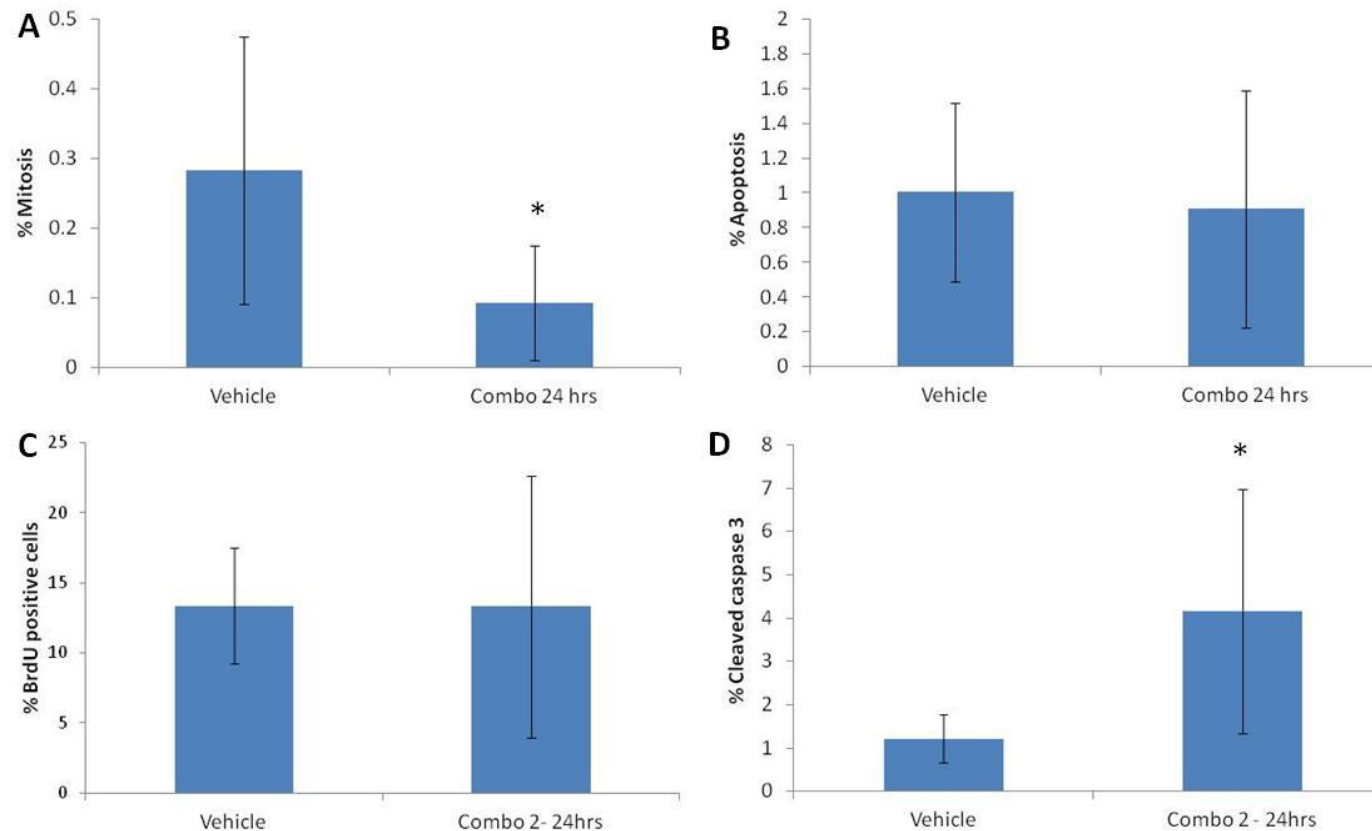


Figure 6.14 Biological effects of combo 2 24 hours post exposure in $Apc^{f/+}$ $Pten^{f/f}$ $Kras^{LSL/+}$ small intestinal tumours (SITs)

Assessment of proliferation in $Apc^{f/+}$ $Pten^{f/f}$ $Kras^{LSL/+}$ SITs 24 hours post exposure to combo 2 by quantification of histological mitosis (**A**) and IHC against BrdU (**C**) revealed a significant reduction in mitotic figures only (p value = 0.0024, $n \geq 15$ tumours, 4 mice, Mann Whitney U test). Additionally, assessment of apoptosis here through quantification of histological apoptotic bodies (**B**) and IHC against cleaved caspase 3 staining (**D**) revealed a pro-apoptotic effect through a significant increase in cleaved caspase 3 staining (p value = 0.0025, $n \geq 15$ tumours, 4 mice, Mann Whitney U test). Error bars represent standard deviation.

Given that PI3K and mTOR signalling was increased 24 hours post exposure to NVP-BE2235, and similarly MEK162 increased mTOR signalling through pS6RP and p4EBP1, it was pertinent to investigate whether the combination alleviate or exacerbated this effect. For this, snap frozen tumours from mice harvested 24 hours post combo 2 were subjected to protein extraction and analysis through western blotting. Proteins from 6 SITs were pooled and following western blot analysis, were incubated with antibodies against various effectors of MAPK and PI3K signalling (Figure 6.15). This, and subsequent densitometry analysis revealed a significant reduction in the phosphorylated and total ERK protein, indicating prolonged inhibition of MAPK signalling. However, a minimal yet significant increase in pAKT473 and large 2.5 fold increase in pAKT308 levels were observed (Figure 6.15, Table 6.5). Despite the increase in PI3K signalling through pAKT, no significant alterations were observed with regards to pS6RP and p4EBP1 which signal downstream of the AKT substrate, mTOR, potentially indicating synergy to stabilise mTOR signalling (Figure 6.15, Table 6.5). These investigations indicate that combo 2 results in prolonged anti-proliferative and pro-apoptotic effects, and when compared to single agents, reduce MAPK signalling and prevent strong activation of PI3K signalling. Whether this results in a beneficial effect long term is addressed in section 6.2.7.

	Vehicle	24hr Combo 2 (p value)
pERK	4235.1 ± 2772.8	344.7 ± 205.6 (0.0404)
T ERK	7500.4 ± 395.3	4816.3 ± 261.1 (0.0404)
pAKT473	5833.4 ± 291.8	6631 ± 102.1 (0.0404)
pAKT308	1517.7 ± 707.2	4094.6 ± 492.6 (0.0404)
pS6RP	5816.0 ± 1622.0	4589.5 ± 1001.5 (0.1914)
p4EBP1	3845.9 ± 3679.1	5960.1 ± 2216.3 (0.5)

Table 6-5 Outline of raw densitometry values from western blot analysis of pooled *Apc^{f/+} Pten^{f/f} Kras^{LSL/+}* SITs 24 hours post exposure to combo 2, n=3, One-tailed Mann Whitney U test was used for statistical analysis

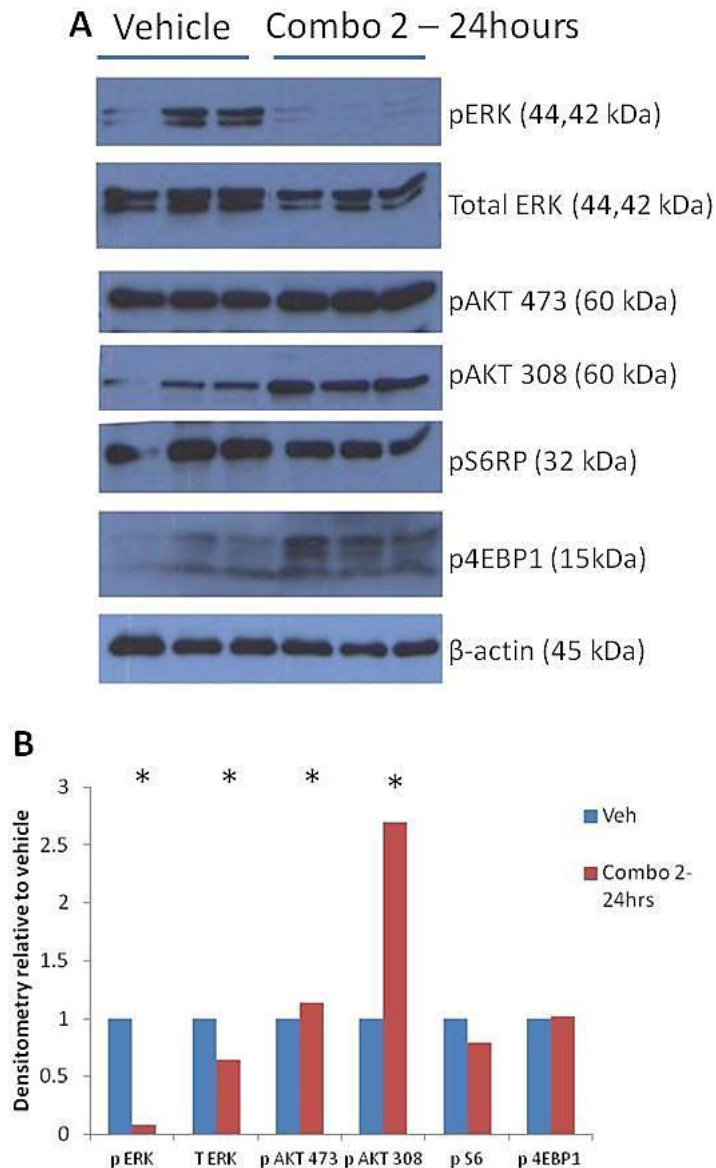


Figure 6.15 Combo 2 led to inhibition of MAPK signalling but increased PI3K signalling 24 hours following exposure

(A) 6 SITs pooled from n=3 mice culled 24 hours following exposure to combo 2 were subjected to western blot analysis and probed for effectors of PI3K/mTOR and MAPK signalling. Immunoblotting revealed substantial inhibition of MAPK signalling, however, an increase in PI3K signalling through pAKT473 and pAKT308. (B) Densitometry analysis was carried out to quantify differences observed from immunoblotting. These are normalised to β -actin as loading control and represented relative to vehicle controls (*p value = 0.0404, n=3, Mann Whitney U test).

6.2.7 Chronic treatment of combined NVP-BEZ235 and MEK162 results in a synergistic survival benefit in $Apc^{f/+}$ $Pten^{f/f}$ $Kras^{LSL/+}$ mice

Previously in sections 4.2.7 and 5.2.7, reduced combined treatment of NVP-BEZ235 and MEK162 (at 35mg/kg NVP-BEZ235 twice daily plus 30mg/kg MEK162 once daily) was found to be well tolerated in $Apc^{f/+}$ $Pten^{f/f}$ mice but not in $Apc^{f/+}$ $Kras^{LSL/+}$ mice. To investigate the combination treatment in $Apc^{f/+}$ $Kras^{LSL/+}$ mice, the dose of combination was further reduced (to 35mg/kg NVP-BEZ235 once daily plus 30mg/kg MEK162 once daily) to ensure tolerability, and this led to an additive increase in survival in comparison to single agent therapy. However, it was not known whether the first combination treatment regimen would be tolerated by $Apc^{f/+}$ $Pten^{f/f}$ $Kras^{LSL/+}$ mice therefore, a cohort of 11 mice were induced and aged until 22 days post induction, at which point they began long term treatment of 35mg/kg NVP-BEZ235 twice-daily plus 30mg/kg MEK162 once daily 1 hour after the first NVP-BEZ235 dose (combo R1). Mice were treated daily and monitored closely for signs of toxicity, until a survival end point. Similarly to $Apc^{f/+}$ $Kras^{LSL/+}$ mice, soon after the experiment began, it was apparent this combination was also toxic for $Apc^{f/+}$ $Pten^{f/f}$ $Kras^{LSL/+}$ mice as 6/11 mice were culled due to dramatic weight loss (weight loss shown on figure 6.16 and survival of mice depicted on (Figure 6.17). Despite this, 5/11 mice displayed some survival benefit compared to vehicle controls with one mouse surviving up to 217 days post induction. In spite of this, the median survival for the whole cohort was found to be 39 days post induction, and not significantly altered from a median survival of 40 days post induction for vehicle controls ($n \geq 11$, p value = 0.118 for Long-Rank and p value = 0.478 for Wilcoxon test) (Figure 6.17).

Given these toxicity issues, the further reduced combination strategy (35mg/kg NVP-BEZ235 once daily plus 30mg/kg MEK162 once daily) which was found to be effective in $Apc^{f/+}$ $Kras^{LSL/+}$ mice, was subsequently used to evaluate the chronic effects of combination therapy in $Apc^{f/+}$ $Pten^{f/f}$ $Kras^{LSL/+}$ mice. Additionally, as NVP-BEZ235 as a twice-daily treatment regimen significantly increased survival of $Apc^{f/+}$ $Pten^{f/f}$ $Kras^{LSL/+}$ mice, a cohort of mice were also administered 35mg/kg NVP-BEZ235 once daily, as a control single agent treatment for the reduced combination therapy. Given that MEK162 had no effect on survival when administered as a twice-daily regimen, it was anticipated that a once-daily treatment regimen would also not have any significant effect on survival and so was an unnecessary control. Interestingly, Kaplan-Meier survival analysis revealed NVP-BEZ235 did not elicit any beneficial effect on survival of $Apc^{f/+}$ $Pten^{f/f}$ $Kras^{LSL/+}$ mice when administered as a once-daily treatment regimen (median survival: NVP-BEZ235 mice = 36 days vs vehicle mice = 40 days post

induction, $n \geq 12$ per cohort, p value ≥ 0.05 for both Log-Rank and Wilcoxon test) (Figure 6.18), indicating that $Apc^{f/+}$ $Pten^{f/f}$ $Kras^{LSL/+}$ mice are particularly sensitive to the dose of NVP-BEZ235. These findings support the dose-dependent effect of NVP-BEZ235 observed in $Apc^{f/+}$ $Kras^{LSL/+}$ mice; however, this effect was more dramatic in $Apc^{f/+}$ $Pten^{f/f}$ $Kras^{LSL/+}$ mice. The further reduced combination treatment (combo R2) here, was well tolerated (Figure 6.16) and significantly increased survival of $Apc^{f/+}$ $Pten^{f/f}$ $Kras^{LSL/+}$ mice from a median of 40 days to 125 days post induction ($n \geq 12$ per cohort, p value ≤ 0.0001 for Log-Rank and Wilcoxon test) (Figure 6.18). As neither single agent controls had any significant beneficial effect on survival of $Apc^{f/+}$ $Pten^{f/f}$ $Kras^{LSL/+}$ mice, the combination treatment here resulted in a synergistic increase in survival, indicating this as a well tolerated and beneficial therapeutic strategy.

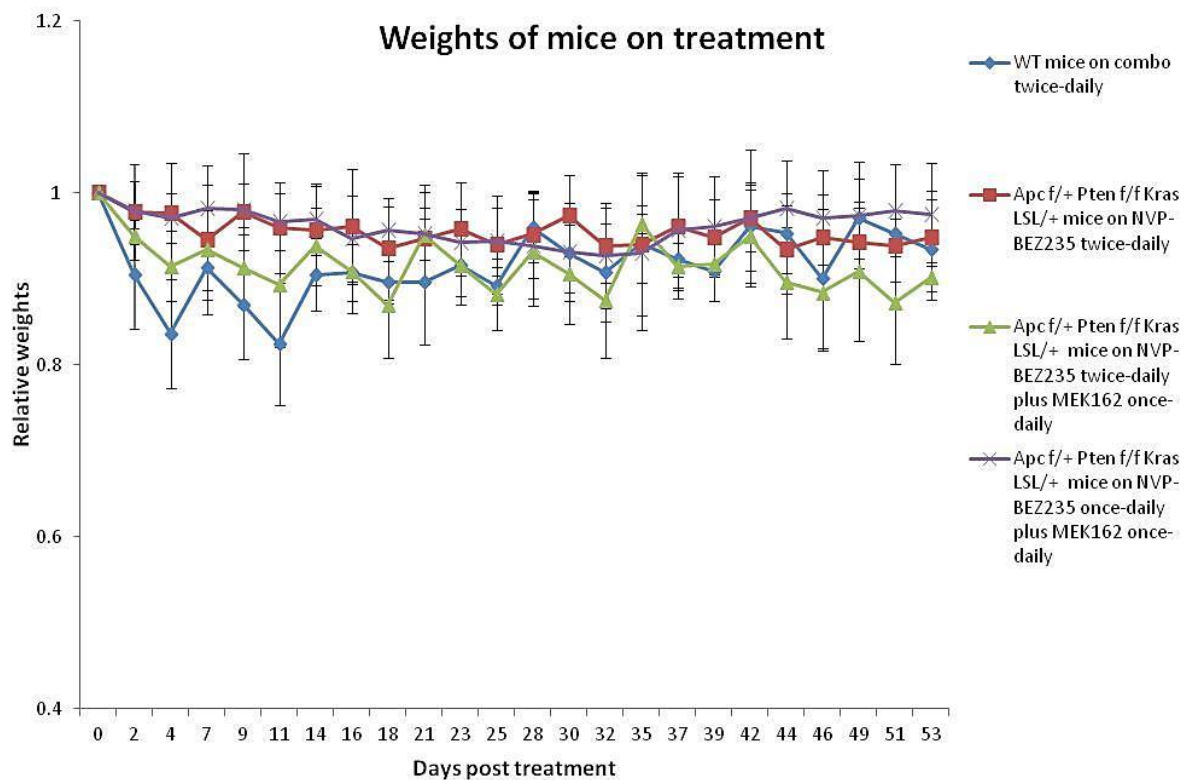


Figure 6.16 Toxicity of combination treatment in $Apc^{f/+} Pten^{f/f} Kras^{LSL/+}$ mice

Similarly to toxicity in $Apc^{f/+} Kras^{LSL/+}$ mice (figure 5.16), administration of 35mg/kg NVP-BEZ235 twice-daily plus 30mg/kg MEK162 once daily, led to notable fluctuations in body weight, n=9/12 mice were culled due 20% original weight loss. A further reduced combination regimen of 35mg/kg NVP-BEZ235 once daily plus 30mg/kg MEK162 once daily (1 hour later) – Combo R2, was subsequently evaluated and appeared to be better tolerated. Weights of wild type mice on twice daily combination is used to illustrate toxicity and single agent NVP-BEZ235 twice daily which was well tolerated in $Apc^{f/+} Pten^{f/f} Kras^{LSL/+}$ mice chosen as a positive comparison.

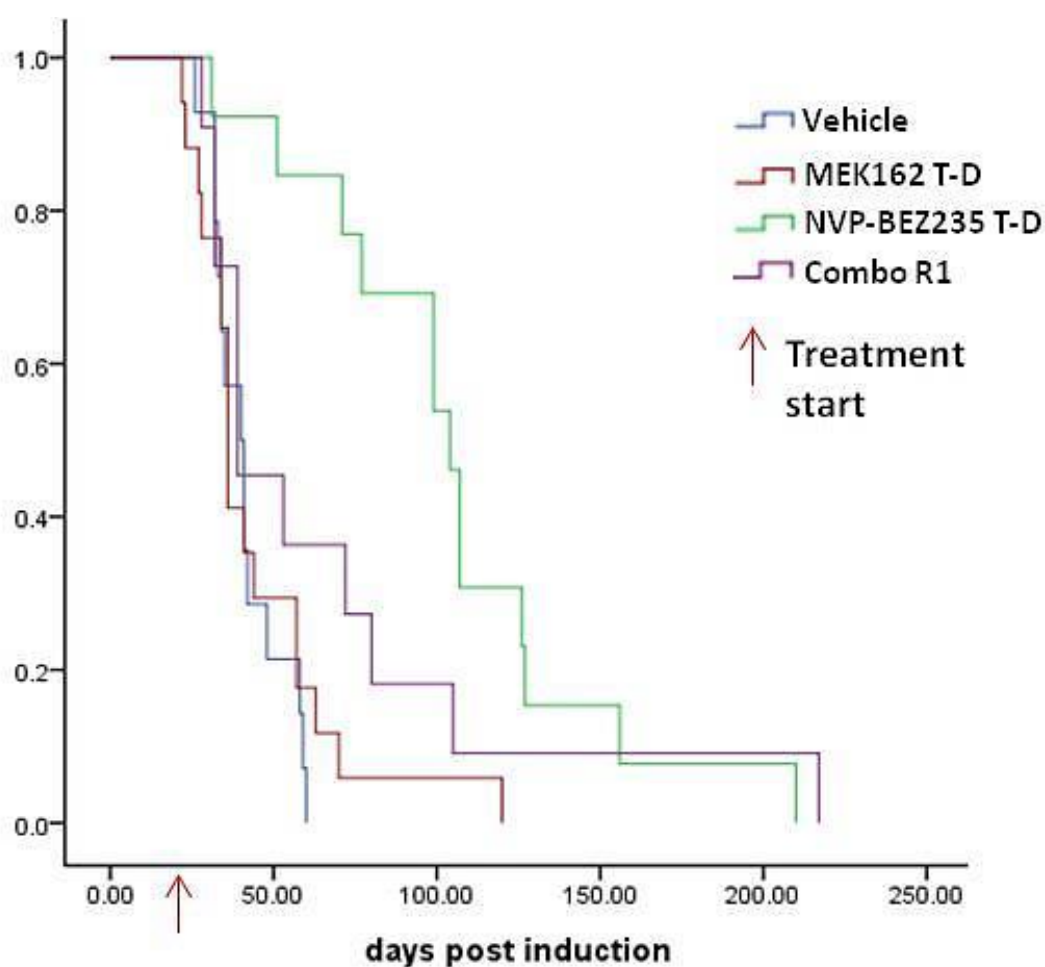


Figure 6.17 Kaplan-Meier survival analysis of $Apc^{f/+}$ $Pten^{f/f}$ $Kras^{LSL/+}$ mice on combination treatment (combo R1) compared to single agent treatment and vehicle controls

$Apc^{f/+}$ $Pten^{f/f}$ $Kras^{LSL/+}$ mice were induced and aged to 22 days post induction, at which point mice received 35mg/kg NVP-BEZ235 twice-daily plus 30mg/kg MEK162 once-daily (1 hour later)- combo R1. This was found to have no significant benefit on median survival of mice due to toxicity, despite some mice appearing to benefit partially. Control dose of twice daily NVP-BEZ235 and MEK162 is also illustrated here. (Median survival: combo 1 = 39 days vs veh = 40 days, vs MEK162 = 36 days and NVP-BEZ235 = 104 days post induction, p values ≥ 0.05 for all Log-Rank and wilcoxon test comparisons $n \geq 12$ mice per cohort).

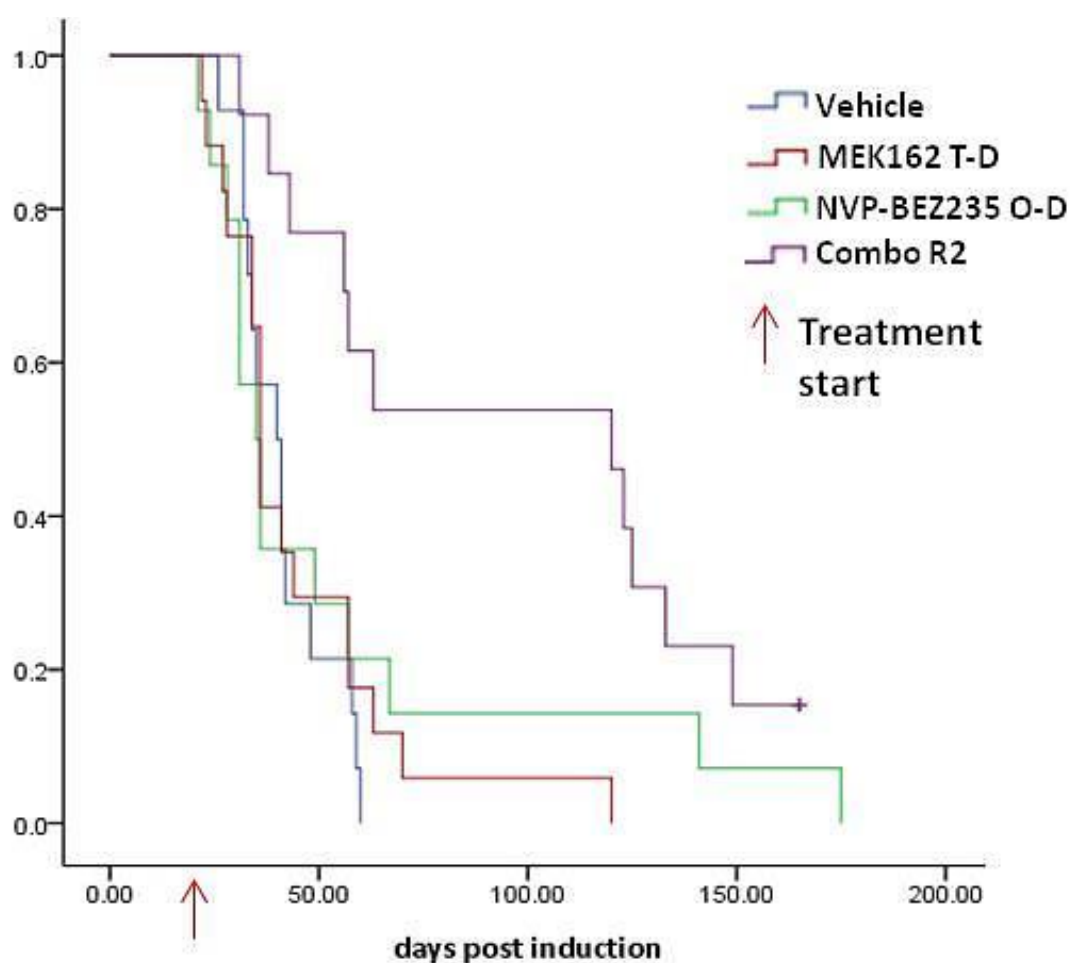


Figure 6.18 Kaplan-Meier survival analysis of $Apc^{f/+} Pten^{f/f} Kras^{LSL/+}$ mice on further reduced combo 2 (Combo R2) dose compared to vehicle, MEK162 T-D and NVP-BEZ235 O-D controls

$Apc^{f/+} Pten^{f/f} Kras^{LSL/+}$ mice were induced and aged to 22 days post induction, at which point mice received 35mg/kg NVP-BEZ235 once-daily plus 30mg/kg MEK162 once-daily (1 hour later)- combo R2. Additionally, a reduced once-daily treatment of NVP-BEZ235 was conducted as a control for the reduced combination. Reduced combination (combo R2) was found to synergistically increase survival of mice from 40 days (vehicle controls) to 125 days post induction (p value ≤ 0.0001 for all Log-Rank and wilcoxon test comparisons $n \geq 13$ mice per cohort). Interestingly, once-daily NVP-BEZ235 had no benefit on survival of $Apc^{f/+} Pten^{f/f} Kras^{LSL/+}$ mice (median survival = 36 days post induction p value ≥ 0.05 for both Log-Rank and wilcoxon test comparisons $n \geq 13$ mice per cohort)

6.2.8 Tumour burden analysis of $Apc^{f/+}$ $Pten^{f/f}$ $Kras^{LSL/+}$ mice on various treatments

Having identified that NVP-BEZ235 as a single agent and in combination with MEK162 is beneficial in extending longevity of $Apc^{f/+}$ $Pten^{f/f}$ $Kras^{LSL/+}$ mice, the effect of these and control treatments on tumour burden was next evaluated. For this, the total number of tumours present at death was scored from H&E stained sections of the small intestines, and tumours were also staged according to tumour severity (described previously in methods section 2.7.4). In chapters 4 and 5, analysis of tumour burden also involved analysis of total tumour area per mouse however, in $Apc^{f/+}$ $Pten^{f/f}$ $Kras^{LSL/+}$ mice the edge of individual tumours was often not clearly visible, therefore it was difficult to accurately measure individual tumours macroscopically. The parameters of tumour burden were also evaluated in a cohort of mice culled at the treatment start point which in this tumour model was 22 days post induction.

The number of tumours present in mice from each cohort was scored blind from 3 H&E stained small intestine sections to increase the probability of scoring all tumours present. These were averaged per section and further averaged per mouse for each cohort. As shown in Figure 6.19 A, the total number of tumours in vehicle treated mice was not significantly altered compared to the cohort of mice culled at 22 days post induction (the start cohort) (Median number of tumours: start = 29.5, vehicle = 44 p value = 0.217, $n \geq 8$, Mann Whitney U test). This indicates that treatment in these mice was not prophylaxis and mice bore statistically similar number of tumours at the start as they would have done at death. Interestingly, mice on NVP-BEZ235 T-D, MEK162 and combo R2 at death, had similar median number of tumours to both start and vehicle cohorts suggesting that these particular treatments resulted in tumour growth stasis, regardless of the effect on survival of mice (Median number of tumours: start = 29.5, vehicle = 44, NVP-BEZ235 T-D = 34.5 p value = 0.787 for start and p value = 0.215 for vehicle comparison, MEK162 = 30.3 p value = 0.856 for start and p value = 0.0644 for vehicle comparison, combo R2 = 30.7 p value = 0.592 for start and p value = 0.0525 for vehicle comparison, $n \geq 8$, Mann Whitney U test) (Figure 6.19 A).

Whilst treatment of $Apc^{f/+}$ $Pten^{f/f}$ $Kras^{LSL/+}$ mice with reduced dose NVP-BEZ235 (O-D) had no effect on survival of mice, analysis of tumour number following treatment indicated mice had significantly more tumours in comparison with the start cohort and the twice-daily NVP-BEZ235 (T-D) treatment, with a trend towards increased tumours number in comparison with the vehicle treated cohorts (median number of tumours: start = 29.5, vehicle = 44, NVP-

BEZ235 T-D = 34.5, NVP-BEZ235 O-D = 62.2; p value = 0.0228 for start cohort, p value = 0.133 for vehicle cohort, p value = 0.0014 for NVP-BEZ235 T-D comparison $n \geq 8$, Mann Whitney U test) (Figure 6.19 A). These observations suggest an increase in tumour burden with NVP-BEZ235 O-D treatment in $Apc^{f/+} Pten^{f/f} Kras^{LSL/+}$ mice.

Although combo R1 was found to be toxic for the majority of mice in the cohort, tumour numbers were found to be significantly reduced in comparison to the start and vehicle cohorts (median number of tumours: start = 29.5, vehicle = 44, combo R1 = 13.2; p value = 0.0456 for start and p value = 0.0011 for vehicle comparisons, $n \geq 6$, Mann Whitney U test) (Figure 6.19 A). These observations suggest that in the absence of toxicity, this treatment regimen may have proven beneficial for $Apc^{f/+} Pten^{f/f} Kras^{LSL/+}$ mice.

To address the effect of treatment on tumour severity in $Apc^{f/+} Pten^{f/f} Kras^{LSL/+}$ mice, tumours on H&E stained sections of the small intestine were scored according to the criteria for grading described in section 2.7.4. The average number of each grade was calculated and is displayed as a proportion of the total number of tumours due to differences observed in the total number of tumours at death (Figure 6.19 A). Similarly to $Apc^{f/+} Kras^{LSL/+}$ mice, the majority of tumours present in all $Apc^{f/+} Pten^{f/f} Kras^{LSL/+}$ mice are the less invasive microadenomas and adenomas, and so therefore, treatments predominantly altered the proportions of these. Tumour severity scoring in vehicle treated mice indicated a trend for reduced microadenomas, but a significant increase in the proportion of adenomas in comparison to the start cohort (proportion of mAds: start = 86.5%, vehicle = 67% p value = 0.699; proportion of Ads: start = 12%, vehicle = 31% p value = 0.0018, $n \geq 8$, Mann Whitney U test) (Figure 6.19 B). This observation highlights that although the number of lesions between the start and vehicle cohort are not significantly different, tumour growth is observed between the start of treatment and at death in vehicle treated mice.

Assessment of tumours in treated cohorts revealed NVP-BEZ235 T-D treatment had no substantial effect on severity of lesions present in $Apc^{f/+} Pten^{f/f} Kras^{LSL/+}$ mice, although mice had significantly reduced adenomas in comparison with vehicle treated mice (proportion of mAds: start = 86.5%, vehicle = 67%, NVP-BEZ235 T-D = 78% p value = 0.847 for start and p value = 0.603 for vehicle comparison; proportion of Ads: start = 12%, vehicle = 31%, NVP-BEZ235 T-D = 19.5% p value = 0.132 for start and p value = 0.0114 for vehicle cohort; proportion of EIAs: start = 1.5%, vehicle = 2%, NVP-BEZ235 T-D = 2.3% p value = 0.4 for start and p value = 0.447 for vehicle cohort, $n \geq 8$, Mann Whitney U test) (Figure 6.19 B). Interestingly, the reduced NVP-BEZ235 treatment (once daily, O-D) significantly increased the

proportion of adenomas and EIAs present in $Apc^{f/+}$ $Pten^{f/f}$ $Kras^{LSL/+}$ mice, indicating treatment augmented tumour progression, due to the lack of significant survival benefit obtained from this treatment (proportion of mAds: start = 86.5%, vehicle = 67%, NVP-BEZ235 O-D = 53% p value = 0.616 for start and p value = 0.751 for vehicle comparison; proportion of Ads: start = 12%, vehicle = 31%, NVP-BEZ235 O-D = 32% p value = 0.003 for start and p value = 0.1571 for vehicle cohort; proportion of EIAs: start = 1.5%, vehicle = 2%, NVP-BEZ235 O-D = 14% p value = 0.0004 for start and p value = 0.0001 for vehicle cohort, $n \geq 8$, Mann Whitney U test) (Figure 6.19 B).

Scoring of tumour severity in MEK162 treated $Apc^{f/+}$ $Pten^{f/f}$ $Kras^{LSL/+}$ mice revealed significant differences in tumour severity in comparison to the start and vehicle cohorts. Here, although the proportion of microadenomas was not found to be significantly reduced, adenomas were increased in comparison to vehicle treated mice and EIAs were increased in comparison to both the start and vehicle cohorts, highlighting progression of tumourigenesis (proportion of mAds: start = 86.5%, vehicle = 67%, MEK162 = 69% p value = 0.294 for start and p value = 0.1916 for vehicle comparison; proportion of Ads: start = 12%, vehicle = 31%, MEK162 = 24% p value = 0.119 for start and p value = 0.0051 for vehicle cohort; proportion of EIAs: start = 1.5%, vehicle = 2%, MEK162 = 6.8% p value = 0.0035 for start and p value = 0.0144 for vehicle cohort, $n \geq 8$, Mann Whitney U test) (Figure 6.19 B). These findings of tumour progression with MEK162 treatment also suggest an exacerbated effect on tumourigenesis, similar to NVP-BEZ235 O-D treatment, as treatment had no benefit on survival of mice.

The proportion of microadenomas and adenomas in mice following long term combo R1 were significantly reduced in comparison to vehicle treatment mice and also appeared to be proportionally more invasive. However, this later observation was not statistically significant perhaps because mice had significantly less tumours in total (proportion of mAds: start = 86.5%, vehicle = 67%, combo R1 = 63.5% p value = 0.0088 for start and p value = 0.0027 for vehicle comparison; proportion of Ads: start = 12%, vehicle = 31%, combo R1 = 29% p value = 0.824 for start and p value = 0.194 for vehicle cohort; proportion of EIAs: start = 1.5%, vehicle = 2%, combo R1 = 6.61% p value = 0.824 for start and p value = 0.18 for vehicle cohort, $n \geq 6$, Mann Whitney U test) (Figure 6.19 B).

Scoring of tumour severity in mice treated with combo R2 revealed significant indications of tumour progression. Here, mice presented with a significant reduction in the proportion of microadenomas and an increase in the proportion of adenomas in comparison to vehicle treated mice, and also a significant increase in the proportion of EIAs in comparison to both

start and vehicle treated mice (proportion of mAds: start = 86.5%, vehicle = 67%, combo R2 = 49% p value = 0.0574 for start and p value = 0.0289 for vehicle comparison; proportion of Ads: start = 12%, vehicle = 31%, combo R2 = 28% p value = 0.137 for start and p value = 0.127 for vehicle cohort; proportion of EIAs: start = 1.5%, vehicle = 2%, combo R2 = 22% p value = 0.0021 for start and p value = 0.0036 for vehicle cohort, $n \geq 8$, Mann Whitney U test) (Figure 6.19 B). The observation of significantly more invasive lesions are present at death in combo R2 treated mice, together with the increased lifespan of mice indicates increased tumour burden and may be indicative of resistant tumour growth.

Interestingly, during the assessment of histological sections for scoring of tumour severity, distinct lesions which lacked the epithelial mucosal layer were notable. Closer analysis of these lesions revealed these to be superficial ulcers which had lost most or all of their epithelial cells, and were left with an inflamed basal layer (Figure 6.20). Further analysis of tumours revealed varied central areas of ulceration denoting potentially, the beginning stages of the ulceration process. The presence of these lesions was scored blind and interestingly, these were identified to only be present in cohorts exposed to NVP-BEZ235 (the % of mice which presented with ulcerated lesions: Start cohort = 0, vehicle = 0, NVP-BEZ235 T-D cohort = 50%, NVP-BEZ235 O-D cohort = 33%, MEK162 cohort = 0, combo R1 cohort = 72%, combo R2 = 63%)(Figure 6.20). Additionally, the presence of ulcerated lesions did not correlate to treatments which increased survival as NVP-BEZ235 O-D and combo R1 treatments had comparable numbers of mice with ulcerated lesions to their corresponding higher dose regimens. The reasons for the presence of these ulcerated lesions are currently unclear however it is hypothesised that due to loss of epithelial cells, a regenerative stromal response may have been activated to heal over the basal layer.

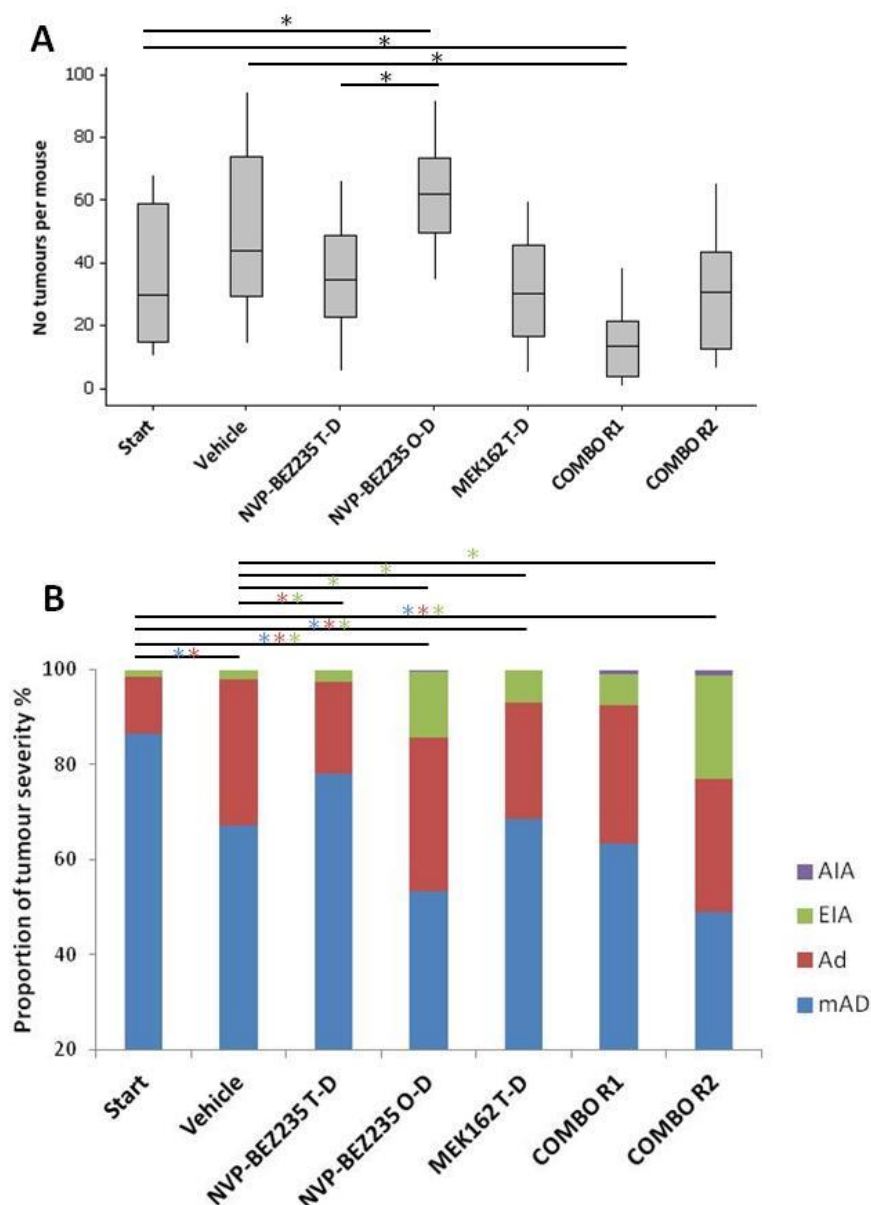


Figure 6.19 Tumour burden analysis of $Apc^{f/+} Pten^{f/f} Kras^{LSL/+}$ mice on all long term treatments

(A) $Apc^{f/+} Pten^{f/f} Kras^{LSL/+}$ mice on NVP-BEZ235 O-D had significantly increased tumours at death compared to the start cohort. Additionally, mice on combo R1 had significantly reduced tumours at death compared to start and vehicle cohorts. **(B)** Key: mAd – microadenoma, Ad – adenoma, EIA – early invasive adenocarcinoma, AIA – advanced invasive adenocarcinoma. Staging of tumours at death revealed a significant reduction in mAds and an increase in Ads with vehicle, NVP-BEZ235 T-D, MEK162 and combo R2 treatments. An increase in EIAs in all cohorts except the vehicle and NVP-BEZ235 T-D cohort was observed in comparison with the start cohort. Additionally, an increase in EIAs was observed in NVP-BEZ235 T-D and O-D, MEK162 and combo R2 cohorts compared to vehicle controls. Furthermore, a significant reduction in Ads was observed with the NVP-BEZ235 T-D cohort in comparison to the vehicle treated cohort (*p value ≤ 0.05 , Mann Whitney U test).

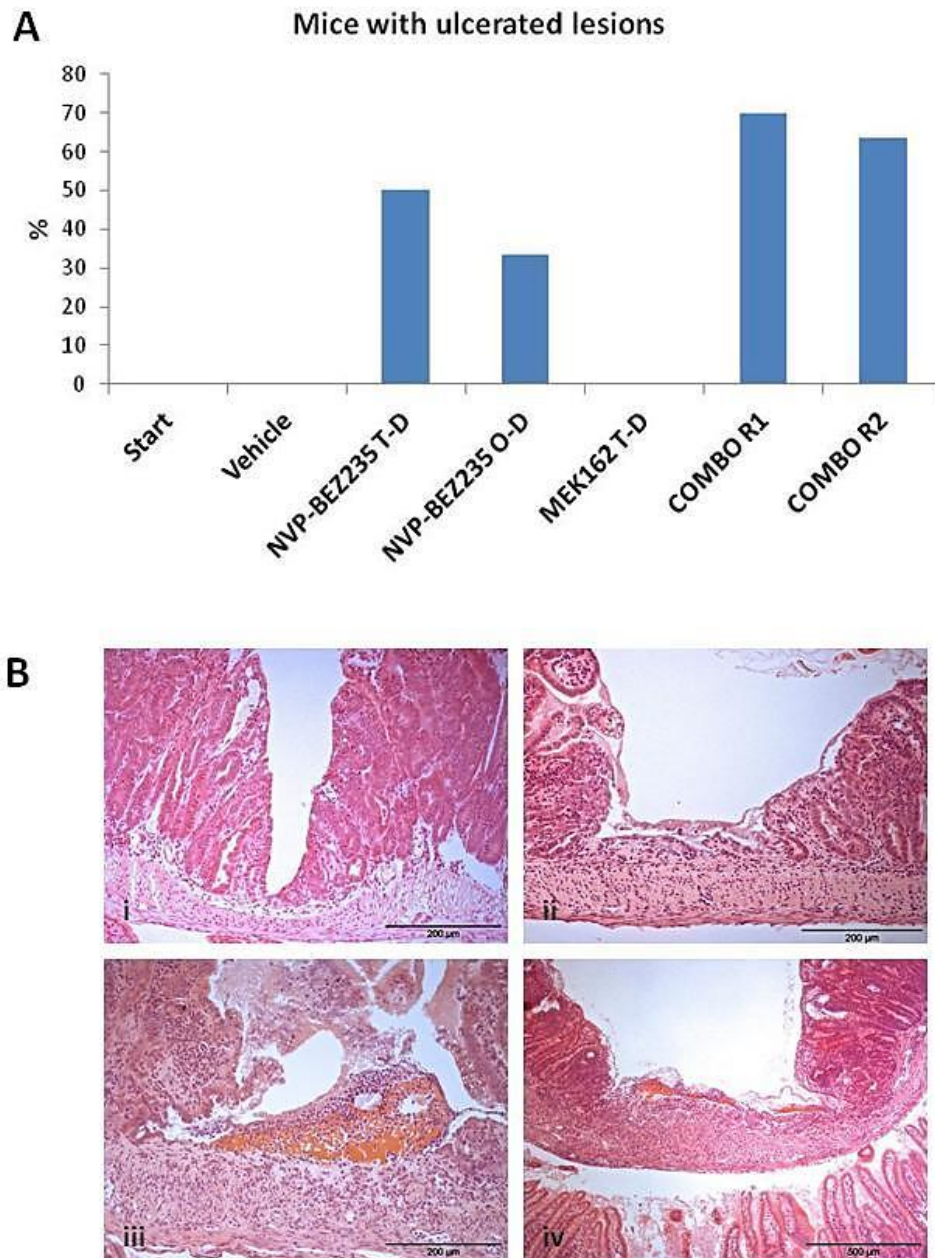


Figure 6.20 Ulceration of tumours in $Apc^{f/+} Pten^{f/f} Kras^{LSL/+}$ mice on long term treatments

(A) Histological analysis of $Apc^{f/+} Pten^{f/f} Kras^{LSL/+}$ small intestine sections revealed tumours with varying signs of ulceration. Scoring of the total number of mice which had ulcerated lesions revealed approximately 50% of mice on NVP-BEZ235 T-D had tumours with ulceration whereas less mice (approximately 30%) of mice on NVP-BEZ235 O-D had ulcerated lesions. Furthermore, 70% of mice on combo R1 had lesions with signs of ulceration and similarly 62% of mice on combo R2 bore ulcerated lesions. **(B)** H&E images of the varying degree of ulceration. Some adenomas with small signs of ulceration were observed as in (i) as well as large areas of ulceration showing signs of inflammatory response and also with and without surrounding tumour tissue were observed (ii), (iii) and (iv).

6.3 Discussion

6.3.1 The effects of acute and chronic NVP-BEZ235 in *Apc^{f/+} Pten^{f/f} Kras^{LSL/+}* mice

Mutations in the oncogene KRAS and those resulting in activation of PI3K signalling co-exist in approximately a third of all human CRC. In light of this, work described in this chapter investigated therapeutic targeting of the PI3K pathway with the dual PI3K/mTOR inhibitor NVP-BEZ235 and the MAPK pathway by inhibition of MEK1/2 through MEK162, as rational therapeutic strategies for this tumour sub-group. These investigations employed the use of the *Apc^{f/+} Pten^{f/f} Kras^{LSL/+}* mouse model where, heterozygous deletion of *Apc* and homozygous deletion of *Pten* together with activation of oncogenic *Kras* is driven by the VillinCreER transgene. This leads to development of invasive adenocarcinoma in the small intestine driven by activation of AKT and ERK, and a reduced lifespan of just 41 days post induction (Davies EJ, unpublished). For all experiments described in this chapter, 10 week old mice were induced by i.p injections of Tamoxifen and allowed to age either until the long term intervention start point of 22 days post induction, or until they presented with distinct symptoms of tumour burden (paling feet, bloating, rectal bleeding). At this point they received a single dose of treatment and were harvested at short time points for investigation of anti-tumour and pharmacodynamic effects.

Acutely, NVP-BEZ235 led to inhibition of all PI3K and mTOR effectors assessed, including pAKT at Ser473 and Thr308, pS6RP as well as p4EBP1 (Figure 6.3). Additionally, a significant increase in histological apoptosis and cleaved caspase 3 scoring, together with no detectable effect on mitosis, indicated favourable pro-apoptotic effects following NVP-BEZ235 (Figure 6.1, 6.2). Given the role of PI3K signalling in controlling survival and apoptosis, the increase in levels of apoptosis may be attributable to the reduction of signalling, potentially through reduced phosphorylation of pro-apoptotic proteins including BAD and BIM (She et al., 2010). Interestingly, NVP-BEZ235 also led to a significant reduction in the levels of pERK a downstream effector of MAPK signalling (Figure 6.3). This was surprising given that recent findings suggest mTORC1 inhibition by rapamycin, upstream of pS6RP and p4EBP1, led to activation of MAPK signalling through pERK rather than inhibition (Carracedo et al., 2008b). This has formally been evidenced through expression of the rapamycin insensitive-constitutively active S6 Kinase and pharmacological inhibition of PI3K, both of which led to reduced MAPK activation upon rapamycin treatment (Carracedo et al., 2008a). Interestingly, a recent study investigating the non-receptor tyrosine kinase SYK has evidenced a role for this protein in regulating mTOR signalling in lymphoma. Furthermore, the effects of SYK have been

confirmed to be PI3K dependent and interestingly, inhibition of SYK led to downregulation of MEK and ERK signalling in some AML cell lines. Nevertheless, the functions of SYK are limited to hematopoietic cells and so identification of a similar protein in epithelial cells may be attributable to the observations here. The mechanism by which PI3K and mTOR inhibition in $Apc^{f/+}$ $Pten^{f/f}$ $Kras^{LSL/+}$ tumours led to a reduction in MAPK signalling through pERK, is still unclear and requires further investigation, as this may identify a novel protein interaction which controls feedback loops affecting both signalling pathways.

Despite the favourable anti-tumour and pharmacodynamic effects characterised at 4 hours, NVP-BEZ235 led to a significant increase in PI3K signalling, reduced histological apoptosis and increased proliferation at 24 hours (Figure 6.1, 6.2, 6.3). Surprisingly, cleaved caspase 3 was still found to be significantly increased at 24 hours contradicting previous apoptosis scoring, but possibly highlighting an on-going shift in the delicate balance between cell death and survival in response to treatment. The increase in PI3K signalling observed here, may be attributable to feedback loops activated to increase signalling, and may be characteristic of a re-balancing mechanism to restore the initially reduced PI3K signalling.

Subsequently, a twice-daily administration regimen was selected for the long term treatment experiment to ensure inhibition of signalling. For this, mice were randomised to receive either 0.5% Methyl cellulose (vehicle treatment) or 35mg/kg NVP-BEZ235 twice-daily by oral gavage, from 22 days post induction until a survival end point. Kaplan-Meier survival analysis revealed administration of NVP-BEZ235 increased survival from 40 days to 104 days post induction, more than doubling the lifespan of $Apc^{f/+}$ $Pten^{f/f}$ $Kras^{LSL/+}$ mice (Figure 6.5). Analysis of tumour burden at death indicated that the NVP-BEZ235 treated cohort had comparable tumour numbers to the start cohort and vehicle treated mice, as well as a similar tumour severity profile, indicating tumour growth stasis with increased survival (Figure 6.19). Interestingly, reduced treatment of NVP-BEZ235 to a once-daily regimen as a control arm for combination treatment (with MEK162) had no beneficial effect on survival of mice (Figure 6.17). Additionally, tumour burden analysis in this cohort indicated that treatment augmented tumour progression as mice had significantly fewer benign lesions and more invasive adenocarcinomas characterised by sub-mucosal invasion (Figure 6.19). Although these observations corroborate findings from chapter 5 of dose-dependent effects of NVP-BEZ235, $Apc^{f/+}$ $Pten^{f/f}$ $Kras^{LSL/+}$ mice were found to be more sensitive to the dose of NVP-BEZ235 than $Apc^{f/+}$ $Kras^{LSL/+}$ mice. I postulate that these later observations may be attributable to the increased PI3K/mTOR signalling observed at 24 hours following NVP-BEZ235, causing non-

response to treatment and promoting progression of tumourigenesis. Studies by Kinross et al. corroborated the dose dependent effects of PI3K/mTOR pathway inhibitors as low dose PF-04691502 (Pfizer) also mitigated the survival benefit shown by the higher dose in a Kras mutant and Pten deficient tumour setting (Kinross et al., 2011). Nevertheless, NVP-BEZ235 treatment significantly increased longevity of $Apc^{f/+} Pten^{f/f} Kras^{LSL/+}$ mice, highlighting this as an efficacious therapeutic strategy for this tumour sub-group.

Interestingly, a range of ulcerated lesions were observed in response to PI3K/mTOR inhibition. Although these were not correlated to a survival response, these lesions represent effective killing of tumour cells from drug treatment. Additionally, no correlation was observed with presence of these lesions and increased drug treatment (Figure 6.20). Such lesions are thought to be precursors from which an epithelial layer could regenerate or alternatively, a superficial lesion would persist. Additionally, it is not known whether the immune cells present in the larger lesions were recruited during treatment to kill tumour cells or whether immune cells are present to aid the healing process. Nevertheless, the presence of these lesions shows effective and quick killing of tumour cells following treatment and the observation that these lesions are only present in the cohorts treated with NVP-BEZ235 (including combination cohorts) indicates this as the main treatment inducing these lesions.

6.3.2 MEK inhibition induces favourable anti-tumour and pharmacodynamic effects however does not increase survival of $Apc^{f/+} Pten^{f/f} Kras^{LSL/+}$ mice

Given the concurrent activation of oncogenic Kras in this Pten deficient tumour setting, the effects of MEK inhibition were next evaluated in an acute exposure setting and in a long term therapeutic intervention setting. Previously, mutations activating PI3K signalling have proven to reduce sensitivity of Kras mutant tumours to MEK inhibition. This was evidenced in a number of tumour models including xenograft models of colorectal cancer (Wee et al., 2009) and a GEM model of lung cancer (Chen et al., 2012b). To further evaluate this in a CRC setting, I employed the MEK inhibitor MEK162 for use in our autochthonous mouse model of intestinal cancer mutant for Apc, Pten and Kras. Acutely, MEK162 led to prolonged inhibition of MAPK signalling through pERK (Figure 6.8). As described previously, this has implications for cancer cell survival due to the involvement of MAPK/RAS/ERK signalling in promoting cell survival and inhibition of apoptosis (Johnson and Lapadat, 2002), and may be attributable to the increase in cleaved caspase 3 staining observed 4 hours post exposure to MEK162 (Figure 6.7). Interestingly, at this 4 hour time point, substantial inhibition of PI3K signalling was also observed, as evidenced by significantly reduced levels of pAKT at Ser473 and Thr308, and

pS6RP as well as a trend towards reduced p4EBP1 levels (Figure 6.8). The cross-talk of signalling observed here may be due to interactions between MEK and TSC2 (Ma et al., 2007) which, together with TSC1, act to modulate mTORC1 signalling, directly upstream pS6RP and p4EBP1. Despite this, the reduction of pAKT at Ser473 mediated by mTORC2 and at Thr308 mediated by PDK1 is not accounted for. Further investigations of these effects may uncover novel feedback mechanisms.

Despite the surprising inhibition of PI3K signalling in $Apc^{f/+}$ $Pten^{f/f}$ $Kras^{LSL/+}$ tumours immediately following MEK162, probing of pathway effectors in tumour samples 24 hours post MEK162 revealed an increase in PI3K/mTORC1 signalling evidenced through increased pS6RP and p4EBP1 (Figure 6.8). This could be attributable to the increase in cellular proliferation as identified through increased BrdU scoring in tumours, however the mechanism for this is yet to be defined (Figure 6.7). The apparent cross-talk between MAPK and PI3K pathways observed here are likely to result from negative feedback loops, however it remains to be established whether these are downstream of pERK through RSK mediated regulation of TSC2 (Roux et al., 2007, O'Reilly et al., 2006), due to the promiscuous nature of Kras (Kodaki et al., 1994) or downstream of mTOR which can lead to activation of PI3K signalling through regulation of receptor tyrosine kinases, including IGF-1 (O'Reilly et al., 2006).

Nevertheless, MEK inhibition was further investigated in this tumour model in a long term therapeutic setting. Given the favourable immediate effects of MEK162, it was hypothesised that treatment may provide some benefit for $Apc^{f/+}$ $Pten^{f/f}$ $Kras^{LSL/+}$ mice, however MEK162 administered at 30mg/kg twice-daily had no effect on survival of mice (Figure 6.10). Kaplan Meier survival analysis showed mice to have a median survival of 36 days compared to 40 days post induction for vehicle treated mice. Tumour burden analysis of $Apc^{f/+}$ $Pten^{f/f}$ $Kras^{LSL/+}$ mice at death revealed that mice on MEK162 had the same number of lesions at death in comparison to the start and vehicle treated cohorts however, mice had a higher proportion of invasive lesions, as characterised by invasion into the sub-mucosal layer (Figure 6.19). Similarly to the observations for the once-daily NVP-BE235 treatment, I hypothesise that the tumour progression observed with MEK162 treatment is perhaps due to increased PI3K signalling detected 24 hours after a single dose of MEK162.

6.3.3 Combination therapy synergistically increases survival of $Apc^{f/+}$ $Pten^{f/f}$ $Kras^{LSL/+}$ mice

Given the therapeutic efficacy of PI3K/mTOR inhibition but the lack of influence from chronic MEK inhibition, even though favourable effects on PI3K signalling were initially noted, the efficacy of combination therapy was next investigated in this tumour context. The rationale for combination therapy here stems from observation that mutations activating PI3K signalling tend to co-exist with Kras mutations and predict non-response to MEK inhibition (Balmanno et al., 2009, Chen et al., 2012b, Dry et al., 2010), as described previously (section 4.3.2). A number of studies have previously characterised the benefits of this in multiple *in vivo* tumour models. Kinross et al showed increased efficacy of dual PI3K/mTOR and MEK inhibition in the $Kras^{G12D}$ $Pten$ deleted mouse model of ovarian cancer, Engelman et al evidenced the combination therapy in the $Kras^{G12D}$ and PIK3CA H1047R lung cancer model whilst Miller et al. showed efficacy in the TPO- $Kras^{G12D}$ $Pten$ deleted thyroid tumour model (Kinross et al., 2011, Engelman et al., 2008, Miller et al., 2009).

In this study, I first evaluated the short term anti-tumour and pharmacodynamic effects of the three differing combination strategies to identify whether compound mutant tumours were sensitive to the schedule of inhibitor administration similarly to $Apc^{f/+}$ $Pten^{f/f}$ tumours, or not so, similarly to $Apc^{f/+}$ $Kras^{LSL/+}$ tumours. Western blot analysis for effectors of MAPK and PI3K signalling revealed no stark differences between the three schedules, similar to $Apc^{f/+}$ $Kras^{LSL/+}$ tumours. Here, all three combination strategies led to a reduction in levels of pERK and pS6RP indicating inhibition of MAPK and PI3K/mTOR signalling (Figure 6.13). Additionally, combo 1 led to moderate inhibition of pAKT308, combo 3 led to inhibition of pAKT473 and both combo 2 and 3 led to inhibition of p4EBP1 (Figure 6.13). Also similarly to $Apc^{f/+}$ $Kras^{LSL/+}$ tumours, the ability of NVP-BE2235 to effectively reduce levels of pAKT was reduced in the combination treatment however, unlike $Apc^{f/+}$ $Kras^{LSL/+}$ tumours, these effects cannot be attributed to an additive effect (Figure 6.13). In this case, single agent NVP-BE2235 led to complete inhibition of PI3K/mTOR signalling, and single agent MEK162 reduced MAPK signalling and also led to inhibition of PI3K signalling. Previous studies investigating combination therapy have reported complete loss of signalling at pAKT, pS6RP and pERK (Kinross et al., 2011) however, this may be due to differences in the agents used, doses or the regimen adopted for treatment. Nevertheless, all three combination strategies increased apoptosis, as detected through scoring of histological apoptosis and cleaved caspase 3 (Figure 6.11. 6.12). Therefore, to remain consistent between the three models assessed for combination therapy, combination

strategy 2 which involved administration of NVP-BEZ235 prior to MEK162, was employed for all further combinatorial experiments.

Subsequently, combo 2 was investigated at a 24 hour time point post administration to further assess the anti-tumour or pharmacodynamic effects. Although a reduction in proliferation and increase in apoptosis was observed (Figure 6.14), PI3K signalling was found to be predominantly increased through pAKT at Ser473 and Thr308 as well as p4EBP1 (Figure 6.15). Despite this, levels of pERK were found to be reduced potentially indicating synergy as previously single agent MEK162 moderately reduced pERK and single agent NVP-BEZ235 had no effect on MAPK signalling 24 hours post exposure (Figure 6.8).

Despite the moderately favourable pharmacodynamic effects, the selected combination strategy was next investigated in a therapeutic setting. As with $Apc^{f/+} Kras^{LSL/+}$ mice, in the first instance combination therapy administered to $Apc^{f/+} Pten^{f/f} Kras^{LSL/+}$ mice from 22 days post induction involved twice-daily NVP-BEZ235 plus once-daily MEK162, 1 hour after the initial NVP-BEZ235 dose (combo R1), as tolerability of this regimen in this tumour setting was not known. Shortly after the experiment began, toxic effects as illustrated by substantial weight loss was apparent in $Apc^{f/+} Pten^{f/f} Kras^{LSL/+}$ mice and led to 6/11 mice being culled due to weight loss. Surprisingly, 5/11 mice showed some advantage as observed by Kaplan-Meier survival analysis on Figure 6.17. As discussed previously in section 5.3.3, the reasons as to why this combination strategy was tolerated in $Apc^{f/+} Pten^{f/f}$ mice and not in $Apc^{f/+} Pten^{f/f} Kras^{LSL/+}$ or $Apc^{f/+} Kras^{LSL/+}$ mice is currently unclear. The observation that both $Apc^{f/+} Kras^{LSL/+}$ and $Apc^{f/+} Pten^{f/f} Kras^{LSL/+}$ models are driven by the VillinCreER^T transgene and the $Apc^{f/+} Pten^{f/f}$ model is driven by the AhCreER^T suggests that the differences in tolerability may be due to the differences in experimental systems within these cohorts. When induced, the VillinCreER^T transgene, leads to activation of genetic modifications in all intestinal cells. A recent study in the Clarke lab investigating the effects of $Apc^{f/+} Pten^{f/f} Kras^{LSL/+}$ alterations on normal intestinal homeostasis found these mutations result in an increased number of cells per half villus and a significant reduction in the number of enteroendocrine and paneth cells in comparison to controls, similar to the effects of $Apc^{f/+} Kras^{LSL/+}$ within the intestinal epithelium (Davies EJ, unpublished). The lack of these absorptive differentiated cells may be the cause of reduced nutrient intake in the intestines, which subsequently leads to weight loss and death of mice, when challenged by the combination therapy however, these observations need further investigation. Despite this, no gross alterations in the histological architecture of the small or large intestines were observed, similar to the $Apc^{f/+} Kras^{LSL/+}$ mice, indicating that either the

effect on normal intestinal homeostasis is minimal or that the toxic effects may be due to alternative factors as described previously (section 5.3.3).

Due to the toxicity issues described above, the further reduced combination dose as with $Apc^{f/+}$ $Kras^{LSL/+}$ mice was next investigated. This involved once-daily administration of 35mg/kg NVP-BEZ235 plus 30mg/kg MEK162 once-daily, an hour following the NVP-BEZ235 dose (combo R2). Interestingly, this was found to be well tolerated in $Apc^{f/+}$ $Pten^{f/f}$ $Kras^{LSL/+}$ mice, as shown in Figure 6.16, and led to a synergistic increase in survival from 40 days post induction to 125 days post induction, when administered from 22 days post induction (Figure 6.18). These effects were found to be synergistic as although single agent NVP-BEZ235 displayed efficacy when administered twice-daily, the control for the combination therapy which involved once-daily administration of NVP-BEZ235 had no beneficial effect on survival. The synergistic effects observed here are surprising given the lack of favourable pharmacodynamics from short term experiments but perhaps investigation of the combination at further short time points may provide some insight into the synergistic mechanisms. Surprisingly, tumour burden analysis revealed that although the number of lesions in $Apc^{f/+}$ $Pten^{f/f}$ $Kras^{LSL/+}$ mice on combo R2 was unaltered in comparison to the start and vehicle cohorts, tumours were significantly more invasive, as characterised by submucosal invasion (Figure 6.19). These later findings suggest tumour progression and corroborate previous findings where increased PI3K signalling observed at short time points, led to tumour progression after chronic treatment. The exception here is that mice had increased median survival and therefore these observations may indicate resistant tumour growth. Together, the investigations in this chapter are the first to show synergistic effects of PI3K/mTOR and MEK inhibition in an autochthonous mouse model of intestinal cancer driven by concurrent loss of Pten and activation of Kras.

6.4 Summary

In summary, the work described in this chapter indicate combined targeting of PI3K/mTOR signalling through NVP-BEZ235 and MEK inhibition through MEK162 as a beneficial therapeutic strategy for $Apc^{f/+}$ $Pten^{f/f}$ $Kras^{LSL/+}$ mice. Results also indicate dose-dependent effects of NVP-BEZ235 however, $Apc^{f/+}$ $Pten^{f/f}$ $Kras^{LSL/+}$ appeared more sensitive to the dose, possibly due to activation of negative feedback signalling activated by mutant Kras in this setting. Additionally, work described in this chapter corroborates previous findings that concurrent mutations in the PI3K signalling cascade predict non-response of the otherwise sensitive Kras mutant tumours, to MEK inhibition.

6.5 Further work

6.5.1 Further investigation of feedback mechanisms in *Apc^{f/+} Pten^{f/f} Kras^{LSL/+}* tumours

Analysis of the immediate pharmacodynamic effects following PI3K/mTOR or MEK inhibition in *Apc^{f/+} Pten^{f/f} Kras^{LSL/+}* tumours uncovered a number of puzzling effects on parallel signalling cascades. Firstly, although PI3K/mTOR inhibition led to complete reduction of pathway effectors, this also resulted in inhibition of MAPK signalling through pERK. Subsequently, PI3K/mTOR signalling was found to be increased at 24 hours following the initial reduction in signalling at 4 hours. Furthermore, acute MEK inhibition reduced PI3K and mTOR signalling components but increased expression of these at the 24 hour time point. The observations summarised above of collateral signalling effects may be associated with convergence of pathways at mTOR. Further probing of intracellular signalling components upstream mTOR including TSC2 and TSC1 as well as downstream of mTOR including S6K-IRS-1, may be insightful.

6.5.2 Further evaluation of synergy between NVP-BEZ235 and MEK162 in *Apc^{f/+} Pten^{f/f} Kras^{LSL/+}* mice

Investigation of the three combination strategies in *Apc^{f/+} Pten^{f/f} Kras^{LSL/+}* tumours revealed that no stark differences between the three strategies. Nevertheless, combination strategy 2 was taken forward for further investigations. Here, although an increase in PI3K/mTOR signalling was observed at short time points, chronic dosing led to a synergistic increase in survival. Investigation at further time point for example at 1, 2, 3, 8 or 12 hours post exposure, may help dissect any potential synergistic effects which may have led to the observed effects. Furthermore, to formally identify the differences between the combination strategies, investigation of combination strategies 1 and 3 in the long term setting may also be insightful for evaluating synergy.

6.5.3 Mechanisms of resistance to chronic PI3K and combination therapy

Mutations activating oncogenic Kras and those leading to aberrant activation of PI3K signalling co-exist in a third of all human CRCs. The work described in this chapter highlights that perhaps a dual PI3K/mTOR inhibitor in combination with a MEK inhibitor could be beneficial for Kras mutant and PI3K activated tumours. Despite this, resistance to treatments is frequently observed and therefore characterisation of any mechanisms used by tumours to escape treatment may provide insightful information. For this, immunohistochemistry for effectors of both signalling pathways together with scoring of proliferation and apoptosis

could be used to determine whether tumours were still responding to treatment or not when harvested at death. Additionally, as described in 5.5.3, these could then be correlated to tumour severity to identify whether tumour progression is associated with non-response of resistance tumour growth.

7 *Characterisation and delivery of anti-cancer ‘ProTide’ agents into a mouse model of colorectal cancer*

7.1 *Introduction*

Whilst work described in chapters 3-6 evaluated a number of established small molecule inhibitors which specifically targeted pathways known to be deregulated in genetically engineered mouse models, this thesis also aimed to assess novel therapeutic compounds designed to improve the efficacy of existing compounds.

The chemotherapeutic agent 5-fluorouracil (5-FU) remains the cornerstone of therapeutic intervention for CRC despite the promise of targeted therapy. 5-FU is an anti-metabolite drug (Rutman et al., 1954) which functions by inhibiting essential biosynthesis and by incorporating into molecules such as DNA or RNA and inhibiting their normal function. The cytotoxic effects of 5-FU are therefore attributed to misincorporation into DNA and RNA and also, its ability to inhibit the nucleotide synthetic enzyme thymidylate synthase (TS) (Longley et al., 2003). Despite the continued use of 5-FU based chemotherapy, response rates in the first-line setting for advanced CRCs are only 10-15% (Johnston and Kaye, 2001), highlighting an urgent need for new and effective therapeutic strategies.

5-FU is a pyrimidine nucleoside derivative and belongs to the family of cytotoxic nucleoside analogues, which includes cladribine and fludarabine (used against low grade blood malignancies) as well as gemcitabine (used against pancreatic and bladder cancers), all of which require metabolic activation in their target cell to the bio-active tri-phosphate form (Galmarini et al., 2001)(Figure 7.1). This requirement can often limit their therapeutic potential due to a number of factors. These include poor metabolism to activate the mono-phosphate form, rapid deactivation of the bio-active molecule, reduced active transport which is required to allow entry into the cell in the initial stages, and most often, development of resistance, either through kinases, polymerases or transporters (Mehellou et al., 2009).

In an effort to address these issues, particularly to improve the delivery of such agents, prodrug technologies which aim to deliver the bio-active nucleoside monophosphates into cells have been utilised, to improve the therapeutic potential of anti-cancer nucleosides. This approach involves using the mono-phosphate form of the nucleoside and masking the charge of the phosphate form by addition of phosphoramidate groups, in order to allow passive cell

membrane penetration. Subsequently upon entering the cell, the masking phosphoramidate groups are enzymatically cleaved to release the bio-active phosphorylated nucleoside molecule (Mehellou et al., 2009). This phosphoramidate method (also known as the ProTide method) developed by McGuigan et al. has successfully been applied to numerous antiviral nucleosides (Bourdin et al., 2013, Madela and McGuigan, 2012) and more recently has been applied to the anti-cancer agent gemcitabine to create NUC1031 which is currently undergoing phase 1/2 clinical trials in humans with pancreatic cancer (Saif et al., 2012, Jordheim et al., 2013).

The main aim of this study was to utilise the ProTide approach to allow passive entry of compounds which aim to target the cause of 5-FU resistance³. When metabolised, 5-FU is converted into fluorodeoxyuridine monophosphate (FdUMP), fluorodeoxyuridine triphosphate (FdUTP) and fluorouridine triphosphate (FUTP) (Figure 7.1), all of which disrupt RNA synthesis and the inhibitory actions of TS (Longley et al., 2003). The normal physiological function of TS is to catalyse the reduction of deoxyuridine monophosphate (dUMP) to deoxythymidine monophosphate (dTMP), providing a *de novo* source of thymidylate (Roberts et al., 2006). Subsequently, FdUMP forms a tertiary complex with the enzyme TS, and CH₂THF (5,10-methylenetetrahydrofolate, a methyl donor) which blocks binding of dUMP, inhibiting dTMP synthesis (Santi et al., 1974, Sommer and Santi, 1974). Despite this, overexpression of TS is widely regarded as the major molecular mechanism of resistance to 5-FU in humans; high levels of TS prior to treatment have been shown to predict poor response (Johnston et al., 1992, Priest et al., 1980) but also, increased RNA expression and protein expression through an auto-regulatory feedback mechanism, has been previously shown to mediate 5-FU resistance (Chu et al., 1993b, Chu et al., 1993a). Given these findings, we sought to exploit the ProTide approach to target TS overexpressing cancer cells with the anti-viral agent Brivudin (BDVU) commonly used against Herpes Simplex Virus (HSV) and Varicella Zoster Virus (VZV) (Figure 7.2).

³ Some data presented in this chapter was collected and analysed together with Dr Trevor Hay

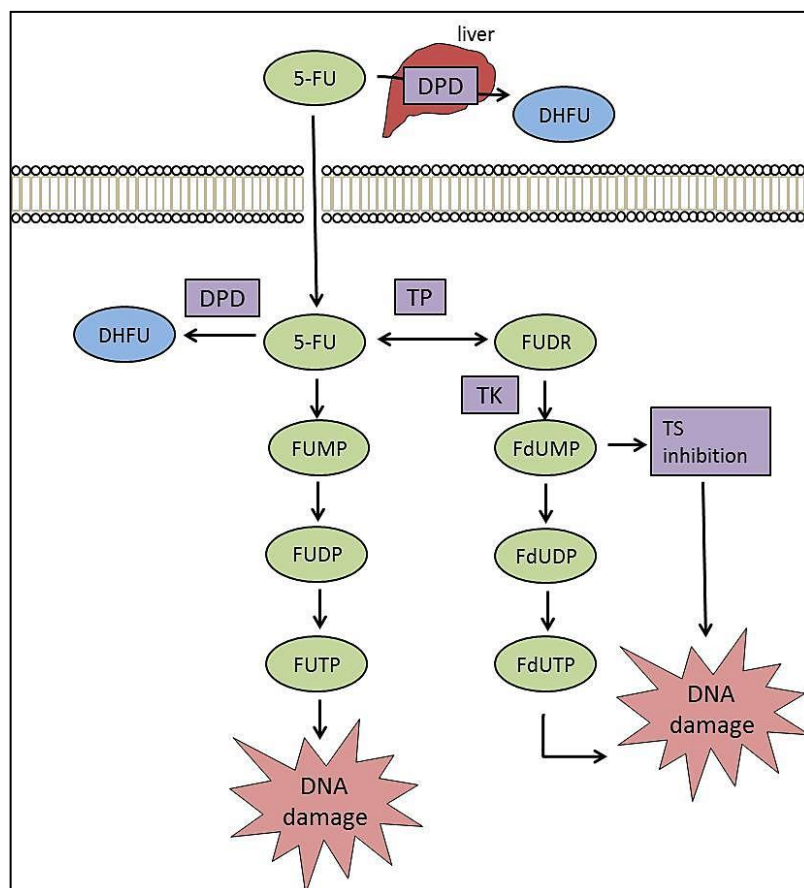


Figure 7.1 Schematic summarising metabolism of 5-FU

5-FU is converted to three active metabolites: fluorodeoxyuridine monophosphate (FdUMP) through thymidine phosphorylase (TP) and thymidine kinase (TK), followed by subsequent phosphorylations to yield fluorodeoxyuridine triphosphate (FdUTP) and fluorouridine triphosphate (FUTP) through sequential phosphorylations. Dihydropyrimidine dehydrogenase (DPD) mediated conversion of 5-FU to dihydrofluorouracil (DHFU) is the rate limiting step of 5-FU catabolism in normal and tumour cells. Up to 80% of administered 5-FU is broken down by DPD in the liver

The metabolites of BVdU (BVdUMP) have been shown to act as an alternative competitive substrate for TS *in vitro* (Lackey et al., 2001). Additionally, previous work has shown BVdUMP is converted into cytotoxic products by intracellular TS without causing activation of the enzyme (Lackey et al., 2001). However, as the charge of BVdUMP prevents entry into the cell, the molecule was converted into a ProTide form, to allow better entry of the bio-active form of the compound. Recently, the phosphoramidate technology was applied to BVdUMP to yield

NB1011 (Thymectacin, New Biotics). Thymectacin has previously been shown to result in cell cytotoxicity and accumulation of BVdUMP in TS overexpressing and hence 5-FU resistant, human colorectal cancer cells (H630-R10) and breast carcinoma cells (MCF7TDX) in comparison with normal counterpart cell lines (Lackey et al., 2001). Despite this, McGuigan et al found thymectacin to be less potent than the parent agent (BVDU) *in vitro* due to poor intracellular delivery of the BVDU monophosphate (McGuigan et al., 2002).

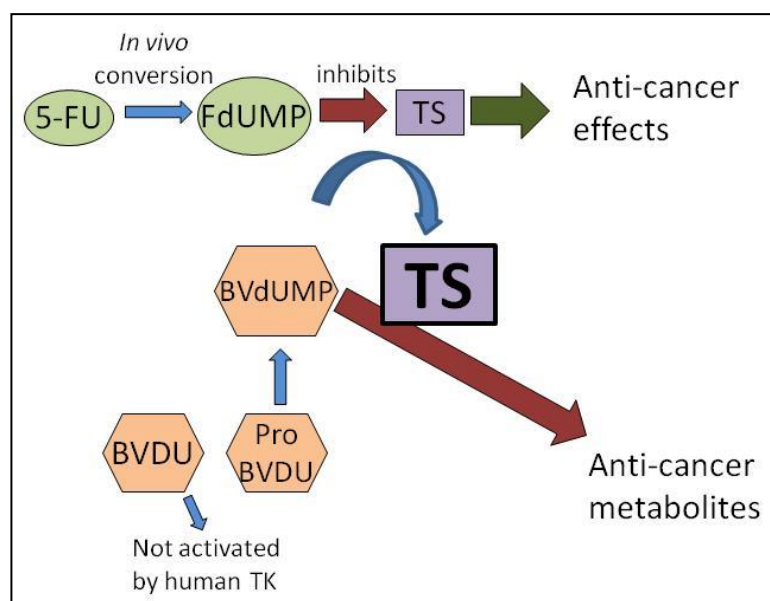


Figure 7.2 Schematic summarising the concept of using ProTide BVDU to target upregulated TS in 5-FU resistant cells.

The 5-FU metabolite FdUMP inhibits the enzyme TS which leads to anti-cancer effects due to the role of TS in cellular proliferation and DNA synthesis. However, cells become resistant to 5-FU simply by upregulating expression of TS. Therefore, the hypothesis was to utilise BVDU, which is not activated by the human enzyme TK, and using the ProTide technology to allow better entry of the BVDU metabolite BVdUMP into the cell. Subsequently, BVdUMP is converted into anti-cancer metabolites by the excess TS, and elicits anti-tumour effects.

In light of these findings, a small family of analogues of thymectacin with modifications in the aryl, ester, aromatic and amino acid regions were prepared (by Dr Stephanie Rats and Dr Sahar Khandil, Professor Chris McGuigans research group, Cardiff University) and evaluated in this chapter. These were initially evaluated *in vitro* against MCF7 (breast cancer) and counterpart MCF7TDX (TS overexpressing) cell lines to determine half maximal inhibitory concentrations (IC50s) in comparison to the parent compound BVDU and thymectacin. Potent ProTide

compounds were then selected for further evaluation by a colony forming assay to establish their effects on proliferation. These compounds were also assessed *in vivo* in the AhCreER driven $Apc^{f/+} Pten^{f/f}$ ($Apc^{f/+} Pten^{f/f}$) mouse model of invasive intestinal adenocarcinoma, in a short term dosing experiment to assess the anti-tumour effects of the selected compounds. Given the reduced efficacy of 5-FU in the advanced tumour setting, the $Apc^{f/+} Pten^{f/f}$ tumour model was chosen to assess these novel agents due to the invasive disease phenotype but also the relatively short latency of tumour development. From these studies, two lead ProTide compounds were then selected for evaluation in a therapeutic setting. For this, the compounds were administered daily to a cohort of $Apc^{f/+} Pten^{f/f}$ mice, from a chosen start point to a survival end point, to determine the effect of continuous treatment on survival. Furthermore, as the compounds evaluated are hypothesised to be more active in a 5-FU resistant and hence TS upregulated tumour setting, I next sought to develop mice bearing TS upregulated tumours, from continuous 5-FU treatment. Although 5-FU treatment in the clinic varies according to several factors, including age of patient and stage of disease, it is regularly administered as a bolus regimen which often involves a high dose for a short period of time - for example for 5 days, every 4 weeks. To mimic the clinical setting, a dose of 50mg/kg once weekly from 60 days post induction was initially selected. Three additional regimens of 5-FU treatment were also undertaken which involved administration of 50mg/kg once weekly from 50 days post induction, 25mg/kg tri-weekly from 60 days post induction and 100mg/kg once weekly from 60 days post induction, to further investigate 5-FU treatment and subsequent resistance.

7.2 Results

7.2.1 Cell viability assay of thymectacin phosphoramidates in MCF7 and MCF7TDX cell lines

To confirm upregulation of TS in MCF7TDX cells in comparison with parent MCF7 cells, cell extracts were prepared, subjected to RNA extraction and corresponding cDNA synthesis (methods section 2.9.4, 2.10). Levels of TS were quantified by qRTPCR and revealed a significant 90 fold increase in levels of TS (ΔCT values: MCF7 cells = 16.05 ± 0.41 , MCF7TDX cells = 9.56 ± 0.03 , p value = 0.0404, n=3, One-tailed Mann Whitney U test) (Figure 7.3).

Having confirmed increased levels of TS mRNA in MCF7TDX cells compared to MCF7 cells, the effects of various thymectacin ProTides on cellular viability was next evaluated using the cell titre blue assay 72 hours following treatment (described in methods section 2.9.5). As outlined

in Table 7.1, thymectacin showed improved activity in comparison with the parent compound BVDU in both MCF7 and MCF7TDX cells however, thymectacin failed to show increased potency in the TS upregulated MCF7TDX cells in comparison with controls (IC₅₀ values: BVDU >250 µM in MCF7 and MCF7TDX cells, thymectacin = 101µM in MCF7 cells and 113.5 µM in MCF7TDX cells). These later findings are in contrast to those reported by Lackey et al whereby thymectacin was found to be 69 fold more active in MCF7TDX cells in comparison with MCF7 cells (IC₅₀ values: MCF7 = 207µM vs MCF7TDX = 3µM) (Lackey et al., 2001). Thymectacin ProTides assessed by the cell titre blue cell viability assay showed variable potency in comparison with thymectacin in MCF7 cells. Of the 15 ProTide compounds evaluated, 5 showed poor activity *in vitro* with IC₅₀ values of >250µM (CPF476, CPF481, CPF486, CPF489 and CPF494) (Table 7.1), therefore showing less potency than thymectacin and similar potency to the BVDU in MCF7 cells. Although 3 of these compounds showed increased potency in MCF7TDX cells (IC₅₀ values: CPF476 > 250µM in MCF7 cells vs 16.6µM in MCF7TDX cells; CPF481 > 250µM in MCF7 cells vs 137µM in MCF7TDX cells; and CPF486 > 250µM in MCF7 cells vs 112.5 µM in MCF7TDX cells) (Table 7.1), more efficacious compounds were available. Additionally, compounds such as CPF474 and CPF485 were also eliminated from further evaluation due to only moderate *in vitro* activity (IC₅₀ values: CPF474 = 61.6µM vs 8.8µM in MCF7TDX cells; CPF485 = 105µM vs 43.7µM). Compounds selected for further evaluation not only showed potency in MCF cells- IC₅₀ values of <20µM, but also showed increased potency in MCF7TDX cells- IC₅₀ values of <10µM. These include CPF472, CPF473, CPF552, CPF555 and CPF3172 (Table 7.1).

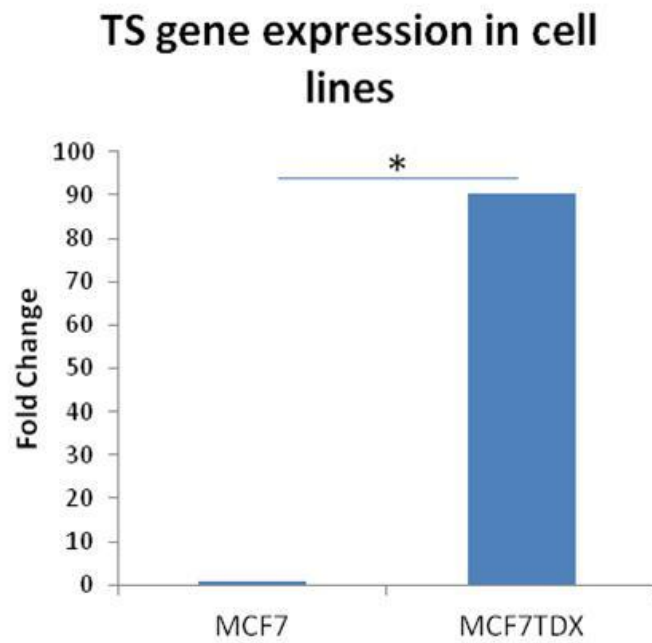


Figure 7.3 Increased expression of TS in MCF7TDX cancer cells

Quantitative-RTPCR analysis of TS in MCF7 and MCF7TDX cells revealed a significant 90 fold increase in TS expression in MCF7TDX cells (Δ CT MCF7 cells = 16.05 ± 0.41 , MCF7TDX cells = 9.56 ± 0.03 , p value = 0.0404, Mann Whitney U test).

<i>Compound</i>	<i>MCF7 IC50 (μM)</i>	<i>MCF7TDX IC50 (μM)</i>
<i>BVDU</i>	>250	>250
<i>Thymectacin</i>	101.3	113.5
<i>CPF472</i>	4.3	3.4
<i>CPF473</i>	6.1	2.7
<i>CPF474</i>	61.6	8.8
<i>CPF476</i>	>250	16.6
<i>CPF477</i>	5.5	4.8
<i>CPF481</i>	>250	137.0
<i>CP7485</i>	105.4	43.7
<i>CPF486</i>	>250	112.5
<i>CPF487</i>	20.2	4.7
<i>CPF489</i>	>250	>250
<i>CPF490</i>	4.1	5.6
<i>CPF494</i>	>250	>250
<i>CPF552</i>	14.44	5.33
<i>CPF555</i>	13.1	6.9
<i>CPF3172</i>	3.7	2.6

Table 7-1 IC50 values (μM) of ProTide compounds assessed by cell viability assay

IC50 values of various ProTide agents, BVDU and thymectacin assessed in MCF7 and MCF7TDX cells. Cells were exposed to agents for 72 hours and then assayed using the Cell titer blue reagent to assess cell viability. Values represent an average of 6 biological repeats.

7.2.2 Colony forming assay of selected thymectacin ProTides in MCF7 and MCF7TDX cell lines

In order to evaluate the clonogenic potential of the selected ProTide compounds i.e the proportion of cells able to extensively replicate following drug treatment, a colony forming assay was performed using both MCF7 and MCF7TDX cell lines (as described in methods section 2.9.6). As observed in Figure 7.4, all five compounds selected (CPF473, CPF473, CPF552, CPF555 and CPF3172) were more effective than thymectacin in inhibiting colony formation in both MCF7 and MCF7TDX cell lines. Interestingly, CPF473, CPF555 and CPF3172 displayed less potency than CPF472 and CPF552 (Figure 7.4). Here, all colonies were killed with 25 μ M, in comparison to 100 μ M with CPF473, CPF555 and CPF3172. Nevertheless, CPF473, CPF555 and CPF3172 displayed increased potency in MCF7TDX cells as more colonies were killed with the 50 μ M concentration, albeit this varied between the compounds (Figure 7.4). Here, more colonies were killed with CPF3172 administrations in comparison with CPF473 and CPF555 in MCF7TDX cells, and so this compound was regarded as a favourable candidate for further evaluation. CPF555 was eliminated from further evaluation as was found to be the least potent compound in MCF7TDX cells with regards to colony forming ability.

Although CPF472 and CPF552 displayed increased efficacy in inhibiting colony formation in comparison with thymectacin, CPF473, CPF555 and CPF3172, only CPF472 showed increased potency in the TS upregulated MCF7TDX cells and therefore progressed for further evaluation (Figure 7.4). All remaining four compounds and thymectacin were next evaluated *in vivo* to determine which, if any, resulted in favourable anti-tumour effects in intestinal tumours from short term exposure, as described in section 7.2.3.

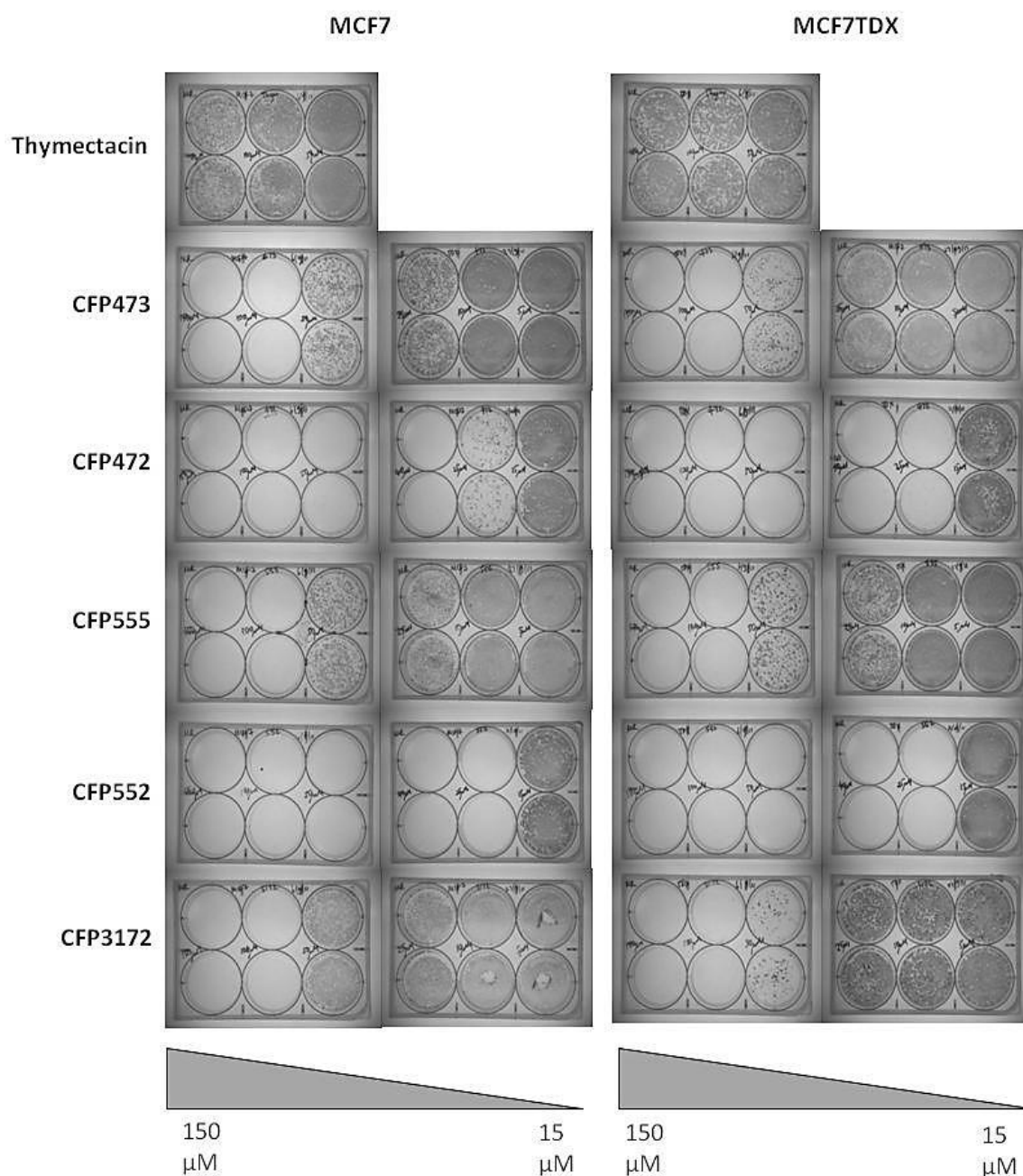


Figure 7.4 Colony forming assay comparing cell growth in MCF7 and MCF7TDX cells

A colony forming assay was conducted on 5 selected ProTide agents and thymectacin to evaluate clonogenic potential of agents in MCF7 and MCF7TDX cells. All compounds were shown to be more potent than thymectacin in both MCF7 and MCF7TDX cells. Interestingly, CFP472 and CFP3172 were shown to be more potent in TS overexpressing MCF7TDX cell lines in comparison with MCF7 cells

7.2.3 *In vivo anti-tumour effects of thymectacin and selected ProTide agents*

The $Apc^{f/+}$ $Pten^{f/f}$ tumour model of invasive intestinal adenocarcinoma was utilised to determine the anti-tumour potential of selected ProTide agents and thymectacin in an invasive tumour setting. Here, 10 week old mice were induced and aged to 85 days post induction at which point mice were known to carry a tumour burden (it was previously established that tumours were present at 77 days post induction -chapter 4, median survival for $Apc^{f/+}$ $Pten^{f/f}$ mice is 100 days post induction). A cohort of 4 mice (per treatment) were administered with 50mg/kg of thymectacin, CPF472, CPF473, CPF552, CPF3172 or vehicle once daily by oral gavage for 4 consecutive days. Mice were culled 6 hours following the final dose and dissected as described previously (section 2.4).

Following exposure to selected ProTide compounds or vehicle, the anti-tumour effects on small intestinal tumours (SITs) were characterised by assessment of histological mitosis and apoptosis from H&E stained slides (Figure 7.5). Scoring of mitotic figures revealed a significant reduction in mitotic figures from CPF472 exposure only (vehicle = 0.48 ± 0.18 , CPF472 = 0.28 ± 0.21 p value = 0.05, $n \geq 10$ tumours, 4 mice, Mann Whitney U test) (Figure 7.5 A). Thymectacin, CPF473, CPF552 and CPF3172 had no significant effect on levels of mitosis (vehicle = 0.48 ± 0.18 ; thymectacin = 0.84 ± 0.49 , p value = 0.153; CPF473 = 0.32 ± 0.16 , p value = 0.298; CPF552 = 0.89 ± 0.61 , p value = 0.259; CPF3172 = 0.47 ± 0.17 , p value = 0.773, $n \geq 10$ tumours, 4 mice, Mann Whitney U test) (Figure 7.5 A). Scoring of histological apoptosis revealed thymectacin led to a significant reduction in levels of apoptosis whereas CPF473 and CPF552 had no effect on apoptosis (vehicle = 0.82 ± 0.24 , thymectacin = 0.42 ± 0.14 , p value = 0.032; CPF473 = 0.84 ± 0.34 , p value = 0.81; CPF552 = 0.93 ± 0.48 , p values = 0.668, $n \geq 10$ tumours, 4 mice, Mann Whitney U test) (Figure 7.5 B). CPF472 led to a trend towards increased apoptosis and CPF3172 resulted in a significant increase in apoptosis (vehicle = 0.82 ± 0.24 ; CPF472 = 1.26 ± 0.67 , p value = 0.119, CPF3172 = 1.53 ± 0.7 , p value = 0.0119; $n \geq 10$ tumours, 4 mice, Mann Whitney U test) (Figure 7.5 B), identifying these as perhaps more effective compounds *in vivo*.

To further characterise the anti-tumour effects of the selected ProTide compounds in comparison with thymectacin *in vivo*, IHC for BrdU and cleaved caspase 3 was performed and subsequently scored (Figure 7.6). This revealed thymectacin exposure resulted in significantly reduced BrdU positive cells in comparison with vehicle controls (vehicle = 33.7 ± 2.06 ; thymectacin = 23.1 ± 3.78 , p value = 0.0107, $n \geq 4$ tumours from at least 2 mice, Mann Whitney U test) (Figure 7.6 A), indicating a reduction in cells in the S phase of the cell cycle. No

significant effect was observed with CPF472, CPF473, CPF552 or CPF3172 exposure (vehicle = 33.7 ± 2.06 ; CPF472 = 27.2 ± 7.78 , p value = 0.391; CPF473 = 31.1 ± 4.15 , p value = 0.471; CPF552 = 31.5 ± 7.14 , p value = 0.55; CPF3172 = 38.5 ± 4.32 , p value = 0.051, $n \geq 10$ tumours, 4 mice, Mann Whitney U test) (Figure 7.6 A). Finally, scoring of cleaved caspase 3, to further characterise any pro-apoptotic effect from ProTide or thymectacin treatment in $Apc^{f/+}$ $Pten^{f/f}$ SITs, revealed that thymectacin exposure resulted in substantially reduced staining, corroborating histological apoptosis findings, whilst the ProTide agents had no significant effect on cleaved caspase 3 staining (vehicle = 5.7 ± 2.16 ; thymectacin = 0.65 ± 0.3 , p value = 0.0005; CPF472 = 7.07 ± 2.07 , p value = 0.203; CPF473 = 5.21 ± 1.77 , p value = 0.936; CPF552 = 5.09 ± 2.23 , p value = 0.531; CPF3172 = 7.03 ± 3.79 , p value = 0.629, $n \geq 10$ tumours, 4 mice, Mann Whitney U test) (Figure 7.6 B)

The anti-tumour effects characterised here, together with the results from the cell viability and colony forming assays performed on the selected ProTide compounds and thymectacin are summarised in table 7.2. These reveal CPF472 and CPF3172 were more effective compounds than CPF473 and CPF552 in comparison with thymectacin, and were therefore selected as lead compounds for further evaluation in a chronic treatment setting. As an additional control, thymectacin was also selected for chronic treatment to determine whether ProTide compounds were indeed more effective in a survival setting. CPF473 and CPF552 were eliminated from further characterisation as they failed to display any anti-proliferative or pro-apoptotic effects in tumours.

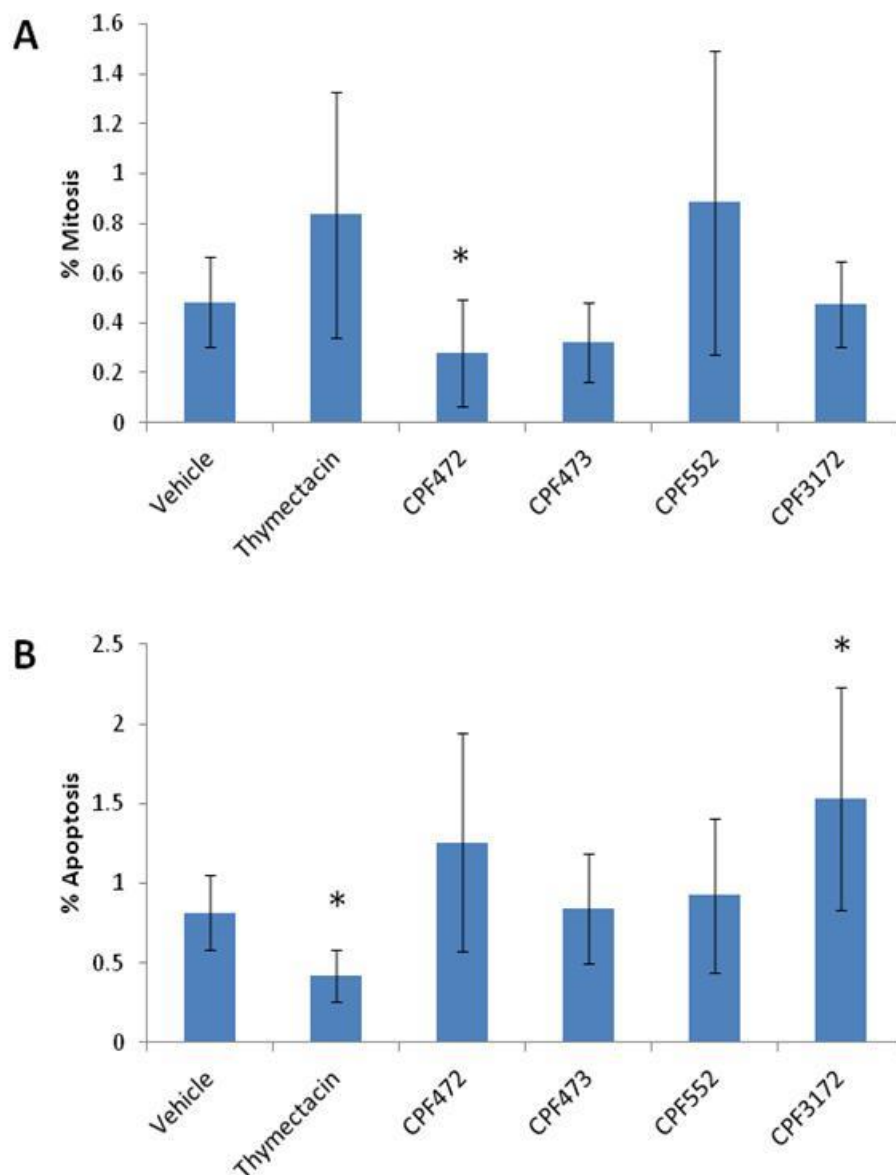


Figure 7.5 Assessment of anti-proliferative and pro-apoptotic effects in $Apc^{f/+} Pten^{f/f}$ tumours following short term treatment of selected ProTides and thymectacin.

$Apc^{f/+} Pten^{f/f}$ mice were administered with 50mg/kg of selected ProTide agents CPF472, CPF473, CPF555 or CPF3172 or thymectacin for 4 consecutive days. Following exposure, assessment of histological mitosis revealed only CPF472 resulted in a significant reduction in levels of mitosis in tumours. Thymectacin and CPF552 resulted in a trend towards increased levels whereas CPF473 and CPF3172 had no effect on levels of mitosis. Scoring of histological apoptosis revealed thymectacin resulted in a significant reduction in levels whereas CPF3972 significantly increased apoptosis in tumours following exposure. CPF472, CPF473 and CPF552 had no effect on apoptosis in $Apc^{f/+} Pten^{f/f}$ tumours. (p value ≤ 0.05 , $n \geq 10$ tumours, 4 mice, Mann Whitney U test). Error bars represent standard deviation.

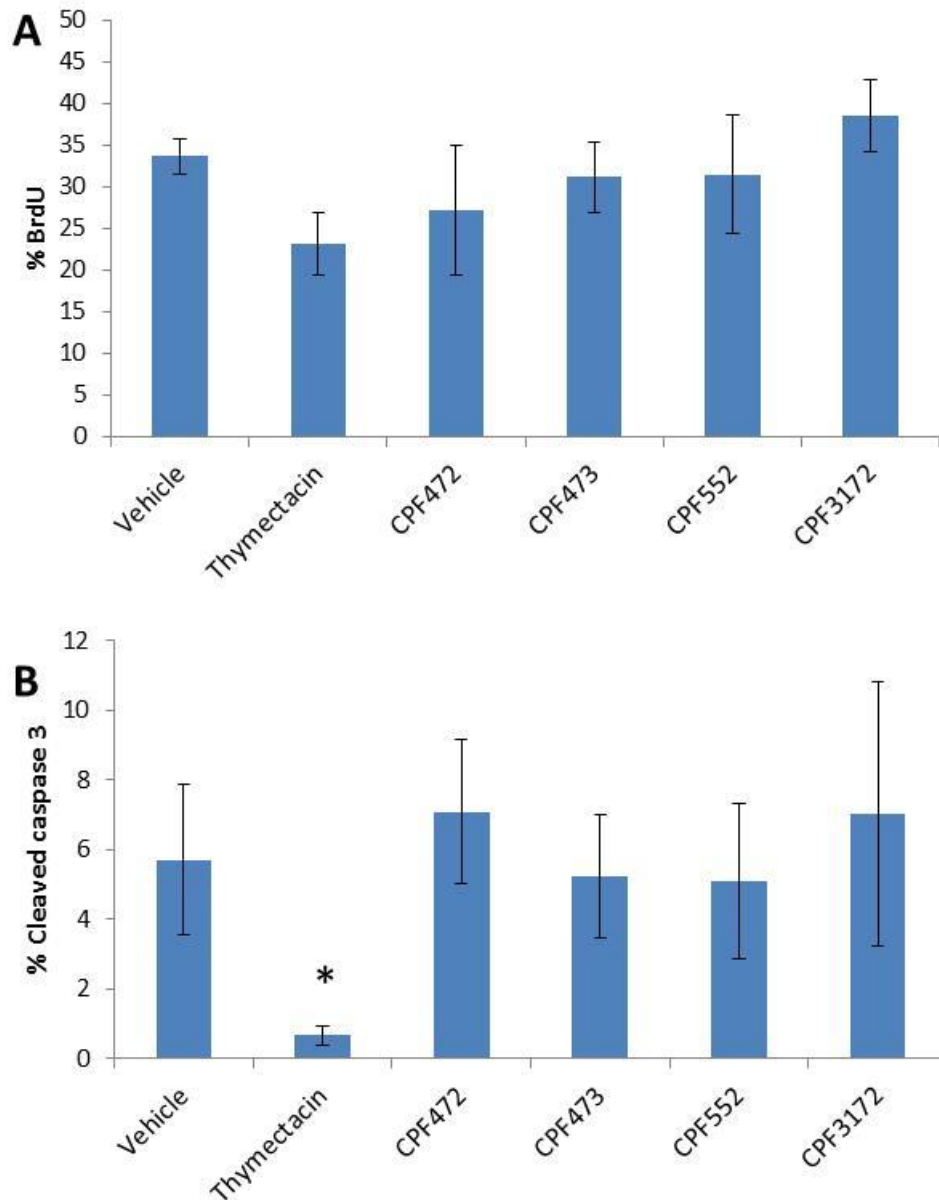


Figure 7.6 Further assessment of anti-proliferative and pro-apoptotic effects through BrdU and cleaved caspase 3 scoring in $Apc^{f/+}$ $Pten^{f/f}$ tumours following short term treatment of selected ProTides and thymectacin.

Scoring of BrdU (**A**) and cleaved caspase 3 (**B**) in $Apc^{f/+}$ $Pten^{f/f}$ mice exposed to 50mg/kg of selected ProTide agents CFP472, CFP473, CPF555 or CFP3172 or thymectacin for 4 consecutive days. Thymectacin treatment resulted in a significant decrease in BrdU scoring indicating an anti-proliferative effect, however also resulted in a significant reduction in cleaved caspase 3 scoring, signifying an anti-apoptotic effect. ProTides had no significant effect on BrdU scoring or cleaved caspase 3. p value ≤ 0.05 , $n \geq 4$ tumours, at least 2 mice, Mann Whitney U test). Error bars represent standard deviation





















	Thymectacin	CPF472	CPF473	CPF552	CPF3172
Cell viability assay (IC50 in MCF7→MCF7TDX cells, µM)	101.3→113.5	4.3→3.4	6.1→2.7	14.4→5.3	3.7→2.6
Colony forming assay (growth in MCF7→MCF7TDX cells, µM)	No difference at 150µM	Reduction from 25µM→15µM	Reduction at 50µM	No difference at 15µM	Reduction at 50µM
Histological mitosis					
Histological apoptosis					
BrdU scoring					
Cleaved caspase 3 scoring					

Table 7-2 Summary of short term in vitro and in vivo anti-tumour effects of selected

ProTides and thymectacin. Table shows the average IC50 values in MCF7 and MCF7TDX cells, differences observed in colony forming ability and short term *in vivo* effects of ProTides and thymectacin. Blue horizontal arrow indicates no difference, green arrow indicates anti-tumour effects and red arrow indicates pro-tumour effects.

7.2.4 Long term treatment of lead ProTide agents in the $Apc^{f/+}$ $Pten^{f/f}$ tumour model

To investigate the therapeutic potential of the selected ProTide agents CPF472 and CPF3172, a long term treatment experiment was conducted (similar to those in Chapter 4) to determine their effect on survival, in comparison to vehicle and thymectacin treatment. For this, a cohort of 15 mice per cohort, were induced and aged to 77 days post induction at which point daily treatment commenced. Mice were randomly selected to receive either 75mg/kg of CPF472, CPF3172, thymectacin or the equivalent vehicle volume once daily, until a survival end point (anaemia, bloating, $\geq 10\%$ loss of body weight).

Continuous treatment of CPF472, CPF3172 and thymectacin was found to be well tolerated in $Apc^{f/+}$ $Pten^{f/f}$ mice (according to body weight), however CPF472 and CPF3172 failed to significantly increase survival of mice (median survival of vehicle mice = 94, CPF472 = 107, p value = 0.61, CPF3172 = 112, p value = 0.203, $n \geq 15$, Log Rank method) (Figure 7.7). Surprisingly, daily thymectacin treatment significantly increased median survival of $Apc^{f/+}$ $Pten^{f/f}$ mice from 94 to 133 days post induction (p value = 0.029, $n \geq 15$, Log Rank method) (Figure 7.7).

These findings were surprising, given the lack of efficacy in *in vitro* experiments from thymectacin exposure and in comparison, the potency of CPF472 and CPF3172 in these settings. Despite this, it was postulated that CPF472 and CPF3172 may be more effective in the 5-FU resistant and hence TS upregulated setting. To model this, I next investigated the effects of chronic 5-FU treatment to determine whether this led to an increase in TS in $Apc^{f/+}$ $Pten^{f/f}$ tumours.

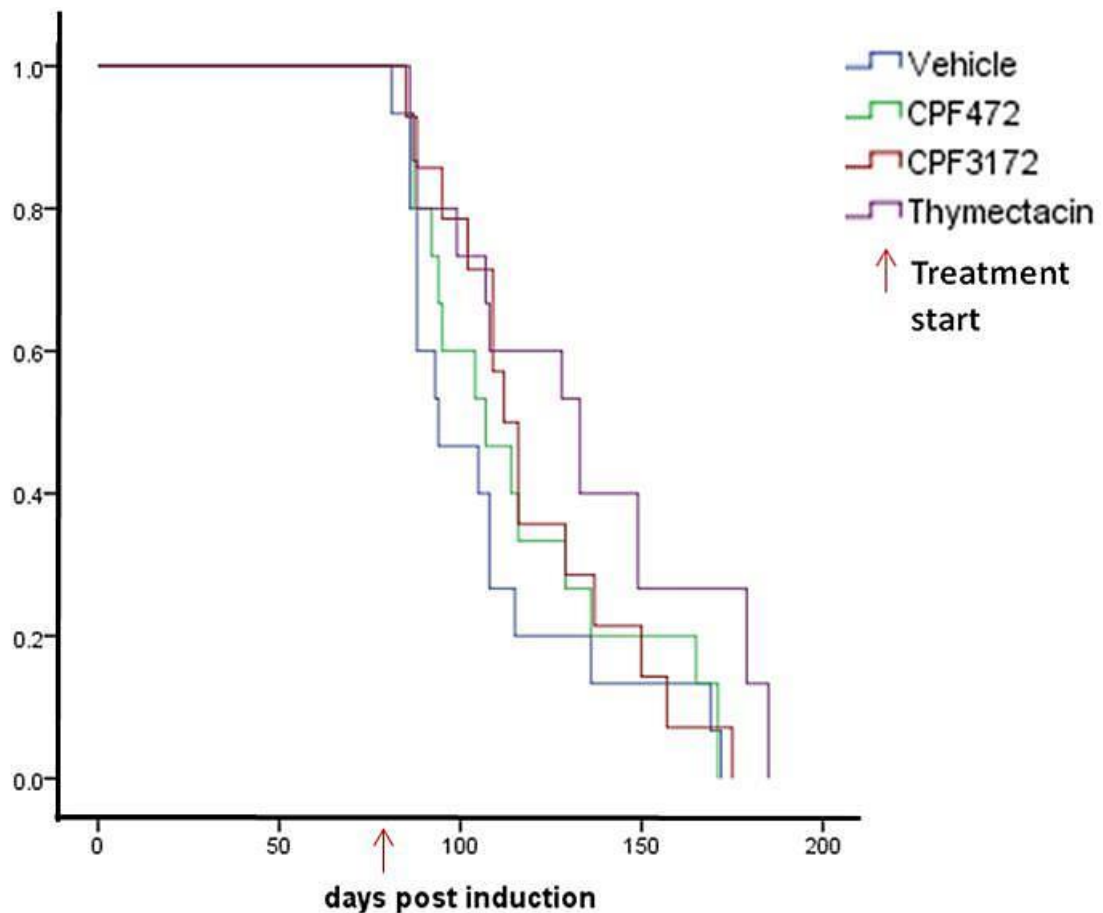


Figure 7.7 Kaplan Meier survival analysis of $Apc^{f/+} Pten^{f/f}$ mice on long term CPF472, CPF3172 or thymectacin treatment.

$Apc^{f/+} Pten^{f/f}$ mice were induced and aged to 77 days post induction, at which point mice were randomised to receive either vehicle control or 75mg/kg of CFP472, CFP3172 or thymectain once daily until a survival end point. Continuous ProTide treatment resulted in no significant benefit in median survival of $Apc^{f/+} Pten^{f/f}$ mice (median survival of 107 and 112 days post induction for CPF472 and CFP3172, respectively, p value ≥ 0.05 for both, $n \geq 10$ mice per cohort, Log Rank method) whereas daily thymectacin treatment significantly increased median survival of mice from 94 days to 133 days post induction (p value = 0.029, $n \geq 10$ mice per cohort, Log Rank method)

7.2.5 Investigation of chronic 5-FU treatment

Prior to 5-FU treatment, it was important to determine the basal levels of TS expression in tumours in comparison with normal small intestine tissue. For this, a cohort of 3 mice which presented with symptoms of tumour burden (paling feet, bloating, rectal bleeding) were culled, then normal small intestine and tumour tissue was dissected and snap frozen (as outlined methods section 2.4) for TS expression analysis. Following RNA and corresponding cDNA synthesis, qRT-PCR analysis revealed a 2-fold increase in $Apc^{f/+}$ $Pten^{f/f}$ tumours, in comparison with small intestinal tissue (Δ CT values: Small intestine normal (SIN) tissue = 9.48 ± 0.127 ; small intestine tumour (SIT) = 8.32 ± 0.131 , p value = 0.0404) (figure 7.8). This finding was not surprising, given the role of TS in DNA replication however, it was pertinent to determine this given that 5-FU has previously been shown to be ineffective in TS upregulated tumours.

To determine the effects of 5-FU treatment in $Apc^{f/+}$ $Pten^{f/f}$ mice, a chronic dosing strategy was employed firstly, to investigate the effects of treatment on increasing longevity of mice and secondly, to establish whether tumours established resistance to 5-FU by increasing expression of TS. Given that $Apc^{f/+}$ $Pten^{f/f}$ mice are often culled shortly after presenting with symptoms of disease, 5-FU treatment was commenced prior to the onset of disease symptoms to allow more time for tumours to develop resistance. The four strategies used for 5-FU treatment were as follows; 50mg/kg 5-FU weekly from 60 days post induction, 50mg/kg 5-FU weekly from 50 days post induction, 25mg/kg 5-FU tri-weekly from 57 days post induction and 100mg/kg 5-FU weekly from 60 days post induction, all administered by i.p injection, until a survival end point. Treatment regimens were found to be well tolerated by mice, except for the 100mg/kg 5-FU strategy which resulted in weight loss 24 hours following the dose administration. Subsequent Kaplan Meier survival analysis revealed this regimen had no significant effect on increasing longevity of mice (median survivals: vehicle = 94 days, 100mg/kg 5-FU = 98 days post induction, p value = 0.665, $n \geq 6$ per cohort, Log Rank method) (Figure 7.9). Interestingly, out of the three tolerated regimens, the only significant increase in median survival was observed with the 50mg/kg 5-FU regimen that commenced at 50 days post induction (median survivals: vehicle = 94 days, 50mg/kg 5-FU day 60 = 120 days, p value = 0.09, 50mg/kg 5-FU day 50 = 131 days, p value = 0.006, 25mg/kg 5-FU tri-weekly = 120 days post induction p value = 0.349, $n \geq 8$, Log Rank method) (Figure 7.9). Given the differences observed increase in median survivals, tumours from mice in various cohorts were analysed for expression of TS.

To assess the expression of TS in SITs from $Apc^{f/+}$ $Pten^{f/f}$ mice exposed to 5-FU, individual tumours snap frozen at dissection were subjected to RNA extraction, cDNA synthesis and qRT-PCR analysis. Analysis to evaluate the expression of TS was conducted in individual tumours (as described in methods section 2.10). It was hypothesised that tumours from mice culled following short exposure to 5-FU would show no alteration in levels of TS indicating no response to 5-FU, whilst those tumours from mice exposed to 5-FU for longer periods of time would present with increased levels of TS.

In comparison with tumours from untreated mice, those exposed to only 1 weekly doses of 50mg/kg 5-FU from days 60 post induction (culled at 61 days post induction) showed no significant difference in levels of TS, indicating 5-FU had no effect on TS expression levels here (Figure 7.10 A). Additionally, no obvious increase in expression of TS was observed in tumours from mice exposed to 11 or 14 weekly doses of 50mg/kg 5-FU from 60 days post induction, although three tumours (from two mice culled at 127 and 148 days post induction) trended towards an increase in TS expression (Figure 7.10 A, B). Interestingly, a high degree of variability was notable within tumours from the same mouse, which may be reflective of the proliferative nature of the tumours given the normal physiological function of TS in DNA replication. Interestingly, three out of six tumours analysed following exposure to 28 weekly doses of 50mg/kg 5-FU (culled at 246 days post induction) from 60 days post induction had reduced TS expression, perhaps indicating tumours were responding to 5-FU treatment but not resistant at this time (Figure 7.10 C).

A similar trend to that described above of no significant alteration in TS expression was observed in mice exposed to 7 weekly doses of 50mg/kg 5-FU (culled at 101 days post induction) from 50 days post induction (Figure 7.11 A). Finally, assessment of tumours from mice which survived the longest (culled at 303 days post induction following 36 weekly doses of 50mg/kg 5-FU) also failed to show an increased TS expression in the majority of tumours (Figure 7.10 B, C). Only one tumour from six showed a 2.5 fold increase in TS expression and may be indicative of differences in the proliferative nature of tumours and not of a single resistant tumour (Figure 7.10 C).

In summary, the findings from these investigations suggest that $Apc^{f/+}$ $Pten^{f/f}$ mice showed little to no responsiveness to 5-FU treatment. This could be due to the severe tumour phenotype present in this model or alternatively the regimens chosen for 5-FU administration in these mice were not appropriate to observe a substantial beneficial effect. The later observation suggests further investigation of the metabolism of 5-FU is required to better

understand the effects of 5-FU. Nevertheless, the findings here are in concert with clinical evaluations of 5-FU, which report limited overall benefits in patients of only 10-15%. Furthermore, expression analysis of TS in long term 5-FU treated tumours which appeared to have some response to 5-FU, failed to reveal an increase in TS expression. This may be due to alternative mechanisms of resistance or tumours not being 'truly resistant'.

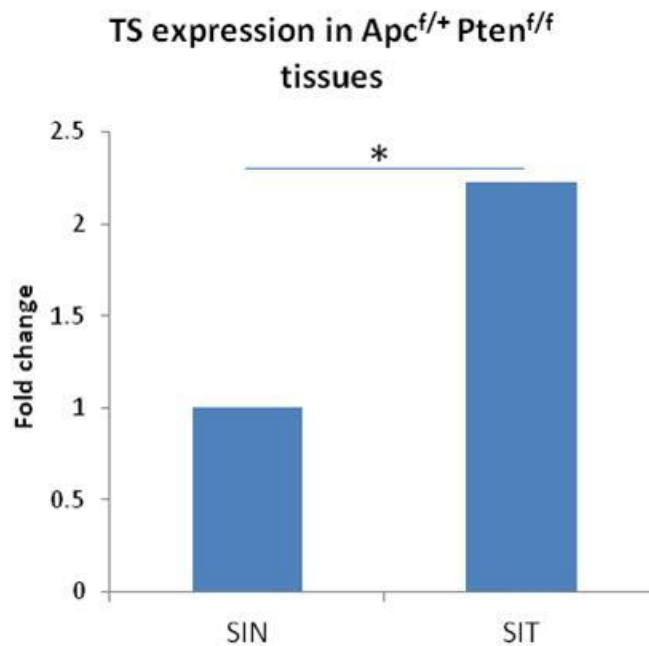


Figure 7.8 Increased expression of TS in $Apc^{f/+}$ $Pten^{f/f}$ small intestinal tumours (SITs) in comparison with normal small intestinal tissue (SIN).

Quantitative-RT-PCR analysis of TS in small intestinal normal (SIN) tissue from $Apc^{f/+}$ $Pten^{f/f}$ mice in comparison with small intestinal tumour (SIT) tissue revealed a significant two-fold increase in TS expression. (ΔCT SIN = 0.948 ± 0.127 , SIN = 8.32 ± 0.131 , p value = 0.0404, n= 3 mice, Mann Whitney U test)

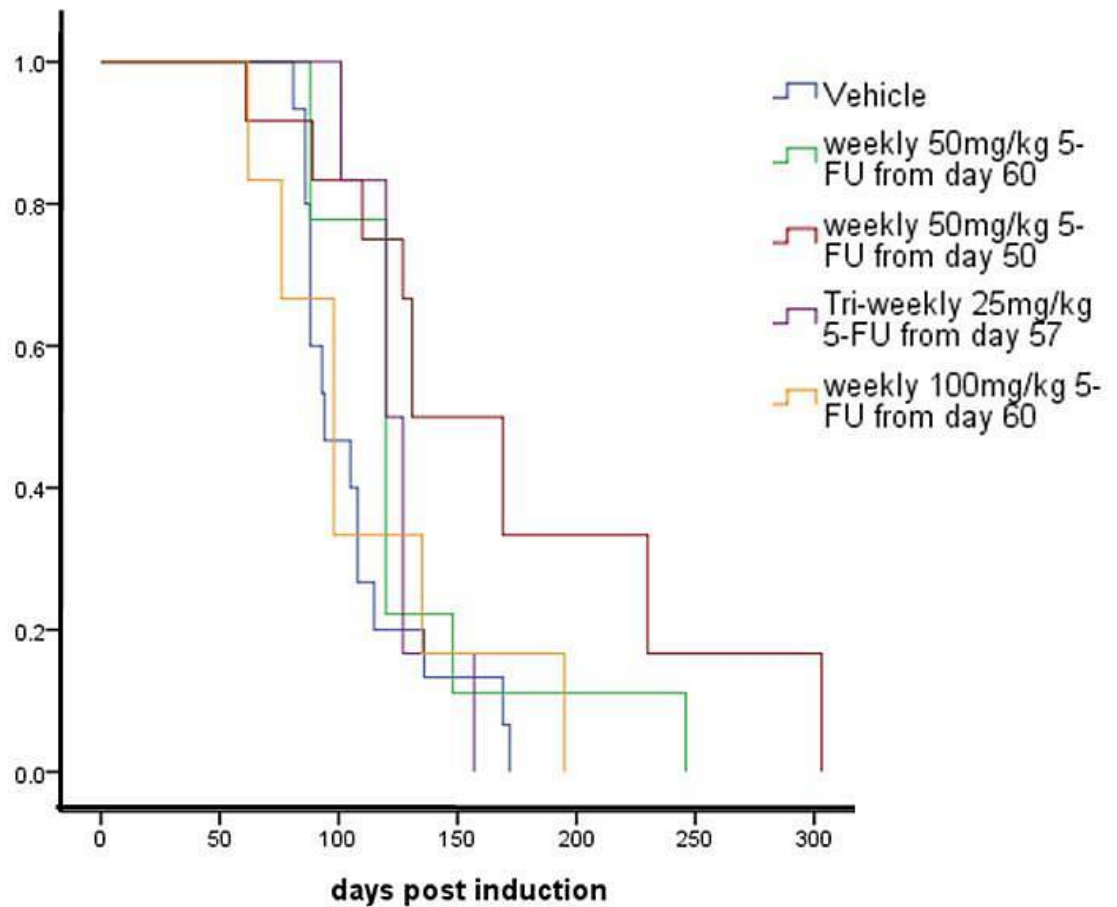


Figure 7.9 Kaplan Meier survival analysis of $Apc^{f/+}$ $Pten^{f/f}$ mice on long term 5-FU treatment.

$Apc^{f/+}$ $Pten^{f/f}$ mice were induced and aged prior to start of various 5-FU treatment regimens, as outlined above. Weekly 50mg/kg 5-FU treatment from day 60, tri-weekly 25mg/kg 5-FU from day 57 or weekly 100mg/kg 5-FU from day 60 post induction had no significant effect on median survival of $Apc^{f/+}$ $Pten^{f/f}$ mice. Only weekly administration of 50mg/kg 5-FU from day 50 post induction significantly increased survival of $Apc^{f/+}$ $Pten^{f/f}$ mice from a median of 94 to 131 days post induction. (50mg/kg 5-FU from 50 days post induction p value = 0.006, for all other treatments p \geq 0.05, n \geq 10 mice per cohort, Log Rank method)

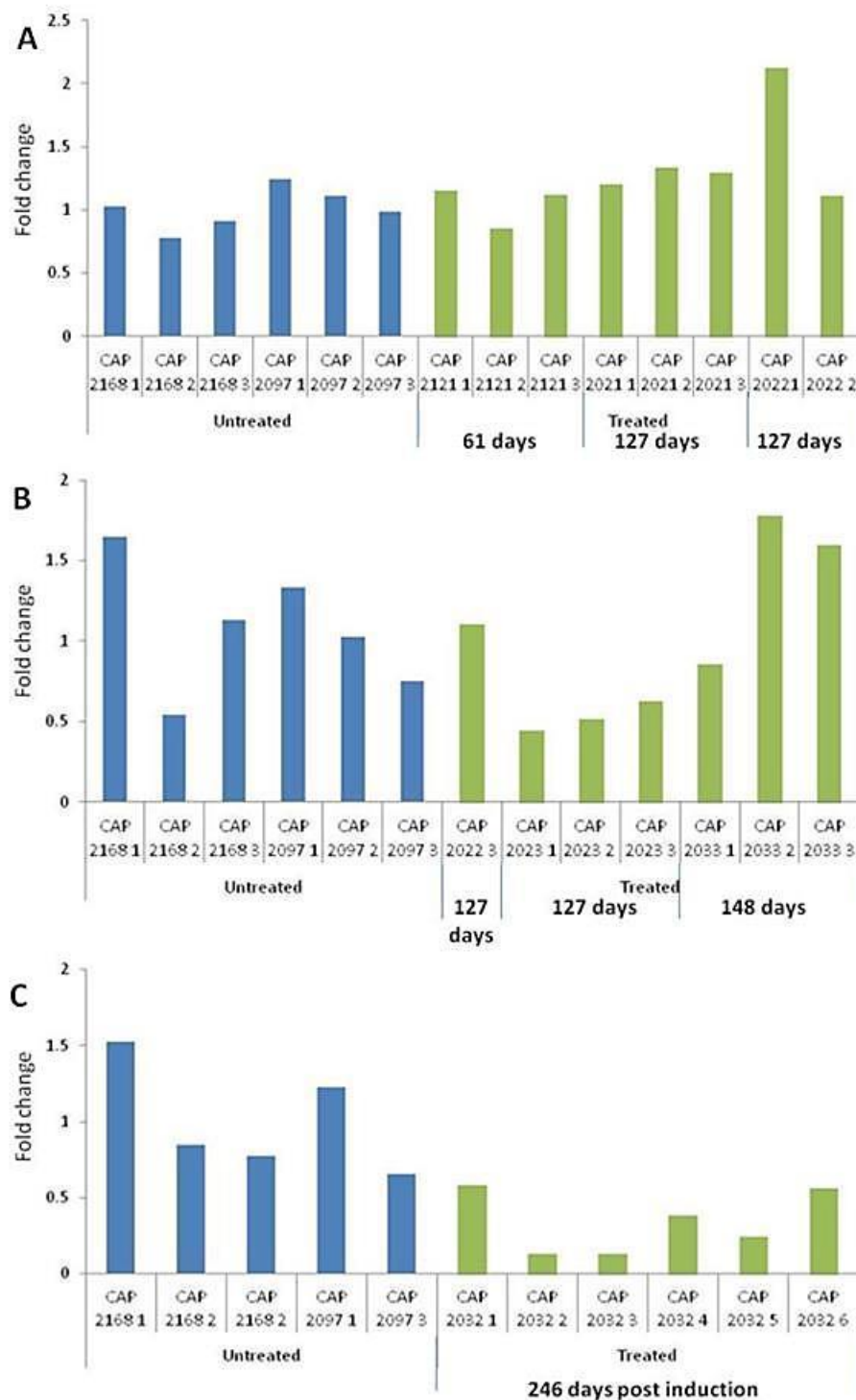


Figure 7.10 quantitative-RT-PCR analysis of individual untreated $Apc^{f/+}$ $Pten^{f/f}$ tumours in comparison with those exposed to 50mg/kg 5-FU treatment from day 60 post induction for varied periods of time.

Expression analysis of TS in small intestinal tumours (SITs) from untreated $Apc^{f/+}$ $Pten^{f/f}$ mice in comparison with those exposed to 5-FU up to 148 days post induction showed no significant difference in TS expression. Interestingly, some tumours from one mouse exposed to 5-FU up to 246 days post induction showed reduced levels of TS (ΔCT values of treated tumours were normalised to the averaged ΔCT s of untreated tumours to calculate $\Delta\Delta CT$ values).

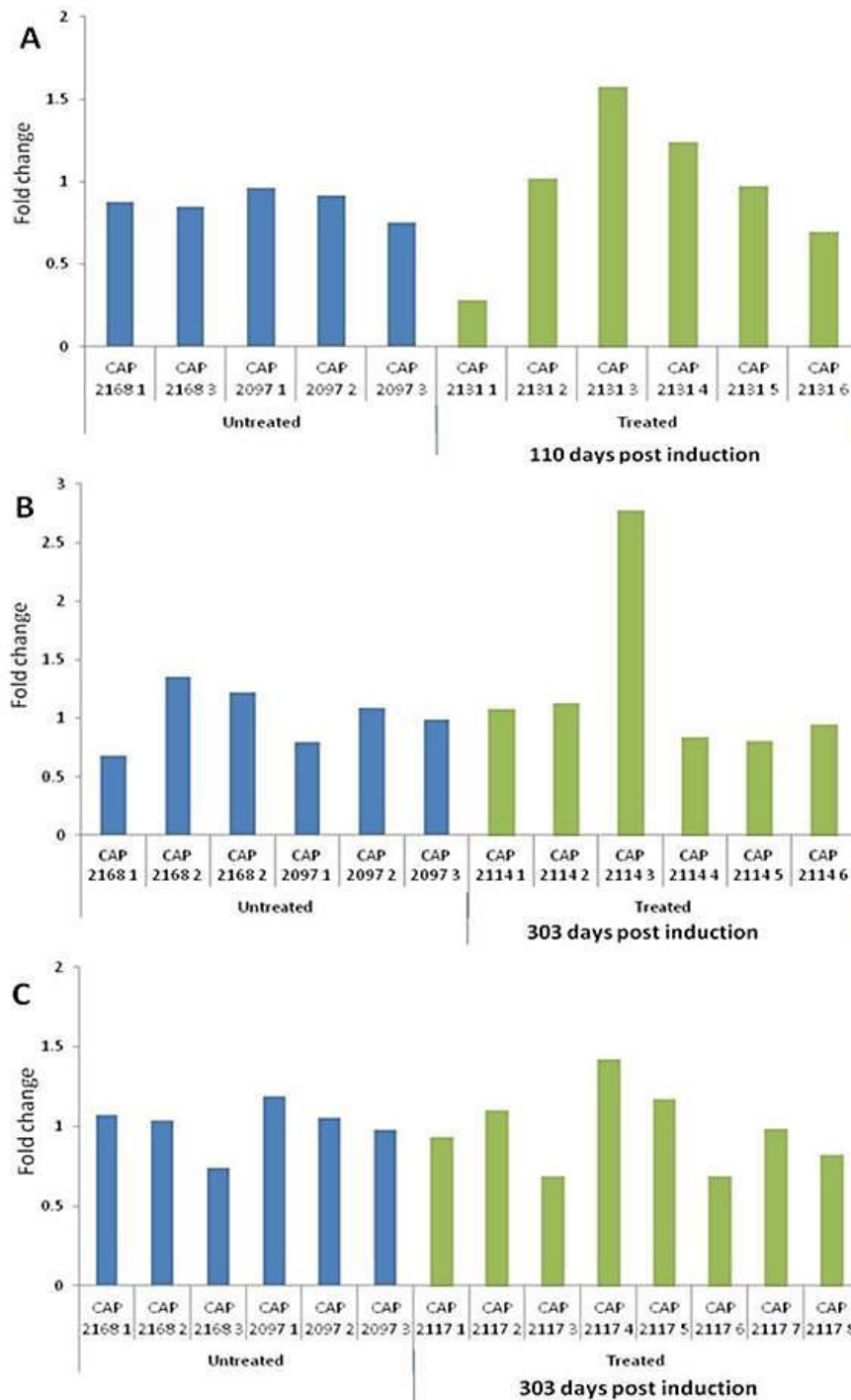


Figure 7.11 quantitative-RTPCR analysis of individual untreated $Apc^{f/+}$ $Pten^{f/f}$ tumours in comparison with those exposed to 50mg/kg 5-FU treatment from day 50 post induction for varied periods of time

Expression analysis of TS in small intestinal tumours (SITs) from untreated $Apc^{f/+}$ $Pten^{f/f}$ mice in comparison with those exposed to 5-FU showed either up to 110 days or 303 days post induction showed mostly unaltered TS expression. One tumour from a mouse exposed to 5-FU for up to 303 days showed increased expression of TS of 2.5 fold. (Δ CT values of treated tumours were normalised to the averaged Δ CTs of untreated tumours to calculate $\Delta\Delta$ CT values)

7.3 Discussion

7.3.1 *In vitro and in vivo characterisation of ProTide compounds*

The ProTide approach has previously proved effective in increasing the therapeutic potential of a number of anti-viral agents and more recently anti-cancer nucleoside agents, such as gemcitabine. This approach involves the use of phosphoramidate groups to mask the charge on the mono-phosphate form of the nucleoside, eliminating the requirement of the initial rate-limiting step in the metabolism of the nucleoside agent, whilst also improving the intracellular delivery of the compound. Once into the cell, the additional phosphoramidate groups are enzymatically cleaved to release the pre-formed monophosphate nucleoside for further phosphorylations. Hence, a widespread library with different alterations in the amino acid, aromatic moiety, ester, or the Br constituent of BVDUMP was synthesised and initially evaluated *in vitro*.

Initial *in vitro* characterisation of ProTide agents involved a cell titer blue cell viability assay, conducted 72 hours following ProTide exposure in both MCF7 and TS overexpressing MCF7TDX cells. Compounds were found to have varied cytotoxic effects from this assay in comparison with Thymectacin and also the parent compound BVDU (Table 7.1). The most active compounds from this assay were further evaluated *in vitro* using a colony forming assay, which also involved 72 hours of drug exposure, to examine the ability of ProTide agents to inhibit cell growth. From this, all compounds were found to have improved efficacy in comparison with Thymectacin, however only 3 compounds were found to be notably more effective in MCF7TDX cells in comparison with MCF7 cells – CPF472, CPF473 and CPF3172 (Figure 7.4). Whilst CPF552 was not found to have increased potency in the MCF7TDX cells, the observation that colony growth was completely killed with the 25µM concentration (in both cell lines) indicated this to be a potent compound nevertheless (Figure 7.4). Finally, despite the improved efficacy of CPF555 in comparison with Thymectacin in the *in vitro* cell viability and colony forming assays, this compound was not further evaluated due to lack of potency in comparison with the remaining ProTide agents.

Subsequently the four remaining ProTide agents were evaluated in an *in vivo* tumour setting. For these evaluations, the AhCreER driven $Apc^{f/+}$ $Pten^{f/f}$ tumour model was selected due to the invasive nature of the tumour phenotype present and the reduced latency for tumour development in comparison with $Apc^{f/+}$ controls. Following induction, $Apc^{f/+}$ $Pten^{f/f}$ mice aged to 85 days post induction were administered consecutive doses of 50mg/kg thymectacin,

CPF472, CPF473, CPF552, CPF3172 or vehicle once daily for four days and culled 6 hours following the final dose. Tumours from mice exposed to the ProTide agents or thymectacin were evaluated for anti-tumour effects, in comparison with vehicle treated tumours (Figures 7.5, 7.6). Whilst both CPF472 and CPF3172 induced favourable pro-apoptotic effects, CPF473 and CPF552 induced no biological effect in $Apc^{f/+}$ $Pten^{f/f}$ tumours, indicating lack of *in vivo* efficacy (Figures 7.5, 7.6). This lack of *in vivo* efficacy may be due to a number of factors including *in vivo* metabolism of the agents as well as lipophilicity which vastly differs in *in vitro* and *in vivo* systems. From anti-proliferative investigations, only CPF472 reduced proliferation in $Apc^{f/+}$ $Pten^{f/f}$ tumours, showing further favourable *in vivo* efficacy. Whilst thymectacin treatment resulted in a reduction of cells in the S phase of the cell cycle, treatment also induced anti-apoptotic effects in tumours as detected by scoring of histological apoptosis and cleaved caspase 3 staining (Figures 7.5, 7.6). From the short term *in vivo* study, ProTides CPF472 and CPF3172 were chosen for further *in vivo* investigations, given their favourable anti-tumour effects from short term treatments. This would formally determine their efficacy in a long term therapeutic setting and ultimately determine whether continuous treatment can improve survival of $Apc^{f/+}$ $Pten^{f/f}$ mice.

Despite the anti-tumour effects of CPF472 and CPF3172 in the short term *in vivo* experiment, both compounds failed to significantly increase survival of $Apc^{f/+}$ $Pten^{f/f}$ mice when administered at 75mg/kg daily. CPF472 treated $Apc^{f/+}$ $Pten^{f/f}$ mice from 77 days post induction, had a median survival of 107 days whilst CPF3172 treatment increased survival of equivalent mice to 112 days post induction (vehicle cohort had a median survival of 94 days post induction) (Figure 7.7). Surprisingly, continuous thymectacin treatment significantly improved survival of mice to 133 days post induction indicating increased potency in comparison with CPF472 and CPF3172 (Figure 7.7). These findings were particularly surprising given the lack of efficacy of thymectacin in the *in vitro* cell viability and colony forming assays, as well as the short term *in vivo* experiment. However, these findings to some extent corroborate previous studies which reported efficacy of thymectacin *in vivo*. Lackey et al reported that whilst thymectacin failed to show efficacy in MCF7 cells in comparison with MCF7TDX cells ($IC_{50} = 207\mu M$ in MCF7 vs $IC_{50} = 3\mu M$ in MCF7TDX), continuous treatment significantly inhibited growth in both MCF7 and MCF7TDX xenograft settings comparably (Lackey et al., 2001), further suggesting the *in vivo* efficacy of thymectacin is not reflected from *in vitro* studies. Whilst findings in this chapter corroborate the lack of efficacy of thymectacin in MCF7 cells but potency in the *in vivo* setting, this study did not find

thymectacin to be increasingly potent in MCF7TDX cells, but this perhaps could be attributed to differences in the *in vitro* experiments conducted.

These findings suggest further characterisation and validation of CPF472 and CPF3172 is required with regards to *in vivo* stability, lipophilicity and metabolism. These further investigations are required to determine *in vivo* uptake of ProTide agents in tumour cells, enzymatic cleavage of the additional phosphoramidate groups and accumulation of BVDUMP *in vivo* to understand the lack of *in vivo* efficacy.

7.3.2 Alternative mechanisms of resistance to 5-FU

5-FU remains the most widely used chemotherapeutic agent for the treatment of CRC, despite the very modest response rates of only 10-15% as first line therapy in patients (Johnston and Kaye, 2001). Efforts to understand the mechanisms by which 5-FU causes cytotoxicity in cells and subsequently how tumours develop resistance to 5-FU are essential for predicting response and also for developing methods to overcome resistance. As described previously, when metabolised, 5-FU is converted into several metabolites including FdUMP, FdUTP as well as FUTP which disrupt RNA synthesis and inhibit the actions of TS (Figure 7.1) (Longley et al., 2003). In particular, the 5-FU metabolite FdUMP binds to the nucleotide binding site of TS, forming a stable tertiary structure with the enzyme and CH₂THF (a methyl donor) to block binding of the normal substrate dUMP, subsequently inhibiting dTMP synthesis. Furthermore, dUTP can be misincorporated into DNA causing false nucleotide incorporation, excision and repair, subsequently causing DNA strand breaks and cell death (Yoshioka et al., 1987, Mitrovski et al., 1994). In addition, misincorporation of the 5-FU metabolite FUTP into RNA can also disrupt normal RNA processing and function, and has previously been associated with loss of clonogenic potential in human colorectal cancer cell lines (Glazer and Lloyd, 1982).

Given the role of TS in mediating the cytotoxic effects of 5-FU in cancer cells, it is not surprising that a number of studies have shown TS expression to be a key determinant of sensitivity and resistance to 5-FU. Clinical investigations have previously evaluated TS levels by immunohistochemistry as well as RT-PCR techniques to show improved response of 5-FU in patients with low tumoural TS expression (Johnston et al., 1995, Edler et al., 1997). Additionally, 5-FU treatment has been shown to increase TS expression in both cell lines and tumours, and is regarded as a mechanism of resistance, as increased TS expression would

result in increased TS protein levels which would facilitate enzymatic recovery (Chu et al., 1993a, Longley et al., 2003).

Studies in this chapter aimed to model TS overexpression through 5-FU exposure, in the $Apc^{f/+}$ $Pten^{f/f}$ tumour model to further investigate the therapeutic potential of novel BVDUMP ProTide agents previously evaluated in this chapter. To achieve 5-FU response and subsequent resistance, four differing dosing strategies were employed, to mimic the clinical setting. These involved once weekly 50mg/kg 5-FU either from day 60 or 50 post induction, 25mg/kg tri-weekly from day 57 post induction and 100mg/kg once weekly from day 60 post induction, all of which were administered to a survival end point (Figure 7.9). Whilst the 100mg/kg treatment was found to induce mild toxicity effects, Kaplan Meier survival analysis revealed only the 50mg/kg once weekly from day 50 post induction had a significant effect on increasing median survival of $Apc^{f/+}$ $Pten^{f/f}$ mice in comparison with vehicle treatment (Figure 7.9). Mice in this cohort appeared to respond to 5-FU treatment, however as mice are culled at a survival end point, it was thought that tumours may have become resistant to 5-FU treatment. Surprisingly the equivalent dose of 50mg/kg weekly but from day 60 and the 25mg/kg tri-weekly regimen from day 57 failed to significantly increase survival of mice (Figure 7.9). This may be attributable to the presence of fewer tumours or perhaps less invasive tumours at day 50 in comparison with day 57 or 60 post induction. To evaluate whether tumours from the responding cohort resulted in increased levels of TS, qRT-PCR analysis was used to assess levels of TS mRNA expression in individual tumours, in comparison with a cohort of untreated tumours (Figure 7.10, 7.11). Although qRT-PCR analysis did not show increased levels of TS with increased exposure to 5-FU, this did reveal variation between tumours from the same mouse, which may be attributable to differences in the basal levels of proliferation between less or more invasive lesions. Alternatively, these findings suggest that in $Apc^{f/+}$ $Pten^{f/f}$ mice, TS overexpression may not be the primary mechanism of resistance to 5-FU (Figure 7.10, 7.11).

Whilst TS overexpression is often regarded as the primary mechanism of resistance to 5-FU, a number of other biological factors have also been implicated in determining response and resistance to 5-FU, and may be attributable to the non-response or resistance following 5-FU treatment in $Apc^{f/+}$ $Pten^{f/f}$ tumours. The enzyme thymidine phosphorylase (TP) which can reversibly convert 5-FU to FUDR, which can subsequently be converted to the active metabolite FdUMP is also implicated in non-response and resistance to 5-FU although the current literature is contradictory (Longley et al., 2003). TP overexpression in cell culture and

xenografts has previously shown sensitivity to 5-FU however mRNA expression analysis of colorectal tumours with high levels of TP were shown to be less likely to respond to 5-FU (Evrard et al., 1999, Metzger et al., 1998). These contrasting findings however, may be attributable to the observation that TP is also an angiogenic endothelial cell growth factor which has been associated with more invasive disease, less likely to respond to chemotherapy (Takebayashi et al., 1996).

Additionally, the rate-limiting enzyme of 5-FU catabolism dihydropyrimidine dehydrogenase (DPD) which converts 5-FU to dihydrofluorouracil (DHFU) is also implicated in non-response to 5-FU (Diasio and Johnson, 1999, Johnson et al., 1999). DPD is abundantly expressed in the liver where it leads to more than 80% of 5-FU catabolism. Therefore patients deficient in DPD show toxicity to 5-FU due to decreased drug catabolism (Johnson et al., 1999). Despite this, *in vitro* studies and expression analyses of patient samples have also shown DPD overexpression confers resistance to 5-FU (Takebe et al., 2001, Salonga et al., 2000), perhaps reflecting higher DPD mediated degradation of 5-FU in tumours.

As well as TP and DPD expression, mutations in several genes have also been associated with poor response to 5-FU including microsatellite instability inducing genes such as *MLH1*, *MSH2* and *MSH6* (Claij and te Riele, 1999), as well as loss of the tumour suppressor protein p53, which mediates DNA integrity and response to DNA damage (Bunz et al., 1999). Disruption of both alleles of the *p53* gene or the pro-apoptotic gene *BAX* can result in cells resistant to apoptosis induced by 5-FU (Bunz et al., 1999, Zhang et al., 2000). This has also been validated in clinical studies through p53 overexpression as a surrogate marker of p53 mutations (Ahnen et al., 1998).

7.4 Summary

This study evaluated novel compounds synthesised using the phosphoramidate prodrug approach applied to the anti-viral agent BVDU. These nucleoside ProTide derivatives demonstrated increased biological activity in comparison to the parent compound BVDU as well as thymectacin, a BVDU prodrug, currently under pre-clinical evaluation. Despite improved *in vitro* and short term *in vivo* activity of selected ProTide agents in comparison with thymectacin, the selected lead ProTide agents were found to be less efficacious than thymectacin in increasing survival of tumour bearing *Apc^{f/+} Pten^{f/f}* mice. Despite this, it was hypothesised these agents would be more active in a TS overexpressing tumour setting, a key enzyme implicated in resistance to 5-FU given that the metabolite of BVDU is a substrate for

TS. However, continuous 5-FU treatment did not result in increased expression of TS, suggesting an alternative mechanism of resistance may be attributable to 5-FU resistance in the $Apc^{f/+}$ $Pten^{f/f}$ mouse model. Therefore the hypothesis that these ProTide agents would be more active in the TS upregulated tumour setting remains to be tested *in vivo*.

7.5 Further work

7.5.1 Further *in vivo* investigations of ProTides agents

Whilst the short term *in vivo* characterisation of selected ProTide agents presented in this chapter showed that the two lead ProTide agents induced favourable biological activity in tumours, these effects were not correlated to long term activity of the compounds. Therefore, it would be useful to conduct a short term dose escalation study, whereby accumulation of BVDU metabolites are detected in the tumours and correlated to biological activity. Such experiments may help determine how well the compounds are getting into the tumours and also how well they are metabolised to release the bioactive phosphate nucleoside. Additionally, these experiments may help determine the most effective dose to use for long term therapeutic studies, as in the study presented here, although a high dose administered, it was not determined whether a higher dose could be used instead. Moreover, such experiments may help determine whether any solubility or lipophilicity issues are preventing effective delivery of compounds into the tumours. To conduct these experiments, mass spectrometry may be required to detect accumulation of BVDUMP in tumours.

7.5.2 Modulation of 5-FU in the $Apc^{f/+}$ $Pten^{f/f}$ tumour model

As mentioned previously, 5-FU treatment was only efficacious in $Apc^{f/+}$ $Pten^{f/f}$ mice when administered at 50mg/kg from day 50 post induction, in comparison to the alternative treatment regimens. However, it is not known whether this is the optimal treatment regimen for 5-FU in mice. Additionally, target validation studies were not conducted to determine whether 5-FU treatment resulted in reduced TS expression. Conducting such experiments may identify a better treatment regimen for 5-FU in mice which may result in an improved response. For this, it would be useful to administer a single dose of 5-FU, at varying concentrations, and investigate the effects on tumour TS expression from day 1 to 7, as treatment was most commonly administered weekly. This may yield informative findings regarding the modulation of 5-FU in the $Apc^{f/+}$ $Pten^{f/f}$ tumour model.

Furthermore, alternative mechanisms of resistance to 5-FU treatment have been described and include increased expression of the enzyme TP or depletion of DPD, both of which are

involved in the catabolism of 5-FU. Also, mutations in a number of genes including *p53*, *BAX* and microsatellite instability inducing genes are commonly associated with resistance. Investigation these would be useful to further explore resistance in *Apc*^{f/+} *Pten*^{f/f} tumours following 5-FU treatment.

8 General Discussion

8.1 *The use of genetically engineered mouse models for pre-clinical studies*

As the third most commonly diagnosed malignancy, colorectal cancer (CRC) leads to more than 16,000 deaths annually (Cancer Research, UK). The high mortality rate associated with CRC is often attributed to patients presenting with late stage disease in the clinic, and also the lack of correlative early symptoms to diagnose the disease. The current treatment strategies for CRC predominantly rely on the use of combinations of cytotoxic agents, which include 5-fluorouracil (5-FU), irinotecan and oxaliplatin in either the FOLFOX or FOLFIRI regimen (FOLinic acid, Fluorouracil and OXaliplatin or FOLinic acid, Fluorouracil and IRinotecan, respectively, Cancer Research, UK), with the addition of anti-epidermal growth factor receptor (EGFR) targeted agents such as cetuximab and panitumumab more recently. Despite this, CRC is the second most common cause of death by cancer, indicating mortality rates remain high. Subsequently, the need for more effective treatment strategies is urgent.

Recently, efforts to identify further mutations involved in CRC by sequencing have increased with the availability of new technologies. Such systematic characterisation of somatic mutations within cancer genomes not only increase our understanding of the disease, but also help to identify novel therapeutic targets. Despite this, the fact that only 1 in 10 novel compounds successful at phase I evaluations is eventually approved by regulators, highlights major flaws in the pre-clinical development process (Johnston and Kaye, 2001). This high attrition rate is often attributed to poor pre-clinical strategies such as the use of xenografted human tumours in immune-compromised mice, which fail to accurately predict the *in vivo* efficacy of novel agents. Furthermore, these fail to recapitulate a number of processes involved in human cancer such as the sporadic nature of tumour formation, the tumour microenvironment, as well as angiogenesis. A number of notable failures in the clinic from promising xenograft studies highlight this issue. For example, thiazolidinediones (TZDs) which are antagonists of PPAR- γ (peroxisome proliferator-activated receptor γ) showed impressive anti-tumour activity in cultured and xenografted colon cancer cell lines (Sarraf et al., 1998). However, in the clinic, these were a clear failure for patients with CRC, and led to rapid progression of disease (Kulke et al., 2002). Similarly, novel anti-angiogenesis agents such as endostatin and angiostatin, showed potent anti-cancer effects in xenografts and human cancer cell lines (Boehm et al., 1997, O'Reilly et al., 1996, Holmgren et al., 1995), however

have yet to demonstrate any single-agent activity against CRC (Twombly, 2002, Thomas et al., 2003). Furthermore, farnesyltransferase inhibitors (FTIs) expected to inhibit RAS function showed activity in xenograft studies, however were less active in human cancers (Kohl et al., 1994, Omer et al., 2000, Berndt et al., 2011). Studies of these in genetically engineered mouse models (GEMMs) showed that anti-tumour activity of FTIs was not RAS dependent. As well as the lack of predictive power of xenograft studies for clinical trials, these provide limited information regarding the genetic or epigenetic mutations present in tumours which could help predict the response of a particular tumour to novel agents (such as Kras or Pten/PIK3CA gene mutation status in anti-EGFR trials).

GEMMs which develop tumours within the tissue of interest with an intact immune system may better recapitulate the human disease and furthermore, may better predict the efficacy of novel agents *in vivo*. Evidence for this was clearly provided by Olive et al. assessing the efficacy of the chemotherapeutic agent gemcitabine in models of pancreatic cancer. This study found that whilst gemcitabine showed activity in xenografts, the limited activity of this in GEMMs was due to the presence of tumour associated stromal tissue and that depletion of this with a Hedgehog pathway inhibitor, led to better delivery and efficacy of gemcitabine *in vivo* (Olive et al., 2009).

Given the discussions presented here, the overall aim of this thesis was to investigate novel therapeutic strategies for CRC using autochthonous mouse models. Recent studies within the Clarke lab have generated mouse models of invasive intestinal adenocarcinomas mutant for the tumour suppressor proteins Apc and Pten as well as the oncogene Kras, using two intestinal specific transgenes, namely the AhCreER and VillinCreER transgenes (Marsh et al., 2008, Davies et al., *in press*). One aspect of work outlined in this thesis was to utilise these models to investigate therapeutic agents which target relevant pathways primarily driving tumourigenesis in these models, namely the PI3K and MAPK signalling pathways.

8.1.1 PI3K/mTOR inhibitor treatment in increasing lifespan of GEMMs

The rationale behind the use of a PI3K/mTOR inhibitor in Apc^{f/+} Pten^{f/f} mice stemmed from the observation that tumour progression in these mice coincides with increased levels of pAKT as reported by Marsh et al., and as confirmed in chapter 3 (Marsh et al., 2008). Furthermore, the PI3K pathway was found to be elevated in Apc^{f/+} Kras^{LSL/+} colon tumours (chapter 3), not surprising given that oncogenic Kras also impinges on the PI3K pathway (Kodaki et al., 1994).

Moreover, presence of all three genetic mutations driven by the VillinCreER transgene resulted in increased tumour number, progression and substantially reduced lifespan of mice (Davies et al., *in press*). All three tumour models present as useful pre-clinical models given the well-defined survival profiles, and genetic differences which could help distinguish between responding and non-responding tumours.

As hypothesised, long term PI3K and mTOR inhibition using NVP-BEZ235 significantly increased lifespan of all three tumour models (summarised in table 8.1, chapters 4-6), highlighting the importance of PI3K/mTOR signalling in tumours and suggesting this as a beneficial therapeutic strategy for Pten deleted and Kras activated colorectal cancers. Whilst the dependence of these tumour models on PI3K signalling could be attributed to the genetic alterations present, i.e. Pten deletion and oncogenic Kras activation, targeting of the PI3K/mTOR signalling pathway has long been associated with increased longevity. mTOR which is a serine/threonine protein kinase of the PI3K pathway, is a master regulator of cellular growth and metabolism, and modulation of mTOR complex 1 (mTORC1) coincides with increased longevity (Stanfel et al., 2009). Whilst mTORC1 is activated by insulin and growth factor signalling through the PI3K and AKT pathway, it can also be activated by environmental nutrients (such as amino acids), and repressed by AMPK, a key sensor of cellular energy (Johnson et al., 2013). Subsequently, mTORC1 can increase protein synthesis through pS6 kinases and 4EBP1, as well as promote lipid biosynthesis, activate autophagy, regulate glucose metabolism and mitochondrial function, all of which are known to contribute to increasing longevity (Johnson et al., 2013). Given the extensive beneficial effects of mTORC1 inhibition, the increase in longevity observed in $Apc^{f/+} Pten^{f/f}$, $Apc^{f/+} Kras^{LSL/+}$ and $Apc^{f/+} Pten^{f/f} Kras^{LSL/+}$ mice following NVP-BEZ235 treatment (chapters 4-6) may to some extent be attributable to the effects of mTORC1 inhibition as opposed to the presence of genetic mutations which render tumours sensitive to PI3K pathway inhibition. Furthermore, given that NVP-BEZ235 treatment also increased survival of $Apc^{f/+}$ mice (summarised in table 8.1, chapter 3), tumours from which do not show activation of PI3K signalling, it could be suggested that the benefits of NVP-BEZ235 are to some extent not associated with the presence of PI3K pathway genetic alterations. Also of interest is the association of mTORC1 inhibition with rejuvenation of stem cell function in a number of tissues. Yilmaz et al showed that rapamycin mediated mTORC1 inhibition, protected against loss of intestinal stem cell function during aging by protecting the stem cell niche (Yilmaz et al., 2012), perhaps implicating an alternative mechanism for NVP-BEZ235 induced longevity. Nevertheless, NVP-BEZ235 treatment in $Apc^{f/+} Pten^{f/f}$, $Apc^{f/+} Kras^{LSL/+}$ and $Apc^{f/+} Pten^{f/f} Kras^{LSL/+}$ mice more than doubled survival of mice whereas treatment in $Apc^{f/+}$ mice only

increased survival by 100 days (vehicle = 270 days vs NVP-BEZ235 = 371 days post induction) (chapters 4-6), suggesting increased benefits in the stratified Pten deficient and Kras mutant genetic tumour settings.

These findings have direct relevance to the clinic highlighting the potential benefits of PI3K/mTOR inhibitors for increasing longevity of PI3K and KRAS mutant, as well as wild-type tumours. It may be useful to assess the effects of PI3K inhibition and mTORC1 inhibition independently using specific inhibitors (Pan-PI3K inhibitors vs rapamycin which preferentially inhibits mTORC1) to assess the independent effects on survival of Pten deficient, Kras activated and wild-type tumour bearing mice.

8.1.2 *Pten deletion as a marker of non-response to MEK inhibitor treatment*

Prior to MEK inhibitor treatment experiments, the levels of MAPK pathway activation was assessed through immunoblotting for pERK, a key MAPK pathway effector, in colon and small intestinal tumours from $Apc^{f/+}$, $Apc^{f/+}$ $Kras^{LSL/+}$, $Apc^{f/+}$ $Pten^{f/f}$ and $Apc^{f/+}$ $Pten^{f/f}$ $Kras^{LSL/+}$ mice (chapter 3). Whilst these experiments confirmed activation of MAPK signalling in $Apc^{f/+}$ $Kras^{LSL/+}$ colon and small intestinal tumours in comparison with $Apc^{f/+}$ controls, surprisingly, levels of pERK were also found to be increased in $Apc^{f/+}$ $Pten^{f/f}$ and not in $Apc^{f/+}$ $Pten^{f/f}$ $Kras^{LSL/+}$ small intestinal tumours. Whilst the reasons for increased MAPK signalling in $Apc^{f/+}$ $Pten^{f/f}$ tumours are not fully understood, the lack of MAPK signalling in $Apc^{f/+}$ $Pten^{f/f}$ $Kras^{LSL/+}$ tumours may be attributable to increased tumour burden within a substantially reduced lifespan. Despite the differences in pathway activation, long term MEK inhibition was investigated in all four models. Subsequently, MEK inhibition through MEK162 was found to significantly increase survival of $Apc^{f/+}$ and $Apc^{f/+}$ $Kras^{LSL/+}$ mice (summarised in table 8.1, chapter 3, 5) and deletion of Pten emerged as a marker of non-response to MEK inhibitor treatment, independently (in the $Apc^{f/+}$ $Pten^{f/f}$ mice) but also in the context of Kras mutant tumours (in the $Apc^{f/+}$ $Pten^{f/f}$ $Kras^{LSL/+}$ mice) (chapter 4, 6). These findings are in accordance with previous studies and provide evidence for the notion that Kras mutational status alone is not sufficient as a prognostic marker for response to MEK inhibition (Chen et al., 2012b). Moreover, mutations activating the PI3K pathway such as Pten deletion could also be used to predict non-response of Kras wild-type tumours to MEK inhibition given the increased survival benefit observed in $Apc^{f/+}$ mice (summarised in table 8.1, chapter 3-4).

8.1.3 Combinatorial therapy in *Kras* mutant and *Pten* deficient tumour settings

Despite the attractiveness of combination therapy, there is currently little data in the literature to advise on the most appropriate dosing schedule for the combination of PI3K and MEK inhibitors. This is crucial, as whilst agents may be effective as single agents, antagonism between two agents when combined, especially given cross-talk between the two pathways may be evident. Furthermore, due to overlapping sensitivities, the combination may result in no net clinical gain when administered jointly (Dancey and Chen, 2006). To address some of these issues, three varied combination strategies which differed in the order of agent administered was investigated. Here, MEK162 was administered 1 hour prior to (combo 1), post (combo 2) or at the same time (combo 3) as NVP-BEZ235 to determine whether scheduling is key to achieve concomitant pathway inhibition. Interestingly, sensitivity to the scheduling was primarily detected in $Apc^{f/+} Pten^{f/f}$ tumours whereby MEK162 administered prior to or at the same time as NVP-BEZ235 diminished sensitivity of *Pten* deficient tumours to complete PI3K and mTOR inhibition (chapter 4). Given that the most favourable anti-tumour effects, in terms of increased apoptosis and reduced proliferation, were also observed by this strategy, it was surprising that long term administration provided no additional benefits to single agent NVP-BEZ235 (summarised in table 8.1, chapter 4). These findings suggest that MAPK signalling is not required for tumour maintenance in $Apc^{f/+} Pten^{f/f}$ mice, despite the increase in signalling observed through pERK in chapter 3.

In direct contrast to the $Apc^{f/+} Pten^{f/f}$ setting, $Apc^{f/+} Kras^{LSL/+}$ and $Apc^{f/+} Pten^{f/f} Kras^{LSL/+}$ tumours in response to the combination strategies displayed less efficacy and less variation in inhibition of both pathways (chapter 5, 6). Nevertheless, the observation that chronic administration of the combination increased median survival additively in $Apc^{f/+} Kras^{LSL/+}$ mice and synergistically in $Apc^{f/+} Pten^{f/f} Kras^{LSL/+}$ mice indicates that whilst some antagonism may be suggested by the short term combination studies, the two pathways are essential in tumour maintenance (chapter 5, 6). These data suggest that combination therapy in *Kras* mutant settings could provide substantial benefits in the clinical setting. To formally determine whether scheduling of the PI3K/mTOR inhibitor NVP-BEZ235, and MEK inhibitor MEK162 is crucial in $Apc^{f/+} Kras^{LSL/+}$ and $Apc^{f/+} Pten^{f/f} Kras^{LSL/+}$ mice, long term treatment experiments with the combo 1 and combo 3 strategies could be conducted. These findings may also be crucial for translation into the clinic.

<i>Treatment</i>	<i>Parameters assessed</i>	<i>Genotype</i>			
		Apc^{f/+}	Apc^{f/+} Pten^{f/f}	Apc^{f/+} Kras^{LSL/+}	Apc^{f/+} Kras^{LSL/+} Pten^{f/f}
MEK162	Survival	270→401 DPI	No effect	153→287 DPI	No effect
	Tumour number	No effect	No effect	Reduction in SIT and colon polyps	No effect
	Tumour area	No effect	No effect	Smaller lesions in SI only, no effect on colon tumours	N/A
	Tumour progression	No effect	No effect	No effect	More invasive SI lesions
NVP-BEZ235	Survival	270→370 DPI	99→266 DPI	153→343 DPI	41→104 DPI
	Tumour number	No effect	Less tumours	No effect	No effect
	Tumour area	No effect	Increased tumour area	Smaller lesions in SI only, no effect on colon tumours	N/A
	Tumour progression	No effect in colon, less invasive lesions in SI	More invasive SI lesions	Less invasive lesions in SI, no effect in colon	More invasive SI lesions
Combination	Survival	N/A	99→270 DPI	153 →389 DPI	41→125 DPI
	Tumour number	N/A	Less tumours in SI	Less colon tumours, no difference in SI	No effect
	Tumour area	N/A	Increased area	No difference in colon, smaller SI lesions	N/A
	Tumour progression	N/A	Fewer benign and more invasive SI lesions	No effect in colon, less invasive lesions in SI	More invasive SI lesions

Table 8.1 Summary of outcomes from long term treatments with NVP-BEZ235 and MEK162

8.1.4 The MRC FOCUS 4 trial

The findings reported in this thesis regarding the efficacy of PI3K and MEK inhibitors have major clinical implications. In terms of predictions, the studies here suggest dual PI3K and mTOR targeting could be useful for Pten deficient and hence PI3K activated tumours, whilst combined targeting of PI3K/mTOR and MAPK signaling could be clinically beneficial for Kras mutant as well as compound Pten deficient and Kras mutant tumours. These predictions are particularly pertinent given the start of the MRC FOCUS-4 trial in January 2013. This trial aims to conduct a molecularly stratified phase II trial for metastatic CRC using similar parameters addressed in this thesis. As outlined in the schematic below (figure 8.1), this trial aims to determine the molecular sub-group of tumours following a course of standard chemotherapy, and subsequently treat with molecularly targeted agents until a primary end point of progression free survival (PFS). Additionally, this trial aims to conduct regular biopsies to address target validation as well as to investigate changes in pathology or mechanisms of resistance following novel agent treatments. For *B-RAF* mutant tumours which lead to activation of MAPK signalling downstream of KRAS, this trial aims to assess combinatorial anti-B-raf and anti-EGFR targeted agents whereas for *KRAS* mutant tumours, this trial aims to use an AKT inhibitor in combination with a MEK inhibitor. Additionally, for *PIK3CA* mutant tumours resulting in activation of the PI3K pathway, this trial aims to use a dual PI3K and mTOR inhibitor. In the event of no mutations in *B-RAF*, *KRAS* or *PIK3CA*, patients will be administered an anti-EGFR targeted agent (Maughan, 2012).

Interestingly, whilst B-RAF and KRAS mutations are known to be mutually exclusive, a third of human CRCs are known to accumulate KRAS and PI3K pathway activating mutations. The FOCUS-4 trial does not currently outline the course of proposed targeted therapy for these patients, but findings from this thesis indicate beneficial effects of combined MEK and PI3K/mTOR inhibitor treatment (chapter 6). Additionally, findings from this thesis indicate equipotent effects of independent PI3K/mTOR and MEK inhibition in the Kras mutant tumour setting (chapter 5). Currently, the FOCUS 4 trial does not include control arms for the proposed combination therapy (AKT inhibitor plus MEK inhibitor treatment) which patients with KRAS mutant tumours will be stratified to receive. If included, this would provide insightful information regarding the predictive nature of the GEMMs used in this study, and could clearly indicate the potential benefits of combination therapy. Furthermore, findings from this study suggest importance of scheduling, particularly as agents target closely

associated signalling pathways, an aspect which is not currently addressed by the FOCUS 4 trial.

Finally, given the direct relevance of findings from this thesis to the FOCUS-4 trial, it would be useful to investigate mechanisms of resistance to such molecularly targeted agents in our genetically defined mouse models, to provide further information to the clinic.

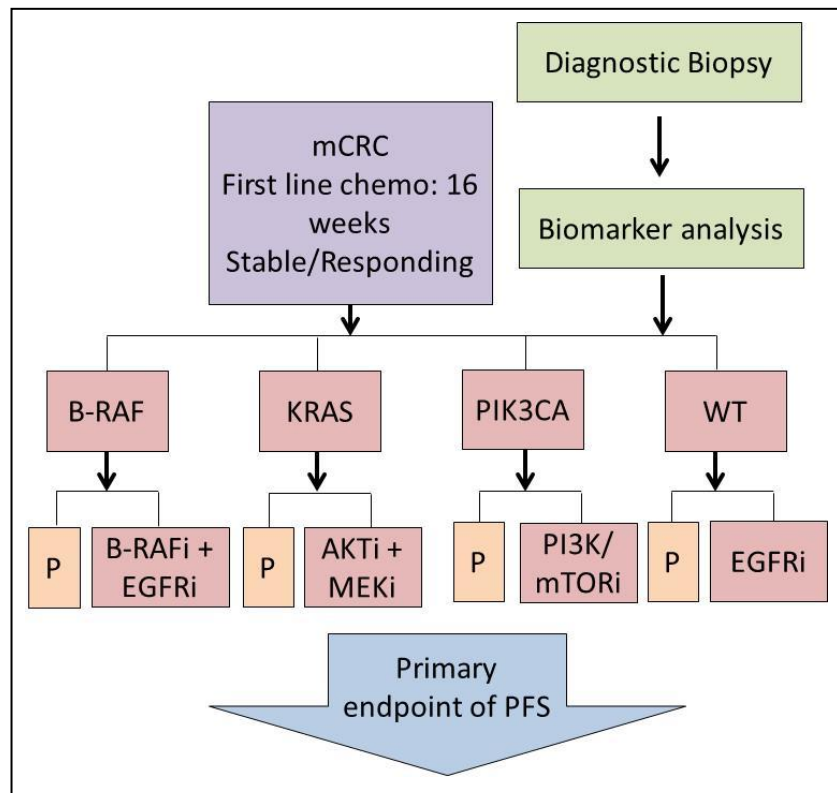


Figure 8.1 Outline of the MRC-FOCUS 4 phase II clinical trial

Following a diagnostic biopsy, patients with metastatic CRC will be recruited to the FOCUS 4 trial. During an initial treatment of first line chemotherapy for up to 16 weeks, tumours will be analysed for genetic alterations in the following genes: *B-RAF*, *KRAS* or *PIK3CA*. The stable or responding patients will subsequently be stratified upon genetic alterations detected within tumours, to receive either a combination of B-RAF and EGFR inhibitor treatment, AKT and MEK inhibitor treatment or a dual PI3K/mTOR inhibitor treatment for relevant disease. In the event of no genetic mutations in any of the three genes evaluated, patients will receive anti-EGFR targeted therapy. Patients will receive therapy to a primary end point of progression free survival (PFS). It is anticipated that these molecularly targeted agents will improve PFS in patients.

8.1.5 The drug discovery and development process applied to 5-FU

Another novel aspect of work outlined in this thesis involved applying the drug discovery and development process to overcome 5-fluorouracil (5-FU) resistance. Whilst targeted therapy holds great promise for the treatment of CRC, 5-FU remains the cornerstone of treatment for CRC as 5-FU based chemotherapy continually improves overall and progression-free survival of patients with resected disease. Despite this, in the advanced stage setting, response rates to 5-FU are modest, at only 10-15% (Johnston and Kaye, 2001). This highlights an urgent need in the clinic to improve prospects for patients.

The current drug discovery and development process is an inefficient process as reflected by the high attrition rate of potential anti-cancer agents. As outlined by Sharpless and DePinho, the root of the problem with regards to drug discovery and development relates to a number of needs: firstly, a robust rate-limiting cancer target; secondly, identification of effective and tolerated lead compounds for the target; thirdly, a clear genetic or cellular context in which the target is required for maintenance of a fully established tumour; and finally, identification of biomarkers for drug efficacy which are translatable into early phase clinical trials (Sharpless and Depinho, 2006).

Non-response and resistance of patients to 5-FU coincides with elevation of the target enzyme thymidylate synthase (TS) albeit this varies greatly between patients (Li et al., 2001). Nevertheless, TS presents as a rational therapeutic target given its central role on thymidine synthesis and cellular proliferation. The rationale behind the use of the anti-viral agent Brivudin (BVDU) as a parent compound to target increased expression of TS stemmed from the observation that TS was capable of using the metabolite of BVDU- BVDUMP, as a substrate and converting this to thiethyl-deoxyuridylate derivatives (these then have anti-tumour properties) (Barr et al., 1983). The charged nature of BVDUMP however prevents passive entry of the compounds into the cell. Therefore, the phosphoramidate technology was used to mask the charged nature of BVDUMP using temporary ester, aryl, amino acid or aromatic moieties to facilitate intracellular delivery of BVDUMP. In light of these observations, a small family of analogues of thymectacin (a phosphoramidate derivative of BVDUMP, currently under clinical evaluation) were prepared and evaluated *in vitro* in an effort to identify lead compounds which displayed efficacy in the MCF7 cancer cells but also showed increased efficacy in the TS overexpressing MCF7TDX cells (chapter 7). Whilst the lead compounds following *in vitro* evaluations showed increased potency in comparison with thymectacin and the parent BVDU compound, these showed varied biological effects in an *in vivo* setting (chapter 7).

Furthermore, due to the lack of a robust biomarker of sensitivity, it was not ascertained whether effective intracellular delivery of BVDUMP was indeed achieved or whether the additional temporary moieties were appropriately cleaved to release the active nucleoside molecule *in vivo*. Knowledge of this would provide useful information for further optimization of the ProTide agents and to improve the efficacy of the lead compounds in the *in vivo* setting. One major caveat of the research presented here was the lack of a 5-FU induced TS upregulated tumour model to evaluate efficacy of the lead ProTide agents. Nevertheless, the relevance of the AhCreER Apc^{f/+} Pten^{f/f} mouse model of invasive adenocarcinoma remains strong. As mentioned previously, the response rates of 5-FU in an advanced human tumour setting remain low. This was directly modelled in the AhCreER Apc^{f/+} Pten^{f/f} mouse model, where efficacy of 5-FU treatment, even in a prophylactic setting, fell short of the efficacy observed from the PI3K/mTOR inhibitor NVP-BEZ235 treatment. Interestingly, in this invasive model of adenocarcinoma, thymectacin treatment resulted in a similar increase in median survival in comparison with 5-FU treatment (median survival thymectacin= 133 days, 5-FU = 131 days, vehicle =94 days post induction) indicating equally beneficial effects.

Nevertheless, the studies presented in this thesis highlight the relevance of genetically engineered mouse models in generating clinically relevant hypotheses which following further clinical evaluation, may improve outcomes for patients with CRC.

Bibliography

- Cancer Research UK* [Online]. Available: <http://www.cancerresearchuk.org/cancer-info/cancerstats/world/colorectal-cancer-world/colorectal-cancer-world>.
- AHNEN, D. J., FEIGL, P., QUAN, G., FENOGLIO-PREISER, C., LOVATO, L. C., BUNN, P. A., STEMMERMAN, G., WELLS, J. D., MACDONALD, J. S. & MEYSKENS, F. L. 1998. Ki-ras mutation and p53 overexpression predict the clinical behavior of colorectal cancer: a Southwest Oncology Group study. *Cancer Res*, 58, 1149-58.
- AKSAMITIENE, E., KHOLODENKO, B. N., KOLCH, W., HOEK, J. B. & KIYATKIN, A. 2010. PI3K/Akt-sensitive MEK-independent compensatory circuit of ERK activation in ER-positive PI3K-mutant T47D breast cancer cells. *Cell Signal*, 22, 1369-78.
- AKSAMITIENE, E., KIYATKIN, A. & KHOLODENKO, B. N. 2012. Cross-talk between mitogenic Ras/MAPK and survival PI3K/Akt pathways: a fine balance. *Biochem Soc Trans*, 40, 139-46.
- AL-KHOURI, A. M., MA, Y., TOGO, S. H., WILLIAMS, S. & MUSTELIN, T. 2005. Cooperative phosphorylation of the tumor suppressor phosphatase and tensin homologue (PTEN) by casein kinases and glycogen synthase kinase 3 β . *J Biol Chem*, 280, 35195-202.
- ALESSI, D. R., JAMES, S. R., DOWNES, C. P., HOLMES, A. B., GAFFNEY, P. R., REESE, C. B. & COHEN, P. 1997. Characterization of a 3-phosphoinositide-dependent protein kinase which phosphorylates and activates protein kinase B α . *Curr Biol*, 7, 261-9.
- ALLEN, L. F., SEBOLT-LEOPOLD, J. & MEYER, M. B. 2003. CI-1040 (PD184352), a targeted signal transduction inhibitor of MEK (MAPKK). *Semin Oncol*, 30, 105-16.
- ANDREU, P., COLNOT, S., GODARD, C., GAD, S., CHAFEY, P., NIWA-KAWAKITA, M., LAURENT-PUIG, P., KAHN, A., ROBINE, S., PERRET, C. & ROMAGNOLO, B. 2005. Crypt-restricted proliferation and commitment to the Paneth cell lineage following Apc loss in the mouse intestine. *Development*, 132, 1443-51.
- AUCLAIR, B. A., BENOIT, Y. D., RIVARD, N., MISHINA, Y. & PERREAULT, N. 2007. Bone morphogenetic protein signaling is essential for terminal differentiation of the intestinal secretory cell lineage. *Gastroenterology*, 133, 887-96.
- BALMANNO, K., CHELL, S. D., GILLINGS, A. S., HAYAT, S. & COOK, S. J. 2009. Intrinsic resistance to the MEK1/2 inhibitor AZD6244 (ARRY-142886) is associated with weak ERK1/2 signalling and/or strong PI3K signalling in colorectal cancer cell lines. *Int J Cancer*, 125, 2332-41.
- BARDELLI, A. & SIENA, S. 2010. Molecular mechanisms of resistance to cetuximab and panitumumab in colorectal cancer. *J Clin Oncol*, 28, 1254-61.
- BARKER, N. & CLEVERS, H. 2006. Mining the Wnt pathway for cancer therapeutics. *Nat Rev Drug Discov*, 5, 997-1014.
- BARKER, N., RIDGWAY, R. A., VAN ES, J. H., VAN DE WETERING, M., BEGTHEL, H., VAN DEN BORN, M., DANENBERG, E., CLARKE, A. R., SANSOM, O. J. & CLEVERS, H. 2009. Crypt stem cells as the cells-of-origin of intestinal cancer. *Nature*, 457, 608-11.
- BARKER, N., VAN ES, J. H., KUIPERS, J., KUJALA, P., VAN DEN BORN, M., COZIJNSEN, M., HAEGEBARTH, A., KORVING, J., BEGTHEL, H., PETERS, P. J. & CLEVERS, H. 2007. Identification of stem cells in small intestine and colon by marker gene Lgr5. *Nature*, 449, 1003-7.
- BARR, P. J., OPPENHEIMER, N. J. & SANTI, D. V. 1983. Thymidylate synthetase-catalyzed conversions of E-5-(2-bromovinyl)-2'-deoxyuridylate. *J Biol Chem*, 258, 13627-31.
- BATLLE, E., HENDERSON, J. T., BEGTHEL, H., VAN DEN BORN, M. M., SANCHO, E., HULS, G., MEELDIJK, J., ROBERTSON, J., VAN DE WETERING, M., PAWSON, T. & CLEVERS, H. 2002. Beta-catenin and TCF mediate cell positioning in the intestinal epithelium by controlling the expression of EphB/ephrinB. *Cell*, 111, 251-63.
- BENDELL, J. C., NEMUNAITIS, J., VUKELJA, S. J., HAGENSTAD, C., CAMPOS, L. T., HERMANN, R. C., SPORTELLI, P., GARDNER, L. & RICHARDS, D. A. 2011. Randomized placebo-

- controlled phase II trial of perifosine plus capecitabine as second- or third-line therapy in patients with metastatic colorectal cancer. *J Clin Oncol*, 29, 4394-400.
- BENNECKE, M., KRIEGL, L., BAJBOUJ, M., RETZLAFF, K., ROBINE, S., JUNG, A., ARKAN, M. C., KIRCHNER, T. & GRETEN, F. R. 2010. Ink4a/Arf and oncogene-induced senescence prevent tumor progression during alternative colorectal tumorigenesis. *Cancer Cell*, 18, 135-46.
- BENVENUTI, S., SARTORE-BIANCHI, A., DI NICOLANTONIO, F., ZANON, C., MORONI, M., VERONESE, S., SIENA, S. & BARDELLI, A. 2007. Oncogenic activation of the RAS/RAF signaling pathway impairs the response of metastatic colorectal cancers to anti-epidermal growth factor receptor antibody therapies. *Cancer Res*, 67, 2643-8.
- BEPPU, H., MWIZERWA, O. N., BEPPU, Y., DATTWYLER, M. P., LAUWERS, G. Y., BLOCH, K. D. & GOLDSTEIN, A. M. 2008. Stromal inactivation of BMPRII leads to colorectal epithelial overgrowth and polyp formation. *Oncogene*, 27, 1063-70.
- BERGE, E., THOMPSON, C. & MESSERSMITH, W. 2011. Development of novel targeted agents in the treatment of metastatic colorectal cancer. *Clin Colorectal Cancer*, 10, 266-78.
- BERGERS, G. & BENJAMIN, L. E. 2003. Tumorigenesis and the angiogenic switch. *Nat Rev Cancer*, 3, 401-10.
- BERNDT, N., HAMILTON, A. D. & SEBTI, S. M. 2011. Targeting protein prenylation for cancer therapy. *Nat Rev Cancer*, 11, 775-91.
- BLASER, B., WASELLE, L., DORMOND-MEUWLY, A., DUFOUR, M., ROULIN, D., DEMARTINES, N. & DORMOND, O. 2012. Antitumor activities of ATP-competitive inhibitors of mTOR in colon cancer cells. *BMC Cancer*, 12, 86.
- BLUMENTHAL, G. M. & DENNIS, P. A. 2008. PTEN hamartoma tumor syndromes. *Eur J Hum Genet*, 16, 1289-300.
- BOEHM, T., FOLKMAN, J., BROWDER, T. & O'REILLY, M. S. 1997. Antiangiogenic therapy of experimental cancer does not induce acquired drug resistance. *Nature*, 390, 404-7.
- BOON, E. M., KELLER, J. J., WORMHOUDT, T. A., GIARDIELLO, F. M., OFFERHAUS, G. J., VAN DER NEUT, R. & PALS, S. T. 2004. Sulindac targets nuclear beta-catenin accumulation and Wnt signalling in adenomas of patients with familial adenomatous polyposis and in human colorectal cancer cell lines. *Br J Cancer*, 90, 224-9.
- BOS, J. L., FEARON, E. R., HAMILTON, S. R., VERLAAN-DE VRIES, M., VAN BOOM, J. H., VAN DER EB, A. J. & VOGELSTEIN, B. 1987. Prevalence of ras gene mutations in human colorectal cancers. *Nature*, 327, 293-7.
- BOURDIN, C., MCGUIGAN, C., BRANCALE, A., CHAMBERLAIN, S., VERNACHIO, J., HUTCHINS, J., GOROVITS, E., KOLYKHALOV, A., MUHAMMAD, J., PATTI, J., HENSON, G., BLEIMAN, B., BRYANT, K. D., GANGULY, B., HUNLEY, D., OBIKHOD, A., WALTERS, C. R., WANG, J., RAMAMURTY, C. V., BATTINA, S. K. & SRIVINAS RAO, C. 2013. Synthesis and evaluation against hepatitis C virus of 7-deaza analogues of 2'-C-methyl-6-O-methyl guanosine nucleoside and L-Alanine ester phosphoramidates. *Bioorg Med Chem Lett*, 23, 2260-4.
- BRACHO-VALDÉS, I., MORENO-ALVAREZ, P., VALENCIA-MARTÍNEZ, I., ROBLES-MOLINA, E., CHÁVEZ-VARGAS, L. & VÁZQUEZ-PRADO, J. 2011. mTORC1- and mTORC2-interacting proteins keep their multifunctional partners focused. *IUBMB Life*, 63, 896-914.
- BUNZ, F., HWANG, P. M., TORRANCE, C., WALDMAN, T., ZHANG, Y., DILLEHAY, L., WILLIAMS, J., LENGAUER, C., KINZLER, K. W. & VOGELSTEIN, B. 1999. Disruption of p53 in human cancer cells alters the responses to therapeutic agents. *J Clin Invest*, 104, 263-9.
- CANCER GENOME ATLAS NETWORK 2012. Comprehensive molecular characterization of human colon and rectal cancer. *Nature*, 487, 330-7.
- CANTLEY, L. C. 2002. The phosphoinositide 3-kinase pathway. *Science*, 296, 1655-7.
- CARPTEN, J. D., FABER, A. L., HORN, C., DONOHO, G. P., BRIGGS, S. L., ROBBINS, C. M., HOSTETTER, G., BOGUSLAWSKI, S., MOSES, T. Y., SAVAGE, S., UHLIK, M., LIN, A., DU, J., QIAN, Y. W., ZECKNER, D. J., TUCKER-KELLOGG, G., TOUCHMAN, J., PATEL, K.,

- MOUSSES, S., BITTNER, M., SCHEVITZ, R., LAI, M. H., BLANCHARD, K. L. & THOMAS, J. E. 2007. A transforming mutation in the pleckstrin homology domain of AKT1 in cancer. *Nature*, 448, 439-44.
- CARRACEDO, A., BASELGA, J. & PANDOLFI, P. P. 2008a. Deconstructing feedback-signaling networks to improve anticancer therapy with mTORC1 inhibitors. *Cell Cycle*, 7, 3805-9.
- CARRACEDO, A., MA, L., TERUYA-FELDSTEIN, J., ROJO, F., SALMENA, L., ALIMONTI, A., EGIA, A., SASAKI, A. T., THOMAS, G., KOZMA, S. C., PAPA, A., NARDELLA, C., CANTLEY, L. C., BASELGA, J. & PANDOLFI, P. P. 2008b. Inhibition of mTORC1 leads to MAPK pathway activation through a PI3K-dependent feedback loop in human cancer. *J Clin Invest*, 118, 3065-74.
- CHAUDHARY, A., KING, W. G., MATTALIANO, M. D., FROST, J. A., DIAZ, B., MORRISON, D. K., COBB, M. H., MARSHALL, M. S. & BRUGGE, J. S. 2000. Phosphatidylinositol 3-kinase regulates Raf1 through Pak phosphorylation of serine 338. *Curr Biol*, 10, 551-4.
- CHEN, B., DODGE, M. E., TANG, W., LU, J., MA, Z., FAN, C. W., WEI, S., HAO, W., KILGORE, J., WILLIAMS, N. S., ROTH, M. G., AMATRUDA, J. F., CHEN, C. & LUM, L. 2009. Small molecule-mediated disruption of Wnt-dependent signaling in tissue regeneration and cancer. *Nat Chem Biol*, 5, 100-7.
- CHEN, J., LI, Y., YU, T. S., MCKAY, R. M., BURNS, D. K., KERNIE, S. G. & PARADA, L. F. 2012a. A restricted cell population propagates glioblastoma growth after chemotherapy. *Nature*, 488, 522-6.
- CHEN, W. S., XU, P. Z., GOTTLÖB, K., CHEN, M. L., SOKOL, K., SHIYANOVA, T., RONINSON, I., WENG, W., SUZUKI, R., TOBE, K., KADOWAKI, T. & HAY, N. 2001. Growth retardation and increased apoptosis in mice with homozygous disruption of the Akt1 gene. *Genes Dev*, 15, 2203-8.
- CHEN, X. G., LIU, F., SONG, X. F., WANG, Z. H., DONG, Z. Q., HU, Z. Q., LAN, R. Z., GUAN, W., ZHOU, T. G., XU, X. M., LEI, H., YE, Z. Q., PENG, E. J., DU, L. H. & ZHUANG, Q. Y. 2010. Rapamycin regulates Akt and ERK phosphorylation through mTORC1 and mTORC2 signaling pathways. *Mol Carcinog*, 49, 603-10.
- CHEN, Z., CHENG, K., WALTON, Z., WANG, Y., EBI, H., SHIMAMURA, T., LIU, Y., TUPPER, T., OUYANG, J., LI, J., GAO, P., WOO, M. S., XU, C., YANAGITA, M., ALTABEF, A., WANG, S., LEE, C., NAKADA, Y., PEÑA, C. G., SUN, Y., FRANCHETTI, Y., YAO, C., SAUR, A., CAMERON, M. D., NISHINO, M., HAYES, D. N., WILKERSON, M. D., ROBERTS, P. J., LEE, C. B., BARDEESY, N., BUTANEY, M., CHIRIEAC, L. R., COSTA, D. B., JACKMAN, D., SHARPLESS, N. E., CASTRILLON, D. H., DEMETRI, G. D., JÄNNE, P. A., PANDOLFI, P. P., CANTLEY, L. C., KUNG, A. L., ENGELMAN, J. A. & WONG, K. K. 2012b. A murine lung cancer co-clinical trial identifies genetic modifiers of therapeutic response. *Nature*, 483, 613-7.
- CHENG, H. & LEBLOND, C. P. 1974. Origin, differentiation and renewal of the four main epithelial cell types in the mouse small intestine. V. Unitarian Theory of the origin of the four epithelial cell types. *Am J Anat*, 141, 537-61.
- CHU, E., KOELLER, D. M., JOHNSTON, P. G., ZINN, S. & ALLEGRA, C. J. 1993a. Regulation of thymidylate synthase in human colon cancer cells treated with 5-fluorouracil and interferon-gamma. *Mol Pharmacol*, 43, 527-33.
- CHU, E., VOELLER, D., KOELLER, D. M., DRAKE, J. C., TAKIMOTO, C. H., MALEY, G. F., MALEY, F. & ALLEGRA, C. J. 1993b. Identification of an RNA binding site for human thymidylate synthase. *Proc Natl Acad Sci U S A*, 90, 517-21.
- CIARDIELLO, F., KIM, N., SAEKI, T., DONO, R., PERSICO, M. G., PLOWMAN, G. D., GARRIGUES, J., RADKE, S., TODARO, G. J. & SALOMON, D. S. 1991. Differential expression of epidermal growth factor-related proteins in human colorectal tumors. *Proc Natl Acad Sci U S A*, 88, 7792-6.

- CLAIJ, N. & TE RIELE, H. 1999. Microsatellite instability in human cancer: a prognostic marker for chemotherapy? *Exp Cell Res*, 246, 1-10.
- CLARKE, A. R., CUMMINGS, M. C. & HARRISON, D. J. 1995. Interaction between murine germline mutations in p53 and APC predisposes to pancreatic neoplasia but not to increased intestinal malignancy. *Oncogene*, 11, 1913-20.
- CLEVERS, H. 2006. Wnt/beta-catenin signaling in development and disease. *Cell*, 127, 469-80.
- COHEN, P. & FRAME, S. 2001. The renaissance of GSK3. *Nat Rev Mol Cell Biol*, 2, 769-76.
- COHEN, Y., XING, M., MAMBO, E., GUO, Z., WU, G., TRINK, B., BELLER, U., WESTRA, W. H., LADENSON, P. W. & SIDRANSKY, D. 2003. BRAF mutation in papillary thyroid carcinoma. *J Natl Cancer Inst*, 95, 625-7.
- COOPER, M. K., PORTER, J. A., YOUNG, K. E. & BEACHY, P. A. 1998. Teratogen-mediated inhibition of target tissue response to Shh signaling. *Science*, 280, 1603-7.
- CORCORAN, R. B., CHENG, K. A., HATA, A. N., FABER, A. C., EBI, H., COFFEE, E. M., GRENINGER, P., BROWN, R. D., GODFREY, J. T., COHOON, T. J., SONG, Y., LIFSHITS, E., HUNG, K. E., SHIODA, T., DIAS-SANTAGATA, D., SINGH, A., SETTLEMAN, J., BENES, C. H., MINO-KENUDSON, M., WONG, K. K. & ENGELMAN, J. A. 2013. Synthetic lethal interaction of combined BCL-XL and MEK inhibition promotes tumor regressions in KRAS mutant cancer models. *Cancer Cell*, 23, 121-8.
- CORCORAN, R. B., EBI, H., TURKE, A. B., COFFEE, E. M., NISHINO, M., COGDILL, A. P., BROWN, R. D., DELLA PELLE, P., DIAS-SANTAGATA, D., HUNG, K. E., FLAHERTY, K. T., PIRIS, A., WARGO, J. A., SETTLEMAN, J., MINO-KENUDSON, M. & ENGELMAN, J. A. 2012. EGFR-mediated re-activation of MAPK signaling contributes to insensitivity of BRAF mutant colorectal cancers to RAF inhibition with vemurafenib. *Cancer Discov*, 2, 227-35.
- COUSSENS, L. M. & WERB, Z. 2002. Inflammation and cancer. *Nature*, 420, 860-7.
- CREAMER, B. 1967. The turnover of the epithelium of the small intestine. *Br Med Bull*, 23, 226-30.
- DACHS, G. U., TUPPER, J. & TOZER, G. M. 2005. From bench to bedside for gene-directed enzyme prodrug therapy of cancer. *Anticancer Drugs*, 16, 349-59.
- DALERBA, P., DYLLA, S. J., PARK, I. K., LIU, R., WANG, X., CHO, R. W., HOEY, T., GURNEY, A., HUANG, E. H., SIMEONE, D. M., SHELTON, A. A., PARMIANI, G., CASTELLI, C. & CLARKE, M. F. 2007. Phenotypic characterization of human colorectal cancer stem cells. *Proc Natl Acad Sci U S A*, 104, 10158-63.
- DANCEY, J. E. & CHEN, H. X. 2006. Strategies for optimizing combinations of molecularly targeted anticancer agents. *Nat Rev Drug Discov*, 5, 649-59.
- DANIEL, V. C., MARCHIONNI, L., HIERMAN, J. S., RHODES, J. T., DEVEREUX, W. L., RUDIN, C. M., YUNG, R., PARMIGIANI, G., DORSCH, M., PEACOCK, C. D. & WATKINS, D. N. 2009. A primary xenograft model of small-cell lung cancer reveals irreversible changes in gene expression imposed by culture in vitro. *Cancer Res*, 69, 3364-73.
- DAVIES, E., MARSH, V., MENIEL, V., WILLIAMS, G. & CLARKE, A. *in press*. Pten loss and Kras mutation predisposes to metastatic carcinoma of the murine small intestine.
- DAVIES, H., BIGNELL, G. R., COX, C., STEPHENS, P., EDKINS, S., CLEGG, S., TEAGUE, J., WOFFENDIN, H., GARNETT, M. J., BOTTOMLEY, W., DAVIS, N., DICKS, E., EWING, R., FLOYD, Y., GRAY, K., HALL, S., HAWES, R., HUGHES, J., KOSMIDOU, V., MENZIES, A., MOULD, C., PARKER, A., STEVENS, C., WATT, S., HOOPER, S., WILSON, R., JAYATILAKE, H., GUSTERSON, B. A., COOPER, C., SHIPLEY, J., HARGRAVE, D., PRITCHARD-JONES, K., MAITLAND, N., CHENEVIX-TRENCH, G., RIGGINS, G. J., BIGNER, D. D., PALMIERI, G., COSSU, A., FLANAGAN, A., NICHOLSON, A., HO, J. W., LEUNG, S. Y., YUEN, S. T., WEBER, B. L., SEIGLER, H. F., DARROW, T. L., PATERSON, H., MARAIS, R., MARSHALL, C. J., WOOSTER, R., STRATTON, M. R. & FUTREAL, P. A. 2002. Mutations of the BRAF gene in human cancer. *Nature*, 417, 949-54.

- DE LA CHAPELLE, A. 2004. Genetic predisposition to colorectal cancer. *Nat Rev Cancer*, 4, 769-80.
- DE LA COSTE, A., ROMAGNOLO, B., BILLUART, P., RENARD, C. A., BUENDIA, M. A., SOUBRANE, O., FABRE, M., CHELLY, J., BELDJORD, C., KAHN, A. & PERRET, C. 1998. Somatic mutations of the beta-catenin gene are frequent in mouse and human hepatocellular carcinomas. *Proc Natl Acad Sci U S A*, 95, 8847-51.
- DE RAEDT, T., WALTON, Z., YECIES, J. L., LI, D., CHEN, Y., MALONE, C. F., MAERTENS, O., JEONG, S. M., BRONSON, R. T., LEBLEU, V., KALLURI, R., NORMANT, E., HAIGIS, M. C., MANNING, B. D., WONG, K. K., MACLEOD, K. F. & CICHOWSKI, K. 2011. Exploiting cancer cell vulnerabilities to develop a combination therapy for ras-driven tumors. *Cancer Cell*, 20, 400-13.
- DECAUDIN, D. 2011. Primary human tumor xenografted models ('tumorgrafts') for good management of patients with cancer. *Anticancer Drugs*, 22, 827-41.
- DI NICOLANTONIO, F., MARTINI, M., MOLINARI, F., SARTORE-BIANCHI, A., ARENA, S., SALETTI, P., DE DOSSO, S., MAZZUCHELLI, L., FRATTINI, M., SIENA, S. & BARDELLI, A. 2008. Wild-type BRAF is required for response to panitumumab or cetuximab in metastatic colorectal cancer. *J Clin Oncol*, 26, 5705-12.
- DIASIO, R. B. & JOHNSON, M. R. 1999. Dihydropyrimidine dehydrogenase: its role in 5-fluorouracil clinical toxicity and tumor resistance. *Clin Cancer Res*, 5, 2672-3.
- DIAZ, L. A., WILLIAMS, R. T., WU, J., KINDE, I., HECHT, J. R., BERLIN, J., ALLEN, B., BOZIC, I., REITER, J. G., NOWAK, M. A., KINZLER, K. W., OLINER, K. S. & VOGELSTEIN, B. 2012. The molecular evolution of acquired resistance to targeted EGFR blockade in colorectal cancers. *Nature*, 486, 537-40.
- DIHLMANN, S., SIERMANN, A. & VON KNEBEL DOEBERITZ, M. 2001. The nonsteroidal anti-inflammatory drugs aspirin and indomethacin attenuate beta-catenin/TCF-4 signaling. *Oncogene*, 20, 645-53.
- DOETSCHMAN, T., GREGG, R. G., MAEDA, N., HOOPER, M. L., MELTON, D. W., THOMPSON, S. & SMITHIES, O. 1987. Targetted correction of a mutant HPRT gene in mouse embryonic stem cells. *Nature*, 330, 576-8.
- DOUILLARD, J. Y. & GROUP, V.-S. 2000. Irinotecan and high-dose fluorouracil/leucovorin for metastatic colorectal cancer. *Oncology (Williston Park)*, 14, 51-5.
- DOWNWARD, J. 2003. Targeting RAS signalling pathways in cancer therapy. *Nat Rev Cancer*, 3, 11-22.
- DRIESSENS, G., BECK, B., CAAUWE, A., SIMONS, B. D. & BLANPAIN, C. 2012. Defining the mode of tumour growth by clonal analysis. *Nature*, 488, 527-30.
- DRY, J. R., PAVEY, S., PRATILAS, C. A., HARBRON, C., RUNSWICK, S., HODGSON, D., CHRESTA, C., MCCORMACK, R., BYRNE, N., COCKERILL, M., GRAHAM, A., BERAN, G., CASSIDY, A., HAGGERTY, C., BROWN, H., ELLISON, G., DERING, J., TAYLOR, B. S., STARK, M., BONAZZI, V., RAVISHANKAR, S., PACKER, L., XING, F., SOLIT, D. B., FINN, R. S., ROSEN, N., HAYWARD, N. K., FRENCH, T. & SMITH, P. D. 2010. Transcriptional pathway signatures predict MEK addiction and response to selumetinib (AZD6244). *Cancer Res*, 70, 2264-73.
- DYMECKI, S. M. 1996. Flp recombinase promotes site-specific DNA recombination in embryonic stem cells and transgenic mice. *Proc Natl Acad Sci U S A*, 93, 6191-6.
- EBI, H., CORCORAN, R. B., SINGH, A., CHEN, Z., SONG, Y., LIFSHITS, E., RYAN, D. P., MEYERHARDT, J. A., BENES, C., SETTLEMAN, J., WONG, K. K., CANTLEY, L. C. & ENGELMAN, J. A. 2011. Receptor tyrosine kinases exert dominant control over PI3K signaling in human KRAS mutant colorectal cancers. *J Clin Invest*, 121, 4311-21.
- ECHELARD, Y., EPSTEIN, D. J., ST-JACQUES, B., SHEN, L., MOHLER, J., MCMAHON, J. A. & MCMAHON, A. P. 1993. Sonic hedgehog, a member of a family of putative signaling molecules, is implicated in the regulation of CNS polarity. *Cell*, 75, 1417-30.

- EDLER, D., BLOMGREN, H., ALLEGRA, C. J., JOHNSTON, P. G., LAGERSTEDT, U., MAGNUSSON, I. & RAGNHAMMAR, P. 1997. Immunohistochemical determination of thymidylate synthase in colorectal cancer--methodological studies. *Eur J Cancer*, 33, 2278-81.
- EL MARJOU, F., JANSSEN, K. P., CHANG, B. H., LI, M., HINDIE, V., CHAN, L., LOUVARD, D., CHAMBON, P., METZGER, D. & ROBINE, S. 2004. Tissue-specific and inducible Cre-mediated recombination in the gut epithelium. *Genesis*, 39, 186-93.
- EMAMI, K. H., NGUYEN, C., MA, H., KIM, D. H., JEONG, K. W., EGUCHI, M., MOON, R. T., TEO, J. L., OH, S. W., KIM, H. Y., MOON, S. H., HA, J. R. & KAHN, M. 2004. A small molecule inhibitor of beta-catenin/CREB-binding protein transcription [corrected]. *Proc Natl Acad Sci U S A*, 101, 12682-7.
- END, D. W., SMETS, G., TODD, A. V., APPLGATE, T. L., FUERY, C. J., ANGIBAUD, P., VENET, M., SANZ, G., POIGNET, H., SKRZAT, S., DEVINE, A., WOUTERS, W. & BOWDEN, C. 2001. Characterization of the antitumor effects of the selective farnesyl protein transferase inhibitor R115777 in vivo and in vitro. *Cancer Res*, 61, 131-7.
- ENGELMAN, J. A. 2009. Targeting PI3K signalling in cancer: opportunities, challenges and limitations. *Nat Rev Cancer*, 9, 550-62.
- ENGELMAN, J. A., CHEN, L., TAN, X., CROSBY, K., GUIMARAES, A. R., UPADHYAY, R., MAIRA, M., MCNAMARA, K., PERERA, S. A., SONG, Y., CHIRIEAC, L. R., KAUR, R., LIGHTBOWN, A., SIMENDINGER, J., LI, T., PADERA, R. F., GARCÍA-ECHEVERRÍA, C., WEISSLEDER, R., MAHMOOD, U., CANTLEY, L. C. & WONG, K. K. 2008. Effective use of PI3K and MEK inhibitors to treat mutant Kras G12D and PIK3CA H1047R murine lung cancers. *Nat Med*, 14, 1351-6.
- ENGELMAN, J. A., LUO, J. & CANTLEY, L. C. 2006. The evolution of phosphatidylinositol 3-kinases as regulators of growth and metabolism. *Nat Rev Genet*, 7, 606-19.
- ETTMAYER, P., AMIDON, G. L., CLEMENT, B. & TESTA, B. 2004. Lessons learned from marketed and investigational prodrugs. *J Med Chem*, 47, 2393-404.
- EVANS, M. J. & KAUFMAN, M. H. 1981. Establishment in culture of pluripotential cells from mouse embryos. *Nature*, 292, 154-6.
- EVRARD, A., CUQ, P., CICCOLINI, J., VIAN, L. & CANO, J. P. 1999. Increased cytotoxicity and bystander effect of 5-fluorouracil and 5-deoxy-5-fluorouridine in human colorectal cancer cells transfected with thymidine phosphorylase. *Br J Cancer*, 80, 1726-33.
- FALCHOOK, G. S., LONG, G. V., KURZROCK, R., KIM, K. B., ARKENAU, T. H., BROWN, M. P., HAMID, O., INFANTE, J. R., MILLWARD, M., PAVLICK, A. C., O'DAY, S. J., BLACKMAN, S. C., CURTIS, C. M., LEBOWITZ, P., MA, B., OUELLET, D. & KEFFORD, R. F. 2012. Dabrafenib in patients with melanoma, untreated brain metastases, and other solid tumours: a phase 1 dose-escalation trial. *Lancet*, 379, 1893-901.
- FALCON, B. L., BARR, S., GOKHALE, P. C., CHOU, J., FOGARTY, J., DEPEILLE, P., MIGLARESE, M., EPSTEIN, D. M. & MCDONALD, D. M. 2011. Reduced VEGF production, angiogenesis, and vascular regrowth contribute to the antitumor properties of dual mTORC1/mTORC2 inhibitors. *Cancer Res*, 71, 1573-83.
- FAZELI, A., DICKINSON, S. L., HERMISTON, M. L., TIGHE, R. V., STEEN, R. G., SMALL, C. G., STOECKLI, E. T., KEINO-MASU, K., MASU, M., RAYBURN, H., SIMONS, J., BRONSON, R. T., GORDON, J. I., TESSIER-LAVIGNE, M. & WEINBERG, R. A. 1997. Phenotype of mice lacking functional Deleted in colorectal cancer (Dcc) gene. *Nature*, 386, 796-804.
- FEARNHEAD, N. S., WILDING, J. L. & BODMER, W. F. 2002. Genetics of colorectal cancer: hereditary aspects and overview of colorectal tumorigenesis. *Br Med Bull*, 64, 27-43.
- FEARON, E. R., CHO, K. R., NIGRO, J. M., KERN, S. E., SIMONS, J. W., RUPPERT, J. M., HAMILTON, S. R., PREISINGER, A. C., THOMAS, G. & KINZLER, K. W. 1990. Identification of a chromosome 18q gene that is altered in colorectal cancers. *Science*, 247, 49-56.
- FEARON, E. R. & VOGELSTEIN, B. 1990. A genetic model for colorectal tumorigenesis. *Cell*, 61, 759-67.

- FEIL, R., WAGNER, J., METZGER, D. & CHAMBON, P. 1997. Regulation of Cre recombinase activity by mutated estrogen receptor ligand-binding domains. *Biochem Biophys Res Commun*, 237, 752-7.
- FODDE, R., SMITS, R. & CLEVERS, H. 2001. APC, signal transduction and genetic instability in colorectal cancer. *Nat Rev Cancer*, 1, 55-67.
- FOUKAS, L. C., CLARET, M., PEARCE, W., OKKENHAUG, K., MEEK, S., PESKETT, E., SANCHO, S., SMITH, A. J., WITHERS, D. J. & VANHAESEBROECK, B. 2006. Critical role for the p110alpha phosphoinositide-3-OH kinase in growth and metabolic regulation. *Nature*, 441, 366-70.
- FRATTINI, M., SALETTI, P., ROMAGNANI, E., MARTIN, V., MOLINARI, F., GHISLETTA, M., CAMPONOV, A., ETIENNE, L. L., CAVALLI, F. & MAZZUCHELLI, L. 2007. PTEN loss of expression predicts cetuximab efficacy in metastatic colorectal cancer patients. *Br J Cancer*, 97, 1139-45.
- FRE, S., HUYGHE, M., MOURIKIS, P., ROBINE, S., LOUVARD, D. & ARTAVANIS-TSAKONAS, S. 2005. Notch signals control the fate of immature progenitor cells in the intestine. *Nature*, 435, 964-8.
- FUCHS, E., TUMBAR, T. & GUASCH, G. 2004. Socializing with the neighbors: stem cells and their niche. *Cell*, 116, 769-78.
- GALMARINI, C. M., MACKEY, J. R. & DUMONTET, C. 2001. Nucleoside analogues: mechanisms of drug resistance and reversal strategies. *Leukemia*, 15, 875-90.
- GARCIA-ECHEVERRIA, C. & SELLERS, W. R. 2008. Drug discovery approaches targeting the PI3K/Akt pathway in cancer. *Oncogene*, 27, 5511-26.
- GERBE, F., BRULIN, B., MAKRINI, L., LEGRAVEREND, C. & JAY, P. 2009. DCAMKL-1 expression identifies Tuft cells rather than stem cells in the adult mouse intestinal epithelium. *Gastroenterology*, 137, 2179-80; author reply 2180-1.
- GERBE, F., VAN ES, J. H., MAKRINI, L., BRULIN, B., MELLITZER, G., ROBINE, S., ROMAGNOLO, B., SHROYER, N. F., BOURGAUX, J. F., PIGNODEL, C., CLEVERS, H. & JAY, P. 2011. Distinct ATOH1 and Neurog3 requirements define tuft cells as a new secretory cell type in the intestinal epithelium. *J Cell Biol*, 192, 767-80.
- GIACCHETTI, S., PERPOINT, B., ZIDANI, R., LE BAIL, N., FAGGIUOLO, R., FOCAN, C., CHOLLET, P., LLORY, J. F., LETOURNEAU, Y., COUDERT, B., BERTHEAUT-CVITKOVIC, F., LARREGAIN-FOURNIER, D., LE ROL, A., WALTER, S., ADAM, R., MISSET, J. L. & LÉVI, F. 2000. Phase III multicenter randomized trial of oxaliplatin added to chronomodulated fluorouracil-leucovorin as first-line treatment of metastatic colorectal cancer. *J Clin Oncol*, 18, 136-47.
- GILBERT, L. A. & HEMANN, M. T. 2010. DNA damage-mediated induction of a chemoresistant niche. *Cell*, 143, 355-66.
- GLAZER, R. I. & LLOYD, L. S. 1982. Association of cell lethality with incorporation of 5-fluorouracil and 5-fluorouridine into nuclear RNA in human colon carcinoma cells in culture. *Mol Pharmacol*, 21, 468-73.
- GLUSKER, P., RECHT, L. & LANE, B. 2006. Reversible posterior leukoencephalopathy syndrome and bevacizumab. *N Engl J Med*, 354, 980-2; discussion 980-2.
- GOSSEN, M. & BUJARD, H. 1992. Tight control of gene expression in mammalian cells by tetracycline-responsive promoters. *Proc Natl Acad Sci U S A*, 89, 5547-51.
- GREGORIEFF, A., PINTO, D., BEGTHEL, H., DESTREÉ, O., KIELMAN, M. & CLEVERS, H. 2005. Expression pattern of Wnt signaling components in the adult intestine. *Gastroenterology*, 129, 626-38.
- GROSSMANN, J., WALTHER, K., ARTINGER, M., RÜMMELE, P., WOENCKHAUS, M. & SCHÖLMERICH, J. 2002. Induction of apoptosis before shedding of human intestinal epithelial cells. *Am J Gastroenterol*, 97, 1421-8.

- GROTHEY, A. & GOLDBERG, R. M. 2004. A review of oxaliplatin and its clinical use in colorectal cancer. *Expert Opin Pharmacother*, 5, 2159-70.
- GSCHWIND, A., FISCHER, O. M. & ULLRICH, A. 2004. The discovery of receptor tyrosine kinases: targets for cancer therapy. *Nat Rev Cancer*, 4, 361-70.
- GUARNER, F. & MALAGELADA, J. R. 2003. Gut flora in health and disease. *Lancet*, 361, 512-9.
- GUERTIN, D. A., STEVENS, D. M., THOREEN, C. C., BURDS, A. A., KALAANY, N. Y., MOFFAT, J., BROWN, M., FITZGERALD, K. J. & SABATINI, D. M. 2006. Ablation in mice of the mTORC components raptor, rictor, or mLST8 reveals that mTORC2 is required for signaling to Akt-FOXO and PKC α , but not S6K1. *Dev Cell*, 11, 859-71.
- GUIJARRO-MUÑOZ, I., SÁNCHEZ, A., MARTÍNEZ-MARTÍNEZ, E., GARCÍA, J. M., SALAS, C., PROVENCIO, M., ALVAREZ-VALLINA, L. & SANZ, L. 2013. Gene expression profiling identifies EPHB4 as a potential predictive biomarker in colorectal cancer patients treated with bevacizumab. *Med Oncol*, 30, 572.
- H, M. F. 2006. Fundamentals of Anatomy & Physiology. 7th ed.: Pearson.
- HAAGENSEN, E. J., KYLE, S., BEALE, G. S., MAXWELL, R. J. & NEWELL, D. R. 2012. The synergistic interaction of MEK and PI3K inhibitors is modulated by mTOR inhibition. *Br J Cancer*, 106, 1386-94.
- HALILOVIC, E., SHE, Q. B., YE, Q., PAGLIARINI, R., SELLERS, W. R., SOLIT, D. B. & ROSEN, N. 2010. PIK3CA mutation uncouples tumor growth and cyclin D1 regulation from MEK/ERK and mutant KRAS signaling. *Cancer Res*, 70, 6804-14.
- HALL, P. A., COATES, P. J., ANSARI, B. & HOPWOOD, D. 1994. Regulation of cell number in the mammalian gastrointestinal tract: the importance of apoptosis. *J Cell Sci*, 107 (Pt 12), 3569-77.
- HARADA, N., TAMAI, Y., ISHIKAWA, T., SAUER, B., TAKAKU, K., OSHIMA, M. & TAKETO, M. M. 1999. Intestinal polyposis in mice with a dominant stable mutation of the beta-catenin gene. *EMBO J*, 18, 5931-42.
- HARAMIS, A. P., BEGTHEL, H., VAN DEN BORN, M., VAN ES, J., JONKHEER, S., OFFERHAUS, G. J. & CLEVERS, H. 2004. De novo crypt formation and juvenile polyposis on BMP inhibition in mouse intestine. *Science*, 303, 1684-6.
- HARRINGTON, L. S., FINDLAY, G. M. & LAMB, R. F. 2005. Restraining PI3K: mTOR signalling goes back to the membrane. *Trends Biochem Sci*, 30, 35-42.
- HAYSTEAD, T. A., DENT, P., WU, J., HAYSTEAD, C. M. & STURGILL, T. W. 1992. Ordered phosphorylation of p42mapk by MAP kinase kinase. *FEBS Lett*, 306, 17-22.
- HE, B., BARG, R. N., YOU, L., XU, Z., REGUART, N., MIKAMI, I., BATRA, S., ROSELL, R. & JABLONS, D. M. 2005a. Wnt signaling in stem cells and non-small-cell lung cancer. *Clin Lung Cancer*, 7, 54-60.
- HE, B., REGUART, N., YOU, L., MAZIERES, J., XU, Z., LEE, A. Y., MIKAMI, I., MCCORMICK, F. & JABLONS, D. M. 2005b. Blockade of Wnt-1 signaling induces apoptosis in human colorectal cancer cells containing downstream mutations. *Oncogene*, 24, 3054-8.
- HE, B., YOU, L., UEMATSU, K., XU, Z., LEE, A. Y., MATSANGOU, M., MCCORMICK, F. & JABLONS, D. M. 2004a. A monoclonal antibody against Wnt-1 induces apoptosis in human cancer cells. *Neoplasia*, 6, 7-14.
- HE, S., NAKADA, D. & MORRISON, S. J. 2009. Mechanisms of stem cell self-renewal. *Annu Rev Cell Dev Biol*, 25, 377-406.
- HE, X. C., ZHANG, J., TONG, W. G., TAWFIK, O., ROSS, J., SCOVILLE, D. H., TIAN, Q., ZENG, X., HE, X., WIEDEMANN, L. M., MISHINA, Y. & LI, L. 2004b. BMP signaling inhibits intestinal stem cell self-renewal through suppression of Wnt-beta-catenin signaling. *Nat Genet*, 36, 1117-21.
- HERNLUND, E., OLOFSSON, M. H., FAYAD, W., FRYKNÄS, M., LESIAK-MIECZKOWSKA, K., ZHANG, X., BRNJIC, S., SCHMIDT, V., D'ARCY, P., SJÖBLOM, T., DE MILITO, A., LARSSON, R. & LINDER, S. 2012. The phosphoinositide 3-kinase/mammalian target of rapamycin

- inhibitor NVP-BEZ235 is effective in inhibiting regrowth of tumour cells after cytotoxic therapy. *Eur J Cancer*, 48, 396-406.
- HOFMANN, I., WEISS, A., ELAIN, G., SCHWAEDERLE, M., STERKER, D., ROMANET, V., SCHMELZLE, T., LAI, A., BRACHMANN, S. M., BENTIREN-ALJ, M., ROBERTS, T. M., SELLERS, W. R., HOFMANN, F. & MAIRA, S. M. 2012. K-RAS mutant pancreatic tumors show higher sensitivity to MEK than to PI3K inhibition in vivo. *PLoS One*, 7, e44146.
- HOLMGREN, L., O'REILLY, M. S. & FOLKMAN, J. 1995. Dormancy of micrometastases: balanced proliferation and apoptosis in the presence of angiogenesis suppression. *Nat Med*, 1, 149-53.
- HOLT, S. V., LOGIE, A., DAVIES, B. R., ALFEREZ, D., RUNSWICK, S., FENTON, S., CHRESTA, C. M., GU, Y., ZHANG, J., WU, Y. L., WILKINSON, R. W., GUICHARD, S. M. & SMITH, P. D. 2012. Enhanced apoptosis and tumor growth suppression elicited by combination of MEK (selumetinib) and mTOR kinase inhibitors (AZD8055). *Cancer Res*, 72, 1804-13.
- HORIE, Y., SUZUKI, A., KATAOKA, E., SASAKI, T., HAMADA, K., SASAKI, J., MIZUNO, K., HASEGAWA, G., KISHIMOTO, H., IIZUKA, M., NAITO, M., ENOMOTO, K., WATANABE, S., MAK, T. W. & NAKANO, T. 2004. Hepatocyte-specific Pten deficiency results in steatohepatitis and hepatocellular carcinomas. *J Clin Invest*, 113, 1774-83.
- HOWE, J. R., ROTH, S., RINGOLD, J. C., SUMMERS, R. W., JÄRVINEN, H. J., SISTONEN, P., TOMLINSON, I. P., HOULSTON, R. S., BEVAN, S., MITROS, F. A., STONE, E. M. & AALTONEN, L. A. 1998. Mutations in the SMAD4/DPC4 gene in juvenile polyposis. *Science*, 280, 1086-8.
- HUANG, E. H., HYNES, M. J., ZHANG, T., GINESTIER, C., DONTU, G., APPELMAN, H., FIELDS, J. Z., WICHA, M. S. & BOMAN, B. M. 2009a. Aldehyde dehydrogenase 1 is a marker for normal and malignant human colonic stem cells (SC) and tracks SC overpopulation during colon tumorigenesis. *Cancer Res*, 69, 3382-9.
- HUANG, S. M., MISHINA, Y. M., LIU, S., CHEUNG, A., STEGMEIER, F., MICHAUD, G. A., CHARLAT, O., WIELLETTE, E., ZHANG, Y., WIESSNER, S., HILD, M., SHI, X., WILSON, C. J., MICKANIN, C., MYER, V., FAZAL, A., TOMLINSON, R., SERLUCA, F., SHAO, W., CHENG, H., SHULTZ, M., RAU, C., SCHIRLE, M., SCHLEGL, J., GHIDELLI, S., FAWELL, S., LU, C., CURTIS, D., KIRSCHNER, M. W., LENGAUER, C., FINAN, P. M., TALLARICO, J. A., BOUWMEESTER, T., PORTER, J. A., BAUER, A. & CONG, F. 2009b. Tankyrase inhibition stabilizes axin and antagonizes Wnt signalling. *Nature*, 461, 614-20.
- HUYNH, H., CHOW, P. K. & SOO, K. C. 2007a. AZD6244 and doxorubicin induce growth suppression and apoptosis in mouse models of hepatocellular carcinoma. *Mol Cancer Ther*, 6, 2468-76.
- HUYNH, H., SOO, K. C., CHOW, P. K. & TRAN, E. 2007b. Targeted inhibition of the extracellular signal-regulated kinase kinase pathway with AZD6244 (ARRY-142886) in the treatment of hepatocellular carcinoma. *Mol Cancer Ther*, 6, 138-46.
- HYNES, N. E. & LANE, H. A. 2005. ERBB receptors and cancer: the complexity of targeted inhibitors. *Nat Rev Cancer*, 5, 341-54.
- IACOPETTA, B., RUSSO, A., BAZAN, V., DARDANONI, G., GEBBIA, N., SOUSSI, T., KERR, D., ELSALEH, H., SOONG, R., KANDIOLER, D., JANSCHKE, E., KAPPEL, S., LUNG, M., LEUNG, C. S., KO, J. M., YUEN, S., HO, J., LEUNG, S. Y., CRAPEZ, E., DUFFOUR, J., YCHOU, M., LEAHY, D. T., O'DONOGHUE, D. P., AGNESE, V., CASCIO, S., DI FEDE, G., CHIECOBIANCHI, L., BERTORELLE, R., BELLUCO, C., GIARETTI, W., CASTAGNOLA, P., RICEVUTO, E., FICORELLA, C., BOSARI, S., ARIZZI, C. D., MIYAKI, M., ONDA, M., KAMPMAN, E., DIERGAARDE, B., ROYDS, J., LOTHE, R. A., DIEP, C. B., MELING, G. I., OSTROWSKI, J., TRZECIAK, L., GUZINSKA-USTYMOWICZ, K., ZALEWSKI, B., CAPELLÁ, G. M., MORENO, V., PEINADO, M. A., LÖNNROTH, C., LUNDHOLM, K., SUN, X. F., JANSSON, A., BOUZOURENE, H., HSIEH, L. L., TANG, R., SMITH, D. R., ALLEN-MERSH, T. G., KHAN, Z. A., SHORTHOUSE, A. J., SILVERMAN, M. L., KATO, S., ISHIOKA, C. & GROUP, T.-C. C.

2006. Functional categories of TP53 mutation in colorectal cancer: results of an International Collaborative Study. *Ann Oncol*, 17, 842-7.
- IKENOUE, T., HIKIBA, Y., KANAI, F., TANAKA, Y., IMAMURA, J., IMAMURA, T., OHTA, M., IJICHI, H., TATEISHI, K., KAWAKAMI, T., ARAGAKI, J., MATSUMURA, M., KAWABE, T. & OMATA, M. 2003. Functional analysis of mutations within the kinase activation segment of B-Raf in human colorectal tumors. *Cancer Res*, 63, 8132-7.
- IRELAND, H., KEMP, R., HOUGHTON, C., HOWARD, L., CLARKE, A. R., SANSOM, O. J. & WINTON, D. J. 2004. Inducible Cre-mediated control of gene expression in the murine gastrointestinal tract: effect of loss of beta-catenin. *Gastroenterology*, 126, 1236-46.
- JACINTO, E., FACCHINETTI, V., LIU, D., SOTO, N., WEI, S., JUNG, S. Y., HUANG, Q., QIN, J. & SU, B. 2006. SIN1/MIP1 maintains rictor-mTOR complex integrity and regulates Akt phosphorylation and substrate specificity. *Cell*, 127, 125-37.
- JANSSEN, K. P., ALBERICI, P., FSIHI, H., GASPAR, C., BREUKEL, C., FRANKEN, P., ROSTY, C., ABAL, M., EL MARJOU, F., SMITS, R., LOUVARD, D., FODDE, R. & ROBINE, S. 2006. APC and oncogenic KRAS are synergistic in enhancing Wnt signaling in intestinal tumor formation and progression. *Gastroenterology*, 131, 1096-109.
- JENSEN, J., PEDERSEN, E. E., GALANTE, P., HALD, J., HELLER, R. S., ISHIBASHI, M., KAGEYAMA, R., GUILLEMOT, F., SERUP, P. & MADSEN, O. D. 2000. Control of endodermal endocrine development by Hes-1. *Nat Genet*, 24, 36-44.
- JIA, S., LIU, Z., ZHANG, S., LIU, P., ZHANG, L., LEE, S. H., ZHANG, J., SIGNORETTI, S., LODA, M., ROBERTS, T. M. & ZHAO, J. J. 2008. Essential roles of PI(3)K-p110beta in cell growth, metabolism and tumorigenesis. *Nature*, 454, 776-9.
- JIANG, Y., PRUNIER, C. & HOWE, P. H. 2008. The inhibitory effects of Disabled-2 (Dab2) on Wnt signaling are mediated through Axin. *Oncogene*, 27, 1865-75.
- JIN, K., TENG, L., SHEN, Y., HE, K., XU, Z. & LI, G. 2010. Patient-derived human tumour tissue xenografts in immunodeficient mice: a systematic review. *Clin Transl Oncol*, 12, 473-80.
- JING, J., GRESHOCK, J., HOLBROOK, J. D., GILMARTIN, A., ZHANG, X., MCNEIL, E., CONWAY, T., MOY, C., LAQUERRE, S., BACHMAN, K., WOOSTER, R. & DEGENHARDT, Y. 2012. Comprehensive predictive biomarker analysis for MEK inhibitor GSK1120212. *Mol Cancer Ther*, 11, 720-9.
- JOHNSON, G. L. & LAPADAT, R. 2002. Mitogen-activated protein kinase pathways mediated by ERK, JNK, and p38 protein kinases. *Science*, 298, 1911-2.
- JOHNSON, M. R., HAGEBOUTROS, A., WANG, K., HIGH, L., SMITH, J. B. & DIASIO, R. B. 1999. Life-threatening toxicity in a dihydropyrimidine dehydrogenase-deficient patient after treatment with topical 5-fluorouracil. *Clin Cancer Res*, 5, 2006-11.
- JOHNSON, S. C., RABINOVITCH, P. S. & KAEBERLEIN, M. 2013. mTOR is a key modulator of ageing and age-related disease. *Nature*, 493, 338-45.
- JOHNSTON, P. G., DRAKE, J. C., TREPEL, J. & ALLEGRA, C. J. 1992. Immunological quantitation of thymidylate synthase using the monoclonal antibody TS 106 in 5-fluorouracil-sensitive and -resistant human cancer cell lines. *Cancer Res*, 52, 4306-12.
- JOHNSTON, P. G. & KAYE, S. 2001. Capecitabine: a novel agent for the treatment of solid tumors. *Anticancer Drugs*, 12, 639-46.
- JOHNSTON, P. G., LENZ, H. J., LEICHMAN, C. G., DANENBERG, K. D., ALLEGRA, C. J., DANENBERG, P. V. & LEICHMAN, L. 1995. Thymidylate synthase gene and protein expression correlate and are associated with response to 5-fluorouracil in human colorectal and gastric tumors. *Cancer Res*, 55, 1407-12.
- JONKER, D. J., O'CALLAGHAN, C. J., KARAPETIS, C. S., ZALCBERG, J. R., TU, D., AU, H. J., BERRY, S. R., KRAHN, M., PRICE, T., SIMES, R. J., TEBBUTT, N. C., VAN HAZEL, G., WIERZBICKI, R., LANGER, C. & MOORE, M. J. 2007. Cetuximab for the treatment of colorectal cancer. *N Engl J Med*, 357, 2040-8.

- JORDHEIM, L. P., DURANTEL, D., ZOULIM, F. & DUMONTET, C. 2013. Advances in the development of nucleoside and nucleotide analogues for cancer and viral diseases. *Nat Rev Drug Discov*, 12, 447-64.
- KABBINAVAR, F. F., SCHULZ, J., MCCLEOD, M., PATEL, T., HAMM, J. T., HECHT, J. R., MASS, R., PERROU, B., NELSON, B. & NOVOTNY, W. F. 2005. Addition of bevacizumab to bolus fluorouracil and leucovorin in first-line metastatic colorectal cancer: results of a randomized phase II trial. *J Clin Oncol*, 23, 3697-705.
- KARAPETIS, C. S., KHAMBATA-FORD, S., JONKER, D. J., O'CALLAGHAN, C. J., TU, D., TEBBUTT, N. C., SIMES, R. J., CHALCHAL, H., SHAPIRO, J. D., ROBITAILLE, S., PRICE, T. J., SHEPHERD, L., AU, H. J., LANGER, C., MOORE, M. J. & ZALCBERG, J. R. 2008. K-ras mutations and benefit from cetuximab in advanced colorectal cancer. *N Engl J Med*, 359, 1757-65.
- KEEFE, D. M. & BATEMAN, E. H. 2012. Tumor control versus adverse events with targeted anticancer therapies. *Nat Rev Clin Oncol*, 9, 98-109.
- KEMP, R., IRELAND, H., CLAYTON, E., HOUGHTON, C., HOWARD, L. & WINTON, D. J. 2004. Elimination of background recombination: somatic induction of Cre by combined transcriptional regulation and hormone binding affinity. *Nucleic Acids Res*, 32, e92.
- KIM, B. G., LI, C., QIAO, W., MAMURA, M., KASPRZAK, B., KASPERCZAK, B., ANVER, M., WOLFRAIM, L., HONG, S., MUSHINSKI, E., POTTER, M., KIM, S. J., FU, X. Y., DENG, C. & LETTERIO, J. J. 2006. Smad4 signalling in T cells is required for suppression of gastrointestinal cancer. *Nature*, 441, 1015-9.
- KINROSS, K. M., BROWN, D. V., KLEINSCHMIDT, M., JACKSON, S., CHRISTENSEN, J., CULLINANE, C., HICKS, R. J., JOHNSTONE, R. W. & MCARTHUR, G. A. 2011. In vivo activity of combined PI3K/mTOR and MEK inhibition in a Kras(G12D);Pten deletion mouse model of ovarian cancer. *Mol Cancer Ther*, 10, 1440-9.
- KINZLER, K. W. & VOGELSTEIN, B. 1996. Lessons from hereditary colorectal cancer. *Cell*, 87, 159-70.
- KIYATKIN, A., AKSAMITIENE, E., MARKEVICH, N. I., BORISOV, N. M., HOEK, J. B. & KHOLODENKO, B. N. 2006. Scaffolding protein Grb2-associated binder 1 sustains epidermal growth factor-induced mitogenic and survival signaling by multiple positive feedback loops. *J Biol Chem*, 281, 19925-38.
- KNOX, R. J. & CONNORS, T. A. 1997. Prodrugs in Cancer Chemotherapy. *Pathol Oncol Res*, 3, 309-324.
- KODAKI, T., WOSCHOLSKI, R., HALLBERG, B., RODRIGUEZ-VICIANA, P., DOWNWARD, J. & PARKER, P. J. 1994. The activation of phosphatidylinositol 3-kinase by Ras. *Curr Biol*, 4, 798-806.
- KOHL, N. E., WILSON, F. R., MOSSER, S. D., GIULIANI, E., DESOLMS, S. J., CONNER, M. W., ANTHONY, N. J., HOLTZ, W. J., GOMEZ, R. P. & LEE, T. J. 1994. Protein farnesyltransferase inhibitors block the growth of ras-dependent tumors in nude mice. *Proc Natl Acad Sci U S A*, 91, 9141-5.
- KORINEK, V., BARKER, N., MOERER, P., VAN DONSELAAR, E., HULS, G., PETERS, P. J. & CLEVERS, H. 1998. Depletion of epithelial stem-cell compartments in the small intestine of mice lacking Tcf-4. *Nat Genet*, 19, 379-83.
- KULKE, M. H., DEMETRI, G. D., SHARPLESS, N. E., RYAN, D. P., SHIVDASANI, R., CLARK, J. S., SPIEGELMAN, B. M., KIM, H., MAYER, R. J. & FUCHS, C. S. 2002. A phase II study of troglitazone, an activator of the PPARgamma receptor, in patients with chemotherapy-resistant metastatic colorectal cancer. *Cancer J*, 8, 395-9.
- KUPERWASSER, C., CHAVARRIA, T., WU, M., MAGRANE, G., GRAY, J. W., CAREY, L., RICHARDSON, A. & WEINBERG, R. A. 2004. Reconstruction of functionally normal and malignant human breast tissues in mice. *Proc Natl Acad Sci U S A*, 101, 4966-71.
- KUROSU, H., MAEHAMA, T., OKADA, T., YAMAMOTO, T., HOSHINO, S., FUKUI, Y., UI, M., HAZEKI, O. & KATADA, T. 1997. Heterodimeric phosphoinositide 3-kinase consisting of

- p85 and p110 β is synergistically activated by the β gamma subunits of G proteins and phosphotyrosyl peptide. *J Biol Chem*, 272, 24252-6.
- L, W. P., R, W., M, D. & H, B. L. 1989. Gray's anatomy. 37th ed.: Churchill Livingstone.
- LACKEY, D. B., GROZIAK, M. P., SERGEEVA, M., BERYT, M., BOYER, C., STROUD, R. M., SAYRE, P., PARK, J. W., JOHNSTON, P., SLAMON, D., SHEPARD, H. M. & PEGRAM, M. 2001. Enzyme-catalyzed therapeutic agent (ECTA) design: activation of the antitumor ECTA compound NB1011 by thymidylate synthase. *Biochem Pharmacol*, 61, 179-89.
- LAPLANTE, M. & SABATINI, D. M. 2012. mTOR signaling in growth control and disease. *Cell*, 149, 274-93.
- LEDWITH, B. J., MANAM, S., KRAYNAK, A. R., NICHOLS, W. W. & BRADLEY, M. O. 1990. Antisense-fos RNA causes partial reversion of the transformed phenotypes induced by the c-Ha-ras oncogene. *Mol Cell Biol*, 10, 1545-55.
- LEE, S. H., HU, L. L., GONZALEZ-NAVAJAS, J., SEO, G. S., SHEN, C., BRICK, J., HERDMAN, S., VARKI, N., CORR, M., LEE, J. & RAZ, E. 2010. ERK activation drives intestinal tumorigenesis in Apc(min/+) mice. *Nat Med*, 16, 665-70.
- LI, L. & CLEVERS, H. 2010. Coexistence of quiescent and active adult stem cells in mammals. *Science*, 327, 542-5.
- LI, Q., BOYER, C., LEE, J. Y. & SHEPARD, H. M. 2001. A novel approach to thymidylate synthase as a target for cancer chemotherapy. *Mol Pharmacol*, 59, 446-52.
- LI, X., MADISON, B. B., ZACHARIAS, W., KOLTERUD, A., STATES, D. & GUMUCIO, D. L. 2007. Deconvoluting the intestine: molecular evidence for a major role of the mesenchyme in the modulation of signaling cross talk. *Physiol Genomics*, 29, 290-301.
- LIN, J. H. 2008. Applications and limitations of genetically modified mouse models in drug discovery and development. *Curr Drug Metab*, 9, 419-38.
- LITTLE, M. P. & WRIGHT, E. G. 2003. A stochastic carcinogenesis model incorporating genomic instability fitted to colon cancer data. *Math Biosci*, 183, 111-34.
- LIU, D. & XING, M. 2008. Potent inhibition of thyroid cancer cells by the MEK inhibitor PD0325901 and its potentiation by suppression of the PI3K and NF-kappaB pathways. *Thyroid*, 18, 853-64.
- LIU, P., CHENG, H., SANTIAGO, S., RAEDER, M., ZHANG, F., ISABELLA, A., YANG, J., SEMAAN, D. J., CHEN, C., FOX, E. A., GRAY, N. S., MONAHAN, J., SCHLEGEL, R., BEROUKHIM, R., MILLS, G. B. & ZHAO, J. J. 2011. Oncogenic PIK3CA-driven mammary tumors frequently recur via PI3K pathway-dependent and PI3K pathway-independent mechanisms. *Nat Med*, 17, 1116-20.
- LIÈVRE, A., BACHET, J. B., BOIGE, V., CAYRE, A., LE CORRE, D., BUC, E., YCHOU, M., BOUCHÉ, O., LANDI, B., LOUVET, C., ANDRÉ, T., BIBEAU, F., DIEBOLD, M. D., ROUGIER, P., DUCREUX, M., TOMASIC, G., EMILE, J. F., PENAULT-LLORCA, F. & LAURENT-PUIG, P. 2008. KRAS mutations as an independent prognostic factor in patients with advanced colorectal cancer treated with cetuximab. *J Clin Oncol*, 26, 374-9.
- LOBO, N. A., SHIMONO, Y., QIAN, D. & CLARKE, M. F. 2007. The biology of cancer stem cells. *Annu Rev Cell Dev Biol*, 23, 675-99.
- LONGLEY, D. B., HARKIN, D. P. & JOHNSTON, P. G. 2003. 5-fluorouracil: mechanisms of action and clinical strategies. *Nat Rev Cancer*, 3, 330-8.
- MA, L., CHEN, Z., ERDJUMENT-BROMAGE, H., TEMPST, P. & PANDOLFI, P. P. 2005. Phosphorylation and functional inactivation of TSC2 by Erk implications for tuberous sclerosis and cancer pathogenesis. *Cell*, 121, 179-93.
- MA, L., TERUYA-FELDSTEIN, J., BONNER, P., BERNARDI, R., FRANZ, D. N., WITTE, D., CORDON-CARDO, C. & PANDOLFI, P. P. 2007. Identification of S664 TSC2 phosphorylation as a marker for extracellular signal-regulated kinase mediated mTOR activation in tuberous sclerosis and human cancer. *Cancer Res*, 67, 7106-12.

- MADELA, K. & MCGUIGAN, C. 2012. Progress in the development of anti-hepatitis C virus nucleoside and nucleotide prodrugs. *Future Med Chem*, 4, 625-50.
- MADISON, B. B., BRAUNSTEIN, K., KUIZON, E., PORTMAN, K., QIAO, X. T. & GUMUCIO, D. L. 2005. Epithelial hedgehog signals pattern the intestinal crypt-villus axis. *Development*, 132, 279-89.
- MAEKAWA, M., NISHIDA, E. & TANOUE, T. 2002. Identification of the Anti-proliferative protein Tob as a MAPK substrate. *J Biol Chem*, 277, 37783-7.
- MAHATO, R., TAI, W. & CHENG, K. 2011. Prodrugs for improving tumor targetability and efficiency. *Adv Drug Deliv Rev*, 63, 659-70.
- MAIRA, S. M., STAUFFER, F., BRUEGGEN, J., FURET, P., SCHNELL, C., FRITSCH, C., BRACHMANN, S., CHÈNE, P., DE POVER, A., SCHOEMAKER, K., FABBRO, D., GABRIEL, D., SIMONEN, M., MURPHY, L., FINAN, P., SELLERS, W. & GARCÍA-ECHEVERRÍA, C. 2008. Identification and characterization of NVP-BEZ235, a new orally available dual phosphatidylinositol 3-kinase/mammalian target of rapamycin inhibitor with potent in vivo antitumor activity. *Mol Cancer Ther*, 7, 1851-63.
- MAIRA, S. M., STAUFFER, F., SCHNELL, C. & GARCÍA-ECHEVERRÍA, C. 2009. PI3K inhibitors for cancer treatment: where do we stand? *Biochem Soc Trans*, 37, 265-72.
- MARIGO, V., DAVEY, R. A., ZUO, Y., CUNNINGHAM, J. M. & TABIN, C. J. 1996. Biochemical evidence that patched is the Hedgehog receptor. *Nature*, 384, 176-9.
- MARSH, V., WINTON, D. J., WILLIAMS, G. T., DUBOIS, N., TRUMPP, A., SANSOM, O. J. & CLARKE, A. R. 2008. Epithelial Pten is dispensable for intestinal homeostasis but suppresses adenoma development and progression after Apc mutation. *Nat Genet*, 40, 1436-44.
- MARTINELLI, E., TROIANI, T., D'AIUTO, E., MORGILLO, F., VITAGLIANO, D., CAPASSO, A., COSTANTINO, S., CIUFFREDA, L. P., MEROLLA, F., VECCHIONE, L., DE VRIENDT, V., TEJPAR, S., NAPPI, A., SFORZA, V., MARTINI, G., BERRINO, L., DE PALMA, R. & CIARDIELLO, F. 2013. Antitumor activity of pimasertib, a selective MEK 1/2 inhibitor, in combination with PI3K/mTOR inhibitors or with multi-targeted kinase inhibitors in pimasertib-resistant human lung and colorectal cancer cells. *Int J Cancer*, 0.
- MARTINEZ, M., HOPE, C., PLANUTIC, K., PLANUTIENE, M., PONTELLO, A., DUARTE, B., ALBERS, C. & HOLCOMBE, R. 2010. Dietary grape-derived resveratrol for colon cancer prevention. *J Clin Oncol*.
- MARTINI, F. H. 2006. Fundamentals of Anatomy & Physiology. 7th ed.: Pearson.
- MASSAGUÉ, J. 1998. TGF-beta signal transduction. *Annu Rev Biochem*, 67, 753-91.
- MAUGHAN, T. 2012. FOCUS 3 TO FOCUS 4: the role of stratified medicine in metastatic colorectal cancer http://www.ecmcnetwork.org.uk/prod_consump/groups/cr_common/@ecm/@gen/documents/generalcontent/cr_087352.pdf.
- MAY, R., RIEHL, T. E., HUNT, C., SUREBAN, S. M., ANANT, S. & HOUCHEN, C. W. 2008. Identification of a novel putative gastrointestinal stem cell and adenoma stem cell marker, doublecortin and CaM kinase-like-1, following radiation injury and in adenomatous polyposis coli/multiple intestinal neoplasia mice. *Stem Cells*, 26, 630-7.
- MCGUIGAN, C., BLEWETT, S., SICCARDI, D., ERICHSEN, J. T., ANDREI, G., SNOEK, R., DE CLERCQ, E. & BALZARINI, J. 2002. Alkyloxyphenyl furano pyrimidines as potent and selective anti-VZV agents with enhanced water solubility. *Antivir Chem Chemother*, 13, 91-9.
- MEHELLOU, Y., BALZARINI, J. & MCGUIGAN, C. 2009. Aryloxy phosphoramidate triesters: a technology for delivering monophosphorylated nucleosides and sugars into cells. *ChemMedChem*, 4, 1779-91.
- MENG, R. D., SHELTON, C. C., LI, Y. M., QIN, L. X., NOTTERMAN, D., PATY, P. B. & SCHWARTZ, G. K. 2009. gamma-Secretase inhibitors abrogate oxaliplatin-induced activation of the

- Notch-1 signaling pathway in colon cancer cells resulting in enhanced chemosensitivity. *Cancer Res*, 69, 573-82.
- METZGER, R., DANENBERG, K., LEICHMAN, C. G., SALONGA, D., SCHWARTZ, E. L., WADLER, S., LENZ, H. J., GROSHEN, S., LEICHMAN, L. & DANENBERG, P. V. 1998. High basal level gene expression of thymidine phosphorylase (platelet-derived endothelial cell growth factor) in colorectal tumors is associated with nonresponse to 5-fluorouracil. *Clin Cancer Res*, 4, 2371-6.
- MIGLIARDI, G., SASSI, F., TORTI, D., GALIMI, F., ZANELLA, E. R., BUSCARINO, M., RIBERO, D., MURATORE, A., MASSUCCO, P., PISACANE, A., RISIO, M., CAPUSSOTTI, L., MARSONI, S., DI NICOLANTONIO, F., BARDELLI, A., COMOGLIO, P. M., TRUSOLINO, L. & BERTOTTI, A. 2012. Inhibition of MEK and PI3K/mTOR suppresses tumor growth but does not cause tumor regression in patient-derived xenografts of RAS-mutant colorectal carcinomas. *Clin Cancer Res*, 18, 2515-25.
- MILLER, K. A., YEAGER, N., BAKER, K., LIAO, X. H., REFETTOFF, S. & DI CRISTOFANO, A. 2009. Oncogenic Kras requires simultaneous PI3K signaling to induce ERK activation and transform thyroid epithelial cells in vivo. *Cancer Res*, 69, 3689-94.
- MILLER, R. L. 2011. Transgenic mice: beyond the knockout. *Am J Physiol Renal Physiol*, 300, F291-300.
- MITROVSKI, B., PRESSACCO, J., MANDELBAUM, S. & ERLICHMAN, C. 1994. Biochemical effects of folate-based inhibitors of thymidylate synthase in MGH-U1 cells. *Cancer Chemother Pharmacol*, 35, 109-14.
- MIWA, M., URA, M., NISHIDA, M., SAWADA, N., ISHIKAWA, T., MORI, K., SHIMMA, N., UMEDA, I. & ISHITSUKA, H. 1998. Design of a novel oral fluoropyrimidine carbamate, capecitabine, which generates 5-fluorouracil selectively in tumours by enzymes concentrated in human liver and cancer tissue. *Eur J Cancer*, 34, 1274-81.
- MIYAMOTO, S. & ROSENBERG, D. W. 2011. Role of Notch signaling in colon homeostasis and carcinogenesis. *Cancer Sci*, 102, 1938-42.
- MOGHADDAM, A. A., WOODWARD, M. & HUXLEY, R. 2007. Obesity and risk of colorectal cancer: a meta-analysis of 31 studies with 70,000 events. *Cancer Epidemiol Biomarkers Prev*, 16, 2533-47.
- MONTGOMERY, R. K., CARLONE, D. L., RICHMOND, C. A., FARILLA, L., KRANENDONK, M. E., HENDERSON, D. E., BAFFOUR-AWUAH, N. Y., AMBRUZS, D. M., FOGLI, L. K., ALGRA, S. & BREAU, D. T. 2011. Mouse telomerase reverse transcriptase (mTert) expression marks slowly cycling intestinal stem cells. *Proc Natl Acad Sci U S A*, 108, 179-84.
- MUELLER, A., BACHMANN, E., LINNIG, M., KHILLIMBERGER, K., SCHIMANSKI, C. C., GALLE, P. R. & MOEHLER, M. 2012. Selective PI3K inhibition by BKM120 and BEZ235 alone or in combination with chemotherapy in wild-type and mutated human gastrointestinal cancer cell lines. *Cancer Chemother Pharmacol*, 69, 1601-15.
- MUELLER, M. M. & FUSENIG, N. E. 2004. Friends or foes - bipolar effects of the tumour stroma in cancer. *Nat Rev Cancer*, 4, 839-49.
- MULLER, P. A., CASWELL, P. T., DOYLE, B., IWANICKI, M. P., TAN, E. H., KARIM, S., LUKASHCHUK, N., GILLESPIE, D. A., LUDWIG, R. L., GOSSELIN, P., CROMER, A., BRUGGE, J. S., SANSOM, O. J., NORMAN, J. C. & VOUSDEN, K. H. 2009. Mutant p53 drives invasion by promoting integrin recycling. *Cell*, 139, 1327-41.
- MUNCAN, V., SANSOM, O. J., TERTOOLEN, L., PHESSSE, T. J., BEGTHEL, H., SANCHO, E., COLE, A. M., GREGORIEFF, A., DE ALBORAN, I. M., CLEVERS, H. & CLARKE, A. R. 2006. Rapid loss of intestinal crypts upon conditional deletion of the Wnt/Tcf-4 target gene c-Myc. *Mol Cell Biol*, 26, 8418-26.
- MURPHY, L. O., MACKEIGAN, J. P. & BLENIS, J. 2004. A network of immediate early gene products propagates subtle differences in mitogen-activated protein kinase signal amplitude and duration. *Mol Cell Biol*, 24, 144-53.

- MUÑOZ, J., STANGE, D. E., SCHEPERS, A. G., VAN DE WETERING, M., KOO, B. K., ITZKOVITZ, S., VOLCKMANN, R., KUNG, K. S., KOSTER, J., RADULESCU, S., MYANT, K., VERSTEEG, R., SANSOM, O. J., VAN ES, J. H., BARKER, N., VAN OUDENAARDEN, A., MOHAMMED, S., HECK, A. J. & CLEVERS, H. 2012. The Lgr5 intestinal stem cell signature: robust expression of proposed quiescent '+4' cell markers. *EMBO J*, 31, 3079-91.
- NATH, N., KASHFI, K., CHEN, J. & RIGAS, B. 2003. Nitric oxide-donating aspirin inhibits beta-catenin/T cell factor (TCF) signaling in SW480 colon cancer cells by disrupting the nuclear beta-catenin-TCF association. *Proc Natl Acad Sci U S A*, 100, 12584-9.
- NETWORK, C. G. A. 2012. Comprehensive molecular characterization of human colon and rectal cancer. *Nature*, 487, 330-7.
- O'BRIEN, C. A., POLLETT, A., GALLINGER, S. & DICK, J. E. 2007. A human colon cancer cell capable of initiating tumour growth in immunodeficient mice. *Nature*, 445, 106-10.
- O'GORMAN, S., FOX, D. T. & WAHL, G. M. 1991. Recombinase-mediated gene activation and site-specific integration in mammalian cells. *Science*, 251, 1351-5.
- O'REILLY, K. E., ROJO, F., SHE, Q. B., SOLIT, D., MILLS, G. B., SMITH, D., LANE, H., HOFMANN, F., HICKLIN, D. J., LUDWIG, D. L., BASELGA, J. & ROSEN, N. 2006. mTOR inhibition induces upstream receptor tyrosine kinase signaling and activates Akt. *Cancer Res*, 66, 1500-8.
- O'REILLY, M. S., HOLMGREN, L., CHEN, C. & FOLKMAN, J. 1996. Angiostatin induces and sustains dormancy of human primary tumors in mice. *Nat Med*, 2, 689-92.
- OGINO, S., NOSHO, K., KIRKNER, G. J., SHIMA, K., IRAHARA, N., KURE, S., CHAN, A. T., ENGELMAN, J. A., KRAFT, P., CANTLEY, L. C., GIOVANNUCCI, E. L. & FUCHS, C. S. 2009. PIK3CA mutation is associated with poor prognosis among patients with curatively resected colon cancer. *J Clin Oncol*, 27, 1477-84.
- OH, W. J. & JACINTO, E. 2011. mTOR complex 2 signaling and functions. *Cell Cycle*, 10, 2305-16.
- OLIVE, K. P., JACOBETZ, M. A., DAVIDSON, C. J., GOPINATHAN, A., MCINTYRE, D., HONESS, D., MADHU, B., GOLDGRABEN, M. A., CALDWELL, M. E., ALLARD, D., FRESE, K. K., DENICOLA, G., FEIG, C., COMBS, C., WINTER, S. P., IRELAND-ZECCHINI, H., REICHEL, S., HOWAT, W. J., CHANG, A., DHARA, M., WANG, L., RÜCKERT, F., GRÜTZMANN, R., PILARSKY, C., IZERADJENE, K., HINGORANI, S. R., HUANG, P., DAVIES, S. E., PLUNKETT, W., EGORIN, M., HRUBAN, R. H., WHITEBREAD, N., MCGOVERN, K., ADAMS, J., IACOBUZIO-DONAHUE, C., GRIFFITHS, J. & TUVESON, D. A. 2009. Inhibition of Hedgehog signaling enhances delivery of chemotherapy in a mouse model of pancreatic cancer. *Science*, 324, 1457-61.
- OMER, C. A., CHEN, Z., DIEHL, R. E., CONNER, M. W., CHEN, H. Y., TRUMBAUER, M. E., GOPAL-TRUTER, S., SEEBURGER, G., BHIMNATHWALA, H., ABRAMS, M. T., DAVIDE, J. P., ELLIS, M. S., GIBBS, J. B., GREENBERG, I., KOBLAN, K. S., KRAL, A. M., LIU, D., LOBELL, R. B., MILLER, P. J., MOSSER, S. D., O'NEILL, T. J., RANDS, E., SCHABER, M. D., SENDERAK, E. T., OLIFF, A. & KOHL, N. E. 2000. Mouse mammary tumor virus-Ki-rasB transgenic mice develop mammary carcinomas that can be growth-inhibited by a farnesyl:protein transferase inhibitor. *Cancer Res*, 60, 2680-8.
- ORBAN, P. C., CHUI, D. & MARTH, J. D. 1992. Tissue- and site-specific DNA recombination in transgenic mice. *Proc Natl Acad Sci U S A*, 89, 6861-5.
- ORFORD, K. W. & SCADDEN, D. T. 2008. Deconstructing stem cell self-renewal: genetic insights into cell-cycle regulation. *Nat Rev Genet*, 9, 115-28.
- OWEN, R. L. & JONES, A. L. 1974. Epithelial cell specialization within human Peyer's patches: an ultrastructural study of intestinal lymphoid follicles. *Gastroenterology*, 66, 189-203.
- PAGÈS, G., GUÉRIN, S., GRALL, D., BONINO, F., SMITH, A., ANJUERE, F., AUBERGER, P. & POUYSSÉGUR, J. 1999. Defective thymocyte maturation in p44 MAP kinase (Erk 1) knockout mice. *Science*, 286, 1374-7.
- PARK, I. H., BACHMANN, R., SHIRAZI, H. & CHEN, J. 2002. Regulation of ribosomal S6 kinase 2 by mammalian target of rapamycin. *J Biol Chem*, 277, 31423-9.

- PARKIN, D. M. 2011. 5. Cancers attributable to dietary factors in the UK in 2010. II. Meat consumption. *Br J Cancer*, 105 Suppl 2, S24-26.
- PARMAR, H., YOUNG, P., EMERMAN, J. T., NEVE, R. M., DAIRKEE, S. & CUNHA, G. R. 2002. A novel method for growing human breast epithelium in vivo using mouse and human mammary fibroblasts. *Endocrinology*, 143, 4886-96.
- PARSONS, D. W., WANG, T. L., SAMUELS, Y., BARDELLI, A., CUMMINS, J. M., DELONG, L., SILLIMAN, N., PTAK, J., SZABO, S., WILLSON, J. K., MARKOWITZ, S., KINZLER, K. W., VOGELSTEIN, B., LENGAUER, C. & VELCULESCU, V. E. 2005. Colorectal cancer: mutations in a signalling pathway. *Nature*, 436, 792.
- PEIGNON, G., DURAND, A., CACHEUX, W., AYRAULT, O., TERRIS, B., LAURENT-PUIG, P., SHROYER, N. F., VAN SEUNINGEN, I., HONJO, T., PERRET, C. & ROMAGNOLO, B. 2011. Complex interplay between β -catenin signalling and Notch effectors in intestinal tumorigenesis. *Gut*, 60, 166-76.
- PENDÁS-FRANCO, N., AGUILERA, O., PEREIRA, F., GONZÁLEZ-SANCHO, J. M. & MUÑOZ, A. 2008. Vitamin D and Wnt/beta-catenin pathway in colon cancer: role and regulation of DICKKOPF genes. *Anticancer Res*, 28, 2613-23.
- PERRONE, F., LAMPIS, A., ORSENIGO, M., DI BARTOLOMEO, M., GEVORGYAN, A., LOSA, M., FRATTINI, M., RIVA, C., ANDREOLA, S., BAJETTA, E., BERTARIO, L., LEO, E., PIEROTTI, M. A. & PILOTTI, S. 2009. PI3KCA/PTEN deregulation contributes to impaired responses to cetuximab in metastatic colorectal cancer patients. *Ann Oncol*, 20, 84-90.
- PINTO, D., GREGORIEFF, A., BEGTHEL, H. & CLEVERS, H. 2003. Canonical Wnt signals are essential for homeostasis of the intestinal epithelium. *Genes Dev*, 17, 1709-13.
- POTTEN, C. S., BOOTH, C., TUDOR, G. L., BOOTH, D., BRADY, G., HURLEY, P., ASHTON, G., CLARKE, R., SAKAKIBARA, S. & OKANO, H. 2003. Identification of a putative intestinal stem cell and early lineage marker; musashi-1. *Differentiation*, 71, 28-41.
- POTTEN, C. S., HUME, W. J., REID, P. & CAIRNS, J. 1978. The segregation of DNA in epithelial stem cells. *Cell*, 15, 899-906.
- POWELL, A. E., WANG, Y., LI, Y., POULIN, E. J., MEANS, A. L., WASHINGTON, M. K., HIGGINBOTHAM, J. N., JUCHHEIM, A., PRASAD, N., LEVY, S. E., GUO, Y., SHYR, Y., ARONOW, B. J., HAIGIS, K. M., FRANKLIN, J. L. & COFFEY, R. J. 2012. The pan-ErbB negative regulator Lrig1 is an intestinal stem cell marker that functions as a tumor suppressor. *Cell*, 149, 146-58.
- POWELL, S. M., ZILZ, N., BEAZER-BARCLAY, Y., BRYAN, T. M., HAMILTON, S. R., THIBODEAU, S. N., VOGELSTEIN, B. & KINZLER, K. W. 1992. APC mutations occur early during colorectal tumorigenesis. *Nature*, 359, 235-7.
- PRAHALLAD, A., SUN, C., HUANG, S., DI NICOLANTONIO, F., SALAZAR, R., ZECCHIN, D., BEIJERSBERGEN, R. L., BARDELLI, A. & BERNARDS, R. 2012. Unresponsiveness of colon cancer to BRAF(V600E) inhibition through feedback activation of EGFR. *Nature*, 483, 100-3.
- PRIEST, D. G., LEDFORD, B. E. & DOIG, M. T. 1980. Increased thymidylate synthetase in 5-fluorodeoxyuridine resistant cultured hepatoma cells. *Biochem Pharmacol*, 29, 1549-53.
- PÁLMER, H. G., GONZÁLEZ-SANCHO, J. M., ESPADA, J., BERCIANO, M. T., PUIG, I., BAULIDA, J., QUINTANILLA, M., CANO, A., DE HERREROS, A. G., LAFARGA, M. & MUÑOZ, A. 2001. Vitamin D(3) promotes the differentiation of colon carcinoma cells by the induction of E-cadherin and the inhibition of beta-catenin signaling. *J Cell Biol*, 154, 369-87.
- RADTKE, F. & RAJ, K. 2003. The role of Notch in tumorigenesis: oncogene or tumour suppressor? *Nat Rev Cancer*, 3, 756-67.
- RAJAGOPALAN, H., BARDELLI, A., LENGAUER, C., KINZLER, K. W., VOGELSTEIN, B. & VELCULESCU, V. E. 2002. Tumorigenesis: RAF/RAS oncogenes and mismatch-repair status. *Nature*, 418, 934.

- RAMIREZ, C. & GEBERT, A. 2003. Vimentin-positive cells in the epithelium of rabbit ileal villi represent cup cells but not M-cells. *J Histochem Cytochem*, 51, 1533-44.
- REEDIJK, M., ODORCIC, S., ZHANG, H., CHETTY, R., TENNERT, C., DICKSON, B. C., LOCKWOOD, G., GALLINGER, S. & EGAN, S. E. 2008. Activation of Notch signaling in human colon adenocarcinoma. *Int J Oncol*, 33, 1223-9.
- RESNICK, M. B., ROUTHIER, J., KONKIN, T., SABO, E. & PRICOLO, V. E. 2004. Epidermal growth factor receptor, c-MET, beta-catenin, and p53 expression as prognostic indicators in stage II colon cancer: a tissue microarray study. *Clin Cancer Res*, 10, 3069-75.
- REY, J. P. & ELLIES, D. L. 2010. Wnt modulators in the biotech pipeline. *Dev Dyn*, 239, 102-14.
- RHEE, C. S., SEN, M., LU, D., WU, C., LEONI, L., RUBIN, J., CORR, M. & CARSON, D. A. 2002. Wnt and frizzled receptors as potential targets for immunotherapy in head and neck squamous cell carcinomas. *Oncogene*, 21, 6598-605.
- RICHMAN, S. D., SEYMOUR, M. T., CHAMBERS, P., ELLIOTT, F., DALY, C. L., MEADE, A. M., TAYLOR, G., BARRETT, J. H. & QUIRKE, P. 2009. KRAS and BRAF mutations in advanced colorectal cancer are associated with poor prognosis but do not preclude benefit from oxaliplatin or irinotecan: results from the MRC FOCUS trial. *J Clin Oncol*, 27, 5931-7.
- RINEHART, J., ADJEI, A. A., LORUSSO, P. M., WATERHOUSE, D., HECHT, J. R., NATALE, R. B., HAMID, O., VARTERASIAN, M., ASBURY, P., KALDJIAN, E. P., GULYAS, S., MITCHELL, D. Y., HERRERA, R., SEBOLT-LEOPOLD, J. S. & MEYER, M. B. 2004. Multicenter phase II study of the oral MEK inhibitor, CI-1040, in patients with advanced non-small-cell lung, breast, colon, and pancreatic cancer. *J Clin Oncol*, 22, 4456-62.
- RINI, B. I. 2008. Temsirolimus, an inhibitor of mammalian target of rapamycin. *Clin Cancer Res*, 14, 1286-90.
- RIVEROS-ROSAS, H., JULIAN-SANCHEZ, A. & PINA, E. 1997. Enzymology of ethanol and acetaldehyde metabolism in mammals. *Arch Med Res*, 28, 453-71.
- ROBERTS, P. J., USARY, J. E., DARR, D. B., DILLON, P. M., PFEFFERLE, A. D., WHITTLE, M. C., DUNCAN, J. S., JOHNSON, S. M., COMBEST, A. J., JIN, J., ZAMBONI, W. C., JOHNSON, G. L., PEROU, C. M. & SHARPLESS, N. E. 2012. Combined PI3K/mTOR and MEK inhibition provides broad antitumor activity in faithful murine cancer models. *Clin Cancer Res*, 18, 5290-303.
- ROBERTS, S. A., HYATT, D. C., HONTS, J. E., CHANGCHIEN, L., MALEY, G. F., MALEY, F. & MONTFORT, W. R. 2006. Structure of the Y94F mutant of Escherichia coli thymidylate synthase. *Acta Crystallogr Sect F Struct Biol Cryst Commun*, 62, 840-3.
- ROBLES, A. I. & VARTICOVSKI, L. 2008. Harnessing genetically engineered mouse models for preclinical testing. *Chem Biol Interact*, 171, 159-64.
- RODILLA, V., VILLANUEVA, A., OBRADOR-HEVIA, A., ROBERT-MORENO, A., FERNÁNDEZ-MAJADA, V., GRILLI, A., LÓPEZ-BIGAS, N., BELLORA, N., ALBÀ, M. M., TORRES, F., DUÑACH, M., SANJUAN, X., GONZALEZ, S., GRIDLEY, T., CAPELLA, G., BIGAS, A. & ESPINOSA, L. 2009. Jagged1 is the pathological link between Wnt and Notch pathways in colorectal cancer. *Proc Natl Acad Sci U S A*, 106, 6315-20.
- ROMEO, Y., ZHANG, X. & ROUX, P. P. 2012. Regulation and function of the RSK family of protein kinases. *Biochem J*, 441, 553-69.
- ROPER, J., RICHARDSON, M. P., WANG, W. V., RICHARD, L. G., CHEN, W., COFFEE, E. M., SINNAMON, M. J., LEE, L., CHEN, P. C., BRONSON, R. T., MARTIN, E. S. & HUNG, K. E. 2011. The dual PI3K/mTOR inhibitor NVP-BE2235 induces tumor regression in a genetically engineered mouse model of PIK3CA wild-type colorectal cancer. *PLoS One*, 6, e25132.
- ROTH, S. I. & HELWIG, E. B. 1963. Juvenile polyps of the colon and rectum. *Cancer*, 16, 468-79.
- ROUX, P. P., BALLIF, B. A., ANJUM, R., GYGI, S. P. & BLENIS, J. 2004. Tumor-promoting phorbol esters and activated Ras inactivate the tuberous sclerosis tumor suppressor complex via p90 ribosomal S6 kinase. *Proc Natl Acad Sci U S A*, 101, 13489-94.

- ROUX, P. P., SHAHBAZIAN, D., VU, H., HOLZ, M. K., COHEN, M. S., TAUNTON, J., SONENBERG, N. & BLENIS, J. 2007. RAS/ERK signaling promotes site-specific ribosomal protein S6 phosphorylation via RSK and stimulates cap-dependent translation. *J Biol Chem*, 282, 14056-64.
- RUIZ I ALTABÁ, A. 1999. Gli proteins encode context-dependent positive and negative functions: implications for development and disease. *Development*, 126, 3205-16.
- RUTMAN, R. J., CANTAROW, A. & PASCHKIS, K. E. 1954. Studies in 2-acetylaminofluorene carcinogenesis. III. The utilization of uracil-2-C14 by preneoplastic rat liver and rat hepatoma. *Cancer Res*, 14, 119-23.
- SAIF, M., LEE, Y. & KIM, R. 2012. Harnessing gemcitabine metabolism: a step towards personalized medicine for pancreatic cancer. *Ther Adv Med Oncol*, 4, 341-6.
- SALMENA, L., CARRACEDO, A. & PANDOLFI, P. P. 2008. Tenets of PTEN tumor suppression. *Cell*, 133, 403-14.
- SALONGA, D., DANENBERG, K. D., JOHNSON, M., METZGER, R., GROSHEN, S., TSAO-WEI, D. D., LENZ, H. J., LEICHMAN, C. G., LEICHMAN, L., DIASIO, R. B. & DANENBERG, P. V. 2000. Colorectal tumors responding to 5-fluorouracil have low gene expression levels of dihydropyrimidine dehydrogenase, thymidylate synthase, and thymidine phosphorylase. *Clin Cancer Res*, 6, 1322-7.
- SANGIORGI, E. & CAPECCHI, M. R. 2008. Bmi1 is expressed in vivo in intestinal stem cells. *Nat Genet*, 40, 915-20.
- SANSOM, O. J., MENIEL, V., WILKINS, J. A., COLE, A. M., OIEN, K. A., MARSH, V., JAMIESON, T. J., GUERRA, C., ASHTON, G. H., BARBACID, M. & CLARKE, A. R. 2006. Loss of Apc allows phenotypic manifestation of the transforming properties of an endogenous K-ras oncogene in vivo. *Proc Natl Acad Sci U S A*, 103, 14122-7.
- SANSOM, O. J., MENIEL, V. S., MUNCAN, V., PHESE, T. J., WILKINS, J. A., REED, K. R., VASS, J. K., ATHINEOS, D., CLEVERS, H. & CLARKE, A. R. 2007. Myc deletion rescues Apc deficiency in the small intestine. *Nature*, 446, 676-9.
- SANSOM, O. J., REED, K. R., HAYES, A. J., IRELAND, H., BRINKMANN, H., NEWTON, I. P., BATLLE, E., SIMON-ASSMANN, P., CLEVERS, H., NATHKE, I. S., CLARKE, A. R. & WINTON, D. J. 2004. Loss of Apc in vivo immediately perturbs Wnt signaling, differentiation, and migration. *Genes Dev*, 18, 1385-90.
- SANTI, D. V., MCHENRY, C. S. & SOMMER, H. 1974. Mechanism of interaction of thymidylate synthetase with 5-fluorodeoxyuridylate. *Biochemistry*, 13, 471-81.
- SARRAF, P., MUELLER, E., JONES, D., KING, F. J., DEANGELO, D. J., PARTRIDGE, J. B., HOLDEN, S. A., CHEN, L. B., SINGER, S., FLETCHER, C. & SPIEGELMAN, B. M. 1998. Differentiation and reversal of malignant changes in colon cancer through PPARgamma. *Nat Med*, 4, 1046-52.
- SATO, T., VRIES, R. G., SNIPPERT, H. J., VAN DE WETERING, M., BARKER, N., STANGE, D. E., VAN ES, J. H., ABO, A., KUJALA, P., PETERS, P. J. & CLEVERS, H. 2009. Single Lgr5 stem cells build crypt-villus structures in vitro without a mesenchymal niche. *Nature*, 459, 262-5.
- SAUER, B. & HENDERSON, N. 1988. Site-specific DNA recombination in mammalian cells by the Cre recombinase of bacteriophage P1. *Proc Natl Acad Sci U S A*, 85, 5166-70.
- SCALTRITI, M. & BASELGA, J. 2006. The epidermal growth factor receptor pathway: a model for targeted therapy. *Clin Cancer Res*, 12, 5268-72.
- SCHEPERS, A. G., SNIPPERT, H. J., STANGE, D. E., VAN DEN BORN, M., VAN ES, J. H., VAN DE WETERING, M. & CLEVERS, H. 2012. Lineage tracing reveals Lgr5+ stem cell activity in mouse intestinal adenomas. *Science*, 337, 730-5.
- SCHRÖDER, N. & GOSSLER, A. 2002. Expression of Notch pathway components in fetal and adult mouse small intestine. *Gene Expr Patterns*, 2, 247-50.
- SCHUBBERT, S., SHANNON, K. & BOLLAG, G. 2007. Hyperactive Ras in developmental disorders and cancer. *Nat Rev Cancer*, 7, 295-308.

- SEARFOSS, G. H., JORDAN, W. H., CALLIGARO, D. O., GALBREATH, E. J., SCHIRTZINGER, L. M., BERRIDGE, B. R., GAO, H., HIGGINS, M. A., MAY, P. C. & RYAN, T. P. 2003. Adipsin, a biomarker of gastrointestinal toxicity mediated by a functional gamma-secretase inhibitor. *J Biol Chem*, 278, 46107-16.
- SEBOLT-LEOPOLD, J. S., DUDLEY, D. T., HERRERA, R., VAN BECELAERE, K., WILAND, A., GOWAN, R. C., TECLE, H., BARRETT, S. D., BRIDGES, A., PRZYBRANOWSKI, S., LEOPOLD, W. R. & SALTIEL, A. R. 1999. Blockade of the MAP kinase pathway suppresses growth of colon tumors in vivo. *Nat Med*, 5, 810-6.
- SEBOLT-LEOPOLD, J. S. & HERRERA, R. 2004. Targeting the mitogen-activated protein kinase cascade to treat cancer. *Nat Rev Cancer*, 4, 937-47.
- SEBTI, S. M. & DER, C. J. 2003. Opinion: Searching for the elusive targets of farnesyltransferase inhibitors. *Nat Rev Cancer*, 3, 945-51.
- SHARMA, S. K., PEDLEY, R. B., BHATIA, J., BOXER, G. M., EL-EMIR, E., QURESHI, U., TOLNER, B., LOWE, H., MICHAEL, N. P., MINTON, N., BEGENT, R. H. & CHESTER, K. A. 2005. Sustained tumor regression of human colorectal cancer xenografts using a multifunctional mannosylated fusion protein in antibody-directed enzyme prodrug therapy. *Clin Cancer Res*, 11, 814-25.
- SHARPLESS, N. E. & DEPINHO, R. A. 2006. The mighty mouse: genetically engineered mouse models in cancer drug development. *Nat Rev Drug Discov*, 5, 741-54.
- SHAW, R. J. 2006. Glucose metabolism and cancer. *Curr Opin Cell Biol*, 18, 598-608.
- SHE, Q. B., CHANDARLAPATY, S., YE, Q., LOBO, J., HASKELL, K. M., LEANDER, K. R., DEFEO-JONES, D., HUBER, H. E. & ROSEN, N. 2008. Breast tumor cells with PI3K mutation or HER2 amplification are selectively addicted to Akt signaling. *PLoS One*, 3, e3065.
- SHE, Q. B., HALILOVIC, E., YE, Q., ZHEN, W., SHIRASAWA, S., SASAZUKI, T., SOLIT, D. B. & ROSEN, N. 2010. 4E-BP1 is a key effector of the oncogenic activation of the AKT and ERK signaling pathways that integrates their function in tumors. *Cancer Cell*, 18, 39-51.
- SHIMAMURA, A., BALLIF, B. A., RICHARDS, S. A. & BLENIS, J. 2000. Rsk1 mediates a MEK-MAP kinase cell survival signal. *Curr Biol*, 10, 127-35.
- SIMINOVITCH, L. & AXELRAD, A. A. 1963. Cell-cell interactions in vitro: their relation to differentiation and Carcinogenesis. *Proc Can Cancer Conf*, 5, 149-65.
- SIMMONS, B. H., LEE, J. H., LALWANI, K., GIDDABASAPPA, A., SNIDER, B. A., WONG, A., LAPPIN, P. B., ESWARAKA, J., KAN, J. L., CHRISTENSEN, J. G. & SHOJAEI, F. 2012. Combination of a MEK inhibitor at sub-MTD with a PI3K/mTOR inhibitor significantly suppresses growth of lung adenocarcinoma tumors in Kras(G12D-LSL) mice. *Cancer Chemother Pharmacol*, 70, 213-20.
- SINGER, G., OLDT, R., COHEN, Y., WANG, B. G., SIDRANSKY, D., KURMAN, R. J. & SHIH, I. M. 2003. Mutations in BRAF and KRAS characterize the development of low-grade ovarian serous carcinoma. *J Natl Cancer Inst*, 95, 484-6.
- SINGH, M., LIMA, A., MOLINA, R., HAMILTON, P., CLERMONT, A. C., DEVASTHALI, V., THOMPSON, J. D., CHENG, J. H., BOU RESLAN, H., HO, C. C., CAO, T. C., LEE, C. V., NANNINI, M. A., FUH, G., CARANO, R. A., KOEPPEN, H., YU, R. X., FORREST, W. F., PLOWMAN, G. D. & JOHNSON, L. 2010. Assessing therapeutic responses in Kras mutant cancers using genetically engineered mouse models. *Nat Biotechnol*, 28, 585-93.
- SMITH, G., CAREY, F. A., BEATTIE, J., WILKIE, M. J., LIGHTFOOT, T. J., COXHEAD, J., GARNER, R. C., STEELE, R. J. & WOLF, C. R. 2002. Mutations in APC, Kirsten-ras, and p53--alternative genetic pathways to colorectal cancer. *Proc Natl Acad Sci U S A*, 99, 9433-8.
- SOBRERO, A., GUGLIELMI, A., GROSSI, F., PUGLISI, F. & ASCHELE, C. 2000. Mechanism of action of fluoropyrimidines: relevance to the new developments in colorectal cancer chemotherapy. *Semin Oncol*, 27, 72-7.

- SOMMER, H. & SANTI, D. V. 1974. Purification and amino acid analysis of an active site peptide from thymidylate synthetase containing covalently bound 5-fluoro-2'-deoxyuridylate and methylenetetrahydrofolate. *Biochem Biophys Res Commun*, 57, 689-95.
- STANFEL, M. N., SHAMIEH, L. S., KAEBERLEIN, M. & KENNEDY, B. K. 2009. The TOR pathway comes of age. *Biochim Biophys Acta*, 1790, 1067-74.
- STEINBERG, S. M., BARKIN, J. S., KAPLAN, R. S. & STABLEIN, D. M. 1986. Prognostic indicators of colon tumors. The Gastrointestinal Tumor Study Group experience. *Cancer*, 57, 1866-70.
- STILES, B., WANG, Y., STAHL, A., BASSILIAN, S., LEE, W. P., KIM, Y. J., SHERWIN, R., DEVASKAR, S., LESCHE, R., MAGNUSON, M. A. & WU, H. 2004. Liver-specific deletion of negative regulator Pten results in fatty liver and insulin hypersensitivity [corrected]. *Proc Natl Acad Sci U S A*, 101, 2082-7.
- STURGILL, T. W., RAY, L. B., ERIKSON, E. & MALLER, J. L. 1988. Insulin-stimulated MAP-2 kinase phosphorylates and activates ribosomal protein S6 kinase II. *Nature*, 334, 715-8.
- SU, L. K., KINZLER, K. W., VOGELSTEIN, B., PREISINGER, A. C., MOSER, A. R., LUONGO, C., GOULD, K. A. & DOVE, W. F. 1992. Multiple intestinal neoplasia caused by a mutation in the murine homolog of the APC gene. *Science*, 256, 668-70.
- SUN, Y., CHEN, X. & XIAO, D. 2007. Tetracycline-inducible expression systems: new strategies and practices in the transgenic mouse modeling. *Acta Biochim Biophys Sin (Shanghai)*, 39, 235-46.
- TAKAHASHI-YANAGA, F. & KAHN, M. 2010. Targeting Wnt signaling: can we safely eradicate cancer stem cells? *Clin Cancer Res*, 16, 3153-62.
- TAKEBAYASHI, Y., AKIYAMA, S., AKIBA, S., YAMADA, K., MIYADERA, K., SUMIZAWA, T., YAMADA, Y., MURATA, F. & AIKOU, T. 1996. Clinicopathologic and prognostic significance of an angiogenic factor, thymidine phosphorylase, in human colorectal carcinoma. *J Natl Cancer Inst*, 88, 1110-7.
- TAKEBE, N., ZHAO, S. C., URAL, A. U., JOHNSON, M. R., BANERJEE, D., DIASIO, R. B. & BERTINO, J. R. 2001. Retroviral transduction of human dihydropyrimidine dehydrogenase cDNA confers resistance to 5-fluorouracil in murine hematopoietic progenitor cells and human CD34+-enriched peripheral blood progenitor cells. *Cancer Gene Ther*, 8, 966-73.
- TAKEDA, N., JAIN, R., LEBOEUF, M. R., WANG, Q., LU, M. M. & EPSTEIN, J. A. 2011. Interconversion between intestinal stem cell populations in distinct niches. *Science*, 334, 1420-4.
- TANIGUCHI, K., ROBERTS, L. R., ADERCA, I. N., DONG, X., QIAN, C., MURPHY, L. M., NAGORNEY, D. M., BURGART, L. J., ROCHE, P. C., SMITH, D. I., ROSS, J. A. & LIU, W. 2002. Mutational spectrum of beta-catenin, AXIN1, and AXIN2 in hepatocellular carcinomas and hepatoblastomas. *Oncogene*, 21, 4863-71.
- TEGLUND, S. & TOFTGÅRD, R. 2010. Hedgehog beyond medulloblastoma and basal cell carcinoma. *Biochim Biophys Acta*, 1805, 181-208.
- TENTLER, J. J., NALLAPAREDDY, S., TAN, A. C., SPREAFICO, A., PITTS, T. M., MORELLI, M. P., SELBY, H. M., KACHAEVA, M. I., FLANIGAN, S. A., KULIKOWSKI, G. N., LEONG, S., ARCAROLI, J. J., MESSERSMITH, W. A. & ECKHARDT, S. G. 2010. Identification of predictive markers of response to the MEK1/2 inhibitor selumetinib (AZD6244) in K-ras-mutated colorectal cancer. *Mol Cancer Ther*, 9, 3351-62.
- THIRION, P., MICHIELS, S., PIGNON, J. P., BUYSE, M., BRAUD, A. C., CARLSON, R. W., O'CONNELL, M., SARGENT, P., PIEDBOIS, P. & CANCER, M.-A. G. I. 2004. Modulation of fluorouracil by leucovorin in patients with advanced colorectal cancer: an updated meta-analysis. *J Clin Oncol*, 22, 3766-75.
- THOMAS, J. P., ARZOOMANIAN, R. Z., ALBERTI, D., MARNOCHE, R., LEE, F., FRIEDL, A., TUTSCH, K., DRESEN, A., GEIGER, P., PLUDA, J., FOGLER, W., SCHILLER, J. H. & WILDING, G. 2003.

- Phase I pharmacokinetic and pharmacodynamic study of recombinant human endostatin in patients with advanced solid tumors. *J Clin Oncol*, 21, 223-31.
- THOMAS, K. R. & CAPECCHI, M. R. 1987. Site-directed mutagenesis by gene targeting in mouse embryo-derived stem cells. *Cell*, 51, 503-12.
- TIAN, Q., HE, X. C., HOOD, L. & LI, L. 2005. Bridging the BMP and Wnt pathways by PI3 kinase/Akt and 14-3-3zeta. *Cell Cycle*, 4, 215-6.
- TORBETT, N. E., LUNA-MORAN, A., KNIGHT, Z. A., HOUK, A., MOASSER, M., WEISS, W., SHOKAT, K. M. & STOKOE, D. 2008. A chemical screen in diverse breast cancer cell lines reveals genetic enhancers and suppressors of sensitivity to PI3K isoform-selective inhibition. *Biochem J*, 415, 97-110.
- TORRES, M. A., ELDAR-FINKELMAN, H., KREBS, E. G. & MOON, R. T. 1999. Regulation of ribosomal S6 protein kinase-p90(rsk), glycogen synthase kinase 3, and beta-catenin in early *Xenopus* development. *Mol Cell Biol*, 19, 1427-37.
- TSUCHIYA, K., NAKAMURA, T., OKAMOTO, R., KANAI, T. & WATANABE, M. 2007. Reciprocal targeting of *Hath1* and beta-catenin by Wnt glycogen synthase kinase 3beta in human colon cancer. *Gastroenterology*, 132, 208-20.
- TURKE, A. B., SONG, Y., COSTA, C., COOK, R., ARTEAGA, C. L., ASARA, J. M. & ENGELMAN, J. A. 2012. MEK inhibition leads to PI3K/AKT activation by relieving a negative feedback on ERBB receptors. *Cancer Res*, 72, 3228-37.
- TWOMBLY, R. 2002. First clinical trials of endostatin yield lukewarm results. *J Natl Cancer Inst*, 94, 1520-1.
- VAN DOP, W. A., HEIJMANS, J., BÜLLER, N. V., SNOEK, S. A., ROSEKRANS, S. L., WASSENBERG, E. A., VAN DEN BERGH WEERMAN, M. A., LANSKE, B., CLARKE, A. R., WINTON, D. J., WIJGERDE, M., OFFERHAUS, G. J., HOMMES, D. W., HARDWICK, J. C., DE JONGE, W. J., BIEMOND, I. & VAN DEN BRINK, G. R. 2010. Loss of Indian Hedgehog activates multiple aspects of a wound healing response in the mouse intestine. *Gastroenterology*, 139, 1665-76, 1676.e1-10.
- VAN DOP, W. A., UHMANN, A., WIJGERDE, M., SLEDDENS-LINKELS, E., HEIJMANS, J., OFFERHAUS, G. J., VAN DEN BERGH WEERMAN, M. A., BOECKXSTAENS, G. E., HOMMES, D. W., HARDWICK, J. C., HAHN, H. & VAN DEN BRINK, G. R. 2009. Depletion of the colonic epithelial precursor cell compartment upon conditional activation of the hedgehog pathway. *Gastroenterology*, 136, 2195-2203.e1-7.
- VAN ES, J. H., VAN GIJN, M. E., RICCIO, O., VAN DEN BORN, M., VOOIJS, M., BEGTHEL, H., COZIJNSEN, M., ROBINE, S., WINTON, D. J., RADTKE, F. & CLEVERS, H. 2005. Notch/gamma-secretase inhibition turns proliferative cells in intestinal crypts and adenomas into goblet cells. *Nature*, 435, 959-63.
- VAN MILTENBURG, M. H. & JONKERS, J. 2012. Using genetically engineered mouse models to validate candidate cancer genes and test new therapeutic approaches. *Curr Opin Genet Dev*, 22, 21-7.
- VANDUSSEN, K. L. & SAMUELSON, L. C. 2010. Mouse atonal homolog 1 directs intestinal progenitors to secretory cell rather than absorptive cell fate. *Dev Biol*, 346, 215-23.
- VELHO, S. & HAIGIS, K. M. 2011. Regulation of homeostasis and oncogenesis in the intestinal epithelium by Ras. *Exp Cell Res*, 317, 2732-9.
- VERMEULEN, L., TODARO, M., DE SOUSA MELLO, F., SPRICK, M. R., KEMPER, K., PEREZ ALEA, M., RICHEL, D. J., STASSI, G. & MEDEMA, J. P. 2008. Single-cell cloning of colon cancer stem cells reveals a multi-lineage differentiation capacity. *Proc Natl Acad Sci U S A*, 105, 13427-32.
- VOGELSTEIN, B., FEARON, E. R., HAMILTON, S. R., KERN, S. E., PREISINGER, A. C., LEPPERT, M., NAKAMURA, Y., WHITE, R., SMITS, A. M. & BOS, J. L. 1988. Genetic alterations during colorectal-tumor development. *N Engl J Med*, 319, 525-32.

- VON HOFF, D. D., LORUSSO, P. M., RUDIN, C. M., REDDY, J. C., YAUCH, R. L., TIBES, R., WEISS, G. J., BORAD, M. J., HANN, C. L., BRAHMER, J. R., MACKEY, H. M., LUM, B. L., DARBONNE, W. C., MARSTERS, J. C., DE SAUVAGE, F. J. & LOW, J. A. 2009. Inhibition of the hedgehog pathway in advanced basal-cell carcinoma. *N Engl J Med*, 361, 1164-72.
- VRIES, R. G., HUCH, M. & CLEVERS, H. 2010. Stem cells and cancer of the stomach and intestine. *Mol Oncol*, 4, 373-84.
- WALKO, C. M. & LINDLEY, C. 2005. Capecitabine: a review. *Clin Ther*, 27, 23-44.
- WALTHER, A., JOHNSTONE, E., SWANTON, C., MIDGLEY, R., TOMLINSON, I. & KERR, D. 2009. Genetic prognostic and predictive markers in colorectal cancer. *Nat Rev Cancer*, 9, 489-99.
- WANEBO, H. J., RAO, B., PINSKY, C. M., HOFFMAN, R. G., STEARNS, M., SCHWARTZ, M. K. & OETTGEN, H. F. 1978. Preoperative carcinoembryonic antigen level as a prognostic indicator in colorectal cancer. *N Engl J Med*, 299, 448-51.
- WATSON, A. J. & COLLINS, P. D. 2011. Colon cancer: a civilization disorder. *Dig Dis*, 29, 222-8.
- WATT, F. M. & DRISKELL, R. R. 2010. The therapeutic potential of stem cells. *Philos Trans R Soc Lond B Biol Sci*, 365, 155-63.
- WEE, S., JAGANI, Z., XIANG, K. X., LOO, A., DORSCH, M., YAO, Y. M., SELLERS, W. R., LENGAUER, C. & STEGMEIER, F. 2009. PI3K pathway activation mediates resistance to MEK inhibitors in KRAS mutant cancers. *Cancer Res*, 69, 4286-93.
- WENG, A. P., FERRANDO, A. A., LEE, W., MORRIS, J. P., SILVERMAN, L. B., SANCHEZ-IRIZARRY, C., BLACKLOW, S. C., LOOK, A. T. & ASTER, J. C. 2004. Activating mutations of NOTCH1 in human T cell acute lymphoblastic leukemia. *Science*, 306, 269-71.
- WHEELER, D. L., HUANG, S., KRUSER, T. J., NECHREBECKI, M. M., ARMSTRONG, E. A., BENAVENTE, S., GONDI, V., HSU, K. T. & HARARI, P. M. 2008. Mechanisms of acquired resistance to cetuximab: role of HER (ErbB) family members. *Oncogene*, 27, 3944-56.
- WICHA, M. S., LIU, S. & DONTU, G. 2006. Cancer stem cells: an old idea--a paradigm shift. *Cancer Res*, 66, 1883-90; discussion 1895-6.
- WILLIAMS, J. L., KASHFI, K., OUYANG, N., DEL SOLDATO, P., KOPELOVICH, L. & RIGAS, B. 2004. NO-donating aspirin inhibits intestinal carcinogenesis in Min (APC(Min/+)) mice. *Biochem Biophys Res Commun*, 313, 784-8.
- WILLIAMS, P. L., WARWICK, R., DYSON, M. & BANNISTER, L. H. 1989. Gray's anatomy. 37th ed.: Churchill Livingstone.
- WILLIAMS, S. A., ANDERSON, W. C., SANTAGUIDA, M. T. & DYLLA, S. J. 2013. Patient-derived xenografts, the cancer stem cell paradigm, and cancer pathobiology in the 21st century. *Lab Invest*, 93, 970-82.
- WILLIAMS, T. M., FLECHA, A. R., KELLER, P., RAM, A., KARNAK, D., GALBÁN, S., GALBÁN, C. J., ROSS, B. D., LAWRENCE, T. S., REHEMTULLA, A. & SEBOLT-LEOPOLD, J. 2012. Cotargeting MAPK and PI3K signaling with concurrent radiotherapy as a strategy for the treatment of pancreatic cancer. *Mol Cancer Ther*, 11, 1193-202.
- WOLPIN, B. M. & MAYER, R. J. 2008. Systemic treatment of colorectal cancer. *Gastroenterology*, 134, 1296-310.
- WONG, E. S., FONG, C. W., LIM, J., YUSOFF, P., LOW, B. C., LANGDON, W. Y. & GUY, G. R. 2002. Sprouty2 attenuates epidermal growth factor receptor ubiquitylation and endocytosis, and consequently enhances Ras/ERK signalling. *EMBO J*, 21, 4796-808.
- WOOD, L. D., PARSONS, D. W., JONES, S., LIN, J., SJÖBLÖM, T., LEARY, R. J., SHEN, D., BOCA, S. M., BARBER, T., PTAK, J., SILLIMAN, N., SZABO, S., DEZSO, Z., USTYANSKY, V., NIKOLSKAYA, T., NIKOLSKY, Y., KARCHIN, R., WILSON, P. A., KAMINKER, J. S., ZHANG, Z., CROSHAW, R., WILLIS, J., DAWSON, D., SHIPITSIN, M., WILLSON, J. K., SUKUMAR, S., POLYAK, K., PARK, B. H., PETHIYAGODA, C. L., PANT, P. V., BALLINGER, D. G., SPARKS, A. B., HARTIGAN, J., SMITH, D. R., SUH, E., PAPADOPOULOS, N., BUCKHAULTS, P., MARKOWITZ, S. D., PARMIGIANI, G., KINZLER, K. W., VELCULESCU, V. E. &

- VOGELSTEIN, B. 2007. The genomic landscapes of human breast and colorectal cancers. *Science*, 318, 1108-13.
- WRIGHT, N. A. & ALISON, M. 1984. The Biology of Epithelial Cell Populations. Clarendon, Oxford.
- WÖHRLE, F. U., DALY, R. J. & BRUMMER, T. 2009. Function, regulation and pathological roles of the Gab/DOS docking proteins. *Cell Commun Signal*, 7, 22.
- XIANG, X., ZANG, M., WAELDE, C. A., WEN, R. & LUO, Z. 2002. Phosphorylation of 338SSYY341 regulates specific interaction between Raf-1 and MEK1. *J Biol Chem*, 277, 44996-5003.
- YANG, B., GUO, M., HERMAN, J. G. & CLARK, D. P. 2003. Aberrant promoter methylation profiles of tumor suppressor genes in hepatocellular carcinoma. *Am J Pathol*, 163, 1101-7.
- YANG, Z. Y., WU, X. Y., HUANG, Y. F., DI, M. Y., ZHENG, D. Y., CHEN, J. Z., DING, H., MAO, C. & TANG, J. L. 2013. Promising biomarkers for predicting the outcomes of patients with KRAS wild-type metastatic colorectal cancer treated with anti-epidermal growth factor receptor monoclonal antibodies: A systematic review with meta-analysis. *Int J Cancer*.
- YAUCH, R. L., GOULD, S. E., SCALES, S. J., TANG, T., TIAN, H., AHN, C. P., MARSHALL, D., FU, L., JANUARIO, T., KALLOP, D., NANNINI-PEPE, M., KOTKOW, K., MARSTERS, J. C., RUBIN, L. L. & DE SAUVAGE, F. J. 2008. A paracrine requirement for hedgehog signalling in cancer. *Nature*, 455, 406-10.
- YEH, T. C., MARSH, V., BERNAT, B. A., BALLARD, J., COLWELL, H., EVANS, R. J., PARRY, J., SMITH, D., BRANDHUBER, B. J., GROSS, S., MARLOW, A., HURLEY, B., LYSSIKATOS, J., LEE, P. A., WINKLER, J. D., KOCH, K. & WALLACE, E. 2007. Biological characterization of ARRY-142886 (AZD6244), a potent, highly selective mitogen-activated protein kinase kinase 1/2 inhibitor. *Clin Cancer Res*, 13, 1576-83.
- YILMAZ, Ö., KATAJISTO, P., LAMMING, D. W., GÜLTEKIN, Y., BAUER-ROWE, K. E., SENGUPTA, S., BIRSOY, K., DURSUN, A., YILMAZ, V. O., SELIG, M., NIELSEN, G. P., MINO-KENUDSON, M., ZUKERBERG, L. R., BHAN, A. K., DESHPANDE, V. & SABATINI, D. M. 2012. mTORC1 in the Paneth cell niche couples intestinal stem-cell function to calorie intake. *Nature*, 486, 490-5.
- YOKOTA, T. 2012. Are KRAS/BRAF mutations potent prognostic and/or predictive biomarkers in colorectal cancers? *Anticancer Agents Med Chem*, 12, 163-71.
- YOSHIOKA, A., TANAKA, S., HIRAOKA, O., KOYAMA, Y., HIROTA, Y., AYUSAWA, D., SENO, T., GARRETT, C. & WATAYA, Y. 1987. Deoxyribonucleoside triphosphate imbalance. 5-Fluorodeoxyuridine-induced DNA double strand breaks in mouse FM3A cells and the mechanism of cell death. *J Biol Chem*, 262, 8235-41.
- YU, C. F., LIU, Z. X. & CANTLEY, L. G. 2002. ERK negatively regulates the epidermal growth factor-mediated interaction of Gab1 and the phosphatidylinositol 3-kinase. *J Biol Chem*, 277, 19382-8.
- YU, K., TORAL-BARZA, L., SHI, C., ZHANG, W. G. & ZASK, A. 2008. Response and determinants of cancer cell susceptibility to PI3K inhibitors: combined targeting of PI3K and Mek1 as an effective anticancer strategy. *Cancer Biol Ther*, 7, 307-15.
- YUAN, T. L. & CANTLEY, L. C. 2008. PI3K pathway alterations in cancer: variations on a theme. *Oncogene*, 27, 5497-510.
- YUEN, H. F., ABRAMCZYK, O., MONTGOMERY, G., CHAN, K. K., HUANG, Y. H., SASAZUKI, T., SHIRASAWA, S., GOPESH, S., CHAN, K. W., FENNELL, D., JANNE, P., EL-TANANI, M. & MURRAY, J. T. 2012. Impact of oncogenic driver mutations on feedback between the PI3K and MEK pathways in cancer cells. *Biosci Rep*, 32, 413-22.
- ZACHARIAS, W. J., MADISON, B. B., KRETOVICH, K. E., WALTON, K. D., RICHARDS, N., UDAGER, A. M., LI, X. & GUMUCIO, D. L. 2011. Hedgehog signaling controls homeostasis of adult intestinal smooth muscle. *Dev Biol*, 355, 152-62.

- ZHANG, L., YU, J., PARK, B. H., KINZLER, K. W. & VOGELSTEIN, B. 2000. Role of BAX in the apoptotic response to anticancer agents. *Science*, 290, 989-92.
- ZHANG, X., GUREASKO, J., SHEN, K., COLE, P. A. & KURIYAN, J. 2006. An allosteric mechanism for activation of the kinase domain of epidermal growth factor receptor. *Cell*, 125, 1137-49.
- ZHANG, Z. G., HARSTRICK, A. & RUSTUM, Y. M. 1992. Modulation of fluoropyrimidines: role of dose and schedule of leucovorin administration. *Semin Oncol*, 19, 10-5.
- ZHOU, X. P., WOODFORD-RICHENS, K., LEHTONEN, R., KUROSE, K., ALDRED, M., HAMPEL, H., LAUNONEN, V., VIRTÄ, S., PILARSKI, R., SALOVAARA, R., BODMER, W. F., CONRAD, B. A., DUNLOP, M., HODGSON, S. V., IWAMA, T., JÄRVINEN, H., KELLOKUMPU, I., KIM, J. C., LEGGETT, B., MARKIE, D., MECKLIN, J. P., NEALE, K., PHILLIPS, R., PIRIS, J., ROZEN, P., HOULSTON, R. S., AALTONEN, L. A., TOMLINSON, I. P. & ENG, C. 2001. Germline mutations in BMPR1A/ALK3 cause a subset of cases of juvenile polyposis syndrome and of Cowden and Bannayan-Riley-Ruvalcaba syndromes. *Am J Hum Genet*, 69, 704-11.
- ZHU, L., GIBSON, P., CURRLE, D. S., TONG, Y., RICHARDSON, R. J., BAYAZITOV, I. T., POPPLETON, H., ZAKHARENKO, S., ELLISON, D. W. & GILBERTSON, R. J. 2009. Prominin 1 marks intestinal stem cells that are susceptible to neoplastic transformation. *Nature*, 457, 603-7.
- ZIMMERMANN, S. & MOELLING, K. 1999. Phosphorylation and regulation of Raf by Akt (protein kinase B). *Science*, 286, 1741-4.
- ZWICK, E., HACKEL, P. O., PRENZEL, N. & ULLRICH, A. 1999. The EGF receptor as central transducer of heterologous signalling systems. *Trends Pharmacol Sci*, 20, 408-12.

